University of Liège
Faculty of Applied Sciences
Urban and Environmental Engineering Dept.

Impact of Climate Change on High-Performance Belgian Houses: Thermal Comfort, HVAC Energy Performance, and HVAC GHG Emissions

Thesis Submitted in Partial Fulfillment of the Requirements for the Degree of Doctor of Philosophy in Engineering and Technology Sciences

By **Ramin RAHIF**

Supervisor: **Prof. Dr. Shady ATTIA** (University of Liège)

Jury members: **Prof. Dr. Anne-Claude ROMAIN** (University of Liège)

Prof. Dr. Vincent LEMORT (University of Liège)

Prof. Dr. Jonathan WRIGHT (Loughborough University)

Prof. Dr. Brice TREMEAC (Le Cnam)

Prof. Dr. Philippe ANDRE (University of Liège)

September 2023

I dedicate this work especially to my beloved Mom and Dad, Farzaneh Nezamdoust and Nasser Rahif.

این اثر را به ویژه به مادر و پدر عزیزم، فرزانه نظام دوست و ناصر رهیف تقدیم می‌کنم.

Acknowledgments

I would like to express my deepest gratitude to my supervisor, Prof. Dr. Shady Attia, whose guidance and support have been invaluable throughout my research journey and personal life. Your knowledge, expertise, and unwavering commitment have been truly inspiring, and I cannot thank you enough for all that you have done.

I would also like to extend my sincere appreciation to my committee members and thesis examiners, Prof. Dr. Anne-Claude Romain, Prof. Dr. Vincent Lemort, Prof. Dr. Jonathan Wright, Prof. Dr. Brice Tremeac, and Prof. Dr. Philippe Andre. Your critical feedback and constructive criticism have helped me to refine my work and to produce a better-quality thesis. Your dedication to your field and your commitment to the development of young researchers are truly admirable.

I would also like to express my sincere gratitude to the University of Liège and Walloon Region for providing the funding under the call 'Actions de Recherche Concertées 2019 (ARC)' (funding number: ARC 19/23-05) and the project OCCuPANt. This funding has been instrumental in enabling us to undertake the research and achieve our objectives. I am grateful for the generous support and trust they have bestowed upon us. I would also like to acknowledge the International Energy Agency (IEA) EBC Annex 80 – *"Resilient cooling of buildings"* project for providing me with a valuable opportunity to be a part of this prestigious research team. This project has been an exceptional learning experience, and I am thankful for the knowledge and skills I have gained throughout this journey. I am indebted to Dr. Peter Holzer and Philipp Stern for their exemplary leadership and guidance throughout the project. Finally, I would like to express my appreciation to the entire teams involved in both projects. The collective effort and hard work of the team have been instrumental in the success of the projects.

To my beloved family, Farzaneh Nezamdoust, Nasser Rahif, and Farzin Rahif, I am forever grateful for your unwavering love and support. You have been my constant source of inspiration, and your encouragement has been instrumental in keeping me motivated during difficult times. I cannot thank you enough for everything you have done for me.

I would like to express my sincere gratitude to my dear friends, who have been a constant source of encouragement, support, and fun. To my friends in Belgium, Parinaz Vahdani, Rana Khodaei, Niloufar Shadmanfar, Farid Mehri Sofiani, Saman Nasseri, Hessam Sadr, Alireza Sasani, Mostafa Kazemi, and Ahmad Packnejad. To my friends in Iran, Samaneh Sehat, Fatemeh Sehat, Amin Khoshkholgh, Vafa Sehat, Amir Balvaneh, Farzad Kaka, Arash Bargi, Ali Ranjbar, Behzad Radan, Navid Moradi, and Salar Nasseri. To my friends in Italy, Nazanin Khoshnevis, Aysan Ghandian, Ali Azizi, and Pedram Ghorbanpour. To my friends in Norway, Farimah Piraei, Alireza Norouziasas. Your friendship and support have been invaluable. The memories we have shared together are cherished, and I am thankful for your presence in my life.

Lastly, I would like to thank my colleagues, Waqas Ahmed Mahar, Essam Elnagar, Guirec Ruellan, Çiğdem Yönder, Hicham Arrar, Elhadi Matallah, Muriel Diaz, Deepak Amaripadath, and Mohsen Pourkiaei.

Thank you all from the bottom of my heart.

Table of Contents

Summary

Climate change arising from natural and anthropogenic sources affects the built environment in several ways. One of the major impacts of climate change is the increase in average air temperatures that can lead to more intense, severe, and prolonged heatwaves. This study is developed to project the effect of such warming weather conditions on Belgian high-performance houses and provide an idea of mitigation strategies. The study consists of three main parts (Part I, Part II, and Part III). In Part I, the study investigates a large number of thermal comfort/overheating evaluation methods to find a fit-to-purpose and appropriate method. It then provides a critical and qualitative review of cooling strategies that can be applied as mitigation strategies. In Part II, a comprehensive simulation-based methodological framework is introduced to assess and compare the resistivity of buildings and their cooling strategies to the overheating impact of climate change. This part also provides an extensive weather dataset to estimate the changes in weather conditions and heatwaves in Belgium by the end of the century under different emission scenarios. In Part III, numerical studies are performed to predict the changes in thermal comfort conditions, HVAC energy performance, and HVAC Greenhouse Gas (GHG) emissions in Belgian high-performance houses due to climate change. This part includes the evaluation of a set of active and passive cooling strategies based on uncertainty analysis, sensitivity analysis, and optimization techniques.

The following presents a summary of essential practical information and recommendations obtained from the research:

- In conducting thermal comfort analyses for building designs, it is crucial to utilize asymmetric indices to effectively identify and address potential issues related to overheating and overcooling discomfort. To ensure comprehensive protection against overheating, it is recommended to incorporate both short-term and long-term criteria into the design process, considering not only specific heatwave events but also year-round warm discomfort. As a practical recommendation, this research proposes the use of three valuable indices for overheating assessments in the context of climate change: Indoor Overheating Degree ($IOhD$), Ambient Warmness Degree (AWD), and Climate Change Overheating Resistivity ($CCOR$). These indices can be calculated using the following fomulas:

$$IOD \equiv \frac{\sum_{z=1}^{Z}\sum_{i=1}^{N_{occ}(z)}\left[\left(T_{in,o,z,i} - T_{comf,z,i}\right)^{+} \times t_{i,z}\right]}{\sum_{z=1}^{Z}\sum_{i=1}^{N_{occ}(z)} t_{i,z}}$$

$$AWD \equiv \frac{\sum_{i=1}^{N}[(T_{out,a,i} - T_b)^{+} \times t_i]}{\sum_{i=1}^{N} t_i}$$

$$\frac{1}{CCOR} = \frac{\sum_{Sc=1}^{Sc=M}(IOD_{Sc} - \overline{IOD}) \times (AWD_{Sc} - \overline{AWD})}{\sum_{Sc=1}^{Sc=M}(AWD_{Sc} - \overline{AWD})^2}$$

- When integrating cooling systems into buildings, it is important to prioritize resilience alongside energy efficiency, sustainability, and affordability. Relying solely on energy efficiency might compromise a building's ability to handle extreme events. To ensure resilient cooling, it is important to consider the four criteria of absorptive, adaptive, and restorative capacities, as well as recovery speed from the initial design phase. Combining multiple cooling strategies with different capacities might be necessary, as no single strategy can fulfill all requirements. The most suitable cooling approach can vary depending on the climate.
- For effective building performance simulations in major cities of Belgium, it is highly recommended to utilize the novel meteorological dataset presented in this thesis. This specialized dataset is thoughtfully designed to cater to the unique requirements of such simulations. By incorporating both historical and future weather data on an annual basis, including Typical Meteorological Years (TMYs), Extreme Meteorological Years (XMYs), and detailed information on three types of heatwaves (based on intensity, duration, and highest temperature), this dataset offers invaluable support for accurately assessing and optimizing building performance under various climatic scenarios.
- With global warming continuing, it is crucial to reconsider the conventional heat-preserving design concept in temperate regions. The future weather predictions indicate a shift from heating-dominated to cooling-dominated conditions in these areas in the coming decades. To cope with the rising cooling demand caused by climate change, it is imperative to adopt active cooling systems that are highly efficient. These systems should be combined with passive cooling techniques during the construction of new buildings and the renovation of existing ones. In the specific context of Belgium, promoting electricity-based HVAC systems can significantly contribute to enhancing the carbon neutrality of buildings, taking into account the country's current energy mix for electricity production. it is also advisable to integrate back-up cooling and energy storage systems, such as batteries or fuel cells, to ensure reliable and resilient cooling capabilities during unprecedented events.

Overall, climate change is a global concern. Governments and policymakers must react swiftly by encouraging proactive adaptation to limit its unfavorable consequences. This can be achieved by establishing a clear path for well-adapted building stock with quantitative targets backed up with appropriate inspection, enforcement, and access to finance.

Abbreviations and nomenclature

%POhOR	Percentage of Occupied hours Outside the Range
AC	Air Conditioning, Air Conditioner
AR6	Sixth Assessment Report
ASHRAE	American Society of Heating, Refrigerating and Air-Conditioning Engineers
ATES	Aquifer Thermal Energy Storage
AvgPPD	Averaged PPD
AWD	Ambient Warmness Degree
BCC-CSM2-MR	Beijing Climate Center Climate System Model version 2 - Medium Resolution
BCVF	Building Climate Vulnerability Factor
BLAST	Building Loads Analysis and System Thermodynamics
BPIE	Building Performance Institute Europe
BPSM	Building Performance Simulation and Modelling
CAD	Computer Aided Design
CCAG	Climate Crisis Advisory Group
CCOR	Climate Change Overheating Resistivity
CEH	Copernicus European Health
CIBSE	Chartered Institution of Building Services Engineers
CMIP3	Coupled Model Inter-comparison Project 3
CMIP5	Coupled Model Inter-comparison Project 5
CMIP6	Coupled Model Inter-comparison Project 6
CO	Carbon monoxide
CO_2	Carbon dioxide
COP	Coefficient of Performance
COP27	27th United Nations Climate Change Conference
CORDEX	Coordinated Regional Downscaling Experiment
CSSR	U.S. Climate Science Special Report
Dh	Degree hours
DOAS	Dedicated Outdoor Air Supply
DOE	US Department of Energy
DX	Direct Expansion
EC	European Commission
EEA	European Environment Agency
EH	Exceedance Hours
E-ISSN	Electronic International Standard Serial Number
EN	European Norm
EPBD	Energy Performance of Building Directive
ERA5	fifth generation ECMWF Atmospheric Reanalysis
ESMs	Earth System Models
ESP-r	Environmental Systems Performance - Research
ESRI	Environmental Systems Research Institut
EU	European Union
GA	Genetic Algorithm

GHG	Greenhouse Gas
HBCD	HexaBromoCycloDecane
HFCs	hydrofluorocarbons
HI	Heat Index
HVAC	Heating, Ventilation, and Air conditioning
HWE	Heatwave Event
IDA ICE	IDA Indoor Climate and Energy
IDD	Indoor Discomfort Degree
idf	Input Data File
IEA	International Energy Agency
IEEE	Institute of Electrical and Electronics Engineers
IEQ	Indoor Environmental Quality
IES VE	IES Virtual Environment
IOcD	Indoor Overcooling Degree
IOhD, IOD	Indoor Overheating Degree
IPCC	Intergovernmental Panel on Climate Change
ISO	International Organization for Standardization
ISSN	International Standard Serial Number
LHS	Latin Hypercube Sampling
MAR	Modèle Atmosphérique Régional
MIROC6	Model for Interdisciplinary Research On Climate version 6
MPI-ESM.1.2	Max Planck Institute Earth System Model version 1.2
MS	Member States
NARCCAP	North American Regional Climate Change Assessment Program
NBN	Belgian National Bureau for Standardization *("Bureau voor Normalisatie"* in Dutch and *"Bureau de Normalisation"* in French)
NMF	Neutral Model Format
NO	Nitrogen oxide
NO_2	Nitrogen dioxide
NOAA	U.S. National Oceanic and Atmospheric Administration
NSGA-II	Non-dominated Sorting Genetic Algorithm 2
nZEB	nearly Zero Energy Building
O_3	Ozone
ODP	Ozone Depletion Potential
PBDE	PolyBrominated Diphenyl Ether
PCB	PolyChlorinated Biphenyl
PCM	Phase-Change Material
PCSs	Personal Comfort Systems
PEF	Primary Energy Factor
PFOS	PerFluoroOctane Sulfonate
PMV	Predicted Mean Vote
POP	Persistent Organic Pollutant
PPD	Predicted Percentage of Dissatisfied
PPDOT	PPD Over Time

PPDw	Weighted PPD
RCMs	Regional Climate Models
RCP	Representative Concentration Pathway
RMI	Royal Meteorological Institute of Belgium
RQ	Research Question
SA	Sensitivity Analysis
SDGs	Sustainable Development Goals
SJR	Scimago Journal Rank
SNIP	Source-Normalized Impact per Paper
SSP	Shared Socioeconomic Pathway
TA	Thermal Autonomy
TM	Technical Memorandum
TMY	Typical Meteorological Year
TRL	Technology Readiness Level
TRNSYS	Transient System Simulation Program
UA	Uncertainty Analysis
UHI	Urban Heat Island
UK	United Kingdom
UN	United Nations
VAV	Variable Air Volume
VBA	Visual Basic for Applications
VOC	Volatile Organic Compound
VRF	Variable Refrigerant Flow
We	Weighted Exceedance
WEH	Weighted Exceedance Hours
WHO	World Health Organization
WMO	World Meteorological Organization
WWR	Window-to-Wall Ratio
XMY	eXtreme Meteorological Year

1. Introduction

1.1. Background

1.1.1. Understanding heat and climate: past, present, and future perspectives

Unraveling the past: exploring hot temperatures in historical records

While global warming does not occur uniformly, the overall trend of increasing average global temperature suggests that a greater number of regions are experiencing warming rather than cooling. Figure 1.1 illustrates this trend, indicating a consistent rise in average global land surface temperature at a rate of 0.30℃ per decade since 1980, as reported by the U.S. National Oceanic and Atmospheric Administration (NOAA) [1]. Specifically, when examining Europe, the rate of temperature increase per decade is 0.47℃ (as depicted in Figure 1.1), highlighting that this region is comparatively more affected by global warming.

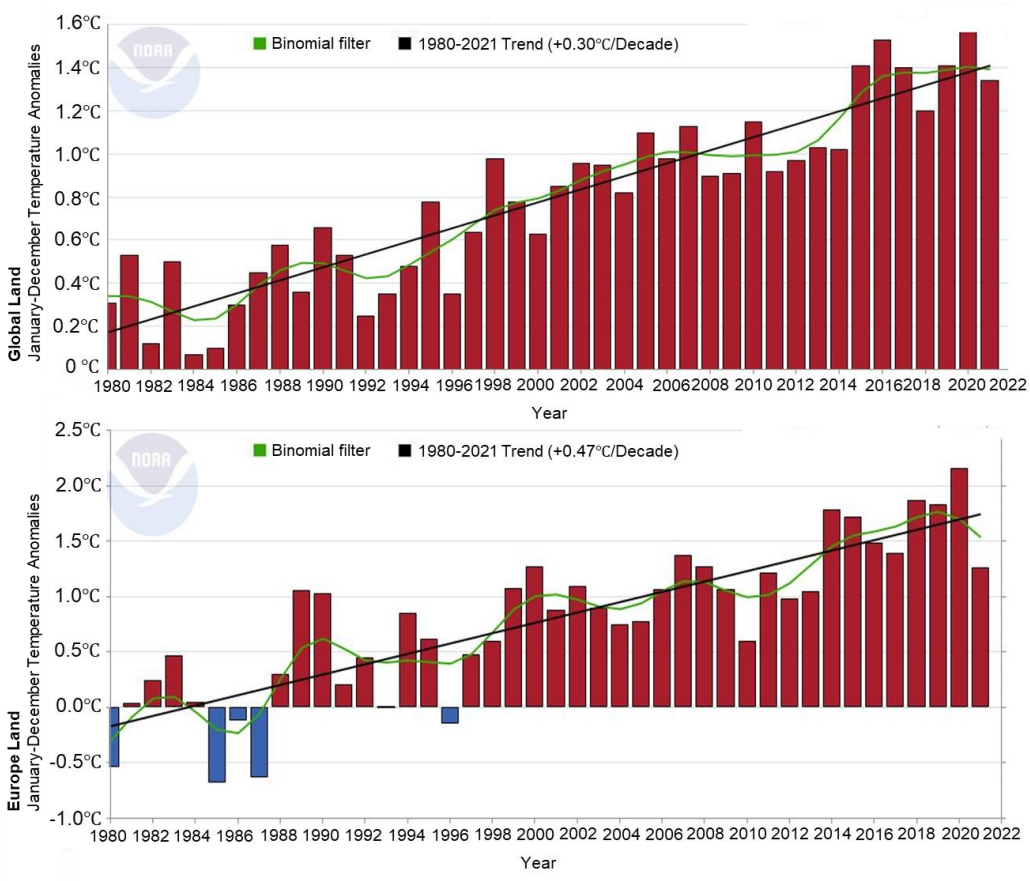

Figure 1.1. Global (upper) and Europe (lower) land temperature time series. The global time series anomalies are with respect to 1901-2000 average. The Europe time series are with respect to 1991-2020 average [1].

The rise in air temperatures contributes to various regional and seasonal temperature extremes, as well as changes in snow cover, sea ice, heavy rainfall, and shifts in plant and animal habitats. In the summer of 2019, Europe witnessed periods of exceptionally high temperatures, with Central and Western regions experiencing multiple heatwaves [2]. These heatwaves were primarily caused by a high-pressure system that transported warm air from Africa, resulting in prolonged periods of elevated temperatures over certain parts of Europe. Consequently, new maximum temperature records were set, such as 42.6℃ in Lingen (Germany), 38.6℃ in Berlin (Germany), 38.9℃ in Doksany (Czech Republic), 35.5℃ in Zurich (Switzerland), 46℃ in Vérargues (France), 40.2℃ in Angleur (Belgium), 40.7℃ in Gilze en Rijen (the Netherlands), 38.2℃ in Radzyń (Poland), 38.7℃ in Cambridge (the UK), 33.4℃ in Bergen (Norway), and 33.7℃ in Emäsalo (Finland) recorded during June and July 2019 [2]. Similarly, the scorching summer of 2003, considered the hottest summer since the 16th century, led to a devastating heatwave responsible for over 30,000 deaths (some estimates suggesting a death toll exceeding 70,000) and caused over 13 billion Euros in financial damages throughout Europe [3]. These instances illustrate Europe's history of experiencing extremely hot weather conditions with severe consequences.

Climate change and beyond: future weather projections and implications

Climate change is the long-term shift in average conditions, such as temperature and rainfall in a region. The main driver of climate change is the Greenhouse effect due to natural or anthropogenic activities. Therefore, the quantity of carbon dioxide and other greenhouse gases that are released in the upcoming decades will determine how much warming Earth will experience in the future. Currently, human activities like burning fossil fuels and cutting forests add about 11 billion metric tons of carbon every year to the atmosphere, which is roughly 40 billion metric tons of carbon dioxide [4]. The amount of carbon in the atmosphere exceeds what can be eliminated by natural processes, causing an annual increase in the overall carbon dioxide concentrations. The Climate Crisis Advisory Group (CCAG) is urging nations to *"buy time"* while reducing emissions *"urgently, deeply, and fast"* and removing *"huge quantities to lower the total from today"* of carbon dioxide and other greenhouse gases from the atmosphere. In 2022, countries in the 27th United Nations Climate Change Conference (more commonly referred to as COP27) agreed to align their emissions strategies with the objective of keeping global warming below 1.5℃.

The U.S. Climate Science Special Report (CSSR) [5] states that if annual emissions keep rising significantly, as they have since 2000, models predict that by the end of this century, the average global temperature will increase by at least 2.78℃ and perhaps as much as 5.67℃. Models also predict that temperatures would still be at least 1.33℃ degrees warmer than in the first half of the 20th century, and possibly up to 3.27℃ degrees warmer, even if annual emissions increase more gradually and start to fall dramatically by 2050. The Intergovernmental Panel on Climate Change (IPCC) estimates global warming based on the Greenhouse Gas (GHG) emission scenarios. Those scenarios are represented by Shared Socioeconomic Pathways (SSPs) in the Sixth Assessment Report (AR6) [6], which are projected scenarios of global socioeconomic evolution by 2100. The SSP scenarios

with corresponding estimated warming in 2041-2060 and 2081-2100 periods are listed in Table 1.1. The likelihood of scenarios is not estimated in the IPCC AR6, but according to a commentary published in 2020 [7], SSP5-8.5 is highly unlikely, SSP3-7.0 is unlikely, and SSP2-4.5 is likely.

Table 1.1. Estimated global warming for Share Socioeconomic Pathways in the IPCC AR6 [8], [9].

SSP No.	Scenario	Estimated warming in ℃ (2041-2060)	Estimated warming in ℃ (2081-2100)	Very likely range in ℃ (2081-2100)
SSP1-1.9	Sustainability – Taking the Green Road (Low challenges to mitigation and adaptation)	1.6	1.4	1.0-1.8
SSP1-2.6	Middle of the Road (Medium challenges to mitigation and adaptation)	1.7	1.8	1.3-2.4
SSP2-4.5	Regional Rivalry – A Rocky Road (High challenges to mitigation and adaptation)	2.0	2.7	2.1-3.5
SSP3-7.0	Inequality – A Road Divided (Low challenges to mitigation, high challenges to adaptation)	2.1	3.6	2.8-4.6
SSP5-8.5	Fossil-fueled Development – Taking the Highway (High challenges to mitigation, low challenges to adaptation)	2.4	4.4	3.3-5.7

Figure 1.2 shows the projected changes in annual mean air temperature between the World Meteorological Organization (WMO) reference period 1981-2010 and 2081-2100 in Europe based on the data from Coupled Model Inter-comparison Project phase 6 (CMIP6) for the forcing scenarios SSP1-2.6 and SSP5-8.5. In terms of the basic patterns of seasonal and regional temperature changes, CMIP6's future temperature estimates are essentially consistent with those of its predecessors (CMIP3 and CMIP5), while CMIP6 anticipates slightly higher warmings across Europe than earlier future climate projections [10]. As shown in Figure 1.2, the annual mean air temperatures are expected to rise in whole Europe, but mainly at the northern and southernmost latitudes, where the SSP1-2.6 and SSP5-8.5 scenarios predict warmings up to 2-3℃ and 5-6℃ by the end of the century, respectively. Therefore, more hot days (mean temperature > 30℃) and tropical nights (minimum temperature > 20℃) [10] are expected, which will greatly worsen the already present temperature stress in the region.

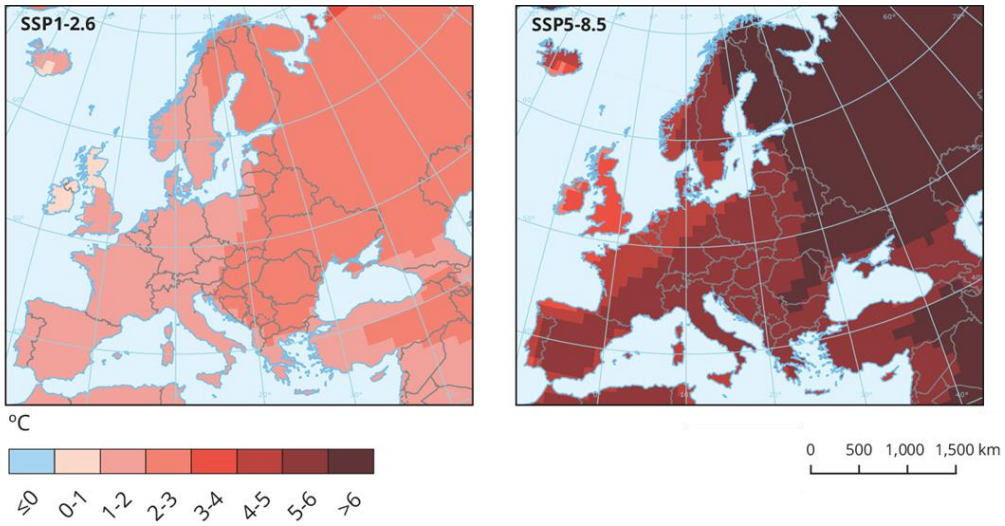

Figure 1.2. Projected changes in annual mean air temperature between the WMO reference period 1981-2010 and 2081-2100 in Europe based on the data of CMIP6 for the forcing scenarios SSP1-2.6 (left) and SSP5-8.5 (right). Retrieved from European Environment Agency (EEA) (www.eea.europa.eu/)

Climate scientists have long warned that climate change will exacerbate the frequency, intensity, and duration of heatwaves, which can have significant impacts on the population, environment, economy, and vital human activities such as agriculture. The record-breaking heatwaves that swept through Europe in recent decades will become the *"average"* summer, even if all countries reduce their greenhouse gas emissions to the level they have promised to by 2035. According to the European Commission (EC), with a 3℃ global warming, an *"intense"* heatwave, which is predicted to occur once every 50 years under the current climate, may occur almost every year in southern Europe, although such events may occur every 3 to 5 years in other regions of Europe. According to [11], depending on the season and region, the intensity and frequency of heatwaves will increase in Europe by at least a factor of 3. Another study predicts that the number of days of dangerous heat (39.4℃ and above) in mid-latitude countries in Western Europe will more than double by 2050 [12]. As a result, it is anticipated that the exacerbation of heatwaves that has been witnessed in vast areas of Europe over the past 30 years will persist (in the winter) or perhaps gain speed (in the summer) until the end of the century.

Unveiling the Urban Heat Island (UHI) effect: heat in the urban landscape

Several definitions of the Urban Heat Island (UHI) effect have been developed in the scientific literature [13]–[16]. Typically, the term *"Urban Heat Island"* refers to the trend of urban regions exhibiting higher temperatures than nearby rural areas. This temperature difference is mostly caused by human activities such as altering green spaces, use of heat-absorbing materials in constructions (e.g., concrete and asphalt), transportation, industrial processes, heat ejection from the HVAC units, etc. [16], [17].

Figure 1.3 illustrates the UHI intensity for 100 European cities, which was created under the Copernicus European Health (CEH) agreement [18]. According to the European Environment Agency (EEA), there is a notable

north-south gradient in the UHI intensity, which can be attributed to climate conditions such as average wind speed and the number of sunny days. Southern Europe shows less noticeable or even detrimental UHI compared to its northern counterparts [19]. This is because the soil in the south dries up quickly during such events, causing the countryside to warm up. In temperate regions, the combination of urbanization and climate change is also expected to result in greater exposure to high temperatures for inhabitants in cities [20]. For example, the Royal Meteorological Institute (RMI) of Belgium reported that during the July 2019 heatwave, temperatures in Brussels were up to 8°C higher than in nearby rural areas, demonstrating the significant impact of the UHI effect on the Brussels metropolitan area [21].

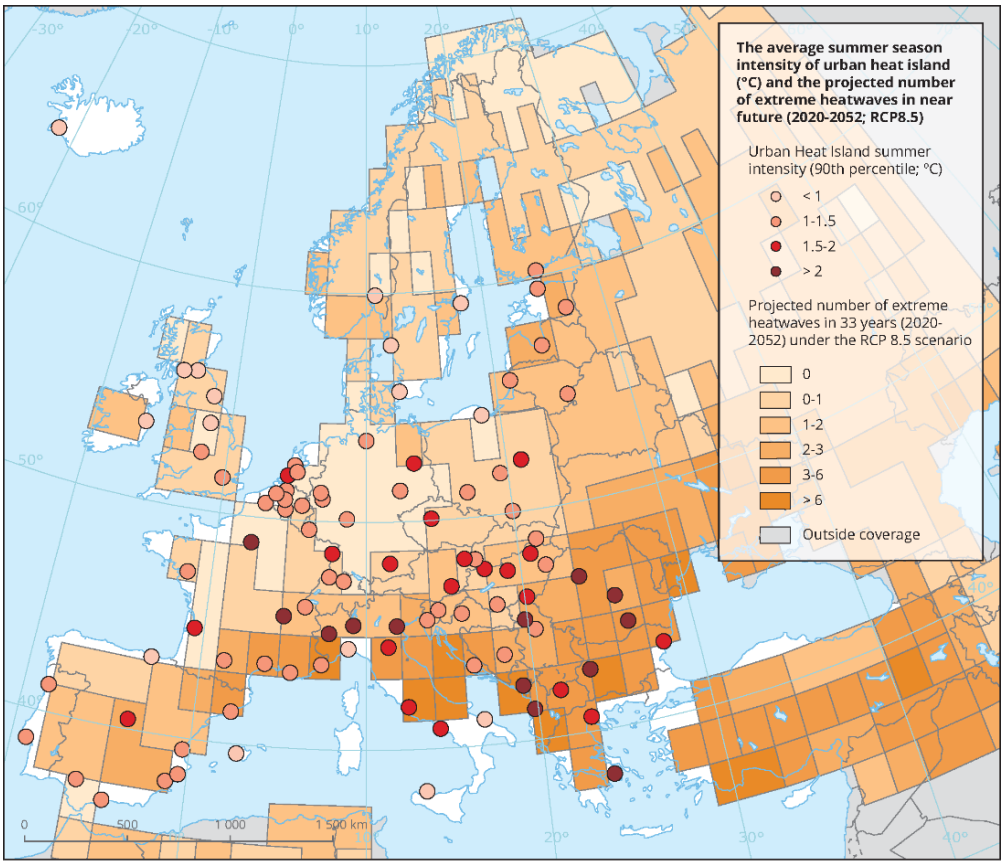

Figure 1.3. The map represents the Urban Heat Island (UHI) effect and the projected number of extreme heatwaves in the near future (2020-2052; RCP8.5) in 100 European cities. Retrieved from European Environment Agency (EEA) (www.eea.europa.eu) (Data source: ©ESRI) [18].

1.1.2. Creating sustainable and comfortable built environments: climate change implications, strategies for overheating prevention and building design concepts

Climate change and indoor air quality: navigating implications for a sustainable future

The growing body of scientific evidence suggests that climate change is expected to have both direct and indirect impacts on buildings [22], [23]. Recent research have extensively reviewed the potential effects of climate

change and mitigation and adaptation measures on the indoor environment, with a specific focus on issues such as building overheating, indoor air quality, and biological contamination [22]–[24]. Figure 1.4, adapted from reference [22], [25], illustrates various pathways through which climate change may alter Indoor Environmental Quality (IEQ).

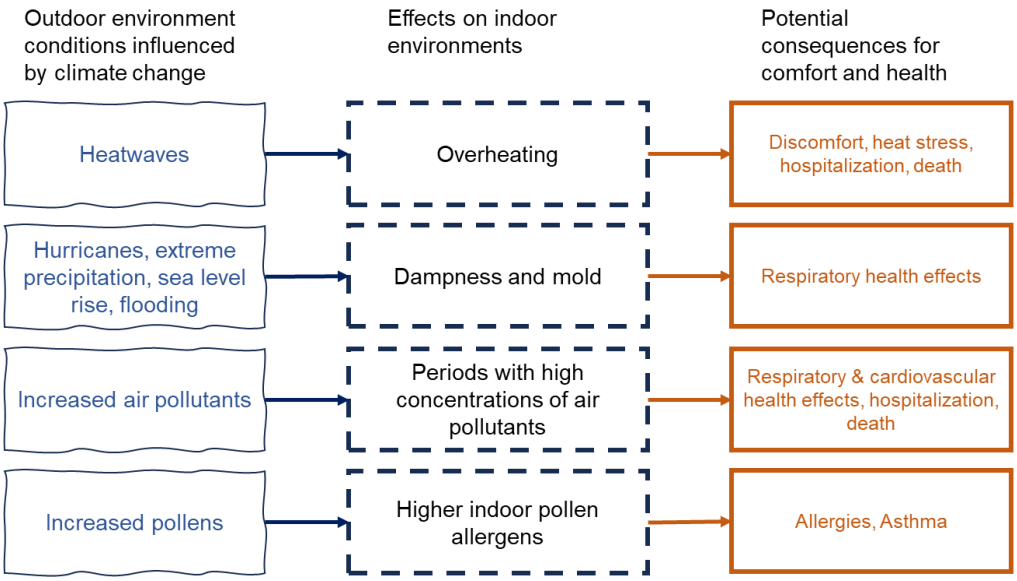

Figure 1.4. Illustrating the impact of climate change on indoor environments and associated comfort and health consequences (adapted from [22], [25], [26]).

- ***Overheating***

As global warming persists, the occurrence of prolonged and severe heatwaves is anticipated to pose a significant threat to public health. Numerous studies have extensively reported the association between elevated outdoor temperatures and increased mortality rates [27]–[29]. While epidemiological research has established a link between high outdoor temperatures and excess deaths, there is a notable lack of evidence regarding the relationship between indoor temperatures and mortality, as indoor temperatures can vary widely from one dwelling to another, even under the same outdoor temperature conditions [30]. Consequently, the definition of an indoor temperature threshold for health risks remains uncertain due to limited and indirect epidemiological data [31], [32].

Furthermore, additional studies have indicated that specific vulnerable populations, such as the elderly, young children, individuals with poor health, and those living in substandard housing without access to air conditioning, are particularly susceptible to heat stress [33], [34]. The elderly, in particular, spend a significant portion of their time indoors, making them more susceptible to indoor overheating during heatwaves [35], [36]. This suggests that a considerable number of heat-related deaths occur among the elderly, who are often indoors, especially at home, rather than among those working outdoors. Indoor overheating, exacerbated by climate change, is emerging as a critical factor contributing to heatwave-related fatalities, especially among vulnerable populations. The link between indoor temperatures and heatwave

mortality highlights the urgent need for comprehensive strategies to address indoor overheating in the context of climate change and safeguard the health and well-being of vulnerable individuals.

- ***Dampness and mold***

In contemporary well-insulated houses, the warm and potentially humid indoor environment creates favorable conditions for the proliferation of dust mites, thereby raising the risk of exposure to allergenic proteins from these organisms [29]. Climate change has the potential to disrupt pest and insect ecosystems, leading to alterations in the prevalence, distribution, and exposure levels of allergens and animal species within households [22]. Furthermore, outdoor climate changes may bring about earlier and prolonged occurrences of seasonal aeroallergens [37]. The extent to which these allergens infiltrate indoor spaces will depend on ventilation rates and penetration factors. Additionally, the rise in water damage and flooding caused by climate change can foster the growth of microbial agents such as mold and bacteria on building surfaces [38]. Moreover, climate change is expected to escalate atmospheric dust levels, particularly during drier summer conditions, which can carry various types of pathogens [39]. Dampness and mold issues in buildings have been closely associated with a substantial increase in respiratory health problems, including asthma symptoms [38], [40]. Although current data are insufficient to precisely predict the magnitude of these health effects, even modest increases in building dampness and mold, as a result of climate change, warrant serious concern. For instance, one can envision the potential health implications and costs if climate change were to cause a 25% increase in dampness and mold in buildings across the United States [25].

- ***Periods with high concentrations of air pollutants***

Elevated levels of outdoor air pollutants can infiltrate indoor environments, leading to the onset of acute and chronic health consequences. Those consequences involve intoxication, cancer, respiratory infections, cardiovascular disease, allergic symptoms and fatalities resulting from exposure to elevated concentrations of ozone (O_3), carbon monoxide (CO), nitrogen dioxide (NO_2), Volatile Organic Compounds (VOCs), Persistent Organic Pollutants (POPs), radon, etc. [26], [41], [42]. Despite significant uncertainty surrounding the impact of climate change on average concentrations of outdoor air pollutants [43], several key pollutants have been identified as susceptible to alteration that are listed below:

- **Ozone (O_3):** ozone, a significant air pollutant, is generated in the outdoor atmosphere through chemical reactions involving Volatile Organic Compounds (VOCs) and nitrogen oxides (NO) in the presence of ultraviolet light from the sun [25]. The rate of these chemical reactions, and consequently, the production of ozone, rises with higher temperatures. Thus, under unchanged conditions, outdoor ozone levels would increase with rising temperatures [25]. According to the IPCC, climate change is expected to reduce global-average tropospheric ozone but increase ozone levels in urban and nearby areas, where a majority of the population resides [6]. Climate change may also influence ozone levels in urban regions due to alterations in

air movement, cloud cover, humidity, and emission rates of reactive VOCs and NO [25]. Additionally, changes in building design, construction, and operation, partly influenced by climate change responses, could potentially impact indoor ozone levels [26]. Warmer summer temperatures might lead occupants of naturally ventilated houses to open their windows more frequently during periods of high outdoor ozone levels [44]. Ozone is known to be an irritant gaseous pollutant, causing adverse health effects such as reduced lung function, exacerbation of chronic respiratory illnesses, increased respiratory hospital admissions, and all-cause mortality, as identified by the World Health Organization (WHO).

- **Combustion products:** elevated indoor concentrations of combustion products, such as carbon monoxide (CO), nitrogen dioxide (NO2), formaldehyde, and acetaldehyde, primarily originate from local traffic emissions, wildfires, tobacco smoking, as well as the use of fossil fuel and biomass-fueled cooking and heating appliances [26], [45], [46]. Within the context of climate change, wildfires stand as the primary contributors to the augmented presence of indoor combustion products. The rise in outdoor temperatures and heat waves due to climate change is expected to foster an increase in wildfires. Moreover, climate change projections indicate a potential escalation in the number and severity of droughts in specific regions, further contributing to the likelihood of wildfires.
- **Volatile organic compounds (VOCs):** VOCs are common indoor air pollutants, including formaldehyde, benzene, and other aromatic hydrocarbons, stem from various sources such as building materials, furniture, paints, consumer products, tobacco smoke, and combustion sources [47], [48]. In the context of climate change and its mitigation policies, the increased airtightness of buildings without adequate mechanical ventilation may lead to higher indoor VOC levels [26]. The health effects associated with VOCs encompass irritation to the eyes or nose, headaches, dizziness, nausea, and allergic reactions [49]. Evidence indicates a potential link between elevated concentrations of VOCs and an increased risk of specific symptoms among infants and their mothers, including wheezing, vomiting, diarrhea, and headaches [50].
- **Persistent Organic Pollutants (POPs):** POPs like PolyChlorinated Biphenyls (PCBs) and PolyBrominated Diphenyl Ethers (PBDEs), are commonly found in indoor environments and have been linked to various adverse health effects, including cancer, immunosuppression, metabolic disorders, neurobehavioral issues, and reproductive disorders [51]. Although global efforts such as the Stockholm Convention are reducing overall POP levels, climate change poses potential challenges to human exposure to these pollutants in indoor settings through direct and indirect mechanisms [26]. For instance, higher indoor temperatures can lead to increased volatile emissions of POPs from household products and materials, resulting in elevated indoor concentrations [52], [53]. Additionally, specific POPs used as brominated flame retardants, like PBDEs, and fabric treatment products, such as PerFluoroOctane Sulfonate (PFOS), may become more significant indoor sources in future climate-controlled buildings [51]. The increased use of thermal wall insulation in houses might also

contribute to indoor contamination with flame retardants like HexaBromoCycloDecane (HBCD), commonly used in insulation materials [26].

- **Radon:** Radon, a naturally occurring radioactive gas emitted from rocks and soils, can infiltrate buildings and reach significant indoor concentrations [54]. Studies have demonstrated seasonal variations of radon in the majority of buildings [55]. Effective ventilation serves as the primary method for removing radon from indoor air, as inadequate ventilation rates can lead to a buildup of radon gas within properties [56]. Consequently, climate change adaptation and mitigation strategies that impact building ventilation may influence radon exposure [57]. It is estimated that radon exposure is responsible for lung cancer deaths, with half of these fatalities occurring among current smokers [26].

- ***Higher indoor pollen allergens***

In northern temperate climates, the early onset of spring and the spread of invasive species like ragweed are introducing novel aeroallergens, leading to increased sensitization [58], [59]. The rising atmospheric carbon dioxide (CO_2) levels have already triggered augmented vegetative growth. Laboratory and field experiments indicate that outdoor pollen levels are expected to increase due to higher CO_2 levels, elevated temperatures, and extended growing seasons linked to human-induced climate change [60], [61]. These changes may have adverse implications for health, including allergic rhinitis, asthma, and atopic dermatitis [62].

This thesis centers its attention on one specific aspect of the mentioned climate change impacts on indoor environmental quality, which is the consequences of overheating. By focusing on this crucial aspect of indoor environmental quality, the thesis seeks to contribute to the development of sustainable and resilient building designs and strategies that can enhance indoor comfort and protect occupants from the adverse effects of rising temperatures caused by climate change.

Building policies for a cooler future: overheating prevention in European buildings

The new recast of the Energy Performance of Building Directive (EPBD) was published in 2021, with a particular focus on ensuring optimal indoor thermal comfort. Member States (MS) have been called upon to review their national regulations linked with the EPBD by the end of 2025 [63]. The primary objective of the EPBD is to promote energy efficiency and achieve decarbonization of buildings in the European Union (EU) by 2050 while also creating a stable environment within these structures. Compliance with the EPBD requires all new buildings within the EU to adhere to nearly Zero Energy Building (nZEB) requirements by the end of 2021, with existing buildings required to comply by 2050. Buildings that meet the nZEB requirements exhibit high levels of energy efficiency, with renewable energy sources covering almost all or a significant portion of the energy use. The EU MS are responsible for developing their unique nZEB requirements based on the overarching definition. Nonetheless, there is a standard framework that

takes into account various factors, including the building's energy use, renewable energy production, and environmental impact.

The status nZEBs in Europe is not consistent across all countries at present. Some nations have already implemented nZEB standards, while others are still in the process of doing so. The European Commission monitors the progress of MS toward achieving the nZEB target and offers assistance and advice to support them in reaching their objectives. Figure 1.5 illustrates that according to the Building Performance Institute Europe (BPIE) factsheet [64], nZEB requirements have been established in all MS since 2021, except for Bulgaria, Hungary, and Greece.

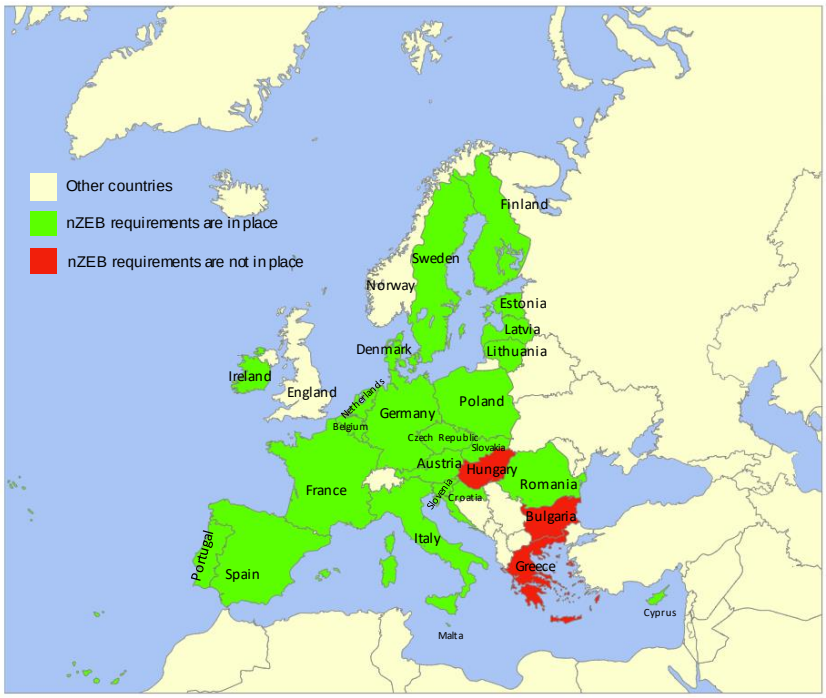

Figure 1.5. The map illustrates the status of nZEB requirements in EU MS. The map is created using an online tool [65].

The EPBD incorporates calculation methods for both residential and non-residential buildings, which are based on the ISO 52016-1 standard [66]. The ISO 52016-1 standard replaces the widely-used ISO 13790 [67] standard, outlining a method for determining energy requirements for heating and cooling, internal temperatures, and sensible and latent heat loads. Similar to its predecessor, the ISO 52016-1 standard includes both monthly and hourly calculation methods. The hourly method in ISO 52016-1 is more sophisticated than the simplified hourly method found in ISO 13790 and is better suited to handle dynamic interactions between building components and system elements [68]. Although each country has its specific regulations with different parameters and thresholds to ensure thermal comfort, they are inspired by this standard. The inconsistency between the calculation methods, along with poor communication between the MS, results in geographic discontinuities in thermal comfort criteria, even in regions with similar climatic conditions. The methods used to calculate overheating in European building codes based on the EPBD are extensively examined in [69], [70]

Focusing on Belgium, the implementation of the EPBD is the responsibility of each region, namely Brussels, Flanders, and Wallonia. The Brussels region, in French *"Région de Bruxelles-Capitale"*, has decided to adopt the criteria outlined by the Passive House standard [71]. Consequently, compliance with overheating regulations in Brussels is achieved by ensuring that the indoor temperature does not exceed 25℃ by 5% during occupied hours throughout the year. Conversely, the Walloon region, in French "*Région Wallonne"*, and the Flemish region, in Dutch *"Vlaams Gewest"*, utilize a quasi-steady-state heat balance method [72], [73]. This involves introducing a time-integrated overheating index, I_{overh} [Kh], which sums up the normalized monthly excess of heat gains in relation to the indoor set-point temperature.

In general, the current European building codes do not sufficiently address climate change implications for overheating evaluations in buildings [69]. These codes are not equipped to handle the challenges presented by climate change in the future. Furthermore, a lack of communication and coordination between countries regarding thermal comfort has resulted in the absence of a standardized approach to address overheating. This is a pressing issue that must be addressed to construct long-term buildings capable of preserving the well-being and health of European residents during current and future heatwaves.

Cooling strategies: mitigating overheating challenges in building design

Cooling strategies, both active and passive, are essential in preventing buildings from overheating. Active cooling strategies utilize mechanical equipment to enhance heat transfer to lower indoor temperatures. Despite their effectiveness, they use large amounts of energy and can be expensive to run. The International Energy Agency (IEA) states that maintaining comfortable indoor temperatures using air conditioners and electric fans currently contributes to ~20% of the total electricity use in buildings worldwide [74]. In contrast, passive cooling strategies rely on natural methods like shading and ventilation to keep indoor temperatures comfortable. Passive cooling strategies consume no to very low energy, tending to be more sustainable and cost-effective than active cooling. However, they may not suffice in extremely hot climates or buildings with high internal heat gains.

A detailed classification of active cooling systems has been proposed by [75] based on the source of energy used to power the cooling units. Active cooling strategies require an external power source and utilize various energy sources, including electricity, natural gas, heat, or solar power, to remove heat from indoor spaces. As shown in Figure 1.6, active cooling strategies can be classified into two primary groups, which are electricity-driven and thermal energy-driven AC units [75].

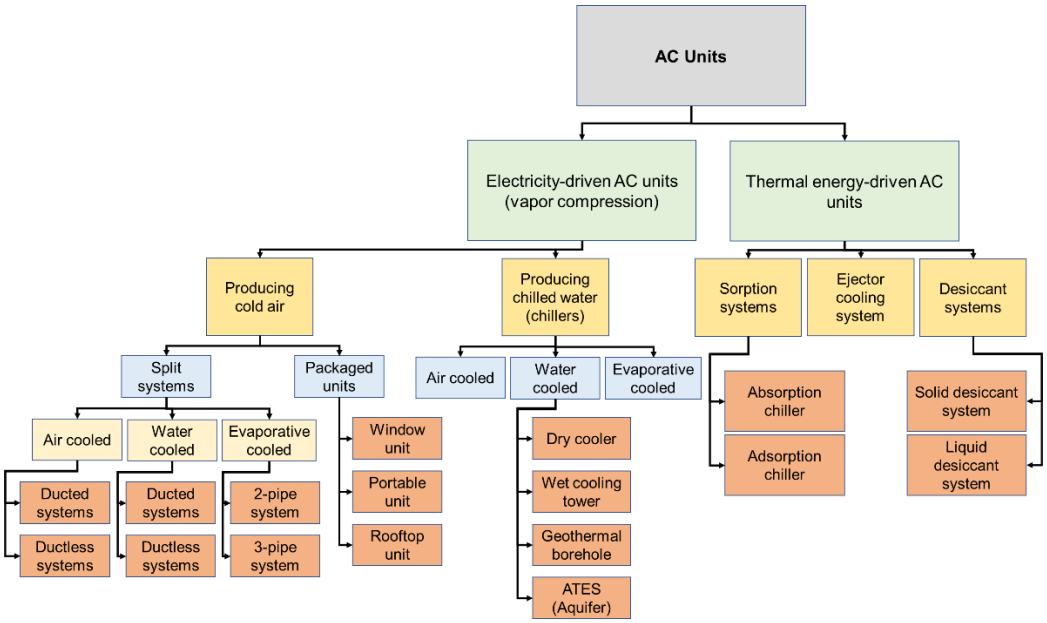

Figure 1.6. Classification of active cooling systems [75].

Passive cooling strategies, in contrast, make use of ambient cooling sinks such as building materials, air, water, and the night sky to counteract the effects of ambient air, direct solar heat gain, and internal heat gain on the building temperature [76]. As shown in Figure 1.7, passive cooling strategies can be classified into three major categories: heat protection, heat modulation, and heat dissipation techniques [77], [78]:

- **Heat protection:** The objective of this technique is to protect the building from excessive amounts of solar heat gains, which can be classified into two main categories: microclimate and solar control strategies. Heat protection can be accomplished by various means, such as shading devices, landscaping, and using water surfaces or active vegetation.
- **Heat modulation:** This technique involves using the thermal storage capacity of the building structure to regulate the amount of heat gained by the building. The stored heat is released at a later and appropriate time to safeguard the building. The effectiveness of this technique largely depends on the type of thermal mass used in the building's construction and the chosen discharge methods, such as free cooling.
- **Heat dissipation:** This technique is useful in situations where the above techniques are insufficient to maintain comfortable conditions. This technique involves removing excess heat from the building and releasing it into a suitable environmental heat sink (e.g., ambient air, water, and the sky) at a lower temperature. The effectiveness of this technique relies on the availability of an environmental heat sink and thermal coupling between the building and the heat sink.

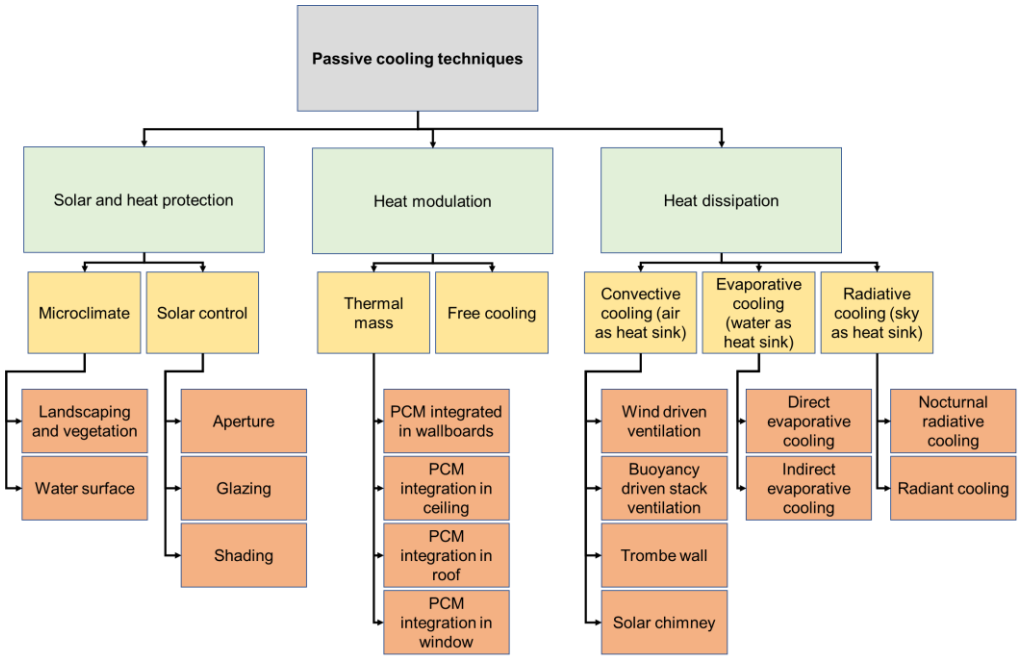

Figure 1.7. Classification of passive cooling techniques [76].

The selection of active and passive cooling strategies (or their combinations) for buildings depends on various factors, including climate, building design, occupancy patterns, ease and cost of installation, operating costs, and cultural limitations [79]. For instance, the climate is a critical factor in selecting a cooling strategy since it determines the level of heat gained from the outdoor environment and the availability of cooling resources. Similarly, a building with high occupancy and internal heat gain may require a more robust cooling system than one with lower occupancy. Additionally, cost and ease of installation may affect the feasibility of certain cooling strategies, especially in developing countries or regions with limited resources. Finally, cultural limitations, such as the use of traditional cooling methods or local customs regarding ventilation, can also play a crucial role in determining the most appropriate cooling strategy for a building.

Climate change poses a significant global challenge for cooling strategies. With the ongoing effects of global warming, the demand for cooling solutions to ensure comfortable indoor environments is expected to escalate. However, changing outdoor weather conditions can have adverse impacts on both active and passive cooling methods, as their design, sizing, and efficiency heavily rely on environmental factors [80].

Regarding active cooling strategies, the efficiency and effectiveness of these strategies are directly influenced by outdoor environmental parameters such as temperature. As the external heat becomes more extreme, cooling systems are forced to work harder to achieve the desired indoor temperatures. This heightened demand places a considerable strain on energy resources and can potentially lead to shortages or failures in the grid as well as higher cooling costs for consumers and businesses alike [81]. Moreover, the efficiency of active cooling components, such as pumps and condensers, is closely tied to specific performance curves derived from outdoor temperature data. As temperatures rise, the performance of these

components may be compromised, leading to reduced cooling efficiency, increased maintenance needs, and, in some cases, system failures. This adds an additional burden on both energy use and maintenance expenses. Likewise, passive cooling techniques are not immune to the influence of a changing climate. For instance, as outdoor temperatures steadily increase, the temperature gradient between indoor and outdoor environments diminishes, resulting in a decline in the capacity of passive cooling methods, such as natural ventilation.

Temperate climates and innovative design concepts: achieving comfort and efficiency

Temperate regions are characterized by relatively moderate mean annual temperatures [82]. The Köppen climate classification designates a climate as *"temperate"* when the mean temperature in the coldest month falls between −3℃ and 18℃ and at least one month averaging above 10℃ [83]. Most temperate regions experience four distinct seasons, with temperatures varying greatly between summer and winter [84]. As shown in Figure 1.8, these climates mainly occur in the middle latitudes (23.5° to 66.5° N/S of the Equator), situated between the tropical and polar regions [85].

Due to its larger landmass and more stable temperatures, the Northern Hemisphere is home to the majority of the world's human population residing in temperate zones [86]. In coastal temperate regions, population densities are typically three times higher than the global average [87]. Over the last century, nearly all temperate coastal regions have experienced net immigration, which has resulted in significant population growth and rapid economic development [88], [89], [90]. This growth has led to the widespread conversion of natural coastal wetlands for agriculture, aquaculture, silviculture, industrial, and residential uses [91]. In Europe, there are several major cities with temperate climates, such as Paris, Berlin, Amsterdam, Brussels, Vienna, and Copenhagen.

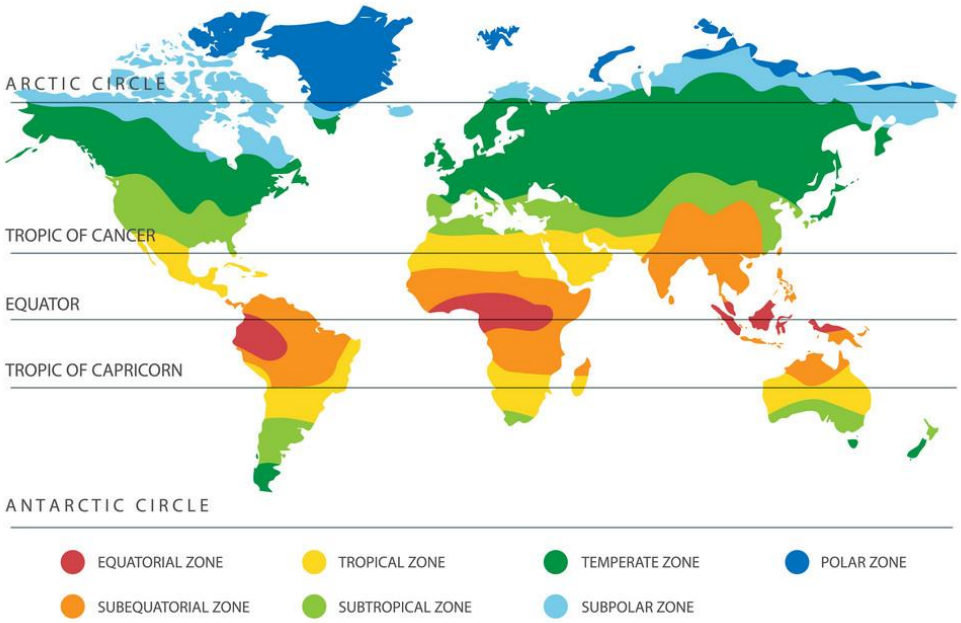

Figure 1.8. World climate map with temperature vectors. Retrieved from www.vectorstock.com/.

In regions with temperate climates, the primary focus of building thermal design is on conserving heat during the winter season [69]. The conventional approach involves the use of passive design techniques along with efficient heating systems to regulate indoor temperatures throughout the year. These strategies typically involve:

- Implementing adequate wall, roof, and floor insulation to retain heat inside the building during winter and keep it out during summer.
- Using a rectangular floor plan with shorter sides facing east and west and a long southern face with larger windows to capture solar energy [92].
- Incorporating high thermal mass to store excess thermal energy and emit it as low-level radiant heat when necessary [93], [94].
- Designing windows to optimize solar gains during winter and reduce heat gains during summer, such as double-glazed windows with low-emissivity coatings [95].
- Utilizing natural ventilation through windows and doors, with mechanical ventilation for extreme weather conditions [96], [97].

In temperate regions, buildings typically are equipped with heating systems and may require cooling systems in the summer as global warming intensifies. To address this issue, energy-efficient systems like heat pumps that use non-GHG refrigerants or district heating and cooling networks are gaining popularity in Europe [98]. These systems show great promise in harnessing renewable energy sources, such as solar, thermal, or geothermal energy, and reducing the dependence on non-renewable energy sources [99].

1.1.3. Building Performance Simulation and Modelling (BPSM)

Definition, methods, and tools

Building Performance Simulation and Modelling (BPSM) involves replicating various aspects of a building through computer-based mathematical models, which are developed using fundamental physical principles and engineering practices [100]. BPSM is a multidisciplinary and problem-oriented approach with a broad scope, which considers dynamic and continuous boundary conditions over time and relies on numerical methods to approximate realistic models with real-world complexities [101]. To achieve this goal, several software tools have been developed that construct physics-based models, requiring substantial input and expert assumptions [102]. Computational simulation stands out as one of the most powerful analysis tools available today. However, it is crucial to understand that simulation does not provide definitive solutions or answers, and ensuring the quality of simulation results can often be challenging [101].

The accuracy of building models and simulations heavily relies on the quality of input data, encompassing factors such as building geometry, construction materials, HVAC systems and components, internal loads, lighting, water heating, control strategies, occupancy and operating schedules, thermostat settings, renewable generation systems, and weather data, among others (as depicted in Figure 1.9) [103], [104]. BPSM software translates this input data into physical equations to generate outputs related to energy consumption, costs, occupant comfort, and more, over various timeframes, such as yearly, hourly, or shorter periods.

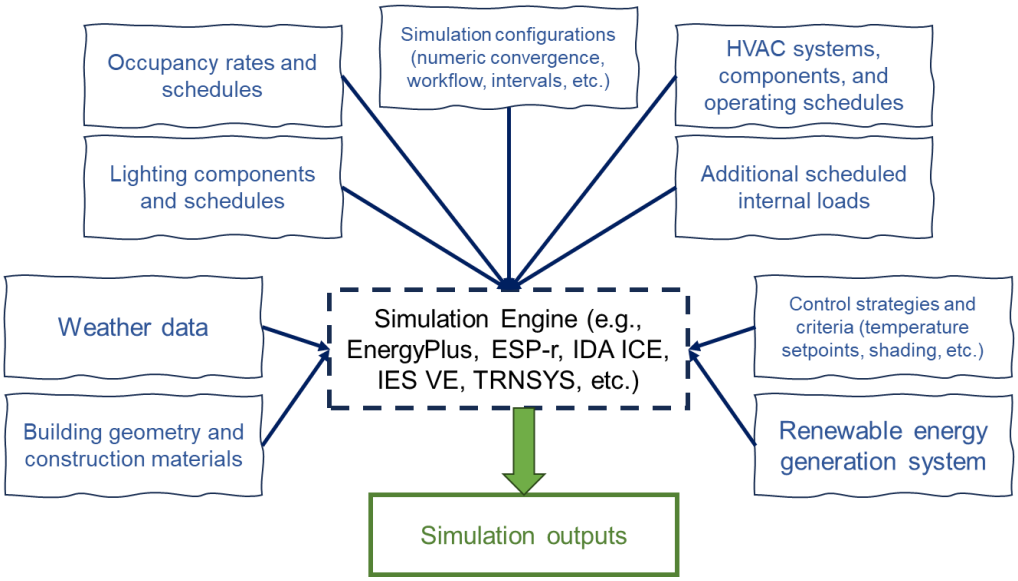

Figure 1.9. General input data required by simulation engines.

According to [105], there are six essential aspects of building design that designers should prioritize and address during the conceptual stage. These aspects encompass metrics, comfort levels, climate considerations, passive strategies, energy efficiency, renewable energy systems, and innovative solutions and technologies. However, integrating these design aspects early

on in the process is a complex and time-consuming endeavor that demands a high level of expertise. Fortunately, BPSM serves as an ideal tool to overcome these barriers. By incorporating BPSM techniques during the initial architectural design phase, designers can leverage its unique ability to provide answers to questions that may be difficult to address through other means.

In modern design practices, designers increasingly rely on BPSM software even during the initial stages of a project to address specific design inquiries. Thess software empower them to predict thermal behavior, evaluate energy costs, and optimize retrofitting measures [106]. They calculate essential variables such as indoor temperatures, heating/cooling needs, HVAC energy use, lighting preferences, occupant comfort, and ventilation levels [64]. In such a way, the designers are able to make informed decisions and ensure compliance with regulations [106]. As indicated in [107], BPSM applications have generally proven their effectiveness in the use scenarios listed below:

- **Architectural Design:** BPSM informs energy-efficient building design by balancing construction costs and operational energy costs, leading to cost reductions in both areas.
- **HVAC Design and Operation:** BPSM helps engineers design efficient HVAC systems and develop effective control strategies.
- **Building Performance Rating:** BPSM assesses building performance for code compliance, green certification, and financial incentives.
- **Building Stock Analysis:** BPSM supports the development of energy codes and aids utilities and local governments in planning energy-efficiency programs.

Over time, the field of BPSM has witnessed the introduction of a wide range of software options, each with its own distinctive features and intended applications [108]. These software tools have been developed to cater to the diverse needs of designers, architects, engineers, and researchers involved in building design and energy analysis. Below is a summary of major BPSM software options derived from [106], serving as valuable resources for professionals engaged in building design and energy analysis:

- **EnergyPlus:** A widely recognized energy simulation software, EnergyPlus was developed in 1996 with sponsorship from the United States Department of Energy (DOE) [109]. It combines features from BLAST and DOE-2 while introducing a new approach that integrates heat balance and a generic HVAC system. Visual building conception and design require third-party software like DesignBuilder.
- **ESP-r:** ESP-r is a comprehensive mathematical software used for project management, offering tools for data coordination, simulation, Computer Aided Design (CAD) applications, performance evaluation, and report generation. It employs complex equations to address various aspects simultaneously, such as geometry, construction, operation, distribution, and heat dissipation [106]. Building geometry can be specified using CAD software or similar tools. However, using

ESP-r requires substantial expertise and entails a significant learning curve.

- **IDA ICE:** IDA ICE is a modular thermal simulation software that utilizes a general system simulation platform. It describes multi-domain physical systems using symbolic equations and the Neutral Model Format (NMF). Users can define tolerances to control solution accuracy and integrate various numerical modeling approaches [106].
- **IES VE:** IES VE is a simulation software tool for comprehensive building analysis. It incorporates ApacheSim, a dynamic thermal simulation tool for evaluating heat transfer processes. The software facilitates detailed modeling and optimization of building systems considering comfort and energy factors. ApacheSim can be linked with MacroFlo for natural ventilation analysis and HVAC Apache for detailed HVAC system analysis.
- **TRNSYS:** TRNSYS is a modular transient system simulation software designed for developing complex energy-related systems. It allows for problem decomposition into smaller components [110], spanning from basic heat pumps to multi-zone building complexes. TRNSYS Simulation Studio offers a graphical user interface for configuring components, while building construction can be performed using TRNBuild [109]. TRNSYS also enables integration with other software tools like Matlab, Excel, and VBA.

Uncertainties

Building performance simulations and models rely on numerous assumptions derived from simplified design guidelines or expert opinions, often based solely on personal judgment [111]. However, it is important to acknowledge that many of the design variables treated as deterministic values are, in fact, subject to uncertainty [111]. As a result, these simulations and models are inherently associated with uncertainties arising from certain input variables [112]. For instance, variables like occupant behavior, thermal properties of the building envelope, and weather conditions possess inherent uncertainties that can significantly influence the outcomes obtained from numerical modellings [111]. It was shown in many studies that such uncertainties can be quite substantial [113]–[115], which makes it imperative to convey these uncertainties to the decision maker [111].

Numerous uncertainties originate from various sources, necessitating a thorough assessment of the associated risks. The significance of evaluating uncertainty in physical experiments directly corresponds to the need for understanding its implications [116]. Failing to quantify the overall error in predictions leaves practitioners uncertain about the accuracy of their results [116]. Therefore, uncertainty analysis plays a critical role in enabling the resolution of the following challenges when applied in simulations [116]:

- **Model realism:** The extent to which the model accurately represents reality, considering its level of detail and fidelity.
- **Input parameters:** Determining appropriate values for input parameters in the absence of measured data.

- **Stochastic processes:** Assessing the impact of assumptions made about future weather, occupancy patterns, and operational factors on the model's predictions.
- **Simulation program capabilities:** Identifying uncertainties associated with the choice of algorithms used for heat and mass transfer processes in the simulation.
- **Design variations:** Understanding the effects of modifying specific aspects of the design on the overall outcomes.

Figure 1.10 illustrates two main categories of uncertainty analysis in building energy assessment: forward and inverse uncertainty quantification [117], [118]. Forward uncertainty analysis, also known as uncertainty propagation, aims to quantify the uncertainty in system outputs that arise from uncertain input variables and mathematical models. On the other hand, inverse uncertainty analysis, also referred to as model calibration, seeks to determine unknown variables using mathematical models and measurement data [119]. So far, a greater emphasis has been placed on forward uncertainty propagation in the field of building energy analysis, as inverse uncertainty quantification is considerably more challenging [119]. Nonetheless, both forward and inverse uncertainty analyses are interconnected [120]. The findings obtained from inverse uncertainty analysis often serve as inputs for forward uncertainty propagation, e,g., it enables the prediction of building energy use based on different energy-saving strategies [119].

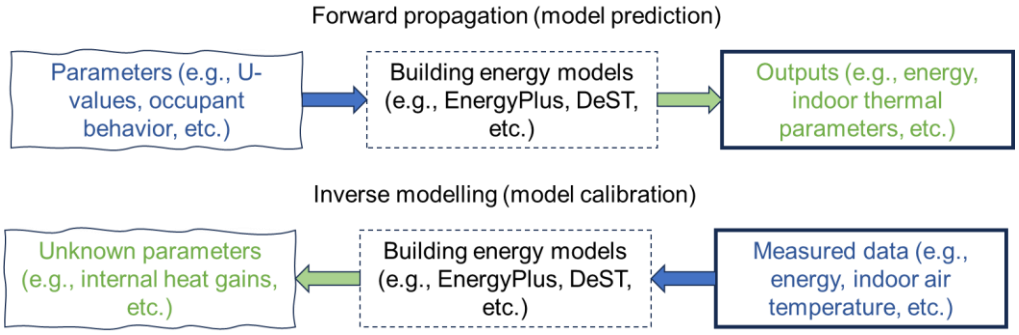

Figure 1.10. Illustration of forward and inverse uncertainty analysis methods applied in building performance analysis [118].

The progress in contemporary uncertainty quantification techniques has significantly improved the methodologies and resources accessible for examining uncertainty analysis in building models [120], [121]. The application of uncertainty analysis has gained extensive utilization in diverse domains of building analysis. These include model calibration [112], [119], life cycle analysis [122], [123], building stock analysis [124], [125], impact and adaptation to climate change , sensitivity analysis [126], [127], spatial analysis [128], [129], and optimization [130], [131].

1.2. Problem statement

Climate change represents an enormous global challenge that is causing significant and widespread impacts across multiple sectors, including the built environment. As mentioned earlier, one specific concern regarding climate

change is its impact on overheating in houses, particularly during the summer months, which has motivated the development of the current thesis. A study conducted in the UK [132] revealed that indoor temperatures in dwellings have been rising at a rate of approximately 1.3℃ per decade between 1978 and 1996. This trend is projected to continue in the future, as many researchers have reported an increase in overheating of buildings due to climate change [26], [133]–[137]. With rising average temperatures and more frequent and intense heatwaves, maintaining comfortable indoor temperatures in buildings has become a critical challenge. Overheating in houses can have some potential effects, including:

- **Thermal discomfort:** Thermal comfort, which is described as "that state of mind that expresses satisfaction with the thermal environment and is assessed by subjective evaluation," can be negatively affected by overheating [138]. Thermal discomfort can result in a lack of satisfaction for building occupants, but it does not necessarily pose a significant threat to their health. It can manifest in several ways, such as feeling too hot or cold, experiencing dryness or humidity, and other related factors.
- **Sleep disruption:** The quality and consistency of sleep can be greatly affected by high indoor temperatures. According to the guidelines set by the Chartered Institution of Building Services Engineers (CIBSE) [139], temperatures above 24℃ degrees Celsius can result in several unfavorable outcomes during sleep, including reduced sleep efficiency, increased sleep fragmentation, and longer time to fall asleep [140]. These outcomes can be counterproductive and result in decreased productivity during the day and potential health issues [141], [142].
- **Reduced productivity:** High indoor temperatures can significantly impact occupants' productivity due to the negative effect of overheating on cognitive performance, including tasks such as perception, memory, and attention [143]–[145]. Studies have shown that overheating incidents can result in a decrease in productivity of up to 10% or more [146]–[148]. It is worth noting that while reduced productivity is primarily a concern in workspaces and educational buildings, it is also becoming an important issue in residential buildings due to the increasing trend toward homeworking [149].
- **Health issues and mortality:** Extended periods of high temperatures can have a cumulative physiological impact on the human body, worsening the leading causes of death worldwide, including respiratory and cardiovascular diseases, diabetes mellitus, and renal disease, as stated by the World Health Organization (WHO). Heatwaves can have acute effects on large populations for brief periods, leading to public health emergencies and excess mortality. The European heatwave of August 2003 is a prime example, resulting in an additional 70,000 deaths throughout Europe. The impact of the 2003 heatwave varied across different cities, with excess deaths ranging from 35.7% in Barcelona, 43.8% in London, to 105.5% in Paris, as illustrated in Figure 1.11 [150]. High indoor temperatures can affect all populations, especially those who are more vulnerable, such as the elderly, infants and children, pregnant women, and individuals with medical conditions.

- **Use of HVAC system:** The changing climate is expected to impact the use of HVAC systems, with a projected 5%-15% decrease in heating demand and a 25%-50% increase in cooling demand across Europe by the 2050s [151]. As a result, households are likely to purchase and use more air conditioning units to combat rising temperatures during the summer months. However, this could lead to excessive strain on cooling system components and the electricity supply grid during future heatwaves, which are expected to increase peak per capita demand by up to 9.5% in temperate regions [152]. This could result in breakdowns and power outages [153], [154].

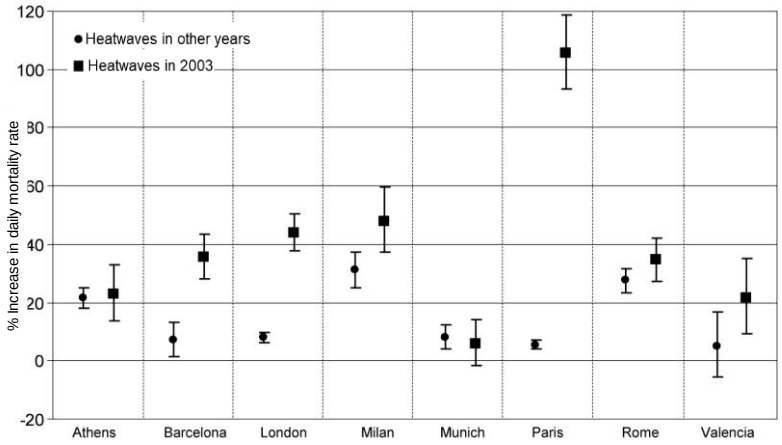

Figure 1.11. The figure shows city-specific estimates of the impact of heatwaves on daily mortality, indicated by the percentage increase and 90% confidence intervals, during the summer of 2003 as well as in other years [150].

The pressing need to tackle the impact of global warming on indoor thermal environments in buildings has motivated this thesis. The thesis centralizes on assessing the impacts of climate change and aims to partially address the issues by offering solutions. In doing so, this thesis aims to contribute towards three of the United Nations (UN) Sustainable Development Goals (SDGs), namely SDG03: Good health and well-being, SDG11: Sustainable cities and communities, and SDG13: Climate action. By offering solutions to assess and mitigate the effects of global warming on indoor thermal environments, this thesis intends to promote healthy and sustainable living conditions while contributing towards climate action.

2. Research framework

2.1. Aim, objectives, and research questions

This Ph.D. research forecasts the impact of climate change on Belgian high-performance houses and provides information on if and which adaptation measures are needed. On the strategic level, this research aims at contributing to a healthy and productive community by indicating the vulnerability of occupants in the indoor environment to the projected impacts of climate change. In other words, the research aims to safeguard human health, comfort, and productivity inside buildings despite a changing climate and achieve this most sustainably, i.e., without compromising climate change mitigation efforts. Furthermore, this Ph.D. research questions the status quo in building regulations and designs about overheating risks and helps the policy-makers design measures to protect the most fragile and often isolated population. In this sense, this Ph.D. research has two-fold objectives to demonstrate (i) a systematic methodology for rapid analysis of overheating risk and comparison of cooling strategies in the context of climate change and (ii) the vulnerability of high-performance Belgian houses to the overheating impact of climate change and how to increase their preparedness to cope with the warming weather conditions.

This Ph.D. research intends to answer the following main research question:

- *What are the likely impacts of climate change on the thermal comfort, HVAC energy performance, and HVAC GHG emissions of high-performance Belgian houses, and how to adapt them?*

The main research question can be broken down into several specific questions that need to be addressed initially. Those questions explore different research gaps that are identified and answered in different scientific publications. In total, seven publications have been published that form the chapters of this thesis. The specific research questions are as follows:

- ***RQ1**. How do current methods assess time-integrated thermal discomfort/overheating in residential buildings in temperate climates in the context of climate change? **(Chapter 01)***
- ***RQ2.** What are the cooling strategies to prevent overheating in buildings? How to classify them and characterize their resiliency against heatwaves and power outages? **(Chapter 02)***
- ***RQ3.** How to quantify and evaluate the resistivity of buildings and their cooling strategies to the overheating impact of climate change using a robust methodology? **(Chapter 03)***
- ***RQ4.** What are the potential weather conditions under different global GHG emission scenarios in Belgium? **(Chapter 04, Chapter 06, & Chapter 07)***
- ***RQ5.** How much impact will climate change have on the thermal comfort, HVAC energy performance, and HVAC GHG emissions of high-performance houses in Belgium? What measures, both active and passive, can be taken to improve thermal comfort and energy efficiency? Can optimized high-performance houses maintain thermal*

comfort levels during unprecedented events? ***(Chapter 05, Chapter 06, & Chapter 07)***

2.2. Thesis outline

As shown in Figure 2.1, this thesis incorporates three principal parts: Part I, Part II, and Part III. Part I is the data collection phase, in which two literature review studies are performed on thermal discomfort/overheating evaluation methods and resilient cooling strategies. In part II, a comprehensive methodology is introduced, followed by prerequisite fulfillment in terms of the weather data. And Part III consists of simulation studies on thermal comfort, HVAC energy performance, and HVAC GHG emissions based on the findings and developments in the previous parts. The chapters in each part include a journal or conference publication that contributes to the accomplishment of the main research questions. In addition, each chapter addresses specific research questions, which are detailed in each publication.

The chapters in this thesis are correlative and integral. Chapter 01 examines different time-integrated thermal discomfort/overheating evaluation methods applicable to temperate regions. This chapter aims to provide a clear picture of the recent methodologies and criteria, highlighting their strengths and limitations using some qualitative measures. This chapter is essential in finding the appropriate thermal comfort metrics and criteria to be implemented in the methodological framework in Chapter 03. Chapter 02 contains a critical review of resilient cooling strategies. In this chapter, a wide range of active and passive cooling strategies are categorized and qualitatively assessed in terms of their resiliency capacities, applicability, and technology readiness level. Chapter 02 forms a major part of the methodological framework in Chapter 03 and helps understand and identify resilient cooling strategies as overheating mitigation measures. Chapter 03 provides the core methodology of this research by providing a simulation-based framework to analyze and compare the resistivity of buildings and their cooling strategies against overheating impact of climate change. The numerical studies follow the methodology introduced in this chapter in Part III. Chapter 04 presents a procedure to generate the historical and future weather data (annual and heatwaves) for building performance simulations in Part III. Chapter 05, Chapter 06, and Chapter 07 are numerical studies as follows. Chapter 05 evaluates the overheating risk in a Belgian Passive house under current and future weather scenarios. Chapter 06 conducts a thermal comfort analysis on a nearly Zero-Energy dwelling in Brussels. It also compares two widely applied HVAC strategies in Belgium in terms of primary energy use and GHG emissions, including uncertainty and sensitivity analysis on HVAC modelling inputs. Chapter 07 entails building optimization regarding thermal comfort and energy performance using passive cooling design strategies and evaluating optimal solutions under heatwaves and the cooling system outage. The subsequent paragraphs describe how each of the three main parts addresses the research questions of the current thesis.

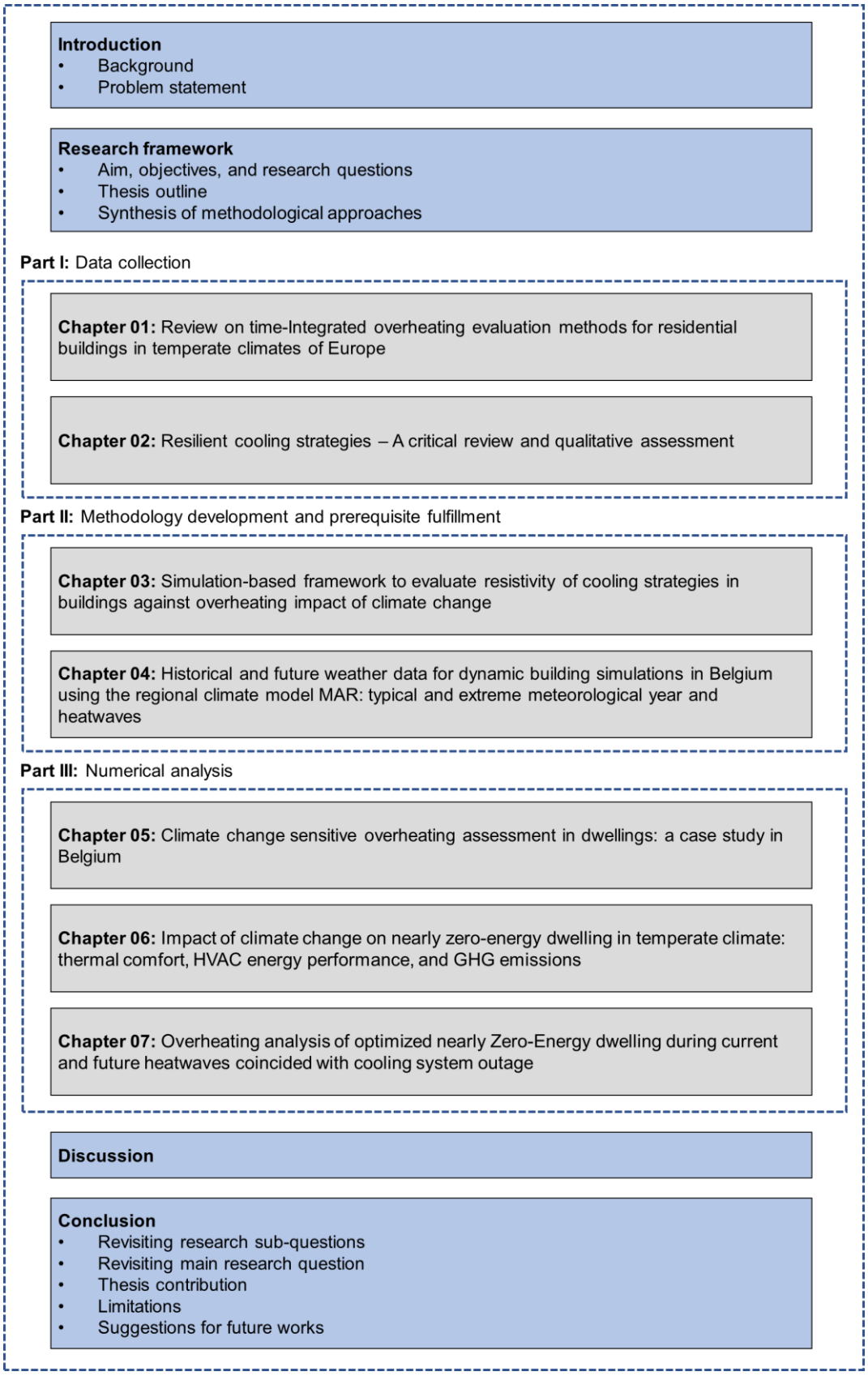

Figure 2.1. Thesis outline

2.3. Synthesis of methodological approaches

Chapter 01. In this chapter, a comprehensive examination of time-integrated overheating evaluation methods is conducted. The research scope is refined by establishing specific boundary conditions related to building type and climate. The primary emphasis is placed on residential buildings, taking into account their prevalence in the European building stock, the vulnerability of certain populations to overheating at homes, and the associated health risks during sleeping hours. The chapter focuses on temperate climates, where the design prioritizes heat preservation during winter, making buildings more susceptible to overheating challenges in the summer.

The target documents considered for the review are categorized into international standards, EPBD regulatory documents, and scientific literature. The selection of international standards such as EN 15251 [155], EN 16798 [156], [157], ISO 7730 [158], ISO 17772 [159], [160], ASHRAE 55 (2017) [138], ASHRAE 55 (2020) [161], CIBSE Guide A (2006) [139], CIBSE TM52 [162], CIBSE Guide A (2015) [163], CIBSE TM59 [164], and Passive House standard [71] is motivated by their extensive integration into building construction and renovation policies within temperate European climates. Additionally, EPBD regulatory documents from Belgium, France, Germany, the UK, and the Netherlands are examined, given their significance in shaping energy efficiency and thermal comfort standards. Moreover, two state-of-the-art methods from the scientific literature [133], [165] are chosen based on their applicability to residential buildings and validation in temperate climates.

The review process entails a thorough analysis of thermal comfort models for both air-conditioned and non-air-conditioned buildings, alongside a critical evaluation of time-integrated overheating indices and criteria. Various measures are employed to qualitatively assess the methods, including dependency on comfort models, dependency on comfort categories, symmetric/asymmetric approaches, consideration of all hours versus occupied hours, normalization to occupied hours, short-term criteria, and long-term criteria.

Chapter 02. The methodology employed in this chapter involves conducting a systematic literature review to provide an overview of existing cooling strategies and assess their resilience under various extreme events. The review process includes a critical analysis of literature obtained from different databases, such as Elsevier (ScienceDirect), IEEE, Google Scholar, Scopus, and SpringerLink. Specific keywords related to resilience, overheating, heatwave, climate change, power outage, disruptive events, and cooling strategies are used to identify relevant peer-reviewed academic literature. Furthermore, additional searches are conducted for each cooling strategy, utilizing specific keywords. The review considers not only peer-reviewed articles but also relevant books and technical reports, with a focus on recent publications.

The analyzed literature is carefully examined to identify the resilient characteristics of cooling strategies based on four criteria: absorptive capacity, adaptive capacity, restorative capacity, and recovery speed.

Absorptive capacity refers to a system's ability to absorb and minimize the impacts of disruptive events, such as the utilization of thermal mass to mitigate temperature increases. Adaptive capacity involves the capability of a system to adjust and modify configurations in response to adverse impacts. Restorative capacity relates to a system's ability to return to normal or improved operation, exemplified by methods like night cooling to dissipate accumulated heat. Recovery speed indicates the rate at which a system can recover, considering factors such as ventilation flow rate and outdoor air temperature.

The cooling strategies are categorized into four distinct groups: reducing heat gains, removing sensible heat, enhancing personal comfort, and removing latent heat. These categories serve as a framework for analyzing the strategies based on their underlying physical principles, typologies, performance in terms of resilience under extreme events, and Technology Readiness Level (TRL) following the guidelines from the U.S. Department of Energy.

Chapter 03. The chapter outlines a research methodology consisting of two main parts: the introduction of the framework and a demonstration case study. The framework is developed through a comprehensive process that includes literature review, consultation of international standards, focus-group discussions, and collaboration among the experts. It encompasses four key steps: specifying reference cities and weather data characterization, identifying building characterization, designing and sizing cooling strategies, and specifying performance indicators and comfort models. This framework is designed to evaluate cooling strategies specifically for addressing overheating discomfort while excluding considerations of overcooling discomfort and heating system performance. It enables a universal comparison of cooling strategies across diverse building typologies and operation modes, considering contemporary and future weather scenarios. The framework also provides flexibility in incorporating weather data with or without the Urban Heat Island (UHI) effect.

Applicability is a crucial aspect of the framework, as it addresses both new and existing buildings. It offers two simulation model approaches: the shoe box model for new buildings and the reference building model for both new and existing buildings. The shoe box model represents a simplified building shape, while the reference building model represents functional buildings in specific locations. The framework allows for the selection of individual or combined cooling strategies, and it accommodates adjustments based on future weather scenarios.

The chapter also introduces the Climate Change Overheating Resistivity ($CCOR$) metric, which serves as an indicator of a building's ability to resist increasing outdoor thermal stress caused by climate change. The $CCOR$ metric is calculated based on the linear regression of Indoor Overheating Degree (IOD) and Ambient Warmness Degree (AWD), considering the relationship between indoor and outdoor thermal conditions. IOD quantifies the risk of indoor overheating by considering the severity and frequency of high indoor temperatures based on multizonal thermal comfort thresholds. While, AWD indicates the severity and frequency of high outdoor temperatures, using a base temperature. Additionally, the chapter suggests utilizing the PMV/PPD comfort models for air-conditioned zones and adaptive

comfort models for non-air-conditioned zones. These models allow for different comfort categories and occupant adaptation, enhancing the accuracy of overheating assessments.

To validate the framework, a demonstration case study is conducted to compare the climate change overheating resistivity of two cooling strategies: Variable Refrigerant Flow (VRF) unit coupled with Dedicated Outdoor Air Supply (DOAS) system and Variable Air Volume (VAV) system. The comparison is performed on a double-zone office building situated in six different locations/climates. The simulations are carried out using the DesignBuilder software, which utilizes the EnergyPlus v8.9 simulation engine. Post-processing of simulation results is performed using MATLAB to calculate key indicators such as IOD, AWD, and $CCOR$. The weather data used for the case study includes present-day Typical Meteorological Year (TMY) data and future weather projections based on the RCP8.5 emission scenario. The case study building incorporates various comfort categories and operational conditions, aligning with established ASHRAE standards and reference models.

Chapter 04. This chapter explores the application of the Regional Climate Model (MAR) *"Modèle Atmosphérique Régional*", to downscale global climate data and generate high-resolution weather outputs. It employs various atmospheric variables such as temperature, pressure, wind, humidity, and sea surface temperature, ensuring comprehensive representation. The chapter initially employs ERA5 reanalysis data to force MAR at its boundaries, replicating the observed climate. It further utilizes three Earth System Models (ESMs) from the Coupled Model Intercomparison Project Phase 6 (CMIP6) database to simulate historical scenarios as well as future scenarios based on different Shared Socioeconomic Pathways (SSPs), with all ESMs driven by the SSP5-8.5 scenario. This approach facilitates the determination of equivalent warming periods for the SSP3-7.0 and SSP2-4.5 scenarios, offering insights into the range of uncertainties without requiring downscaled simulations for all ESMs. The analysis in this chapter focuses on 12 carefully selected cities in Belgium, guided by two key factors. Firstly, these cities are chosen based on their significant size, enabling the observation of notable temperature increases compared to the surrounding rural areas, thereby capturing the UHI effect accurately. Secondly, the selection of these cities takes into account their ability to effectively represent the spatial variability and climatic diversity observed across Belgium, ensuring a comprehensive depiction of the country's climate characteristics.

The chapter also presents the construction of Typical Meteorological Year (TMY) and eXtreme Meteorological Year (XMY) datasets, which are valuable for building simulations. TMYs are composed of representative typical months, while XMYs encompass extreme months. A detailed protocol is provided for constructing these datasets based on ISO 15927-4 [166], focusing on crucial climatic variables such as temperature and solar radiation. Furthermore, the chapter adopts a statistical heatwave definition proposed by [167], which involves calculating temperature thresholds based on percentiles. In this method, heatwave events are identified when the daily mean temperature exceeds a specific threshold, and their duration, maximum temperature, and intensity are characterized. Hourly weather data files are generated for various heatwave criteria, including the longest duration, highest daily average temperature, and highest intensity.

Chapter 05. This chapter investigates how climate change affects thermal comfort and overheating risk in residential buildings. A Passive House case study is conducted, utilizing the dynamic simulation tool EnergyPlus v9.0 to simulate different ventilation rates and four climate scenarios. The model is calibrated using monthly energy uses and hourly indoor air temperature using the recorded data from 2015-2018. The study also calculates the potential of ventilative cooling as a mitigation strategy, and MATLAB is used to process and visualize the simulation results.

The case study takes place in Eupen, Belgium, which has a temperate oceanic climate. The house in the study is a two-level, four-façade lightweight timber construction with a total area of 174 m^2. It complies with the Belgian Passive House requirements, which aim for an annual net energy for heating below 150 MJ/m^2. The building features insulated external walls and utilizes a pellet stove for heating and a gas water boiler for domestic hot water. The infiltration rate is measured at 0.5 ac/h.

To assess overheating, the study employs three metrics: Indoor Overheating Degree (IOD), Ambient Warmness Degree (AWD), and Building Climate Vulnerability Factor ($BCVF$). For the calculation of IOD, bedrooms have a fixed temperature limit of 26℃ based on CIBSE Guide A's [163] static comfort model, while other living areas use Category II of the adaptive thermal comfort model EN 15251 [155]. $BCVF$ represents the vulnerability of the building to overheating based on the correlation between IOD and AWD.

The study considers two historical weather data and two future weather data to analyze the impact of climate change. The historical datasets represent average and extreme climate scenarios, while the future datasets project normal and extreme climates with temperature increases resulting from global warming and the urban heat island effect.

Chapter 06. The methodology in this chapter outlines a two-stage approach. In the first stage, the base case building model is simulated under different historical and future weather scenarios to assess indoor thermal conditions. The second stage involves considering two HVAC system designs (referred to as S01 and S02) using the DesignBuilder v7.0.0 software (which uses EnergyPlus simulation engine). The building and HVAC models are developed in DesignBuilder, and the exported Input Data File (.idf) is utilized in subsequent uncertainty and sensitivity analyses.

The base case building model represents typical naturally ventilated terraced dwellings in Belgium, renovated to meet nearly Zero-Energy Building (nZEB) requirements. It features external insulation, photovoltaic panels, and different conditioned zones. Occupancy schedules, thermal set-points, and comfort models from ISO 17772-1 [159] are applied.

The first HVAC strategy (S01) involves adding a split Air Conditioner (AC) to the existing gas-fired boiler system for cooling purposes. The gas-fired boiler, modeled in DesignBuilder, provides hot water for heating and domestic use using flow splitters, mixers, and a circulating pump. The gas-fired boiler's fuel usage is calculated based on its thermal efficiency and a performance curve. The AC in DesignBuilder is implemented using a unitary single zone module with a DX cooling coil, and its performance under different conditions is defined using default performance curves from the EnergyPlus database.

The second HVAC strategy (S02) utilizes a reversible air-to-water heat pump system for both heating and cooling purposes. To design this system in DesignBuilder, it is necessary to define separate hot- and chilled-water loops. In the hot water loop, an air-to-water heat pump module is employed, which includes an air-to-water DX compression coil as the primary heat source. This coil is connected to a water tank, which serves as a secondary/additional heat source for heating, along with a supplemental heater. On the other hand, the chilled water loop is designed as a high-temperature system, encompassing an air-cooled condenser, an evaporator, and a compressor. The purpose of this loop is to supply chilled water at approximately 18℃. The performance curves and component characteristics for the chilled water loop are derived from the data provided by the manufacturer.

Auto-sizing feature is utilized for thermal capacities and design flow rates of HVAC components based on external design conditions and the building's characteristics. The existing mechanical ventilation system with heat recovery is maintained in both strategies. The study incorporates Uncertainty Analysis (UA) and Sensitivity Analysis (SA) to assess the influence of HVAC model input parameters on heating and cooling primary energy use and HVAC GHG emissions. UA employs Latin Hypercube Sampling (LHS) in the jEPlus tool, while SA employs the Morris method in jEPlus+EA tool.

Chapter 07. The methodology in this chapter aims for optimizing HVAC energy use and thermal comfort in a nearly Zero-Energy terraced dwelling in Belgium as well as further analysis of optimal cases under extreme events. The methodology consists of two main stages: Stage 01 involves multi-objective optimization of passive design strategies to minimize HVAC energy use and thermal discomfort, while Stage 02 analyzes short-term overheating during heatwave events with the cooling system outage.

In Stage 01, the Non-dominated Sorting Genetic Algorithm 2 (NSGA-II) method is used for optimization, considering 13 passive design strategies such as natural ventilation rate, building orientation, solar absorptance of walls and roof, infiltration rate, shading strategies, glazing type, window frame type, and different building constructions. The objective functions are final HVAC energy use and a newly introduced indicator called Indoor Discomfort Degree (IDD).

In Stage 02, the study evaluates a set of optimal solutions obtained in Stage 01 under short-term heatwave conditions coincided with the cooling system outage, using the highest maximal temperature heatwaves over three periods (historical, mid-future, and future). Zonal thermal comfort analysis is conducted, considering maximum operative temperature, Heat Index (HI), and Thermal Autonomy (TA) index. Furthermore, the Climate Change Overheating Resistivity ($CCOR$) index is used to assess the building's resistivity to overheating caused by climate change.

DesignBuilder v7.0.0 software, which uses the EnergyPlus simulation engine, is utilized for both stages. The building model is based on a typical renovated three-floor terraced dwelling with a total area of 259 m², occupied by a four-member family. Initially heated by a gas-fired boiler with natural ventilation, the chapter proposes a mixed-mode approach using a reversible air-to-water heat pump for heating and cooling. The building model includes various zones and is validated through calibration and utility bill comparison.

The HVAC system's design flow rates and thermal capacities are auto-sized based on the building configuration and external weather conditions. The HVAC system's availability schedule aligns with the occupancy schedule.

3. Journal and conference publications

Chapter 01. *Review on time-Integrated overheating evaluation methods for residential buildings in temperate climates of Europe – Journal paper (Appendix A)*

Abstract – Overheating exposure over time can lead to discomfort, productivity reduction, and health issues for the occupants in buildings. The *time-integrated overheating evaluation methods* are introduced to describe, in a synthetic way, the extent of overheating over a span of time and predict the uncomfortable phenomena. This paper reviews the time-integrated overheating evaluation methods that are applicable to residential buildings in temperate climates of Europe. We critically analyze the methods found in (i) 11 international standards, namely, EN 15251 (2006), EN 16798 (2019), ISO 7730 (2004), ISO 17772 (2017-2018), ASHRAE 55 (2017), ASHRAE 55 (2020), CIBSE Guide A (2006), CIBSE TM52 (2013), CIBSE Guide A (2015), CIBSE TM59 (2017), and Passive House (2015), (ii) five national building codes based on the Energy Performance of Building Directive (EPBD) in Belgium, France, Germany, the UK, and the Netherlands, and (iii) two studies in the scientific literature. For each method, we present thermal comfort models along with the time-integrated overheating indices and criteria. The methods are analyzed according to some key measures in order to identify their scope, strength, and limitations. We found that most standards recommend static comfort models for air conditioned buildings and adaptive comfort models for non-air conditioned ones. We also found a promising method based on three indices, namely, Indoor Overheating Degree (IOD), Ambient Warmness Degree (AWD), and overheating escalation factor ($\alpha_{IOD/AWD}$) that allows for a multizonal and climate change-sensitive overheating assessment. Finally, some guidance is provided for practice and future developments.

Role of Ph.D. candidate:

- First author

Journal:

- Energy and Buildings

Journal metrics (Scopus):

- **Scopus coverage years:** 1970, from 1977 to 1979, from 1981 to Present, **Subject area:** Engineering: Civil and Structural Engineering (#10/326 – Q1), Engineering: Mechanical Engineering (#24/601 – Q1), Engineering: Building and Construction (#9/211 – Q1), and Engineering: Electrical and Electronic Engineering (#45/708 – Q1), **Publisher:** Elsevier, **ISSN:** 0378-7788, **CiteScore 2021:** 11.5, **SJR 2021:** 1.682, **SNIP 2021:** 2.069.

Citations:

- **Google Scholar:** 26
- **PlumX:** 22

Reference:

Rahif, R., Amaripadath, D., & Attia, S. (2021). Review on time-integrated overheating evaluation methods for residential buildings in temperate climates of Europe. *Energy and Buildings*, *252*, 111463. https://doi.org/10.1016/j.enbuild.2021.111463 & https://hdl.handle.net/2268/263829

Chapter 02. *Resilient cooling strategies – A critical review and qualitative assessment – Journal paper (Appendix B)*

Abstract – The global effects of climate change will increase the frequency and intensity of extreme events such as heatwaves and power outages, which have consequences for buildings and their cooling systems. Buildings and their cooling systems should be designed and operated to be resilient under such events to protect occupants from potentially dangerous indoor thermal conditions.

This study performed a critical review on the state-of-the-art of cooling strategies, with special attention to their performance under heatwaves and power outages. We proposed a definition of resilient cooling and described four criteria for resilience—absorptive capacity, adaptive capacity, restorative capacity, and recovery speed —and used them to qualitatively evaluate the resilience of each strategy.

The literature review and qualitative analyses show that to attain resilient cooling, the four resilience criteria should be considered in the design phase of a building or during the planning of retrofits. The building and relevant cooling system characteristics should be considered simultaneously to withstand extreme events. A combination of strategies with different resilience capacities, such as a passive envelope strategy coupled with a low-energy space-cooling solution, may be needed to obtain resilient cooling. Finally, a further direction for a quantitative assessment approach has been pointed out.

Role of Ph.D. candidate:

- Co-author (**Contribution:** Investigation, Formal Analysis, Data Curation, Writing – Original Draft, Review, & Editing)

Journal:

- Energy and Buildings

Journal metrics (Scopus):

- **Scopus coverage years:** 1970, from 1977 to 1979, from 1981 to Present, **Subject area:** Engineering: Civil and Structural Engineering (#10/326 – Q1), Engineering: Mechanical Engineering (#24/601 – Q1), Engineering: Building and Construction (#9/211 – Q1), and Engineering: Electrical and Electronic Engineering (#45/708 – Q1), **Publisher:** Elsevier, **ISSN:** 0378-7788, **CiteScore 2021:** 11.5, **SJR 2021:** 1.682, **SNIP 2021:** 2.069.

Citations:

- **Google Scholar:** 57
- **PlumX:** 33

Reference:

Zhang, C., Kazanci, O. B., Levinson, R., Heiselberg, P., Olesen, B. W., Chiesa, G., ... & Zhang, G. (2021). Resilient cooling strategies–A critical review and qualitative assessment. *Energy and Buildings*, *251*, 111312. https://doi.org/10.1016/j.enbuild.2021.111312 & https://hdl.handle.net/2268/262303

Chapter 03. *Simulation-based framework to evaluate resistivity of cooling strategies in buildings against overheating impact of climate change – Journal paper (Appendix C)*

Abstract – Over the last decades overheating in buildings has become a major concern. The situation is expected to worsen due to the current rate of climate change. Many efforts have been made to evaluate the future thermal performance of buildings and cooling technologies. In this paper, the term "climate change overheating resistivity" of cooling strategies is defined, and the calculation method is provided. A comprehensive simulation-based framework is then introduced, enabling the evaluation of a wide range of active and passive cooling strategies. The framework is based on the Indoor Overheating Degree (IOD), Ambient Warmness Degree (AWD), and Climate Change Overheating Resistivity ($CCOR$) as principal indicators allowing a multizonal approach in the quantification of indoor overheating risk and resistivity to climate change.

To test the proposed framework, two air-based cooling strategies including a Variable Refrigerant Flow (VRF) unit coupled with a Dedicated Outdoor Air System (DOAS) (C01) and a Variable Air Volume (VAV) system (C02) are compared in six different locations/climates. The case study is a shoe box model representing a double-zone office building. In general, the C01 shows higher CCOR values between 2.04 and 19.16 than the C02 in different locations. Therefore, the C01 shows superior resistivity to the overheating impact of climate change compared to C02. The maximum $CCOR$ value of 37.46 is resulted for the C01 in Brussels, representing the most resistant case, whereas the minimum $CCOR$ value of 9.24 is achieved for the C02 in Toronto, representing the least resistant case.

Role of Ph.D. candidate:

- First author

Journal:

- Building and Environment

Journal metrics (Scopus):

- **Scopus coverage years:** from 1976 to Present, **Subject area:** Social Sciences: Geography, Planning and Development (#14/747 – Q1), Engineering: Civil and Structural Engineering (#12/326 – Q1), Engineering: Building and Construction (#11/211 – Q1), and Engineering: Environmental Science: Environmental Engineering (#13/173 – Q1), **Publisher:** Elsevier. **ISSN:** 0360-1323, **CiteScore 2021:** 10.7, **SJR 2021:** 1.498, **SNIP 2021:** 2.228.

Citations:

- **Google Scholar:** 23
- **PlumX:** 18

Reference:

Rahif, R., Hamdy, M., Homaei, S., Zhang, C., Holzer, P., & Attia, S. (2022). Simulation-based framework to evaluate resistivity of cooling strategies in buildings against overheating impact of climate change. *Building and Environment*, *208*, 108599.
https://doi.org/10.1016/j.buildenv.2021.108599 & https://hdl.handle.net/2268/265193

Chapter 04. *Historical and future weather data for dynamic building simulations in Belgium using the regional climate model MAR: typical and extreme meteorological year and heatwaves – Journal paper (Appendix D)*

Abstract – Increasing temperatures due to global warming will influence building, heating, and cooling practices. Therefore, this data set aims to provide formatted and adapted meteorological data for specific users who work in building design, architecture, building energy management systems, modelling renewable energy conversion systems, or others interested in this kind of projected weather data. These meteorological data are produced from the regional climate model MAR (Modèle Atmosphérique Régional in French) simulations. This regional model, adapted and validated over Belgium, is forced firstly, by the ERA5 reanalysis, which represents the closest climate to reality and secondly, by three Earth system models (ESMs) from the Sixth Coupled Model Intercomparison Project database, namely, BCC-CSM2-MR, MPI-ESM.1.2, and MIROC6. The main advantage of using the MAR model is that the generated weather data have a high resolution (hourly data and 5 km) and are spatially and temporally homogeneous. The generated weather data follow two protocols. On the one hand, the Typical Meteorological Year (TMY) and eXtreme Meteorological Year (XMY) files are generated largely inspired by the method proposed by the standard ISO 15927-4, allowing the reconstruction of typical and extreme years, while keeping a plausible variability of the meteorological data. On the other hand, the heatwave event (HWE) meteorological data are generated according to a method used to detect the heatwave events and to classify them according to three criteria of the heatwave (the most intense, the longest duration, and the highest temperature). All generated weather data are freely available on the open online repository Zenodo (https://doi.org/10.5281/zenodo.5606983, Doutreloup and Fettweis, 2021) and these data are produced within the framework of the research project OCCuPANt (https://www.occupant.uliege.be/ (last access: 24 June 2022) – ULiège).

Role of Ph.D. candidate:

- Co-author (**Contribution:** Conceptualization, Methodology, Investigation, Validation, Writing – Original Draft, Review, & Editing)

Journal:

- Earth System Science Data

Journal metrics (Scopus):

- **Scopus coverage years:** from 2009 to Present, **Subject area:** Earth and Planetary Sciences: General Earth and Planetary Sciences (#3/191 – Q1), **Publisher:** Copernicus. **ISSN:** 1866-3508, **E-ISSN:** 1866-3516, **CiteScore 2021:** 13.8, **SJR 2021:** 3.657, **SNIP 2021:** 3.034.

Citations:

- **Google Scholar:** 8

Reference:

Doutreloup, S., Fettweis, X., Rahif, R., El Nagar, E., Pourkiaei, S. M., Amaripadath, D., & Attia, S. (2022). Historical and future weather data for dynamic building simulations in Belgium using the regional climate model MAR: typical and extreme meteorological year and heatwaves. *Earth System Science Data*, *14*(7). https://doi.org/10.5194/essd-14-3039-2022 & https://hdl.handle.net/2268/293076

Chapter 05. *Climate change sensitive overheating assessment in dwellings: a case study in Belgium – Peer-reviewed conference paper – International Congress (Appendix E)*

Abstract – Due to the current rate of global warming, overheating in buildings is expected to be more frequent and intense in future climates. High indoor temperature affects occupant productivity, comfort, and health. Thus, it is necessary to predict the thermal performance of buildings concerning climate change. This paper applies a climate change sensitive overheating assessment method to a lightweight timber house in Eupen, Belgium. Three metrics are used, namely Indoor Overheating Degree (IOD), Ambient Warmness Degree (AWD), and Building Climate Vulnerability Factor ($BCVF$). The overheating risk is assessed under four climate scenarios representing historical and future scenarios using dynamic simulation tool EnergyPlus v9.0. This method accounts for overheating severity and frequency, considering zonal occupancy profiles and thermal comfort models. The results indicate $BCVF < 1$ for the Passive House case study showing its high potential in suppressing the outdoor thermal stress in the long-term. Finally, the increase in ventilation rate proves to be an adequate measure by decreasing the zonal peak temperatures up to 10℃ and indoor overheating risk by ~60%.

Role of Ph.D. candidate:

- First author

Conference name, organizers, and location:

- International Building Performance Simulation Association (IBPSA) Building Simulation 2021 (BS2021) - KU Leuven, Boydens engineering, Daidalos Peutz, and Ghent university - Bruges, Belgium.

Citations:

- **Google Scholar:** 3

Reference:

- Rahif, R., Fani, A., & Attia, S. (2021, September). Climate Change Sensitive Overheating Assessment in Dwellings: A Case Study in Belgium. In *Building Simulation 2021 Conference*. KU Leuven, Leuven, Belgium. https://hdl.handle.net/2268/263260

Chapter 06. *Impact of climate change on nearly zero-energy dwelling in temperate climate: thermal comfort, HVAC energy performance, and GHG emissions – Journal paper (Appendix F)*

Abstract – Global warming is widely recognized to affect the built environment in several ways. This paper projects the current and future climate scenarios on a nearly zero-energy dwelling in Brussels. Initially, a time-integrated discomfort assessment is carried out for the base case without any active cooling system. It is found that overheating risk will increase up to 528%, whereas the overcooling risk will decrease up to 32% by the end of the century. It is also resulted that the overheating risk will overlap the overcooling risk by 2090s under high emission scenarios. Subsequently, two commonly applied HVAC strategies are considered, including a gas-fired boiler + an air conditioner (S01) and a reversible air-to-water heat pump (S02). In general, S02 shows ~6-13% and 15-27% less HVAC primary energy use and GHG emissions compared to S01, respectively. By conducting the sensitivity analysis, it is found that the choice of the HVAC strategy, heating set-point, and cooling set-point are among the most influential parameters determining the HVAC primary energy use. Finally, some future recommendations are provided for practice and future research.

Role of Ph.D. candidate:

- First author

Journal:

- Building and Environment

Journal metrics (Scopus):

- **Scopus coverage years:** from 1976 to Present, **Subject area:** Social Sciences: Geography, Planning and Development (#14/747 – Q1), Engineering: Civil and Structural Engineering (#12/326 – Q1), Engineering: Building and Construction (#11/211 – Q1), and Engineering: Environmental Science: Environmental Engineering (#13/173 – Q1), **Publisher:** Elsevier. **ISSN:** 0360-1323, **CiteScore 2021:** 10.7, **SJR 2021:** 1.498, **SNIP 2021:** 2.228.

Citations:

- **Google Scholar:** 12
- **PlumX:** 10

Reference:

Rahif, R., Norouziasas, A., Elnagar, E., Doutreloup, S., Pourkiaei, S. M., Amaripadath, D., ... & Attia, S. (2022). Impact of climate change on nearly zero-energy dwelling in temperate climate: Time-integrated discomfort, HVAC energy performance, and GHG emissions. *Building and Environment*, *223*, 109397. https://doi.org/10.1016/j.buildenv.2022.109397 & https://hdl.handle.net/2268/293674

Chapter 07. *Overheating analysis of optimized nearly Zero-Energy dwelling during current and future heatwaves coincided with cooling system outage – Journal paper (Appendix G)*

Abstract – It is expected that heatwaves will strike more frequently and with higher temperatures with the continuation of global warming. More extreme heatwaves concurrent with disruptions in the cooling system can lead to significant overheating problems in buildings affecting occupants' health, productivity, and comfort. This paper projects current and future heatwaves on an optimized nearly Zero-Energy terraced dwelling in Brussels, assuming the outage of the cooling system. Initially, a multi-objective optimization is performed considering 13 passive design strategies using the Genetic Algorithm (GA) based on the Non-dominated Sorting Genetic Algorithm 2 (NSGA-II) method. It is found that high ventilation rate, low infiltration rate, high insulation, high thermal mass, integration of green roof, and application of operable roller blinds are beneficial in reducing the final HVAC energy use up to 32% and enhancing thermal comfort up to 46%. Subsequently, three optimal solutions are selected and analyzed under the highest maximal temperature heatwaves detected during the 2001-2020, 2041-2060, and 2081-2100 periods. It is found that non of the optimal solutions are able to fully suppress overheating during heatwaves and the cooling system outage. The indoor operative temperatures reach more than 29℃, which can cause serious health issues for the occupants. The situation will be exacerbated in the future since an increase in maximum Heat Index (HI) between 0.28°C-0.49°C, an increase in the maximum operative temperature between 1.34℃-2.33℃, and a decrease in Thermal Autonomy (TA) between 17%-28% are estimated. Finally, some recommendations are provided for practice and future research.

Role of Ph.D. candidate:

- First author

Journal:

- Energy and Buildings

Journal metrics (Scopus):

- **Scopus coverage years:** 1970, from 1977 to 1979, from 1981 to Present, **Subject area:** Engineering: Civil and Structural Engineering (#10/326 – Q1), Engineering: Mechanical Engineering (#24/601 – Q1), Engineering: Building and Construction (#9/211 – Q1), and Engineering: Electrical and Electronic Engineering (#45/708 – Q1), **Publisher:** Elsevier, **ISSN:** 0378-7788, **CiteScore 2021:** 11.5, **SJR 2021:** 1.682, **SNIP 2021:** 2.069.
-

Citations:

- **Google Scholar:** 0
- **PlumX:** 0

Reference:

Rahif, R., Kazemi, M., & Attia, S. (2023). Overheating analysis of optimized nearly Zero-Energy dwelling during current and future heatwaves coincided with cooling system outage. Energy and Buildings, 112998. https://doi.org/10.1016/j.enbuild.2023.112998 & https://hdl.handle.net/2268/301147

4. Discussion

The findings of Chapters 01 to Chapter 07 have been detailed in each publication. This section further discusses the findings and the connections between the chapters and their implications. Figure 4.1 provides a visual representation of the connections between the various chapters, highlighting the interrelatedness of the topics covered.

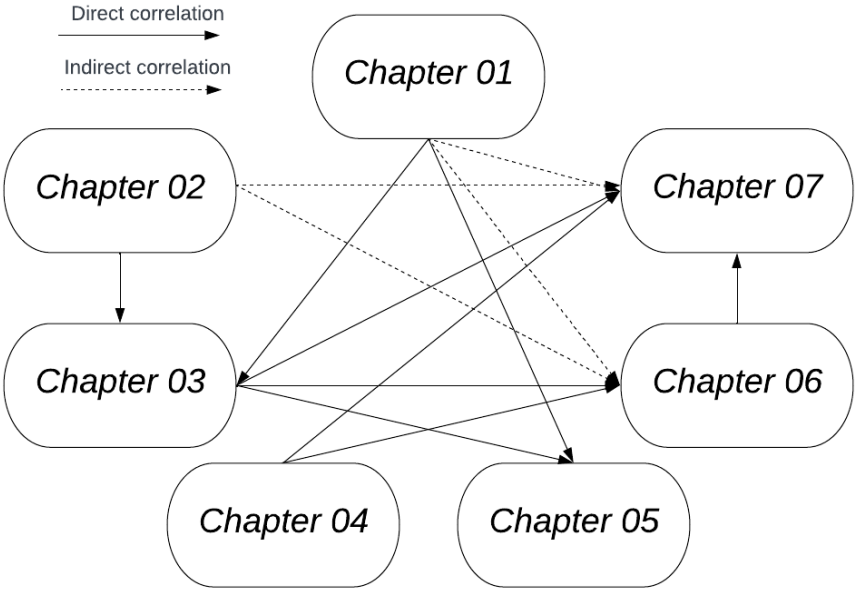

Figure 4.1. Connections among the chapters of the thesis.

Overheating in buildings has become an increasingly pressing issue in recent years due to the effects of climate change and the frequent occurrence of heatwaves. According to [168], heat-related mortality can be more than double by the 2050s and triple by the 2080s. To combat this issue, it is necessary to evaluate the current state of buildings to identify areas where improvements can be made. However, there is currently a lack of comprehensive guidance on how to evaluate overheating in the context of climate change and how to test and apply possible adaptation options. Chapter 01 highlights the fact that building standards and scientific literature have so far paid limited attention to overheating assessments in the context of climate change. Even previous efforts to analyze overheating assessment methods [169]–[172] have failed to address this issue and have instead focused solely on classical evaluation criteria. As a result, current methods are not effective in quantifying and illustrating the evolution of building thermal performance in future climates.

As a result of the review in Chapter 01, initially, the metric of overheating escalation factor ($\alpha_{IOD/AWD}$) (or Building Climate Vulnerability Factor "$BCVF$" as denoted in Chapter 05) is chosen to evaluate the vulnerability of a building and its cooling strategies to climate change. However, while participating in the International Energy Agency (IEA) Annex 80 – *"Resilient cooling of buildings"* project, discussions revealed inaccuracies in its calculation method.

This issue is addressed in Chapter 03 by introducing a new metric called Climate Change Overheating Resistivity ($CCOR$). The $CCOR$ metric is then used in subsequent studies conducted in Chapter 06 and Chapter 07. In addition, to prevent confusion, Indoor Overheating Degree (IOD) is represented by $IOhD$ instead of its original acronym in Chapter 06 and Chapter 07. This change is made after the introduction of the Indoor Overcooling Degree ($IOcD$) metric.

In light of the the current state of the Energy Performance of Buildings Directive (EPBD) in Belgium, it is evident that the Brussels region adheres to the criteria outlined by the Passive House standard, while the Walloon region and the Flemish region adopt a quasi-steady-state heat balance method. However, each method has notable shortcomings that have been extensively discussed in Chapter 01. In shaping the future of EPBD in Belgium, it is advised to prioritize the initial unification of all three regions and shift the focus from heating and heat-preserving concepts to considering cooling and overheating as key factors. Subsequently, a vital step involves the development of dynamic overheating calculation methods based on comfort parameters, as opposed to relying solely on heat balance methods, to more accurately represent occupants' thermal sensation. Ideally, the new method should encompass all six comfort parameters, including relative humidity, metabolic rate, air velocity, air temperature, radiant temperature, and clothing factor. Furthermore, the new method should account for climate change and the urban heat island effect, utilizing current historical data and future climatic scenarios. It is essential to adopt both short-term and long-term criteria to prepare buildings for heatwaves while ensuring general comfort conditions throughout the year. Additionally, provisions should be integrated for the operation of buildings in mixed modes, utilizing Predicted Mean Vote (PMV) - Predicted Percentage of Dissatisfied (PPD) and adaptive models that directly address occupants' comfort, health, and well-being [70], [173]. In parallel with the performance-based approach, it is essential to define prescriptive requirements for building envelopes, encompassing external shading, Window-to-Wall Ratio (WWR) limits, maximum G-values, etc.

Chapter 01 identifies a critical issue that served as the main driving force for developing the methodological framework outlined in Chapter 03, which is later used in Chapter 05, Chapter 06, and Chapter 07. The framework is designed in four steps to address this issue comprehensively: Step 1) specify reference cities and weather data characterization, Step 2) identify building characterization, Step 3) identify and design/size the cooling strategies to be compared, and Step 4) specify performance indicators and comfort models. To follow the standard practice in climate change research, the framework is based on dynamic thermal simulation, which requires computer models to simulate a building's thermal performance under varying weather conditions. Throughout the framework's development, findings from different chapters are incorporated to enhance its comprehensiveness. In Step 3, the framework utilizes the insights collected from Chapter 02, which not only provides a categorization of cooling strategies but also offers a valuable qualitative assessment of their resilience against heatwaves and power outages. This unique contribution had not been discussed in scientific literature before, with prior studies mainly comparing various active and passive cooling strategies in terms of energy performance [97], [174], [175], thermal comfort and air quality [176], capital expenditure [97], [175], and applicability in different

climate zones [76]. In Step 4 of the framework, Chapter 01's contributions become particularly crucial. The chapter's identification of a climate change-sensitive evaluation method in the scientific literature [133] paved the way for the introduction of the Climate Change Overheating Resistivity ($CCOR$) metric. Additionally, Chapter 01 helped in developing a systematic procedure in Step 4 of the framework for selecting thermal comfort models for air conditioned and non-air conditioned zones, especially in mixed/hybrid mode zones. The latter is particularly important given the lack of consensus on the suitability of static and adaptive thermal comfort models for mixed/hybrid mode operation [177].

While historical weather data can be a useful starting point for climate change research, it is essential to supplement it with high-accuracy future weather projections, as outlined in Step 1 of the framework in Chapter 03. In Chapter 04 of the thesis, the focus is on generating future weather data by forcing the *"Modèle Atmosphérique Régional"* (MAR) using Earth System Models (ESMs) from the Coupled Model Intercomparison Project Phase 6 (CMIP6). This approach offers two significant advantages. Firstly, CMIP6 has a relatively small bias compared to its predecessor, CMIP5 [178]. Secondly, the use of MAR dynamical downscaling results in high-resolution climate data and extreme events [179]. Although other projects such as ENSEMBLES [180], NARCCAP [181], and CORDEX [182] have used combinations of several Regional Climate Models (RCMs) to provide high-resolution models achieving 10–20 km of horizontal resolution, the data provided in Chapter 04 the current thesis are at a finer resolution of approximately 5km, which is specifically tuned for Belgium [183]. This allows for a more detailed and accurate analysis of future weather projections, making the research findings more relevant and applicable to the region.

In addition, Chapter 04 provides heatwaves data allowing for the evaluation of buildings under extreme events. Heatwaves have different definitions, such as a period of at least five consecutive days with a maximum temperature higher than 25℃ and at least three days with a maximum temperature above 30℃, according to the Royal Meteorological Institute (RMI) of Belgium [184]. Another definition is a period of at least three consecutive days with a minimum temperature of 18.2℃ and a maximum temperature of 29.6℃ or higher [185]. However, these definitions are static and do not consider climate variations, and may produce inaccurate results when using data from different ESMs. The European Environment Agency's definition is more advanced, defining a heatwave as a period of at least three consecutive days when the daily maximum temperature exceeds the 99th percentile of daily temperature values from May to September in a specific location over the reference climate period. Differently, Chapter 04 uses a statistical method based on three percentiles of daily mean air temperatures to couple the RMI's definition with a more sophisticated approach [167]. This approach overcomes the limitations of static definitions and enables the study of heatwaves across different regions and time periods, respecting the RMI's official definition.

It is important to acknowledge that there exists an inconsistency in the source of weather data used for the simulations throughout the thesis. Specifically, in Chapter 03 and Chapter 05, the weather data is obtained from Meteonorm, while in Chapter 06 and Chapter 07, the simulations rely on the dataset developed in Chapter 04. The use of Meteonorm in the earlier chapters incorporates older versions of emission scenarios, specifically the

Representative Concentration Pathways (RCPs) from the IPCC Fifth Assessment Report (AR5). This inconsistency arises due to two reasons: i) at the time of conducting the research in Chapter 03 and Chapter 05, the weather data based on MAR (Meteorological Regional Climate Model) was not available or complete. and Ii) Chapter 03 encompasses cities in various countries worldwide, whereas the weather data in Chapter 04 is specifically tailored for Belgium.

Chapter 03, Chapter 05, Chapter 06, and Chapter 07 of the thesis are devoted to exploring active and passive cooling strategies. While the original project sought to examine the entire residential building stock in Belgium, this Ph.D. research specifically concentrates on newly built or renovated high-performance houses. This decision arose from the challenge of obtaining benchmark models representing the wide array of building typologies found across the entire building stock in Belgium. Furthermore, the building models utilized in Chapter 05, Chapter 06, and Chapter 07 were not accessible during the initial stages of research, leading to the adoption of a simplified shoe box model in Chapter 03 to evaluate the framework.

As supported by numerous studies, passive cooling design strategies have the potential to reduce heating and cooling demands, creating opportunities to incorporate more efficient HVAC systems with lower capacities throughout the year and potentially delaying their operation [186]–[190]. The findings of this thesis in Chapter 05 and Chapter 07 align with these previous studies, as it concludes that certain passive cooling design strategies can indeed offer thermal comfort and energy efficiency benefits. The following section provides a brief discussion of some of these identified strategies:

- **Natural ventilation:** adequate levels of natural ventilation can help buildings to maintain thermal comfort during the summer months by circulating fresh and relatively cool outdoor air. Natural ventilation can provide higher air change rates using natural systems at almost no cost compared to mechanical systems. The positive impact of natural ventilation on summer thermal comfort and cooling energy efficiency was also confirmed in previous research [133], [191], [192].
- **Low infiltration rate:** by reducing the unwanted penetration of cold air in the winter and hot air in the summer, low levels of infiltration rate can improve thermal comfort and prevent a host of problems associated with indoor air quality, energy use, and moisture damage in buildings [193]. The positive impact of a low infiltration rate on thermal comfort and energy efficiency has also been confirmed by previous research [194]–[196].
- **Low U-values for building envelope components:** incorporating materials and elements with low U-values in the building envelope can help minimize the unwanted heat transfer between indoor and outdoor environments. This is especially crucial for buildings that are heated and cooled actively, as the unwanted heat transfer can lead to wasted energy and may even prompt users to increase the use of heating and cooling systems to maintain the desired temperature. Previous research has also confirmed the positive impact of low U-value building envelope components on both thermal comfort and energy efficiency [197]–[199].
- **Use of thermal mass:** utilizing high thermal mass in various building components functions as a thermal storage system, which can absorb

excess heat and release it when needed. Additionally, it helps reduce peak loads during extreme weather events [200], [201]. Previous research [202]–[205] also confirmed the favorable impact of high thermal mass on thermal comfort and energy efficiency.

- **Green roofs:** green roofs, like insulation, can reduce the thermal conductivity of the roofs, thereby minimizing heat transfer between indoor and outdoor environments. As a result, they can help to reduce heating and cooling loads and improve thermal comfort and energy efficiency in buildings. In addition to these benefits, green roofs can also contribute to decreasing the urban heat island effect, mitigating air pollution, enhancing urban air quality, improving water run-off quality and stormwater management, reducing noise levels, and increasing biodiversity [206]. The positive impact of green roofs on thermal comfort and energy efficiency has also been supported by previous research [207]–[210].
- **Shading devices:** shading devices are a highly effective solution for minimizing solar heat gains and preventing solar radiation from entering buildings. By reducing the amount of solar radiation that enters a building, shading devices can provide significant thermal comfort and energy efficiency benefits, particularly during the hot summer months when buildings are most susceptible to overheating. These devices can be installed on either the interior or exterior of a building and can also enhance the aesthetic value of a building, creating a unique architectural feature that can be both functional and visually appealing. This thesis suggests that roller blinds are highly effective in achieving optimal energy efficiency and thermal comfort. The positive impact of shading devices on thermal comfort and energy efficiency has also been supported by previous research [211]–[214].

Chapter 07 of this thesis emphasizes that optimizing HVAC energy use and maintaining thermal comfort in buildings using passive design strategies requires a trade-off between reducing heating energy use/overcooling and cooling energy use/overheating. Solar radiation is a natural heat source that can be advantageous in winter months but not during the summer months. Thus, it is important to carefully select factors such as orientation, glazing areas, and solar absorptance of roofs and walls that directly impact solar gains in buildings, taking into consideration the climate. While in heating-dominated temperate regions, specifying these factors for higher solar gains can be beneficial under current weather conditions; it may not be the case in the future due to global warming.

Passive cooling design strategies are highly effective means of achieving both thermal comfort and energy efficiency in buildings. However, it is important to note that with the ongoing effects of global warming, the effectiveness of these strategies may begin to decline. As a result, active cooling strategies will become increasingly necessary in the coming decades, particularly during periods of intense heatwaves, to ensure that optimal thermal comfort is maintained. While active cooling systems are capable of reducing temperatures within a building, it is also important to consider their impact on energy use and greenhouse gas emissions. According to the Odyssee database, the rate of households in Europe with air conditioning equipment increased from 14% in 2010 to approximately 20% in 2019, and this trend is expected to continue as the market for active cooling systems,

including reversible systems like heat pumps, continues to expand. In fact, the recently published 'REPowerEU' initiative aims to accelerate the roll-out of heat pumps in order to decrease dependency on Russian fossil fuels, doubling the deployment rate in the next five years.

The European Environment Agency (EEA) has identified heat pumps as promising technologies for reducing energy use and greenhouse gas emissions in buildings, especially when they are powered by electricity from renewable sources [215]. This assertion is supported by Chapter 06 of the current thesis, in which a reversible air-to-water heat pump outperforms a conventional system consisting of a gas-fired boiler and air conditioner. However, it is important to note that heat pumps can still contribute to climate change in two primary ways [135]. First, the generation of electricity used to power heat pumps emits CO_2, and the level of emissions depends on the degree of decarbonization of the electricity-generation system. Second, the use of refrigerants in heat pumps also emits Greenhouse Gases (GHGs), primarily hydrofluorocarbons (HFCs), which have a global warming potential that is thousands or tens of thousands of times higher than that of CO_2. These HFCs may be emitted when refrigerant leakages occur or when refrigerants are improperly disposed of [74].

Finally, it worth highlighting several important aspects regarding the modeling and simulation approaches presented in Chapter 05, Chapter 06, and Chapter 07. One noteworthy point is the reliance on certain hypotheses and assumptions, which can introduce uncertainties into the findings. Specifically, the use of fixed rates for natural ventilation and infiltration is a significant factor contributing to these uncertainties. These rates are strongly influenced by environmental factors, such as the temperature gradient between indoor and outdoor spaces, wind speed, and direction. Given the potential impact of climate change on these environmental factors, it becomes crucial to acknowledge that the rates of natural ventilation and infiltration may be subject to change, adding further complexity to the analysis. Additionally, Chapter 07 introduces the consideration of external shading devices, which are controlled based on an indoor air temperature of 24℃ during occupied hours. However, it is important to recognize that occupants may not always operate these shading devices solely based on indoor air temperature. Other factors, such as diffuse solar radiation incident, glare, and illuminance set-point, can also play a detrimental role in controlling these shading strategies. Additionally, uncertainties stemming from inputs regarding building materials, occupancy patterns, and HVAC components performance further contribute to deviations between simulated and actual performance, influencing energy use predictions and indoor comfort levels. Consequently, the findings from Chapter 05, Chapter 06, and Chapter 07 should be cautiously interpreted, keeping in mind the various sources of uncertainties that can influence the outcomes of the simulations.

5. Conclusions

The primary aim of this Ph.D. research is to address the crucial issue of climate change impacts on high-performance houses in Belgium, where current building construction practices and regulations have increased the risk of overheating. To achieve this goal, the study proposes a rigorous methodology to conduct climate change impact assessments, considering factors such as location, cooling strategy, and building construction and operational properties. By evaluating the impact of climate change on representative high-performance houses, the research determines the extent of the risk of overheating and its potential impact on thermal comfort and energy use. Furthermore, the research suggests and evaluates several active and passive cooling solutions that can be incorporated into houses to mitigate the overheating impact of climate change.

By addressing the research sub-questions (Section 5.1), this section compiles the response to the main research question (Section 5.2), offering valuable insights into the scientific contribution of the research (Section 5.3). It highlights the limitations of the study (Section 5.4), where future research can improve upon the current approach. Finally, it concludes with final remarks and suggestions for future works (Section 5.5) to underscore the importance of continued research on overheating risks and adaptation measures to promote sustainable and resilient house design in the face of climate change.

5.1. Revisiting research sub-questions

The present Ph.D. thesis comprises seven chapters, each corresponding to a peer-reviewed scientific journal or conference paper. Each chapter responds to one or more research sub-questions outlined in the thesis, and collectively they provide an answer to the main research question. In essence, the thesis is a compilation of published research that addresses the central inquiry in a structured and comprehensive manner. The division of the thesis into seven chapters serves to organize the findings and present them in a coherent manner that highlights the significance and relevance of each sub-topic. The approach also facilitates easy access and reference to individual papers for interested readers.

RQ1**. How do current methods assess time-integrated thermal discomfort and overheating in residential buildings in temperate climates in the context of climate change? **(Chapter 01)

The conclusions are obtained from an exhaustive review of time-integrated thermal discomfort/overheating evaluation methods that are relevant to air conditioned and non-air conditioned residential buildings in temperate regions. The review draws on a wide range of sources, including 11 international standards such as EN 15251 [155], EN 16798 [156], [157], ISO 7730 [158], ISO 17772 [159], [160], ASHRAE 55 (2017) [138], ASHRAE 55 (2020) [161], CIBSE Guide A (2006) [139], CIBSE TM52 [162], CIBSE Guide A (2015) [163], CIBSE TM59 [164], and Passive House standard [71], along with five national building codes based on the Energy Performance of

Building Directive (EPBD) in Belgium, France, Germany, the UK, and the Netherlands. Furthermore, two recent methods from scientific literature [133], [165] are also analyzed.

The review covers all aspects of time-integrated thermal discomfort/overheating evaluation, including thermal comfort models, indices, and criteria. To provide a qualitative assessment, several measures are considered, such as the dependency on comfort models and categories, whether the method is symmetric or asymmetric, whether it applies to all hours or just occupied hours in a time span, normalization to occupied hours, and whether it has short-term criteria, and long-term criteria. Overall, this review provides a comprehensive analysis of the various methods available for evaluating time-integrated thermal discomfort/overheating in residential buildings in temperate regions. By examining both international standards and national building codes, as well as recent scientific literature, the review highlights the strengths and weaknesses of each method and offers insights into which approaches are best suited to a particular context. The answer to RQ1 is as follows:

- Time-integrated thermal discomfort/overheating evaluation methods mainly consist of three different parts, including thermal comfort models, time-integrated indices, and criteria.
    - In terms of thermal comfort models, the general recommendation from standards is to use static models for air conditioned buildings and adaptive models for non-air conditioned buildings. However, ISO 7730, CIBSE Guide A (2006), and Passive House standards rely exclusively on static models. Additionally, some standards specify fixed temperature thresholds specifically for bedrooms, such as the CIBSE Guide A recommendation of 26℃, even if an adaptive model is used for other living areas.
    - A series of indices that can be employed with the static comfort model (e.g., Weighted *PPD* ($PPDw$) & Averaged *PPD* ($AvgPPD$)), the adaptive comfort model (e.g., Daily Weighted Exceedance (W_e)), or both (e.g., Percentage of Occupied hours Outside the Range ($\%POhOR$) & Degree hours (Dh)) have been developed to provide time-integrated thermal discomfort/overheating measurements.
    - Some of the time-integrated indices, such as the Percentage of Occupied hours Outside the Range ($\%POhOR_{\mathrm{EN},ISO}$), Averaged *PPD* ($AvgPPD$), *PPD* Over Time ($PPDOT$), Exceedance Hours ($EH$), and Weighted Exceedance Hours (WEH), are symmetric in nature, combining both overheating and overcooling discomfort into a single value. Although these indices provide valuable insights into the overall comfort conditions in buildings, they combine two distinct components of thermal comfort, making it difficult to determine whether a building can effectively address both overheating and overcooling discomfort solely by relying on these indices.
    - None of the two methods mentioned in the scientific literature, as well as ASHRAE 55 and ISO 7730 standards, specify any criteria or thresholds for time-integrated indices.

However, EN 15251 and Passive House standards establish a single value to limit only long-term annual discomfort and overheating, respectively. More recent standards, such as EN 16798 and ISO 17772, establish values to limit short-term (weekly) as well as long-term (monthly and annual) discomfort in buildings. In the case of naturally ventilated buildings, CIBSE TM52 provides criteria to limit seasonal overheating, as well as daily and instant overheating. Additionally, EPBD regulations define annual criteria in Belgium, annual and seasonal criteria in Germany, annual criteria in France, monthly criteria in the UK, and monthly criteria (only for July) in the Netherlands.

- In general, most standards and scientific literature underestimate the impact of climate change. However, Hamdy et al. [133] presented a study that provides a methodology for climate change considerations. They introduced three metrics: Indoor Overheating (IOD) and Ambient Warmness Degree (AWD), and overheating escalation factor ($\alpha_{IOD/AWD}$). By combining these metrics, it is possible to quantify a building's sensitivity and cooling system's response to the increasing frequency and intensity of overheating due to the progressive rise in outdoor air temperature resulting from climate change.

RQ2. *What are the cooling strategies to prevent overheating in buildings? How to classify them and characterize their resiliency against heatwaves and power outages?* ***(Chapter 02)***

Conclusions are drawn from a critical review of the state-of-the-art cooling strategies in existing scientific literature. In this collective work conducted within the International Energy Agency (IEA) Annex 80 – *"Resilient cooling of buildings"* project, cooling strategies are classified. The classification aims to provide a comprehensive overview of different cooling strategies, including their physical principle, typologies, performance with attention to resilience under extreme events (heatwaves and power outages), and technology readiness level (TRL).

A definition of resilient cooling is also provided as *"the capacity of the cooling system integrated with the building that allows it to withstand or recover from disturbances due to disruptions, including heatwaves and power outages, and to adopt the appropriate strategies after failure to mitigate degradation of building performance (deterioration of indoor environmental quality and/or increased need for space cooling energy)."* Finally, the resilience of cooling strategies is evaluated through a qualitative approach that involves conducting focus group discussions among scientific and professional experts in cooling technologies and building science who are participating in the Annex 80 project. The assessment also relies on an extensive review of the existing literature. The answer to RQ2 is as follows:

- Cooling strategies can be classified into four categories based on their approaches to cooling the people or the indoor environment:
    - **Category A:** Reducing heat gains to indoor environments and people indoors (e.g., solar shading and chromogenic glazing technologies, cool envelope materials, green roofs, roof ponds, green facades, ventilated roofs and facades, and thermal mass

utilization). These strategies aim to reduce the need for cooling and can potentially lower energy use and costs.
    - **Category B:** Removing sensible heat from indoor environments (e.g., absorption refrigeration (including desiccant cooling), ventilative cooling including natural ventilation and mechanical ventilation, adiabatic/evaporative cooling, compression refrigeration, ground source cooling, sky radiative cooling, and high-temperature cooling). These strategies are more targeted towards cooling entire spaces and may be more energy intensive.
    - **Category C:** Enhancing personal comfort apart from cooling whole spaces (e.g., personal comfort systems). These strategies aim to provide comfort to individuals rather than cooling an entire space.
    - **Category D:** Removing latent heat from indoor environments (e.g., desiccant humidification). Such strategies remove moisture, which can improve indoor air quality and potentially reduce the need for cooling.
- The cooling strategies can be characterized based on four criteria:
    - **Absorptive capacity** is the degree to which a system is able to absorb the impacts of disruptive events and minimize their consequences with little effort. For example, heavy thermal mass in a building (capacitance) can absorb unwanted solar gain and can minimize and/or delay the air temperature increase in the building without the use of cooling energy.
    - **Adaptive capacity** is the ability to adjust to undesirable situations by undergoing some changes. Adaptive capacity is distinguished from absorptive capacity in that adaptive systems change in response to adverse impacts, especially if the absorptive capacity has been exceeded. For example, a façade solar shade may be activated when the air temperature in the building starts to increase because the storage capacity of the thermal mass has been exceeded.
    - **Restorative capacity** is the ability to return to normal or improved operation. For example, night cooling can remove unwanted heat gain accumulated in the thermal mass during the day and provide a heat sink for the next day.
    - **Recovery speed** is the speed of the recovery process. Recovery may be accelerated if absorption activities are well implemented, and the system can quickly mobilize and effectively use all the resources at its disposal [216]. For example, the speed with which night cooling can remove heat from the building's thermal mass and restore the building to its desired condition depends on the ventilation flow rate and the outdoor air temperature.
- Overall, strategies that aim to reduce heat gains in the indoor environment demonstrate high absorptive capacity under heatwaves, while those with dynamic or flexible controls and Personal Comfort Systems (PCSs) exhibit a high adaptive capacity. Strategies that remove sensible and latent heat show a high restorative capacity. The recovery speed of the cooling strategies depends on various factors

such as their cooling potential, design, and control or operation of the cooling system.

RQ3. *How to quantify and evaluate the resistivity of buildings and their cooling strategies to the overheating impact of climate change using a robust methodology?* ***(Chapter 03)***

To address this research question, the term *"climate change overheating resistivity"* of cooling strategies is initially defined as *"the ability of building cooling strategies to resist the increase of indoor overheating risk against the increase of outdoor thermal severity in a changing climate".* This definition aims to assess to what extent the indoor overheating risk may increase with the rising outdoor thermal stress in future climate scenarios.

Subsequently, a comprehensive simulation-based framework is introduced in four steps, allowing the evaluation of a wide range of buildings with different active and passive cooling strategies. The primary aim of the framework is to provide a practical, cost-effective, and standardized approach based on internationally applicable standards for comparing cooling strategies in various locations and climates. However, the suggested procedure can be customized to compare a set of applicable cooling strategies for a specific building and location. Finally, the proposed framework is tested by comparing two air-based cooling strategies, namely a Variable Refrigerant Flow (VRF) unit coupled with a Dedicated Outdoor Air System (DOAS) and a Variable Air Volume (VAV) system, in six different locations/climates. The answer to RQ3 is as follows:

- To evaluate the resistivity of cooling strategies in buildings to the overheating impact of climate change, a four-step simulation-based framework is introduced, which can be followed as follows:
    - **Step 1** (specify reference cities and weather data characterization): this step involves several crucial components. Firstly, one contemporary (i.e., 2010s) and two future (i.e., 2050s and 2090s) weather scenarios should be selected considering the worst-case emission scenario (e.g., RCP8.5 or SSP5-8.5). Secondly, it is essential to identify the target city or cities where the cooling strategy will be evaluated. The framework suggests 23 reference cities based on their population and growth rate, which cover climate zones 1 to 6 as defined in ASHRAE 169.1 [217]. Nonetheless, other cities can be selected for this purpose. Thirdly, it is recommended to either include or exclude the Urban Heat Island (UHI) effect in urban-related studies. Including the UHI effect improves the accuracy of the weather datasets, while excluding it simplifies the process due to the complexity and limited availability of UHI-included weather data.
    - **Step 2** (identify building characterization): in this step, two approaches for selecting building simulation models are provided by the framework: the shoe box model for new buildings and the reference building model for both new and existing buildings. For shoe box models, the envelope characteristics must comply with ASHRAE 90.1 [218], and ISO 18523-1 [219], ISO 18523-2 [220], and ISO 17772-1 [159] are suggested to define schedules and conditions of building,

zone, and space usage. These include occupancy, operation of technical building systems, hot water usage, internal gains due to occupancy, lighting, and equipment. For reference building models, one should create or select a model that represents a specific building typology and vintage constructed during a particular period in a specific city.

- **Step 3** (identify and design/size the cooling strategies to be compared): to identify the proper cooling strategy, the framework lists a set of active and passive cooling strategies that are categorized and detailed in Chapter 02. The cooling strategy selected to be evaluated through the framework can be an individual or any combination of active and passive cooling strategies. The applicability of the selected cooling strategy in the target cities and climates must be ensured. Active cooling systems typically have a limited lifespan of 15-25 years, and the framework provides two schemes for long-term analysis adjustments: Scheme A, which is non-responsive to climate change, and Scheme B, which is climate change responsive. In Scheme A, the cooling strategy should be designed or sized based on the contemporary weather scenario of the 2010s and should be either kept or replaced with the same strategy for future scenarios. In Scheme B, the cooling strategy should be adjusted at the end of its lifespan based on changes in weather conditions and thus should be designed or sized according to future weather scenarios. The active cooling strategies should be sized for summer design days, while passive cooling strategies should comply with strict acceptable deviation criteria outlined in ISO 17772-2. For mixed/hybrid mode cooling strategies, the building should be considered in a way that it first operates via non-air conditioned mode and then uses air conditioning to moderate extreme weather conditions, as recommended by [177].
- **Step 4** (specify performance indicators and comfort models): three principal indices should be implemented: Indoor Overheating Degree (IOD), Ambient Warmness Degree (AWD), and the newly introduced Climate Change Overheating Resistivity ($CCOR$) metric, which combines IOD and AWD. These metrics allow for a comprehensive multizonal assessment of overheating and building resistivity to the overheating impact of climate change, taking into account both intensity and duration of overheating. Additionally, other overheating indices that are partially analyzed in Chapter 01 can also be employed. With regard to thermal comfort models, it is recommended to employ the category-based PMV/PPD (or static) model for air conditioned zones, as well as the adaptive model for non-air conditioned zones from ISO 17772-1 [159]. For zones with mixed/hybrid cooling modes, the PMV/PPD model or adaptive comfort model should be selected considering various factors, such as the occupants' level of expectancy or vulnerability, as well as energy conservation goals. The comfort category (I, II, III, and IV)

should be determined based on building typology, occupant expectations, and climate context.

RQ4. *What are the potential weather conditions under different global GHG emission scenarios in Belgium?* ***(Chapter 04, Chapter 06, & Chapter 07)***

Conclusions are drawn from simulations of the regional climate model MAR *"Modèle Atmosphérique Régional"* to create weather data for 12 cities in Belgium spanning from 1981-2100. The simulations are conducted by forcing MAR with both ERA5 reanalysis, which closely approximates real climate conditions, and three Earth system models (ESMs) from the Sixth Coupled Model Intercomparison Project (CMIP6) database: BCC-CSM2-MR, MPI-ESM.1.2, and MIROC6. CMIP6 characterizes the average evolution of climate parameters between 1980 and 2014 based on observations and 2015–2100 based on Shared Socioeconomic Pathway (SSP) scenarios [221]. Three SSP scenarios are considered for the generation of future data: i) SSP2-4.5 – CO_2 emissions around current levels until 2050, then falling but not reaching net zero by 2100 (2.7℃ estimated global warming by 2100), ii) SSP3-7.0 – CO_2 emissions double by 2100 (3.6℃ estimated global warming by 2100), and iii) SSP5-8.5 – CO_2 emissions triple by 2075 (4.4℃ estimated global warming by 2100) [8], [9]. The resulting weather data has a spatial resolution of 5 km and temporal resolution of 1 hour, which are used to create Typical Meteorological Year (TMY) and eXtreme Meteorological Year (XMY) files based on ISO 15927-4 standard [166]. This allows for the reconstruction of typical and extreme years while maintaining a reasonable variability of the meteorological data. Additionally, heatwave events are identified and characterized by their duration, highest temperature, and intensity. The answer to RQ4 focusing on Brussels is as follows:

- Climate change will shift Brussels from a heating-dominated to a cooling-dominated city by the 2090s, assuming the worst GHG emission scenario SSP5-8.5.
- The outdoor air temperature is projected to rise 1.11℃ to 4.11℃ per month between 2081-2100 compared to the period between 2001-2020, assuming the SSP5-8.5 scenario. The annual air temperature is expected to increase by 1.1-1.6℃ between 2041-2060 and 1.6-3.2℃ between 2081-2100, depending on the SSP scenario, in comparison to the period between 2001-2020. The $HDD10℃$ is predicted to decrease by 24% between 2041-2060 and 42% between 2081-2100, while the $CDD18℃$ is anticipated to increase by 21% between 2041-2060 and 60% between 2081-2100 across all SSPs compared to the period between 2001-2020.
- It is shown that the highest maximal temperature heatwave happened in 2019 and will most probably happen in 2047 and 2098, respectively, during historical (2001-2020), mid-future (2041-2060 under SSP5-8.5 scenario), and future (2081-2100 under SSP5-8.5 scenario) periods. The duration and average air temperature of heatwaves are predicted to increase with continued global warming. The duration of the highest maximal temperature heatwave is expected to rise from 120 hours (five days) in 2019 to 168 hours (seven days) in 2047 and 240 hours (ten days) in 2098, while the average air temperature during these heatwaves is estimated to increase by 0.94℃ and 3.48℃,

respectively. Furthermore, the intensity of the highest maximal temperature heatwaves is expected to increase by 115% in 2047 and 498% in 2098 due to the increase in temperature and duration of future heatwaves.

RQ5. *How much impact will climate change have on the thermal comfort, HVAC energy performance, and HVAC GHG emissions of high-performance houses in Belgium? What measures, both active and passive, can be taken to improve thermal comfort and energy efficiency? Can optimized high-performance houses maintain thermal comfort levels during unprecedented events?* ***(Chapter 05, Chapter 06, & Chapter 07)***

Conclusions are drawn from the modellings of two high-performance houses located in Belgium in Chapter 05, Chapter 06, and Chapter 07.

Chapter 05 presents the simulation results of a lightweight timber Passive house in Eupen under four weather scenarios: the moderate year of 1965, the extreme year of 2003, a moderate future year projected from 1976 to 2100 with a 2℃ temperature increase due to global warming, and an extreme future year projected from 1976 to 2100 with a 4℃ temperature increase due to global warming and 1.4℃ due to urban heat island effect. Mechanical/natural ventilation is considered as the cooling strategy assuming minimum and maximum ventilation rates based on NBN D50-001 [222] and [133].

Chapter 06 presents a climate change impact assessment for a nearly Zero-Energy terraced house, which serves as a benchmark for the study. The assessment focuses on time-integrated discomfort, HVAC energy performance, and HVAC Greenhouse Gas (GHG) emissions. To conduct the analysis, this chapter utilizes seven weather scenarios based on the regional climate model *"Modèle Atmosphérique Régional"* (MAR), which includes the Typical Meteorological Years (TMYs) for 2001-2020, 2041-2060 (considering SSP2-4.5, SSP3-7.0, and SSP5-8.5 emission scenarios), and 2081-2100 (considering SSP2-4.5, SSP3-7.0, and SSP5-8.5 emission scenarios). In the first stage, the chapter evaluates time-integrated discomfort for the naturally ventilated base case. In the second stage, the chapter compares the evolution of primary energy use and GHG emissions of two commonly applied HVAC strategies: a gas-fired boiler + air conditioner and a reversible air-to-water heat pump. Both strategies include mechanical ventilation with a heat recovery system. During the second stage of the analysis, specific key parameters that characterize the HVAC system undergo Uncertainty Analysis (UA) and Sensitivity Analysis (SA) using the Latin Hypercube Sampling (LHS) and Morris's methods. The primary goal of these analyses is to address uncertainties that may arise from the HVAC input parameters and identify the most influential factors on the HVAC primary energy use, respectively.

Chapter 07 investigates the risk of overheating for the optimized case of the benchmark dwelling discussed in Chapter 06. The assessment is carried out in two stages, using weather data obtained from the Regional Climate Model (MAR). The first stage involves conducting a multi-objective optimization using Genetic Algorithm (GA) based on Non-dominated Sorting Genetic Algorithm 2 (NSGA-II) method, which considers 13 passive design strategies to minimize both final HVAC energy use and time-integrated thermal discomfort. In the second stage, three optimal solutions (i.e., the most energy-efficient solution, the most thermally comfortable solution, and the

compromise solution) are selected from the Pareto front obtained in the first stage to analyze the risk of overheating during the highest maximal temperature heatwaves detected in the 2001–2020, 2041–2060, and 2081–2100 periods that coincide with the cooling system outage. The answer to RQ5 is as follows:

- According to Chapter 05:
  - The Passive House, constructed using lightweight timber, demonstrates significant potential in preventing long-term overheating and maintaining a comfortable thermal environment throughout the year. However, certain vulnerable areas, particularly those with large glazing areas that result in high solar gains, require additional provisions to ensure comfortable conditions, especially in future climates. This is particularly crucial given the ongoing effects of global warming, which are estimated to increase the Indoor Overheating Degree ($IOhD$) by 66%.
  - The use of a mechanical/natural ventilation strategy exhibits a substantial cooling potential of 62.68% when employed at high ventilation rates. However, due to global warming, this potential is projected to decrease.
- According to Chapter 06:
  - As global warming persists, naturally ventilated, nearly-zero energy terraced houses are expected to experience a significant increase in overheating risk. This risk is quantified by the $IOhD$ metric and may increase between 154-528% by the end of the century, depending on the SSP scenario. In contrast, the Indoor Overcooling Degree ($IOcD$) metric, which quantifies the risk of overcooling, is projected to decrease by 21-32%. If the high emission scenario (i.e., SSP5-8.5) occurs, there is a possibility that the overheating risk may overlap the overcooling risk by the 2090s.
  - The use of a reversible air-to-water heat pump leads to a decrease of approximately 6-13% and 15-27% in HVAC primary energy use and Greenhouse Gas (GHG) emissions, respectively, compared to the gas-fired boiler + air conditioner strategy. This reduction is primarily attributed to the heat pump's lower heating primary energy use and its ability to operate in an electricity-based heating mode. The latter is particularly relevant in Belgium, where the current electricity supply conditions (i.e., energy mix and Primary Energy Factor "PEF") make electricity a more environmentally friendly alternative to natural gas.
  - It is predicted that by the 2090s, the reversible air-to-water heat pump strategy will experience a reduction of approximately 4% in HVAC primary energy use, while the gas-fired boiler and air conditioner strategy will see a decrease of about 7%. In terms of greenhouse gas emissions, the reversible air-to-water heat pump is expected to have a 3% decrease, while the gas-fired boiler + air conditioner strategy is anticipated to have a 14ss% reduction by the same period.
  - The HVAC primary energy use for the reversible air-to-water heat pump and gas-fired boiler + air conditioner is most

affected by specific factors. For the former, the heating and cooling set-points and weather scenario have the most significant impact, while for the latter, the fan efficiency, heating COP, and cooling set-point are key factors. It is also shown that selecting the appropriate HVAC system during the early design stages is crucial for achieving energy-efficient buildings.

- According to Chapter 07:
  - To achieve optimal HVAC energy use and thermal comfort in a building through passive design strategies, a balance should be made between reducing heating energy use/overcooling and reducing cooling energy use/overheating. For a specific case study of a nearly Zero-Energy terraced dwelling in a temperate climate, certain design features such as high ventilation rate, low infiltration rate, high insulation, high thermal mass, green roof integration, and operable roller blinds are found to increase energy efficiency by up to 32% and improve thermal comfort by up to 46%.
  - Even in high-performance houses that have been optimized for thermal comfort and energy efficiency, overheating can reach critical and unhealthy levels for the occupants during unprecedented events such as heatwaves that coincide with cooling system outages. Climate change is expected to exacerbate this issue. For example, the highest maximal temperature heatwave in 2098 results in an increase in maximum Heat Index (HI) between 0.28℃ and 0.49℃, an increase in the maximum operative temperature between 1.34℃ and 2.33°℃, and a decrease in Thermal Autonomy (TA) between 17% and 28% compared to the one in 2019.

5.2. Revisiting main research question

What are the likely impacts of climate change on the thermal comfort, HVAC energy performance, and HVAC GHG emissions of high-performance Belgian houses, and how to adapt them?

The main research question has been addressed by dividing the research process into three distinct parts, which are data collection (Part I: Chapter 01 and Chapter 02), methodology development and prerequisite fulfillment (Part II: Chapter 03 and Chapter 04), and numerical analysis (Part III: Chapter 05, Chapter 06, and Chapter 07). Each part is detailed in a specific part of the thesis, with Part I focusing on reviewing and analyzing existing methods, Part II focusing on developing a comprehensive framework, and Part III focusing on presenting the results of climate change impact assessments on high-performance houses. In fact, the two first parts are intended to establish the foundation to conduct the simulations in Part III in order to answer the main research question as follows:

- ***Climate change's effect on thermal comfort:*** The findings from Chapter 05, Chapter 06, and Chapter 07 indicate that climate change will have significant and varied impacts on the thermal comfort of high-performance buildings. While the discomfort caused by overcooling is expected to decrease, the discomfort caused by overheating will

become a major challenge, particularly for naturally ventilated houses. The research conducted in Chapter 04 found that the detached house will experience a 66% increase in the risk of overheating, while the terraced house in Chapter 05 will experience a much higher increase of up to 528% by the end of the century. Furthermore, Chapter 07 demonstrated that extreme events, such as heatwaves and cooling system outages, can pose significant risks to occupants in the future. Therefore, relying solely on passive cooling strategies may not be sufficient to ensure thermal comfort and safety in highly insulated high-performance houses in Belgium, and active cooling systems will likely become necessary.

- ***Climate change's effect on HVAC energy performance and GHG emissions:*** Climate change is anticipated to alter the heating and cooling loads in buildings, leading to a reduction in heating loads and an increase in cooling loads. The net effect on HVAC energy use will vary depending on the efficiency and energy source of the system in use and climate. In Belgium's temperate climate, global warming can result in a decrease in the overall HVAC energy use and HVAC GHG emissions, as revealed in Chapter 06. The research shows that considering a reversible air-to-water heat pump strategy and a gas-fired boiler + air conditioner strategy in a high-performance terraced house will result in estimated reductions of 4% and 7% in HVAC primary energy use by the end of the century, respectively. The same applies to HVAC GHG emissions, with the reversible air-to-water heat pump strategy expected to have a 3% reduction and the gas-fired boiler + air conditioner strategy anticipated to have a 14% reduction. Overall, as shown by the results of the sensitivity analysis in Chapter 06, the choice of the HVAC system plays a major role in determining the changes in HVAC energy and HVAC GHG emissions due to global warming.
- ***Adaptation to climate change:*** Adapting buildings to the overheating impact of climate change requires selecting appropriate active and passive cooling strategies or a combination of both. This can be a challenging task, especially as the effectiveness of different strategies can vary depending on the specific conditions of the building and the surrounding environment. As shown in Chapter 05 and Chapter 07, passive strategies, such as natural ventilation, lowering infiltration rates, insulation, use of thermal mass, green roofs, and shading devices, have been shown to be effective in achieving comfort and energy efficiency benefits in high-performance houses in Belgium. However, as mentioned earlier, the effectiveness of these passive strategies may diminish due to global warming. Therefore, it is important to regularly evaluate and guarantee their performance under different weather scenarios that may be experienced in the future. In situations where active cooling systems are required, it is important to ensure that they are highly efficient and flexible to be coupled to renewable energy sources, such as electricity-based systems. Heat pumps are a promising solution for high-performance houses in Belgium, as indicated in Chapter 06. However, it is important to consider contingency plans for abnormal conditions, such as concurrent heatwaves and cooling system/power outages. In such cases, backup cooling or power systems, such as mini-split systems,

generators, and batteries, should be installed to ensure that the building remains comfortable and cool. By implementing a combination of active and passive cooling strategies and adopting contingency plans for abnormal weather conditions, buildings can be effectively adapted to climate change, thus reducing energy use and improving comfort.

5.3. Thesis contribution

The thesis aims to fill specific knowledge gaps in the field by dedicating each chapter to addressing a particular area. The findings of the thesis can provide valuable insights for researchers, policymakers, building designers and professionals, constructors, and the cooling industry. By highlighting the urgency of climate change adaptation actions, the thesis can help the construction sector move towards developing climate-proof and energy-efficient houses that offer comfort and health benefits to their occupants. The main contributions of the thesis can be summarized as follows:

- By presenting criteria for qualitative evaluation of different methods for assessing time-integrated thermal discomfort/overheating, the thesis contributes to a better understanding of this phenomenon. Specifically, the thesis examines commonly used methods in temperate regions and offers an overview of their strengths and limitations.
- The thesis introduces the concept of resilient cooling and characterizes the resiliency of a wide range of state-of-the-art cooling strategies using a set of qualitative criteria.
- The thesis proposes a multizonal method for climate change-sensitive evaluation of time-integrated overheating in buildings based on three principal metrics ($IOhD$, AWD, and $CCOR$) [133]. Incorporating these metrics allows for an asymmetric and multizonal quantification of overheating and determines the resistivity of buildings and their cooling strategies to global warming.
- The core contribution of this thesis lies in the development of a versatile simulation-based methodological framework that significantly advances the existing knowledge. Firstly, the framework is founded on universally applicable standards, facilitating a standardized comparison of cooling strategies across diverse climatic regions under common boundary conditions. Secondly, it offers a comprehensive approach, enabling the evaluation of various active and passive cooling strategies, while also providing systematic guidance on selecting appropriate comfort models for zones with different cooling modes (air-conditioned, non-air-conditioned, and mixed/hybrid mode). Thirdly, this framework exhibits flexibility by accommodating both residential and non-residential buildings, regardless of their typologies or operation types, encompassing both newly constructed and existing structures. Lastly, the framework incorporates a multi-zonal and climate-change-sensitive perspective to effectively assess overheating risks in buildings.
- The thesis presents a novel meteorological dataset for major cities in Belgium that is tailored and structured to suit building performance simulations. The dataset encompasses both historical and future weather data, presented on an annual basis. The dataset also

includes TMYs, XMYs, and three types of heatwaves for different timeframes.
- The thesis provides the results of a comparative analysis among commonly applied active cooling systems in Belgium and offers an in-depth examination of their sizing. It also identifies passive design strategies that can contribute to both energy efficiency and thermal comfort in high-performance houses using optimization techniques.

Overall, this thesis makes a valuable contribution to the growing body of knowledge on the effect of climate change on the thermal comfort and energy performance of high-performance houses, with a particular focus on temperate climates. The findings on these houses, which were recently constructed or renovated to comply with current Belgian legislation, offer practical insights that can guide policy decisions and inform actions in the construction industry.

5.4. Limitations

Each chapter may have been affected by various limitations, which are described in detail within the chapter. The primary limitations can be summarized as follows:

- Chapter 01 and Chapter 02 of the study both lack quantitative analyses of the methods used to assess overheating and the resiliency characterization of cooling strategies, respectively. This indicates that the study does not utilize numerical data and statistical methods in the analyses, making it difficult to accurately interpret the effectiveness of the methods and strategies.
- The study lacks a specific threshold for $IOhD$ as the principal metric used to quantify the overheating risk in Chapter 03, Chapter 05, Chapter 06, and Chapter 07. Without a defined threshold, this metric can only be used for comparative analysis between different buildings and cooling strategies. However, it does not provide a clear indication of whether a building is experiencing overheating or not.
- The thermal comfort evaluations carried out in different chapters do not consider all influential factors that affect occupants' comfort (i.e., air temperature, radiant temperature, relative humidity, clothing insulation level, metabolic rate, and air velocity). Chapter 03, Chapter 05, and Chapter 06 evaluate thermal comfort based solely on the operative temperature, whereas Chapter 07 takes into account the operative temperature and relative humidity.
- The focus of the thesis is narrowed down to the temperate region of Belgium. This is reflected in various chapters, including Chapter 04, Chapter 05, Chapter 06, and Chapter 07, which specifically deal with the development of weather data, simulation studies, and analysis of results in the context of Belgium.
- The future weather data developed in Chapter 04 does not accurately account for the Urban Heat Island (UHI) effect due to insufficient information on the expected changes in urbanization and human activities. Therefore, the study does not incorporate the potential impact of UHI on the future thermal conditions of the studied cases.

- The study's scope is limited to a few building typologies, namely a high-performance shoe box office model in Chapter 03, a high-performance detached house in Chapter 05, and a benchmark high-performance terraced house in Chapter 06 and Chapter 07. As a consequence, the study's paradigm does not encompass the majority of other residential and non-residential typologies, such as apartments, high-rise buildings, nursing homes, commercial buildings, etc.
- The models presented in Chapter 05, Chapter 06, and Chapter 07 exhibit certain partial oversimplifications. One significant aspect is the use of fixed rates for natural ventilation and infiltration, which introduces uncertainties in the findings. The rates of natural ventilation and infiltration are strongly influenced by environmental factors, such as the temperature gradient between indoor and outdoor spaces, wind speed, and direction. Considering the impact of climate change, where these environmental factors are subject to change, the rates of natural ventilation and infiltration may also be affected, making this an especially critical consideration.
- The investigations in Chapter 03 and Chapter 06 fail to take into account the Ozone Depletion Potential (ODP) of the refrigerant in the HVAC systems. ODP, which reflects the decrease in the ozone layer in the atmosphere caused by halocarbons [223], is a significant factor in determining the sustainability of the HVAC systems [224].

5.5. Suggestions for future works

The Ph.D. thesis identifies several limitations and unsolved issues, which offer various suggestions for future research, elaborated in each chapter. The key concepts can be outlined as follows:

- To advance research in this area, it is suggested to project the impact of global warming on other types of buildings, particularly the old residential building stock in Belgium. The proportion of dwellings built before 1990 in Belgium is 87% [225]–[227], and given the current renovation rate of less than 1% [228], it is anticipated that these old buildings will remain prevalent for several decades in the country.
- It is recommended that future studies focus on enhancing the evaluation techniques for overheating in the context of climate change. The new overheating indices should incorporate all comfort parameters, including relative humidity, metabolic rate, air velocity, air temperature, radiant temperature, and clothing factor provide a holistic and accurate estimation of occupants' thermal sensation. Additionally, these new indices should be accompanied by distinct thresholds that indicate whether a building is experiencing overheating during short-term heatwave events or in the long-term.
- It is suggested that future research should include a comparison between the weather data developed in Chapter 04 and data obtained from other sources such as CORDEX, Meteonorm, WeatherShift, and CCWorldWeatherGen. This can involve analyzing the similarities and differences between the datasets and evaluating the potential impacts of any variations on the results of the study. Moreover, it is suggested that additional research should be conducted to examine the

development of Urban Heat Island (UHI) and its impact on future weather conditions.

- It is recommended that future research should focus on exploring the effectiveness of various combinations of active and passive cooling strategies in improving thermal comfort and energy efficiency in buildings. This can result in the identification of the best possible combinations of cooling strategies for different building types and climates, helping in the development of optimized design guidelines.

References

[1] NOAA National Centers for Environmental information, “Climate at a Glance: Global Time Series,” Nov. 2022. https://www.ncei.noaa.gov/access/monitoring/climate-at-a-glance/global/time-series (accessed Dec. 13, 2022).

[2] I. Smiljanic, S. Lancaster, C. Barroso, I. Trigo, A. Salentinig, and J. Prieto, “Maximum Temperature Records Were Broken in Many Parts of Europe in June and July 2019, Due to a Series of Heatwaves,” 2019.

[3] U. Irfan, “113 degrees in France: why Europe is so vulnerable to extreme heat,” Jun. 28, 2019. Accessed: Dec. 15, 2022. [Online]. Available: https://www.vox.com/world/2019/6/26/18744518/heat-wave-2019-europe-france-germany-spain

[4] R. Lindsey and L. Dahlman, “Climate change: Global temperature,” *Available Online Clim. Gov Accessed 22 March 2021*, 2020.

[5] D. Wuebbles, “US Global change research program: Climate science special report (CSSR),” 2016.

[6] IPCC WGII core writing team, “Summary for Policymakers: Climate Change 2022 - Impacts, Adaptation, and Vulnerability.,” p.7, IPCC Geneva, Switzerland, 2022. Accessed: Sep. 03, 2023. [Online]. Available: https://www.ipcc.ch/report/ar6/wg2/downloads/report/IPCC_AR6_WGII_FinalDraft_FullReport.pdf

[7] Z. Hausfather and G. P. Peters, “Emissions–the ‘business as usual’story is misleading,” 2020.

[8] V. Masson-Delmotte *et al.*, “Climate Change 2021: The Physical Science Basis Contribution of Working Group I to the Sixth Assessment Report of the Intergovernmental Panel on Climate Change,” 2021.

[9] K. Riahi *et al.*, “The Shared Socioeconomic Pathways and their energy, land use, and greenhouse gas emissions implications: An overview,” *Glob. Environ. Change*, vol. 42, pp. 153–168, Jan. 2017, doi: 10.1016/j.gloenvcha.2016.05.009.

[10] D. Carvalho, S. Cardoso Pereira, and A. Rocha, “Future surface temperatures over Europe according to CMIP6 climate projections: an analysis with original and bias-corrected data,” *Clim. Change*, vol. 167, no. 1, pp. 1–17, 2021.

[11] B. Koffi and E. Koffi, “Heat waves across Europe by the end of the 21st century: multiregional climate simulations,” *Clim. Res.*, vol. 36, no. 2, pp. 153–168, 2008.

[12] L. R. Vargas Zeppetello, A. E. Raftery, and D. S. Battisti, “Probabilistic projections of increased heat stress driven by climate change,” *Commun. Earth Environ.*, vol. 3, no. 1, pp. 1–7, 2022.

[13] T. R. Oke, “The energetic basis of the urban heat island,” *Q. J. R. Meteorol. Soc.*, vol. 108, no. 455, pp. 1–24, 1982.

[14] H. Akbari, M. Pomerantz, and H. Taha, “Cool surfaces and shade trees to reduce energy use and improve air quality in urban areas,” *Sol. Energy*, vol. 70, no. 3, pp. 295–310, 2001.

[15] L. Zhao, X. Lee, R. B. Smith, and K. Oleson, “Strong contributions of local background climate to urban heat islands,” *Nature*, vol. 511, no. 7508, pp. 216–219, 2014.

[16] C. Rosenzweig, W. D. Solecki, S. A. Hammer, and S. Mehrotra, *Climate change and cities: First assessment report of the urban climate change research network*. Cambridge University Press, 2011.

[17] H. Taha, “Urban climates and heat islands: albedo, evapotranspiration, and anthropogenic heat,” *Energy Build.*, vol. 25, no. 2, pp. 99–103, 1997.

[18] A. Kazmierczak *et al.*, “Urban adaptation in Europe: how cities and towns respond to climate change,” European Environment Agency (EEA), 9294802701, 2020.

[19] K. Ward, S. Lauf, B. Kleinschmit, and W. Endlicher, “Heat waves and urban heat islands in Europe: A review of relevant drivers,” *Sci. Total Environ.*, vol. 569–570, pp. 527–539, Nov. 2016, doi: 10.1016/j.scitotenv.2016.06.119.
[20] D. Lauwaet *et al.*, “Detailed Urban Heat Island Projections for Cities Worldwide: Dynamical Downscaling CMIP5 Global Climate Models,” *Climate*, vol. 3, no. 2, pp. 391–415, 2015, doi: 10.3390/cli3020391.
[21] Royal Meteorological Institute of Belgium, “Heatwaves of 22-26 July 2019: Analysis of the meteorological and climatological context,” 2019. Accessed: Sep. 03, 2023. [Online]. Available: https://www.meteo.be/en/info/news/heatwaves-of-22-26-july-2019-analysis-of-the-meteorological-and-climatological-context
[22] J. D. Spengler, “Climate change, indoor environments, and health,” *Indoor Air*, vol. 22, no. 2, pp. 89–95, 2012.
[23] D. Crump, “Climate change–health impacts due to changes in the indoor environment; research need,” 2011.
[24] W. W. Nazaroff, “Exploring the consequences of climate change for indoor air quality,” *Environ. Res. Lett.*, vol. 8, no. 1, p. 015022, 2013.
[25] W. J. Fisk, “Review of some effects of climate change on indoor environmental quality and health and associated no-regrets mitigation measures,” *Build. Environ.*, vol. 86, pp. 70–80, Apr. 2015, doi: 10.1016/j.buildenv.2014.12.024.
[26] S. Vardoulakis *et al.*, “Impact of climate change on the domestic indoor environment and associated health risks in the UK,” *Environ. Int.*, vol. 85, pp. 299–313, Dec. 2015, doi: 10.1016/j.envint.2015.09.010.
[27] S. Hajat, S. Vardoulakis, C. Heaviside, and B. Eggen, “Climate change effects on human health: projections of temperature-related mortality for the UK during the 2020s, 2050s and 2080s,” *J Epidemiol Community Health*, vol. 68, no. 7, pp. 641–648, 2014.
[28] B. G. Armstrong *et al.*, “Association of mortality with high temperatures in a temperate climate: England and Wales,” *J. Epidemiol. Community Health*, vol. 65, no. 4, Art. no. 4, Apr. 2011, doi: 10.1136/jech.2009.093161.
[29] S. Vardoulakis, K. Dear, S. Hajat, C. Heaviside, B. Eggen, and A. J. McMichael, “Comparative assessment of the effects of climate change on heat-and cold-related mortality in the United Kingdom and Australia,” *Environ. Health Perspect.*, vol. 122, no. 12, pp. 1285–1292, 2014.
[30] K. Vadodaria, D. L. Loveday, and V. Haines, “Measured winter and spring-time indoor temperatures in UK homes over the period 1969–2010: A review and synthesis,” *Energy Policy*, vol. 64, pp. 252–262, Jan. 2014, doi: 10.1016/j.enpol.2013.07.062.
[31] M. Anderson, C. Carmichael, V. Murray, A. Dengel, and M. Swainson, “Defining indoor heat thresholds for health in the UK,” *Perspect. Public Health*, vol. 133, no. 3, pp. 158–164, 2013.
[32] G. DCLG, “Investigation into overheating in homes: literature review,” *Dep. Communities Local Gov. Lond.*, 2012.
[33] M. Stafoggia *et al.*, “Vulnerability to heat-related mortality: a multicity, population-based, case-crossover analysis,” *Epidemiology*, pp. 315–323, 2006.
[34] M. A. McGeehin and M. Mirabelli, “The potential impacts of climate variability and change on temperature-related morbidity and mortality in the United States.,” *Environ. Health Perspect.*, vol. 109, no. suppl 2, pp. 185–189, 2001.
[35] N. E. Klepeis, A. M. Tsang, and J. V. Behar, “Analysis of the National Human Activity Pattern Survey (NHAPS) respondents from a standpoint of exposure assessment,” *Las Vegas Lab. USEPANER*, 1996.
[36] T. Lanki *et al.*, “Determinants of personal and indoor PM2. 5 and absorbance among elderly subjects with coronary heart disease,” *J. Expo. Sci. Environ. Epidemiol.*, vol. 17, no. 2, pp. 124–133, 2007.
[37] R. Kennedy and M. Smith, “Effects of Aeroallergens on Human Health under Climate Change. In: Health Effects of Climate Change in the UK 2012,” 2012.
[38] N. Clark *et al.*, “Damp indoor spaces and health,” *Wash. DC Inst. Med. Natl. Acad.*, 2004.

[39] P. R. Morey, “Climate change and potential effects on microbial air quality in the built environment,” Washington DC: US Environmental Protection Agency, 2010.
[40] W. J. Fisk, Q. Lei-Gomez, and M. J. Mendell, “Meta-Analyses of the Associations of Respiratory Health Effectswith Dampness and Mold in Homes,” *Indoor Air*, vol. 17, no. LBNL-59363, 2006.
[41] J. A. Raub, M. Mathieu-Nolf, N. B. Hampson, and S. R. Thom, “Carbon monoxide poisoning — a public health perspective,” *Toxicology*, vol. 145, no. 1, pp. 1–14, Apr. 2000, doi: 10.1016/S0300-483X(99)00217-6.
[42] A. De Juniac, I. Kreis, J. Ibison, and V. Murray, “Epidemiology of unintentional carbon monoxide fatalities in the UK,” *Int. J. Environ. Health Res.*, vol. 22, no. 3, pp. 210–219, 2012.
[43] J. P. Dawson, B. J. Bloomer, D. A. Winner, and C. P. Weaver, “Understanding the Meteorological Drivers of U.S. Particulate Matter Concentrations in a Changing Climate,” *Bull. Am. Meteorol. Soc.*, vol. 95, no. 4, pp. 521–532, Apr. 2014, doi: 10.1175/BAMS-D-12-00181.1.
[44] V. Fabi, R. V. Andersen, S. Corgnati, and B. W. Olesen, “Occupants’ window opening behaviour: A literature review of factors influencing occupant behaviour and models,” *Build. Environ.*, vol. 58, pp. 188–198, Dec. 2012, doi: 10.1016/j.buildenv.2012.07.009.
[45] R. J. Delfino *et al.*, “The relationship of respiratory and cardiovascular hospital admissions to the southern California wildfires of 2003,” *Occup. Environ. Med.*, vol. 66, no. 3, pp. 189–197, 2009, doi: 10.1136/oem.2008.041376.
[46] J. Wu, A. M Winer, and R. J Delfino, “Exposure assessment of particulate matter air pollution before, during, and after the 2003 Southern California wildfires,” *Atmos. Environ.*, vol. 40, no. 18, pp. 3333–3348, Jun. 2006, doi: 10.1016/j.atmosenv.2006.01.056.
[47] J. A. Bernstein *et al.*, “The health effects of nonindustrial indoor air pollution,” *J. Allergy Clin. Immunol.*, vol. 121, no. 3, pp. 585–591, Mar. 2008, doi: 10.1016/j.jaci.2007.10.045.
[48] C. Dimitroulopoulou, M. Trantallidi, P. Carrer, G. C. Efthimiou, and J. G. Bartzis, “EPHECT II: Exposure assessment to household consumer products,” *Sci. Total Environ.*, vol. 536, pp. 890–902, Dec. 2015, doi: 10.1016/j.scitotenv.2015.05.138.
[49] A. P. Jones, “Indoor air quality and health,” *Atmos. Environ.*, vol. 33, no. 28, pp. 4535–4564, Dec. 1999, doi: 10.1016/S1352-2310(99)00272-1.
[50] A. Farrow, H. Taylor, K. Northstone, and J. Golding, “Symptoms of Mothers and Infants Related to Total Volatile Organic Compounds in Household Products,” *Arch. Environ. Health Int. J.*, vol. 58, no. 10, pp. 633–641, Oct. 2003, doi: 10.3200/AEOH.58.10.633-641.
[51] UNEP, AMAP., “Climate change and POPs: predicting the impacts,” Report of the UNEP/AMAP expert group. Secretariat of the Stockholm Convention, Geneva, Switzerland.
[52] S. Hazrati and S. Harrad, “Causes of Variability in Concentrations of Polychlorinated Biphenyls and Polybrominated Diphenyl Ethers in Indoor air,” *Environ. Sci. Technol.*, vol. 40, no. 24, pp. 7584–7589, Dec. 2006, doi: 10.1021/es0617082.
[53] L. Lamon, H. von Waldow, M. MacLeod, M. Scheringer, A. Marcomini, and K. Hungerbühler, “Modeling the Global Levels and Distribution of Polychlorinated Biphenyls in Air under a Climate Change Scenario,” *Environ. Sci. Technol.*, vol. 43, no. 15, pp. 5818–5824, Aug. 2009, doi: 10.1021/es900438j.
[54] WHO, *WHO handbook on indoor radon: a public health perspective*. World Health Organization (WHO), 2009.
[55] J. C. H. Miles, C. B. Howarth, and N. Hunter, “Seasonal variation of radon concentrations in UK homes,” *J. Radiol. Prot.*, vol. 32, no. 3, pp. 275–287, 2012, doi: 10.1088/0952-4746/32/3/275.

[56] C. R. Scivyer, “Radon protection for new buildings: a practical solution from the UK,” *Radon Living Environ.*, vol. 272, no. 1, pp. 91–96, May 2001, doi: 10.1016/S0048-9697(01)00670-2.
[57] N. Hunter, C. R. Muirhead, J. C. H. Miles, and J. D. Appleton, “Uncertainties in radon related to house-specific factors and proximity to geological boundaries in England,” *Radiat. Prot. Dosimetry*, vol. 136, no. 1, pp. 17–22, 2009, doi: 10.1093/rpd/ncp148.
[58] R. Asero, “Birch and ragweed pollinosis north of Milan: a model to investigate the effects of exposure to ‘new’ airborne allergens.,” *Allergy*, vol. 57, no. 11, pp. 1063–1066, Nov. 2002, doi: 10.1034/j.1398-9995.2002.23766.x.
[59] S. Voltolini *et al.*, “Trend of herbaceous pollen diffusion and allergic sensitisation in Genoa, Italy,” *Aerobiologia*, vol. 16, no. 2, pp. 245–249, Jun. 2000, doi: 10.1023/A:1007639030473.
[60] C. A. Rogers *et al.*, “Interaction of the onset of spring and elevated atmospheric CO2 on ragweed (Ambrosia artemisiifolia L.) pollen production.,” *Environ. Health Perspect.*, vol. 114, no. 6, pp. 865–869, Jun. 2006, doi: 10.1289/ehp.8549.
[61] B. D. Singer, L. H. Ziska, D. A. Frenz, D. E. Gebhard, and J. G. Straka, “Research note: Increasing Amb a 1 content in common ragweed (Ambrosia artemisiifolia) pollen as a function of rising atmospheric CO(2) concentration.,” *Funct. Plant Biol. FPB*, vol. 32, no. 7, pp. 667–670, Aug. 2005, doi: 10.1071/FP05039.
[62] C. E. Reid and J. L. Gamble, “Aeroallergens, allergic disease, and climate change: impacts and adaptation.,” *EcoHealth*, vol. 6, no. 3, pp. 458–470, Sep. 2009, doi: 10.1007/s10393-009-0261-x.
[63] Buildings Performance Institute Europe, “EPBD RECAST: NEW PROVISIONS NEED SHARPENING TO HIT CLIMATE TARGETS,” BPIE, Brussels, Belgium, 2022. Accessed: Sep. 03, 2023. [Online]. Available: https://www.bpie.eu/wp-content/uploads/2022/01/EPBD-recast-new-provisions-need-sharpening-to-hit-climate-targets.pdf
[64] Buildings Performance Institute Europe, “NEARLY ZERO: A REVIEW OF EU MEMBER STATE IMPLEMENTATION OF NEW BUILD REQUIREMENTS,” BPIE, Brussels, Belgium, 2021. Accessed: Sep. 03, 2023. [Online]. Available: https://www.bpie.eu/wp-content/uploads/2021/06/Nearly-zero_EU-Member-State-Review-062021_Final.pdf.pdf
[65] P. Archer, “Interactive Map of Europ,” 2013. https://philarcher.org/diary/2013/euromap/ (accessed Mar. 16, 2023).
[66] ISO 52016-1, *"ISO 52016-1: Energy performance of buildings — Energy needs for heating and cooling, internal temperatures and sensible and latent heat loads — Part 1: Calculation procedures*. Geneva, Switzerland, 2017.
[67] C. E. de Normalización, *EN ISO 13790: Energy Performance of Buildings: Calculation of Energy Use for Space Heating and Cooling (ISO 13790: 2008).* CEN, 2008.
[68] D. van Dijk, “EN ISO 52016 1: The new International Standard to calculate building energy needs for heating and cooling, internal temperature and heating and cooling loads,” presented at the Proceedings of the Building Simulation, 2019.
[69] R. Rahif, D. Amaripadath, and S. Attia, “Review on Time-Integrated Overheating Evaluation Methods for Residential Buildings in Temperate Climates of Europe,” *Energy Build.*, vol. 252, p. 111463, Dec. 2021, doi: 10.1016/j.enbuild.2021.111463.
[70] S. Attia *et al.*, “Overheating calculation methods in European building energy codes,” 2023.
[71] W. Feist, B. Kaufmann, J. Schnieders, and O. Kah, “Passive house planning package,” *Passive House Inst. Darmstadt Ger.*, 2015.
[72] Vlaams Energie- en Klimaatagentschap, “Bijlage V Bepalingsmethode EPW: BEPALINGSMETHODE VAN HET PEIL VAN PRIMAIR ENERGIEVERBRUIK VAN RESIDENTIËLE EENHEDEN,” Flanders, Belgium, 2020.

[73] Gouvernement Wallon, “Méthode PER 2018: MÉTHODE DE DÉTERMINATION DU NIVEAU DE CONSOMMATION D’ÉNERGIE PRIMAIRE DES UNITES RESIDENTIELLES,” Wallonia, Belgium, 2018.
[74] F. Birol, “The future of cooling: opportunities for energy-efficient air conditioning,” *Int. Energy Agency*, vol. 526, 2018.
[75] E. Elnagar, A. Zeoli, R. Rahif, S. Attia, and V. Lemort, “A qualitative assessment of integrated active cooling systems: A review with a focus on system flexibility and climate resilience,” *Renew. Sustain. Energy Rev.*, vol. 175, p. 113179, Apr. 2023, doi: 10.1016/j.rser.2023.113179.
[76] D. K. Bhamare, M. K. Rathod, and J. Banerjee, “Passive cooling techniques for building and their applicability in different climatic zones—The state of art,” *Energy Build.*, vol. 198, pp. 467–490, Sep. 2019, doi: 10.1016/j.enbuild.2019.06.023.
[77] M. Santamouris and D. Kolokotsa, “Passive cooling dissipation techniques for buildings and other structures: The state of the art,” *Energy Build.*, vol. 57, pp. 74–94, Feb. 2013, doi: 10.1016/j.enbuild.2012.11.002.
[78] N. Geetha and R. Velraj, “Passive cooling methods for energy efficient buildings with and without thermal energy storage–A review,” *Energy Educ. Sci. Technol. Part Energy Sci. Res.*, vol. 29, no. 2, pp. 913–946, 2012.
[79] Arup, “Addressing overheating risk in existing UK homes,” Arup, London, UK, An Arup report commissioned by the Climate Change Committee, 2022. Accessed: Mar. 17, 2023. [Online]. Available: https://www.theccc.org.uk/wp-content/uploads/2022/10/Addressing-overheating-risk-in-existing-UK-homes-Arup.pdf
[80] A. Velashjerdi Farahani, J. Jokisalo, N. Korhonen, K. Jylhä, R. Kosonen, and S. Lestinen, “Performance assessment of ventilative and radiant cooling systems in office buildings during extreme weather conditions under a changing climate,” *J. Build. Eng.*, vol. 57, p. 104951, Oct. 2022, doi: 10.1016/j.jobe.2022.104951.
[81] D. M. Ward, “The effect of weather on grid systems and the reliability of electricity supply,” *Clim. Change*, vol. 121, no. 1, pp. 103–113, 2013.
[82] P. Pratolongo, N. Leonardi, J. R. Kirby, and A. Plater, “Chapter 3 - Temperate Coastal Wetlands: Morphology, Sediment Processes, and Plant Communities,” in *Coastal Wetlands (Second Edition)*, G. M. E. Perillo, E. Wolanski, D. R. Cahoon, and C. S. Hopkinson, Eds., Elsevier, 2019, pp. 105–152. doi: 10.1016/B978-0-444-63893-9.00003-4.
[83] A. Albatayneh, D. Alterman, A. Page, and B. Moghtaderi, “Development of a new metric to characterise the buildings thermal performance in a temperate climate,” *Energy Sustain. Dev.*, vol. 51, pp. 1–12, Aug. 2019, doi: 10.1016/j.esd.2019.04.002.
[84] R. W. McColl, *Encyclopedia of world geography*, vol. 1. Infobase Publishing, 2014.
[85] Education Scotland, “Weather & Climate Change: Climates around the world,” 2016. https://web.archive.org/web/20160414115206/http://www.educationscotland.gov.uk/weatherandclimatechange/climate/worldclimates/temperate.asp (accessed Mar. 20, 2023).
[86] J. E. Cohen and C. Small, “Hypsographic demography: the distribution of human population by altitude,” *Proc. Natl. Acad. Sci.*, vol. 95, no. 24, pp. 14009–14014, 1998.
[87] C. Small and R. J. Nicholls, “A global analysis of human settlement in coastal zones,” *J. Coast. Res.*, pp. 584–599, 2003.
[88] B. Neumann, A. T. Vafeidis, J. Zimmermann, and R. J. Nicholls, “Future coastal population growth and exposure to sea-level rise and coastal flooding-a global assessment,” *PloS One*, vol. 10, no. 3, p. e0118571, 2015.
[89] G. Hugo, “Future demographic change and its interactions with migration and climate change,” *Glob. Environ. Change*, vol. 21, pp. S21–S33, 2011.
[90] K. Smith, “We are seven billion,” *Nat. Clim. Change*, vol. 1, no. 7, pp. 331–335, 2011.

[91] I. Valiela, *Global coastal change*. John Wiley & Sons, 2009.
[92] J. Kachadorian, *The Passive Solar House: Using Solar Design to Cool and Heat Your Home*. Chelsea Green Publishing, 2006.
[93] T. Kuczyński and A. Staszczuk, "Experimental study of the influence of thermal mass on thermal comfort and cooling energy demand in residential buildings," *Energy*, vol. 195, p. 116984, Mar. 2020, doi: 10.1016/j.energy.2020.116984.
[94] Z. Yılmaz, "Evaluation of energy efficient design strategies for different climatic zones: Comparison of thermal performance of buildings in temperate-humid and hot-dry climate," *Energy Build.*, vol. 39, no. 3, pp. 306–316, Mar. 2007, doi: 10.1016/j.enbuild.2006.08.004.
[95] F. D. Ching, *Building construction illustrated*. John Wiley & Sons, 2020.
[96] H. B. Awbi, *Ventilation of buildings*, 2nd ed. London, UK: Routledge, 2003. [Online]. Available: https://doi.org/10.4324/9780203634479
[97] I. Oropeza-Perez and P. A. Østergaard, "Potential of natural ventilation in temperate countries – A case study of Denmark," *Appl. Energy*, vol. 114, pp. 520–530, Feb. 2014, doi: 10.1016/j.apenergy.2013.10.008.
[98] European Environment Agency (EEA), "Cooling buildings sustainably in Europe: exploring the links between climate change mitigation and adaptation, and their social impacts," 2022. https://www.eea.europa.eu/publications/cooling-buildings-sustainably-in-europe (accessed Mar. 22, 2023).
[99] International Energy Agency (IEA), "District heating," 2021. https://www.iea.org/reports/district-heating (accessed Mar. 22, 2023).
[100] P. De Wilde, *Building performance analysis*. John Wiley & Sons, 2018.
[101] J. L. Hensen and R. Lamberts, *Building performance simulation for design and operation*. Routledge, 2012.
[102] T. Hauge Broholt, M. Dahl Knudsen, and S. Petersen, "The robustness of black and grey-box models of thermal building behaviour against weather changes," *Energy Build.*, vol. 275, p. 112460, Nov. 2022, doi: 10.1016/j.enbuild.2022.112460.
[103] T. Maile, M. Fischer, and V. Bazjanac, "Building energy performance simulation tools-a life-cycle and interoperable perspective," *Cent. Integr. Facil. Eng. CIFE Work. Pap.*, vol. 107, pp. 1–49, 2007.
[104] Y. Nugraha Bahar, C. Pere, J. Landrieu, and C. Nicolle, "A thermal simulation tool for building and its interoperability through the building information modeling (BIM) platform," *Buildings*, vol. 3, no. 2, pp. 380–398, 2013.
[105] S. Attia, E. Gratia, A. De Herde, and J. L. M. Hensen, "Simulation-based decision support tool for early stages of zero-energy building design," *Energy Build.*, vol. 49, pp. 2–15, Jun. 2012, doi: 10.1016/j.enbuild.2012.01.028.
[106] J. Sousa, "Energy simulation software for buildings: review and comparison," presented at the International Workshop on Information Technology for Energy Applicatons-IT4Energy, Lisabon, Citeseer, 2012, pp. 1–12.
[107] US Energy Department, "About Building Energy Modeling." https://www.energy.gov/eere/buildings/about-building-energy-modeling (accessed Jul. 11, 2023).
[108] US Energy Department, "Building Energy Software Tools Directory." http://apps1.eere.energy.gov/buildings/tools_directory/subjects.cfm/pagename=subjec (accessed Jul. 11, 2023).
[109] D. B. Crawley, J. W. Hand, M. Kummert, and B. T. Griffith, "Contrasting the capabilities of building energy performance simulation programs," *Build. Environ.*, vol. 43, no. 4, pp. 661–673, 2008, doi: 10.1016/j.buildenv.2006.10.027.
[110] TRNSYS, "A transient SYSTEM Simulation Software tool." Solar Energy Laboratory, Univ. of Wisconsin-Madison; TRANSSOLAR Energietechnik GmbH; CSTB – Centre Scientifique et Technique du Bâtiment; TESS – Thermal Energy Systems Specialists.
[111] S. de Wit and G. Augenbroe, "Analysis of uncertainty in building design evaluations and its implications," *View Energy Bild. Perform. Simul. Start Third*

Millenn., vol. 34, no. 9, pp. 951–958, Oct. 2002, doi: 10.1016/S0378-7788(02)00070-1.
[112] W. Tian, S. Yang, Z. Li, S. Wei, W. Pan, and Y. Liu, “Identifying informative energy data in Bayesian calibration of building energy models,” *Energy Build.*, vol. 119, pp. 363–376, May 2016, doi: 10.1016/j.enbuild.2016.03.042.
[113] W. Tian and P. de Wilde, “Uncertainty and sensitivity analysis of building performance using probabilistic climate projections: A UK case study,” *Autom. Constr.*, vol. 20, no. 8, pp. 1096–1109, Dec. 2011, doi: 10.1016/j.autcon.2011.04.011.
[114] C. J. Hopfe and J. L. M. Hensen, “Uncertainty analysis in building performance simulation for design support,” *Energy Build.*, vol. 43, no. 10, pp. 2798–2805, Oct. 2011, doi: 10.1016/j.enbuild.2011.06.034.
[115] Y. Heo, D. J. Graziano, L. Guzowski, and R. T. Muehleisen, “Evaluation of calibration efficacy under different levels of uncertainty,” *J. Build. Perform. Simul.*, vol. 8, no. 3, pp. 135–144, 2015.
[116] I. A. Macdonald, “Quantifying the effects of uncertainty in building simulation,” 2002.
[117] K. Beven, *Environmental modelling: an uncertain future?* CRC press, 2010.
[118] W. Tian *et al.*, “A review of uncertainty analysis in building energy assessment,” *Renew. Sustain. Energy Rev.*, vol. 93, pp. 285–301, Oct. 2018, doi: 10.1016/j.rser.2018.05.029.
[119] Y. Heo, R. Choudhary, and G. A. Augenbroe, “Calibration of building energy models for retrofit analysis under uncertainty,” *Energy Build.*, vol. 47, pp. 550–560, Apr. 2012, doi: 10.1016/j.enbuild.2011.12.029.
[120] R. C. Smith, *Uncertainty quantification: theory, implementation, and applications*, vol. 12. Siam, 2013.
[121] P. D. Arendt, D. W. Apley, and W. Chen, “Quantification of model uncertainty: Calibration, model discrepancy, and identifiability,” 2012.
[122] R. M. S. F. Almeida, N. M. M. Ramos, and S. Manuel, “Towards a methodology to include building energy simulation uncertainty in the Life Cycle Cost analysis of rehabilitation alternatives,” *J. Build. Eng.*, vol. 2, pp. 44–51, Jun. 2015, doi: 10.1016/j.jobe.2015.04.005.
[123] L. F. Cabeza, L. Rincón, V. Vilariño, G. Pérez, and A. Castell, “Life cycle assessment (LCA) and life cycle energy analysis (LCEA) of buildings and the building sector: A review,” *Renew. Sustain. Energy Rev.*, vol. 29, pp. 394–416, Jan. 2014, doi: 10.1016/j.rser.2013.08.037.
[124] W. Tian and R. Choudhary, “A probabilistic energy model for non-domestic building sectors applied to analysis of school buildings in greater London,” *Energy Build.*, vol. 54, pp. 1–11, Nov. 2012, doi: 10.1016/j.enbuild.2012.06.031.
[125] W. Tian, R. Choudhary, G. Augenbroe, and S. H. Lee, “Importance analysis and meta-model construction with correlated variables in evaluation of thermal performance of campus buildings,” *Build. Environ.*, vol. 92, pp. 61–74, Oct. 2015, doi: 10.1016/j.buildenv.2015.04.021.
[126] P. de Wilde and W. Tian, “Towards probabilistic performance metrics for climate change impact studies,” *Energy Build.*, vol. 43, no. 11, pp. 3013–3018, Nov. 2011, doi: 10.1016/j.enbuild.2011.07.014.
[127] W. Tian and P. de Wilde, “Thermal building simulation using the UKCP09 probabilistic climate projections,” *J. Build. Perform. Simul.*, vol. 4, no. 2, pp. 105–124, 2011.
[128] R. Choudhary and W. Tian, “Influence of district features on energy consumption in non-domestic buildings,” *Build. Res. Inf.*, vol. 42, no. 1, pp. 32–46, 2014.
[129] W. Tian, S. Yang, Q. Meng, and L. Wei, “Spatial Variation of Urban Building Energy Analysis,” presented at the Proceedings of the 14th Inernational IBPSA Building Simulation Conference, Hyderabad, India, 2015, pp. 7–9.
[130] A. T. Rezvan, N. S. Gharneh, and G. B. Gharehpetian, “Robust optimization of distributed generation investment in buildings,” *6th Dubrov. Conf. Sustain. Dev.*

Energy Water Environ. Syst. SDEWES 2011, vol. 48, no. 1, pp. 455–463, Dec. 2012, doi: 10.1016/j.energy.2012.10.011.
[131] A. P. Ramallo-González, T. S. Blight, and D. A. Coley, “New optimisation methodology to uncover robust low energy designs that accounts for occupant behaviour or other unknowns,” *J. Build. Eng.*, vol. 2, pp. 59–68, Jun. 2015, doi: 10.1016/j.jobe.2015.05.001.
[132] A. Mavrogianni *et al.*, “Historic Variations in Winter Indoor Domestic Temperatures and Potential Implications for Body Weight Gain,” *Indoor Built Environ.*, vol. 22, no. 2, pp. 360–375, 2013, doi: 10.1177/1420326X11425966.
[133] M. Hamdy, S. Carlucci, P.-J. Hoes, and J. L. M. Hensen, “The impact of climate change on the overheating risk in dwellings—A Dutch case study,” *Build. Environ.*, vol. 122, pp. 307–323, Sep. 2017, doi: 10.1016/j.buildenv.2017.06.031.
[134] M. Santamouris, “Cooling the buildings – past, present and future,” *Energy Build.*, vol. 128, pp. 617–638, Sep. 2016, doi: 10.1016/j.enbuild.2016.07.034.
[135] R. Escandón, R. Suárez, A. Alonso, and G. M. Mauro, “Is indoor overheating an upcoming risk in southern Spain social housing stocks? Predictive assessment under a climate change scenario,” *Build. Environ.*, vol. 207, p. 108482, Jan. 2022, doi: 10.1016/j.buildenv.2021.108482.
[136] Y. Yang, K. Javanroodi, and V. M. Nik, “Climate change and energy performance of European residential building stocks – A comprehensive impact assessment using climate big data from the coordinated regional climate downscaling experiment,” *Appl. Energy*, vol. 298, p. 117246, Sep. 2021, doi: 10.1016/j.apenergy.2021.117246.
[137] R. Gupta and M. Gregg, “Preventing the overheating of English suburban homes in a warming climate,” *Build. Res. Inf.*, vol. 41, no. 3, pp. 281–300, 2013, doi: 10.1080/09613218.2013.772043.
[138] ASHRAE, *ANSI/ASHRAE Standard 55-2017, Thermal environmental conditions for human occupancy*. Atlanta: ASHRAE, 2017.
[139] CIBSE Guide A, *CIBSE Guide A (2006): Environmetnal Design*. Chartered Institution of Building Services Engineers, London, UK, 2006.
[140] C. Song, T. Zhao, Z. Song, and Y. Liu, “Effects of phased sleeping thermal environment regulation on human thermal comfort and sleep quality,” *Build. Environ.*, vol. 181, p. 107108, Aug. 2020, doi: 10.1016/j.buildenv.2020.107108.
[141] M. R. Rosekind, “Underestimating the societal costs of impaired alertness: safety, health and productivity risks,” *Art Goods Sleep Proc. 2nd Int. Sleep Disord. Forum Yrly. Event Made Possible Sanofi-Aventis*, vol. 6, pp. S21–S25, Jan. 2005, doi: 10.1016/S1389-9457(05)80005-X.
[142] F. S. Luyster, P. J. Strollo Jr, P. C. Zee, and J. K. Walsh, “Sleep: a health imperative,” *Sleep*, vol. 35, no. 6, pp. 727–734, 2012.
[143] O. Seppanen, W. J. Fisk, and Q. Lei, “Effect of temperature on task performance in office environment,” 2006.
[144] A. Baddeley, “Working memory: Theories, models, and controversies,” *Annu. Rev. Psychol.*, vol. 63, pp. 1–29, 2012.
[145] P. Wargocki, J. A. Porras-Salazar, and S. Contreras-Espinoza, “The relationship between classroom temperature and children’s performance in school,” *Build. Environ.*, vol. 157, pp. 197–204, Jun. 2019, doi: 10.1016/j.buildenv.2019.04.046.
[146] P. Wargocki and D. P. Wyon, “Research report on effects of HVAC on student performance,” *ASHRAE J.*, vol. 48, no. 10, p. 22, 2006.
[147] P. Wargocki, D. P. Wyon, Y. K. Baik, G. Clausen, and P. O. Fanger, “Perceived air quality, sick building syndrome (SBS) symptoms and productivity in an office with two different pollution loads,” *Indoor Air*, vol. 9, no. 3, pp. 165–179, 1999.
[148] P. Roelofsen, “The impact of office environments on employee performance: The design of the workplace as a strategy for productivity enhancement,” *J. Facil. Manag.*, vol. 1, no. 3, pp. 247–264, 2002.

[149] S. Phillips, “Working through the pandemic: Accelerating the transition to remote working,” *Bus. Inf. Rev.*, vol. 37, no. 3, pp. 129–134, 2020, doi: 10.1177/0266382120953087.
[150] D. D’Ippoliti *et al.*, “The impact of heat waves on mortality in 9 European cities: results from the EuroHEAT project,” *Environ. Health*, vol. 9, no. 1, pp. 1–9, 2010.
[151] M. A. D. Larsen, S. Petrović, A. Radoszynski, R. McKenna, and O. Balyk, “Climate change impacts on trends and extremes in future heating and cooling demands over Europe,” *Energy Build.*, vol. 226, p. 110397, 2020, doi: 10.1016/j.enbuild.2020.110397.
[152] T. Randazzo, E. De Cian, and M. N. Mistry, “Air conditioning and electricity expenditure: The role of climate in temperate countries,” *Econ. Model.*, vol. 90, pp. 273–287, Aug. 2020, doi: 10.1016/j.econmod.2020.05.001.
[153] B. Ostro, S. Rauch, R. Green, B. Malig, and R. Basu, “The effects of temperature and use of air conditioning on hospitalizations,” *Am. J. Epidemiol.*, vol. 172, no. 9, pp. 1053–1061, 2010, doi: 10.1093/aje/kwq231.
[154] R. S. Kovats and S. Hajat, “Heat Stress and Public Health: A Critical Review,” *Annu. Rev. Public Health*, vol. 29, no. 1, pp. 41–55, Mar. 2008, doi: 10.1146/annurev.publhealth.29.020907.090843.
[155] EN 15251, *EN 15251: Indoor environmental input parameters for design and assessment of energy performance of buildings addressing indoor air quality, thermal environment, lighting and acoustics*. European Committee for Standardization, Brussels, Belgium, 2006.
[156] EN 16798-1, *EN 16798-1: Energy performance of buildings–ventilation for buildings–Part 1: Indoor environmental input parameters for design and assessment of energy performance of buildings addressing indoor air quality, thermal environment, lighting and acoustics*. European Committee for Standardization, Brussels, Belgium, 2019.
[157] EN 16798-2, *EN 16798-2: Energy performance of buildings–ventilation for buildings–Part 2: Interpretation of the requirements in EN 16798-1 - Indoor environmental input parameters for design and assessment of energy performance of buildings addressing indoor air quality, thermal environment, lighting and acoustics*. European Committee for Standardization, Brussels, Belgium, 2019.
[158] ISO 7730, *ISO 7730: Ergonomics of the Thermal Environment. Analytical Determination and Interpretation of Thermal Comfort Using Calculation of the PMV and PPD Indices and Local Thermal Comfort Criteria*. International Standards Organization Geneva, 2004.
[159] ISO 17772-1, *“ISO 17772-1: Energy performance of buildings - Indoor environmental quality. Part 1: Indoor environmental input parameters for the design and assessment of energy performance in buildings”.* Geneva, Switzerland, 2017.
[160] ISO 17772-2, *“ISO 17772-2: Energy performance of buildings - Overall energy performance assessment procedures. Part 2: Guideline for using indoor environmental input parameters for the design and assessment of energy performance of buildings”.* Geneva, Switzerland, 2018.
[161] ANSI/ASHRAE Standard 55, *Standard 55–2020: Thermal Environmental Conditions for Human Occupancy*. American Society of Heating, Refrigerating and Air Conditioning Engineers: Atlanta, GA, USA, 2020.
[162] CIBSE TM52, *CIBSE TM52: The limits of thermal comfort: avoiding overheating in European buildings*. Chartered Institution of Building Services Engineers, London, UK: Chartered Institution of Building Services Engineers, London, UK, 2013.
[163] CIBSE Guide A, *CIBSE Guide A (2015): Environmetnal Design*. Chartered Institution of Building Services Engineers, London, UK, 2015.
[164] CIBSE TM59, *CIBSE TM59: Design methodology for the assessment of overheating risk in homes*. Chartered Institution of Building Services Engineers, London, UK, 2017.

[165] M. Hendel, K. Azos-Diaz, and B. Tremeac, “Behavioral adaptation to heat-related health risks in cities,” *Energy Build.*, vol. 152, pp. 823–829, Oct. 2017, doi: 10.1016/j.enbuild.2016.11.063.
[166] ISO 15927-4, “‘ISO 15927-4: Hygrothermal performance of buildings — Calculation and presentation of climatic data — Part 4: Hourly data for assessing the annual energy use for heating and cooling’.,” p. Geneva, Switzerland, 2005.
[167] G. Ouzeau, J.-M. Soubeyroux, M. Schneider, R. Vautard, and S. Planton, “Heat waves analysis over France in present and future climate: Application of a new method on the EURO-CORDEX ensemble,” *Clim. Serv.*, vol. 4, pp. 1–12, Dec. 2016, doi: 10.1016/j.cliser.2016.09.002.
[168] C. Cheng, “Coauthors, 2009: Differential and combined impacts of extreme temperatures and air pollution on human mortality in south–central Canada. Part II: future estimates,” *Air Qual Atmosphere Health*, vol. 1, pp. 223–235.
[169] S. Carlucci and L. Pagliano, “A review of indices for the long-term evaluation of the general thermal comfort conditions in buildings,” *Energy Build.*, vol. 53, pp. 194–205, Oct. 2012, doi: 10.1016/j.enbuild.2012.06.015.
[170] S. Carlucci, “Thermal comfort assessment of buildings,” *Springer*, 2013, doi: 10.1007/978-88-470-5238-3.
[171] Zero Carbon Hub, “Impacts of Overheating: Evidence Review,” Zero Carbon Hub, London, England, 2015.
[172] NHBC, “Overheating in new homes: A review of the evidence,” National House-Building Council, UK., 2012.
[173] J. Kim and R. de Dear, “Is mixed-mode ventilation a comfortable low-energy solution? A literature review,” *Build. Environ.*, vol. 205, p. 108215, Nov. 2021, doi: 10.1016/j.buildenv.2021.108215.
[174] J. S. Brown and P. A. Domanski, “Review of alternative cooling technologies,” *Appl. Therm. Eng.*, vol. 64, no. 1–2, pp. 252–262, 2014.
[175] B. R. Hughes, H. N. Chaudhry, and S. A. Ghani, “A review of sustainable cooling technologies in buildings,” *Renew. Sustain. Energy Rev.*, vol. 15, no. 6, pp. 3112–3120, 2011.
[176] C. Zhang, M. Pomianowski, P. K. Heiselberg, and T. Yu, “A review of integrated radiant heating/cooling with ventilation systems-Thermal comfort and indoor air quality,” *Energy Build.*, vol. 223, p. 110094, 2020.
[177] T. Parkinson, R. de Dear, and G. Brager, “Nudging the adaptive thermal comfort model,” *Energy Build.*, vol. 206, p. 109559, 2020, doi: 10.1016/j.enbuild.2019.109559.
[178] N. N. Ishizaki, H. Shiogama, N. Hanasaki, and K. Takahashi, “Development of CMIP6-Based Climate Scenarios for Japan Using Statistical Method and Their Applicability to Heat-Related Impact Studies,” *Earth Space Sci.*, vol. 9, no. 11, p. e2022EA002451, 2022.
[179] J. Tang, X. Niu, S. Wang, H. Gao, X. Wang, and J. Wu, “Statistical downscaling and dynamical downscaling of regional climate in China: Present climate evaluations and future climate projections,” *J. Geophys. Res. Atmospheres*, vol. 121, no. 5, pp. 2110–2129, 2016.
[180] P. van der Linden and J. Mitchell editors, “ENSEMBLES: Climate Change and its Impacts: Summary of research and results from the ENSEMBLES project,” *Met Off. Hadley Cent. FitzRoy Road Exeter EX1 3PB UK*, vol. 160, 2009.
[181] L. Mearns *et al.*, “Climate change projections of the North American regional climate change assessment program (NARCCAP),” *Clim. Change*, vol. 120, pp. 965–975, 2013.
[182] D. Jacob *et al.*, “EURO-CORDEX: new high-resolution climate change projections for European impact research,” *Reg. Environ. Change*, vol. 14, pp. 563–578, 2014.
[183] M. Herrera *et al.*, “A review of current and future weather data for building simulation,” *Build. Serv. Eng. Res. Technol.*, vol. 38, no. 5, pp. 602–627, 2017, doi: 10.1177/0143624417705937.

[184] RMI, “Rapport climatique 2020 de l’information aux services climatiques, edited by: Gellens, D., Royal Meteorological Institute of Belgium, Brussels, ISSN 2033-8562,” 2020. Accessed: Aug. 31, 2022. [Online]. Available: https://www.meteo.be/resources/misc/climate_report/RapportClimatique-2020.pdf
[185] E. Brits *et al.*, “Climate change and health: set-up of monitoring of potential effects of climate change on human health and on the health of animals in Belgium. Unit environment and health, Brussels, Belgium,” 2009. Accessed: Aug. 31, 2022. [Online]. Available: https://www.belspo.be/belspo/organisation/publ/pub_ostc/agora/ragjj146_en.pdf (
[186] S. Zahiri and H. Altan, “The effect of passive design strategies on thermal performance of female secondary school buildings during warm season in a hot and dry climate,” *Front. Built Environ.*, vol. 2, p. 3, 2016.
[187] E. Rodriguez-Ubinas *et al.*, “Passive design strategies and performance of Net Energy Plus Houses,” *Energy Build.*, vol. 83, pp. 10–22, 2014.
[188] H. Albayyaa, D. Hagare, and S. Saha, “Energy conservation in residential buildings by incorporating Passive Solar and Energy Efficiency Design Strategies and higher thermal mass,” *Energy Build.*, vol. 182, pp. 205–213, 2019.
[189] E. Mushtaha *et al.*, “The impact of passive design strategies on cooling loads of buildings in temperate climate,” *Case Stud. Therm. Eng.*, vol. 28, p. 101588, 2021.
[190] J. Morrissey, T. Moore, and R. E. Horne, “Affordable passive solar design in a temperate climate: An experiment in residential building orientation,” *Renew. Energy*, vol. 36, no. 2, pp. 568–577, 2011.
[191] R. Becker, I. Goldberger, and M. Paciuk, “Improving energy performance of school buildings while ensuring indoor air quality ventilation,” *Build. Environ.*, vol. 42, no. 9, pp. 3261–3276, 2007, doi: 10.1016/j.buildenv.2006.08.016.
[192] M. Gil-Baez, Á. Barrios-Padura, M. Molina-Huelva, and R. Chacartegui, “Natural ventilation systems in 21st-century for near zero energy school buildings,” *Energy*, vol. 137, pp. 1186–1200, 2017, doi: 10.1016/j.energy.2017.05.188.
[193] C. Younes, C. A. Shdid, and G. Bitsuamlak, “Air infiltration through building envelopes: A review,” *J. Build. Phys.*, vol. 35, no. 3, pp. 267–302, 2012.
[194] K. Hassouneh, A. Alshboul, and A. Al-Salaymeh, “Influence of infiltration on the energy losses in residential buildings in Amman,” *Sustain. Cities Soc.*, vol. 5, pp. 2–7, 2012, doi: 10.1016/j.scs.2012.09.004.
[195] U. Mathur and R. Damle, “Impact of air infiltration rate on the thermal transmittance value of building envelope,” *J. Build. Eng.*, vol. 40, p. 102302, Aug. 2021, doi: 10.1016/j.jobe.2021.102302.
[196] J. Jokisalo, J. Kurnitski, M. Korpi, T. Kalamees, and J. Vinha, “Building leakage, infiltration, and energy performance analyses for Finnish detached houses,” *Build. Environ.*, vol. 44, no. 2, pp. 377–387, 2009, doi: 10.1016/j.buildenv.2008.03.014.
[197] J. Lee, J. Kim, D. Song, J. Kim, and C. Jang, “Impact of external insulation and internal thermal density upon energy consumption of buildings in a temperate climate with four distinct seasons,” *Renew. Sustain. Energy Rev.*, vol. 75, pp. 1081–1088, Aug. 2017, doi: 10.1016/j.rser.2016.11.087.
[198] P. L. Simona, P. Spiru, and I. V. Ion, “Increasing the energy efficiency of buildings by thermal insulation,” *Energy Procedia*, vol. 128, pp. 393–399, 2017.
[199] J.-J. Kim and J. W. Moon, “Impact of insulation on building energy consumption,” presented at the Eleventh International IBPSA Conference, Building Simulation, 2009.
[200] E. Guelpa, “Impact of thermal masses on the peak load in district heating systems,” *Energy*, vol. 214, p. 118849, Jan. 2021, doi: 10.1016/j.energy.2020.118849.

[201] S. B. Pallin, T. Pilet, and R. Starostka, “Variables Influenced by Thermal Mass and its Impact on Energy Performance in Buildings,” Oak Ridge National Lab.(ORNL), Oak Ridge, TN (United States), 2019.
[202] S. A. Al-Sanea, M. F. Zedan, and S. N. Al-Hussain, “Effect of thermal mass on performance of insulated building walls and the concept of energy savings potential,” *Spec. Issue Therm. Energy Manag. Process Ind.*, vol. 89, no. 1, pp. 430–442, Jan. 2012, doi: 10.1016/j.apenergy.2011.08.009.
[203] A. H. Ghoreishi and M. M. Ali, “Contribution of thermal mass to energy performance of buildings: A comparative analysis,” *Int. J. Sustain. Build. Technol. Urban Dev.*, vol. 2, no. 3, pp. 245–252, 2011.
[204] J. Kosny, T. Petrie, D. Gawin, P. Childs, A. Desjarlais, and J. Christian, “Thermal mass-energy savings potential in residential buildings,” *Rep. No Build. Technol. Cent. ORNL*, 2001.
[205] K. Gregory, B. Moghtaderi, H. Sugo, and A. Page, “Effect of thermal mass on the thermal performance of various Australian residential constructions systems,” *Energy Build.*, vol. 40, no. 4, pp. 459–465, 2008.
[206] U. Berardi, A. GhaffarianHoseini, and A. GhaffarianHoseini, “State-of-the-art analysis of the environmental benefits of green roofs,” *Appl. Energy*, vol. 115, pp. 411–428, Feb. 2014, doi: 10.1016/j.apenergy.2013.10.047.
[207] J. Goussous, H. Siam, and H. Alzoubi, “Prospects of green roof technology for energy and thermal benefits in buildings: Case of Jordan,” *Sustain. Cities Soc.*, vol. 14, pp. 425–440, Feb. 2015, doi: 10.1016/j.scs.2014.05.012.
[208] A. Sfakianaki, E. Pagalou, K. Pavlou, M. Santamouris, and M. Assimakopoulos, “Theoretical and experimental analysis of the thermal behaviour of a green roof system installed in two residential buildings in Athens, Greece,” *Int. J. Energy Res.*, vol. 33, no. 12, pp. 1059–1069, 2009, doi: 10.1002/er.1535.
[209] N. R. Netusil, L. Lavelle, S. Dissanayake, and A. W. Ando, “Valuing the public benefits of green roofs,” *Landsc. Urban Plan.*, vol. 224, p. 104426, 2022.
[210] M. Semaan and A. Pearce, “Assessment of the gains and benefits of green roofs in different climates,” *Procedia Eng.*, vol. 145, pp. 333–339, 2016.
[211] H. Sghiouri, A. Mezrhab, M. Karkri, and H. Naji, “Shading devices optimization to enhance thermal comfort and energy performance of a residential building in Morocco,” *J. Build. Eng.*, vol. 18, pp. 292–302, 2018.
[212] S. G. Koç and S. M. Kalfa, “The effects of shading devices on office building energy performance in Mediterranean climate regions,” *J. Build. Eng.*, vol. 44, p. 102653, 2021.
[213] I. R. Maestre, J. L. F. Blázquez, F. J. G. Gallero, and P. R. Cubillas, “Influence of selected solar positions for shading device calculations in building energy performance simulations,” *Energy Build.*, vol. 101, pp. 144–152, 2015.
[214] A. Kirimtat, B. K. Koyunbaba, I. Chatzikonstantinou, and S. Sariyildiz, “Review of simulation modeling for shading devices in buildings,” *Renew. Sustain. Energy Rev.*, vol. 53, pp. 23–49, 2016.
[215] S. Quefelec, “Cooling buildings sustainably in Europe: exploring the links between climate change mitigation and adaptation, and their social impacts,” European Environment Agency, 2022. Accessed: May 04, 2023. [Online]. Available: https://www.eea.europa.eu/publications/cooling-buildings-sustainably-in-europe/cooling-buildings-sustainably-in-europe/#fn7
[216] A. Sharifi and Y. Yamagata, “Principles and criteria for assessing urban energy resilience: A literature review,” *Renew. Sustain. Energy Rev.*, vol. 60, pp. 1654–1677, Jul. 2016, doi: 10.1016/j.rser.2016.03.028.
[217] ASHRAE, *ANSI/ASHRAE Standard 169-2013, Climatic Data for Building Design*. Atlanta: ASHRAE, 2013.
[218] ASHRAE, *ANSI/ASHRAE/IES Standard 90.1-2016: Energy Standard for Buildings Except Low-Rise Residential Buildings*. 2016. [Online]. Available: https://www.techstreet.com/ashrae/ashrae_standards.html
[219] ISO 18523-1, “"ISO 18523-1: Energy performance of buildings — Schedule and condition of building, zone and space usage for energy calculation — Part 1: Non-residential buildings.,” p. Geneva, Switzerland, 2016.

[220] ISO 18523-2, “"ISO 18523-2: Energy performance of buildings — Schedule and condition of building, zone and space usage for energy calculation — Part 2: Residential buildings.,” p. Geneva, Switzerland, 2017.
[221] V. Eyring *et al.*, “Overview of the Coupled Model Intercomparison Project Phase 6 (CMIP6) experimental design and organization,” *Geosci. Model Dev.*, vol. 9, no. 5, pp. 1937–1958, 2016, doi: 10.5194/gmd-9-1937-2016.
[222] D. NBN, “Standard 50-001: Dispositifs de ventilation dans les bâtiments d’habitation. NBN, Brussels, Belgium,” *Dispositifs de ventilation dans les bâtiments d’habitation*, 1991.
[223] C. B. Farinha, J. Jankovic, and M. D. R. Veiga, *Eco-efficient rendering mortars: use of recycled materials*. Woodhead Publishing, 2021.
[224] R. Legg, *Air conditioning system design*. Butterworth-Heinemann, 2017.
[225] “Émissions par secteur Klimaat | Climat.” Accessed: Apr. 27, 2023. [Online]. Available: https://climat.be/en-belgique/climat-et-emissions/emissions-des-gaz-a-effet-de-serre/emissions-par-secteur
[226] FGOV, “CSTC sur base du census des logements,” 2011. Accessed: Apr. 27, 2023. [Online]. Available: Available: https://www.census2011.be/download/downloads_fr.html
[227] S. Attia, A. Mustafa, N. Giry, M. Popineau, M. Cuchet, and N. Gulirmak, “Developing two benchmark models for post-world war II residential buildings,” *Energy Build.*, vol. 244, p. 111052, Aug. 2021, doi: 10.1016/j.enbuild.2021.111052.
[228] G. Ruellan, M. Cools, and S. Attia, “Analysis of the determining factors for the renovation of the Walloon residential building stock,” *Sustainability*, vol. 13, no. 4, p. 2221, 2021, doi: 10.3390/su13042221.

Appendices

Appendix A

Chapter 1: *Review on time-Integrated overheating evaluation methods for residential buildings in temperate climates of Europe*

Energy & Buildings 252 (2021) 111463

Contents lists available at ScienceDirect

Energy & Buildings

journal homepage: www.elsevier.com/locate/enb

Review on Time-Integrated Overheating Evaluation Methods for Residential Buildings in Temperate Climates of Europe

R. Rahif*, D. Amaripadath, S. Attia

Sustainable Building Design Lab, Dept. UEE, Faculty of Applied Sciences, Université de Liege, Belgium

ARTICLE INFO

Article history:
Received 25 May 2021
Revised 31 August 2021
Accepted 11 September 2021
Available online 17 September 2021

Keywords:
Thermal comfort
EPBD
Long-term comfort
International standards
Thermal discomfort
Chronic overheating

ABSTRACT

Overheating exposure over time can lead to discomfort, productivity reduction, and health issues for the occupants in buildings. The *time-integrated overheating evaluation methods* are introduced to describe, in a synthetic way, the extent of overheating over a span of time and predict the uncomfortable phenomena. This paper reviews the time-integrated overheating evaluation methods that are applicable to residential buildings in temperate climates of Europe. We critically analyze the methods found in (i) 11 international standards, namely, EN 15251 (2006), EN 16798 (2019), ISO 7730 (2004), ISO 17772 (2017–2018), ASHRAE 55 (2017), ASHRAE 55 (2020), CIBSE Guide A (2006), CIBSE TM52 (2013), CIBSE Guide A (2015), CIBSE TM59 (2017), and Passive House (2015), (ii) five national building codes based on the Energy Performance of Building Directive (EPBD) in Belgium, France, Germany, the UK, and the Netherlands, and (iii) two studies in the scientific literature. For each method, we present the thermal comfort models along with the time-integrated overheating indices and criteria. The methods are analyzed according to some key measures in order to identify their scope, strength, and limitations. We found that most standards recommend the static comfort models for air-conditioned buildings and the adaptive comfort models for non-air-conditioned ones. We also found a promising method based on three indices, namely, Indoor Overheating Degree (*IOD*), Ambient Warmness Degree (*AWD*), and overheating escalation factor ($\alpha_{IOD/AWD}$) that allows for a multi-zonal and climate change-sensitive overheating assessment. Finally, some guidance is provided for practice and future developments.

Contents

* Corresponding author.
E-mail address: ramin.rahif@uliege.be (R. Rahif).

https://doi.org/10.1016/j.enbuild.2021.111463
0378-7788/

1. Introduction

During the last two decades, extremely hot outdoor conditions have become more intense and frequent in temperate climates of Europe. In summer 2003, the outdoor air temperatures of 35 °C, 37 °C, 38.5 °C, and 40.2 °C were recorded in the Netherlands, France, the UK, and Germany, respectively [1–4]. Royal Meteorological Institute (RMI) of Belgium reported that the Hechtel-Eksel municipality experienced 51 consecutive days with the outdoor air temperature above 25 °C, and a maximum air temperature of 38.8 °C is recorded in the summer of 2018.

Unfortunately, the situation will worsen since the European Environment Agency (EEA) predicts an increase in the annual average air temperature between 1.0 and 2.5 °C by 2021–2050 and between 2.5 and 4 °C by 2071–2100 over Europe. It is expected that Europe's sweltering heatwave in 2003 will become typical weather by the middle of the 21st century [5]. In addition, the Urban Heat Island (UHI) effect that is recognized in more than 400 cities around the world will be exacerbated by climate change [6,7]. The UHI effect, defined as the *"relatively atmospheric warmth of urban areas compared to surrounding countryside"* [8], is predicted to increase the land air temperature in Europe by 2.68 °C (December to February) and 5.06 °C (June to August) in urban areas by 2080–2099 [9]. Such warming outdoor conditions will increase the risk of overheating in indoor environments where people spend most of the time [10].

Overheating in residential buildings has been reported in many temperate regions across Europe [11–15]. High indoor temperatures affect the occupant's health, comfort, and productivity where in severe cases can lead to illness and death [16,17]. According to Housing Health and Safety Rating System (HHSRS) in the UK, the indoor temperature exceeding the maximum threshold of 25 °C can lead to an increase in strokes and mortality [18]. In total, over 35,000 people died in Europe during the summer 2003 heatwave [19], in which 14,729 deaths reported in France [20], 2139 in England and Wales [21], up to 2200 in the Netherlands [1], 7295 in Germany [22], and 1175 in Belgium [23]. To avoid such issues, there is a need for proper definition and criteria for indoor overheating to be considered in the building designs.

A number of methods are introduced for assessing the human thermal response to the surrounding environment in the literature [24]. They aim at describing the human thermal perception from an environment where an individual or a group of people is exposed. In the last twenty years, a new group of methods are proposed for assessing the comfort over a span of time in buildings, which are termed *long-term comfort evaluation methods* [25,26], *chronic overheating evaluation methods* [27], or *time-integrated comfort evaluation methods* [28]. They aim at evaluating the comfort qualities of a building over time and considering all the building zones [29]. The majority of these methods were developed to assess the overheating discomfort, and some of them deal with overheating and overcooling discomfort at the same time, and only a few of them deal with overcooling discomfort [29,30]. Most of the time-integrated comfort evaluation methods have two key decisions in common, the choice of thermal comfort model and the selection of time-integrated discomfort index. Previous research exists by reviewing the existing thermal comfort models and the time-integrated discomfort indices.

Among the reviews on thermal comfort models, Taleghani et al. [31] chronologically reviewed the static and the adaptive comfort models with a detailed analysis of the adaptive comfort models in ASHRAE 55 (2010), EN 15251, and ISSO 74 (2004) (in the Netherlands) standards. It was found that the main difference of the adaptive comfort models relies on the choice of outdoor reference temperature, the extend of acceptable temperature ranges, and databases related to the field studies. Khovalyg et al. [32] extensively reviewed EN 15251, ISO 17772, EN 16798, ISO 7730, ASHRAE 55 (2017), GB/T 50785 (in China), ISHRAE 10,001 (in India), SS 553, and SS 554 (in Singapore) standards, questioning the applicability of their comfort models on regional scales. Carlucci et al. [33] reviewed the adaptive comfort models in ASHRAE 55, EN 15251, EN16798, ISSO 74 (in the Netherlands), and GB/T 50785 standards. Carlucci et al. [33] also revealed that the difference in the choice of outdoor reference temperature is the primary source of discrepancy in deriving the adaptive comfort models. Cheng et al. [34] reviewed the thermoregulatory models for the human body by distinguishing between the psychological models and physiological models. They numerically assessed the UC Berkeley thermal comfort model (UCB) and ISO 14505 thermal comfort model using a detailed Computational Fluid Dynamics (CFD) analysis. They found that the coupling of the UCB model with CFD is complex, hindering its widespread. On the other hand, the ISO 14505 model is more sensitive in warm environments and less sensitive in cold environments, questioning the reliability of the model. The overview of thermal comfort models and indicators is also presented in [24,35–39]. The focus of the above reviews was mainly on investigating the existing models for thermal comfort.

Despite the numerous studies on thermal comfort models, a limited number of documents reviewed the time-integrated discomfort indices. Carlucci et al. [29] systematically reviewed 15 indices, classifying them into four homogenous families (i.e., percentage indices, cumulative indices, risk indices, and averaging indices). Carlucci [40] quantitatively evaluated 16 time-integrated discomfort indices focusing on summer overheating in 54 variants of an office building. It was found that different indices would identify different variants as the optimal case. The gap recognition is then performed through the sensitivity analysis by varying the calculation periods in the time-integrated discomfort indices. Finally, the Long-term Percentage of Dissatisfied (*LPD*) index is proposed, which is a symmetric and comfort model-based discomfort index. Zero Carbon Hub (a non-profit organization to implement zero energy homes policy in the UK) published an evidence review for overheating risk assessment in buildings in 2015 [41]. It covers the methodologies in the Standard Assessment Procedure (SAP), CIBSE Guide A (2006), CIBSE Guide A (2015), CIBSE TM52, Passive House, BB 101, and Part L2A of UK government's building regulations. Also, the UK National House-Building Council (NHBC) provided a report by studying the overheating definitions in several guidelines and regulatory documents in the UK [42]. The two former studies (i.e., [29,40]) are outdated since most standards are superseded and new methods are introduced in the literature and the two latter reports (i.e., [41,42]) are local and focused on the methods mainly implemented in the UK. To overcome the limitations of the above studies, by extending our scope to temperate regions in Europe, we explore the long-lasting standards in addition to those that were not reviewed

Table 1
Summary of reviews on thermal comfort models and overheating evaluation methods.

Author	Ref.	Year	Journal/Institution	Thermal comfort models	Overheating evaluation methods
Roaf et al.	[39]	2010	Architectural Science Review	✓	
Van hoof et al.	[35]	2010	Frontiers in Bioscience	✓	
Carlucci and Pagliano	[29]	2012	Energy and Buildings	✓	✓
NHBC	[42]	2012	NHBC	✓	✓
Cheng et al.	[34]	2012	Building and Environment	✓	
Halawa and Van Hoof	[36]	2012	Energy and Buildings	✓	
Taleghani et al.	[31]	2013	Renewable and Sustainable Energy Reviews	✓	
Carlucci	[40]	2013	Springer	✓	✓
Yang et al.	[37]	2014	Applied Energy	✓	
Zero Carbon Hub	[41]	2015	Zero Carbon Hub	✓	✓
Enescu	[24]	2017	Renewable and Sustainable Energy Reviews	✓	
Carlucci et al.	[33]	2018	Building and Environment	✓	
Khovalyg et al.	[32]	2020	Energy and Buildings	✓	
Zhao et al.	[38]	2021	Energy and Built Environment	✓	

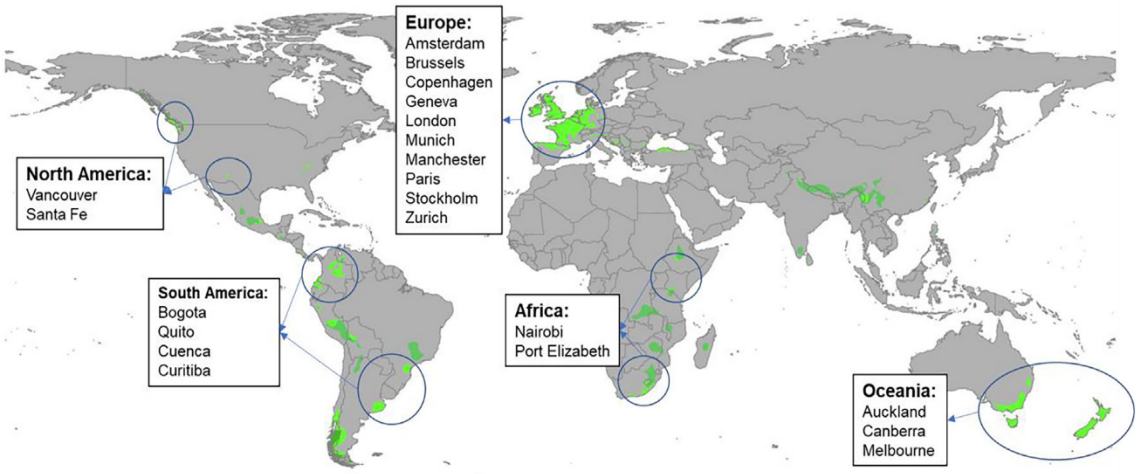

Fig. 1. Cities with Temperate oceanic climate (Cfb) worldwide.

before such as EN 16798, ISO 17772, ASHRAE (2020), CIBSE TM59, and five national codes based on the Energy Performance of Building Directive (EPBD) in Belgium, France, Germany, the UK, and the Netherlands as well as two state-of-the-art methods in the literature [14,43]. Table 1 provides a list of review documents (published after 2010) on thermal comfort models and overheating evaluation methods.

In general, there is a substantial need for a comprehensive review (i.e., thermal comfort models, indices, and criteria) of the time-integrated discomfort evaluation methods focusing on overheating discomfort (we refer to as "time-integrated overheating evaluation methods"). Therefore, as members of the International Energy Agency (IEA) EBC Annex 80 – "Resilient cooling of buildings" project, we initiated this research to address the abovementioned knowledge gap. This paper provides a valuable contribution to the new body of knowledge from an international perspective. Our paper provides insights for overheating assessments in temperate oceanic climate (Cfb) according to Köppen climate classification. Such climate is particularly dominant in Western Europe such as in Brussels that had 2381 Heating Degree Days (HDD) and 38 Cooling Degree Days (CDD) in 2018 [44]. As can be seen in Fig. 1, in addition to many European cities, there are major cities like Auckland, Bogotá, Nairobi, Vancouver, and Santa Fe with similar climate in other regions around the world. Therefore, our study will be useful to improve the understanding of overheating and allow the comparison of overheating evaluation methods globally. We should mention that provisions are required to the generalizability of the results to hot climates.

The main objectives of this paper are, (i) identifying the thermal comfort models suggested for the buildings with and without air-conditioning and (ii) exploring the time-integrated overheating indices and criteria. This paper attempts to respond to the following research questions:

1) What are the thermal comfort models suggested in the standards for the buildings with and without air-conditioning?
2) What are the indices suggested to calculate the time-integrated overheating in residential buildings?
3) What are the threshold values and criteria to limit overheating in buildings?

Our review critically analyzes 95 recent and long-standing documents, including 11 international standards, namely, EN 15251, EN 16798, ISO 7730, ISO 17772, ASHRAE 55 (2017), ASHRAE 55 (2020), CIBSE Guide A (2006), CIBSE TM52, CIBSE Guide A (2015), CIBSE TM59, and Passive House (see Appendix A). We also review five national building codes based on the Energy Performance of Building Directive (EPBD) in Belgium, France, Germany, the UK, and the Netherlands. We highlight the main differences between the new and old versions of the standards. This paper is the first of its kind that focused on the overheating calculation methods specific for residential buildings in temperate climates and thoroughly examined the EPBD regulations. More importantly, we addressed new measures in addition to those in Carlucci et al. [29], such as *all hours or occupied hours in a time span, normalization to occupied hours, short-term criteria, and long-term criteria.* Our

extensive review summarizes the vast body of standards and literature in a brief, informative, and content-rich document that allows the comparison of the most critical thermal comfort models and time-integrated overheating indices.

This paper provides strong support for decision-making for building professionals and designers to assess indoor overheating during the early design stages. Implementing the findings may yield comfort benefits in the buildings. The study outcomes also provide practical recommendations for policymakers to improve the regional and national overheating evaluation methods towards climate change proof residential buildings. The paper is structured as follows. Section 2 presents the review methodology including the boundary conditions, target documents, and measures. Section 3 describes the results of the review on the time-integrated overheating evaluation methods including thermal comfort models (Section 3.1) followed by analyzing overheating/discomfort indices and criteria in international standards (Section 3.2.1), national building codes based on the EPBD (Section 3.2.2) and scientific literature (Section 3.2.3). Section 4 discusses the key findings and Section 5 concludes the paper.

2. Review methodology

This paper performs a review of the time-integrated overheating evaluation methods. As shown in Fig. 2, towards providing a thorough and in-depth review, we narrow our scope by setting boundary conditions on the building type and the climate. Based on the boundary conditions, we then select the target documents to be reviewed. Finally, the review is conducted by applying some existing and newly defined evaluation measures.

2.1. Boundary conditions

As the first boundary condition, we restrict our focus on the methods that are specified for residential buildings. It is since, (i) the majority of European heterogeneous building stock is composed of residential buildings; the share of residential buildings is between 60 and 89% over the Member States and the UK according to the European Union (EU) buildings Factsheet, (ii) people spend most of their time at homes, in particular elderly people who are more vulnerable to overheating exposure [42], and (iii) the overheating during the sleeping time at homes was reported as a major risk to the public health [41,45].

Another boundary condition is that we focus on the methods proposed for temperate climates. In temperate climates, the focus of building thermal design is mainly on preserving the heat during the winter. Such a design concept prevents the dissipation of internal heat loads in buildings and makes them more vulnerable to overheating issues during the hot summertime [27,46,47]. Therefore, we decided to condemn the policy, legislative, and scientific drivers of overheating in temperate climates as one of the high-risk areas and provide recommendations for future improvements.

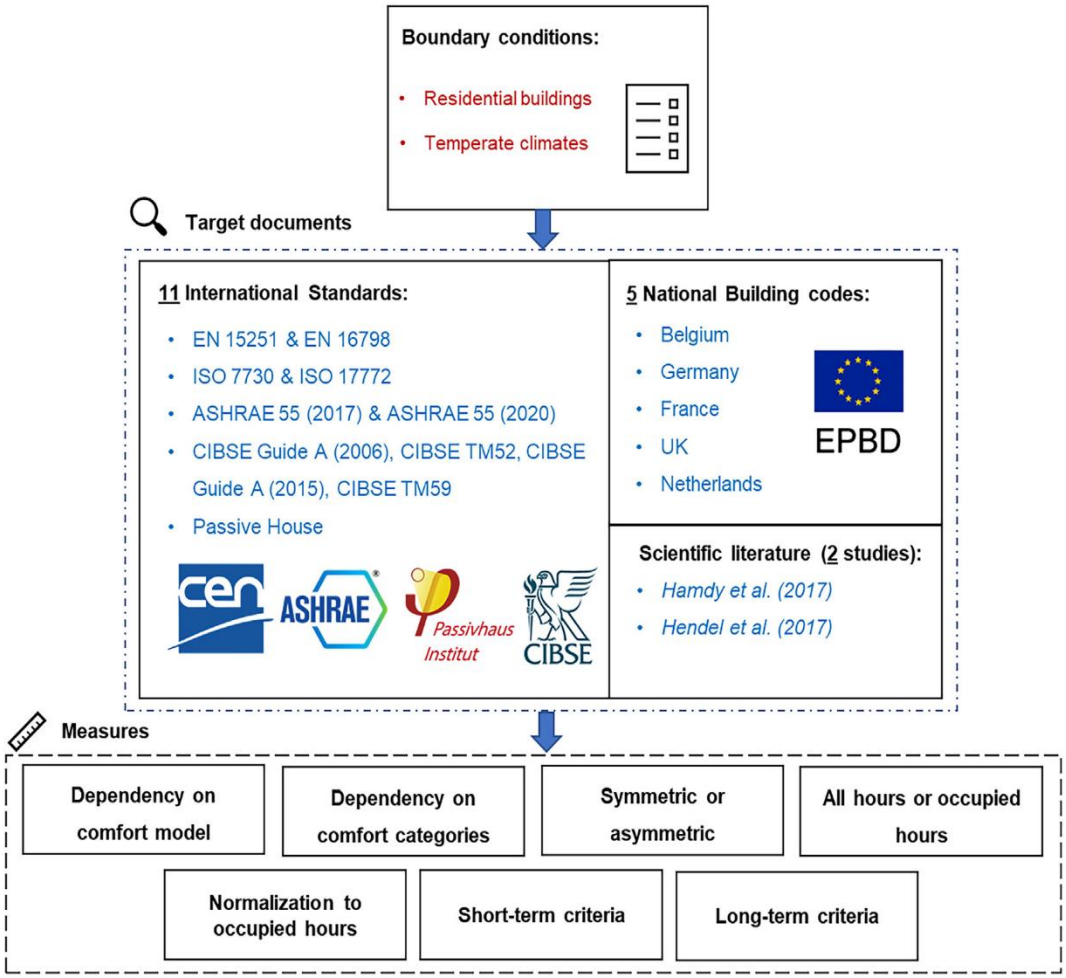

Fig. 2. Study Conceptual Framework (SCF).

2.2. Target documents

The target documents in this paper can be divided into, international standards, EPBD regulatory documents, and scientific literature. For the international standards, we select EN 15251, EN 16798, ISO 7730, ISO 17772, ASHRAE 55 (2017), ASHRAE 55 (2020), CIBSE Guide A (2006), CIBSE TM52, CIBSE Guide A (2015), CIBSE TM59, and Passive House standards. These mostly cited standards [14,48–56] are extensively included within the building construction and renovation policies in temperate climates of Europe. Afterwards, we review the EPBD regulatory documents in Belgium, France, Germany, the UK, and the Netherlands. These five countries form the largest portion of the temperate regions in Europe and together entail 47% of the total population and 30% of the total area considering the EU and the UK [44,57,58]. The EPBD regulations are obligatory and thus play a main role in defining the energy efficiency and thermal comfort in buildings at the European level. Finally, we select two state-of-the-art methods found in the literature [14,43]. For this aim, we set two inclusion criteria: (i) introduced and implemented in residential buildings and (ii) applied and validated for temperate climates in Europe. We exclude the methods in the literature that are previously reviewed by Carlucci et al. [29] or aimed at quantifying the instant overheating phenomena. Our aim is not to provide an extensive review of the methods introduced in the scientific literature, but we intend to take the initiative and provide the basis for future studies in this context. We should also mention that there is no strict limitation on the publication period for the additional documents that form the references of this paper, but priority has been given to recent publications to address the state-of-the-art research.

2.3. Measures

The review is carried out by describing the thermal comfort models for air-conditioned and non-air-conditioned buildings along with a critical analysis of the time-integrated overheating indices and criteria (i.e., threshold values). A previous study by Carlucci et al. [29] defined some measures such as *dependency on a comfort model, dependency on comfort categories, symmetric/asymmetric, and inclusion/exclusion of comfort thresholds*. We further elaborate on those terms and add some new measures including *all hours or occupied hours in a time span, normalization to occupied hours, short-term criteria, and long-term criteria*. Therefore, this study analyzes the time-integrated overheating evaluation methods based on the following measures,

- **Dependency on comfort model:** this measure shows that whether the method is dependent on a comfort model. If yes, which of the static and adaptive comfort models are implemented.
- **Dependency on comfort categories:** this measure shows whether the underlying thermal comfort model of a method relies on comfort categories. Dependency on comfort categories generates discontinuity at the boundaries of the categories and results in different values for overheating if the category changes.
- **Symmetric or asymmetric:** the symmetric methods combine the overheating and overcooling discomfort in a single value, whereas the asymmetric methods only consider overheating discomfort. The symmetric methods do not imply whether the building is unable to suppress overheating or overcooling discomfort.
- **All hours or occupied hours in a time span:** this measure shows whether the method considers all hours or only the occupied hours during a specific time period. The inclusion of unoccupied hours in the calculations raises the uncertainty by including the needless effect of comfort conditions where there is no one in the building.
- **Normalization to occupied hours:** we assess if the index of a method is normalized to the occupied hours. The normalized indices allow the comparison of the buildings with different occupancy profiles.
- **Short-term criteria:** short-term criteria are threshold values on an hourly, daily, or weekly basis to limit the overheating during the heatwave events.
- **Long-term criteria:** long-term criteria are threshold values to limit the extensive overheating during monthly, seasonal, or annual periods.

3. Results

3.1. Thermal comfort models

The evaluation of overheating risks in buildings requires the determination of an appropriate thermal comfort model. The thermal comfort in buildings can be divided into two major models: (a) static and (b) adaptive.

The static comfort models in the comfort standards are mainly based on Fanger's widely accepted *PMV/PPD* model (*PMV* = Predicted Mean Vote and *PPD* = Predicted Percentage Dissatisfied) developed in the 1970 s where six major parameters (air temperature, radiant temperature, relative humidity, metabolic rate, air velocity, and clothing factor) intervene. Those parameters were estimated or measured to evaluate the thermal sensation of the human body in a thermally symmetrical environment while calculating the *PMV* index.

The static comfort models suggested in the *PMV/PPD* ranges in EN, ISO, ASHRAE, and CIBSE standards are listed in Table 2. The EN and ISO standards provide the *PMV/PPD* ranges in different categories reflecting the level of occupant expectation and the indoor environmental quality (see Appendix B), whereas ASHRAE (for the static model) and CIBSE standards do not categorize the thermal environments or as CIBSE TM52 refer to a single category.

Since it is difficult to measure the *PMV* accurately due to high uncertainty in measuring and predicting all comfort parameters, in particular clothing factor and metabolic rate, some standards translate the *PMV/PPD* ranges into the operative temperature scales with some assumptions. As listed in Table 3, EN 15251, EN 16798, ISO 17772, and CIBSE TM52 (following EN 15251) translate the *PMV/PPD* ranges into the operative temperature scales with assumptions on relative humidity (=50% for EN 15251, =40% and = 60% for heating and cooling seasons in EN 16,798 and ISO 17772, respectively), air velocity (<0.1 m/s), metabolic rate (1.2 met), and clothing factor (0.5 clo for summer and 1 clo for winter). Following the same suit, CIBSE Guide A (2006) prescribes the translated operative temperature scales (for $|PMV| < 0,25$) considering the clothing factor between 0.25 and 1.2 clo, metabolic rate between 0.9 and 1.8 met, relative humidity (=50%), and air velocity (<0.15 m/s) over different zones. It is also recommended that the operative temperature ranges can be extended by 1 °C at each end if a PMV of ±0.5 is acceptable. CIBSE Guide A (2015), however, translates the range of $|PMV| < 0,5$ into the operative temperature scales by assumptions on clothing factor between 0.5 and 1.2 clo, metabolic rate between 0.9 and 1.5 met, relative humidity (=50%), and air velocity (<0.15 m/s) over different zones. It also allows fluctuations up to 1 °C at the boundaries. The translated operative temperature thresholds are associated with boundary conditions, therefore are not applicable to the spaces where: (i) the air velocity threshold is violated by the operation of ceiling fan etc., (ii) the relative humidity exceeds the threshold value by humidifying activities such as cooking in the kitchen or drying

Table 2
The PMV/PPD static comfort limits in EN, ISO, ASHRAE, and CIBSE. The presented limits are suggested for residential buildings.

Standard	Operation type*	Category	*PPD* [%] & *PMV* [-]
EN 15,251 (2007)	Mechanically heated and cooled	I	$PPD\% < 6, -0.2 < PMV < +0.2$
		II	$PPD\% < 10, -0.5 < PMV < +0.5$
		III	$PPD\% < 15, -0.7 < PMV < +0.7$
		IV	$PPD\% > 15, PMV < -0.7 or PMV > +0.7$
EN 16798 (2019) & ISO 17772 (2017)	Mechanically heated and cooled	I	$PPD\% < 6, -0.2 < PMV < +0.2$
		II	$PPD\% < 10, -0.5 < PMV < +0.5$
		III	$PPD\% < 15, -0.7 < PMV < +0.7$
		IV	$PPD\% < 25, -1.0 < PMV < +1.0$
ISO 7730 (2005)	All	I	$PPD\% < 6, -0.2 < PMV < +0.2$
		II	$PPD\% < 10, -0.5 < PMV < +0.5$
		III	$PPD\% < 15, -0.7 < PMV < +0.7$
ASHRAE 55 (2017) & ASHRAE 55 (2020)	All	–	$PPD\% < 10, -0.5 < PMV < +0.5$
CIBSE Guide A (2006)	Air-conditioned	–	$PPD\% < 10, -0.25 < PMV < +0.25 PPD\% < 10, -0.5 < PMV < +0.5$(if acceptable)
CIBSE TM52	Mechanically conditioned and naturally conditioned	II (EN 15251)	$PPD\% < 10, -0.5 < PMV < +0.5$
CIBSE Guide A (2015)	Air-conditioned	–	$PPD\% < 10, -0.5 < PMV < +0.5$

*the terminology of each standard is used to name the operation type.

Table 3
The fixed maximum temperature limits in EN, ISO, CIBSE, and Passive House standards. The presented limits are suggested for residential buildings.

Standard	Operation type*	Zone/category	Maximum operative temperature[°C]
EN 15251 (2007)	Mechanically heated and cooled	Living spaces (bedrooms, living rooms, kitchens, etc.)/I	25.5
		Living spaces (bedrooms, living rooms, kitchens, etc.)/II	26
		Living spaces (bedrooms, living rooms, kitchens, etc.)/III	27
EN 16798 (2019) & ISO 17772 (2017)	Mechanically heated and cooled	Living spaces (bedrooms, living rooms, kitchens, etc.)/I	25.5
		Living spaces (bedrooms, living rooms, kitchens, etc.)/II	26
		Living spaces (bedrooms, living rooms, kitchens, etc.)/III	27
		Living spaces (bedrooms, living rooms, kitchens, etc.)/IV	28
CIBSE Guide A (2006)	Air-conditioned	Living rooms, bedrooms, halls, stairs, landings	25 (+1°C if PMV = 0.5 is acceptable)
		Kitchen, toilets	23 (+1°C if PMV = 0.5 is acceptable)
	Free-running	Living room	28
		Bedrooms	26
CIBSE TM52	Mechanically conditioned and naturally conditioned	All/II (EN 15251)	26
CIBSE Guide A (2015)	Air-conditioned	Bathrooms, bedrooms, halls, stairs, landings, kitchen, toilet/II (EN 15251)	26 (+1°C)
	Free-running	Bedrooms	26
CIBSE TM59	Mechanically ventilated	All	26
	Naturally ventilated	Bedrooms	26
Passive House	Without active cooling or with passive cooling	All zones	25

*the terminology of each standard is used to name the operation type.

the clothes inside, and (iii) occupants have activities or clothing that are out-of-range considering the assumptions on metabolic rate and clothing factor.

Differently, some standards provide the static comfort model by proposing fixed temperature thresholds. As indicated in Table 3, CIBSE Guide A (2006) specifies a threshold value denoted as "*benchmark peak temperature*" for free-running buildings which is 3 °C higher than the summer comfort temperature. It defines 25 °C as the summer comfort temperature in the living room at which few people feel uncomfortable. For bedrooms, however, it assigns the summer comfort temperature of 23 °C since sleep may be impaired above 24 °C. Accordingly, the prescribed benchmark peak temperature is 28 °C for the living room and 26 °C for the bedrooms. CIBSE Guide A (2015) and CIBSE TM59 also commonly suggest 26 °C for the bedrooms in naturally ventilated buildings. The Passive House standard sets a maximum threshold value of 25 °C for all living areas in buildings without active cooling or with passive cooling. In the case of fixed temperature thresholds, the effect of other comfort parameters such as relative humidity, clothing factor, metabolic rate, and air velocity is totally neglected in defining comfort.

The adaptive comfort model has been developed during the last twenty years based on a group of field studies taken in real buildings to represent the actual conditions. The adaptive comfort theory accepts that the occupants can adapt to the surrounding thermal environment because of the behavioural, physiological, and psychological actions. Therefore, it suggests reaching a temperature that is positively correlated to a reference outdoor air temperature. And not anymore, a unique and ideal temperature.

To derive the reference outdoor air temperature, EN and ISO standards recommend the "*exponentially weighted running mean outdoor temperature*" (T_{rmo}). The T_{rmo} [A°C] can be calculated by,

Table 4
The adaptive comfort boundaries in EN, ISO, ASHRAE, and CIBSE.

Standard	Operation type*	Category or acceptability	Upper limit[°C]	Lower limit[°C]	T_{rmo} or T_{pmo} applicability range[°C]
EN 15251 (2007)	Without mechanical heating and cooling	I	$0.33T_{rmo}+18.8+2$	$0.33T_{rmo}+18.8-2$	10–30
		II	$0.33T_{rmo}+18.8+3$	$0.33T_{rmo}+18.8-3$	10–30
		III	$0.33T_{rmo}+18.8+4$	$0.33T_{rmo}+18.8-4$	10–30
EN 16798 (2019) & ISO 17772 (2017)	Without mechanical heating and cooling	I	$0.33T_{rmo}+18.8+2$	$0.33T_{rmo}+18.8-3$	10–30
		II	$0.33T_{rmo}+18.8+3$	$0.33T_{rmo}+18.8-4$	10–30
		III	$0.33T_{rmo}+18.8+4$	$0.33T_{rmo}+18.8-5$	10–30
ASHRAE 55 (2017)	Naturally conditioned	80% Acceptability	$0.31T_{pmo}+21.3$	$0.31T_{pmo}+14.3$	10–33.5
		90% Acceptability	$0.31T_{pmo}+20.3$	$0.31T_{pmo}+15.3$	10–33.5
CIBSE TM52	Free-running	II (EN 15251)	$0.33T_{rmo}+18.8+3$	$0.33T_{rmo}+18.8-3$	10–30
CIBSE Guide A (2015) & CIBSE TM59	Naturally ventilated	II (EN 15251)	$0.33T_{rmo}+18.8+3$	$0.33T_{rmo}+18.8-3$	10–30

*the terminology of each standard is used to name the operation type.

$$T_{rmo}=(1-\alpha).\{T_{ed-1}+\alpha T_{ed-2}+\alpha^2 T_{ed-3+\cdots}\} \quad (1)$$

$$T_{rmo}=1/3.8.\{T_{ed-1}+0.8T_{ed-2}+0.6T_{ed-3+}0.5T_{ed-4}+0.4T_{ed-5}+0.3T_{ed-6}+0.2T_{ed-7}\} \quad (2)$$

Where α is the weighting factor between 0 and 1 (recommended value is 0.8), T_{ed-i} is the daily mean outdoor air temperature for i-th previous day [°C]. ASHRAE 55, however, introduces the *"prevailing mean outdoor air temperature"* (T_{pmo}) as the reference outdoor air temperature. The T_{pmo}[°C] is the arithmetic mean of the mean daily outdoor air temperature of all sequential days (no less than seven and no more than 30 days). ASHRAE 55 also permits the use of the weighting method (see Equation (1)) in a way that the weight applied to a day is between 0.6 and 0.9 of that applied to the subsequent day. The formulas to derive the adaptive comfort ranges based on the reference outdoor air temperature and corresponding applicable ranges are summarized in Table 4.

Similar to the static model, EN 15251, EN 16798, and ISO 17772 standards provide category-based adaptive temperature ranges for buildings without mechanical heating and cooling systems. There are some differences in defining the adaptive thermal comfort in EN 15251 compared to EN 16798 and ISO 17772. First, in EN 15251, it is allowable to install mechanical cooling systems; nevertheless, they should not be in operation. EN 15251 also allows mechanical ventilation, which provides unconditioned air during the summer as well as other low-energy technologies such as shutters, night ventilation, fans, etc. However, this information is excluded in EN 16798 and ISO 17772. Second, the metabolic rate of nearly sedentary activity (1–1.3 met) is assumed in EN 15251, while the metabolic rate of sedentary activity (1.2 met) is assumed in EN 16798 and ISO 17772. Third, EN 16798 and ISO 17772 has a more extensive range of adaptive comfort boundaries since the lower temperature limits are 1 °C below the equivalent temperature limits in EN 15251.

ASHRAE 55 (2017) and ASHRAE 55 (2020) recommend the adaptive comfort model (see Table 4) for naturally ventilated buildings in two applicability ranges (see Appendix B). However, there are two changes between both versions: (i) ASHRAE 55 (2020) allows for the installation of a mechanical cooling system as long as the system is not in operation which is not permitted in ASHRAE 55 (2017) and (ii) the range of metabolic rate assumption is extended from 1.0 to 1.3 met in ASHRAE 55 (2017) to 1.0–1.5 met in ASHRAE 55 (2020). The main strength of the ASHRAE 55 standard is its regular revisions and updates (every 3–4 years during the last decade) reflecting the new results from the field studies contributing to the accuracy of its adaptive comfort model [59].

CIBSE TM52, CIBSE Guide A (2015) (not for bedrooms), and CIBSE TM59 (not for bedrooms) commonly adopt Category II of the adaptive comfort model in EN 15251 for free-running and naturally ventilated buildings. It should be mentioned that the ISO 7730, CIBSE Guide A (2006), and Passive House standards do not contain or refer to any adaptive comfort model.

3.2. Time-integrated overheating/discomfort indices and criteria

3.2.1. International standards

3.2.1.1. EN 15251 and EN 16798. Identical time-integrated discomfort indices are established in EN 15251 (Annex F) and EN 16798 (Annex D of Part 2). Three indices are defined, namely Percentage of Occupied hours Outside the Range ($\%POhOR_{EN}$), Degree hours (Dh_{EN}), and *PPD* weighted (*PPDw*).

The $\%POhOR_{EN}$ index shows the percentage of occupied hours when the *PMV* or indoor operative temperature is outside the comfort ranges related to the selected comfort category. It is thus applicable to both static and adaptive comfort models (see Section 3.1). The $\%POhOR_{EN}$ can be calculated using a binary weighting factor (wf_i) that is zero during the time within the comfort ranges and is one during the out-of-range conditions. It is a straightforward index that shows the frequency of discomfort, however, (i) it does not quantify the intensity of discomfort, (ii) it is category-based, it introduces discontinuities at the boundaries of categories that do not correlate to the physics and physiology [29], and (iii) it is symmetric without distinguishing between the overheating and overcooling discomfort.

Provisions are made to restrict the short-term and long-term overheating by defining acceptable deviation thresholds for the $\%POhOR_{EN}$ index during weekly, monthly, and annual periods. EN 15251 recommends the acceptable deviation of 3% (5%) based on working hours (total hours) during daily, weekly, monthly, and yearly periods. Whereas EN 16798-2 suggests 20% (50% as a strict criterion) weekly, 12% (25% as a strict criterion) monthly and 3% (6% as a strict criterion) annual acceptable deviations during the occupied hours. The latter sets criteria for how long short-term and long-term consecutive periods of out-of-range temperatures can be accepted.

The Dh_{EN} index quantifies the time in which the indoor operative temperature exceeds the specified comfort range weighted by a factor (wf_i). The wf_i is a module of the difference between the indoor operative temperature and the lower or upper limit of the comfort range. To calculate the Dh_{EN}, If the comfort ranges are specified in terms of *PMV*, the ranges should be translated into operative temperature scales by assumptions on clothing factor, metabolic rate, relative humidity, and air velocity. Both static and adaptive comfort models are applicable (see Section 3.1). The Dh_{EN} is an asymmetric

Table 5
Summary of overheating/discomfort evaluation methods in EN, ISO, ASHRAE, CIBSE, and Passive House standards.

Standard	Index	Equation	Measures						
			Static (S) / Adaptive (A)	Category-based	Symmetric (S) / Asymmetric (A)	All hours (A) / occupied hours (O)	Normalized to occupied hours	Short-term criterion	Long-term criterion
EN 15251&EN 16798&ISO 17772	Percentage of Occupied hours Outside the Range ($\%POhOR_{EN\ \&\ ISO\ 17772,op}$)	$\%POhOR_{EN\&ISO17772,op} = \frac{\sum_{i=1}^{occupiedhours} wf_i}{\sum_{i=1}^{occ.h} h_i} \times 100$ $where \begin{cases} wf_i = 1; T_{op,i} < T_{op,i,lower} or T_{op,i} > T_{op,i,upper} \\ wf_i = 0; T_{op,i,lower} < T_{op,i} < T_{op,i,upper} \end{cases}$	*S & A*	✓	*S*	**O**	✓	✓(not in EN 15251)	✓
	Percentage of Occupied hours Outside the Range ($\%POhOR_{EN\ \&\ ISO\ 17772,PMV}$)	$\%POhOR_{EN\&ISO17772,PMV} = \frac{\sum_{i=1}^{occupiedhours} wf_i}{\sum_{i=1}^{occupiedhours} h_i} \times 100$ $where \begin{cases} wf_i = 1; PMV_i < PMV_{lower} or PMV_i > PMV_{upper} \\ wf_i = 0; PMV_{lower} < PMV_i < PMV_{upper} \end{cases}$	*S*	✓	*S*	**O**	✓	✓(not in EN 15251)	✓
	Degree hours*($Dh_{EN\ \&\ ISO\ 17772,overh}$)	$Dh_{EN\&ISO17772,overh} = \sum_{i-1}^{occupiedhours} (wf_i \times h_i)$ $where \begin{cases} wf_i = T_{op,i} - T_{op,i,upper}; T_{op,i} > T_{op,i,upper} \\ wf_i = 0; T_{op,i} < T_{i,upper} \end{cases}$	*S & A*	✓	*A*	**O**			
	Weighted PPD* ($PPDw_{EN\ \&\ ISO\ 17772,overh}$)	$PPDw_{EN\&ISO17772,overh} = \sum_{i-1}^{occupiedhours} (wf_i \times h_i)$ $where \begin{cases} wf_i = \frac{PPD_i}{PPD_{upper}}; PMV_i > PMV_{upper} \\ wf_i = 0; PMV_i < PMV_{upper} \end{cases}$	*S*	✓	*A*	**O**			
ISO 7730	Percentage of Occupied hours Outside the Range ($\%POhOR_{ISO\ 7730,op}$)	$\%POhOR_{ISO7730,op} = \frac{\sum_{i=1}^{occupiedhours} wf_i}{\sum_{i=1}^{occupiedhours} h_i} \times 100$ $where \begin{cases} wf_i = 1; T_{op,i} < T_{op,i,lower} or T_{op,i} > T_{op,i,upper} \\ wf_i = 0; T_{op,i,lower} < T_{op,i} < T_{op,i,upper} \end{cases}$	*S*	✓	*S*	**O**	✓		
	Percentage of Occupied hours Outside the Range ($\%POhOR_{ISO\ 7730,PMV}$)	$\%POhOR_{ISO7730,PMV} = \frac{\sum_{i=1}^{occupiedhours} wf_i}{\sum_{i=1}^{occupiedhours} h_i} \times 100$ $where \begin{cases} wf_i = 1; PMV_i < PMV_{lower} or PMV_i > PMV_{upper} \\ wf_i = 0; PMV_{lower} < PMV_i < PMV_{upper} \end{cases}$	*S*	✓	*S*	**O**	✓		
	Degree hours*($Dh_{ISO\ 7730,overh}$)	$Dh_{ISO7730,overh} = \sum_{i-1}^{occupiedhours} (wf_i \times h_i)$ $where \begin{cases} wf_i = 1 + \frlac{\lvert T_{op,i} - T_{op,upper} \rvert}{\lvert T_{Comfort} - T_{op,upper} \rvert}; T_{op,i} > T_{op,i,upper} \\ wf_i = 0; T_{op,i} < T_{op,upper} \end{cases}$	*S*	✓	*A*	**O**			
	Weighted PPD* ($PPDw_{ISO\ 7730,overh}$)	$PPDw_{ISO7730,overh} = \sum_{i-1}^{occupiedhours} (wf_i \times h_i)$ $where \begin{cases} wf_i = \frac{PPD_i}{PPD_{upper}}; PMV_i > PMV_{upper} \\ wf_i = 0; PMV_i < PMV_{upper} \end{cases}$	*S*	✓	*A*	**O**			
	Averaged PPD ($AvgPPD$)	$AvgPPD = \frac{\sum_{i=1}^{occupiedhours} PPD_i}{\sum_{i=1}^{occupiedhours} h_i}$			*S*	**O**	✓		
	PPD over time(PPDOT)	$PPDOT = \sum_{i-1}^{occupiedhours} PPD_i$			*S*	**O**			
ASHRAE 55 (2017) & ASHRAE 55 (2020)	Exceedance Hours(EH_{op})	$EH_{op} = \sum_{i-1}^{occupiedhours} H_{disc}$ $where \begin{cases} H_{disc} = 1; T_{op,i} < T_{op,i,lower} or T_{op,i} > T_{op,i,upper} \\ H_{disc} = 0; T_{op,i,lower} < T_{op,i} < T_{op,i,upper} \end{cases}$	*A*	✓	*S*	**O**			
	Exceedance Hours(EH_{PMV})	$EH_{PMV} = \sum_{i-1}^{occupiedhours} H_{disc}$ $where \begin{cases} H_{disc} = 1; \lvert PMV_i \rvert > 0.5 \\ H_{disc} = 0; \lvert PMV_i \rvert < 0.5 \end{cases}$	*S*		*S*	**O**			
	Weighted Exceedance Hours(WEH_{op})	$WEH_{op} = \sum_{i-1}^{occupiedhours} \Big((T_{op,i} - T_{op,i,upper}) \times H_{disc,warm} + (T_{op,i,lower} - T_{op,i}) \times H_{disc,cold} \Big)$ $where \begin{cases} H_{disc,warm} = 1; T_{op,i} > T_{op,i,upper} \\ H_{disc,cold} = 1; T_{op,i} < T_{op,i,lower} \\ H_{disc,cold} = H_{disc,warm} = 0; T_{op,i,lower} < T_{op,i} < T_{op,i,lower} \end{cases}$	*A*	✓	*S*	**O**			
	Weighted Exceedance Hours(WEH_{PMV})	$WEH_{PMV} = \sum_{i-1}^{occupiedhours} (\lvert PMV_i \rvert - 0.5) \times H_{disc}$ $where \begin{cases} H_{disc} = 1; \lvert PMV_i \rvert > 0.5 \\ H_{disc} = 0; \lvert PMV_i \rvert < 0.5 \end{cases}$	*S*		*S*	**O**			

Table 5 (*continued*)

Standard	Index	Equation	Measures						
			Static (S) / Adaptive (A)	Category-based	Symmetric (S) / Asymmetric (A)	All hours (A) / occupied hours (O)	Normalized to occupied hours	Short-term criterion	Long-term criterion
CIBSE Guide A (2006) & CIBSE Guide A (2015)	Percentage of Occupied hours Outside the Range ($POhOR_{CIBSEGuideA,op}$)	$\%POhOR_{CIBSEGuideA,op} = \frac{\sum_{i=1}^{occupiedhours} wf_i \cdot h_i}{\sum_{i=1}^{occupiedhours} h_i} \times 100$ $where \begin{cases} wf_i = 1; T_{op,i} > T_{op,upper} \\ wf_i = 0; T_{op,i} < T_{op,upper} \end{cases}$	*S*		*A*	**O**	✓		✓
CIBSE Guide A (2015)	Percentage of Occupied hours Outside the Range ($POhOR_{CIBSEGuideA,PMV}$)	$\%POhOR_{CIBSEGuideA,PMV} = \frac{\sum_{i=1}^{occupiedhours} wf_i \cdot h_i}{\sum_{i=1}^{occupiedhours} h_i} \times 100$ $where \begin{cases} wf_i = 1; PMV_i > 0.5 \\ wf_i = 0; PMV_i < 0.5 \end{cases}$	*S*		*A*	**O**	✓		✓
CIBSE TM52[1]	Hours of Exceedance (He) "Criterion (1)"	$\%He = \frac{\sum_{i=1}^{occupiedhours} wf_i \cdot h_i}{\sum_{i=1}^{occupiedhours} h_i} \times 100$ $where \begin{cases} wf_i = 1; T_{op,i} - T_{op,i,upper} > 1^{\circ}C(adaptivemodel) and 0^{\circ}C(staticmodel) \\ wf_i = 0; T_{op,i} - T_{op,i,upper} < 1^{\circ}C(adaptivemodel) and 0^{\circ}C(staticmodel) \end{cases}$	*A*		*A*	**O**	✓		✓
	Daily Weighted Exceedance (W_e) "Criterion (2)"	$W_e = \sum_{i-1}^{occupiedhours,daily} (wf_i \times h_i)$ $where \begin{cases} wf_i = T_{op,i} - T_{op,i,upper}; T_{op,i} > T_{op,i,upper} \\ wf_i = 0; T_{op,i} < T_{op,i,upper} \end{cases}$	*A*		*A*	**O**		✓	
	Upper Limit Temperature (T_{upp}) "Criterion (3)"[2]	$T_{op,i} - T_{op,i,upper} \not> 4^{\circ}C$	*A*		*A*	**O**			
CIBSE TM59	Percentage of Sleeping hours Outside the Range($\%PShOR_{CIBSE\ TM59}$)	$\%PShOR_{CIBSETM59} = \frac{\sum_{d-1}^{d-365} \sum_{10pm}^{7am} wf_i \cdot h_i}{\sum_{d-1}^{d-365} \sum_{10pm}^{7am} h_i} \times 100$ $where \begin{cases} wf_i = 1; T_{op,i} > 26^{\circ}C \\ wf_i = 0; T_{op,i} < 26^{\circ}C \end{cases}$	*S*		*A*	**O**	✓		✓
Passive House	Percentage of hours Outside the Range ($\%PhOR$)	$\%PhOR = \frac{\sum_{i=1}^{annualhours} wf_i \cdot h_i}{\sum_{i=1}^{annualhours} h_i} \times 100$ $where \begin{cases} wf_i = 1; T_{a,i} > 25^{\circ}C \\ wf_i = 0; T_{a,i} < 25^{\circ}C \end{cases}$	*S*		*A*	*A*			✓

* It also has an overcooling specific discomfort index. [1] All three criteria must be taken together, and compliance is achieved by passing any two of them. [2] It is not intended for overheating evaluation over time and is a "right now" and "right here" criterion.

index that should be calculated for overheating period and overcooling period separately. The limit of this index is that, (i) it is category-based, (ii) it lacks the normalization to the number of occupied hours, this makes the comparison of buildings with different occupancy profiles troublesome, (iii) it is only based on the operative temperature and neglects the effects of personal factors (metabolic rate and clothing factor) and environmental parameters (relative humidity and air velocity) in the determination of thermal comfort, and (iv) no maximum thresholds are prescribed to limit the short-term and long-term overheating.

The *PPDw* index is proposed only for the *PMV/PPD* model (see Section 3.1). It assumes the time (occupied hours) in which the *PMV* exceeds the comfort boundaries is weighted with a weighting factor (wf_i). The wfi is a module that quantifies the measured or simulated *PPD* over the corresponding *PPD* limit. Similar to the *Dh* index, the assessment of overheating and overcooling discomfort is separated, making it asymmetric. The *PPDw* allows the consideration of the hourly percentage of dissatisfaction accumulation over time. However, the limitation of this index is that (i) it is only based on *PMV/PPD* model, (ii) it is not normalized to the number of occupied hours, (iii) no maximum thresholds are prescribed, and (iv) it is category-based. The time-integrated overheating/discomfort indices in EN 15251 and EN 16798 standards are listed in Table 5.

3.2.1.2. ISO 7730 and ISO 17772. For time-integrated thermal discomfort assessment, ISO 7730 provides five methods, namely Percentage of Occupied hours Outside the Range ($\%POhOR_{ISO\ 7730}$), Degree hours ($Dh_{ISO\ 7730}$), *PPD* weighted ($PPDw_{ISO\ 7730}$), average *PPD* (*avgPPD*), and *PPD* Over Time (*PPDOT*) criteria.

The $\%POhOR_{ISO\ 7730}$ is similar to $\%POhOR_{EN}$. The $Dh_{ISO\ 7730}$ index however has some differences compared to the Dh_{EN} index related to the calculation of weighting factor (wf_i). Based on the ISO 7730 formulation of wf_i, it penalizes the recurrence of exceedance and weights the discomfort by the amplitude of the comfort range (i.e., it results in higher discomfort for the same exceedance where the stricter thermal conditions are assigned such as in Category I) [29]. The only difference in the calculation of the $PPDw_{ISO\ 7730}$ compared to the $PPDw_{EN}$ is that the ISO 7730 method increases the value of the $PPDw_{ISO\ 7730}$ even if the *PMV* is equal to the upper or lower limit of the comfort range.

The average *PPD* (*avgPPD*) index shows the average *PPD* calculated over the occupied hours. The *avgPPD* does not rely on the limits of any specific comfort category; it quantifies the accumulation of discomfort over time without the problem of discontinuity at the boundaries of the comfort categories. It is a useful index to compare and optimize the thermal comfort performance of different buildings independent of the occupancy expectation levels. However, (i) this index is only applicable to the *PMV/PPD* model and (ii) it is symmetric.

The *PPD* Over Time (*PPDOT*) consists of the summation of all *PPDs* during the occupied hours. The *PPDOT* does not depend on the limits of comfort categories. This index has some disadvantages such as, (i) it is only based on the *PMV/PPD* model, (ii) it is symmetric, and (iii) it is not normalized to the occupied hours. ISO 7730 includes threshold limits on none of the above indices to limit the short-term and long-term overheating/discomfort.

All the recommendations on time-integrated overheating/discomfort indices and criteria in ISO 17772 are identical to that of EN 16,798 (see Section 3.2.1.1). Table 5 summarizes all the time-integrated overheating/discomfort indices in ISO 7730 and ISO 17772.

3.2.1.3. ASHRAE 55 (2017) and ASHRAE (2020). For time-integrated thermal discomfort assessment, both versions of ASHRAE 55 provide two principal and identical indices in informative Appendix L, namely, Exceedance Hours (*EH*) and Weighted Exceedance Hours (*WEH*). Moreover, some metrics such as expected number of episodes, rate of change exceedance, and local discomfort exceedances within a time period of interest exist in ASHRAE 55; however, the calculation methods are not presented.

The *EH* index shows the number of occupied exceedance hours when the *PMV* or the operative temperature is outside the static and adaptive comfort zone boundaries (see Section 3.1). The *EH* can be calculated using a binary weighting factor (H_{disc}). The H_{disc} is one during the out-of-range conditions and is zero during the time within the comfort zone. The *EH* index quantifies the general discomfort without distinguishing between overheating and overcooling discomfort. This index can be criticized since, (i) it does not include the intensity of discomfort, (ii) no limits are prescribed as the acceptable deviation of the *EH* index, (iii) it is symmetric, (iv) it is category-based if adaptive comfort model is applied, and (v) it is not normalized to the occupied hours.

The *WEH* quantifies the severity of discomfort during the occupied hours which is analogous to the Degree hours index described in Section 3.2.1.1. To calculate the *WEH*, ASHRAE 55 provides a formula based on the *PMV* for the static comfort model and a formula based on operative temperature for the adaptive comfort model. The *WEH* based on the *PMV* is the summation of the $|PMV|$-0.5 weighted by the binary weighting factor (H_{disc}) during the occupied hours. And, the *WEH* based on the operative temperature consists of the summation of two factors during the occupied hours, (i) the difference between the operative temperature and minimum adaptive comfort threshold (if $T_{op,i} < T_{op,i,lower}$) weighted by the H_{disc} and (ii) the difference between the operative temperature and maximum adaptive comfort threshold (if $T_{op,i} > T_{op,i,upper}$) weighted by the H_{disc}. The *WEH* has some limitations since, (i) it is not normalized to the occupied hours, (ii) no limits are prescribed as the acceptable deviation of the *WEH* index, (iii) it is symmetric, and (iv) it is category-based if the adaptive comfort model is applied. All the time-integrated discomfort indices in ASHRAE 55 are summarized in Table 5.

3.2.1.4. CIBSE Guide A (2006), CIBSE TM52, CIBSE Guide A (2015), and CIBSE TM59.

CIBSE Guide A (2006). CIBSE Guide A (2006) defines Percentage of Occupied hours Outside the Range ($\%POhOR_{CIBSE\ Guide\ A,op}$) as a single index to assess the time-integrated overheating, only for naturally ventilated buildings. The $\%POhOR_{CIBSE\ Guide\ A,op}$ index consists of the summation of all occupied hours exceeding the fixed maximum operative temperature limit (i.e., benchmark peak temperature) (see Section 3.1) over the total number of occupied hours. The $\%POhOR_{CIBSE\ Guide\ A,op}$ is an asymmetric index focusing on overheating discomfort. According to CIBSE Guide A (2006) overheating criteria, the $\%POhOR_{CIBSE\ Guide\ A,op}$ should not exceed more than 1% during the occupied hours year-round in the bedrooms and living room in dwellings. It can be criticized since, (i) it is based on operative temperature and does not take into account the influential personal factors (i.e., clothing factor and metabolic rate) and environmental parameters (i.e., relative humidity and air velocity) in the determination of thermal comfort, (ii) only a long-term annual overheating criterion is prescribed, and (iii) it does not consider the intensity of overheating.

CIBSE TM52. CIBSE TM52 introduces a method consisting of three criteria for time-integrated overheating evaluation, only for free-running buildings. The criterion (1) and criterion (2) are concerned with time-integrated overheating; however, the criterion (3) is a "right now" and "right here" approach to limit the instant overheating in buildings. The three criteria, taken together, provide a holistic approach to overheating risk assessment and a zone or building that fails any two of the three criteria is classed as overheated.

Criterion (1) uses the Hours of exceedance ($He_{CIBSE\ TM52}$) index that is the percentage of hours when the indoor operative temperature is exceeding the maximum temperature limit (see Section 3.1) by one or greater than one degree K over the total number of occupied hours. The $He_{CIBSE\ TM52}$ should be calculated during a typical non-heating season (1 May to 30 September). According to its definition, the $He_{CIBSE\ TM52}$ is an asymmetric index focusing on overheating discomfort during the summertime. For $He_{CIBSE\ TM52}$ index, CIBSE TM52 allows for a maximum deviation of 3% during the occupied hours. The criterion (1) can be criticized since, (i) it neglects the intensity of overheating, (ii) it is specific for the period from May to September, it excludes the potential overheating events that can happen in other periods [60], (iii) it is based on operative temperature and does not take into account the influential personal factors (i.e., clothing factor and metabolic rate) and environmental parameters (i.e., relative humidity and air velocity) in the determination of thermal comfort, and (iv) it sets a criterion only to limit long-term overheating.

In criterion (2), CIBSE TM52 defines the daily Weighted exceedance (W_e) index to deal with the severity of overheating within any one day. The W_e index resembles the Degree hours metric quantifying the number of exceedance hours weighted by a factor (WF). The WF is the module of the difference between the operative temperature and maximum temperature limit (see Section 3.1) (similar to the wf_i in the calculation of Dh). The W_e is an asymmetric index concerned with overheating discomfort. CIBSE TM52 allows the W_e index to reach equal to or<6 in any one day setting a short-term (daily) criterion to limit the overheating during the heatwave events. The criterion (2) has some limitations such as, (i) it is not normalized to the occupied hours, (ii) it is only based on the operative temperature and does not take into account the influential personal factors (i.e., clothing factor and metabolic rate) and environmental parameters (i.e., relative humidity and air velocity) in the determination of thermal comfort, and (iii) it sets a criterion only to limit short-term overheating.

The criterion (3) is simply setting an absolute maximum value, in which the indoor operative temperature shall not exceed by 4 K. It sets a limit beyond the adaptation actions will be insufficient to restore the personal comfort aiming at covering the extreme heatwave events in the future climates. This asymmetric criterion does not account for the accumulation of overheating over time. It can be criticized because it only assigns a threshold value for operative temperature but not for other environmental parameters such as relative humidity and air velocity.

CIBSE Guide A (2015). For time-integrated overheating evaluation in mechanically cooled and naturally ventilated buildings, CIBSE Guide A (2015) uses the Percentage of Occupied hours Outside the Range ($\%POhOR_{CIBSE\ Guide\ A}$) index that shows the exceedance hours over the upper comfort threshold represented in *PMV* or operative temperature scale (see Section 3.1). It is thus an asymmetric index. To limit the long-term overheating, the calculated $\%POhOR_{CIBSE\ Guide\ A}$ should not exceed the maximum limit of comfort for more than 3% during the occupied hours. We can criticize this index since, (i) it only considers the frequency of overheating, and (ii) only a long-term (annual) threshold value is prescribed.

For time-integrated overheating evaluation in free-running buildings, CIBSE Guide A (2015) follows the three criteria that are previously described in CIBSE TM52.

CIBSE TM59. The criteria for homes predominantly mechanically conditioned follows the CIBSE fixed temperature test which states that all zones should not exceed an operative temperature of 26 °C for more than 3% of the annual occupied hours.

For homes predominantly naturally ventilated, CIBSE TM59 requires compliance based on passing the two following criteria, (i) in living rooms, kitchens, and bedrooms, the criterion (1) of CIBSE TM52 should be respected, and (ii) in the bedrooms during the sleeping hours from 10 pm to 7 am, the operative temperature should not exceed 26 °C for more than 1% of total annual hours. The latter leads to the definition of an asymmetric index called Percentage of Sleeping hours Outside the Range ($\%PShOR_{CIBSE\ TM59}$).

Overall, following the two above criteria of CIBSE TM59 has some limitations, (i) both criteria are based on operative temperature and do not take into account the influential personal factors (i.e., clothing factor and metabolic rate) and environmental parameters (i.e., relative humidity and air velocity) in the determination of thermal comfort, and, (ii) both criteria neglects the intensity of overheating, (iii) both criteria set threshold values to limit long-term overheating (i.e., seasonal and annual), (iv) the $\%PShOR_{CIBSE\ TM59}$ index makes a rough estimation regarding the sleeping time and duration, and (v) the threshold selection for $\%PShOR_{CIBSE\ TM59}$ is contentious, for instance, World Health Organization (WHO) suggests a threshold of 24 °C for bedrooms.

All the time-integrated overheating indices in CIBSE norms are summarized in Table 5.

3.2.1.5. Passive house. Regarding the time-integrated overheating evaluation in buildings without active cooling or with passive cooling, the Passive House standard contains an asymmetric index called the Percentage of hours outside the range (*%PhOR*) (see Table 5). The *%PhOR* index shows the percentage of hours (occupied and unoccupied) exceeding the pre-defined threshold value of 25 °C. For a building to comply with the requirements of Passive House standard, the *%PhOR* should not exceed 10% throughout the year for all living areas. This approach can be criticized since, (i) it only sets a long-term (annual) overheating criterion, (ii) it is only based on the operative temperature and does not take into account the influential personal factors (i.e., clothing factor and metabolic rate) and environmental parameters (i.e., relative humidity and air velocity) in the determination of thermal comfort, (iii) it includes the discomfort hours during the unoccupied periods, and (iv) it neglects the intensity of overheating.

3.2.2. National building codes based on the Energy Performance of building Directive (EPBD)

In 2012, the European Commission established a legislative framework that includes the Energy Performance of Building Directive (EPBD) [61]. The EPBD aims at promoting energy efficiency and decarbonized building stock by 2050 s as well as creating a stable environment in buildings. General regulations made by EPBD must be interpreted and implemented by the Member States in the national building regulations. In this section, we investigate the overheating evaluation methods in the national building codes of Belgium, Germany, France, the UK, and the Netherlands.

Belgium. In Belgium, each region (i.e., Brussels, Flanders, and Wallonia) is in charge of implementing the EPBD individually. The region of Brussels *"Région de Bruxelles-Capitale"* decided to adopt the criteria defined by Passive House standard for the residential buildings that are new or assimilated to new [62,63]. The overheating compliance in Brussels is achieved by not exceeding 25 °C by 5% during the occupied hours throughout the year. On the other hand, the regions of Wallonia *"Région wallonne"* and Flanders *"Vlaams Gewest"* establish a quasi-steady-state heat balance method derived from ISO 13790 for new and renovated residential buildings without active cooling [64]. Accordingly, a time-integrated overheating index I_{overh} [Kh] is introduced which sums up the normalized monthly excess of heat gains $Q_{excess\ norm,\ m}$ [Kh] in relation to the indoor set-point temperature,

$$I_{overh} = \sum_{m=1}^{12} Q_{excessnorm,m}[Kh] \quad (3)$$

$$Q_{excessnorm,m} = \frac{\left(1 - \eta_{util,overh,m}\right) \cdot Q_{g,overh,m}}{H_{T,overh} + H_{V,overh,m}} \cdot \frac{1000}{3,6} \quad (4)$$

Where $\eta_{util,overh,m}$ [-] is the utilization factor depending on the ratio between the monthly heat loss and heat gain, $Q_{g,overh,m}$ is the monthly solar and internal heat gains [MJ], $H_{T,overh}$ is the conduction heat transfer coefficient [W/K], and $H_{V,overh,m}$ is the monthly ventilation heat transfer coefficient [W/K]. An acceptable range of ($1000\ Kh < I_{overh} < 6500\ Kh$) over the annual period is recommended.

This method has some disadvantages such as, (i) it is calculated by heat balance equations, it does not take into account the influential personal factors (i.e., clothing factor and metabolic rate) and environmental parameters (i.e., air temperature, radiant temperature, relative humidity, and air velocity) in the determination of thermal comfort, (ii) it neglects the adaptation actions taken by the occupants, (iii) it is based on monthly averages of heat loads and thus not able to track short-term heatwave events, (iv) it is not normalized to the occupied hours, (v) it takes into account the unoccupied hours, and (vi) only a long-term (annual) threshold value is suggested.

Germany. In Germany, the national building code based on the EPBD was translated into DIN 4108 [65] to define the overheating calculation method and criteria for buildings with and without passive cooling. The method in DIN 4108 consists of two criteria for overheating protection, and compliance is achieved through passing one of them.

Criterion (1) is a simplified method with standardized boundary conditions. Accordingly, the summer overheating protection must be ensured in the most critical room in terms of solar and endogenous heat gains. For this aim, the solar transmittance S_{vorh} [-] index is proposed which is the function of room size, window size, window type, and solar shading devices,

$$S_{vorh} = \frac{\sum_j (A_{W,j} \times g_{tot,j})}{A_G} \quad (5)$$

Where $A_{W,j}$ is window area of zone j [m^2], $g_{tot,j}$ is total energy transmittance of the glazing including sun protection of zone j [-], and A_G is the net floor area [m^2]. The calculated S_{vorh} [-] should not exceed the maximum value of solar transmittance S_{zul} [-] calculated by,

$$S_{zul} = S_1 + S_2 + S_3 + S_4 + S_5 + S_6 \quad (6)$$

$$S_{vorh} \leq S_{zul} \quad (7)$$

The S_1 to S_6 are proportional solar input parameters given in DIN 4108 as following,

S_1 for night ventilation type, climatic region, and usage
S_2 for the base area correction factor
S_3 for solar protection of glass
S_4 for window pitch
S_5 for window orientation
S_6 for passive cooling

Criterion (1) directly concerns with the solar gains through the glazing areas. It has some limitations such as, (i) it excludes the internal gains induced by the equipment and occupants, (ii) It does not accumulate the overheating discomfort over time (i.e., time-independent), (iii) it neglects the influential personal factors (i.e., clothing factor and metabolic rate) and environmental parameters (i.e., air temperature, radiant temperature, relative humidity, and air velocity) in the determination of thermal comfort, and (iv) the notion of occupant adaptation is undermined. It was shown by Krone et al. [66] that only compliance to the first criterion does not guarantee a comfortable thermal environment in buildings.

In Criterion (2), the symmetric Degree hours (*Dh*) index should be calculated for the most critical room of the building via the simulation. The reference temperature for the *Dh* calculation depends on climatic region (i.e, 25 °C for "Klimaregion A" Rostock, 26 °C for "Klimaregion B" Potsdam, and 27 °C for "Klimaregion C" Mannheim). The compliance is required on the value of *Dh* which should not exceed the specified value of 1200 Kh during the year. Criterion (2) overcomes the first two limitations of the criterion (1), however, (i) it still neglects the influential personal factors (i.e., clothing factor and metabolic rate) and environmental parameters (i.e., relative humidity and air velocity) in the determination of thermal comfort, (ii) it is not providing any criteria to limit the short-term overheating events, and (iii) it does not allow for occupant adaptation, and (iv) it is not normalized to the occupied hours.

France. In France, the EPBD is translated into a standard called *"Règlementation Environnementale"* (RE2020) [67]. The RE2020 uses the Degree hours (*Dh*) index to evaluate the discomfort during the summer in new residential buildings. The reference temperature for the *Dh* calculation should be derived from the maximum temperature limits of the Category II of the adaptive comfort model in EN 15251 (see Section 3.2.1.1). According to RE2020, the symmetric *Dh* should be evaluated for a weather scenario similar to that of 2003 heatwaves. The RE2020 sets a maximum threshold of 1250 Kh corresponding to a period of 25 days when the indoor operative temperature is continuously at 30 °C during the day and 28 °C at night. The criterion is applied to all climate zones across the country. Also, RE2020 sets the lowest threshold at 350 Kh beyond the penalties that will be applied in the calculation of energy performance.

The time-integrated overheating evaluation method in RE2020 has some limitations: (i) it imposes criterion only to limit the long-term overheating, (ii) it is based on operative temperature neglecting the personal factors (i.e., clothing factor and metabolic rate) and environmental parameters (i.e., air temperature, relative humidity, and air velocity) in the determination of thermal comfort, (iii) even though France consists of the regions with very different climatic characterization (the Oceanic to the Mediterranean), the same comfort zone boundaries are suggested, and (iv) it is not normalized to the occupied hours.

Uk. In the UK, the overheating evaluation method according to the EPBD is included within the Approved Document L1A for new dwellings [68] (there is no method for overheating evaluation in existing dwellings in Approved Document L1B [69]). The Approved Document L1A is updated regularly by the DCLG. It worth mentioning that the DCLG review report in 2014 did not present any proposed actions to the overheating calculation method [70]. Hence, the latest edition of the Approved Document L1A in 2013 with amendments in 2016 follows the same method and criteria of its previous edition published in 2013 [71] which enforces the SAP [72] to set the overheating criteria. We should also mention that according to [73], a recent draft of a consultation document on changes to Approved Document L by the UK government, there is an ongoing effort to replace the SAP methodology with more recent methodologies proposed for residential buildings such as the one in CIBSE TM59.

The SAP provides the overheating assessment method in Appendix P requiring the compliance to "overheating check". The SAP procedure introduces an internal threshold index ($T_{threshold}$) for overheating evaluation during the summer. The $T_{threshold}$ [°C] is used to estimate the likelihood of high internal temperatures. The $T_{threshold}$ is calculated by summing up the mean external temperature during the summer month T_e^{summer}, the ratio of monthly

heat gains and heat losses, and an increment related to the building thermal mass ΔT_{mass}. The formula to calculate the T_e^{summer} is,

$$T_{threshold} = T_e^{summer} + G/H + T_{mass} \quad (8)$$

Where G is the sum of monthly solar and internal gains [W] and H is the monthly ventilation and fabric heat loss [W]. The ΔT_{mass} can be calculated by,

$$\Delta T_{mass} = 2.0 - 0.007 \times TMP if TMP < 285 \quad (9)$$

Where TMP is the thermal mass parameter for building envelope components [kJ/m^{2}K]. According to the SAP, the $T_{threshold}$ should be calculated for June, July and August. The level of likelihood of high internal temperatures during hot weather conditions is listed in Table 6. The disadvantages of the SAP method are, (i) it is specific for summertime overheating evaluation, (ii) It does not consider the influential personal factors (i.e., metabolic rate and clothing) and environmental parameters (i.e., radiant temperature, relative humidity, and air velocity) in the determination of thermal comfort, (iii) it neglects the occupant adaptation, (iv) it takes into account the unoccupied hours, (v) it is not normalized to the occupied hours, and (v) only the long-term (i.e., monthly) overheating is characterized. It was shown by McLeod and Swainson [27] that in complex building typologies that are inherently vulnerable to overheating such as a single-sided dwelling with high internal gains in the urban context, the steady-state procedure of SAP is not reliable in validating the design performance.

Netherlands. In the Netherlands, the EPBD was interpreted and included within NTA 8800 [74]. NTA 8800 contains the methods and criteria for overheating assessment in Almost Energy Neutral Buildings (BENG) (in Dutch *"Bijna Energie Neutrale Gebouwen"*). The overheating evaluation requires the determination of dimensionless index TO_{juli}. The value is calculated depending on the façade surface per orientation. For instance, a terraced house has two outcomes, and a corner house has three outcomes. The TO_{juli} should be calculated for the month of July using the formula below,

$$TO_{juli,or,zi} = \frac{(Q_{C,nd,juli,or,zi} - Q_{C,HP,juli,or,zi}) \times 1000}{(H_{C,D,juli,or,zi} + H_{gr,an,juli,or,zi} + H_{C,ve,juli,or,zi}) \times h_{juli}} \quad (10)$$

Where $Q_{C,nd,juli,or,zi}$ is cooling demand for orientation or in zone zi [kWh], $Q_{C,HP,juli,or,zi}$ is the extracted energy from the cooling unit by the booster heat pump for orientation or in zone zi [kWh], $H_{C,D,juli,or,zi}$ is direct heat transfer coefficient by transmission between the heated space and the outdoor air except for the ground floor for orientation or in zone zi [W/K], $H_{gr,an,juli,or,zi}$ is the direct heat transfer coefficient by the transmission for building elements in thermal contact with the ground for orientation or in zone zi [W/K], $H_{C,ve,juli,or,zi}$ is the direct heat transfer coefficient through ventilation for orientation or in zone zi [W/K], and h_{juli} is the total time over the month of July. The TO_{juli} is an indication number derived from the average cooling requirement of the entire building. A maximum limit value of 1 is specified for the TO_{juli}. It should be mentioned that If the building is provided with cooling, there is then no need for the calculation of the TO_{juli}.

NTA 8800 also provides a method based on the weighted limit temperature (*GTO*) to calculate the risk of overheating more accurately when the TO_{juli} slightly exceeds its limit value. In the *GTO* method, the hours of when the actual or calculated *PMV* exceeds the limit value of +0.5 are weighted proportional to the *PPD* as shown in Table 7. The formula to calculate the *GTO* is,

$$GTO = \sum Wf_{i,NTA8800} \quad (11)$$

The *GTO* is calculated for the living areas with a threshold value of 450. The method provided by NTA 8800 for overheating evaluation has some limitations such as, (i) by only using the TO_{juli} index it is not possible to track and limit the short-term (i.e., hourly, daily, and weekly) overheating events, (ii) TO_{juli} takes into account the unoccupied hours, (iii) the TO_{juli} is calculated by heat balance equations, it does not take into account the influential personal factors (i.e., clothing factor and metabolic rate) and environmental parameters (i.e., air temperature, radiant temperature, relative humidity, and air velocity) in the determination of thermal comfort, (iv) the *GTO* index is not normalized to the occupied hours, (v) both methods are specific for the long-term overheating during the month of July and neglect overheating occurrence in other months even during the summer, and (vi) both mehtods exclude the occupant adaptation notion.

In Table 8, we summarize the overheating assessment methods in EPBD regulatory documents in five abovementioned countries with some key information. The occupant adaptation to the ther-

Table 6
The threshold temperature ranges corresponding to the likelihood of high internal temperatures.

$T_{threshold}$[°C]	Likelihood of high internal temperatures during hot weather
> 23.5°C	Not significant
22°C – 23.5°C	Slight
22°C – 23.5°C	Medium
> 23.5°C	High

Table 7
The $Wf_{i,\ NTA\ 8800}$ corresponding to the PMV and PPD values for the calculation of GTO.

PMV [-]	PPD [%]	$Wf_{i,\ NTA\ 8800}$ [-]
0	5	0
0,5	10	1,0
0,7	15	1,5
1,0	26	2,6

Table 8
Summary of overheating assessment methods in national building codes based on the EPBD.

Country	Regulatory documents based on EPBD	Static model	Adaptive model	Based on heat balance	Based on comfort parameters	Multizonal or single-zone approach
Belgium (Brussels)	Réglementation sur la Performance Energêtique des Bâtiments (PEB Brussels)	✓			✓	Multi-zonal
Belgium (Wallonia and Flanders)	Réglementation sur la Performance Energêtique des Bâtiments (PEB Wallonia)Energieprestatie en Binnenklimaat (EPB Flanders)	✓		✓		Single zone
Germany	Deutsches Institut für Normung (DIN) 4108-6	✓		✓(Criterion 1)	✓(Criterion 2)	Multi-zonal
France	Règlementation Environnementale(RE2020)		✓		✓	Multi-zonal
UK	Approved Document L1A	✓		✓		Single zone
Netherlands	Netherlands Technical Agreement (NTA) 8800	✓		✓(Criterion 1)	✓(Criterion 2)	Multi-zonal

mal environment is largely neglected in the reviewed building codes except for France. The building codes in Belgium (Wallonia and Flanders), Germany, the UK, and the Netherlands have only or at least one criterion based on the steady-state heat balance equations. The heat balance approach does not fully represent the occupant thermal sensation which is determined by six major parameters (i.e., air temperature, radiant temperature, relative humidity, air velocity, metabolic rate, and clothing,). The evidence of compliance in Belgium (Wallonia and Flanders) and the UK is provided by considering the heat balance of the whole building as a single zone. This approach prevents the identification of the most critical zones within a building and includes the effect of trivial zones (e.g., attic, warehouse etc.) in overheating assessments.

3.2.3. Scientific literature

3.2.3.1. Indoor overheating Degree (IOD), Ambient Warmness Degree (AWD), and overheating escalation factor ($\alpha_{IOD/AWD}$). Hamdy et al. [14] proposed a climate change-sensitive overheating evaluation method based on three indices called Indoor Overheating Degree (*IOD*), Ambient Warmness Degree (*AWD*), and Overheating Escalation Factor). The Indoor Overheating Degree (*IOD*) index is the summation of the temperature difference between the indoor operative temperature and a preferred comfort temperature averaged over the total number of zonal occupied hours. In other words, it incorporates the frequency by integrating the intensity over the occupied hours in different building zones. The *IOD* [°C] can be calculated by,

$$IOD = \frac{\sum_{z=1}^{Z}\sum_{i=1}^{N_{occ}(z)}\left[\left(T_{op,i,z} - T_{op,i,z,upper}\right)^{+} \times h_{i,z}\right]}{\sum_{z=1}^{Z}\sum_{i=1}^{N_{occ}(z)} h_{i,z}} \quad (12)$$

Where z is zone counter, i is occupied hour counter, Z is total building zones, N_{occ} (z) is the total number of zonal occupied hours, $T_{op,i,z}$ is the indoor operative temperature in zone z at time step i [°C], $T_{op,i,z,upper}$ is the maximum comfort threshold in zone z at time step i [°C], and *h* is the time step [1 h]. Only positive values of the difference $(T_{op,i,z}\text{-}T_{op,i,z,upper})^{+}$ are considered. Both static and adaptive temperature limits can be used as comfort thresholds. The authors recommended two types of comfort models, (i) the static comfort model of CIBSE Guide A [75], and (ii) the adaptive comfort models by [76,77].

The *IOD* is an asymmetric and multi-zonal index that allows for considering the occupancy profiles of each zone, separately. Such an approach makes it easier to use zone-specific comfort models to reflect the occupant behaviour and adaptation opportunities within a zone. However, it is only based on operative temperature and thus neglects the influential personal factors (i.e., clothing factor and metabolic rate) and environmental parameters (i.e., relative humidity and air velocity) in the determination of thermal comfort. Another drawback is that there are no threshold values recommended to limit the short-term and long-term overheating.

The second index is the Ambient Warmness Degree (AWD_b) that shows the severity of outdoor thermal conditions. The AWD_b [°C] consists of averaging the cooling Degree hours over the total number of building occupied hours,

$$AWD_b = \frac{\sum_{i=1}^{N}\left[\left(T_{a,i} - T_b\right)^{+} \times h_i\right]}{\sum_{i=1}^{N} h} \quad (13)$$

Where T_a is the outdoor dry-bulb air temperature [°C], T_b is the base temperature [°C], N is the total number of occupied hours when $T_{a,i} \geqslant T_b$. The choice of base temperature is context-specific depending on the climate and building characteristics (e.g., age, construction type, occupancy type etc.). The T_b of 18 °C is suggested by the authors appropriate for temperate climates. The main drawback regarding the calculation of the AWD_b index is that it does not include the effect of solar radiation on outdoor thermal severity. It raises uncertainty since the same AWD_b values result in two climates that have the same outdoor air temperature profiles but with different profiles of solar irradiance.

The AWD_b was established and normalized by building occupied hours to be coupled with the *IOD* index through the dimensionless third index ($\alpha_{IOD/AWD}$). Basically, the ($\alpha_{IOD/AWD}$) index couples the indoor and outdoor thermal environments showing the sensitivity of a building to outdoor thermal stress. The ($\alpha_{IOD/AWD}$) [-] is calculated by,

$$\alpha_{IOD/AWD} = \frac{IOD}{AWD_b} \quad (14)$$

$\alpha_{IOD/AWD} > 1$ means that the building is unable to suppress outdoor thermal stress. $\alpha_{IOD/AWD} < 1$ means that the building can suppress some of the outdoor thermal stress. It is suggested that the *IOD* and AWD_b indices be calculated under multiple contemporary and future weather scenarios. Afterwards, by assuming a linear regression between both parameters, one can calculate the $\alpha_{IOD/AWD}$. In this case, the $\alpha_{IOD/AWD}$ shows the sensitivity of a building to the progressive rise in outdoor air temperature due to the impact of climate change.

3.2.3.2. Heat exposure index (HEI). Hendel et al. [43] suggested Heat Exposure Index (*HEI*) which is a cumulative index focusing on overheating discomfort during sleeping time. The *HEI* index is resulted by integrating the difference between the indoor air temperature $T_{a,i}$ [°C] and a set-point temperature $T_{set\text{-}point}$ [°C] over the sleeping time (11 pm-7am). Only the positive values of the difference $(T_{a,i} - T_{set\text{-}point})^{+}$ is considered. The *HEI* is calculated by,

$$HEI = \int_{11pm}^{7am} \left(T_{a,i} - T_{set-point}\right)^{+}_{T_{a,i} \geq T_{set\ point}} dt \quad (15)$$

A set-point temperature of 26 °C is suggested by the authors based on the work of [78]. The *HEI* is an asymmetric index focusing on overheating during sleeping time. It incorporates the intensity and the length of time when the indoor air temperature is exceeding the set-point temperature. The calculation method is not index-specific, and other indices such as the Universal Thermal Climate Index (*UTCI*) can be used instead of air temperature.

The *HEI* index has some limitations such as: (i) it makes a rough estimation regarding the sleeping time and duration, (ii) the threshold selection is contentious considering the threshold of 24 °C suggested by WHO for bedrooms, (iii) it neglects the day-time overheating periods (iv) it does not consider other influential environmental parameters (i.e., radiant temperature, relative humidity, air velocity) and personal factors (i.e., metabolic rate and clothing factor) in the determination of thermal comfort, (v) it is not normalized to the occupied hours, and (vi) it is specific for short-term overheating evaluation and no threshold value is prescribed.

4. Discussion

This paper initially reviews the static and adaptive comfort models suggested by different standards to derive the threshold values in *PMV/PPD* or operative temperature scales to be implemented in the overheating/discomfort calculations. Numerous studies discussed the applicability of the static and adaptive comfort models in buildings with different cooling modes (air-conditioned, non-air-conditioned, and mixed-mode) [79–87]. It was reported in [88–90] that the static comfort models are performing well in air-conditioned spaces. However, such models overestimate the discomfort and technically predict more heating or cooling loads to provide a thermally comfortable environment [91]. On the other hand, the adaptive comfort models are

suggested for naturally ventilated ones where the occupants have more connection to the outdoor environment [33,92]. Although there is still no consensus on the choice of comfort model in mixed-mode buildings, it was shown by Parkinson et al. [92] that these buildings are more closely aligned to naturally ventilated buildings in determining the neutral temperatures, and thus the adaptive comfort model is preferable.

It worth mentioning that the concept of occupant adaptation is more elaborated in thermally asymmetrical environments through the thermoregulatory models of the human body. Cheng et al. [34] reviewed such models and grouped them into physiological and psychological models. Thermoregulatory models deal with the whole or segmented human body interaction with the adjacent portion of the thermal environment. Therefore, they require detailed modelling (via numerical methods such as Computational Fluid Dynamics) or extensive point-in-space measurements to accurately reveal the distribution of environmental parameters (e.g., relative humidity, temperature etc.) through space. Two main factors are preventing their widespread, (i) there is a complexity associated with the detailed analysis of the thermal environment and segmentation of the human body, and (ii) they are environment-specific (i.e., sensitive to hot or cold environments) and thus not comprehensive enough [34].

Despite all the research into thermal comfort, there are still questions about the appropriateness of using it as a framework for assessing the issues such as morbidity and mortality [93,94]. The findings of [93] outline the lack of sufficient and direct epidemiological evidence concerning the adverse health effects due to high-temperature exposure. Whereas the mortality rate is increased during extreme events (e.g., heat waves) are positively associated with mortality. In addition, there is a lack of true understanding in the existing thermal comfort models when it comes to the most vulnerable population like the elderly people [42,95]. As a result, further research into thermal comfort and its effect on morbidity and mortality rate is required to solidify our understanding and instigate the policy changes.

Our review on time-integrated overheating indices led to significant findings in this context. We found that some indices such as Percentage of Occupied hours Outside the Range ($\%POhOR_{EN\ \&\ ISO\ 17772}$ and $\%POhOR_{ISO\ 7730}$), Averaged PPD (*AvgPPD*), *PPD* Over Time (*PPDOT*), Exceedance Hours (*EH*), and Weighted Exceedance Hours (*WEH*) are symmetric. It means that they synthesize both overheating discomfort and overcooling discomfort in a single value. Although such indices provide useful insights on general comfort conditions in buildings, but they mix up two very different aspects of thermal comfort. Therefore, the sole use of these indices does not imply whether the building can overcome the overheating discomfort or overcooling discomfort.

Through our review, we attempt to distinguish between the criteria prescribed to limit short-term (hourly, daily, and weekly) and long-term (monthly, seasonal, and annual) overheating or discomfort. To ensure an acceptable thermal environment throughout the year, it is necessary to consider both short-term and long-term overheating criteria in building design and retrofit strategies. A building only complying with the short-term overheating criteria will be able to suppress the short-term heatwave events but might not be able to maintain an acceptable thermal environment in the long-term (i.e., design for heatwave). Differently, a building complying with only the long-term overheating criteria will be able to maintain an acceptable thermal environment in the long-term but might not be able to withstand short-term heatwave events (i.e., design for climate).

Surprisingly, none of the previous studies as well as ASHRAE 55 and ISO 7730 standards prescribed any threshold values. EN 15251 and Passive House standards provide a single value to limit only the long-term annual discomfort and overheating, respectively. While more recent standards such as EN 16798 and ISO 17772 prescribe values to limit short-term (only weekly) and long-term (monthly and annual) discomfort in buildings. The CIBSE TM52 provides criteria to limit seasonal overheating as well as daily and instant overheating in naturally ventilated buildings. The EPBD regulations define annual criterion in Belgium, annual and seasonal criteria in Germany, annual criterion in France, monthly criterion in the UK, and monthly (only for July) criterion in the Netherlands. It shows that setting comprehensive criteria to fully limit short-term and long-term overheating (or discomfort) phenomena was not so far that much of interest in building design and operation policies.

The building experts commonly agree that there is a growing risk of overheating in buildings due to the impact of climate change. The only study that examined overheating in the context of climate change is the work of Hamdy et al. [14] (see Section 3.2.3.1). They introduced the overheating escalation factor ($\alpha_{IOD/AWD}$) index by coupling the Indoor Overheating (*IOD*) and Ambient Warmness Degree (*AWD*) indices. The $_{IOD/AWD}$ seems a promising index by integrating the rate of change in intensity and frequency of overheating in relation to the progressive rise in outdoor air temperature. In other words, it estimates the thermal sensitivity of a building to the overheating impact of climate change. A reliable value calculated for the $_{IOD/AWD}$ index allows the building designer to simply predict the evolution of overheating risks without requiring a whole building thermal modelling. It is also a useful index to compare the effectiveness of different active and passive cooling technologies on the thermal resistivity of buildings against the overheating impact of climate change.

5. Conclusion

In this paper, we have comprehensively reviewed the time-integrated overheating/discomfort evaluation methods proposed for residential buildings in temperate climates in terms of thermal comfort models, indices, and criteria. We explored EN 15251, EN 16798, ISO 7730, ISO 17772, ASHRAE 55 (2017), ASHRAE 55 (2020), CIBSE Guide A (2006), CIBSE TM52, CIBSE Guide A (2015), CIBSE TM59, and Passive House standards (Section 3.2.1). We also look into five national building codes based on the Energy Performance of Building Directive (EPBD) in Belgium, France, Germany, the UK, and the Netherlands (Section 3.2.2) as well as two studies found in the scientific literature (Section 3.2.3). To summarize the significant recommendations and future research ideas, we provide the list below:

- In line with most standards, we suggest the static comfort models for air-conditioned buildings (see Table 2 and Table 3) and the adaptive comfort models for non-air-conditioned buildings both in living areas (see Table 4). The provisions are required in the bedrooms not to exceed the maximum threshold of 24 °C suggested by the WHO.
- We recommend using the asymmetric indices to detect the shortcomings of the building thermal design in the matter of overheating and overcooling discomfort, individually.
- We recommend considering full criteria for overheating (i.e., short-term and long-term) in building designs. This prevents overheating not only during a specific period (e.g., heatwave events), but also warm discomfort throughout the year.
- We recommend further exploring and validating the climate change-sensitive method based on three indices *IOD*, *AWD*, and $\alpha_{IOD/AWD}$ by applying them on real multizonal buildings. Future research can also go in the direction of developing climate-change sensitive overheating evaluation methods.

- Future research is suggested to introduce time-integrated overheating indices by including more and more comfort parameters (i.e., relative humidity, metabolic rate, air velocity, air temperature, radiant temperature, and clothing factor). The new indices should be normalized to the occupied hours enabling a fair comparison between the buildings with different occupancy profiles.
- Future research is also recommended to review the overheating evaluation methods in non-residential buildings and in other climatic zones. Future research can analyze overheating calculation methods in the EPBD regulatory documents in other EU Member States.

Last but not least, the study is restricted to two major limitations. First, our review was limited to the methods and criteria proposed for overheating evaluations in residential buildings in temperate climates. Second, our study lacks the comparison and validation of the time-integrated overheating evaluation methods in a quantitative manner.

Declaration of Competing Interest

The authors declare that they have no known competing financial interests or personal relationships that could have appeared to influence the work reported in this paper.

Acknowledgement

This research was funded by the Walloon Region under the call 'Actions de Recherche Concertées 2019 (ARC)' (funding number: ARC 19/23-05) and the project OCCuPANt, on the Impacts Of Climate Change on the indoor environmental and energy PerformAnce of buildiNgs in Belgium during summer. The authors would like to gratefully acknowledge the Walloon Region and the University of Liege for funding. We would like to also acknowledge the Sustainable Building Design (SBD) lab at the Faculty of Applied Sciences at the University of Liege for valuable support during the content analysis and curation of the data. This study is a part of the International Energy Agency (IEA) EBC Annex 80 – "Resilient cooling of buildings" project activities to define resilient cooling in residential buildings.

Appendix A

Table A.1 contains the origin and a short description of the international standards analyzed in this paper. These standards are widely adopted in temperate regions of Europe to assess the indoor environmental quality, in particular thermal comfort during the design and operation of residential buildings.

Appendix B

ISO and EN establish categories to define the static and adaptive comfort models reflecting the level of occupant expectation and indoor environmental quality. Similarly, ASHRAE 55 sets two ranges of acceptability 80% and 90% when defining the adaptive comfort model. The comfort categories are summarized in Table B.1.

Table A1
General description of comfort standards.

Standards	Origin	Description
EN 15251 and EN 16798	European (based in Brussels, Belgium)	EN 15251 was prepared by the Comité Européen de Normalisation (CEN) in 2006 as an essential requirement to EU Directive 2002/91/EC on Energy Performance of Building Directive (EPBD) covering both residential and non-residential buildings. In 2019, the CEN published EN 16798–1 and EN 16798–2, replacing the parts of EN 15,251 related to indoor environmental input parameters including the criteria for thermal comfort. EN 16798–1 contains the thermal comfort models and EN 16798–2 contains the methods for time-integrated discomfort assessment. All the above documents are still in force.
ISO 7730 and ISO 17772	International (based in Geneva, Switzerland)	ISO (International Organization for Standardization) is a worldwide federation of national standard bodies that published ISO 7730 in 2004 containing the ergonomics of thermal environment and still remains in action. The ISO also published ISO 17772-1 in 2017 and ISO 17772-2 in 2018 defining indoor environmental quality and overall energy performance assessments, respectively. ISO 17772-1 contains the thermal comfort models and ISO 17772-2 contains the methods for time-integrated discomfort assessment.
ASHRAE 55 (2017) and ASHRAE 55 (2020)	United States	ASHRAE 55 (2017) was published in 2017 by the American Society of Heating, Ventilation, and Air-conditioning Engineers (ASHRAE) containing thermal environmental conditions for human occupancy in all building types. The ASHRAE 55 specifies the acceptable conditions for thermal environments during the design, operation, and commissioning of occupied spaces. The latest version of ASHRAE 55 was recently published in 2020, with some minor changes superseding the version 2017.
CIBSE Guide A (2006), CIBSE TM52, CIBSE Guide A (2015), and CIBSE TM59	UK	CIBSE Guide A was published in 2006 by Charted Institution of Building Services Engineering (CIBSE), which is a standard setter and authority on building services as the primary UK technical reference for the designers and installers of Heating, Ventilation, and Air-Conditioning (HVAC) systems. Due to the increased risk of overheating, CIBSE formed an overheating task force to define and address the overheating risks in buildings. The outcome of this overheating task force activities was published as CIBSE TM52 in 2013. Subsequently, a newer version of CIBSE Guide A was published in 2015, superseding the version 2006 with some changes and included the overheating criteria developed in CIBSE TM52 for naturally ventilated buildings. CIBSE TM59 was also published in 2017 to provide a design methodology for the assessment of overheating risk in homes. All the above documents, except CIBSE Guide A (2006), are still in force.
Passive House	Germany	The Passive House is a voluntary standard provided by Passive House Institute (PHI) defining complete criteria for indoor environmental quality and energy efficiency in buildings. The Passive House standard aims at achieving a comfortable environment year-round with very low energy consumption. The evidence of compliance with the Passive House standard must be provided through a design tool called *"Passive House Planning Package (PHPP)"*.

Table B1
Comfort category applicability in EN, ISO and ASHRAE.

ISO 7730 Cat.	EN 15251, EN 16798, and ISO 17772 Cat.	Category description
A	I	High level of expectation recommended for spaces occupied by very fragile and sensitive persons with special requirements such as handicapped, sick, very young children and elderly persons
B	II	Normal level of expectation recommended for new buildings and renovations
C	III	Moderate level of expectation suggested for existing buildings
	IV (EN 16798)	Low level of expectation that compromises the comfort but not the occupants' health
	IV (EN 15251)	Out-of-range values acceptable for limited periods
ASHRAE 55 Cat.		
90% acceptability		When higher standard of thermal comfort is desired
80% acceptability		For typical applications

References

[1] J. Garssen, C. Harmsen, J. De Beer. The effect of the summer 2003 heat wave on mortality in the Netherlands, Eurosurveillance 10(7) 2005 13SP 557-14, 10.2807/esm.10.07.00557-en.

[2] M. Perry, N. Golding. Range of environmental temperature conditions in the United Kingdom, Met Office, Department of Transport, Exeter, UK, 2011. [Online]. Available: https://www.onr.org.uk/transport/temperature-range-report.pdf.

[3] P. Pirard et al., Summary of the mortality impact assessment of the 2003 heat wave in France, Eurosurveillance 10 (7) (2005) 7–8.

[4] A.H. Fink, T. Brücher, A. Krüger, G.C. Leckebusch, J.G. Pinto, U. Ulbrich, The 2003 European summer heatwaves and drought–synoptic diagnosis and impacts, Weather 59 (8) (2004) 209–216.

[5] B.E. Johansen, The encyclopedia of global warming science and technology, ABC-CLIO, Santa Barbara, California, 2009.

[6] M. Santamouris, Innovating to zero the building sector in Europe: Minimising the energy consumption, eradication of the energy poverty and mitigating the local climate change, Sol. Energy 128 (2016) 61–94, https://doi.org/10.1016/j.solener.2016.01.021.

[7] M. Santamouris et al., Urban heat island and overheating characteristics in Sydney, Australia. An analysis of multiyear measurements, Sustainability 9 (5) (2017) 712, https://doi.org/10.3390/su9050712.

[8] T. Oke. The heat island of the urban boundary layer: characteristics, causes and effects, in Wind climate in cities, Springer, 1995, pp. 81–107.

[9] K. Oleson, Contrasts between urban and rural climate in CCSM4 CMIP5 climate change scenarios, J. Clim. 25 (5) (2012) 1390–1412, https://doi.org/10.1175/JCLI-D-11-00098.1.

[10] A.-T. Nguyen, S. Reiter, P. Rigo, A review on simulation-based optimization methods applied to building performance analysis, Appl. Energy 113 (2014) 1043–1058, https://doi.org/10.1016/j.apenergy.2013.08.061Get, rights and content.

[11] E. Oikonomou, M. Davies, A. Mavrogianni, P. Biddulph, P. Wilkinson, M. Kolokotroni, Modelling the relative importance of the urban heat island and the thermal quality of dwellings for overheating in London, Build. Environ. 57 (2012) 223–238, https://doi.org/10.1016/j.buildenv.2012.04.002.

[12] A. Mavrogianni, A. Pathan, E. Oikonomou, P. Biddulph, P. Symonds, M. Davies, Inhabitant actions and summer overheating risk in London dwellings, Build. Res. Inf. 45 (1–2) (2017), https://doi.org/10.1080/09613218.2016.1208431.

[13] T. Psomas, P. Heiselberg, K. Duer, E. Bjørn, Overheating risk barriers to energy renovations of single family houses: multicriteria analysis and assessment, Energy Build. 117 (2016) 138–148, https://doi.org/10.1016/j.enbuild.2016.02.031.

[14] M. Hamdy, S. Carlucci, P.-J. Hoes, J.L.M. Hensen, The impact of climate change on the overheating risk in dwellings—A Dutch case study, Build. Environ. 122 (Sep. 2017) 307–323, https://doi.org/10.1016/j.buildenv.2017.06.031.

[15] P. Symonds et al., Overheating in English dwellings: comparing modelled and monitored large-scale datasets, Build. Res. Inf., 45(1–2) 2016 10.1080/09613218.2016.1224675.

[16] L. Lan, K. Tsuzuki, Y. Liu, Z. Lian, Thermal environment and sleep quality: a review, Energy Build. 149 (2017) 101–113, https://doi.org/10.1016/j.enbuild.2017.05.043Get.

[17] H. Hooyberghs, S. Verbeke, D. Lauwaet, H. Costa, G. Floater, K. De Ridder, Influence of climate change on summer cooling costs and heat stress in urban office buildings, Clim. Change 144 (4) (2017) 721–735, https://doi.org/10.1007/s10584-017-2058-1.

[18] HHSRS, "HHSRS Guidance for Landlords and Property-Related Professionals," London, UK, 2006. [Online]. Available: https://www.gov.uk/government/publications/housing-health-and-safety-rating-system-guidance-for-landlords-and-property-related-professionals.

[19] G. Brücker, Vulnerable populations: lessons learnt from the summer 2003 heat waves in Europe, Eurosurveillance 10 (7) (2005) 1–2, https://doi.org/10.2807/esm.10.07.00551-en.

[20] A. Fouillet et al., Excess mortality related to the August 2003 heat wave in France, Int. Arch. Occup. Environ. Health 80 (1) (2006) 16–24, https://doi.org/10.1007/s00420-006-0089-4.

[21] H. Johnson, S. Kovats, G. McGregor, J. Stedman, M. Gibbs, H. Walton, The impact of the 2003 heat wave on daily mortality in England and Wales and the use of rapid weekly mortality estimates, Eurosurveillance 10 (7) (2005) 15–16, https://doi.org/10.2807/esm.10.07.00558-en.

[22] J.-M. Robine, S. L. Cheung, S. Le Roy, H. Van Oyen, F. R. Herrmann. Report on excess mortality in Europe during summer 2003, EU Community Action Programme Public Health Grant Agreem. 2005114 2007 28.

[23] J.-M. Robine et al., Death toll exceeded 70,000 in Europe during the summer of 2003, C. R. Biol., 331(2) 2008 10.1016/j.crvi.2007.12.001.

[24] D. Enescu, A review of thermal comfort models and indicators for indoor environments, Renew. Sustain. Energy Rev. 79 (Nov. 2017) 1353–1379, https://doi.org/10.1016/j.rser.2017.05.175.

[25] EN 15251, EN 15251: Indoor environmental input parameters for design and assessment of energy performance of buildings addressing indoor air quality, thermal environment, lighting and acoustics. European Committee for Standardization, Brussels, Belgium, 2006.

[26] ISO 7730, ISO 7730: Ergonomics of the Thermal Environment. Analytical Determination and Interpretation of Thermal Comfort Using Calculation of the PMV and PPD Indices and Local Thermal Comfort Criteria. International Standards Organization Geneva, 2004.

[27] R.S. McLeod, M. Swainson, Chronic overheating in low carbon urban developments in a temperate climate, Renew. Sustain. Energy Rev. 74 (Jul. 2017) 201–220, https://doi.org/10.1016/j.rser.2016.09.106.

[28] ANSI/ASHRAE Standard 55, Standard 55–2017: Thermal Environmental Conditions for Human Occupancy. American Society of Heating, Refrigerating and Air Conditioning Engineers: Atlanta, GA, USA, 2017.

[29] S. Carlucci, L. Pagliano, A review of indices for the long-term evaluation of the general thermal comfort conditions in buildings, Energy Build. 53 (2012) 194–205, https://doi.org/10.1016/j.enbuild.2012.06.015.

[30] M. Beshir, J.D. Ramsey, Heat stress indices: a review paper, Int. J. Ind. Ergon. 3 (2) (1988) 89–102.

[31] M. Taleghani, M. Tenpierik, S. Kurvers, A. van den Dobbelsteen, A review into thermal comfort in buildings, Renew. Sustain. Energy Rev. 26 (2013) 201–215, https://doi.org/10.1016/j.rser.2013.05.050.

[32] D. Khovalyg et al., "Critical review of standards for indoor thermal environment and air quality," Energy Build. 2020 109819 10.1016/j.enbuild.2020.109819.

[33] S. Carlucci, L. Bai, R. de Dear, L. Yang, Review of adaptive thermal comfort models in built environmental regulatory documents, Build. Environ. 137 (2018) 73–89, https://doi.org/10.1016/j.buildenv.2018.03.053.

[34] Y. Cheng, J. Niu, N. Gao, Thermal comfort models: a review and numerical investigation, Int. Workshop Vent. Comf. Health Transp. Veh. 47 (2012) 13–22, https://doi.org/10.1016/j.buildenv.2011.05.011.

[35] J. Van Hoof, M. Mazej, J.L. Hensen, Thermal comfort: research and practice, Front. Biosci. 15 (2) (2010) 765–788, https://doi.org/10.2741/3645.

[36] E. Halawa, J. van Hoof, The adaptive approach to thermal comfort: a critical overview, Energy Build. 51 (2012) 101–110, https://doi.org/10.1016/j.enbuild.2012.04.011.

[37] L. Yang, H. Yan, J.C. Lam, Thermal comfort and building energy consumption implications – A review, Appl. Energy 115 (2014) 164–173, https://doi.org/10.1016/j.apenergy.2013.10.062.

[38] Q. Zhao, Z. Lian, D. Lai, Thermal comfort models and their developments: a review, Energy Built Environ. 2 (1) (Jan. 2021) 21–33, https://doi.org/10.1016/j.enbenv.2020.05.007.

[39] S. Roaf, F. Nicol, M. Humphreys, P. Tuohy, A. Boerstra, Twentieth century standards for thermal comfort: promoting high energy buildings, Archit. Sci. Rev. 53 (1) (2010) 65–77, https://doi.org/10.3763/asre.2009.0111.

[40] S. Carlucci. Thermal comfort assessment of buildings, Springer, 2013, 10.1007/978-88-470-5238-3.

[41] Zero Carbon Hub, Impacts of Overheating: Evidence Review, Zero Carbon Hub, London, England, 2015.

[42] NHBC. Overheating in new homes: A review of the evidence, National House-Building Council, UK., 2012.

[43] M. Hendel, K. Azos-Diaz, B. Tremeac, Behavioral adaptation to heat-related health risks in cities, Energy Build. 152 (2017) 823–829, https://doi.org/10.1016/j.enbuild.2016.11.063.

[44] European Commission (EC), "Eurostat - Tables, Graphs and Maps Interface (TGM) table," 2017. Accessed: May 19, 2021. [Online]. Available: https://ec.europa.eu/eurostat/web/main/help/first-visit/tgm.
[45] R.S. Kovats, S. Hajat, Heat stress and public health: a critical review, Annu. Rev. Public Health 29 (1) (2008) 41–55, https://doi.org/10.1146/annurev.publhealth.29.020907.090843.
[46] K.J. Lomas, S.M. Porritt, Overheating in buildings: lessons from research, Build. Res. Inf. (2017), https://doi.org/10.1080/09613218.2017.1256136.
[47] S. Yannas, J. Rodríguez-Álvarez, Domestic overheating in a temperate climate: feedback from London Residential Schemes, Sustain. Cities Soc. 59 (2020), https://doi.org/10.1016/j.scs.2020.102189 102189.
[48] A. Mavrogianni et al., The impact of occupancy patterns, occupant-controlled ventilation and shading on indoor overheating risk in domestic environments, Build. Environ. 78 (2014) 183–198, https://doi.org/10.1016/j.buildenv.2014.04.008.
[49] T. Psomas, P. Heiselberg, K. Duer, M.M. Andersen. Comparison and statistical analysis of long-term overheating indices applied on energy renovated dwellings in temperate climates, Indoor Built Environ. 27(3) 2018 10.1177/1420326X16683435.
[50] R. Birchmore, K. Davies, P. Etherington, R. Tait, A. Pivac. Overheating in Auckland homes: testing and interventions in full-scale and simulated houses, Build. Res. Inf. 45(1–2) 2016, 10.1080/09613218.2017.1232857.
[51] H. Elsharkawy, S. Zahiri, The significance of occupancy profiles in determining post retrofit indoor thermal comfort, overheating risk and building energy performance, Build. Environ. 172 (2020), https://doi.org/10.1016/j.buildenv.2020.106676 106676.
[52] M.J. Fletcher, D.K. Johnston, D.W. Glew, J.M. Parker, An empirical evaluation of temporal overheating in an assisted living Passivhaus dwelling in the UK, Build. Environ. 121 (2017) 106–118, https://doi.org/10.1016/j.buildenv.2017.05.024.
[53] A. Pathan, A. Mavrogianni, A. Summerfield, T. Oreszczyn, M. Davies, Monitoring summer indoor overheating in the London housing stock, Energy Build. 141 (2017) 361–378, https://doi.org/10.1016/j.enbuild.2017.02.049.
[54] M. Mulville, S. Stravoravdis, The impact of regulations on overheating risk in dwellings, Build. Res. Inf. 44 (5–6) (2016) Aug, https://doi.org/10.1080/09613218.2016.1153355.
[55] W.V. Lee, K. Steemers. Exposure duration in overheating assessments: a retrofit modelling study, Build. Res. Inf. 45(1–2) 2016, 10.1080/09613218.2017.1252614.
[56] L. Rodrigues, V. Sougkakis, M. Gillott. Investigating the potential of adding thermal mass to mitigate overheating in a super-insulated low-energy timber house, Int. J. Low-Carbon Technol. 11(3) 2016 10.1093/ijlct/ctv003.
[57] United Nations (UN), "World Population Prospects - Population Division"," United Nations. Accessed: May 19, 2021. [Online]. Available: https://population.un.org/wpp/Download/Standard/Population/.
[58] United Nations (UN), "Demographic Yearbook - Table 3: Population by sex, rate of population increase, surface area and density," United Nations Statistics division, 2014. Accessed: May 19, 2021. [Online]. Available: http://unstats.un.org/unsd/demographic/products/dyb/dyb2012/Table03.pdf.
[59] R. De Vecchi, M.J. Sorgato, M. Pacheco, C. Cândido, R. Lamberts, ASHRAE 55 adaptive model application in hot and humid climates: the Brazilian case, Archit. Sci. Rev. 58 (1) (2015) 93–101, https://doi.org/10.1080/00038628.2014.981145.
[60] Y. Yuan, J. Shim, S. Lee, D. Song, J. Kim, Prediction for overheating risk based on deep learning in a zero energy building, Sustainability 12 (21) (2020) 8974, https://doi.org/10.3390/su12218974.
[61] E. Recast, Directive 2010/31/EU of the European Parliament and of the Council of 19 May 2010 on the energy performance of buildings (recast), Off. J. Eur. Union 18 (06) (2010) 2010.
[62] IBGE, "Performance Energétique des Bâtiments: Guide des exigences et des procédures de la réglementation Travaux PEB en Région de Bruxelles Capitale," Brussels, Belgium, 2017.
[63] Vlaams Energie- en Klimaatagentschap, Bijlage V Bepalingsmethode EPW: BEPALINGSMETHODE VAN HET PEIL VAN PRIMAIR ENERGIEVERBRUIK VAN RESIDENTIËLE EENHEDEN, Flanders, Belgium, 2020.
[64] Gouvernement Wallon, "Méthode PER 2018: MÉTHODE DE DÉTERMINATION DU NIVEAU DE CONSOMMATION D'ÉNERGIE PRIMAIRE DES UNITES RESIDENTIELLES," Wallonia, Belgium, 2018.
[65] V. Fux, "Thermische Gebäudesimulation zum sommerlichen Wärmeschutz nach DIN 4108-2: 2013," Hochsch. Für Tech. Stuttg., 2013.
[66] U. Krone, F. Ascione, N. Bianco, T. Tschirner, O. Böttcher, Prescriptive-and performance-based approaches of the present and previous German DIN 4108–2. Hourly energy simulation for comparing the effectiveness of the methods, Energy Procedia 75 (2015) 1315–1324.
[67] Ministère de la transition écologique, "Réglementation environnementale RE2020," France, 2020.
[68] HM Government, "The Building Regulations 2010: Conservation of fuel and power in new dwellings, Approved Document L1A," 2013 edition incorporating 2016 amendments, UK.
[69] HM Government, "The Building Regulations 2010: Conservation of fuel and power in existing dwellings, Approved Document L1B," 2010 edition incorporating 2010, 2011, 2013. 2016 , and 2018 amendments, UK.
[70] DCLG, "Housing Standards Review: Summary of Responses," Department for Communities and Local Government, London, UK, ISBN: 978-1-4098-4178-4, 2014. [Online]. Available: https://www.gov.uk/government/consultations/housing-standards-review-consultation.
[71] HM Government, "The Building Regulations 2010: Conservation of fuel and power in new dwellings, Approved Document L1A," 2013 edition, UK.
[72] BRE (DECC), "SAP 2012: The Government's Standard Assessment Procedure for Energy Rating of Dwellings," Watford, UK, 2012.
[73] UK Government, "Approved Document [X] – Overheating." Jan. 2021. Accessed: Aug. 30, 2021. [Online]. Available: https://assets.publishing.service.gov.uk/government/uploads/system/uploads/attachment data/file/953752/Draft guidance on heating.pdf.
[74] NTA 8800, NTA 8800: Energieprestatie van gebouwen-Bepalingsmethode. Royal Netherlands Standardization Institute, Delft, Netherlands, 2019.
[75] BRE (DECC), "SAP 2012: The Government's Standard Assessment Procedure for Energy Rating of Dwellings," Watford, UK, 2012.
[76] I. I. Publicatie, "74; Thermische behaaglijkheid e eisen voor de binnentemperatuur in gebouwen, Stichting ISSO," Rotterdam Neth., 2004.
[77] A.C. van der Linden, A.C. Boerstra, A.K. Raue, S.R. Kurvers, R.J. de Dear, Adaptive temperature limits: a new guideline in The Netherlands: A new approach for the assessment of building performance with respect to thermal indoor climate, Energy Build. 38 (1) (2006) 8–17, https://doi.org/10.1016/j.enbuild.2005.02.008.
[78] N. Willand, I. Ridley, A. Pears, Relationship of thermal performance rating, summer indoor temperatures and cooling energy use in 107 homes in Melbourne, Australia, Energy Build. 113 (2016) 159–168, https://doi.org/10.1016/j.enbuild.2015.12.032.
[79] J.F. Nicol, I.A. Raja, A. Allaudin, G.N. Jamy, Climatic variations in comfortable temperatures: the Pakistan projects, Energy Build. 30 (3) (1999) 261–279, https://doi.org/10.1016/S0378-7788(99)00011-0.
[80] I. Fato, F. Martellotta, C. Chiancarella, Thermal comfort in the climatic conditions of Southern Italy, Trans.-Am. Soc. Heat. Refrig. AIR Cond. Eng. 110 (2) (2004) 578–593.
[81] R.J. De Dear, A. Auliciems, Validation of the predicted mean vote model of thermal comfort in six Australian field studies, ASHRAE Trans. 91 (2 B) (1985) 452–468.
[82] G.E. Schiller, A comparison of measured and predicted comfort in office buildings, ASHRAE Trans. 96 (1) (1990) 609–622.
[83] J.F. Busch, Thermal responses to the Thai office environment, ASHRAE Trans. 96 (1) (1990) 859–872.
[84] J.F. Busch, A tale of two populations: thermal comfort in air-conditioned and naturally ventilated offices in Thailand, Energy Build. 18 (3) (1992) 235–249, https://doi.org/10.1016/0378-7788(92)90016-A.
[85] K. van der Linden, A.C. Boerstra, A.K. Raue, S.R. Kurvers, Thermal indoor climate building performance characterized by human comfort response, Energy Build. 34 (7) (2002) 737–744, https://doi.org/10.1016/S0378-7788(01)00144-X.
[86] S. Heidari, S. Sharples, A comparative analysis of short-term and long-term thermal comfort surveys in Iran, Energy Build. 34 (6) (2002) 607–614, https://doi.org/10.1016/S0378-7788(02)00011-7.
[87] N. Yamtraipat, J. Khedari, J. Hirunlabh, Thermal comfort standards for air conditioned buildings in hot and humid Thailand considering additional factors of acclimatization and education level, Sol. Energy 78 (4) (2005) 504–517, https://doi.org/10.1016/j.solener.2004.07.006.
[88] R. De Dear and G. S. Brager, "Developing an adaptive model of thermal comfort and preference," UC Berkeley Cent. Built Environ., 1998, Accessed: Feb. 03, 2020. [Online]. Available: https://escholarship.org/uc/item/4qq2p9c6.
[89] W.A. Andreasi, R. Lamberts, C. Cândido, Thermal acceptability assessment in buildings located in hot and humid regions in Brazil, Build. Environ. 45 (5) (2010) 1225–1232, https://doi.org/10.1016/j.buildenv.2009.11.005.
[90] P. Ole Fanger, J. Toftum. Extension of the PMV model to non-air-conditioned buildings in warm climates, Energy Build. 34(6) 2002 533–536 10.1016/S0378-7788(02)00003-8.
[91] M.A. Humphreys, J. Fergus Nicol. The validity of ISO-PMV for predicting comfort votes in every-day thermal environments, Energy Build. 34(6) 2002 667–684 10.1016/S0378-7788(02)00018-X.
[92] T. Parkinson, R. de Dear, G. Brager, Nudging the adaptive thermal comfort model, Energy Build. 206 (2020), https://doi.org/10.1016/j.enbuild.2019.109559 109559.
[93] R. Basu, J.M. Samet, Relation between elevated ambient temperature and mortality: a review of the epidemiologic evidence, Epidemiol. Rev. 24 (2) (2002) 190–202, https://doi.org/10.1093/epirev/mxf007.
[94] B.R. Hughes, H.N. Chaudhry, S.A. Ghani, A review of sustainable cooling technologies in buildings, Renew. Sustain. Energy Rev. 15 (6) (2011) 3112–3120, https://doi.org/10.1016/j.rser.2011.03.032.
[95] C. Hughes, S. Natarajan, Summer thermal comfort and overheating in the elderly, Build. Serv. Eng. Res. Technol. 40 (4) (2019) 426–445, https://doi.org/10.1177/0143624419844518.

Appendix B

Chapter 2: *Resilient cooling strategies – A critical review and qualitative assessment*

Energy & Buildings 251 (2021) 111312

Contents lists available at ScienceDirect

Energy & Buildings

journal homepage: www.elsevier.com/locate/enb

Resilient cooling strategies – A critical review and qualitative assessment

Chen Zhang [a,*], Ongun Berk Kazanci [b], Ronnen Levinson [c], Per Heiselberg [a], Bjarne W. Olesen [b], Giacomo Chiesa [d], Behzad Sodagar [e], Zhengtao Ai [f], Stephen Selkowitz [c], Michele Zinzi [g], Ardeshir Mahdavi [h], Helene Teufl [h], Maria Kolokotroni [i], Agnese Salvati [i], Emmanuel Bozonnet [j], Feryal Chtioui [j], Patrick Salagnac [j], Ramin Rahif [k], Shady Attia [k], Vincent Lemort [l], Essam Elnagar [l], Hilde Breesch [m], Abantika Sengupta [m], Liangzhu Leon Wang [n], Dahai Qi [o], Philipp Stern [p], Nari Yoon [c,t], Dragos-Ioan Bogatu [d], Ricardo Forgiarini Rupp [b], Taha Arghand [q], Saqib Javed [q], Jan Akander [r], Abolfazl Hayati [r], Mathias Cehlin [r], Sana Sayadi [r], Sadegh Forghani [r], Hui Zhang [s], Edward Arens [s], Guoqiang Zhang [f]

[a] Department of the Built Environment, Aalborg University, Denmark
[b] International Centre for Indoor Environment and Energy - ICIEE, Department of Civil Engineering, Technical University of Denmark, Denmark
[c] Building Technology and Urban Systems Division, Lawrence Berkeley National Laboratory, USA
[d] Department of Architecture and Design, Politecnico di Torino, Italy
[e] School of Architecture and the Built Environment, University of Lincoln, UK
[f] Department of Building Environment and Energy, Hunan University, China
[g] ENEA Italian National Agency for New Technologies, Energy and Sustainable Economic Development, Italy
[h] Department of Building Physics and Building Ecology, TU Wien, Austria
[i] Institute for Energy Futures, Brunel University London, Kingston Lane, Uxbridge UB8 3PH, UK
[j] LaSIE, University of La Rochelle, France
[k] Sustainable Building Design Lab, Dept. UEE, Faculty of Applied Sciences, Université de Liège, Belgium
[l] Thermodynamics Laboratory, Aerospace and Mechanical Engineering Department, Faculty of Applied Sciences, Université de Liège, Belgium
[m] Building Physics and Sustainable Design, Department of Civil Engineering, KU Leuven, Ghent and Aalst Technology Campuses, Belgium
[n] Building, Civil, and Environmental Engineering, Concordia University, Canada
[o] Department of Civil and Building Engineering, Université de Sherbrooke, Canada
[p] Institute of Building Research & Innovation, Austria
[q] Division of Building Services Engineering, Department of Architecture and Civil Engineering, Chalmers University of Technology, Sweden
[r] Faculty of Engineering and Sustainable Development, University of Gävle, Sweden
[s] Center for the Built Environment, University of California, Berkeley, CA, USA
[t] School of Civil, Environmental and Architectural Engineering, Korea University, Republic of Korea

ARTICLE INFO

Article history:
Received 2 February 2021
Revised 15 June 2021
Accepted 26 July 2021
Available online 29 July 2021

Keywords:
Building cooling
Resilient
Climate change
Heatwave
Power outage
Qualitative analysis
Passive cooling
Active cooling
Low-energy cooling
Critical review

ABSTRACT

The global effects of climate change will increase the frequency and intensity of extreme events such as heatwaves and power outages, which have consequences for buildings and their cooling systems. Buildings and their cooling systems should be designed and operated to be resilient under such events to protect occupants from potentially dangerous indoor thermal conditions.

This study performed a critical review on the state-of-the-art of cooling strategies, with special attention to their performance under heatwaves and power outages. We proposed a definition of resilient cooling and described four criteria for resilience—absorptive capacity, adaptive capacity, restorative capacity, and recovery speed —and used them to qualitatively evaluate the resilience of each strategy.

The literature review and qualitative analyses show that to attain resilient cooling, the four resilience criteria should be considered in the design phase of a building or during the planning of retrofits. The building and relevant cooling system characteristics should be considered simultaneously to withstand extreme events. A combination of strategies with different resilience capacities, such as a passive envelope strategy coupled with a low-energy space-cooling solution, may be needed to obtain resilient cooling. Finally, a further direction for a quantitative assessment approach has been pointed out.

* Corresponding author.
E-mail address: cz@build.aau.dk (C. Zhang).

https://doi.org/10.1016/j.enbuild.2021.111312
0378-7788/

1. Introduction

Climate change and extreme heat are critical issues faced by all countries. The Intergovernmental Panel on Climate Change (IPCC) defines climate extreme as "the occurrence of a value of a weather or climate variable above (or below) a threshold value near the upper (or lower) ends of the range of observed values of the variable" [1]. The long duration and high intensity heatwaves are becoming a potential natural hazard that presents significant risk and challenge to humans, buildings, and building-related systems. The extremely high temperatures can cause heatstroke, heat exhaustion and other heat-related diseases, which are particularly dangerous for vulnerable populations, such as the elderly or low-income communities [2]. A most well-known hazard was the European heatwave 2003, which resulted in 14,800 excess deaths in France; 74% of these excess deaths occurred indoors [3]. EuroHEAT estimated that the increase in mortality ranges from 7.6% to 33.6% during heatwaves by analyzing the impact of long heatwaves in nine European cities (Athens, Barcelona, Budapest, London, Milan, Munich, Paris, Rome and Valencia) [4].

Resilience is a concept widely applied in disaster risk management. It refers to "*the ability of a system and its components parts to anticipate, absorb, accommodate, or recover from the effects of a hazardous event in a timely and efficient manner, including through ensuring the preservation, restoration, or improvement of its essential basic structures and functions*", as defined by IPCC [5]. Resiliency in the context of the building environment refers to the ability of buildings and their systems to continue functioning as intended in the face of natural hazards imposed by climate change [6]. Buildings shelter humans from the outdoor environment and it is crucial that buildings maintain safe thermal conditions during extreme events, such as heatwaves. Current building and building-related system designs strongly focus on energy efficiency to mitigate climate change through reducing carbon emissions. However, energy efficient strategies (technologies and practices) are not always consistent with strategies that improve resilience to extreme heat; often there is a trade-off between these two objectives [7]. Ren et al. [8] contend that "Excessive striving for energy efficiency" could compromise a building's ability to maintain comfortable thermal conditions during heatwaves, such as higher insulation and airtightness. Another limitation for current building and building system design is the use of typical weather or historical weather files for the calculation of cooling demand and evaluation of the effectiveness of cooling strategies [9,10]. As a consequence, the building and its systems may not be prepared to cope with heatwaves or climate change. This is supported by the findings of several studies [11,12,13], which show that the low-energy cooling strategies that work well today might not remain effective under long-term climate change, or in extreme events such as a heatwave or a power failure.

Like energy efficiency, sustainability and economic affordability, resilience should be considered as an important property of buildings and their systems in the early design phase. Ceré et al. [14] note that resilience is already part of recent architectural and structural building design practices.

The recently formed International Energy Agency (IEA) Energy in Buildings and Communities Programme (EBC) Annex 80 "Resilient Cooling of Buildings" addresses this need by developing, assessing and communicating strategies for resilient cooling and overheating protection against climate change and the consequent hazards or events [15]. Many cooling technologies and solutions

Table 1
Definitions provided in literature for the concepts of resilience.

Ref	Definition	Characteristics	Threats	Scale	Year
[29]	"Building resilience is defined as a building's ability to withstand severe weather and natural disasters along with its ability to recover in a timely and efficient manner if it does incur damages."	Withstand, recover, rapidity	Climate and natural disasters	Building	2013
[26]	"A resilient building is a building that not only is robust but also can fulfill its functional requirements (withstand) during a major disruption. Its performance might even be disrupted but has to recover to an acceptable level in a timely manner in order to avoid disaster impacts."	Withstand, absorb, recover, rapidity	Climate extremes	Building	2019
[24]	"A resilient built environment as one designed, located, built, operated, and maintained in a way that maximizes the ability of built assets, associated support system (physical and institutional) and the people that reside or work within the built asset, to withstand, recover from, and mitigate the impacts of threats."	Withstand, recover, mitigate	Natural hazards (geo-hazards and hydro-meteorological hazards)	Built environment	2008
[14]	"The intrinsic ability of the built environment to react positively before, during and after the presence of the adversely exogenous input (e.g., landslides), i.e., the ability to absorb external disturbances, in order to maintain the system's original states or reach a new set of steady states for serving its normal functionalities."	Vulnerability, adaptive capacity, recoverability	Geo-environmental hazards	Built environment	2017
[21]	"Resilient urban energy system needs to be capable of "planning and preparing for", "absorbing", "recovering from", and "adapting" to any adverse events that may happen in the future. The complex, dynamic, and adaptive systems (e.g. cities) would not necessarily return to an equilibrium state."	Preparation, absorption, recovery, adaptation	Disruptions in energy supply	Urban energy systems	2016
[27]	"Resilience can be understood as the ability of the system to reduce the chances of a shock, to absorb a shock if it occurs (abrupt reduction of performance) and to recover quickly after a shock (re-establish normal performance)."	Robustness, redundancy, resourcefulness, rapidity	Earthquake	Community (technical, organization, social, economic)	2003
[5]	"The ability of a system and its component parts to anticipate, absorb, accommodate, or recover from the effects of a hazardous event in a timely and efficient manner, including through ensuring the preservation, restoration, or improvement of its essential basic structures and functions."	Anticipate, absorb, accommodate, recover	Climate extremes and disasters	System	2012
[28]	"Resilience is a continuous process starting from a reliable initial condition, followed by a vulnerability-survivability state after a disruptive event and eventually a recoverability phase aimed at achieving a new stable equilibrium condition."	N/A	Flood	Infrastructure system	2012

are available both in the market and are under development. Previous studies have systematically compared various active and passive cooling strategies in terms of energy performance [16,17,18], thermal comfort and air quality [19], capital expenditure [16,18] and applicability in different climate zones [20]. However, the resilience of cooling strategies has not been widely discussed in the literature and it lacks a clear definition of resilient cooling and the criteria for assessing it.

The present study aims to fill this knowledge gap. First, we define resilient cooling and propose the criteria that can be used to assess the resilience of a cooling strategy. Second, we review the state-of-the-art of existing cooling strategies, assessing their physical principle, typologies, and performance, with special attention to resilience, applicability and technology readiness level. Finally, we use the proposed resilience criteria to qualitatively evaluate cooling strategies under various extreme events, such as, heatwaves and power outages.

2. Resilience and characteristics of resilient cooling

This section reviews the definition of resilience and the characteristics of resilient systems, and further discusses resilient cooling and the criteria for assessing it.

The concept of resilience originated in physics and psychology, where it described the ability of an object to return to its initial condition after a disruption [21,22]. The definition and interpretation of resilience vary from one discipline to another. Table 1 summarizes various definitions of resilience within the context of buildings and building-related systems.

One critical prerequisite for a comprehensive definition of resilience is to identify the threats or external perturbations to the systems, which can be summarized into an essential question as "resilience to what?"[23]. The threats faced by buildings and building-related systems are diverse and include both natural hazards and human hazards. Natural hazards can further be divided into geo-hazards, such as earthquakes, tsunamis, landslides, hydro-meteorological hazards (e.g., hurricanes and floods), wind storms and extreme temperature [24]. In the concept of resilient cooling, the building and its systems are mainly challenged by extreme heat events (heatwaves) and power outages. High power demand from air-conditioning during a heatwave strains and destabilizes the electrical grid [25]. Extreme heat can also impede power generation. For example, during the heatwave in 2003, the river water levels in France dropped so low that the cooling process of nuclear reactors became impossible and the nuclear power plants had to shut down [26].

Bruneau et al. [27] proposed four dimensions of resilience: technical, organizational, social, and economic. This study will mainly discuss resilient cooling from the technical point of view and the other dimensions will be treated as supplementary conditions. The resilience researches [5,21,27] considered various scales from micro (building or building element) to macro (district, city, or urban). The current study will address the resilience of building-scale cooling strategies over the life of the building.

Some studies tended to define resilience by considering the phases that systems undergo with external disruptions (initial condition, vulnerability-survivability state, recoverability state, new stable equilibrium state) [14,28], but most defined resilience through its features and systems abilities [5,21,24,26,27,29]. Several words commonly found in the literature to characterize resilient systems include "absorb", "withstand", "recover", and "rapidity". Therefore, this study proposes to summarize the resilient characteristics of cooling strategies by four criteria – absorptive capacity, adaptive capacity, restorative capacity and recovery speed.

- **Absorptive capacity** is the degree to which a system is able to absorb the impacts of disruptive events and minimize their consequences with little effort. For example, heavy thermal mass in a building (capacitance) can absorb unwanted solar gain and can minimize and/or delay the air temperature increase in the building without the use of cooling energy.
- **Adaptive capacity** is the ability to adjust undesirable situations by undergoing some changes. The system can learn from the event, evaluate the system performance and modify its configurations, and make it more flexible to future disruptions. Adaptive capacity is distinguished from absorptive capacity in that adaptive systems change in response to adverse impacts, especially if the absorptive capacity has been exceeded. For example, a façade solar shade may be activated, when the air temperature in the building starts to increase because the storage capacity of the thermal mass has been exceeded.
- **Restorative capacity** is the ability to return to normal or improved operation. For example, night cooling can remove unwanted heat gain accumulated in the thermal mass during the day and provide a heat sink for the next day.
- **Recovery speed** is the speed of the recovery process. Recovery may be accelerated if absorption activities are well implemented and the system can quickly mobilize and effectively use all the resources at its disposal [21]. For example, the speed with which night cooling can remove heat from the building's thermal mass and restore the building to its desired condition depends on the ventilation flow rate and the outdoor air temperature.

Therefore, Annex 80 defines resilient cooling as a capacity of the cooling system integrated with the building that allows it to withstand or recover from disturbances due to disruptions, including heatwaves and power outages, and to adopt the appropriate strategies after failure to mitigate degradation of building performance (deterioration of indoor environmental quality and/or increased need for space cooling energy) [23].

3. Review method

To provide an overview of the state-of-the-art of existing cooling strategies, and assessing their resilience under various extreme events, a systematic literature review was performed. The review was carried out through a critical analysis of existing literature. Different databases have been used to identify peer-reviewed academic literature, including Elsevier (ScienceDirect), IEEE, Google Scholar, Scopus, SpringerLink. To address the resilience of cooling strategies under extreme events, the keywords for the search included resilience, overheating, heatwave, climate change, power outage, disruptive events, cooling strategies/solutions/techniques. Additional searches were performed by combining the keywords for each cooling strategy. Take ventilative cooling as an example, the following keywords were used: ventilative cooling, ventilation, natural/mechanic/hybrid ventilation, night cooling, air-based system. Besides peer-reviewed articles, relevant books and technical reports have also been taken into account. There was no strict limitation on the publication period, but priority has been given to recent publications to address the state-of-the-art research. Table 2 summarizes the statistic of reviewed literature for different cooling strategies.

4. Resilient cooling strategies

Annex 80 has created four cooling-strategy categories based on their approaches to cooling people or the indoor environment.

Table 2
Statistic of reviewed literature for different cooling strategies.

Cooling strategies	Number of references	Year of publication
Solar shading/glazing	172	1982–2020
Cool envelope materials	256	1975–2021
Green roofs, roof pond, and green facades	39	1969–2020
Ventilated roofs and facades	47	2001–2020
Thermal mass including PCMs	89	1982–2020
Ventilative cooling	84	1996–2021
Adiabatic/evaporative cooling	33	1991–2020
Compression refrigeration	9	2008–2019
Absorption refrigeration including desiccant cooling	10	1992–2019
Ground source cooling	79	1987–2020
Sky radiative cooling	32	2002–2021
High-temperature cooling system: Radiant cooling	28	1995–2020
Personal comfort systems	26	1979–2020
Dehumidification including desiccant dehumidification	27	1993–2020

A. Reducing heat gains to indoor environments and people indoors
B. Removing sensible heat from indoor environments
C. Enhancing personal comfort apart from cooling whole spaces
D. Removing latent heat from indoor environments

This section will review the above cooling strategies from the following aspects: physical principle, typologies, performance with attention to resilience under extreme events, and technology readiness level (TRL). The technology readiness level is based on the guidelines from the U.S. Department of Energy [30].

4.1. Reduce heat gains to indoor environments and people indoors

4.1.1. Advanced solar shading/advanced glazing technologies

Windows are inserted into walls and roofs to provide a view to the outdoors for occupants, and to admit and control daylight, sunlight, and air. While windows usually comprise only a small fraction of the overall envelope area (typically 5–35%) the impacts of these transparent surfaces on cooling energy use, peak cooling loads, and occupant comfort can be very large. Windows (glass, sash, and frame elements) are commonly accompanied by shading systems. When mounted on the building exterior, shading devices are more effective in managing solar loads, but more costly. The combined ability of window and shading technologies to provide resilient cooling depends on the intrinsic properties of the window/glazing package as modified by any shading technologies. Shading elements are commonly relied upon to manage solar gain in the event of a heatwave or power outage.

To better assess the window/glazing/shading response in terms of resilience it is useful to divide the available technology options into static and dynamic technologies, and to further divide dynamic solutions into manually operated and automatically operated.

Glazing technologies manage cooling loads from solar gain by absorbing, transmitting, and reflecting solar energy by virtue of the materials used in the construction of the glass and glazing system. Traditional clear glass has a very high solar transmittance; glazing systems used in most windows today use body tints and coatings for absorption and reflection, and can be further combined into multiple glazings in an insulated glazing unit with two or more glazing layers that provide a wide range of thermal management capabilities. Several thousand different variants of glass are commercially available with documented wavelength-dependent optical properties [31]. The solar properties of the complete glass package in a window, optimized for structural needs as well as energy control, can be readily determined by simulation [32,33]. The most effective and widely used glazing products incorporate low thermal-infrared emittance ("low-E") coatings which can serve two purposes. All reduce the window thermal transmittance ("U-value") and when properly positioned within an insulating glass unit will reduce solar heat gain. Some low-E coatings provide spectral control and admit most daylight [visible transmittance (Tv) > 60%] while effectively reducing solar gain [solar heat gain coefficient (SHGC) less than 0.30]. A wide range of light-transmitting glazings is available with a light-to-solar-gain-ratio (LSG = Tv/SHGC) ranging from 0.5 to 2.3 [34]. The ability to admit daylight but minimize solar heat gain can reduce building cooling loads attributable to electric lighting.

Glazings with fixed solar optical and thermal properties do not have the flexibility to respond dynamically to changing environmental conditions or to grid demands. After a 20-year R&D effort manufacturers have commercialized several different "smart glazing" products. Thermochromic glass technologies have solar optical properties that vary moderately with temperature [35,36]. The solar-optical properties of electrochromic and liquid crystal-based glazings are altered over a wide range with an applied voltage [37,38]. These show promising performance in laboratory studies and field studies in buildings but adoption has been slow because they are expensive and require new sensors and controls. There is a significant global investment in ongoing R&D regarding new or enhanced electrochromic solutions, as well as in other active glazing technologies based on liquid crystal devices. This is expected to provide new market options in the near term [39,40]. One approach is to control visible transmittance and NIR transmittance independently. This facilitates improved performance in northern climates, and the window can reduce SHGC in warmer climates but still admit daylight [41,42]. An emerging technology solution incorporates transparent or semi-transparent photovoltaic layers in the glazing to manage solar heat gain and generate electricity [43].

Shading solutions for windows are diverse in terms of function, materials, and operation in both homes and commercial buildings. Shading systems can be static or dynamic, and are mounted either exterior or interior to the glazing [44–50]. More complex solutions utilize the cavities between glazing and shading layers to manage air flow and heat removal or recovery; these ventilated facades are discussed in more detail in section 4.1.4. The best-known shading solutions are operable shades, blinds, and drapes on the interior, and screens, shades, blinds and fins/overhangs on the exterior [51–53]. The newest generation of exterior solar shading can incorporate power generation (i.e., PV arrays) in the shading elements [54]. Since the solar loads depend on ever-changing solar position, even fixed shading solutions will have an annual performance that varies with latitude, orientation, and geometry. An interior operable shading system will always be less efficient than a similar exterior system since the absorbed solar radiation is trapped within the building [49]. Operable systems have limited effectiveness and resilience if they are not triggered and operated appropriately in response to climatic stress. The promise of improved controls, wireless sensors, and better integration with building control systems should reduce costs and improve reliability [55–58]. Ongoing studies on occupant response to glare and preferences in managing the tradeoffs between daylight control, solar control, and glare [59,60] are influencing design and deployment trends for the years ahead.

Market availability and acceptance varies across these technology solutions and also by region. Both spectrally selective static glazing as well as high insulating glazing solutions, are widely

available. Active and passive smart glazing solutions are still offered by a limited number of companies globally. Fixed exterior shading systems are available in the global market, although they are infrequently used in many countries and for multiple building types. Multiple solutions for operable interior or exterior shading systems are also widely available. Exterior systems are in use in Europe but less widely in the U.S. These systems are commonly operated manually. Automated or motorized solutions are limited but they are entering the market in increasing volumes.

4.1.2. Cool envelope materials

A cool envelope material (CEM), typically a reflective roof or wall product, provides a solar-opaque surface that reduces net radiative heat gain at the envelope [(solar absorption - fluorescence) + (thermal infrared absorption – thermal infrared emission] to decrease heat flow into the occupied space [61–65]. Strategies include static high solar reflectance (light-colored or ultrabright-white CEM) [66–72], static high near-infrared (NIR) reflectance (cool-colored CEM) [73–82], temperature-sensitive high solar reflectance (thermochromic CEM) [66,83–86], angle-sensitive high solar reflectance (directionally selective reflector CEM) [87–89], static solar retroreflection (solar-retroreflective CEM) [90,91], and static near-unity solar reflectance + static selective thermal emittance (daytime sky radiator CEM) [92–94].

Except for daytime sky radiators, CEMs reduce heat flow into the occupied space but do not increase heat flow out of the occupied space. Therefore, CEMs must be coupled with heat modulating strategies, such as thermal storage, or heat-dissipating strategies, such as night ventilation, evaporative cooling, or mechanical cooling, if the outside air is uncomfortably or dangerously hot.

CEMs save cooling energy in an air-conditioned building when power is available; lower indoor temperatures in an unconditioned ("free-running") building when power is unavailable, or the building lacks cooling equipment, and provide a combination of energy savings and indoor temperature reduction when power is available, but the cooling equipment is undersized for an exceptionally hot day. Hernández-Pérez et al. [95] summarize cooling load or cooling energy savings simulated in over 20 studies; additional simulations can be found in later studies [63,66,84,96–108]. They also review space temperature reductions measured or simulated in over 30 studies and discomfort hour reductions simulated in 4 studies; later works also report reductions in indoor temperature [102–119] or discomfort hours [97,101,110–112,114,120], with heat-wave benefits assessed by Porritt et al. [121,122]. Cool-roof monitoring studies have measured reductions of about 1 to 3 K in top-floor air temperature [98,99,123–126] and up to about 5 K in top-floor operative temperature [112,127].

The ability of a CEM to reduce the envelope's net radiative heat gain on a sunny day provides an "absorptive" capacity for heat resilience by helping the cooling equipment meet its load, or by diminishing the temperature rise in an unconditioned building. As passive solar-control measures, CEMs help whenever the sun shines, and continue to mitigate unwanted solar heat gain during a power outage or heatwave. However, their absorptive capacities diminish when cloudy, hazy, or smoky skies reduce incident sunlight. A thermochromic CEM may provide adaptive capacity if a heat event accelerates its switch from low to high solar reflectance. While CEMs do not directly provide restorative or recovery capacity, their abilities to reduce heat flow into the occupied space make it easier for heat-modulating and heat-dissipating strategies to moderate interior temperatures.

Both white and cool-colored roof materials are mature technologies that are widely available to both building owners and building contractors [68,128], and identifiable via mature product rating systems provided by the Cool Roof Rating Council [129] and the European Cool Roofs Council [130,131]. Cool wall materials, such as light-colored paints, claddings, and sidings, and some cool-colored wall products, are similarly mature and available (Appendix P of [70]), but their product rating system is still under development [132]. Some novel CEMS such as directionally selective reflectors are specialty products with limited availability; other CEMs, such as daytime radiators, solar retroreflectors, fluorescent cool colors, and thermochromics remain under development.

4.1.3. Green roofs, roof pond, green facades (evaporative envelope surfaces)

Evaporation on the outside of the building envelope is an efficient cooling technique, which can be managed with vegetated surfaces, water films, ponds, and sprays [133–136] (Fig. 1).

The primary difference between façades (green or watered, Fig. 1a,b,c) and roofs (green roof or roof pond, Fig. 1d,e) is linked to the vertical water runoff, which amplifies the thermal transfer due to the increased sensible and convective heat transfer in the water stream. Moreover, evaporative façades require continuous water spray or water supply to permanently irrigate the upper part, while roof ponds and green roofs may adapt more easily to various climate conditions without water supply.

The water retention potential is a key design parameter for roof ponds [137] and green roofs [138]. A permanent water supply may be required (for façades, or during dry periods), which brings out the optimal control of the evaporative dynamic for a resilient cooling strategy, and low water consumption. E.g., to increase the evaporation process of a roof pond, Erell et al. [139] recommended

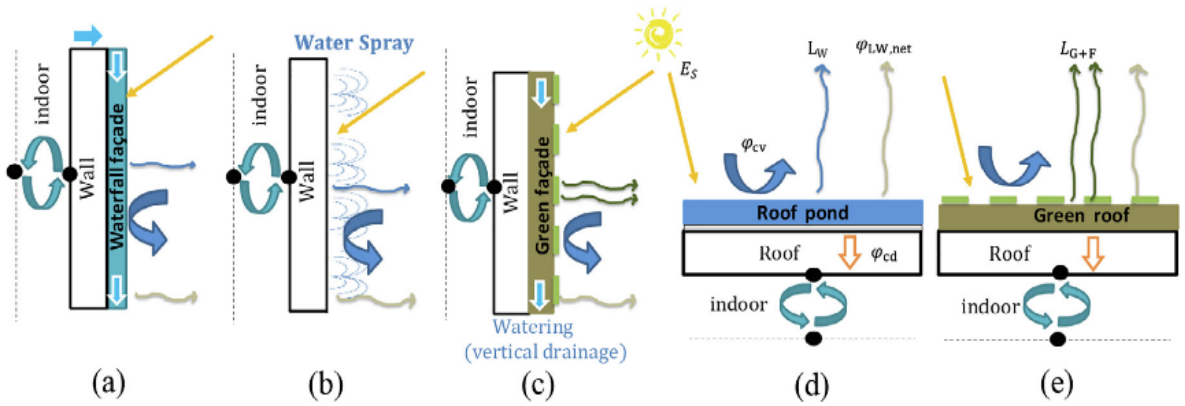

Fig. 1. Heat transfer in evaporative envelope surfaces, including (a) a waterfall façade, (b) a spraying system, (c) a green façade, (d) a roof pond, and (e) a green roof. (For interpretation of the references to color in this figure legend, the reader is referred to the web version of this article.)

droplet sizes of 0.5 to 1 mm, spray rates of about 1–1.5 volumes of the roof pond per hour, and a spray height of 50 cm.

Innovative evaporative envelopes include the combinations of increased albedo, the development of porous materials, or movable claddings [140,141].

However, for hot, temperate and even cold climates, evaporative envelope surfaces demonstrated strong cooling effects of the roof and façades surfaces for summer conditions [142,143]. E.g., the surface temperature of the south-oriented wall can decrease by 9.8 °C in Moscow, and 18.7 °C in Riyadh [139], while energy cooling loads can decrease up to 100% in Brasilia and Hong Kong with green roof and façades. These cooling techniques are also widely recommended for their stormwater retention potential, and their impact on sewer overflow, which translates into some local policies such as the Toronto (Canada) green roof policy [144]. This can be an efficient solution even considering the effects of climate change, but some parameters like plant species [145] or roof water retention capacity may have to be adapted.

Regarding evaporative surfaces, the most advanced TRL (TRL 9) concerns green roofs and façades, which are widely available, and included in policies and standards. However, few alternatives for water retention systems on roofs exists, e.g., typical gravel roofs (TRL 9). Most of these alternatives are only at a research or prototype stage, including various roof pond typologies with/without radiative protections, or porous material, all mainly available as lab prototypes, or full-scale experiments (TRL 4–6) [146].

4.1.4. Ventilated roofs and ventilated facades (ventilated envelope surfaces)

Ventilated roofs and façades have been widely developed as an adaptive element for both winter heat recovery and summer heat dissipation. An additional opaque or transparent cladding forms a ventilated double-skin, which allows various airflow strategies (see Fig. 2) to cool the external side when required. Ventilation patterns and additional controls, such as venetian blinds [147–150], make these techniques highly adaptable to seasonal changes and climate change.

The air-tightness and winter solar gains of the closed cavity façade (Fig. 2a) are a good option for temperate climates, while it can support high temperatures (up to 90 °C) with a long service life without maintenance [138]. Yet, overheating of the air gap under extreme summer conditions has led to the development of more performant solutions, such as movable blinds and natural ventilation. The solar heat gains observed in an experimental setup in China were reduced from 330 to 28 W/m^2 with Venetian blinds [149]. The cooling performance is improved with ventilation openings designed to remove heat, and outdoor or indoor air ventilation strategies [151]. The indoor ventilation can be designed with air outlets through the roof [152] or the wall (Fig. 2b,e), which can be efficient for air-conditioned buildings even in extreme hot climates. Driven by the outside air–gap stack effect (amplified by solar gains), the airflow may be intensified by the mechanical ventilation system of the building. Similarly, outdoor air can be used as the heat sink for the double-skin air gap (Fig. 2c,d). The study of a ventilated pitched roof in Djibouti [153] demonstrated a heat gain reduction of about 50% for the building, which underlines the effectiveness of this ventilation technique in extreme summer conditions, given the high solar gains of the roof, and the temperature differences between the roof and outdoor air.

The ventilation rate is a key parameter for this technique's cooling efficiency. This ventilation rate is highly dependent on the opening design. Then, the design and the optimal perforation rate of outdoor façade claddings vary greatly depending on the location and orientations [154,155]. The optimal perforated percentage varies between seasons, and variations between 10 and 60% were found to be optimum for Japan [143]. However, these optimal cooling performances will drop under extreme heatwave events and climate change, due to the outdoor air temperature increase. Yet, some design parameters such as solar orientation [156] and prevailing wind direction [156,157], will be much less sensitive to climate change.

Regarding ventilated surfaces, double-skin façades are very well developed in the construction sector, from the first Trombe walls in the 1920's to the transparent double-skins for high-rise office buildings [158] (TRL 9). These techniques include many innovations, such as the perforated and the closed cavity façades; yet many lab developments are still ongoing (TRL 6), and some biomimetic solutions are arising, such as adaptive façades similar to a natural foliage [159] (TRL8). Ventilated roof for cooling can be found in research studies [153] (TRL5-6), but very few construction products are available for this typology [160] (TRL9).

4.1.5. Thermal mass utilization including PCM

Thermal Energy Storage (TES) systems absorb, store, and release thermal energy on a cyclical basis (usually daily) to regulate internal temperature and improve thermal comfort in buildings [161]. Thermal energy can be stored as a change in internal energy of a material as sensible heat (e.g., ground, water tanks and aquifer energy storage), latent heat (e.g., Phase Change Materials, including organic and inorganic substances and ice storage), or chemical energy (e.g., thermochemical storage). It should be noted that the cooling capacity (in [kWh]) of a latent thermal energy storage comprises both a fraction of sensible and a fraction of latent energy.

TES systems increase the generation capacity by releasing the stored energy during high demand which allows a smaller production unit to be installed.. TES systems operate as a cost-saving measure by shifting the energy demand to low-tariff periods [162]. TES systems also increase the cooling system reliability and can easily be integrated with other functions such as on-site fire protection water storages [163]. However, TES system performance is not guaranteed during the days with small temperature swings. Storage cycle efficiency (i.e., long-term heat loss reduction) and high

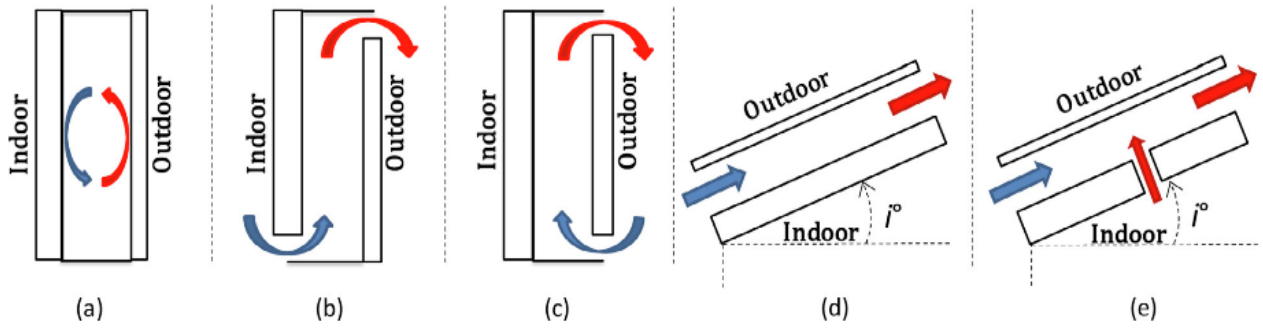

Fig. 2. Typologies of ventilated envelope surfaces: (a) closed cavity façade; (b) exhaust air façade; (c) outdoor air curtain façade; (d) ventilated roof; (e) ventilated roof coupled to a natural ventilation of the building.

investment cost in latent and thermochemical heat storage are further limitations of TES systems [164].

The performance of a TES is characterized by its storage capacity and its ability to provide cooling or heating power as a function of the state of charge of the storage. TES systems have shown to be effective measures in reducing peak indoor air temperature and dampening temperature variations in buildings during extreme events such as heatwaves or power outages. TES cooling performance under extreme conditions is highly sensitive to the temperature gradient between cyclic cold (e.g., night) and warm (e.g., day) periods. For instance, consecutive days with high nighttime outdoor temperatures deteriorate the cooling capacity of TES systems significantly [165]. Kuczyński & Staszczuk [166] indicated that the cooling effect and efficiency of increased thermal mass do not change during the heatwaves and remain independent of the duration and distribution of heatwaves. In their analysis, the use of concrete ground floors and walls in a detached single-family house, combined with nighttime ventilation and shading devices, substantially reduces the risk of overheating and the need for the installation of active cooling systems.

PCMs are applied mostly for energy-saving purposes but have shown some advantages in reducing overheating hours and improving thermal comfort. Similar to increased thermal mass, installing PCMs can reduce indoor air temperature variations [167]. The effectiveness of PCMs in overheating reduction in buildings relies on PCM properties and climate [168]. Some studies report a 50% reduction of discomfort hours [169,170]. However, Kuznik et al. [171] found that while the use of PCMs is beneficial in some periods during the year, it is not effective in very hot days because it remains liquid throughout the day. According to Ramakrishnan et al. [172] who optimized PCM melt temperature for resiliency, parametric optimization for the current heatwave events will not work for future heatwaves. Baniassadi et al. [173] analyzed the effectiveness of wall-integrated PCMs during the loss of air conditioning (i.e., power outage) coincident with heatwaves. They found that although PCM application can mitigate overheating during power outages, its resiliency is highly correlated to temporal factors (initiation time and duration of a power outage), PCM properties, and climate. They stated that the PCM melt temperature is a crucial factor in determining its resiliency. In most climates, the optimum melt temperature for resiliency differs from the optimum temperature for energy efficiency [173]. Considering the fact that energy efficiency is the main driver of the installation of PCMs, in most cases, there is no significant added resiliency advantage by using PCMs [173]. However, in some climates, there is a chance to select a melt temperature that has benefits for both energy efficiency and resiliency [174].

Common materials for thermal mass utilization are concrete, stone or masonry, bricks, and tiles. These materials are available all around the world as they do not necessarily require special technology to be produced. TES systems based on sensible heat such as water tank or underground storage methods are widely available, but devices based on latent heat such as PCM are mostly under development. The higher costs of PCMs is a barrier to widely enter the markets. The cost difference between sensible TES and PCM is even higher in active applications. Another barrier is related to the stability of the PCM materials. Further research and development are needed in PCM to adopt these technologies in more cost-effective manner.

4.2. Remove sensible heat from indoor environments

4.2.1. Ventilative cooling

Ventilative cooling (VC) uses the cooling potential of the outdoor air, and can be achieved with natural solutions (either by wind-driven or buoyancy-driven flows), mechanical technologies (fan), or a combination of both (i.e., mixed-mode or hybrid ventilation). Some studies [175,176] categorized VC into daytime comfort ventilation (or direct cooling) and night cooling (or indirect cooling). Daytime comfort ventilation introduces the flow of outdoor air through the building during the day to directly remove heat gains. It aims to improve the occupant's thermal comfort via convective heat transfer, increasing the evaporative cooling effect on the occupants' skin, and decreasing indoor air temperature. Night cooling has a double effect: on the one side it utilizes the building's thermal mass during the night, where thermal mass works as a heat sink during the occupied period, and, on the other side, it decreases indoor air temperature during the night hours.

The cooling performance of ventilation systems under extreme events is strongly correlated to ventilation types (natural or mechanical), building characteristics, local climate and occupant behavior [177,178]. Alessandrini et al. [179] investigated the overheating risk in a naturally ventilated dwelling during heatwaves under the weather condition of France, Paris. They observed that by natural ventilation, the maximum indoor operative temperature could be maintained 6–9 °C lower than the maximum outdoor temperature which reached 39 °C during the five days of heatwaves. Their study demonstrates that a well-designed natural ventilation system can mitigate the surging cooling demand during an extreme heat event. Architectural elements such as a solar chimney, atrium, or double-skin façade can help facilitate natural ventilation. A study by Lomas and Ji [180] demonstrated that buildings with such architectural elements integrated with advanced ventilation controls could provide greater resilience to future climate change than single-side natural ventilation.

However, ventilative cooling will be less beneficial when climate change makes heatwave events more frequent [181]. Artman et al. [182] quantified the effect of global warming on the night-time ventilative cooling potential in Europe. They compared the climatic cooling potential (CCP) index between monitored climate conditions (1961–1990, European Climate Assessment and Dataset) and possible future climate conditions (2071–2100, IPCC SRES scenarios A2, more divided world, and B2 [183], world more divided but more ecological). Their study indicated that future warming would have a significant impact on the night-time ventilative cooling potential across Europe. The CCP was expected to decrease by 20–50% in Central and Northern Europe by the end of the 21st century. At the same time, for Southern Europe, CCP was found to become negligible in summer and decrease by 20–55% during the transient season at the end of the 21st century. Campaniço et al. [177] evaluated the impact of climate change on direct ventilation for the Iberian Peninsula area. They predicted a 20% reduction of CCP in the future climate (2070–2100) along the annual cycle and up to 60% reduction in the summer season. The impact of climate change on the uncertainty of thermal comfort in a naturally ventilated office was investigated by Breesch and Janssens [184]. The probability of discomfort increases significantly when recent and warmer weather data sets are assumed. To reduce the risk of overheating in a warming climate, natural night ventilation should be combined with additional measures, such as mechanical ventilation coupled with cooling coil or passive cooling strategies (earth-air heat exchanger, indirect evaporative cooling), or increased thermal storage in the building. Mechanical ventilation increases resiliency, on the other hand, it will increase energy consumption. It is therefore recommended to perform a full life-cycle assessment to ensure energy efficiency and overheating resilience over the long-term building life span [185].

Natural ventilation through openings and other passive devices is widely available for most applications. Traditional examples developed through centuries of trial and error are modified to provide contemporary solutions. Mechanical ventilation techniques and solutions are also readily available for most applications. Both

natural and mechanical solutions are available on the marked reaching a TRL 9, although specific innovative solutions and control techniques are under development at different TRL levels.

4.2.2. Adiabatic/evaporative cooling

Evaporative cooling is based on an adiabatic process in which the sensible air temperature is reduced. Evaporative cooling may be classified into two main approaches: direct coolers (e.g., desert coolers) and indirect coolers (e.g., evaporative chiller units for fan coil) [186,187]. Direct evaporative cooling (DEC) evaporates the water directly into the air stream, while indirect evaporative cooling (IDEC) evaporates water into a secondary air stream. The secondary air stream cools the main air stream through a heat exchanger without adding humidity.

Direct evaporative cooling systems have been well known since ancient times. Several historical buildings in hot (and dry) climates show DEC solutions, such as the Ziza Palace in Palermo, Italy, or Red Ford in Delhi, India [188,189]. The efficiencies of DEC systems depend on the local wet bulb temperature depression, and they are best suited to hot and dry locations. Performance of IDEC depends on wet bulb effectiveness, dew point effectiveness, cooling power, power consumption, and coefficient of performance [190]. Water scarcity may limit the application of evaporative cooling systems in desert or semi-desert areas.

The impact of climate change on the cooling potential of evaporative cooling has been studied by Campaniço et al. [177]. The climatic cooling potential index has been calculated under past (1970–2000) and future weather conditions (2070–2100) in the Iberian Peninsula. A 10%-15% decrease in CCP (ventilative cooling) is expected in the further climate due to increased outdoor temperature, while evaporative cooling is shown to be more resilient to climate changes than ventilative cooling. Osman et al. [191] found that building design strategies in a hot and arid region should shift from natural ventilation to more active cooling by the year 2070, and that two-stage evaporative cooling comprised of DEC and IDEC is the most resilient strategy for all of Khartoum's seasons in the future climate. Furthermore, the population of arid regions is growing and climate changes are increasing human thermal stress in arid areas. Evaporative cooling solutions and green infrastructure (evapotranspiration from vegetation) are essential technologies supporting resilience, although the potential reduction in water availability requires high efficiency solutions.

Passive DEC systems are generally low cost, nevertheless, they need high maintenance to avoid microorganisms and connected diseases (e.g. legionella). DEC may be a valid dissipative system for open or semi-open spaces, in where the growth of air absolute humidity is mitigated by natural air movements [192,193]. In enclosed spaces, DEC systems can be controlled to prevent too high humidity values by adopting a control system. From the TRL point of view, several DEC systems have been installed in different building typologies. This technology is at the market level (TRL9), nevertheless, new researches are under development for new porous materials, and to develop specific systems connected to ventilative cooling solutions. In these cases, lower TRL may be found. Finally, movable simpler evaporation solutions (e.g. personal evaporator fan systems) independent by building system integration are commercialized in everyday shops.

4.2.3. Compression refrigeration

Vapor compression refrigeration is certainly the most used "active" technology to produce a cooling effect. The system mainly comprises an evaporator, a compressor, a condenser and an expansion device. A working fluid (refrigerant) successively flows through these components and follows a thermodynamic cycle [43].

Vapor Compression Air Conditioning units (ACs) can be classified by the heat source and heat sink (e.g. air, glycol–water, water, or soil), function (AC unit-cooling, heat pump-heating, reversible ACs- heating or cooling modes, AC with heat recovery – heating and cooling simultaneously), compressor technology, refrigerant type (natural or synthetic)), configuration [194] (packaged units (including window ACs and rooftop units), split ACs (including ductless mini-split systems, ductless multi-split systems and central ducted split-systems) and chillers (air-cooled, water-cooled, evaporative cooled). The other classification of interest when considering resilient technologies is cooling capacity. Vapor compression refrigerant technology covers a large range of cooling capacities going from a few hundred watts (household refrigerators) to tens of megawatts (industrial chillers and large-scale heat pumps) [44].

The cooling capacity of compression refrigeration systems is more constrained by the design and size of the machine than by the available capacity of the natural heat sink. Even though the COP of the system might decrease due to the high outdoor temperature during heatwaves, a well-designed system can still retain sufficient cooling capacity to confront the heatwave, indicating that compression refrigeration technology provides a high adaptive capacity. Hajidavalloo and Eghtedari [195] investigated the impact of outdoor air temperature on the COP of a split-air-conditioner with an air-cooled condenser. They found that when the outdoor temperature increases to 49 °C from 35 °C, the cooling capacity of this air-conditioner decreases to 5.6 kW from 6.8 kW, and COP decreases to 3.14 from 4.56. The study also found that this problem could be mitigated by using an evaporative-cooled condenser, which maintained the cooling capacity of the air-conditioner at 6.7 kW when the outdoor air temperature was 49 °C.

Vapor compression systems rely on electricity and are not very robust to the power outage. An approach to increase its robustness is to connect with local electricity production, such as photovoltaic (PV) panels in buildings. Chillers are more likely to operate simultaneously to PV electricity production compared with heat pumps, i.e., the highest cooling demand usually coincides with the large intensity of solar radiation. It is hence a good candidate to improve building self-consumption. On the other hand, chillers connected to energy storage (batteries, thermal storage units of building thermal mass) can also apply as a backup solution to the management of electrical grids by the flexibility provided by such combinations. This flexibility is activated by a time of use tariff as a demand side management (DSM) mechanism. It should be stressed that heatwaves lead to electricity peak demands on the grid and DSM mechanisms become of paramount importance. Average cooling demand around the world is responsible for 15% of peak electricity demand; but during hot days, cooling can be responsible for up to 50% and more of residential peak electricity demand [196]. Moreover, for buildings equipped with on-site generation, the use of thermal storage combined with specific net-metering programs can promote better load matching between production and consumption [197]. Another approach is to integrate the vapor compression system with ice storage systems, which can help limit the impact on the electricity grid of highly fluctuating distributed renewable energy sources. Actually, they offer a mechanism of building electricity consumption flexibility that can take profit of dynamic electricity rates.

Vapor-compression ACs for buildings, with a wide range of capacities and numerous configurations, show TRL values of 9. In 2020, roughly 2 billion AC units were in operation in the world, with residential ACs representing 68% of these units [196]. The market of AC units is growing in an accelerated way, with estimated sales increasing by 10% between 2018 and 2019 (mainly in emerging and developing countries) [196]. Building contractors and engineering offices define the most appropriate cooling/heat-

ing plants depending on the availabilities of heat sink/heat source, on the building characteristics, on the ease of installation, on the cost of the solutions, on the cost of energy (and the presence of local electricity production), on local regulation/incentives, but also on the customer's expectations. AC efficiency rating varies from one country to another, but it is always an image of the ratio of the cooling effect to the electricity consumption (W/W). Average efficiency rating of installed AC units has increased by 15% between 2010 and 2020 [196], but still far behind the most efficient products on the market [196].

4.2.4. Absorption refrigeration including desiccant cooling

Desiccant cooling systems were developed to handle sensible and latent heat loads independently [198]. The dehumidifier absorbs the moisture of the supplied air and afterward will pass to the regeneration unit to recover its initial moisture absorption capability [199]. The dry supplied air stream passes the cooling unit for sensible cooling and is then routed to the conditioned space. Additional heat exchangers could be added on different points such as economizers to increase the system efficiency.

Desiccant systems are classified as solid or liquid desiccators [200]. A rotary wheel with solid dehumidifiers is a compact system made from matrix-shaped parallel channels coated with desiccant material, such as SiO_2, $TiSiO_4$, or Al_2O_3, that operate continuously with low corrosion probability [198]. The liquid desiccant materials, such as ClLi, LiBr, $CaCl_2$, TEG HCOONa, HCOOK, CH_3COONa, CH_3COOK, or a combination of these solutions, ideally should be stable, odorless, non-toxic, non-flammable, inexpensive, non-crystalized in the operating temperature range, non-corrosive and non-volatile with good heat transfer characteristics and low surface vapor pressure at the contacting temperature [201]. The low cooling capacity of solid desiccants and the corrosivity of liquid desiccants are important limitations. Therefore, new desiccants including bio-desiccants, composite desiccants, and polymer desiccants have been introduced; some of them could provide an absorption capacity 2–3 times of traditional absorbers [202].

The major benefits of absorption cooling are discussed in Refs. [198,203,204]. The system uses eco-friendly fluids including air and water, which have no negative impact on the environment. It could operate with diverse thermal energy sources, even low-grade resources, in the regenerators. The required electrical energy can be less than 25 % of conventional refrigeration systems and this technique acts as an energy-efficient method, especially for hot dry and hot humid areas. Finally, the desiccant cooling system works near atmospheric pressure, which makes them easy to construct, install, preserve and maintain. The major limitation of desiccant cooling is that it needs an additional heat source for regenerating the desiccant to provide stable operation [199]. However, the heating power can be provided by any source such as the waste heat from industries through a district heating network or via solar collectors or ground source heat pumps. This improves the overall efficiency of desiccant coolers because the heat requirement can be gained from sources with lower primary energy factor, i.e. waste heat from a combined heat and power plant, industry or solar energy which are also available during the cooling season. Moreover, to make the system more environmentally friendly, the required electrical power can be provided by renewable sources, for example, tidal energy in marine facilities, solar cells, or wind turbines.

High outdoor air temperature during a heatwave might decrease the efficiency of absorption refrigeration systems, depending on the type and design of the systems. Kim et al. [205] simulated the cooling performance of an air-cooled LiBr–water absorption chiller in extremely hot weather. It was found that when the ambient temperature increases to 50 °C from 35 °C, the cooling capacity of the absorption chiller decreases 37.5% and 35.6% for direct air-cooled chiller and indirect air-cooled chiller compared with their cooling capacity at 35 °C, respectively. Grzebielec et al. [206] confirmed that the outdoor air temperature plays an important role in the efficiency of absorption refrigeration. However, by using a spray-evaporative heat exchanger, the effect of outdoor temperature can be reduced and the average cooling capacity can be up to 44% higher than those with dry air cooler devices.

Although the absorption refrigeration systems are partially activated by thermal energy, the systems are not robust during the power outage events because the cooling water distribution system cannot operate without power input. Like compression refrigeration, the system could integrate local electricity production and energy storage to increase its resilience during the power outage.

Desiccator wheels are used for residential and primarily for non-residential purposes. However, these usually use a simple system with basic equipment and more advanced systems are not widely implemented, though. Desiccant cooling technology could be categorized in TRL 9 according to the Technology Readiness Assessment Guide issued by the U.S. Department of Energy [207]. TRL 9 signifies that the technology operates and can achieve defined requirements. For instance, desiccators can be used in various applications and are available in the market [208,209]; therefore as a mature technology providing cool and dry air, desiccant coolers can be categorized in TRL9.

4.2.5. Ground source cooling

The working principle of ground-source cooling is based on the fact that the ground temperature below approximately 10 m remains fairly constant all year round at about mean annual ambient air temperature [210]. Thus, ground temperature over the cooling period is less or not affected by hourly and daily temperature variations, regardless of outside air temperature. It rejects heat to the ground by circulating a working fluid through ground heat exchangers. Based on the heat transfer medium (air or liquid), the system can be further categorized as an earth-to-air heat exchanger (EAHE) or a borehole heat exchanger (BHE). Ground-source cooling can also be classified as direct ground cooling (passive) or ground-source heat pump (active). The direct-ground cooling system utilizes ground as the only source for cooling the working fluid without any mechanical refrigeration. In a ground-source heat pump system, the cooling is provided through a mechanical refrigeration system using the ground as a sink for dissipating the heat [211]. Ground source systems may also be used to pre-heat a heat transfer medium in winter seasons, nevertheless, for this paper, only their cooling potential is analyzed.

Since the subsurface temperature below a certain depth is insensitive to seasonal and diurnal variations, ground-source cooling shows a high resilience under heatwaves. However, the cooling capacity of ground-source cooling might be affected by climate change. The sensitivity of ground-source cooling (EAHE) to future climate was investigated by Chiesa et al. [212] considering historical and future North America climate conditions - future climate were based on Five General Circulation Models (GCMs) from the CMIP5 (Coupled Model Intercomparison Project Phase 5) multi-model ensembles [213]. Results showed an expected reduction in climate EAHE sensible cooling dissipative potential in future years, while variations in the soil surface average temperature were identified to be a synthetic index to analyze variations in EAHE cooling potentials.

Several measurement studies have shown that ground-source systems perform better under peak-load conditions than under off-peak load conditions [214–216]. This is partly because under peak load conditions the ground heat transfer is higher, due to a larger temperature difference between working fluid and the ground. The percentage share of the parasitic energy consumption

of circulation pumps and other auxiliary equipment under peak load conditions is also lower. Passive ground-cooling systems have larger absorptive capacities than active ground-cooling systems because they are bigger and because of their greater ability to adjust the working fluid conditions to match the cooling demand of the building. The systems can adjust to extreme events including heatwaves in many ways, such as by pre-cooling the building at night and off-peak periods, by using active thermal energy storage systems like chilled water or ice storage for load shifting, or by reducing peak loads at the expense of lower thermal comfort. The restorative capacity of ground-source cooling systems under heatwaves is high, as the heat injected into the ground is dissipated to the earth surrounding the ground heat exchanger. This can be done using dry coolers at nighttime when the ambient air temperature is lower. Depending on the soil's thermal diffusivity, it can take several hours to a few days for the system to fully recover from heat injections to the ground [217,218]. However, the impact of different recovery times have on the restorative capacity of the ground is generally considered in the design of ground-cooling systems.

The resilience of ground-source cooling systems to power outages depends on the degree of disruption and the type of the ground cooling system. The ground-source heat pump systems require substantial electrical energy to operate the refrigeration cycle and the auxiliary components. The direct-ground cooling systems require much less electricity as the only energy input to the system is the work required to drive the circulation pumps.

At the system level, ground-source cooling is a fully mature technology at TRL 9. It has been used worldwide for several decades and there are thousands of actual systems operating over the full range of possible conditions. There exists a great wealth of knowledge concerning design methods, installation procedures, operating practices, and application examples in literature. Moreover, there are several scientific and professional bodies defining norms and standards, protocols and guidelines, and best practices at local, national, and international levels. At the subsystem level, the heat exchangers and grouting materials used in ground-source cooling systems are widely available commercially and are at TRL 9. Nevertheless, there is still ongoing research into developing innovative heat exchanger designs and materials to enhance the ground heat transfer. The TRLs of the new developments range from early lab-scale (TRL 1–3) to commercial demonstration (TRL 8).

4.2.6. Sky radiative cooling

Sky radiative cooling represents the passive process in which any object located on the Earth's surface (sky facing terrestrial object or surface) releases heat to the sky through net loss of long-wave (thermal infrared) radiation [219,220]. The incident solar radiation during the day, the convective heat transfer (for a higher outdoor air temperature than the radiator temperature), and cloud coverage can have a negative impact on the net cooling output [92,221–226]. Thus, currently, this technology is mostly associated with nighttime, when the sky can reach temperatures below 0 °C [222,227] and there is no incident solar radiation. Still, the radiative heat exchange with the sky can take place both during night and day. Heat can be released in the broadband (4–30 μm) or a selective band (8–13 μm), the latter leading to a higher efficiency during an all-day cycle [92,228]. Thus, ideal material properties for radiative cooling should present a maximum reflectivity in the short-wave range (0.25–2.8 μm) to reflect solar radiation while the emissivity should be as close as possible to unity especially in the atmospheric window band (8–13 μm) and zero otherwise [92,228].

In buildings, roof paints can be employed as a passive radiative cooling solution to increase both solar reflectivity and emissivity of the surfaces, although this may increase the heating energy use during the heating season [92,228]. However, buildings can also make use of roof ponds, movable insulation systems, radiators, or existing solar heating systems integrated as passive or active systems (with or without pumps and fans) that extract the heat from the indoor environment and release it to the sky [92,226,228]. This way, sky radiative cooling presents the ability to restore the indoor thermal environment to its original state, making it a resilient cooling technology.

Nevertheless, as the cooling potential is influenced by air temperature, relative humidity, air speed, and clouds (e.g. the cooling potential is decreased in very hot and humid environments) [222,224–226] its restorative capacity is dependent on the outdoor climate. Thus, like other renewable energy technologies (e.g. wind, solar), its recovery speed (rapidity of the restorative capacity) can vary as well with the outdoor environmental conditions. Furthermore, the presence of solar radiation makes sky radiative cooling time dependent. As objects (e.g. other buildings) can block the radiative heat exchange with the sky while lack of space can drastically reduce the surface area facing it [220,228], their restorative and recovery capacities can be further limited in dense urban environments. Clouds, if present for a short and long period (hours to days), will reduce both its restorative and recovery capacity for the respective period. Still, even for a clear sky when the radiative heat exchange is not hindered by clouds, the convective heat exchange could counter its effect for a high outdoor temperature [221–226]. Therefore, the best sky radiative cooling solution must be chosen according to the climate and setting (high versus low building density), i.e. good planning is required for a high exploitation potential.

If used passively, sky radiative cooling cannot be adequately controlled and relies solely on favorable environmental conditions and material properties to achieve its maximum potential. However, reduced time dependency and a constant recovery speed could be achieved by employing night radiative cooling actively combined with different storage techniques (e.g. building thermal mass, storage tanks). This would allow the system to store cooling during periods with favorable conditions and use it at later times when the sky radiative cooling potential is limited. Furthermore, when using the technology actively, parameters such as the flow rate of the heat storage medium can be controlled [220,221,223,229], allowing higher exploitation (higher recovery speed), especially during periods when the potential is high, thus using the available resources in a timely manner.

After heatwaves, the sky radiative cooling's restorative capacity was rated as low to moderate, as the cooling capacity could be reduced by increased humidity and outdoor temperatures also during night time [92,225,228]. For example, an increase in relative humidity (50 to 100%) and outdoor air temperature (9 K) could reduce the cooling power of thermal solar collectors by 18% to 41%, respectively [225]. However, recent progress in solar reflective materials with high emissivity in the atmospheric window may further enhance the sky radiative cooling's restorative capacity as cooling could be achieved concurrently with the demand, i.e. during the day [92,228]. Blackouts would not pose an issue and thus the sky radiative cooling restorative capacity after blackouts was rated as moderate. The recovery speed on the other hand could vary between low and high depending on the way sky radiative technology is employed, passively or actively. If the technology is passively used, no additional auxiliary energy (e.g. pumping power) would be required to start the process. Therefore, in those situations, the recovery speed can vary from low (unfavorable environmental conditions) to high (favorable environmental conditions) during both heatwaves and blackouts. On the other hand, active use could ensure an increased recovery speed through an increased flow rate of the heat transfer medium (e.g. air, water).

Although not an issue for short-term blackouts, one challenge for active use during a long-term blackout, e.g. days, would be ensuring the circulation of the heat transfer medium. In those situations, without backup power the recovery speed would be low.

As the sky is a free cooling source, night sky radiative cooling is a renewable technology available for any consumer. Moreover, it is ready for market implementation since it can be employed through existing technologies such as solar collectors and PV/Ts [222,223,225]. However, further development and research can improve and optimise both the equipment and the systems employed, especially for daytime use [92,228]. Although it can be used directly by any consumer, the experience of design engineers and building contractors might improve its use leading to an optimum operation of the desired application.

4.2.7. High-temperature cooling system: Radiant cooling

A hydronic radiant cooling system refers to a system in which water is the heat carrier and more than half of the heat exchange with the conditioned space is by radiation [230,231]. Heat transfer from indoor spaces is by a combination of radiation and convection via cooled surfaces. The convection is usually natural, unless the air movement over the conditioned surface has been enhanced—e.g., by supplying air from a ventilation diffuser. These systems employ high-temperature cooling, where the heat-transfer medium is near room temperature. The system conditions large surfaces in indoor spaces, usually floors, ceilings, and walls, and the large conditioned surface areas make it possible to cool indoor spaces with a small temperature difference between the conditioned surfaces and the room. Supply water temperatures in radiant systems are usually 16 – 23 °C for cooling.

Radiant cooling systems can be classified as radiant cooling panels, radiant surface systems, and thermally active building systems (TABS) [230]. Radiant panel systems and radiant surface systems can be used in both new buildings and renovated buildings. However, TABS needs to be installed in the construction phase of a building, which limits the use of TABS in renovation projects. To address this limitation and to bring the benefits of TABS to renovation projects and to lightweight buildings, a particular type of radiant ceiling panels has been emerging. This technology combines PCMs with radiant ceiling panels to create a similar system to TABS—i.e., PCM radiant ceiling panels. Pipes are embedded in the PCM. Water is circulated in pipes to control the charging (melting) and discharging (freezing) behavior of PCM, which in turn controls the thermal environment in indoor spaces. This is a promising solution and has been proven to perform similar to TABS in terms of operation, energy performance, heat removal from rooms, and resulting thermal indoor environment [232–235].

Radiant cooling systems have many benefits compared to more conventional (e.g., all-air) cooling systems. The use of high-temperature cooling enables the system to couple to natural heat sources and sinks, such as ground, lake water, or seawater [236–238]. It also creates favorable operating conditions for heating and cooling plants (mainly due to operating temperature ranges and return temperatures), increasing the efficiencies of heat pumps, chillers, and boilers [81 83]. Radiant cooling systems have the possibility of transferring peak cooling loads to off-peak hours, reducing peak power demand [237]. Further benefits of radiant systems have been summarized by Kazanci [206]. One of the major characteristics of radiant systems is that they address only sensible heating and cooling loads. Therefore, they need to be coupled with ventilation systems, usually in the form of a dedicated outdoor air system (DOAS). The main function of ventilation systems is to regulate humidity (i.e., to dehumidify the air) and provide fresh air to indoor spaces [230]. There are various combinations according to the location of radiant surfaces and air distribution principles. A summary of the coupled system configurations and their performance in terms of thermal comfort and air quality have been systematically discussed in [239].

Radiant heating and cooling systems can be applied in almost all climates and building types. The main challenge for using radiant cooling systems is avoiding condensation; therefore, its applications in humid climate zones require careful design and operation considerations. Studies have shown that when properly designed, controlled, and coupled with an appropriate ventilation system, radiant cooling systems can also be applied in hot-humid climate zones without problems [240–243].

Radiant systems have similar characteristics under heatwaves and power outages. The absorptive and adaptive capacities of radiant systems under heatwaves and power outages range from low to high - low for radiant ceiling panels, high for TABS, and in between those two systems for the radiant surface systems. This is because these systems have different amounts of thermal mass, and, therefore have different operations, heat removal, and heat storage characteristics. For example, due to the available thermal mass, TABS can provide cooling even if there is no active heat removal from the TABS structure for a period (e.g., no chilled water circulation in the pipes in case of a power failure) and under a heatwave, the pre-cooled thermal mass will be able to absorb a certain amount heat from the space.

The restorative and recovery capacities of radiant systems under heatwaves and power outages are high. This is because all system types have the ability to return to normal or improved operation once the heatwave is over or power is back, and this can be done immediately.

The previously described radiant cooling systems (i.e., radiant cooling panels, radiant surface systems, and TABS) are available in the market. These systems and their components can be purchased by building owners (e.g., for a residential building) and also by building contractors. Note that, whereas the radiant ceiling panels with PCMs that were described in this chapter, are not yet available in the market, all of their individual components are market available (i.e., PCMs, piping, and metal panels).

4.3. Enhance personal comfort apart from space cooling: Personal comfort system

A personal comfort system (PCS), also known as personalized conditioning system, is a device to heat and/or cool individual occupants directly or heat and/or cool the immediate thermal environment of an individual occupant, under the control of the occupant without affecting the thermal environment of other occupants [244].

In contrast to total volume systems which condition entire indoor spaces, PCS devices condition the immediate surroundings of the occupants, creating micro-environments that can (1) extend the range of temperatures that is generally perceived as comfortable, thereby reducing the energy used by mechanical space conditioning; and (2) accommodate the interpersonal thermal differences that are inherent in any occupancy, thereby increasing the percentage of comfort in the space over that possible with uniform environmental control. The improved comfort may also increase occupants' productivity.

Cooling PCS devices may involve the following technologies:

- Vertical-axis ceiling fans and horizontal-axis wall fans (such fixed fans differ from pure PCS devices in that they may be operated under imposed central control or under group or individual control)
- Small desktop-scale fans or stand fans
- Furniture-integrated fan jets
- Devices combining fans with misting/evaporative cooling

- Cooled chairs, with convective/conductive cooled heat absorbing surfaces
- Cooled desktop surfaces
- Workstation micro-air-conditioning units including personalized ventilation, some including phase change material storage
- Radiant panels (these are currently used less for PCS than for room heat load extraction)
- Conductive wearables
- Fan-ventilated clothing ensembles
- Variable clothing insulation: flexible dress codes, variable porosity fabrics.

PCS devices offer both comfort and energy benefits. PCS devices use very small amounts of energy, making them inherently suitable for resilience applications and adaptable for use during energy emergencies. PCS devices allow occupants to personally control their thermal microenvironments and thereby satisfy their individual comfort requirements. Such comfort requirements differ due to variations in gender, age, body mass, clothing habits, and metabolic rate, and thermal adaptation [245]. The only published case of a field study of office workers reporting 100% satisfaction involved PCS installed in each workstation [246]. In a large-scale field study, Kroner and Stark-Martin [247] suggested that it is possible to increase productivity by at least 2% using PCS.

PCS devices offer an opportunity to save HVAC energy in buildings. Since it is possible to relax the room temperature range in either the hot or cold direction due to the use of personalized heating, ventilation or cooling, total HVAC energy use can be reduced at a rate of 10% per K room temperature setpoint relaxation [248,249]. Savings of this magnitude exceed those of virtually any energy-conserving technology available in the industry. Widening the temperature range for energy must continue to ensure occupants' comfort, or at least provide the same level of comfort as in current buildings. Occupants themselves require far less energy to heat and cool than does the entire indoor space that houses them. PCS offers the opportunity to accomplish this. With small amounts of energy, it can provide individual comfort within a broader range of indoor ambient temperatures (varying over both time and space).

The application of PCS enables relaxing the temperature requirements for the ambient zones in buildings. This is based on the assumption that the occupants have available to them individually controlled PCS devices at their workstations and that there is general elevated air movement provided in other zones of the building where they may spend time. Advantages for resilience include

- Flexibility in space heating and cooling temperature setpoints - the possibility of extended setpoints compared to traditional systems such as extending the room temperatures below 20 °C in the heating season and extending the room temperatures above 26 °C in the cooling season; these temperatures are based on the Category II of EN 16798–1:2019 [250]. This possibility will allow operating flexibility and will not load the cooling plant unnecessarily during an extreme event (e.g., a heatwave) or coming back to normal operation after an extreme event, and occupants can still be comfortable at high indoor temperatures, as they would have personalized cooling systems.
- Possibility of reduced-size cooling plant or a plant that is run part-time during periods beneficial to the electricity grid and supply sources.

PCS devices have no absorptive capacity under heatwaves, as absorptive capacity mainly relates to building envelope and structure. Under heatwaves, PCS devices have a high adaptive capacity as PCS or the user controlling the PCS can adjust its cooling output until its maximum capacity.

PCS devices have no absorptive capacity under power outage events, as absorptive capacity mainly relates to building envelope and structure. Assuming that there are no batteries or emergency power generators during the power outage, PCS have a low adaptive capacity as only certain PCS technologies will be able to keep on functioning (such as conductive wearables, fan-ventilated clothing ensembles or PCM assisted PCS).

PCS devices have high restorative and recovery capacities under heatwaves and power outage events, as the PCS will be functioning normally once the heatwave or power outage is over, and it will be able to recover immediately as long as the system has not been physically damaged.

PCS devices are applicable in all climate zones. The above-listed PCS devices are commercially available; however, their availability could change from country to country. Even though there are commercially available products, the technology is not as mature as some of the other technologies e.g., compression refrigeration.

4.4. Remove latent heat from indoor environments: High-performance dehumidification including desiccant dehumidification

Removing latent heat from indoor environments through dehumidification is an essential and important method, especially in hot and humid climates, to reduce cooling load and increase human comfort [251]. In high-performance buildings, the percentage of dehumidification energy consumption from the building's total energy consumption can be as high as 13–22 % [252]. There are many dehumidification methods reported in the literature and applied in practice, including desiccant dehumidification, refrigeration dehumidification, ventilation dehumidification, and thermos-electric dehumidification. Desiccant dehumidification is to utilize the humidity-absorbing material to absorb moisture. Refrigeration dehumidification uses a conventional vapor compression cycle to dehumidify the humid air through cool-reheat processes. Thermos-electric dehumidification is to utilize the thermoelectric effect (Peltier effect) to convert electricity into a temperature difference across a Peltier module. The module includes cold-side heat sink and hot-side heat source. Humid air driven by the fan flows over the cold side heat sink and the air is dehumidified. Ventilation dehumidification replaces humid indoor air with dry outdoor air.

Dehumidification technologies absorb the impacts of heatwaves by decreasing the humidity of indoor air, which improves the comfort level and relieves part of the pressure of other cooling systems. Desiccant refrigeration (see Section 4.2.4) and thermos-electric dehumidification technologies work in principle in areas with humidity higher than comfort level, while ventilation dehumidification technology works in areas with dry outdoor air. Desiccant, refrigeration, thermoelectric dehumidification, and mechanical ventilation dehumidification each require electricity and therefore are not very robust to power outages. Ventilation dehumidification through natural means could operate during a power outage, but its capacity to remove latent heat depends on building characteristics, local climate, and occupant behavior (see Section 4.2.1). Although dehumidification technologies could improve the thermal comfort level during a heatwave or recovery the thermal condition after a heatwave, their cooling capacity is limited due to the fact, they only take care of the latent heat in the indoor environment.

All these technologies have been well developed and commercial products are available in the market in the forms of either large dehumidification plants or small household dehumidifiers. Both individual consumers and building contractors are quite free to

purchase dehumidification products, although the desiccant dehumidification plants are usually purchased by building contractors.

5. Assessment and comparison of resilient cooling strategies

A qualitative assessment of the resilience of cooling strategies is performed based on the criteria developed in Section 2. The resilience criteria include absorptive capacity, adaptive capacity, restorative capacity and recovery speed. Different disruptions or extreme events will have different effects on the cooling systems. 'Temperature hazard' was identified as the primary risk associated with the cooling strategies in buildings, which represents the overheating risk in buildings that threatens human health, activities and productivity [253]. Heatwave and associated power outages are identified as major disruptions because they have direct impacts on the thermal environment of buildings and they are listed as dominant threats faced by cooling systems, as stated by Attia et al.[23]. Therefore, the four resilient cooling criteria are evaluated separately for two extreme events in this study: heatwave or power outage. The resilient cooling strategies assessment framework is illustrated in Fig. 4.

We present the following approach to evaluate the resilience characteristics.

- **Absorptive capacity** can be calculated as the ratio of the absorbed heat load (or heat storage) to the change in heat load during a certain disruption.
- **Adaptive capacity** can be calculated as the ratio of the heat load reduction to the change in heat load during a certain disruption.
- **Restorative capacity** can be calculated as the ratio of the heat removed from the building to the heat stored after a certain disruption.
- **Recovery speed** can be calculated as the time required to remove the stored heat from a building until reaching a designed thermal condition.

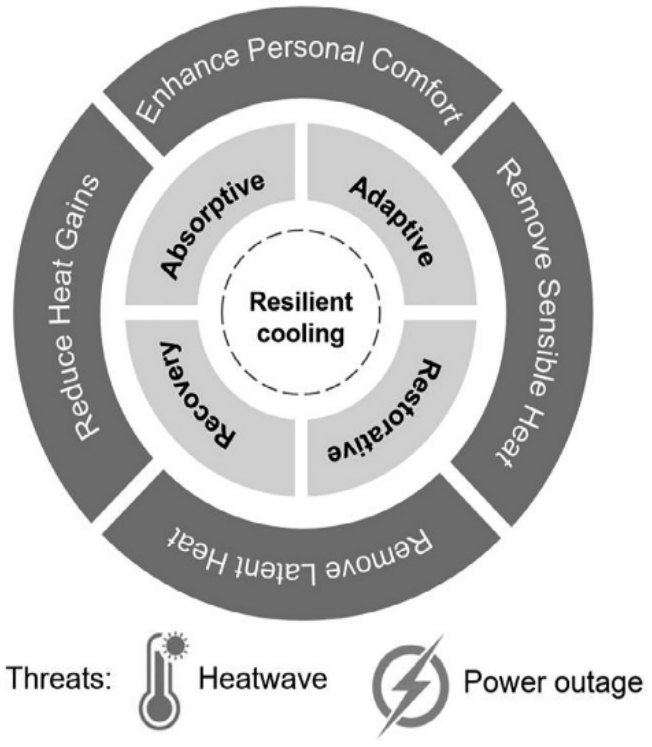

Fig. 4. Resilient cooling strategies assessment framework.

The resilience capacities can be evaluated into three categories: high, moderate and low. For recovery speed, high is within one hour, moderate is several hours, and low is one or more days. The other capacities are categorized by the following criteria:

- High: the strategy can maintain or even increase its cooling or heat-load-reduction capacity during a certain event. For example, a building's heat load might double during a heatwave or power outage due to the extreme high outdoor temperature or the failure of the mechanical cooling system. (The strategy can increase its cooling capacity to deal with a high heat load during a heatwave or power outage.)
- Moderate: the strategy can maintain its cooling or heat-load-reduction capacity most of the time during a certain event. (The strategy keeps the same cooling capacity during a heatwave or power outage.)
- Low: the strategy will experience a decrease in cooling or heat-load-reduction capacity during a certain event. (The strategy reduces cooling capacity during a heatwave or power outage.)

Besides the resilience capacities under extreme events, the cooling strategy's applicability in terms of climate zone and technology readiness level are summarized in Table 3. The climate zone classification is based on ASHRAE Standard 169 [254], as illustrated in Fig. 5.

A qualitative method is used in this study, which relies on the literature review carried out in Section 4 and focus group discussion. IEA-EBC Annex 80 participants were invited to provide evaluations of the resiliency capacities for all cooling strategies based on the categories proposed above. The participants are scientific and professional experts in the field of cooling technologies and building environments. The collected results were compared and discussed within the focus group based on the results of the literature review and their expertise and experience, to reach a final rating for each cooling strategy.

Table 3 presents assessment results of different cooling strategies where addresses the four resiliency criteria, application and technology readiness level. We obverse that cooling strategies contributing to reducing heat gains to the indoor environment generally show a moderate to high absorptive capacity under heatwaves. These strategies, such as solar shading/glazing, cool envelop materials, ventilated or evaporated envelop and thermal mass, mainly relate to the design of building structure and envelope, and should be considered in the early design phase of the buildings.

The cooling strategies with dynamic or flexible control present a high adaptive capacity under heatwaves. For example, a well-designed mechanical cooling system, such as compression refrigeration, absorption refrigeration, or active cooling with natural heat sink, could adjust its cooling capacity to fulfill the demand based on the change of the indoor and outdoor conditions or even prepare the system before the extreme event occurs if predictive control is available. However, active cooling systems strongly rely on the power supply and are not robust to the power outage. As mentioned in Section 4, an alternative approach to increase their robustness is to have local or on-site power production or connected to electrical or thermal energy storage. Another group of cooling strategies that show a high adaptive capacity under heatwaves is PCS devices, such as local fans, local cooled surfaces, or wearable systems. Instead of providing space cooling, these devices could enhance personal heat loss, and allow thermal comfort with higher ambient temperatures. In addition, PCS allow personal control of the microenvironment without affecting the thermal environment of other occupants. Even though PCS devices require a power supply, they could reduce cooling plant size or run part-time during periods beneficial to the electricity grid and supply sources.

Table 3
Assessment of cooling strategies, in term of resilience capacities, applicability, and technology readiness.

Cooling-strategy categories	Cooling strategies	Resilience under extreme events								Climate zone	Technology readiness level (TRL)
		Heatwave				Power outage					
		Absorptive capacity	Adaptive capacity	Restorative capacity	Recovery speed	Absorptive capacity	Adaptive capacity	Restorative capacity	Recovery speed		
A	Static solar shading/glazing	Low-Moderate	Low	N/A	N/A	Low-Moderate	Low	N/A	N/A	All	9
	Dynamic solar shading/glazing	Moderate-High	High	N/A	N/A	Low	Low	N/A	N/A	All	9
	Cool envelope materials	High	N/A (High for thermochromic CEMS)	N/A	N/A	High	N/A (High for thermochromic CEMS)	N/A	N/A	All (preferable for 0-4B)	Light-colored and cool-colored CEMs: 9; other CEMs: 4–6
	Green roofs, roof pond, and green facades	High	Moderate- High (Low for some plant species)	Moderate-High (Low for some plant species)	Moderate-High (Low for some plant species)	High	Moderate-High (Low for some plant species)	Moderate - High (Low for some plant species)	Moderate-High (Low for some plant species)	All	Green roofs and façades: 9 - roof ponds and evaporative systems: 4–8
	Ventilated roofs and facades	Low-Moderate	Moderate - High	Moderate-High	Moderate-High	Moderate-High for passive system; Low for activity system	Moderate for passive systems; N/A for active systems	Moderate - High	Moderate-High	All	4–9
	Thermal mass including PCMs	High	N/A	Low-High	Moderate	High	N/A	Low - High	Moderate	All (less effective 0–2)	4–9
B	Passive ventilative cooling	Low	Moderate	Moderate	Low - Moderate	Moderate-High	Moderate	Moderate	Low - Moderate	All (less effective in 0A, 0B, 1A, 1B)	9
	Active ventilative cooling	Moderate	High	High	Moderate - High	Low	N/A	High	Moderate - High		
	Adiabatic/ evaporative cooling	Moderate	High	High	Moderate - High	Moderate	Moderate	High	Moderate-High	All except 0A, 1A	9
	Compression refrigeration	N/A	High	High	High	N/A	N/A	High	High	All	9
	Absorption refrigeration including desiccant cooling	N/A	High	High	High	N/A	N/A	High	High	All (preferable 0A,1A, 2A)	9
	Passive ground source cooling	Moderate	Moderate	High	Moderate - High	High	Moderate	High	Moderate - High	All	9
	Active ground source cooling	High	High	High	Moderate - High	N/A	N/A	High	Moderate - High		
	Sky radiative cooling	N/A	N/A	Low-Moderate	Low-Moderate	N/A	N/A	Moderate	Low - Moderate	Increased performance in climates that are cold or with high seasonal variation (4, 5, 6) and dry (C, B) compared to hot and warm (2, 3) humid (A) climates.	7–9
	High-temperature cooling system: Radiant cooling	Low - High	Low - High	High	Moderate - High	Low - High	Low - High	High	Moderate - High	All	9

Table 3 (*continued*)

Cooling-strategy categories	Cooling strategies	Resilience under extreme events								Climate zone	Technology readiness level (TRL)
		Heatwave				Power outage					
		Absorptive capacity	Adaptive capacity	Restorative capacity	Recovery speed	Absorptive capacity	Adaptive capacity	Restorative capacity	Recovery speed		
C	Personal comfort systems	N/A	High	High	High	N/A	N/A or Low (e.g., fan-ventilated clothing ensembles)	High	High	All	5–9
D	Dehumidification including desiccant dehumidification	N/A	Moderate- High	Moderate	Moderate	N/A	N/A	Moderate	Moderate	All (preferable 0A,1A, 2A)	9

The cooling strategies used to remove sensible and latent heat present moderate to high restorative capacity. Mechanical cooling systems, such as compression refrigeration and absorption refrigeration can efficiently remove the surplus heat from the indoor environment in a timely manner regardless of the outdoor climate. However, the cooling systems utilizing natural heat sinks can remove the surplus heat only when there is a temperature difference between heat sinks and the indoor environment. Depending on the physical properties of natural heat sinks, ground-source cooling and evaporative cooling are more efficient than ventilative cooling under heatwaves. The recovery speed of cooling systems is influenced by the cooling potential (cooling capacity of mechanical systems, the temperature difference between natural heat sinks and indoor environment for natural or hybrid systems), design of the cooling system (for example, the window opening area and amount of thermal mass), and control or operation of the cooling system (for example, occupant behavior on window opening). In some situations, a certain cooling or building design might benefit to one resilience criteria but results in a negative impact on the other criteria. For example, a building with heavy thermal mass might have a high absorptive capacity, but have a low recovery speed due to all the stored energy that needs to be removed before the indoor environment can return to acceptable thermal conditions.

6. Discussion

6.1. Findings and recommendations

This section presents the primary findings of this study and provides recommendations to the building designers and engineers on how to address resiliency characteristics in the early design stages.

1. Resilience should be considered as an important property for cooling systems integrated with the building, together with energy efficiency, sustainability and economic affordability. Energy efficient cooling strategy does not equal to resilient cooling strategy. Sometimes, "Excessive striving for energy efficiency" could compromise a building's ability to maintain comfortable thermal conditions during extreme events.
2. The resilient characteristics of cooling strategies are summarized by four criteria – absorptive capacity, adaptive capacity, restorative capacity and recovery speed. The definition of the criteria and a qualitative approach for evaluating the resilience characteristics are proposed in this study.
3. As suggested by Attia et al. [23] and Miller et al. [253], the assessment of resilience must be based on the identification of a specific threat or disruption. 'Temperature hazard' is identified as the primary risk associated with the cooling systems in buildings, and heatwave and associated power outages are identified as major disruptions since they have direct impacts on the thermal environment of buildings.
4. Cooling strategies for reducing heat gains to the indoor environment present high absorptive capacity under heatwaves. These cooling strategies strongly relate to the design of building structure and envelope, and should be considered in the early building design phase. Cooling strategies with dynamic or flexible control present a high adaptive capacity under heatwaves. These strategies could adjust their operating mode depending on the indoor and outdoor condition or even prepare the systems or buildings before the extreme event occurs. PCS devices also present high adaptive capacity, which could allow thermal comfort with relatively higher ambient temperatures and provide personal control over the microenvironment without affecting the thermal environment of other occupants. Cooling

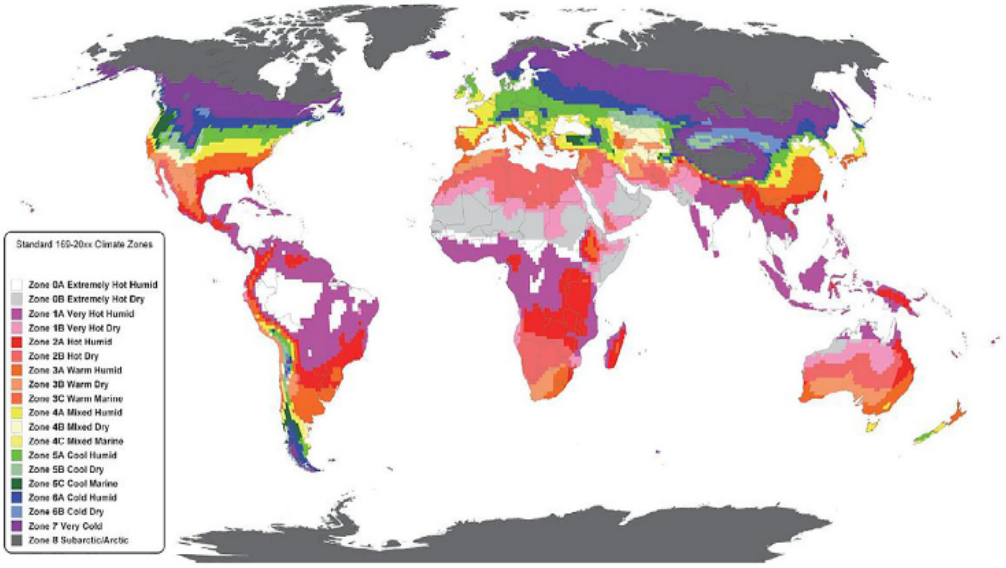

Fig. 5. Climate zone classification scheme used in ASHRAE Standard 169 [254]

strategies for removing sensible and latent heat present high restorative capacity. The mechanical cooling systems can remove surplus heat from the indoor environment efficiently without being influenced by the outdoor climate. For those cooling strategies that use natural heat sinks, such as air, water, ground and sky, the temperature difference between the heat sink and indoor environment is critical for the efficiency of these cooling strategies. The recovery speed (rapidity) of cooling strategies depends on multiply factors, such as cooling potential, design of the cooling system and control or operation of the cooling system.

5. To attain resilient cooling, the four resilience criteria should be considered from the design phase. The building and relevant cooling system characteristics should be considered simultaneously to withstand extreme events. The literature review indicates that a single cooling strategy normally does not contain all the capacities or high levels of capacities. Therefore, a combination of cooling strategies with different capacities might be needed to obtain resilient cooling, and there may not be a universally optimal solution as certain cooling strategies might perform better in certain climates.

6.2. Limitation and future directions

The study applies a qualitative approach to assess the resilience of various cooling strategies. Some limitations observed by using the qualitative approach, are explained below.

First of all, the amount of literature that discussed the resilience of cooling strategies under extreme events is limited. The literature review indicated that resilience is still a relatively new concept for the development, characterization and evaluation of cooling strategies. The current researches strongly focus on the energy efficiency and performance of the system under 'typical' operating conditions. However, the systems perform and respond to the disruptions, and the strategies for increasing the system resilience require future research. Secondly, the literature studies analyzed cooling performance under very different boundary conditions, from weather datasets, reference building, system design and operation, to performance indicators, which is difficult to conduct a direct comparison between different cooling strategies based on the results of these studies. Finally, the resiliency capacities proposed in the current study are qualitative and theoretical concepts. Even though we proposed categories for evaluation (low, moderate and high), the outcome is a rather subjective assessment of resilience than reaching an objective measure.

As a consequence, it is a challenge to provide a concrete assessment and direct comparison between different cooling strategies based on the qualitative approach. There is a strong need for a more technical or quantitative resilience assessment methodology. A numerical approach with consistent and measurable metrics for the characterization of resilience capacities will be the further direction of Annex 80.

7. Conclusions

Resilience should be considered as an important property of the cooling systems integrated with buildings, to cope with extreme events such as heatwaves and power outages. This study performs a systematic literature review on the state-of-the-art of cooling strategies, with special attention to their performance under extreme events. A definition of resilient cooling is developed and four criteria are proposed to describe resilience characteristics, including absorptive capacity, adaptive capacity, restorative capacity, and recovery speed. The developed resilience characterization scheme is used to assess the resilience of various cooling strategies qualitatively.

The literature review indicates that resilience capacities depend on many parameters: the function of cooling strategies (reducing heat gains, removing sensible/latent heat, or enhancing personal comfort), the driven forces (passive or active), design feature, and control and operation of the cooling system. A single cooling strategy normally does not contain all the resilience capacities, therefore, a combination of cooling strategies with different capacities is important to obtain resilient cooling of buildings.

The limitation of the qualitative resilience assessment approach is discussed. There is a strong need for a quantitative assessment framework with specified boundary conditions and consistent and measurable performance indicators. A numerical-based approach will be developed and discussed in further study.

Declaration of Competing Interest

The authors declare that they have no known competing financial interests or personal relationships that could have appeared to influence the work reported in this paper.

Acknowledgement

The authors would like to thank all the participants of the IEA-EBC Annex 80: Resilient Cooling of Buildings.

The research is supported by Det Energiteknologisk Udviklings- og Demonstrationsprogram (EUDP) under grant 64018-0578. It was also supported by the Assistant Secretary for Energy Efficiency and Renewable Energy, Building Technologies Office of the U.S. Department of Energy under Contract No. DE-AC02-05CH11231.

References

[1] The Intergovernmental Panel on Climate Change, "IPCC DDC Glossary," 2020. https://www.ipcc-data.org/guidelines/pages/glossary/glossary_c.html (accessed Jun. 12, 2020).

[2] Centers for Disease Control and Preventation, "About Extreme Heat Natural Disasters and Severe Weather CDC." https://www.cdc.gov/disasters/extremeheat/heat_guide.html (accessed Jun. 17, 2020).

[3] E. Cadot, V.G. Rodwin, A. Spira, In the heat of the summer: Lessons from the heat waves in Paris, Journal of Urban Health 84 (4) (Jul. 2007) 466–468, https://doi.org/10.1007/s11524-007-9161-y.

[4] "WHO/Europe Climate change - Heat threatens health: key figures for Europe." https://www.euro.who.int/en/health-topics/environment-and-health/Climate-change/activities/public-health-responses-to-weather-extremes2/heathealth-action-plans/heat-threatens-health-key-figures-for-europe (accessed Jun. 15, 2020).

[5] C. B. Field et al., Managing the Risks of Extreme Events and Disasters to Advance Climate Change Adaptation: Special Report of the Intergovernmental Panel on Climate Change, vol. 9781107025. Cambridge University Press, 2012. 10.1017/CBO9781139177245.009.

[6] Y. Alfraidi, A. Boussabaine, Design Resilient Building Strategies in Face of Climate Change, World Academy of Science, Engineering and 9 (1) (2015) 23–28.

[7] A. Baniassadi and D. J. Sailor, "Synergies and trade-o ff s between energy e ffi ciency and resiliency to extreme heat – A case study," Building and Environment, vol. 132, no. August 2017, pp. 263–272, 2018, 10.1016/j.buildenv.2018.01.037.

[8] Z. Ren, X. Wang, and D. Chen, "Heat stress within energy efficient dwellings in Australia," vol. 8628, 2014, 10.1080/00038628.2014.903568.

[9] A.P. Ramallo-González, M.E. Eames, S. Natarajan, D. Fosas-de-Pando, D.A. Coley, An analytical heat wave definition based on the impact on buildings and occupants, Energy and Buildings 216 (2020), https://doi.org/10.1016/j.enbuild.2020.109923.

[10] A. Dodoo, L. Gustavsson, Energy use and overheating risk of Swedish multi-storey residential buildings under different climate scenarios, Energy 97 (Feb. 2016) 534–548, https://doi.org/10.1016/j.energy.2015.12.086.

[11] H. Wang, Q. Chen, Impact of climate change heating and cooling energy use in buildings in the United States, Energy and Buildings 82 (2014) (2014) 428–436, https://doi.org/10.1016/j.enbuild.2014.07.034.

[12] M. Steeman, A. Janssens, M. De Paepe, Performance evaluation of indirect evaporative cooling using whole-building hygrothermal simulations, Applied Thermal Engineering 29 (14–15) (2009) 2870–2875, https://doi.org/10.1016/j.applthermaleng.2009.02.004.

[13] H. Breesch, B. Merema, A. Versele, Ventilative Cooling in a School Building: Evaluation of the Measured Performances, Fluids 3 (4) (Sep. 2018) 68, https://doi.org/10.3390/fluids3040068.

[14] G. Ceré, Y. Rezgui, and W. Zhao, "Critical review of existing built environment resilience frameworks: Directions for future research," International Journal of Disaster Risk Reduction, vol. 25, no. September, pp. 173–189, 2017, 10.1016/j.ijdrr.2017.09.018.

[15] Annex 80 IEA EBC, "IEA EBC Annex on Resilient Cooling for Residential and Small Commercial Buildings Draft Annex Text," pp. 1–13, 2018.

[16] I. Oropeza-Perez and P. A. Østergaard, "Active and passive cooling methods for dwellings: A review," Renewable and Sustainable Energy Reviews, vol. 82, no. October 2017, pp. 531–544, 2018, 10.1016/j.rser.2017.09.059.

[17] J. Steven Brown, P.A. Domanski, Review of alternative cooling technologies, Applied Thermal Engineering 64 (1–2) (2014) 252–262, https://doi.org/10.1016/j.applthermaleng.2013.12.014.

[18] B.R. Hughes, H.N. Chaudhry, S.A. Ghani, A review of sustainable cooling technologies in buildings, Renewable and Sustainable Energy Reviews 15 (6) (2011) 3112–3120, https://doi.org/10.1016/j.rser.2011.03.032.

[19] C. Zhang, M. Pomianowski, P. Kvols, T. Yu, A review of integrated radiant heating / cooling with ventilation systems- Thermal comfort and indoor air quality, Energy & Buildings 223 (2020), https://doi.org/10.1016/j.enbuild.2020.110094 110094.

[20] D.K. Bhamare, M.K. Rathod, J. Banerjee, Passive cooling techniques for building and their applicability in different climatic zones - The State of Art, Energy & Buildings (2019), https://doi.org/10.1016/j.enbuild.2019.06.023.

[21] A. Sharifi, Y. Yamagata, Principles and criteria for assessing urban energy resilience: A literature review, Renewable and Sustainable Energy Reviews 60 (2016) 1654–1677, https://doi.org/10.1016/j.rser.2016.03.028.

[22] A. Sharifi and Y. Yamagata, "Major Principles and Criteria for Development of an Urban Resilience Assessment Index," no. June, 2014.

[23] S. Attia et al., Resilient cooling of buildings to protect against heat waves and power outages: Key concepts and definition, Energy and Buildings 239 (May 2021), 110869, https://doi.org/10.1016/j.enbuild.2021.110869.

[24] L. Bosher, Hazards and the Built Environment- Attaining Built-in Resilience, 1st Editio. Routledge, 2008.

[25] D. Burillo, M. V. Chester, S. Pincetl, and E. Fournier, "Electricity infrastructure vulnerabilities due to long-term growth and extreme heat from climate change in Los Angeles County," Energy Policy, vol. 128, no. December 2018, pp. 943–953, 2019, 10.1016/j.enpol.2018.12.053.

[26] A. Moazami, S. Carlucci, and S. Geving, "Robust and resilient buildings: A framework for defining the protection against climate uncertainty," IOP Conference Series: Materials Science and Engineering, vol. 609, no. 7, 2019, 10.1088/1757-899X/609/7/072068.

[27] M. Bruneau et al., A Framework to Quantitatively Assess and Enhance the Seismic Resilience of Communities, Earthquake Spectra 19 (4) (2003) 733–752, https://doi.org/10.1193/1.1623497.

[28] D. Henry, J. Emmanuel Ramirez-Marquez, Generic metrics and quantitative approaches for system resilience as a function of time, Reliability Engineering and System Safety 99 (2012) 114–122, https://doi.org/10.1016/j.ress.2011.09.002.

[29] H. Mallawarachchi, L. De Silva, and R. Rameezedeen, "Green buildings, resilience ability and the challenge of disaster risk," International Conference on Building Resilience, no. September, 2015.

[30] US Department of Energy, "Technology Readiness Assessment Guide," 2011. [Online]. Available: http://www.springerreference.com/index/doi/10.1007/SpringerReference 24357.

[31] "IGDB Windows and Daylighting," 2020. https://windows.lbl.gov/software/igdb (accessed May 14, 2020).

[32] M. Rubin, K. von Rottkay, R. Powles, Window optics, Solar Energy 62 (3) (Mar. 1998) 149–161, https://doi.org/10.1016/S0038-092X(98)00010-3.

[33] "WINDOW Windows and Daylighting," 2019. https://windows.lbl.gov/software/window (accessed May 14, 2020).

[34] M. Rubin, R. Powles, K. Von Rottkay, Models for the angle-dependent optical properties of coated glazing materials, Solar Energy 66 (4) (Jul. 1999) 267–276, https://doi.org/10.1016/S0038-092X(99)00029-8.

[35] M. Aburas, V. Soebarto, T. Williamson, R. Liang, H. Ebendorff-Heidepriem, Y. Wu, Thermochromic smart window technologies for building application: A review, Applied Energy 255 (Dec. 2019), https://doi.org/10.1016/j.apenergy.2019.113522 113522.

[36] E. S. Lee et al., "A Pilot Demonstration of Electrochromic and Thermochromic Windows in the Denver Federal Center, Building 41, Denver, Colorado," LBNL–1005095, 1249497, Jul. 2013. 10.2172/1249497.

[37] M. Casini, Active dynamic windows for buildings: A review, Renewable Energy 119 (Apr. 2018) 923–934, https://doi.org/10.1016/j.renene.2017.12.049.

[38] A. Piccolo, F. Simone, Performance requirements for electrochromic smart window, Journal of Building Engineering 3 (Sep. 2015) 94–103, https://doi.org/10.1016/j.jobe.2015.07.002.

[39] C. G. Granqvist, M. A. Arvizu, İ. Bayrak Pehlivan, H.-Y. Qu, R.-T. Wen, and G. A. Niklasson, "Electrochromic materials and devices for energy efficiency and human comfort in buildings: A critical review," Electrochimica Acta, vol. 259, pp. 1170–1182, Jan. 2018, 10.1016/j.electacta.2017.11.169.

[40] E.S. Lee, "Innovative Glazing Materials", in *Handbook of Energy Efficiency in Buildings*, Butterworth Heinemann (2019) 358–372.

[41] N. DeForest et al., Regional performance targets for transparent near-infrared switching electrochromic window glazings, Building and Environment 61 (Mar. 2013) 160–168, https://doi.org/10.1016/j.buildenv.2012.12.004.

[42] N. DeForest et al., United States energy and CO2 savings potential from deployment of near-infrared electrochromic window glazings, Building and Environment 89 (Jul. 2015) 107–117, https://doi.org/10.1016/j.buildenv.2015.02.021.

[43] R.R. Lunt, V. Bulovic, Transparent, near-infrared organic photovoltaic solar cells for window and energy-scavenging applications, Applied Physics Letters 98 (Mar. 2011), https://doi.org/10.1063/1.3567516 113305.

[44] A. Tzempelikos, A Review of Optical Properties of Shading Devices, Advances in Building Energy Research 2 (1) (Jan. 2008) 211–239, https://doi.org/10.3763/aber.2008.0207.

[45] L. Bellia, C. Marino, F. Minichiello, A. Pedace, An Overview on Solar Shading Systems for Buildings, Energy Procedia 62 (Jan. 2014) 309–317, https://doi.org/10.1016/j.egypro.2014.12.392.

[46] S. Attia, S. Bilir, T. Safy, C. Struck, R. Loonen, F. Goia, Current trends and future challenges in the performance assessment of adaptive façade systems, Energy and Buildings 179 (Nov. 2018) 165–182, https://doi.org/10.1016/j.enbuild.2018.09.017.

[47] Y.-H. Perng, Y.-Y. Huang, Investigation of technological trends in shading devices through patent analysis, Journal of Civil Engineering and Management 22 (6) (2016) 818–830, https://doi.org/10.3846/13923730.2014.914091.

[48] S. Hoffmann, E.S. Lee, A. McNeil, L. Fernandes, D. Vidanovic, A. Thanachareonkit, Balancing daylight, glare, and energy-efficiency goals: An evaluation of exterior coplanar shading systems using complex fenestration modeling tools, Energy and Buildings 112 (Jan. 2016) 279–298, https://doi.org/10.1016/j.enbuild.2015.12.009.

[49] A. Kirimtat, B.K. Koyunbaba, I. Chatzikonstantinou, S. Sariyildiz, Review of simulation modeling for shading devices in buildings, Renewable and Sustainable Energy Reviews 53 (Jan. 2016) 23–49, https://doi.org/10.1016/j.rser.2015.08.020.

[50] G. Yun, K.C. Yoon, K.S. Kim, The influence of shading control strategies on the visual comfort and energy demand of office buildings, Energy and Buildings 84 (Dec. 2014) 70–85, https://doi.org/10.1016/j.enbuild.2014.07.040.

[51] "ES-SO, European Solar Shading Organization," 2020. https://www.es-so.com/ (accessed May 17, 2020).

[52] Attachment Energy Rating Council, "AERC - Attachments Energy Rating Council," AERC, 2020. https://aercnet.org/ (accessed May 17, 2020).

[53] T.E. Kuhn, State of the art of advanced solar control devices for buildings, Solar Energy 154 (Sep. 2017) 112–133, https://doi.org/10.1016/j.solener.2016.12.044.

[54] X. Zhang, S.-K. Lau, S.S.Y. Lau, Y. Zhao, Photovoltaic integrated shading devices (PVSDs): A review, Solar Energy 170 (Aug. 2018) 947–968, https://doi.org/10.1016/j.solener.2018.05.067.

[55] M.H. Oh, K.H. Lee, J.H. Yoon, Automated control strategies of inside slat-type blind considering visual comfort and building energy performance, Energy and Buildings 55 (Dec. 2012) 728–737, https://doi.org/10.1016/j.enbuild.2012.09.019.

[56] A. Tzempelikos, H. Shen, Comparative control strategies for roller shades with respect to daylighting and energy performance, Building and Environment 67 (Sep. 2013) 179–192, https://doi.org/10.1016/j.buildenv.2013.05.016.

[57] G.R. Newsham, Manual Control of Window Blinds and Electric Lighting: Implications for Comfort and Energy Consumption, Indoor Environment 3 (3) (May 1994) 135–144, https://doi.org/10.1177/1420326X9400300307.

[58] A. Luna-Navarro, R. Loonen, M. Juaristi, A. Monge-Barrio, S. Attia, and M. Overend, "Occupant-Facade interaction: A review and classification scheme," Building and Environment, p. 106880, Apr. 2020, 10.1016/j.buildenv.2020.106880.

[59] K. Van Den Wymelenberg, Patterns of occupant interaction with window blinds: A literature review, Energy and Buildings 51 (Aug. 2012) 165–176, https://doi.org/10.1016/j.enbuild.2012.05.008.

[60] S. Hoffmann, E. Lee, Potential energy savings with exterior shades in large office buildings and the impact of discomfort glare, LBNL–187170 1248922 (2015) Apr, https://doi.org/10.2172/1248922.

[61] R. Levinson, H. Akbari, J. Reilly, Cooler tile-roofed buildings with near-infrared-reflective non-white coatings, Building and Environment 42 (7) (2007) 2591–2605, https://doi.org/10.1016/j.buildenv.2006.06.005.

[62] R. Levinson, H. Akbari, Potential benefits of cool roofs on commercial buildings: Conserving energy, saving money, and reducing emission of greenhouse gases and air pollutants, Energy Efficiency 3 (1) (2010) 53–109, https://doi.org/10.1007/s12053-008-9038-2.

[63] P.J. Rosado, R. Levinson, Potential benefits of cool walls on residential and commercial buildings across California and the United States: conserving energy, saving money, and reducing emission of greenhouse gases and air pollutants, Energy and Buildings 199 (2019) 588–607, https://doi.org/10.1016/j.enbuild.2019.02.028.

[64] H. Akbari and S. Konopacki, "The Impact of Reflectivity and Emissivity of Roofs on Building Cooling and Heating Energy Use," in Thermal VII: Thermal Performance of the Exterior Envelopes of Buildings VII, Miami, FL, 1998, pp. 29–39. [Online]. Available: https://pdfs.semanticscholar.org/ac35/f5e37a3f1ac9010c5d0d4d4215a8aab6e203.pdf

[65] S. Konopacki, H. Akbari, M. Pomerantz, S. Gabersek, and L. Gartland, "Cooling energy savings potential of light-colored roofs for residential and commercial buildings in 11 US metropolitan areas," LBNL-39433, May 1997. 10.2172/510556.

[66] J. Testa, M. Krarti, A review of benefits and limitations of static and switchable cool roof systems, Renewable and Sustainable Energy Reviews 77 (Sep. 2017) 451–460, https://doi.org/10.1016/j.rser.2017.04.030.

[67] R. Levinson, H. Akbari, S. Konopacki, S. Bretz, Inclusion of cool roofs in nonresidential Title 24 prescriptive requirements, Energy Policy 33 (2) (2005) 151–170, https://doi.org/10.1016/S0301-4215(03)00206-4.

[68] Global Cool Cities Alliance, "A Practical Guide to Cool Roofs and Cool Pavements," Jan. 2012. [Online]. Available: https://CoolRoofToolkit.org

[69] M. Santamouris, A. Synnefa, T. Karlessi, Using advanced cool materials in the urban built environment to mitigate heat islands and improve thermal comfort conditions, Solar Energy 85 (12) (Dec. 2011) 3085–3102, https://doi.org/10.1016/j.solener.2010.12.023.

[70] R. Levinson et al., "Solar-Reflective 'Cool' Walls: Benefits, Technologies, and Implementation," California Energy Commission, Sacramento, CA, CEC-500-2019-040; also LBNL-2001296, Apr. 2019. [Online]. Available: http://dx.doi.org/10.20357/B7SP4H

[71] X. Li, J. Peoples, P. Yao, X. Ruan, Ultrawhite BaSO4 Paints and Films for Remarkable Daytime Subambient Radiative Cooling, ACS Appl. Mater. Interfaces 13 (18) (May 2021) 21733–21739, https://doi.org/10.1021/acsami.1c02368.

[72] X. Li, J. Peoples, Z. Huang, Z. Zhao, J. Qiu, X. Ruan, Full Daytime Sub-ambient Radiative Cooling in Commercial-like Paints with High Figure of Merit, CR-PHYS-SC 1 (10) (2020) Oct, https://doi.org/10.1016/j.xcrp.2020.100221.

[73] R. Levinson et al., Methods of creating solar-reflective nonwhite surfaces and their application to residential roofing materials, Solar Energy Materials and Solar Cells 91 (4) (2007) 304–314, https://doi.org/10.1016/j.solmat.2006.06.062.

[74] R. Levinson, P. Berdahl, H. Akbari, Solar spectral optical properties of pigments - Part I: Model for deriving scattering and absorption coefficients from transmittance and reflectance measurements, Solar Energy Materials and Solar Cells 89 (4) (2005) 319–349, https://doi.org/10.1016/j.solmat.2004.11.012.

[75] R. Levinson, P. Berdahl, H. Akbari, Solar spectral optical properties of pigments - Part II: Survey of common colorants, Solar Energy Materials and Solar Cells 89 (4) (2005) 351–389, https://doi.org/10.1016/j.solmat.2004.11.013.

[76] R. Levinson, P. Berdahl, and H. Akbari, "Lawrence Berkeley National Laboratory Pigment Database," 2005. http://pigments.lbl.gov

[77] R.F. Brady, L.V. Wake, Principles and formulations for organic coatings with tailored infrared properties, Progress in Organic Coatings 20 (1) (Mar. 1992) 1–25, https://doi.org/10.1016/0033-0655(92)85001-C.

[78] R. Levinson, H. Akbari, P. Berdahl, K. Wood, W. Skilton, J. Petersheim, A novel technique for the production of cool colored concrete tile and asphalt shingle roofing products, Solar Energy Materials and Solar Cells 94 (6) (2010) 946–954, https://doi.org/10.1016/j.solmat.2009.12.012.

[79] A. Synnefa, M. Santamouris, K. Apostolakis, On the development, optical properties and thermal performance of cool colored coatings for the urban environment, Solar Energy 81 (4) (Apr. 2007) 488–497, https://doi.org/10.1016/j.solener.2006.08.005.

[80] R. Levinson et al., "Next-generation factory-produced cool asphalt shingles: Phase 1 final report," Lawrence Berkeley National Laboratory, Berkeley, CA, LBNL-2001007, Nov. 2016. Accessed: Feb. 04, 2020. [Online]. Available: https://escholarship.org/uc/item/2t3602nt

[81] P. Berdahl, S.S. Chen, H. Destaillats, T.W. Kirchstetter, R. Levinson, M.A. Zalich, Fluorescent cooling of objects exposed to sunlight - The ruby example, Solar Energy Materials and Solar Cells 157 (2016) 312–317, https://doi.org/10.1016/j.solmat.2016.05.058.

[82] P. Berdahl, S.K. Boocock, G.C.-Y. Chan, S.S. Chen, R.M. Levinson, M.A. Zalich, High quantum yield of the Egyptian blue family of infrared phosphors ($MCuSi_4O_{10}$, M = Ca, Sr, Ba), Journal of Applied Physics 123 (19) (May 2018), https://doi.org/10.1063/1.5019808 193103.

[83] S. Garshasbi, M. Santamouris, Using advanced thermochromic technologies in the built environment: Recent development and potential to decrease the energy consumption and fight urban overheating, Solar Energy Materials and Solar Cells 191 (Mar. 2019) 21–32, https://doi.org/10.1016/j.solmat.2018.10.023.

[84] J. Testa, M. Krarti, Evaluation of energy savings potential of variable reflective roofing systems for US buildings, Sustainable Cities and Society 31 (May 2017) 62–73, https://doi.org/10.1016/j.scs.2017.01.016.

[85] T. Karlessi, M. Santamouris, K. Apostolakis, A. Synnefa, I. Livada, Development and testing of thermochromic coatings for buildings and urban structures, Solar Energy 83 (4) (Apr. 2009) 538–551, https://doi.org/10.1016/j.solener.2008.10.005.

[86] M. Zinzi, S. Agnoli, G. Ulpiani, and B. Mattoni, "On the potential of switching cool roofs to optimize the thermal response of residential buildings in the Mediterranean region," Energy and Buildings, p. 110698, Dec. 2020, 10.1016/j.enbuild.2020.110698.

[87] H. Akbari, D. Kolokotsa, Three decades of urban heat islands and mitigation technologies research, Energy and Buildings 133 (Dec. 2016) 834–842, https://doi.org/10.1016/j.enbuild.2016.09.067.

[88] K. M. Bailey, "CoolAngle shingles," 2020. http://coolangle.com/coolangle-shingles

[89] K. M. Bailey and M. E. Ewing, "Roofing material with directionally dependent properties," US20110183112A1, Jul. 28, 2011 Accessed: Mar. 16, 2020. [Online]. Available: https://patents.google.com/patent/US20110183112A1/en

[90] J. Yuan, K. Emura, C. Farnham, Potential for application of retroreflective materials instead of highly reflective materials for urban heat island mitigation, Urban Studies Research 2016 (2016) 1–10, https://doi.org/10.1155/2016/3626294.

[91] R. Levinson, S. Chen, J. Slack, H. Goudey, T. Harima, P. Berdahl, Design, characterization, and fabrication of solar-retroreflective cool-wall materials, Solar Energy Materials and Solar Cells 206 (Mar. 2020), https://doi.org/10.1016/j.solmat.2019.110117 110117.

[92] M. Santamouris and J. Feng, "Recent Progress in Daytime Radiative Cooling: Is It the Air Conditioner of the Future?," Buildings, vol. 8, no. 12, Art. no. 12, Dec. 2018, 10.3390/buildings8120168.

[93] D. Zhao et al., Radiative sky cooling: Fundamental principles, materials, and applications, Applied Physics Reviews 6 (2) (Apr. 2019), https://doi.org/10.1063/1.5087281 021306.

[94] S. Catalanotti, V. Cuomo, G. Piro, D. Ruggi, V. Silvestrini, G. Troise, The radiative cooling of selective surfaces, Solar Energy 17 (2) (May 1975) 83–89, https://doi.org/10.1016/0038-092X(75)90062-6.

[95] I. Hernández-Pérez, G. Álvarez, J. Xamán, I. Zavala-Guillén, J. Arce, E. Simá, Thermal performance of reflective materials applied to exterior building components—A review, Energy and Buildings 80 (Sep. 2014) 81–105, https://doi.org/10.1016/j.enbuild.2014.05.008.

[96] S. Algarni, D. Nutter, Influence of dust accumulation on building roof thermal performance and radiant heat gain in hot-dry climates, Energy and Buildings 104 (Oct. 2015) 181–190, https://doi.org/10.1016/j.enbuild.2015.07.018.

[97] A. Baniassadi, D.J. Sailor, P.J. Crank, G.A. Ban-Weiss, Direct and indirect effects of high-albedo roofs on energy consumption and thermal comfort of

residential buildings, Energy and Buildings 178 (Nov. 2018) 71–83, https://doi.org/10.1016/j.enbuild.2018.08.048.
[98] Y. Gao et al., Cool roofs in China: Policy review, building simulations, and proof-of-concept experiments, Energy Policy vol. 74, no. C (2014) 190–214, https://doi.org/10.1016/j.enpol.2014.05.036.
[99] Y. Gao, D. Shi, R. Levinson, R. Guo, C. Lin, J. Ge, Thermal performance and energy savings of white and sedum-tray garden roof: A case study in a Chongqing office building, Energy and Buildings 156 (Dec. 2017) 343–359, https://doi.org/10.1016/j.enbuild.2017.09.091.
[100] M. Hosseini, H. Akbari, Effect of cool roofs on commercial buildings energy use in cold climates, Energy and Buildings 114 (Feb. 2016) 143–155, https://doi.org/10.1016/j.enbuild.2015.05.050.
[101] M. Kolokotroni et al., Cool roofs: High tech low cost solution for energy efficiency and thermal comfort in low rise low income houses in high solar radiation countries, Energy and Buildings 176 (Oct. 2018) 58–70, https://doi.org/10.1016/j.enbuild.2018.07.005.
[102] E. Mastrapostoli, T. Karlessi, A. Pantazaras, D. Kolokotsa, K. Gobakis, M. Santamouris, On the cooling potential of cool roofs in cold climates: Use of cool fluorocarbon coatings to enhance the optical properties and the energy performance of industrial buildings, Energy and Buildings 69 (Feb. 2014) 417–425, https://doi.org/10.1016/j.enbuild.2013.10.024.
[103] S. Pushkar, O. Verbitsky, Life cycle assessments of white flat and red or white pitched roofs for residential buildings in Israel, Journal of Green Building 12 (2) (Mar. 2017) 95–111, https://doi.org/10.3992/1943-4618.12.2.95.
[104] M. Seifhashemi, B.R. Capra, W. Millller, J. Bell, The potential for cool roofs to improve the energy efficiency of single storey warehouse-type retail buildings in Australia: A simulation case study, Energy and Buildings 158 (Jan. 2018) 1393–1403, https://doi.org/10.1016/j.enbuild.2017.11.034.
[105] D. Shi, Y. Gao, R. Guo, R. Levinson, Z. Sun, and B. Li, "Life cycle assessment of white roof and sedum-tray garden roof for office buildings in China," Sustainable Cities and Society, vol. 46, no. July 2018, p. 101390, 2019, 10.1016/j.scs.2018.12.018.
[106] M. Zinzi, Characterisation and assessment of near infrared reflective paintings for building facade applications, Energy and Buildings 114 (Feb. 2016) 206–213, https://doi.org/10.1016/j.enbuild.2015.05.048.
[107] M. Zinzi, Exploring the potentialities of cool facades to improve the thermal response of Mediterranean residential buildings, Solar Energy 135 (Oct. 2016) 386–397, https://doi.org/10.1016/j.solener.2016.06.021.
[108] M. Zinzi, E. Carnielo, A. Federici, Preliminary studies of a cool roofs' energy-rating system in Italy, Advances in Building Energy Research 8 (1) (Jan. 2014) 84–96, https://doi.org/10.1080/17512549.2014.890539.
[109] C. Fabiani, V.L. Castaldo, A.L. Pisello, Thermochromic materials for indoor thermal comfort improvement: Finite difference modeling and validation in a real case-study building, Applied Energy 262 (Mar. 2020), https://doi.org/10.1016/j.apenergy.2019.114147 114147.
[110] M. Dabaieh, O. Wanas, M.A. Hegazy, E. Johansson, Reducing cooling demands in a hot dry climate: A simulation study for non-insulated passive cool roof thermal performance in residential buildings, Energy and Buildings 89 (Feb. 2015) 142–152, https://doi.org/10.1016/j.enbuild.2014.12.034.
[111] V. Garg et al., Assessment of the impact of cool roofs in rural buildings in India, Energy and Buildings 114 (Feb. 2016) 156–163, https://doi.org/10.1016/j.enbuild.2015.06.043.
[112] A.L. Pisello, F. Cotana, The thermal effect of an innovative cool roof on residential buildings in Italy: Results from two years of continuous monitoring, Energy and Buildings 69 (Feb. 2014) 154–164, https://doi.org/10.1016/j.enbuild.2013.10.031.
[113] P. Samani, V. Leal, A. Mendes, N. Correia, Comparison of passive cooling techniques in improving thermal comfort of occupants of a pre-fabricated building, Energy and Buildings 120 (May 2016) 30–44, https://doi.org/10.1016/j.enbuild.2016.03.055.
[114] E.-H. Drissi Lamrhari and B. Benhamou, "Thermal behavior and energy saving analysis of a flat with different energy efficiency measures in six climates," Build. Simul., vol. 11, no. 6, pp. 1123–1144, Dec. 2018, 10.1007/s12273-018-0467-3.
[115] D. Dias, J. Machado, V. Leal, A. Mendes, Impact of using cool paints on energy demand and thermal comfort of a residential building, Applied Thermal Engineering 65 (1) (Apr. 2014) 273–281, https://doi.org/10.1016/j.applthermaleng.2013.12.056.
[116] N. Nazarian, N. Dumas, J. Kleissl, L. Norford, Effectiveness of cool walls on cooling load and urban temperature in a tropical climate, Energy and Buildings 187 (Mar. 2019) 144–162, https://doi.org/10.1016/j.enbuild.2019.01.022.
[117] N.L. Alchapar, E.N. Correa, 6 - Comparison of the performance of different facade materials for reducing building cooling needs, in: F. Pacheco-Torgal, J. A. Labrincha, L.F. Cabeza, C.-.G. Granqvist (Eds.), Eco-Efficient Materials for Mitigating Building Cooling Needs, Woodhead Publishing, Oxford, 2015, pp. 155–194, https://doi.org/10.1016/B978-1-78242-380-5.00006-6.
[118] A. Gagliano, M. Detommaso, F. Nocera, G. Evola, A multi-criteria methodology for comparing the energy and environmental behavior of cool, green and traditional roofs, Building and Environment 90 (Aug. 2015) 71–81, https://doi.org/10.1016/j.buildenv.2015.02.043.
[119] K.T. Zingre et al., Modeling of cool roof heat transfer in tropical climate, Renewable Energy 75 (Mar. 2015) 210–223, https://doi.org/10.1016/j.renene.2014.09.045.
[120] W. Ma, C. Xiang, L. Li, G. Liu, Impact of cool roof on energy consumption for a railway station, Indoor and Built Environment 24 (8) (Jun. 2015) 1095–1109, https://doi.org/10.1177/1420326X15592941.
[121] S. Porritt, L. Shao, P. Cropper, C. Goodier, Adapting dwellings for heat waves, Sustainable Cities and Society 1 (2) (Jul. 2011) 81–90, https://doi.org/10.1016/j.scs.2011.02.004.
[122] S.M. Porritt, P.C. Cropper, L. Shao, C.I. Goodier, Ranking of interventions to reduce dwelling overheating during heat waves, Energy and Buildings 55 (Dec. 2012) 16–27, https://doi.org/10.1016/j.enbuild.2012.01.043.
[123] M. Zinzi, G. Fasano, Properties and performance of advanced reflective paints to reduce the cooling loads in buildings and mitigate the heat island effect in urban areas, International Journal of Sustainable Energy 28 (1–3) (Sep. 2009) 123–139, https://doi.org/10.1080/14786450802453314.
[124] A. Synnefa, M. Saliari, M. Santamouris, Experimental and numerical assessment of the impact of increased roof reflectance on a school building in Athens, Energy and Buildings 55 (Dec. 2012) 7–15, https://doi.org/10.1016/j.enbuild.2012.01.044.
[125] C. Romeo, M. Zinzi, Impact of a cool roof application on the energy and comfort performance in an existing non-residential building. A Sicilian case study, Energy and Buildings 67 (Dec. 2013) 647–657, https://doi.org/10.1016/j.enbuild.2011.07.023.
[126] R. Guo et al., Optimization of cool roof and night ventilation in office buildings: A case study in Xiamen, China, Renewable Energy 147 (Mar. 2020) 2279–2294, https://doi.org/10.1016/j.renene.2019.10.032.
[127] M. Kolokotroni, B.L. Gowreesunker, R. Giridharan, Cool roof technology in London: An experimental and modelling study, Energy and Buildings 67 (Dec. 2013) 658–667, https://doi.org/10.1016/j.enbuild.2011.07.011.
[128] B. Urban and K. Roth, "Guidelines for Selecting Cool Roofs," Fraunhofer Center for Sustainable Energy Systems and Oak Ridge National Laboratory, Version 1.2, Jul. 2010. [Online]. Available: https://www.nps.gov/tps/sustainability/greendocs/doe coolroofguide-sm.pdf
[129] Cool Roof Rating Council, "Rated Products Directory," 2018. https://coolroofs.org/directory
[130] European Cool Roofs Council Technical Committee, Product Rating Manual. 2017. Accessed: Apr. 08, 2020. [Online]. Available: https://coolroofcouncil.eu/wp-content/uploads/2019/05/ECRC-Product-rating-manual 2017.pdf
[131] European Cool Roofs Council, "Product Rating Database," 2020. https://coolroofcouncil.eu/product-rating-database (accessed Apr. 08, 2020).
[132] Cool Roof Rating Council, "CRRC to Rate Exterior Wall Products." Oct. 06, 2020. Accessed: Mar. 20, 2021. [Online]. Available: https://coolroofs.org/documents/CRRC Wall Rating Program Approval Press Release - 2020-10-07.pdf
[133] B. Raji, M. J. Tenpierik, and A. Dobbelsteen, "The impact of greening systems on building energy performance: A literature review," Renewable and Sustainable Energy Reviews, vol. 45, pp. 610–623, May 2015, 10/gcv7ks.
[134] D.J. Sailor, A green roof model for building energy simulation programs, Energy and Buildings 40 (8) (Jan. 2008) 1466–1478, https://doi.org/10.1016/j.enbuild.2008.02.001.
[135] M. Santamouris et al., Investigating and analysing the energy and environmental performance of an experimental green roof system installed in a nursery school building in Athens, Greece, Energy 32 (9) (Sep. 2007) 1781–1788, https://doi.org/10.1016/j.energy.2006.11.011.
[136] A. Sharifi, Y. Yamagata, Roof ponds as passive heating and cooling systems: A systematic review, Applied Energy 160 (Dec. 2015) 336–357, https://doi.org/10.1016/j.apenergy.2015.09.061.
[137] S. Raeissi, M. Taheri, Cooling load reduction of buildings using passive roof options, Renewable Energy 7 (3) (Mar. 1996) 301–313, https://doi.org/10.1016/0960-1481(95)00123-9.
[138] N.H. Wong, D.K.W. Cheong, H. Yan, J. Soh, C.L. Ong, A. Sia, The effects of rooftop garden on energy consumption of a commercial building in Singapore, Energy and Buildings 35 (4) (May 2003) 353–364, https://doi.org/10.1016/S0378-7788(02)00108-1.
[139] E. Erell, S. Yannas, and J. L. Molina, "Roof Cooling Techniques," in The 23rd Conference on Passive and Low Energy Architecture, Geneva, Switzerland, Sep. 2006, vol. 2, pp. 571–576.
[140] N.D. Kaushika, S.K. Rao, Non-convective roof pond with movable insulation for passive solar space heating in cold climates, Building and Environment 18 (1) (Jan. 1983) 9–17, https://doi.org/10.1016/0360-1323(83)90014-8.
[141] S. M. S. Shokri Kuehni, E. Bou-Zeid, C. Webb, and N. Shokri, "Roof cooling by direct evaporation from a porous layer," Energy and Buildings, vol. 127, pp. 521–528, Sep. 2016, 10.1016/j.enbuild.2016.06.019.
[142] I. Jaffal, S.-E. Ouldboukhitine, R. Belarbi, A comprehensive study of the impact of green roofs on building energy performance, Renewable Energy 43 (Jul. 2012) 157–164, https://doi.org/10.1016/j.renene.2011.12.004.
[143] E. Alexandri, P. Jones, Temperature decreases in an urban canyon due to green walls and green roofs in diverse climates, Building and Environment 43 (4) (Apr. 2008) 480–493, https://doi.org/10.1016/j.buildenv.2006.10.055.
[144] B. Doug, D. Hitesh, L. James, and M. Paul, "Report on the Environmental Benefits and Costs of Green Roof Technology for the City of Toronto," University Library of Munich, Germany, 70526, Oct. 2005. Accessed: Jan. 29, 2020. [Online]. Available: https://ideas.repec.org/p/pra/mprapa/70526.html
[145] T.-C. Liu, G.-S. Shyu, W.-T. Fang, S.-Y. Liu, B.-Y. Cheng, Drought tolerance and thermal effect measurements for plants suitable for extensive green roof planting in humid subtropical climates, Energy and Buildings 47 (Apr. 2012) 180–188, https://doi.org/10.1016/j.enbuild.2011.11.043.

[146] S. Yannas, E. Erell, J.L. Molina, *Roof Cooling Techniques: A Design Handbook*. Earthscan (2006).

[147] Y. Ji, M.J. Cook, V. Hanby, D.G. Infield, D.L. Loveday, L. Mei, CFD modelling of naturally ventilated double-skin facades with Venetian blinds, Journal of Building Performance Simulation 1 (3) (Sep. 2008) 185–196, https://doi.org/10.1080/19401490802478303.

[148] A. Velasco, S. Jiménez García, A. Guardo, A. Fontanals, and M. Egusquiza, "Assessment of the Use of Venetian Blinds as Solar Thermal Collectors in Double Skin Facades in Mediterranean Climates," Energies, vol. 10, no. 11, Art. no. 11, Nov. 2017, 10.3390/en10111825.

[149] Y. Wang, Y. Chen, C. Li, Airflow modeling based on zonal method for natural ventilated double skin façade with Venetian blinds, Energy and Buildings 191 (May 2019) 211–223, https://doi.org/10.1016/j.enbuild.2019.03.025.

[150] X. Xu, Z. Yang, Natural ventilation in the double skin facade with venetian blind, Energy and Buildings 40 (8) (Jan. 2008) 1498–1504, https://doi.org/10.1016/j.enbuild.2008.02.012.

[151] S. Fantucci, V. Serra, M. Perino, Dynamic Insulation Systems: Experimental Analysis on a Parietodynamic Wall, Energy Procedia 78 (Nov. 2015) 549–554, https://doi.org/10.1016/j.egypro.2015.11.734.

[152] J. Hirunlabh, S. Wachirapuwadon, N. Pratinthong, J. Khedari, New configurations of a roof solar collector maximizing natural ventilation, Building and Environment 36 (3) (Apr. 2001) 383–391, https://doi.org/10.1016/S0360-1323(00)00016-0.

[153] A.I. Omar, J. Virgone, E. Vergnault, D. David, A.I. Idriss, Energy Saving Potential with a Double-Skin Roof Ventilated by Natural Convection in Djibouti, Energy Procedia 140 (Dec. 2017) 361–373, https://doi.org/10.1016/j.egypro.2017.11.149.

[154] J.M. Blanco, A. Buruaga, E. Rojí, J. Cuadrado, B. Pelaz, Energy assessment and optimization of perforated metal sheet double skin façades through Design Builder; A case study in Spain, Energy and Buildings 111 (Jan. 2016) 326–336, https://doi.org/10.1016/j.enbuild.2015.11.053.

[155] T. Srisamranrungruang, K. Hiyama, Balancing of natural ventilation, daylight, thermal effect for a building with double-skin perforated facade (DSPF), Energy and Buildings 210 (Mar. 2020), https://doi.org/10.1016/j.enbuild.2020.109765 109765.

[156] S. Barbosa, K. Ip, Perspectives of double skin façades for naturally ventilated buildings: A review, Renewable and Sustainable Energy Reviews 40 (Dec. 2014) 1019–1029, https://doi.org/10.1016/j.rser.2014.07.192.

[157] E. Gratia, A. De Herde, Is day natural ventilation still possible in office buildings with a double-skin façade?, Building and Environment 39 (4) (Apr 2004) 399–409, https://doi.org/10.1016/j.buildenv.2003.10.006.

[158] H. Poirazis, "Double Skin Façades for Office Buildings," Lund University, LUND, Sweden, Literature Review Report No EBD-R–04/3 ISBN 91-85147-02-8, 2004. [Online]. Available: http://www.ebd.lth.se/fileadmin/energi byggnadsdesign/images/Publikationer/Bok-EBD-R3-G5 alt 2 Harris.pdf

[159] P. Jarjat, T. Nenov, and S. Ware, "Pho'liage® - A Biomimetic Façade which increases Building Energy Efficiency," ARTBUILD, p. 50, Dec. 2019.

[160] Vent-A-Roof, "Revolutionary Roof Ventilation System - Vent-A-Roof Australia," Vent-A-Roof, 2020. https://ventaroof.com.au/ (accessed Apr. 17, 2020).

[161] N. H. Steven Tay, M. Belusko, M. Liu, and F. Bruno, "Chapter 1 - Introduction," in High Temperature Thermal Storage Systems Using Phase Change Materials, L. F. Cabeza and N. H. S. Tay, Eds. Academic Press, 2018, pp. 1–4. 10.1016/B978-0-12-805323-2.00001-1.

[162] M. Pomianowski, P. Heiselberg, Y. Zhang, Review of thermal energy storage technologies based on PCM application in buildings, Energy and Buildings 67 (Dec. 2013) 56–69, https://doi.org/10.1016/j.enbuild.2013.08.006.

[163] I. Dincer, M. Rosen, Thermal energy storage: systems and applications, John Wiley & Sons, 2002.

[164] J. Lizana, R. Chacartegui, A. Barrios-Padura, J.M. Valverde, Advances in thermal energy storage materials and their applications towards zero energy buildings: A critical review, Applied Energy 203 (Oct. 2017) 219–239, https://doi.org/10.1016/j.apenergy.2017.06.008.

[165] J. West, J. Braun, Modeling Partial Charging and Discharging of Area-Constrained Ice Storage Tanks, HVAC&R Res. 5 (3) (Jul. 1999) 209–228, https://doi.org/10.1080/10789669.1999.10391234.

[166] T. Kuczyński, A. Staszczuk, Experimental study of the influence of thermal mass on thermal comfort and cooling energy demand in residential buildings, Energy 195 (Mar. 2020), https://doi.org/10.1016/j.energy.2020.116984 116984.

[167] G. Zhou, Y. Zhang, X. Wang, K. Lin, W. Xiao, An assessment of mixed type PCM-gypsum and shape-stabilized PCM plates in a building for passive solar heating, Solar energy 81 (11) (2007) 1351–1360, https://doi.org/10.1016/j.solener.2007.01.014.

[168] M. Alam, H. Jamil, J. Sanjayan, J. Wilson, Energy saving potential of phase change materials in major Australian cities, Energy and Buildings 78 (Aug. 2014) 192–201, https://doi.org/10.1016/j.enbuild.2014.04.027.

[169] H. Jamil, M. Alam, J. Sanjayan, J. Wilson, Investigation of PCM as retrofitting option to enhance occupant thermal comfort in a modern residential building, Energy and Buildings 133 (2016) 217–229, https://doi.org/10.1016/j.enbuild.2016.09.064.

[170] J. Sage-Lauck, D. Sailor, Evaluation of phase change materials for improving thermal comfort in a super-insulated residential building, Energy and Buildings 79 (2014) 32–40, https://doi.org/10.1016/j.enbuild.2014.04.028.

[171] F. Kuznik, J. Virgone, K. Johannes, In-situ study of thermal comfort enhancement in a renovated building equipped with phase change material wallboard, Renewable Energy 36 (5) (2011) 1458–1462, https://doi.org/10.1016/j.renene.2010.11.008.

[172] S. Ramakrishnan, X. Wang, J. Sanjayan, J. Wilson, Thermal performance of buildings integrated with phase change materials to reduce heat stress risks during extreme heatwave events, Applied Energy 194 (May 2017) 410–421, https://doi.org/10.1016/j.apenergy.2016.04.084.

[173] A. Baniassadi, D.J. Sailor, H.J. Bryan, Effectiveness of phase change materials for improving the resiliency of residential buildings to extreme thermal conditions, Solar Energy 188 (Aug. 2019) 190–199, https://doi.org/10.1016/j.solener.2019.06.011.

[174] H.W. Samuelson, A. Baniassadi, P.I. Gonzalez, Beyond energy savings: Investigating the co-benefits of heat resilient architecture, Energy 204 (Aug. 2020), https://doi.org/10.1016/j.energy.2020.117886 117886.

[175] G. Carrilho da Graça, Q. Chen, L.R. Glicksman, L.K. Norford, Simulation of wind-driven ventilative cooling systems for an apartment building in Beijing and Shanghai, Energy and Buildings 34 (1) (2002) 1–11, https://doi.org/10.1016/S0378-7788(01)00083-4.

[176] R. Yao, B. Li, K. Steemers, A. Short, Assessing the natural ventilation cooling potential of office buildings in different climate zones in China, Renewable Energy 34 (12) (Dec. 2009) 2697–2705, https://doi.org/10.1016/j.renene.2009.05.015.

[177] H. Campaniço, P.M.M. Soares, R.M. Cardoso, P. Hollmuller, Impact of climate change on building cooling potential of direct ventilation and evaporative cooling: A high resolution view for the Iberian Peninsula, Energy and Buildings 192 (Jun. 2019) 31–44, https://doi.org/10.1016/j.enbuild.2019.03.017.

[178] V. Geros, M. Santamouris, A. Tsangrasoulis, G. Guarracino, Experimental evaluation of night ventilation phenomena, Energy and Buildings 29 (2) (1999) 141–154, https://doi.org/10.1016/S0378-7788(98)00056-5.

[179] J.-M. Alessandrini, J. Ribéron, D. Da Silva, Will naturally ventilated dwellings remain safe during heatwaves?, Energy and Buildings 183 (Jan 2019) 408–417, https://doi.org/10.1016/j.enbuild.2018.10.033.

[180] K.J. Lomas, Y. Ji, Resilience of naturally ventilated buildings to climate change: Advanced natural ventilation and hospital wards, Energy and Buildings 41 (6) (2009) 629–653, https://doi.org/10.1016/j.enbuild.2009.01.001.

[181] M. Hamdy, S. Carlucci, P.-J. Hoes, J.L.M. Hensen, The impact of climate change on the overheating risk in dwellings—A Dutch case study, Building and Environment 122 (Sep. 2017) 307–323, https://doi.org/10.1016/j.buildenv.2017.06.031.

[182] N. Artmann, D. Gyalistras, H. Manz, P. Heiselberg, Impact of climate warming on passive night cooling potential, Building Research and Information 36 (2) (2008) 111–128, https://doi.org/10.1080/09613210701621919.

[183] N. Nakićenović and Intergovernmental Panel on Climate Change, Eds., Special report on emissions scenarios: a special report of Working Group III of the Intergovernmental Panel on Climate Change. Cambridge ; New York: Cambridge University Press, 2000.

[184] H. Breesch, A. Janssens, Performance evaluation of passive cooling in office buildings based on uncertainty and sensitivity analysis, Solar Energy 84 (8) (2010) 1453–1467, https://doi.org/10.1016/j.solener.2010.05.008.

[185] E. Burman and D. Mumovic, "The impact of ventilation strategy on overheating resilience and energy performance of schools against climate change: the evidence from two UK secondary schools," 2018. [Online]. Available: https://discovery.ucl.ac.uk/id/eprint/10055059

[186] E. Erell, "Evaporative cooling," in Advances in passive cooling, London: Earthscan, 2007, pp. 228–261.

[187] P. Rajagopalan, "Recent Advances in Passive Cooling Techniques", in *Cooling Energy Solutions for Buildings and Cities*, World Scientific, Singapore, 2020.

[188] B. Ford, R. Schiano-Phan, and E. Francis, Eds., The architecture and engineering of downdraught cooling. A design sourcebook. UK: PHDCpress, 2010.

[189] G. Chiesa, "Early Design Strategies for Passive Cooling of Buildings: Lessons Learned from Italian Archetypes," in Sustainable Vernacular Architecture, A. Sayigh, Ed. Cham: Springer International Publishing, 2019, pp. 377–408. 10.1007/978-3-030-06185-2 17.

[190] M. Santamouris, Ed., Advances in Passive Cooling. London: Earthscan, 2007.

[191] M.M. Osman, H. Sevinc, Adaptation of climate-responsive building design strategies and resilience to climate change in the hot/arid region of Khartoum, Sudan, Sustainable Cities and Society 47 (May 2019), https://doi.org/10.1016/j.scs.2019.101429 101429.

[192] E. Erell, D. Pearlmutter, Y. Etzion, A multi-stage down-draft evaporative cool tower for semi-enclosed spaces: aerodynamic performance, Solar Energy 82 (2008) 420–429.

[193] D. Pearlmutter, E. Erell, Y. Etzion, A multi-stage down-draft evaporative cool tower for semi-enclosed spaces: experiments with a water spraying system, Solar Energy 82 (2008) 430–440.

[194] "The Future of Cooling – Analysis," IEA. https://www.iea.org/reports/the-future-of-cooling (accessed Jun. 04, 2020).

[195] E. Hajidavalloo, H. Eghtedari, Performance improvement of air-cooled refrigeration system by using evaporatively cooled air condenser, International Journal of Refrigeration 33 (5) (Aug. 2010) 982–988, https://doi.org/10.1016/j.ijrefrig.2010.02.001.

[196] "Cooling," IEA. https://www.iea.org/reports/cooling (accessed Jun. 01, 2021).

[197] E. Georges, J.E. Braun, V. Lemort, A general methodology for optimal load management with distributed renewable energy generation and storage in residential housing, Journal of Building Performance Simulation 10 (2017) 224–241, https://doi.org/10.1080/19401493.2016.1211738.
[198] D. La, Y. J. Dai, Y. Li, R. Z. Wang, and T. S. Ge, "Technical development of rotary desiccant dehumidification and air conditioning: A review," Renewable and Sustainable Energy Reviews, vol. 14, no. 1. Pergamon, pp. 130–147, Jan. 2010. 10.1016/j.rser.2009.07.016.
[199] K. Daou, R. Z. Wang, and Z. Z. Xia, "Desiccant cooling air conditioning: A review," Renewable and Sustainable Energy Reviews, vol. 10, no. 2. Pergamon, pp. 55–77, Apr. 2006. 10.1016/j.rser.2004.09.010.
[200] G.Q. Qiu, S.B. Riffat, Experimental investigation on a novel air dehumidifier using liquid desiccant, International Journal of Green Energy 7 (2) (Mar. 2010) 174–180, https://doi.org/10.1080/15435071003673666.
[201] A. A. M. Sayigh and J. C. McVeigh, Solar air conditioning and refrigeration. Pergamon Press, 1992.
[202] M. Sahlot and S. B. Riffat, "Desiccant cooling systems: a review," International Journal of Low-Carbon Technologies, p. ctv032, Jan. 2016, 10.1093/ijlct/ctv032.
[203] D.G. Waugaman, A. Kini, C.F. Kettleborough, A review of desiccant cooling systems, Journal of Energy Resources Technology, Transactions of the ASME 115 (1) (1993) 1–8, https://doi.org/10.1115/1.2905965.
[204] P. Niemann, F. Richter, A. Speerforck, G. Schmitz, Desiccant-Assisted Air Conditioning System Relying on Solar and Geothermal Energy during Summer and Winter, Energies 12 (16) (Aug. 2019) 3175, https://doi.org/10.3390/en12163175.
[205] D. S. Kim and C. A. Infante Ferreira, "Air-cooled LiBr–water absorption chillers for solar air conditioning in extremely hot weathers," Energy Conversion and Management, vol. 50, no. 4, pp. 1018–1025, Apr. 2009, 10.1016/j.enconman.2008.12.021.
[206] A. Grzebielec, R. Laskowski, A. Ruciński, "Influence of Outside Temperature on the Operation of the Adsorption Chiller", presented at the Environmental Engineering, Vilnius Gediminas Technical University, Lithuania (Aug. 2017), https://doi.org/10.3846/enviro.2017.255.
[207] U.S. DoE, Technology readiness assessment guide, DOE G 413 (2011) 3–4.
[208] "Alfa Laval Kathabar," Alfa Laval. https://www.alfalaval.us/microsites/consistentlyperfect/kathabar-technology/liquid-desiccant/ (accessed May 25, 2021).
[209] "DesiCool - Munters." https://www.munters.com/en/munters/products/dehumidifiers/desicool/?country=SE (accessed May 27, 2021).
[210] C.O. Popiel, J. Wojtkowiak, B. Biernacka, Measurements of temperature distribution in ground, Experimental thermal and fluid science 25 (5) (2001) 301–309.
[211] G. Hellström, B. Sanner, Experiences with the Borehole Heat Exchanger, Megastock 1997 (1997) 247–252, https://doi.org/10.1007/978-3-319-70548-4_447.
[212] G. Chiesa, A. Zajch, Contrasting climate-based approaches and building simulations for the investigation of Earth-to-air heat exchanger (EAHE) cooling sensitivity to building dimensions and future climate scenarios in North America, Energy and Buildings 227 (Nov. 2020), https://doi.org/10.1016/j.enbuild.2020.110410 110410.
[213] K.E. Taylor, R.J. Stouffer, G.A. Meehl, An Overview of CMIP5 and the Experiment Design, Bulletin of the American Meteorological Society 93 (4) (Apr. 2012) 485–498, https://doi.org/10.1175/BAMS-D-11-00094.1.
[214] D. Spitler and S. Gehlin, "Measured Performance of a Mixed-Use Commercial-Building Ground Source Heat Pump System in Sweden," Energies, vol. 12, no. 10, 2019, 10.3390/en12102020.
[215] P. Filipsson, A. Trüschel, J. Gräslund, J. Dalenbäck, Performance evaluation of a direct ground-coupled self-regulating active chilled beam system, Energy and Buildings 209 (2020), https://doi.org/10.1016/j.enbuild.2019.109691.
[216] H. Liu, H. Zhang, S. Javed, Long-Term Performance Measurement and Analysis, Energies 13 (17) (2020) 1–30, https://doi.org/10.3390/en13174527.
[217] Y. Shang, M. Dong, S. Li, Intermittent experimental study of a vertical ground source heat pump system, Applied Energy 136 (2014) 628–635, https://doi.org/10.1016/j.apenergy.2014.09.072.
[218] S. Javed, J. Claesson, and B. Ra, "Recovery times after thermal response tests on vertical borehole heat exchangers," 2011.
[219] M. I. Ahmad, H. Jarimi, and S. Riffat, Nocturnal Cooling Technology for Building Applications. Singapore: Springer Singapore, 2019. Accessed: May 12, 2020. [Online]. Available: http://link.springer.com/10.1007/978-981-13-5835-7
[220] M. G. Meir, J. B. Rekstad, and O. M. Løvvik, "A STUDY OF A POLYMER-BASED RADIATIVE COOLING SYSTEM," vol. 73, no. 6, pp. 403–417, 2002.
[221] D.-I. Bogatu, O.B. Kazanci, B.W. Olesen, A Preliminary Analysis on the Night Cooling Potential of Photovoltaic/thermal (PV/T) Panels for European Cities, E3S Web Conf. 111 (2019) 01055, https://doi.org/10.1051/e3sconf/201911101055.
[222] U. Eicker and A. Dalibard, "Photovoltaic–thermal collectors for night radiative cooling of buildings," Solar Energy, vol. 85, no. 7, pp. 1322–1335, Luglio 2011, 10.1016/j.solener.2011.03.015.
[223] E. Hosseinzadeh, H. Taherian, An Experimental and Analytical Study of a Radiative Cooling System with Unglazed Flat Plate Collectors, International Journal of Green Energy 9 (8) (Nov. 2012) 766–779, https://doi.org/10.1080/15435075.2011.641189.
[224] G. D. Joubert and R. T. Dobson, "Modelling and testing a passive night-sky radiation system," J. energy South. Afr., vol. 28, no. 1, p. 76, Mar. 2017, 10.17159/2413-3051/2017/v28i1a1550.
[225] T. Q. Pêan, L. Gennari, O. B. Kazanci, E. Bourdakis, and B. W. Olesen, "Influence of the environmental parameters on nocturnal radiative cooling capacity of solar collectors," p. 11, 2016.
[226] S. Zhang, J. Niu, Cooling performance of nocturnal radiative cooling combined with microencapsulated phase change material (MPCM) slurry storage, Energy and Buildings 54 (Nov. 2012) 122–130, https://doi.org/10.1016/j.enbuild.2012.07.041.
[227] M. Hu, G. Pei, Q. Wang, J. Li, Field test and preliminary analysis of a combined diurnal solar heating and nocturnal radiative cooling system, Applied Energy 179 (2016) 899–908, https://doi.org/10.1016/j.apenergy.2016.07.066.
[228] A.S. Farooq, P. Zhang, Y. Gao, R. Gulfam, Emerging radiative materials and prospective applications of radiative sky cooling - A review, Renewable and Sustainable Energy Reviews 144 (Jul. 2021), https://doi.org/10.1016/j.rser.2021.110910 110910.
[229] X. Xu, R. Niu, G. Feng, An Experimental and Analytical Study of a Radiative Cooling System with Flat Plate Collectors, Procedia Engineering 121 (2015) 1574–1581, https://doi.org/10.1016/j.proeng.2015.09.180.
[230] J. Babiak, B. W. Olesen, and D. Petras, Low temperature heating and high temperature cooling. Brussels: REHVA - Federation of European Heating, Ventilation and Air Conditioning Associations, 2009. [Online]. Available: https://www.rehva.eu/eshop/detail/no07-low-temperature-heating-and-high-temperature-cooling
[231] O. B. Kazanci, Low temperature heating and high temperature cooling in buildings: PhD Thesis. Kgs. Lyngby: DTU Civil Engineering, Technical University of Denmark, 2016. [Online]. Available: https://backend.orbit.dtu.dk/ws/files/126945749/Thesis til orbit.pdf
[232] J.Q. Allerhand, O.B. Kazanci, B.W. Olesen, Energy and thermal comfort performance evaluation of PCM ceiling panels for cooling a renovated office room, E3S Web Conf. 111 (2019) 03020, https://doi.org/10.1051/e3sconf/201911103020.
[233] J.Q. Allerhand, O.B. Kazanci, B.W. Olesen, Investigation of the influence of operation conditions on the discharge of PCM ceiling panels, E3S Web Conf. 111 (2019) 03021, https://doi.org/10.1051/e3sconf/201911103021.
[234] L. Bergia Boccardo, O. B. Kazanci, J. Quesada Allerhand, and B. W. Olesen, "Economic comparison of TABS, PCM ceiling panels and all-air systems for cooling offices," Energy and Buildings, vol. 205, p. 109527, Dec. 2019, 10.1016/j.enbuild.2019.109527.
[235] D.-I. Bogatu, E. Bourdakis, O.B. Kazanci, B.W. Olesen, Experimental Comparison of Radiant Ceiling Panels and Ceiling Panels Containing Phase Change material (PCM), E3S Web Conf. 111 (2019) 01072, https://doi.org/10.1051/e3sconf/201911101072.
[236] H. E. Feustel and C. Stetiu, "Hydronic radiant cooling - preliminary assessment," Energy and Buildings, p. 13, 1995, 10.1016/0378-7788(95)00922-K.
[237] B. Lehmann, V. Dorer, M. Koschenz, Application range of thermally activated building systems tabs, Energy and Buildings 39 (5) (May 2007) 593–598, https://doi.org/10.1016/j.enbuild.2006.09.009.
[238] B. Olesen, Radiant Floor Cooling Systems, ASHRAE Journal 50 (9) (2008) 16–22.
[239] C. Zhang, M. Pomianowski, P.K. Heiselberg, T. Yu, A review of integrated radiant heating/cooling with ventilation systems- Thermal comfort and indoor air quality, Energy and Buildings 223 (Sep. 2020), https://doi.org/10.1016/j.enbuild.2020.110094 110094.
[240] D. W. Kessling, S. Holst, and M. Schuler, "New Bangkok International Airport, NBIA," Proceedings of the Fourteenth Symposium on Improving Building Systems in Hot and Humid Climates, pp. 269–277, 2004.
[241] J.L. Niu, L.Z. Zhang, H.G. Zuo, Energy savings potential of chilled-ceiling combined with desiccant cooling in hot and humid climates, Energy and Buildings 34 (5) (Jun. 2002) 487–495, https://doi.org/10.1016/S0378-7788(01)00132-3.
[242] G. Sastry, P. Rumsey, VAV vs. Radiant: Side-by-Side Comparison, ASHRAE Journal 56 (5) (2014) 16–24.
[243] C. Stetiu, Energy and peak power savings potential of radiant cooling systems in US commercial buildings, Energy and Buildings 30 (2) (1999) 127–138, https://doi.org/10.1016/S0378-7788(98)00080-2.
[244] ASHRAE, ANSI/ASHRAE Standard 55-2017, Thermal environmental conditions for human occupancy. Atlanta: ASHRAE, 2017.
[245] Z. Wang et al., Revisiting individual and group differences in thermal comfort based on ASHRAE database, Energy and Buildings 219 (Jul. 2020), https://doi.org/10.1016/j.enbuild.2020.110017 110017.
[246] F. Bauman, A. Baughman, G. Carter, and E. A. Arens, "A Field Study of PEM (Personal Environmental Module) Performance in Bank of America's San Francisco Office Buildings," University of California, Berkeley, CEDR-01-97, 1997. [Online]. Available: https://escholarship.org/uc/item/717760bz
[247] W.M. Kroner, J.A. Stark-Martin, Environmentally Responsive Workstations and Office Worker Productivity, ASHRAE Transactions 100 (2) (1994) 750–755.
[248] T. Hoyt, E. Arens, H. Zhang, Extending air temperature setpoints: Simulated energy savings and design considerations for new and retrofit buildings, Building and Environment 88 (Jun. 2015) 89–96, https://doi.org/10.1016/j.buildenv.2014.09.010.

[249] T. Lund Madsen and B. Saxhof, "An unconventional method for reduction of the energy consumption for heating of buildings," in Proceedings of the Second International CIB Symposium on Energy Conservation in the Built Environment, Copenhagen, 1979, pp. 623–633.
[250] European Committee for Standardization, EN 16798-1:2019 - Energy performance of buildings - Part 1: Indoor environmental input parameters for design and assessment of energy performance of buildings addressing indoor air quality, thermal environment, lighting and acoustics. Brussels, 2019. [Online]. Available: https://standards.cen.eu/dyn/www/f?p=204:110:0::::FSP PROJECT,FSP ORG ID:41425,6138&cs=11EDD0CE838BCEF1A1EFA39A24B6C9890
[251] M. Mujahid Rafique, P. Gandhidasan, S. Rehman, L.M. Al-Hadhrami, "A review on desiccant based evaporative cooling systems", May, Renewable and Sustainable Energy Reviews 45 (2015) 145–159, https://doi.org/10.1016/j.rser.2015.01.051.
[252] X. Fang, J. Winkler, D. Christensen, Using EnergyPlus to perform dehumidification analysis on Building America homes, HVAC&R Research 17 (3) (Jun. 2011) 268–283, https://doi.org/10.1080/10789669.2011.564260.
[253] W. Miller et al., Conceptualising a resilient cooling system: A socio-technical approach, City and Environment Interactions 11 (Aug. 2021), https://doi.org/10.1016/j.cacint.2021.100065 100065.
[254] ASHRAE, ANSI/ASHRAE Standard 169-2013, Climatic Data for Building Design. Atlanta: ASHRAE, 2013.

Appendix C

Chapter 3: *Simulation-based framework to evaluate resistivity of cooling strategies in buildings against overheating impact of climate change*

Building and Environment 208 (2022) 108599

Contents lists available at ScienceDirect

Building and Environment

journal homepage: www.elsevier.com/locate/buildenv

Simulation-based framework to evaluate resistivity of cooling strategies in buildings against overheating impact of climate change

R. Rahif [a,*], M. Hamdy [b], S. Homaei [b], C. Zhang [c], P. Holzer [d], S. Attia [a]

[a] Sustainable Building Design Lab, Dept. UEE, Faculty of Applied Science, Université de Liege, Belgium
[b] Department of Civil and Environmental Engineering, Norwegian University of Science and Technology, Norway
[c] Aalborg University, Department of the Built Environment, Thomas Manns Vej 23, 9220, Aalborg Øst, Denmark
[d] Institute of Building Research and Innovation, Wipplingerstraße, 23/3, 1010, Vienna, Austria

ARTICLE INFO

Keywords:
Thermal comfort
Global warming
Overheating
Cooling strategy
Climate change

ABSTRACT

Over the last decades overheating in buildings has become a major concern. The situation is expected to worsen due to the current rate of climate change. Many efforts have been made to evaluate the future thermal performance of buildings and cooling technologies. In this paper, the term "climate change overheating resistivity" of cooling strategies is defined, and the calculation method is provided. A comprehensive simulation-based framework is then introduced, enabling the evaluation of a wide range of active and passive cooling strategies. The framework is based on the Indoor Overheating Degree (IOD), Ambient Warmness Degree (AWD), and Climate Change Overheating Resistivity (CCOR) as principal indicators allowing a multi-zonal approach in the quantification of indoor overheating risk and resistivity to climate change.

To test the proposed framework, two air-based cooling strategies including a Variable Refrigerant Flow (VRF) unit coupled with a Dedicated Outdoor Air System (DOAS) (C01) and a Variable Air Volume (VAV) system (C02) are compared in six different locations/climates. The case study is a shoe box model representing a double-zone office building. In general, the C01 shows higher *CCOR* values between 2.04 and 19.16 than the C02 in different locations. Therefore, the C01 shows superior resistivity to the overheating impact of climate change compared to C02. The maximum CCOR value of 37.46 is resulted for the C01 in Brussels, representing the most resistant case, whereas the minimum CCOR value of 9.24 is achieved for the C02 in Toronto, representing the least resistant case.

1. Introduction

During the last decade, the concept of resistivity of buildings and cooling strategies emerged in several studies [1]. The term resistivity appeared under different names including: Resistance, Resilience, Robustness, and other terms. For example, Attia et al. [1] defines cooling resistance as the building system's ability to maintain the initial design conditions during the disturbances such as heatwaves or power outages. This paper defines so-called "climate change overheating resistivity" as the ability of building cooling strategies to resist the increase of indoor overheating risk against the increase of outdoor thermal severity in a changing climate. In other words, the climate change overheating resistivity shows to what extend the indoor overheating risk will increase with the increase of outdoor thermal stress under future climate scenarios. This definition targets the ability of cooling strategies in buildings to maintain an acceptable thermal environment against the gradual worsening of weather conditions due to climate change, whereas the definition in Ref. [1] targets the ability of cooling strategies to suppress the short-term overheating incidents. There is a universal need to understand the notion of climate change overheating resistivity as a key factor in characterizing the future thermal performance of cooling strategies in buildings.

Despite the important role of opting for the implementation of climate change overheating resistive cooling strategies in buildings, it is being overlooked in the fight against climate change. Climate change overheating resistive cooling strategy improves the preparedness of the building for more intense and frequent overheating events in the future. The more the cooling strategy is resistant, the higher it is able to maintain a comfortable and healthy environment for the occupants in buildings. The concept of climate change overheating resistivity must be

* Corresponding author.
E mail address: ramin.rahif@uliege.be (R. Rahif).

https://doi.org/10.1016/j.buildenv.2021.108599
Received 7 September 2021; Received in revised form 15 November 2021; Accepted 16 November 2021
Available online 19 November 2021

standardized through the regulation and policies to be strictly implemented in the building cooling requirements.

Several studies highlighted the importance of cooling strategies in mitigating the overheating impacts of climate change [2–4]. The cooling demand in buildings is predicted to encounter unprecedented growth with the continuation of global warming [5–7]. The increase in cooling demand will be further aggravated with the increase of internal gains related to growing occupancy densities [8]. The cooling strategies will become inexorable to remove sensible/latent heating loads, prevent heat gains to the indoor environment, or enhance personal comfort. Therefore, the cooling strategies are expected to play the main role in reducing the overheating risks in buildings and hence ensure comfortable environments in future climates.

The first question considered in evaluating the scientific literature is, *"what are the simulation-based studies that assessed the performance of cooling strategies in relation to climate change?"*. In response to the first question, some relevant studies are presented as follows. O'Donovan et al. [9] investigated ten passive cooling control strategies applied on a Nearly Zero Energy Building (NZEB). Each strategy uses different combinations of passive cooling systems such as day-time ventilation, nighttime ventilation, and dynamic solar shading. For different combinations of passive cooling systems, an increase in indoor operative temperature between 0.1°*C* and 0.3°*C* in Dublin (maritime climate) and between 1°*C* and 1.9°*C* in Budapest (continental climate) was resulted by 2050s. It was also mentioned that the passive cooling strategies (and their combination) are able to maintain 57–95% comfortable occupied hours. Chiesa & Zajch [10] investigated the sensitivity of Earth-to Air Heat Exchangers (EAHE) to climate change in nine different locations across Northern America. Using Local and Residual Cooling Degree Hour (CDH_{loc} and CDH_{res}) to calculate the virtual control of EAHE, they found a significant reduction in the cooling potential of the EAHE system for Representative Concentration Pathway (RCP) 4.5 and 8.5 scenarios by 2061–2090. Rey-Hernández et al. [11] studied the impact of climate change on the indoor operative temperature of a zero energy and carbon office building located in Valladolid, Spain. The cooling system consists of a chiller system backed up with an adsorption chiller connected to an Air Handling Unit (AHU). By using the CCWorldWeatherGen tool to produce future weather files, they found an increase in indoor air temperature of ∼ 1°*C* between 2020 and 2050 and ∼ 1.7°*C* between 2050 and 2080. Ibrahim & Pelsmakers [12] investigated the increase in indoor overheating risk in a PassivHaus retrofit case study using PassiveHaus Planning Package (PHPP) [13] metric. For the period between High Emission Scenarios (HiES) of 2050 and 2080, the study results show an increase in overheating frequency by 6% for roof insulation, 7% for wall insulation, 6% for reduced glazing size, 5% for nighttime ventilation, 5% for internal and external shading devices, and 3% for reduced glazing G-value.

There is a study by Hamdy et al. [14] that introduced the Overheating Escalation Factor (OEF) metric corresponding to the inverse of climate change overheating resistivity factor within this paper. The *OEF* shows the sensitivity of a building to increasing outdoor thermal severity. By morphing the historical data (1964/1965 and 2003), they generated future and worst future weather scenarios. By applying in total 4 weather scenarios, they found the *OEF* values between 0.1 and 0.989 in Dutch dwellings. It means that there are some dwellings (with only natural ventilation) that are very close to become overheated in the future.

The second question considered in evaluating the scientific literature is, *"do those studies allow for a universal and comprehensive evaluation of the resistivity of cooling strategies against the overheating impact of climate change?"*. In response to the second question, four criteria are set for a systematic analysis as follows.

- **Universality:** this criterion evaluates whether the study is conducted for a universal evaluation of cooling strategies. Most studies focus on a specific location and climate based on the national or regional standards for comfort models and definition of building characteristics.
- **Function-independency:** this criterion investigates whether the study is focused on a specific building typology and function mode. Function-dependent studies focus on specific residential or non-residential buildings. Therefore, they do not contain full guidance on how to define the operational properties, schedules, and comfort categories for different building types.
- **Comfort model-independency:** this criterion evaluates whether the study has provisions regarding the flexible selection of the static and adaptive comfort models. Such a provision enables the evaluation of both active and passive cooling strategies with different cooling modes (air conditioned, non-air conditioned, and mixed/hybrid modes).
- **Resistivity evaluation:** this criterion examines whether the study contains resistivity evaluation against overheating impact of climate change. The main factor for the resistivity evaluation is the use of specific metrics (e.g. *OEF*, *CCOR*, etc.) that relate the indoor and outdoor thermal environments while incorporating multiple historical and future weather scenarios. Such metrics show, via a single value, to what extend the thermal performance of the cooling strategies in buildings are affected due to the changes in outdoor thermal conditions over time.

The results of the literature analysis based on the four abovementioned criteria are presented in Table 1.

Until now, there is a lack of comprehensive universal method to evaluate and compare the climate change overheating resistivity of cooling strategies. As part of the International Energy Agency (IEA) EBC Annex 80 – "Resilient cooling of buildings" project activities, this paper is developed to address the abovementioned knowledge gaps. The aim of this research is to broaden the comparative analysis among cooling strategies to global scales. The main research question is:

- How to evaluate the climate change overheating resistivity of cooling strategies worldwide?

The main research question can be divided into:

- Q1: How to characterize the climate data and building models in a consistent way to universally compare the cooling strategies?

Table 1
A list of studies in the literature concerning the thermal performance evaluation of buildings/cooling strategies under future climate scenarios.

Scientific article	Universality	Function-independency	Comfort model-independency	Resistivity evaluation
O'Donovan et al. [9]	×	×	×	×
Lomas & Ji [15]	×	×	×	×
Hanby & Smith [16]	×	×	✓	×
K.J. Lomas & Giridharan [17]	×	×	×	×
Gupta & Gregg [18]	×	×	×	×
Sajjadian et al. [19]	✓	×	×	×
Hamdy et al. [14]	×	×	✓	✓
Ibrahim & Pelsmakers [12]	×	×	×	×
Pagliano et al. [20]	×	×	✓	×
Chiesa & Zajch [10]	✓	×	×	×

- Q2: How to quantify and evaluate the climate change overheating resistivity of cooling strategies in buildings?
- Q3: How to test the evaluation framework?

This paper provides a generic simulation-based framework contributing to the body of knowledge in several ways. First, the framework is based on universally applicable standards enabling, with common boundary conditions, a universal comparison of cooling strategies in different climatic regions. Second, the framework is comprehensive; it allows for the comparison of a wide range of active and passive cooling strategies by providing systematic guidance on how to select the comfort models for the zones with different cooling modes (air conditioned, non-air conditioned, and mixed/hybrid mode). The framework is also not limited to any building typology and operation type; it encompasses residential and non-residential buildings, whether they are newly built or existing buildings. Third, the framework identifies and includes a multi-zonal and climate-change sensitive approach in the quantification of overheating risks in buildings. More importantly, a new fit-to-purpose metric called "Climate Change Overheating Resistivity (CCOR)" is introduced to quantify the resistivity of cooling strategies against overheating impacts of climate change. Finally, a Variable Refrigerant Flow (VRF) unit coupled with a Dedicated Outdoor Air Supply (DOAS) and a Variable Air Volume (VAV) system are compared in six reference cities to test the framework. Detailed information on their sizing is also presented.

The proposed framework can provide strong support for the building professionals to assess and compare different cooling strategies in the early design stage and retrofit of the new and existing buildings, respectively. Implementing the methodology may yield to thermal resiliency benefits in the buildings. Also, the research outcomes can inform the cooling industry regarding the resistivity of cooling strategies against climate change in different regions. It can instigate technical improvements towards more resistive cooling concepts. It also sheds light on the importance of resistivity requirements to be embedded in the regional and national building codes in defining thermal comfort requirements. The current paper is organized as follows. In Section 2, the methodology, including the framework is provided (Section 2.1) and the demonstration case (Section 2.2). Section 3 presents the results. Section 4 discusses the key findings, recommendations, strengths, limitations, and implications on the practice of the study and suggests potential future research. And, Section 5 concludes the paper.

2. Methodology

Fig. 1 shows the research methodology of the current paper. The methodology consists of two main parts. In the first part, the framework is introduced relying on the literature review, International standards, focus-group discussions, and follow-up discussions among the authors. In the second part, a demonstration case to test the proposed framework is provided.

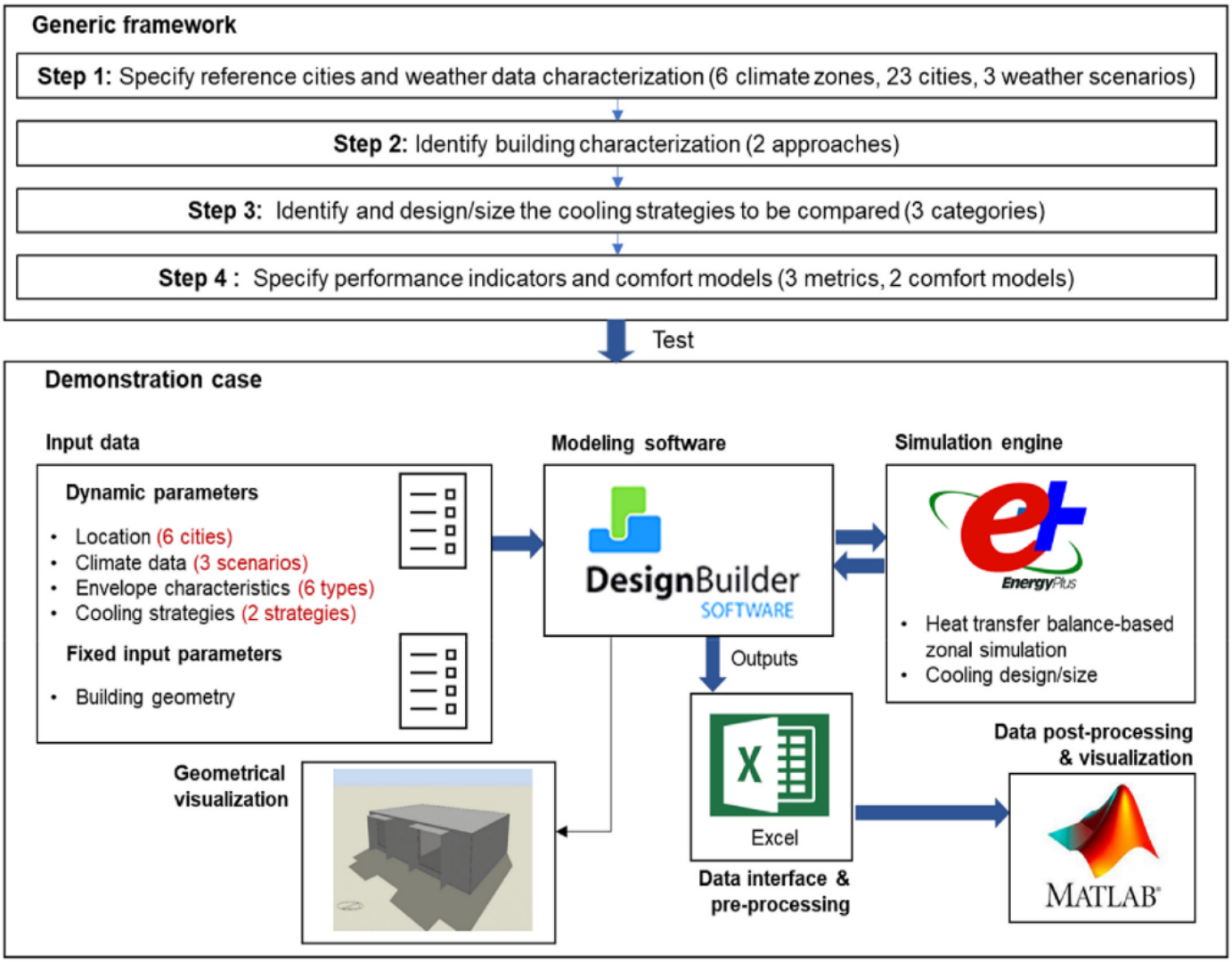

Fig. 1. Study conceptual framework (SCF).

2.1. Generic framework

Thermal discomfort in buildings can be divided into overheating discomfort and overcooling discomfort. Many researchers highlighted that with the continuation of global warming, overheating will become the increasing cause of thermal discomfort in buildings in most regions [21–25]. Therefore, the scope of the current framework is narrowed to the overheating discomfort and the evaluation of cooling strategies. In other words, the overcooling discomfort and heating system performance are excluded.

As shown in Fig. 2, the proposed framework consists of four main steps, 1) specify reference cities and weather data characterization (Section 2.1.1), 2) identify building characterization (Section 2.1.2), 3) identify and design/size the cooling strategies to be compared (Section 2.1.3), and 4) specify performance indicators and comfort models (Section 2.1.4). The framework allows a universal comparison of a wide range of active and passive cooling strategies. It encompasses almost the entire building typologies and function modes. The framework is also flexible to be used as a fast decision-support tool with recommending simple shoe box models as well as to more sophisticated analysis via reference building models. As mentioned earlier, the principal aim of the framework is to provide a standardized method (based on Internationally applicable standards) for a universal (different locations and climates) comparison of cooling strategies. However, for practical use, one can select a specific location and building and follow the suggested procedure to compare a set of applicable cooling strategies.

2.1.1. Step 1: specify reference cities and weather data characterization

Weather files are major prerequisites in any study related to climate change. The weather data requirements for the current framework is inspired by the work of (IEA) EBC Annex 80 - Weather Data Task Force. First, it necessitates the use of one contemporary (i.e. 2010s) and two future (i.e. 2050s and 2090s) weather scenarios. Future weather data projections are grouped according to the concentration and emission scenarios that are called Representative Concentrations Pathways (RCPs) to represent the 21st century. RCPs are based on energy, land use and cover, technological, socioeconomic, Green House Gas (GHG) emissions, and air pollutant assumptions [26]. With the current climate change mitigation efforts, the actual temperatures expected to be much higher than the projections in RCP2.6 (low emission scenario), RCP4.5 (medium-low emission scenario), and RCP6 (medium-high emission scenario) [27]. So, the framework requires future weather files based on RCP8.5 (high emission scenario). Current state-of-the-art approaches and tools to produce future global projections and weather files are widely discussed in Refs. [28–30].

Second, the framework recommends 23 cities (see Fig. 2) representing the climate zones 1 to 6 in ASHRAE 169.1 [31] classification. Multiple reference cities are assigned for each climate zone based on the population and the rate of growth.

Third, the framework allows both UHI effect included and excluded weather data. Including the UHI effect, especially in urban-related studies, quantifies the anthropogenic impacts on the evolution of outdoor thermal conditions [32]. Doing so contributes to more realistic weather data input for the simulations. However, due to limitations in obtaining such accurate weather data, the framework allows the use of weather files without UHI effects as an alternative.

2.1.2. Step 2: identify building characterization

The framework is applicable for evaluations in both new and existing buildings. The "existing buildings" are the buildings that are already in existence or constructed and authorized prior to the effective date of the current national or regional building regulations. Differently, the "new buildings" are the buildings that are already constructed or will be constructed after the effective date of the current national or regional building regulations. The framework provides two approaches for the selection of the building simulation models, the shoe box model (new buildings) and the reference building model (new and existing buildings).

The shoe box model is a basic and simplified model of a building that represents a building or its division as a rectangular box. The shoe box models can be made very quickly and therefore valuable to make early design decisions. In the case of shoe box models, the envelope characteristics must comply with ASHRAE 90.1 [33]. It is a widely accepted standard that specifies requirements for building envelope thermal properties for high-performance buildings (except for low-rise residential buildings) for each climate zone. The International standards ISO 18523- [34] and ISO 18253–2 [35] as well as ISO 17772–1 [36] are suggested to define schedules and condition of building, zone and space usage, including occupancy, operation of technical building systems, hot water usage, internal gains due to occupancy, lighting and equipment.

The reference building models are "*buildings characterized by and representative of their functionality and geographic location, including indoor and outdoor climate conditions*" (Annex III of the EPBD recast). The reference buildings can be created statistically (theoretical model) or by expert assumptions and previous studies (example model) or by selecting a real typical building [37]. Consequently, all the input parameters regarding the geometry, envelope properties, and operational conditions (schedule and condition of building, zone and space usage) can be derived by statistical analysis or expert assumptions or should reflect real typical conditions. Establishing reference building models provides a credible and robust model to evaluate the energy needs and retrofit measures [38] as well as thermal comfort and climate change adaptation measures. There are several studies that developed reference building models such as for educational buildings in Belgium [39], in Italy [40], in Ireland [41], in Australia [42], for office buildings in Korea [43], in England and Wales [44], for commercial buildings and residential buildings in the United States [33,45,46], and for residential buildings in thirteen European countries (Germany, Greece, Slovenia, Italy, France, Ireland, Belgium, Poland, Austria, Bulgaria, Sweden, Czech Republic, and Denmark) within the TABULA IEE-EU followed by EPISCOPE IEE-EU projects. In the case of reference building models, the users should create or select (e.g. from the above studies) representing a specific building typology and vintage (i.e., constructed during a specific new or old period) in the target reference city.

2.1.3. Step 3: identify and design/size the cooling strategies to be compared

Choosing a cooling strategy for buildings is challenging, especially when the designers are concerned with the impact of their choices on the resistivity against climate change. The framework lists a set of active and passive cooling strategies that are categorized by Ref. [4] as part of (IEA) EBC Annex 80 - Subtask B activities into four main categories (A, B, C, and D) based on their approaches in cooling the people or the indoor environment.

In category A, there are cooling strategies that reduce heat gains to the indoor environment and the occupants. It consists of solar shading and chromogenic glazing technologies, cool envelope materials, green roofs, roof ponds, green facades, ventilated roofs and facades, and thermal mass utilization. In category B, there are cooling strategies that remove sensible heat from indoor environments. It consists of absorption refrigeration (including desiccant cooling), ventilative cooling including Natural Ventilation (NV) and Mechanical Ventilation (MV), adiabatic/evaporative cooling, compression refrigeration, ground source cooling, sky radiative cooling, and high-temperature cooling (including radiant cooling). In category C, there are cooling strategies that enhance personal comfort apart from space cooling such as personal comfort systems. In category D, there are cooling strategies that remove latent heat from indoor environments such as high-performance dehumidification (including desiccant humidification). However, the framework cannot be used for category D due to the lack of relative humidity factor within the performance indicators (Step 4).

The cooling strategy (C_n) selected to be evaluated through the framework can be an individual or any combination of active and

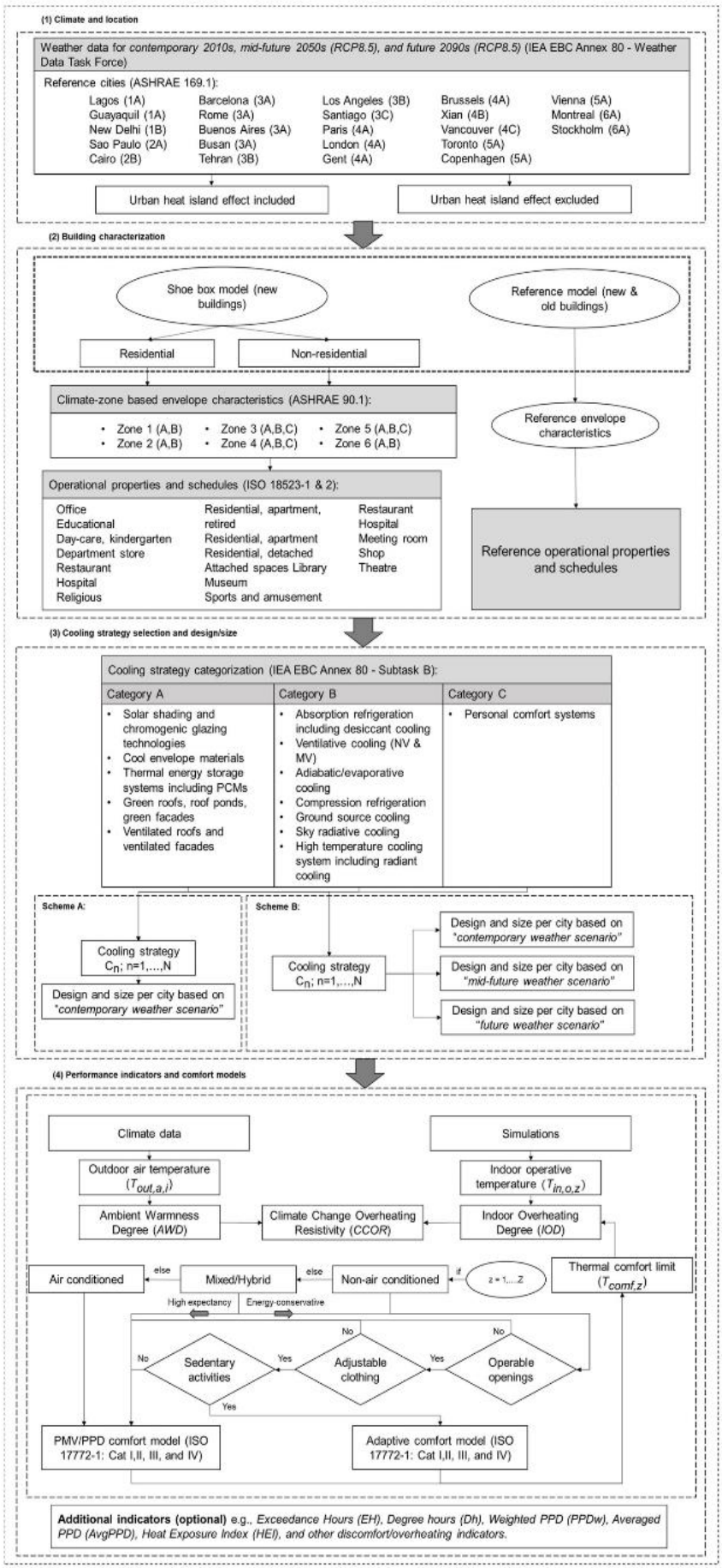

Fig. 2. The generic simulation-based framework to evaluate the climate change overheating resistivity of cooling strategies in buildings.

passive cooling strategies. The applicability of the selected cooling strategy in the target climates must be ensured while incorporating the different locations. Also, most active cooling systems have a life span of 15–25 years, depending on the type of the system and other contributing factors. Therefore, the framework allows for system adjustments through the long-term analysis period. It means that the cooling strategy characteristics can be changed in the mid-future and future scenarios.

Two schemes for cooling strategy adjustment is proposed within the framework. Scheme A: the C_n is designed or sized to provide an acceptable thermal environment in each reference city based on the *"contemporary weather scenario 2010s"* and is kept or replaced with the same for future scenarios, Scheme B: the C_n is adjusted at the end of its life span considering the changes in weather conditions, and thus is designed or sized based on future weather scenarios. In this case, it is possible to predict the thermal performance of the building if the cooling strategy design is not climate change-responsive (scheme A) or is climate change-responsive (scheme B).

Attaining the indoor thermal conditions always within the comfort limits can lead to oversizing the building cooling strategies. For the active strategies, the cooling strategy must be sized to summer design days. While for passive cooling strategies, the design should comply with the strict acceptable deviations criteria by Ref. [47]. It allows weekly 20%, monthly 12%, and yearly 3% deviations from the maximum comfort limits (Section 2.1.4.2) during the occupied hours. For mixed/hybrid mode cooling strategies, it is recommended that the building first operates via non-air conditioned cooling technology and use air conditioning to temper the weather extremes [48].

2.1.4. Step 4: specify performance indicators and comfort models

2.1.4.1. Performance indicators. There are several metrics introduced in the standards and scientific literature to quantify the time-integrated overheating in buildings. The time-integrated overheating indices describe, in a synthetic way, the extend of discomfort over time and predict the uncomfortable phenomena. Those indicators were extensively reviewed by Refs. [49,50]. Following the recommendations of [49], a climate change-sensitive overheating calculation method developed by Ref. [14] is selected that fits the scope of the current paper. Hamdy et al. [49] introduced a methodology based on two principal indicators, namely, Indoor Overheating Degree (IOD) (for the indoor environment) and Ambient Warmness Degree (AWD) (for the outdoor environment).

The *IOD* metric provides a multi-zonal approach in the quantification of intensity and frequency of overheating risks in buildings. Such a multi-zonal approach allows the implementation of zonal thermal comfort models (i.e., PMV/PPD and adaptive models) and requirements (i.e., comfort categories). Therefore, it is possible to assign variable comfort models with regard to the cooling mode and occupant adaptation opportunities in different zones of a building. It also tracks the zonal occupancy profiles and therefore excludes the effect of unoccupied zones in overheating calculations. The *IOD* [°C] is the summation of positive values of the difference between zonal indoor operative temperature $T_{in,o,z}$ and the zonal thermal comfort limit $T_{comf,z}$ (PMV/PPD or adaptive comfort limits) averaged over the sum of the total number of zonal occupied hours $N_{occ}(z)$ [–],

$$IOD \equiv \frac{\sum_{z\ 1}^{Z}\sum_{i\ 1}^{N_{occ}(z)}\left[\left(T_{in,o,z,i}-T_{comf,z,i}\right)^{+}\times t_{i,z}\right]}{\sum_{z\ 1}^{Z}\sum_{i\ 1}^{N_{occ}(z)}t_{i,z}} \tag{2}$$

where t is the time step (1h), i is occupied hour counter [–], z is building zone counter [–], Z is total building zones [–].

The *AWD* [°C] metric is used to quantify the severity of outdoor thermal conditions by averaging the Cooling Degree hours (*CDh*) calculated for a base temperature (T_b) of 18 °C [14] over the total number of building occupied hours,

$$AWD \equiv \frac{\sum_{i\ 1}^{N}\left[\left(T_{out,a,i}-T_b\right)^{+}\times t_i\right]}{\sum_{i\ 1}^{N}t_i} \tag{3}$$

where $T_{out,a,i}$ is the outdoor dry-bulb air temperature and N is the total number of building occupied hours. Only the positive values of $(T_{out,a,i}-T_b)^{+}$ are taken into account in the summation.

In this paper, the Climate Change Overheating Resistivity (CCORF) metric is introduced to couple the outdoor and indoor environments quantifying the climate change overheating resistivity of cooling strategies in buildings. The *CCOR* [–] shows the rate of change in the *IOD* with an increasing *AWD* due to the impact of climate change. It can be calculated using the linear regression methods assuming linearity between the *IOD* and *AWD*,

$$\frac{1}{CCOR}=\frac{\sum_{Sc\ 1}^{Sc\ M}\left(IOD_{Sc}-\overline{IOD}\right)\times\left(AWD_{Sc}-\overline{AWD}\right)}{\sum_{Sc\ 1}^{Sc\ M}\left(AWD_{Sc}-\overline{AWD}\right)^{2}} \tag{4}$$

where *Sc* is the weather scenario counter, *M* is the total number of weather scenarios, and $\overline{IOD}$ and $\overline{AWD}$ are the average of total *IODs* and *AWDs*. $CCOR > 1$ means that the building is able to suppress the increasing outdoor thermal stress due to climate change, and $CCOR < 1$ means the building is unable to suppress increasing outdoor thermal stress due to climate change.

The framework is also open for the implementation of additional user-specific metrics such as Exceedance Hours (EH), Degree hours (Dh), Weighted PPD (PPDw) [47,51], Averaged PPD (AvgPPD) [52], Heat Exposure Index (HEI) [53], and other discomfort/overheating indicators.

2.1.4.2. Thermal comfort models. The evaluation of overheating risks in buildings requires the determination of thermal comfort criteria. Thermal comfort defined as *"that condition of mind which expresses satisfaction with the thermal environment"* [52] has two main approaches: PMV/PPD (static) and adaptive.

The PMV/PPD comfort model assumes the human body as a passive recipient of its immediate environment [54], thus defining static thermal criteria. It has been shown that the PMV/PPD comfort model works well in air-conditioned spaces [55–57]. The framework suggests the use of the Category-based PMV/PPD model of [36] for the air-conditioned zones (Table 2).

The adaptive comfort model, however, allows a chance for occupant adaptation (e.g. operable openings, activity and clothing adjustments) and provides variable thermal comfort limits based on outdoor running mean temperature T_{rmo} [36],

$$T_{rmo}=(1-\alpha).\left\{T_{ed-1}+\alpha T_{ed-2}+\alpha^{2}T_{ed-3+\ldots}\right\} \tag{1}$$

where α is reference value between 0 and 1, $T_{ed\ i}$ is daily mean outdoor air temperature for $i-th$ previous day [°C]. The adaptive comfort model presents a valuable alternative in an energy-constrained world and is recommended by most standards to non-air conditioned buildings [58,59]. Therefore, the framework suggests the use of the Category-based adaptive comfort model of [36] for non-air conditioned zones (Table 3). In the adaptive comfort model, the occupants should have access to operable openings (e.g. windows, vents, and doors etc.) and

Table 2
PMV/PPD comfort model ranges by ISO 17772–1.

Categories	PPD [%] & PMV [–]
I (high-quality environment)	$PPD\% < 6\ ,\ -0.2 < PMV < +0.2$
II (medium-quality environment)	$PPD\% < 10\ ,\ -0.5 < PMV < +0.5$
III (moderate-quality environment)	$PPD\% < 15\ ,\ -0.7 < PMV < +0.7$
IV (low-quality environment)	$PPD\% < 25\ ,\ -1.0 < PMV < +1.0$

Table 3
Adaptive comfort model ranges by ISO 17772–1.

Categories	Upper limit [°C]	Lower limit [°C]	T_{rmo} range [°C]
I (high-quality environment)	$0.33T_{rmo} + 18.8 + 2$	$0.33T_{rmo} + 18.8 - 3$	10–30
II (medium-quality environment)	$0.33T_{rmo} + 18.8 + 3$	$0.33T_{rmo} + 18.8 - 4$	10–30
III (moderate-quality environment)	$0.33T_{rmo} + 18.8 + 4$	$0.33T_{rmo} + 18.8 - 5$	10–30

mainly sedentary activities (~ 1.2 *met*). They should also be able to adjust their clothing.

Different categories reflect the expected indoor environmental quality [50]. Category I is recommended for the high level of expectancy that is expected by very sensitive and fragile occupants such as the elderly, very young, and sick. Category II corresponds to the normal level of expectation and should be used for new buildings and renovations. Category III is the acceptable and moderate level of expectation and may be used for existing buildings. Category IV (only for the PMV/PPD model) defines the out of the range values that can be accepted for a limited part of the year.

So far, there is no sufficient Internationally applicable comfort model for mixed/hybrid cooling operation mode [48]. For mixed/hybrid cooling mode zone, the framework suggests the selection of either PMV/PPD model (high levels of expectancy or vulnerability of occupants) or the adaptive comfort model (energy-conservative purposes). The comfort Category (I, II, III, and IV) should be selected depending on building typology, occupant expectation, and climate context.

2.2. Demonstration case

To test the framework, in this section a demonstration case is provied to compare the climate change overheating resistivity of two cooling strategies, 1) Variable Refrigerant Flow (VRF) unit coupled with Dedicated Outdoor Air Supply (DOAS) system, and 2) Variable Air Volume (VAV) system. Those strategies applied on a double-zone office building under the operation of two cooling technologies in six different locations/climates.

2.2.1. Simulation program

In this paper, the DesignBuilder software based on EnergyPlus v8.9 simulation engine is used to conduct the simulations. EnergyPlus is developed by the U.S. Department Of Energy (U.S. DOE) as one of twenty major building energy simulation programs to run the simulations [60]. EnergyPlus contains an integrated heat and mass balance module and a building system module. Zone heating and cooling loads are calculated based on heat balance method recommended by Ref. [61]. The calculated loads are then passed to building HVAC module to calculate heating and cooling system, plant, and electric system response [62]. The HVAC simulation results via EnergyPlus have shown a close agreement with well-known simulation tools such as TRNSYS, ESP-r, and DOE-2.1E [63,64]. The simulations' results are then post-processed using a MATLAB script to calculate the *IOD*, *AWD*, and *CCOR*.

2.2.2. Weather data

To demonstrate the first step of the framework, six cities are selected including New Delhi, Cairo, Buenos Aires, Brussels, Toronto, and Stockholm covering zones 1 to 6 in ASHRAE 169.1 climatic classification [31]. Heating and Cooling Degree Days (HDD10°*C* and CDD18°*C*) averaged over 2016–2020 for the selected cities are summarized in Table 4.

Three weather scenarios are generated for each city. *Scenario 01* is the TMY [65] weather data constructed based on the recorded data in each weather station. It includes the solar radiation values for 1996–2015 and other parameters (i.e. air temperature, dew-point temperature, wind speed, wind direction, and precipitation properties) for 2000–2019. *Scenario 02* and Scenario *03* are future weather projections based on RCP8.5 defined by IPCC Fifth Assessment Report (AR5) [66]. To generate the future weather data, a representative subset (10 out of 35) of CMIP5 models are used for averaging the weather parameters [67]. All weather files are derived from Meteonorm v8 which is a combination of climate database, spatial interpolation tool and a stochastic weather generator, with global radiation data obtained from the Global Energy Balance Archive (GEBA) [28,29].

Table 4
Weather station location and climate characteristics of New Delhi, Cairo, Buenos Aires, Brussels, Toronto, and Stockholm (HDD10°*C* and CDD18°*C* averaged over 2016–2020).

City	Country	Coordinates (weather station)	Climate zone	HDD10°*C*	CDD18°*C*
New Delhi	India	28.6° N, 77.2° E	1B	24	3130
Cairo	Egypt	30.1° N, 31.3° E	2B	5	2327
Buenos Aires	Argentina	34.8° S, 58.5° W	3A	75	1034
Brussels	Belgium	50.9° N, 4.5° E	4A	780	258
Toronto	Canada	43.7° N, 79.4° W	5A	1630	494
Stockholm	Sweden	59.3° N, 18.1° E	6A	1501	171

2.2.3. Case study

The case study is assumed to be a double-zone office building formed by two adjacent identical zones (i.e., office room and administration room). Different comfort categories (i.e., comfort Category II and I) and operational conditions (i.e., occupancy density and heat loads by equipment) are considered for each zone. Each zone corresponds to the BESTEST 630 model [68]. It has east- and west- oriented windows (3 m $\times$ 2 m) with permanent solar shading devices (overhang and sidefins). The total building area is 96 m^2. The envelope characteristics are

Table 5
Building envelope characteristics for six cities (ASHRAE 90.1).

		Assembly maximum [W/m^2K]	Insulation Min. R-value [m^2K/W]
New Delhi	Roof	U-0.048	R-20 c.i.*
	Walls	U-0.089	R-13
	Floors	U-0.282	–
	Windows	U-0.45	–
Cairo	Roof	U-0.039	R-25 c.i.
	Walls	U-0.089	R-13
	Floors	U-0.033	R-30
	Windows	U-0.36	–
Buenos Aires	Roof	U-0.039	R-25 c.i.
	Walls	U-0.089	R-13
	Floors	U-0.033	R-30
	Windows	U-0.32	–
Brussels	Roof	U-0.029	R-35 c.i.
	Walls	U-0.058	R-13.0 + R-7.5 c.i.
	Floors	U-0.030	R-38.0
	Windows	U-0.32	–
Toronto	Roof	U-0.029	R-35 c.i.
	Walls	U-0.046	R-13.0 + R-12.5 c.i.
	Floors	U-0.030	R-38.0
	Windows	U-0.29	–
Stockholm	Roof	U-0.029	R-35 c.i.
	Walls	U-0.046	R-13.0 + R-12.5 c.i.
	Floors	U-0.024	R-38.0+ R-7.5 c.i.
	Windows	U-0.29	–

● Continuous insulation.

defined per city (climate zone) based on [33] and are summarized in Table 5. The case study is illustrated in Fig. 3.

The occupancy densities of 0.1 *person*/m^2 and 0.025 *person*/ m^2 are set for the office room and the administration room. Heat gains by the lighting and appliances of 12 W/m^2 is considered for the office room. Heat gains by the lighting and appliances of 12 W/m^2 and 4 W/m^2 are assigned for the administration room. It is also assumed that the occupants have the generic winter 1 clo and summer 0.5 clo clothing, and metabolic rate of 1.2 met (sedentary activity). All the information regarding the lighting, equipment, and occupancy schedules can be found in Ref. [34].

2.2.4. Cooling strategies

2.2.4.1. VRF + DOAS system. The first cooling strategy (C01) includes the Variable Refrigerant Flow (VRF) air-conditioning unit coupled with a Dedicated Outdoor Air Supply (DOAS). The VRF system uses an electric expansion valve and a variable-speed compressor to vary the refrigerant flow rate to each terminal unit to meet the zonal thermal loads. There are two types of VRF systems: Heat Pump (HP) and Heat Recovery (HR). In VRF-HP, all zones must be either in heating or cooling mode. In VRF-HR, the system is able to operate in the heating and cooling modes simultaneously. This paper applies VRF-HR system by default performance curves in the EnergyPlus such as the polynomial performance curve (VRFCoolCapFTBoundary) for the cooling capacity ratio boundary curve from the manufacturer's data [69]. The VRF-HR is implemented in v8.6. EnergyPlus and validated by Ref. [70]. The default input values are mostly used for the VRF-HR system as described in Table 6 [62,70]. However, some input values are modified in this study, including the increase of maximum outdoor air temperature in cooling only mode to 50°*C* to avoid the system disruption in the hot climates of New Delhi and Cairo. The Coefficient Of Performance (COP) values of 3.23 and 3.2 are set for cooling and heating, respectively, as minimum efficiency requirements [33,62]. The VRF-HR unit is operated by load priority master thermostat control type. It means that the total zone load is used to vary the zonal operating mode as being either heating or cooling. A Constant Air Volume (CAV) Air Handling Unit (AHU) is coupled to the VRF-HR system as DOAS to handle the latent loads and provide ventilation rates as per [36,71]. The input values for DOAS system are also presented in Table 6.

2.2.4.2. VAV system. The second cooling strategy (C02) is Variable Air Volume (VAV) system that consists of an AHU and Air Distribution Units (ADUs). The supply air is heated or cooled with heating and cooling coils centrally in AHU and the thermal capacity is controlled by varying the supply air volume via the dampers installed in the zonal ADUs. At full cooling capacity, the damper is fully open and the fan operates at maximum speed to supply the maximum air flow rate. With decreasing the cooling demand, the damper closes until it reaches the zone minimum ventilation air requirements as per [36]. In this study, the default AHU is used for the VAV system which contains a variable speed fans. Such AHU supplies variable airflow at a constant temperature having additional precision in temperature control [72]. The VAV models in EnergyPlus have been validated by Ref. [73]. In this paper, the VAV system is modeled using mostly the default input values or the values derived from Refs. [62,74,75] as listed in Table 6.

For both C01 and C02, all thermal capacities and design flow rates are auto-sized to design days by EnergyPlus based on the reference cities' external design conditions and the building configuration. Assuming a non climate change-responsive design (scheme A), the cooling strategies are not re-sized for future climates. The C01 and C02 are schematically shown in Fig. 4. The two technologies are among widely available (TRL~9) and applicable cooling technologies for the selected climate zones [4,62].

2.2.5. Zonal comfort criteria

Two air conditioned cooling strategies are selected for the case study. Therefore, the PMV/PPD comfort model is considered for both zones [36]. A Distinct comfort categories for the office room and the administration room are considered. The comfort Category II is set for the office room due to the normal level of expectation that should be used for the new buildings [76]. It corresponds to a fixed maximum indoor operative temperature limit of 26°*C*. The minimum ventilation rate requirement for Category II is 1.4 l/s.m^2. Assuming a high level of expectation for the occupants in the administration room, the comfort Category I is selected for this zone. It corresponds to a fixed maximum indoor operative temperature limit of 25.5°*C*. The minimum ventilation rate requirement for Category I is 2 l/s.m^2. The cooling and heating

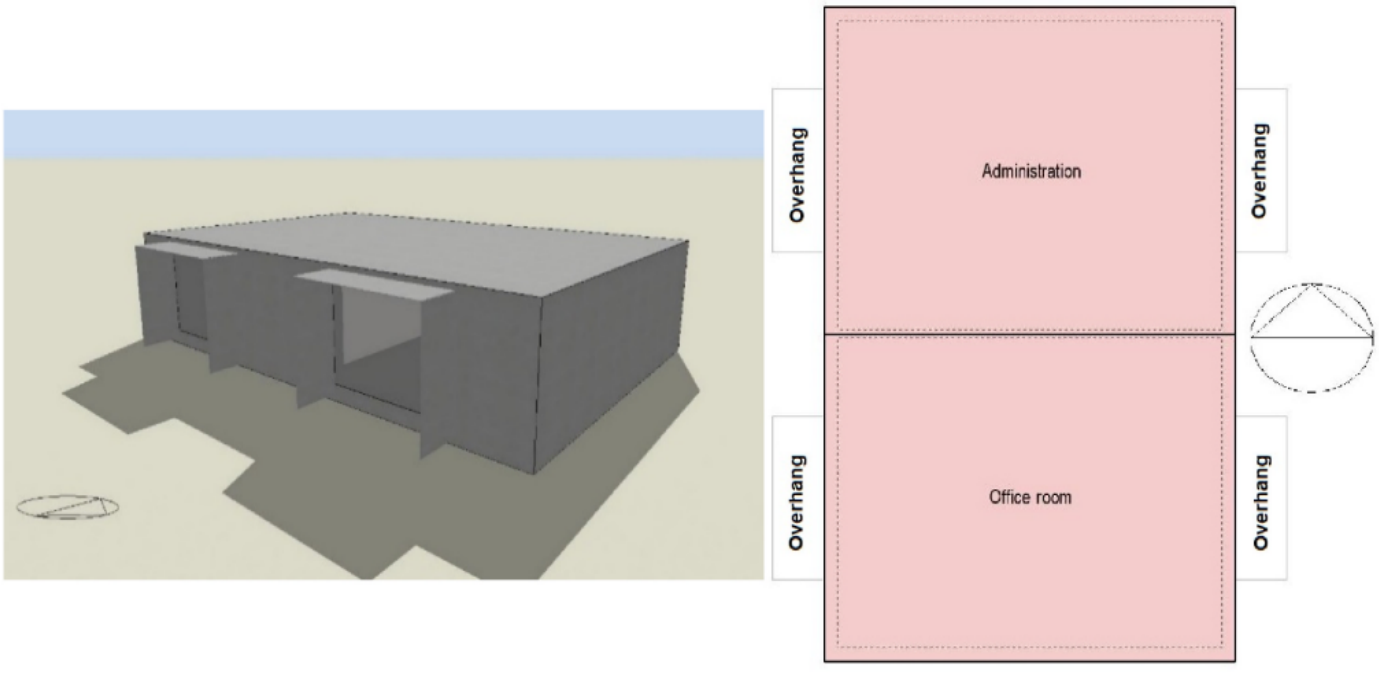

Fig. 3. The case study 3D view (left) and floor plan (right).

Table 6
The HVAC model inputs for C01 (VRF + DOAS) and C02 (VAV).

	C01 (VRF + DOAS)	C02 (VAV)
Set-points temperatures (occupied hours)	24.5°*C* for cooling/22°*C* for heating	24.5°*C* for cooling/22°*C* for heating
Set-back temperatures (unoccupied hours)	26.6°*C* for cooling/ 15.5°*C* for heating	26.6°*C* for cooling/15.5°*C* for heating
Minimum fresh air	1.4 l/s.m^2 (office room)/ 2 l/s.m^2 (Administration)	1.4 l/s.m^2 (office room)/2 l/ s.m^2 (Administration)
Fuel type	Electricity	Electricity (cooling)/Gas (heating)
Defrost strategy/ capacity	Resistive/Auto-sized	N/A
Condenser type	Air-cooled	Air-cooled
Heating	VRF outdoor unit	Gas furnace inside the packaged air conditioning unit
Cooling	VRF outdoor unit	Air-cooled chiller inside the packaged air conditioning unit
Total cooling capacity	Auto-sized to design days per city	Auto-sized to design days per city
Cooling COP	3.23	3.39
Total heating capacity	Auto-sized to design days per city	Auto-sized to design days per city
Heating COP	3.20	0.8 (gas burner efficiency)
Minimum outdoor temperature in cooling mode	−6°*C*	N/A
Maximum outdoor temperature in cooling mode	50°*C*	N/A
Minimum outdoor temperature in heating mode	−20°*C*	N/A
Maximum outdoor temperature in heating mode	40°*C*	N/A
Indoor unit supply air flow rates	Auto-sized to design days per city	Auto-sized to design days per city
Indoor fan efficiency/ type/pressure rise	0.7/constant volume/100 pa	N/A
Indoor cooling coil	VRF DX cooling coil	N/A
Indoor heating coil	VRF DX heating coil	N/A
AHU type	CAV	VAV
AHU supply air flow rates	Auto-sized to design days per city	Auto-sized to design days per city
AHU fan efficiency/ type/pressure rise	0.7/constant volume/600 pa	0.7/variable volume/600 pa
Supply air set-point manager	Preheat coil: Always 5°*C*	Air loop cooling: Always 14°*C*
AHU cooling coil	N/A	Water cooling coil
AHU heating coil	Electric heating coil	Water heating coil

set-point temperatures of 24.5°*C* and 22°*C* are set, respectively [36].

3. Results

Following the instructions given by the framework (see Fig. 2), this section is allocated to show the results of totally 36 simulation cases which are the combination of two cooling strategies (C01 and C02) and three weather scenarios (2010s, 2050s, and 2090s) in six locations (New Delhi, Cairo, Buenos Aires, Brussels, Toronto, and Stockholm). The simulations are run for annual period to cover the overheating incidents in winter and intermediate seasons as well. It should be mentioned that the heating system performance and cold discomfort is not in the scope of the current study.

3.1. Outdoor thermal conditions

The annual distribution of hourly outdoor air temperature for Scenario 01, Scenario 02, and Scenario 03 are illustrated in Fig. 5. The minimum, maximum, and average outdoor air temperature, Direct Normal Irradiance (DNI), Diffuse Horizontal Irradiance (DHI), *HDD10°C*, and *CDD18°C* over the annual period as well as *AWD* are summarized in Table 7. The increase in average and maximum outdoor air temperature is about 2.97–5.97°*C* and 3.5–6.5°*C* for the six reference cities by 2090s. In the cooling-dominated climates of New Delhi and Cairo, the AWD increases by 23% and 30% in the 2090s. It corresponds to CDD18°*C* variation of +42% and +62%, respectively, and HDD10°*C* tends to be zero in the future (i.e., 2050s and 2090s). New Delhi has the highest average and maximum outdoor air temperature of 29.15°*C* and 49.9°*C*, and has the highest AWD of 14.87°*C* in the 2090s. In the heating-dominated climates of Toronto and Brussels, both are expected to shift to cooling-dominated zones by increasing 248% and 224% in CDD18 °C and a decrease of 59% and 56% in HDD10°*C* by 2090s, respectively. In Toronto, higher maximum outdoor air temperature of around 2–4.1°*C* and higher CDD18°*C* of around 208–643 are resulted compared to Brussels. Therefore, Toronto shows higher AWD by 1.32°*C* in the 2010s, 2.7°*C* in the 2050s, and 3.89°*C* in the 2090s than in Brussels. Toronto has the highest increase in average outdoor air temperature by 5.97°*C*, maximum outdoor air temperature by 6.5°*C*, and AWD by 4.06°*C* in the 2090s. In Stockholm, although the CDD18°*C* increases by 313% in the 2090s, it still remains as a heating-dominated city with HDD10°*C* of 824 and CDD18°*C* of 413. Stockholm has the lowest average and maximum outdoor air temperature of 7.53°*C* and 30.20°*C* and therefore has the lowest AWD of 3.84°*C* in the 2010s.

3.2. Indoor operative temperature and exceedance hours (EH)

Fig. 6 shows the distribution of annual indoor operative temperature and Exceedance Hours (EH) (additional indicators) over the cooling set-point of 24.5°*C* in the office room and the administration room. The maximum indoor operative temperature fixed thresholds of 25.5°*C* of Category I (administration room) and 26°*C* of Category II (office room) are illustrated based on the static comfort model of ISO 17772–1. Table 8 summarizes the *IOD*, maximum indoor operative temperature, and *EH* for each scenario in six cities under the operation of C01 and C02.

In this study, the highest maximum indoor operative temperature of 34.98°*C* and the highest increase in maximum indoor operative temperature of 6.91°*C* are resulted for Toronto by 2090s. The highest *EH* of 625 and the highest increase in *EH* of 576 are also calculated for Toronto during the same period. It is due to the fact that, first, even though Toronto is classified as cool-humid climate (5A), more extreme up to 40.60°*C* and frequent hot weather conditions are expected by 2090s (similar to Buenos Aires) (see Table 7). Second, in line with the findings of [14,77], higher insulation levels in Toronto based on ASHRAE 90.1 requirements exacerbate the intensity and frequency of high indoor temperatures.

The ranges of the maximum indoor operative temperature difference between the office room and the administration room are 0.96–1.98°*C* for C01 and 0.63–2.07°*C* for C02. The ranges of the difference between the *EH* in the office room and the administration room are 16–143 for C01 and 19–131 for C02. The office room experiences higher maximum indoor operative temperatures and more overheating hours than the administration room. It is normal because of the higher internal gains by the office equipment and the higher number of occupants. However, the C01 shows more consistent zonal temperature control and therefore lower zonal temperature gradients [73]. The difference in the number of exceedance hours among the office room and administration room increases with global warming up to 346% (in Cairo). As a result, the office room is expected to have a relatively higher increase in the frequency of high indoor temperatures than the administration room due to climate change.

The C01 shows a lower maximum indoor operative temperature by 0.5–2.74°*C* in the office room (except for New Delhi) and 0.5–2.67°*C* in the administration room than C02. It shows that the C01 performs better

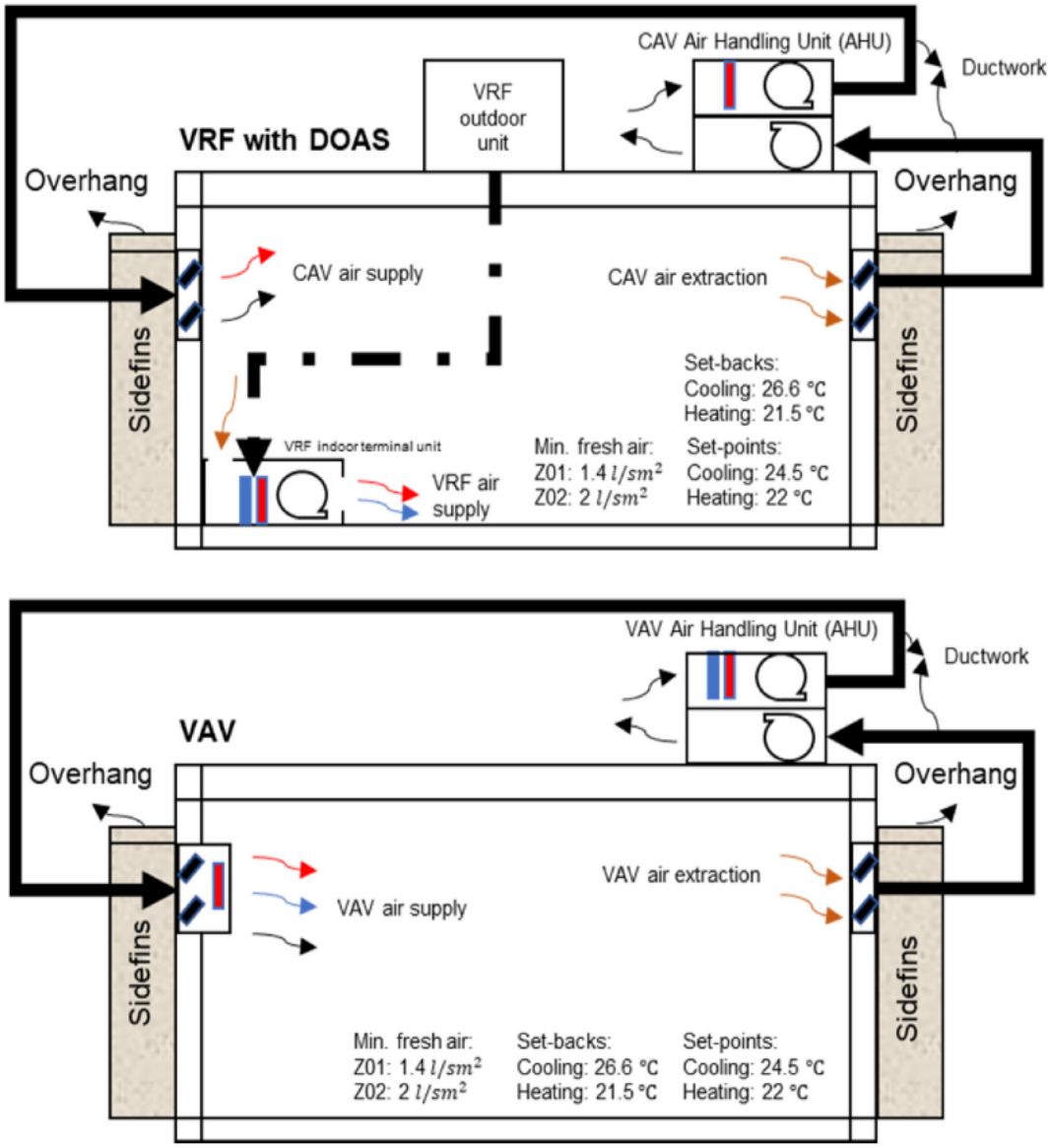

Fig. 4. Graphical representation of C01 (VRF with DOAS) (upper) and C02 (VAV) (lower).

in dampening the maximum indoor operative temperatures. The C01 results in higher *EH* between 1 and 56 (in office room) and 3–82 (in administration room) in relatively warmer climates of New Delhi, Cairo, and Buenos aires. However, the C02 shows lower *EH* between 2 and 57 (in office room) and 2–122 (in administration room) in Brussels, Toronto, and Stockholm. Both the above differences regarding the maximum indoor operative temperature and *EH* between the C01 and C02 increase with global warming. Overall, C01 performs better in reducing the maximum indoor operative temperatures in all climates and *EH* in Brussels, Toronto and Stockholm. At the same time, C02 has better performance in reducing the *EH* in New Delhi, Cairo, and Buenos Aires.

3.3. *Overheating risk and climate change overheating resistivity*

This section presents the results of the Indoor Overheating Risk (IOD) and Climate Change Overheating Resistivity (CCOR) of the selected cooling strategies. The *IOD* represents the intensity and frequency of overheating in buildings considering zonal comfort criteria. The *CCOR* quantifies the increase in the *IOD* corresponding to an increase in the *AWD*. Fig. 7 shows the linear regression models representing *IOD* as *AWD*. It shows a direct correlation between *IOD* and *AWD*; that is, when the *AWD* increases, overheating risk increases as well. The climate scenarios, namely 2010s, 2050s, and 2090s are represented by their *AWD* in each city.

Fig. 7 shows that the overheating conditions are becoming more intense and frequent with the increase of *AWD*. Since the C01 and C02 are sized to design days based on the *"Contemporary weather scenario 2010s"*, very low *IOD* values between 0.005 and 0.012 are calculated for this scenario.

In this study, the highest value of *IOD* 0.46°*C* is calculated for Toronto by 2090s associated with the maximum indoor operative temperature of 34.98°*C* and the *EH* of 589 under the operation of C02. It means that the current building configuration (i.e., the envelope complying with ASHRAE 90.1 standard and C02 as the cooling strategy) in Toronto is expected to have the highest risk of overheating in the future. In all cases, with the continuation of global warming the difference of *IOD* between C01 and C02 increases, especially in Brussels, Toronto, and Buenos Aires where higher differences up to 0.182 are observed. It shows that C02 is more affected by climate change than C01.

The *CCOR* values vary between 9.24 and 37.46 depending on the city and cooling strategy. However, it is > 1 for all cases. It shows that the cooling strategies (C01 and C02) selected and sized for the current weather conditions will be able to maintain an acceptable thermal environment and suppress global warming [14]. It is normal since the case study is equipped with active cooling systems, making it more

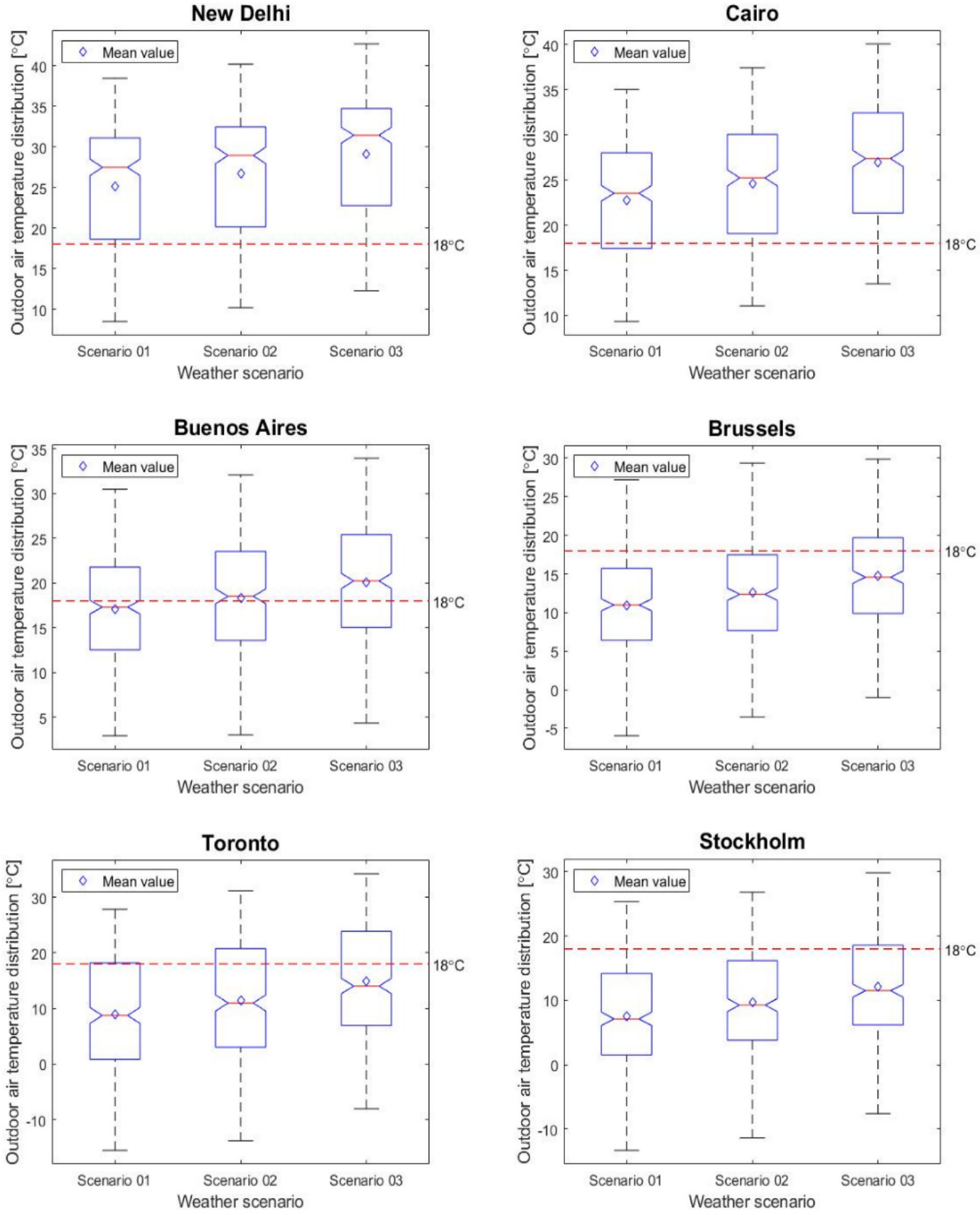

Fig. 5. Distribution of annual outdoor air temperature for Scenario 01 (2010s), Scenario 02 (2050s), and Scenario 03 (2090s).

resistant to climate change impacts but with different levels of success. The case study with C02 in Toronto has the lowest *CCOR* of 9.24 representing the case that affected most by climate change. On the other hand, the case study with C01 in Brussels has the highest *CCOR* of 37.46 and therefore is the most resistant case in this paper. In the analysis, the C01 always has higher *CCOR* values than C02, showing its superior resistance toward climate change. Especially in relatively cold climates of Brussels, Toronto, and Stockholm, the differences between the *CCOR* values among C01 and C02 are 19.16, 6.04, and 14.41, respectively. It was shown that most design variants such as internal heat gain, building

Table 7
Summary of average, minimum, and maximum outdoor air temperature, Direct Normal Irradiance (DNI), Diffuse Horizontal Irradiance (DHI), HDD10°C, CDD18°C, and AWD for three scenarios in all cities.

		Scenario 01	Scenario 02	Scenario 03
New Delhi	$T_{out,ave}$ [°C]	25.11	26.65	29.15
	$T_{out,max}$ [°C]	44.90	46.80	49.9
	$T_{out,min}$ [°C]	3.70	5.30	7.50
	DNI [W/m^2]	166.93	147.47	142.28
	DHI [W/m^2]	99.08	100.75	102.71
	AWD [°C]	12.12	13.05	14.87
	HDD10°C	2.51	0	0
	CDD18°C	2911	3355	4149
Cairo	$T_{out,ave}$ [°C]	22.80	24.63	26.99
	$T_{out,max}$ [°C]	41.80	44	46.9
	$T_{out,min}$ [°C]	5.60	7.40	9.30
	DNI [W/m^2]	185.36	176.62	179.95
	DHI [W/m^2]	94.24	96.88	95.69
	AWD [°C]	9.39	10.59	12.16
	HDD10°C	1	0	0
	CDD18°C	2052	2581	3325
Buenos Aires	$T_{out,ave}$ [°C]	17.11	18.33	20.08
	$T_{out,max}$ [°C]	37.50	39.10	41
	$T_{out,min}$ [°C]	−2.70	−1.70	−0.50
	DNI [W/m^2]	198.75	189.61	187.88
	DHI [W/m^2]	77.53	80.43	82.12
	AWD [°C]	6.49	7.40	8.42
	HDD10°C	135	109	55
	CDD18°C	777	1048	1446
Brussels	$T_{out,ave}$ [°C]	10.93	12.58	14.70
	$T_{out,max}$ [°C]	32.10	33.90	36.50
	$T_{out,min}$ [°C]	−7	−5.70	−3.40
	DNI [W/m^2]	101.95	115.44	117.58
	DHI [W/m^2]	65.94	65.03	66.47
	AWD [°C]	3.64	4.59	5.13
	HDD10°C	804	572	325
	CDD18°C	134	264	467
Toronto	$T_{out,ave}$ [°C]	8.99	11.40	14.96
	$T_{out,max}$ [°C]	34.10	36.60	40.60
	$T_{out,min}$ [°C]	−18.90	−16.40	−11.10
	DNI [W/m^2]	138.58	143.01	141.83
	DHI [W/m^2]	71.80	72.68	73.30
	AWD [°C]	4.96	7.29	9.02
	HDD10°C	1794	1405	782
	CDD18°C	342	663	1110
Stockholm	$T_{out,ave}$ [°C]	7.53	9.63	12.20
	$T_{out,max}$ [°C]	30.20	32.10	34.60
	$T_{out,min}$ [°C]	−15.70	−13.30	−10.60
	DNI [W/m^2]	130.22	133.42	138.46
	DHI [W/m^2]	53.30	54	52.31
	AWD [°C]	3.84	4.53	5.96
	HDD10°C	1742	1280	824
	CDD18°C	100	189	413

archetype, construction period, orientation, solar shading option are not key aspects to describe the resistivity to climate change [14]. However, the study shows that the selection of the active cooling system has a sound effect in determining the comfort conditions in buildings in the future. The relative potential to adapt to climate change metric P is quantified via the difference between the *IOD* resulted by C01 and C02 in the 2090s $(IOD_{C01,2090s} - IOD_{C02,2090s})^+$ over the Max $[IOD_{C01,2090s}, IOD_{C02,2090s}]$ [14]. By calculating the P, the C02 shows to have 13%, 29%, 8%, 51%, 39%, and 49% more potential to adapt compared to C01 in New Delhi, Cairo, Buenos Aires, Brussels, Toronto, and Stockholm, respectively.

4. Discussion

4.1. Findings and recommendations

More intense and frequent overheating events are expected with the continuation of global warming. Comparative building performance simulations seek to evaluate different strategies or measures in buildings concerning climate change with identical boundary conditions. Therefore, a generic simulation-based framework is developed that allows performing a relative comparison of individual or multiple cooling technologies in the frame of the (IEA) EBC Annex 80 – "Resilient cooling of buildings" project. The framework considers all function types (i.e., residential and non-residential), comfort categories (i.e., I, II, III, and IV), and cooling strategies (i.e., conditioned air, non-conditioned air, and mixed/hybrid mode). And, the selection of weather data and comfort criteria are based on unique approaches for climate change overheating resistivity evaluations in buildings.

Through the efforts to assign the building models in the framework, it was found that while in the North America especially in the United States, the creation of benchmark building models has consistently evolved [78–80], it is a recently emerging concept in other regions [39,40,43,81]. For example, after introducing the Energy Performance of Building Directive (EPBD) in Europe in 2003 which was implemented after in 2008, the projects such as the TABULA and the EPISCOPE started to create a central and structured depository of building stocks. However, there is still a substantial knowledge gap in the reliable benchmark models for different building typologies, vintages, and functions. Therefore, the framework is open to the implementation of the shoe box models for basic early design decisions and reference models for more sophisticated analyses.

The framework uses *IOD*, *AWD*, and *CCOR* as principal indicators to calculate the indoor overheating risk, the severity of the outdoor thermal environment, and climate change overheating resistivity of cooling strategies in buildings. The *IOD* metric allows a multi-zonal approach representing the real situations in buildings including zones with variable thermal comfort models (i.e., PMV/PPD and adaptive models) and requirements (e.g., comfort categories) tracing the occupied hours in each zone of the building (Section 2.1.4.2). Therefore, the framework is flexible and allows for personalization to evaluate cooling strategies under real and artificial conditions at zone levels. The *AWD* is a useful metric to quantify the severity of outdoor thermal conditions. However, it does not take into account the effect of solar radiation. As a result, it underestimates the severity of the outdoor thermal environment during the days with high solar radiation and low air temperatures.

The proposed methodology is tested by comparing C01 (VRF unit with DOAS) and C02 (VAV system) cooling strategies on a double-zone (i.e., office room and administration room) shoe box model in New Delhi, Cairo, Buenos Aires, Brussels, Toronto, and Stockholm (Section 2.2). Both systems are able to suppress the outdoor warming conditions by the end of this century. The C01 showed reduced maximum indoor operative temperature as well as *EH* compared to C02 leading to lower overheating risks (Table 8) and higher climate change overheating resistivity (Fig. 7). It shows that the C02 system is more prone to outdoor temperature increase and thus has less potential to overcome the climate change impacts. Although the VAV system cooling capacity can be increased by an increase in the amount of inlet air or by decreasing the inlet air temperature, it can lead to droughts and cold discomfort due to excessively high air velocities associated with low air temperatures [82]. The superior performance of C01 over C02 is more evident in Brussels, Toronto, and Stockholm. However, it should be mentioned that in this paper, a maximum temperature of 50°C is set as the temperature above the VRF system does not operate. Such assumption ensures the operation of the VRF system throughout the year in the selected reference cities

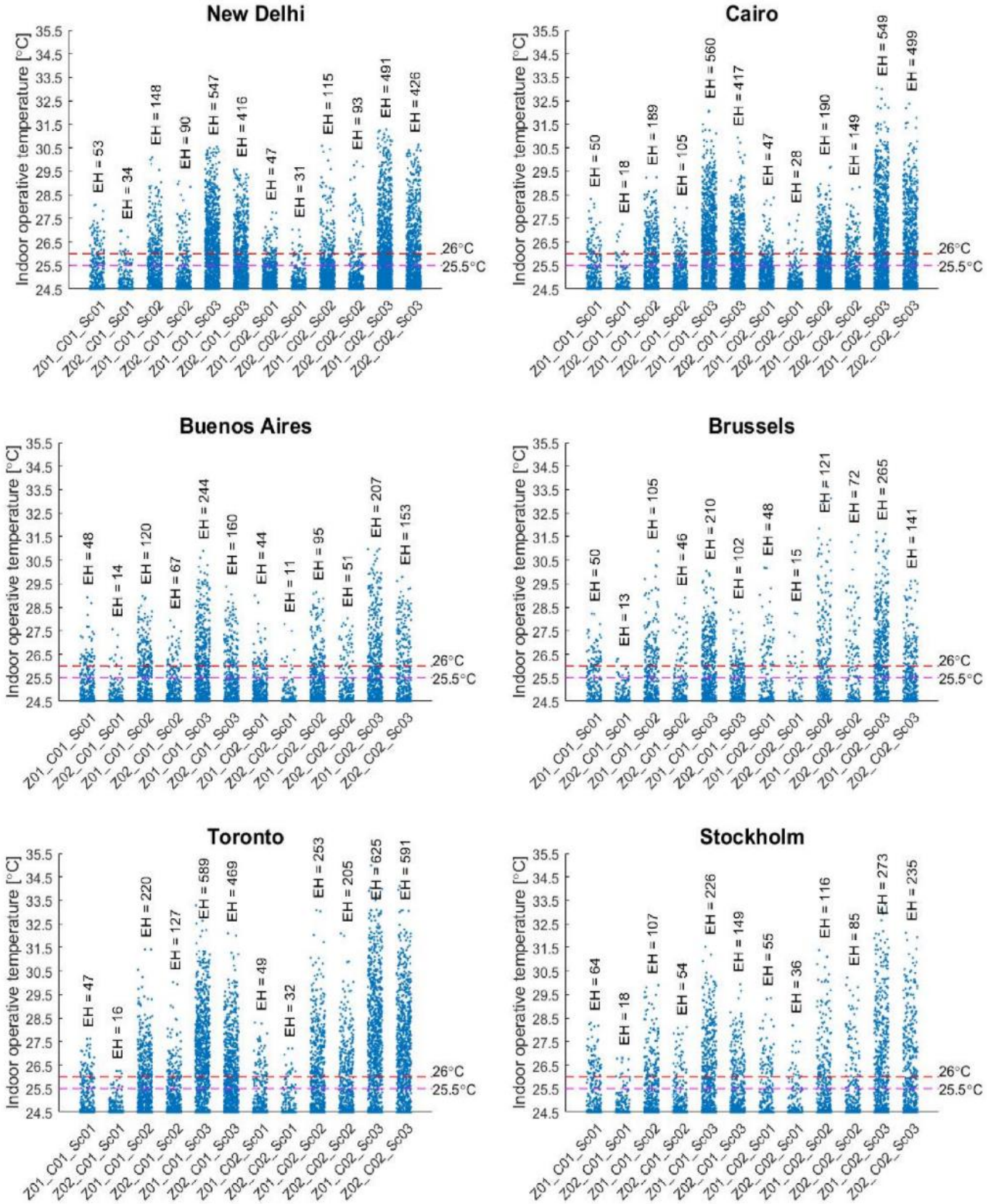

Fig. 6. Annual distribution of indoor operative temperature over cooling set-point of 24.5°C in office room and administration room for C01 and C02 during the occupied hours. The maximum indoor operative temperature threshold of 25.5°C is assigned for comfort Category I (administration room) and 26°C for Category II (office room). Exceedance Hours (EH) are shown for each zone per cooling strategy per scenario.

considering the weather data used in this study. Also, a previous study by Ref. [73] showed the energy-saving potential of the VRF system between 14 and 39% over the VAV system in all climatic zones across the U.S. Consequently, the VRF unit with DOAS seems to offer better performance in comparison to the VAV system in both energy-saving and thermal comfort aspects.

To summarize the significant recommendations, the list below is provided:

Table 8
Summary of IOD, exceedance hours, and maximum indoor operative temperature during occupied hours in the office room and the administration room.

			C01		C02	
			Office room (Z01)	Administration room (Z02)	Office room (Z01)	Administration room (Z02)
New Delhi	Scenario 01	IOD [°C]	0.0075		0.0058	
		$EH\,[-]\,(T_{i,max})\,[°C]$	47 (28.07)	31 (26.97)	53 (27.75)	34 (27.02)
	Scenario 02	IOD [°C]	0.0362		0.0361	
		$EH\,[-]\,(T_{i,max})\,[°C]$	115 (30.09)	93 (29.07)	148 (30.58)	90 (29.91)
	Scenario 03	IOD [°C]	0.1891		0.2162	
		$EH\,[-]\,(T_{i,max})\,[°C]$	491 (30.54)	426 (29.58)	547 (31.27)	416 (30.64)
Cairo	Scenario 01	IOD [°C]	0.0066		0.0075	
		$EH\,[-]\,(T_{i,max})\,[°C]$	50 (28.32)	18 (27.24)	47 (28.37)	28 (27.65)
	Scenario 02	IOD [°C]	0.0357		0.0447	
		$EH\,[-]\,(T_{i,max})\,[°C]$	189 (29.24)	105 (27.96)	190 (29.69)	149 (28.81)
	Scenario 03	IOD [°C]	0.2087		0.2946	
		$EH\,[-]\,(T_{i,max})\,[°C]$	560 (32.07)	417 (30.93)	549 (33.05)	499 (32.37)
Buenos Aires	Scenario 01	IOD [°C]	0.0063		0.0050	
		$EH\,[-]\,(T_{i,max})\,[°C]$	44 (28.92)	11 (27.57)	48 (28.99)	14 (27.78)
	Scenario 02	IOD [°C]	0.0235		0.0229	
		$EH\,[-]\,(T_{i,max})\,[°C]$	95 (28.97)	51 (27.93)	120 (29.13)	67 (28.02)
	Scenario 03	IOD [°C]	0.0792		0.0862	
		$EH\,[-]\,(T_{i,max})\,[°C]$	207 (30.89)	153 (29.37)	244 (30.97)	160 (29.78)
Brussels	Scenario 01	IOD [°C]	0.0055		0.0107	
		$EH\,[-]\,(T_{i,max})\,[°C]$	48 (28.22)	15 (26.31)	50 (30.18)	13 (28.24)
	Scenario 02	IOD [°C]	0.0261		0.0544	
		$EH\,[-]\,(T_{i,max})\,[°C]$	121 (30.87)	72 (28.89)	105 (33.61)	46 (31.56)
	Scenario 03	IOD [°C]	0.0461		0.0935	
		$EH\,[-]\,(T_{i,max})\,[°C]$	265 (30.03)	141 (28.37)	210 (31.68)	102 (29.61)
Toronto	Scenario 01	IOD [°C]	0.0046		0.0081	
		$EH\,[-]\,(T_{i,max})\,[°C]$	49 (27.62)	32 (26.25)	47 (28.30)	16 (27.20)
	Scenario 02	IOD [°C]	0.0558		0.1087	
		$EH\,[-]\,(T_{i,max})\,[°C]$	253 (31.42)	205 (30.02)	220 (33.08)	127 (32.09)
	Scenario 03	IOD [°C]	0.2810		0.4636	
		$EH\,[-]\,(T_{i,max})\,[°C]$	625 (33.29)	591 (32.09)	589 (34.98)	469 (34.11)
Stockholm	Scenario 01	IOD [°C]	0.0088		0.0122	
		$EH\,[-]\,(T_{i,max})\,[°C]$	55 (28.29)	36 (26.82)	64 (29.34)	18 (28.19)
	Scenario 02	IOD [°C]	0.0259		0.0461	
		$EH\,[-]\,(T_{i,max})\,[°C]$	116 (29.88)	85 (28.11)	107 (31.38)	54 (30.21)
	Scenario 03	IOD [°C]	0.0819		0.1602	
		$EH\,[-]\,(T_{i,max})\,[°C]$	273 (31.53)	235 (29.93)	226 (33.33)	149 (32.12)

- It is recommended to use the proposed framework to assess the indoor overheating risks in buildings and conduct comparative studies on the climate change overheating resistivity of different cooling strategies in buildings.
- It is also recommended to implement *IOD*, *AWD*, and *CCOR* as three principal indicators in climate change sensitive overheating evaluations. Designers and decision-makers can use these indicators for a multi-zonal comparison of building designs and their cooling strategies in the context of climate change.
- It is recommended to include additional weather files with intermediate periods (e.g., 2030s, 2040s, 2060s, etc.), which contributes to the CCOR's accuracy as the inverse slope of the linear regression line between the *IOD* and the *AWD*.
- It is recommended to further explore the potential of the VRF unit coupled with the DOAS as a promising strategy in enhancing the resistivity of buildings against overheating impacts of climate change.

4.2. Strength and limitations

There is an ongoing concern regarding the overheating risks that will be encountered more in future climates. There is no common guidance so far for evaluating the climate change overheating resistivity of cooling strategies to overcome the potential overheating issues in buildings. For this aim, the paper develops a comprehensive framework that can be followed step by step to compare the climate change overheating resistivity of a wide range of cooling strategies in buildings. The first strength of the study relies on the strong intellectual support via long-lasting brainstorming sessions by the members of (IEA) EBC Annex 80 – "Resilient cooling of buildings" project. The study provides a well-established framework based on universally applicable standards and state-of-the-art methods. This paper also provides the basis to compare different cooling strategies worldwide. The study's strength also relates to the implementation of a multi-zonal and climate change sensitive approach in the quantification of overheating risk as well as quantification of climate change overheating resistivity of cooling strategies. The proposed framework is also tested by comparing the C01 (VRF with DOAS) and C02 (VAV) cooling strategies in six reference cities. Despite the numerous previous studies on both above systems [83–87], there is no comparative study on their impact on the climate change overheating resistivity with detailed information on the system design and sizing.

However, the study has some limitations. First, this paper considers a shoe box model as the case study due to the restrictions in obtaining region-specific reference models. Second, the focus was on the thermal

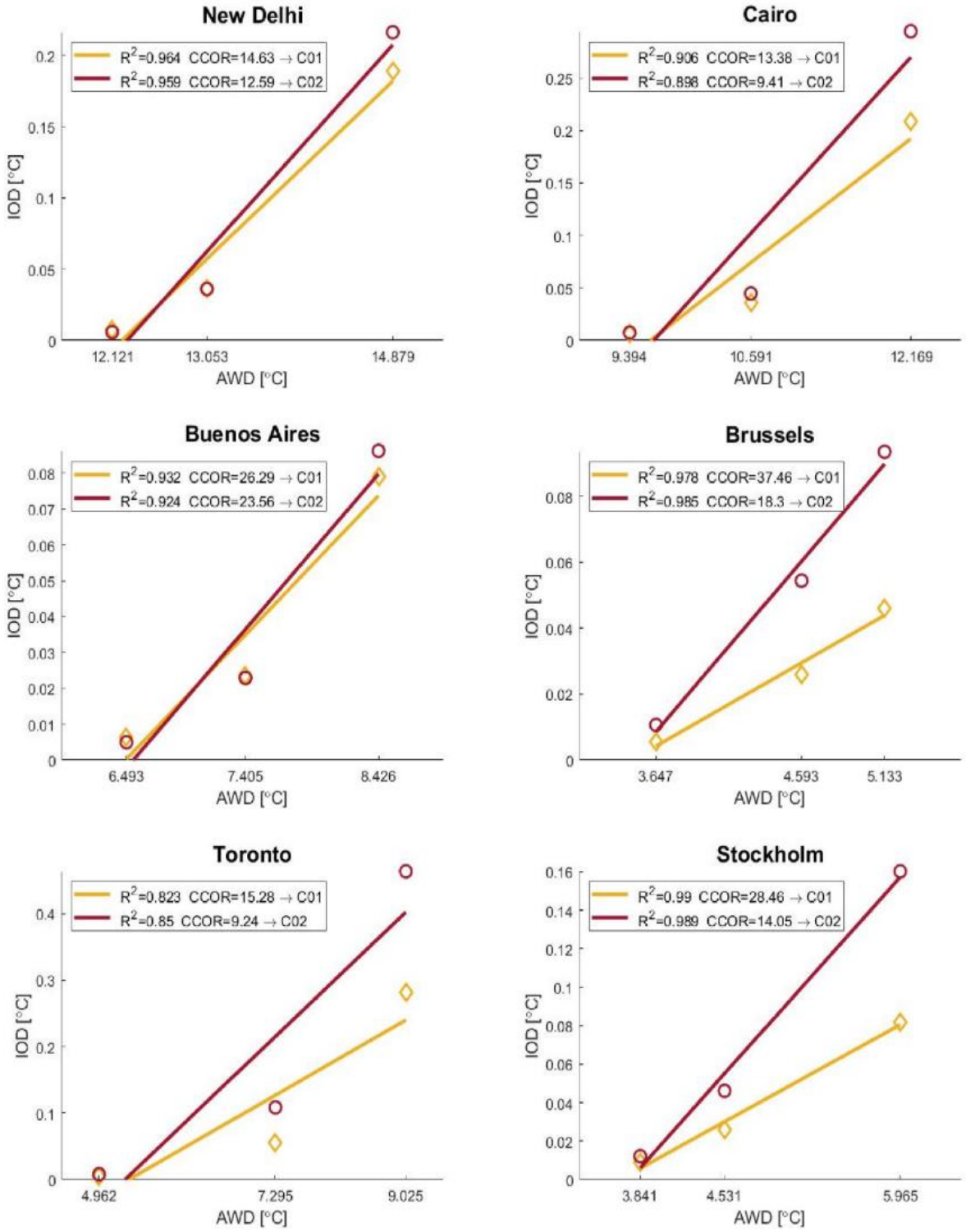

Fig. 7. IOD versus AWD. The slope of the regression line inverse shows the CCOR per city per cooling strategy.

comfort aspect, neglecting the energy performance of the selected cooling strategies. Third, spatial, cultural, and occupant behavioural differences are not considered in the selected cities to accurately define simulation parameters such as clothing factor, metabolic rate, control strategies, etc. Fourth, the weather data applied in the current study are generated using an autoregressive model very similar to the morphing technique [88]. It means that the same weather events are assumed to occur in the future in the same way as they do under the current climate, with the only difference being a linear shift in temperature throughout the year. Fourth, the effect of heat stress is not only dependent on air temperature or operative temperature. Considerations for relative humidity and other comfort parameters such as clothing factor, metabolic rate, and air velocity are also important in determining thermal comfort. Those parameters are neglected within the evaluation framework of the current study. Therefore, more accurate studies are suggested to overcome the limitations of this paper.

4.3. Implication on practice and future research

One of the implications of the current work is to interpret and include the proposed framework and recommendations in future revisions of national, regional, or local building regulations. Most regulations, such as the EPBD in Europe, do not provide a straightforward method to assess the indoor overheating risk and have no considerations for

climate change. Consequently, the indoor overheating risks arising from global warming are undermined in building designs. Also, the study establishes the foundation for the experts of the field such as the members of (IEA) EBC Annex 80 – "Resilient cooling of buildings" project to compare the resilient cooling strategies in different climate zones worldwide. The results will be communicated publicly to disseminate knowledge and raise community awareness to adapt the buildings to worsening outdoor conditions.

As some areas of the framework yet remain undemonstrated, some potential research recommendations are provided. First, future research is recommended to incorporate other reference cities specified in the framework using more accurate and reliable weather files. Second, even though the use of multi-zonal shoe box models provides preliminary but valuable insights into the performance of cooling strategies in a simple and fast way, the future research is recommended to apply real residential and non-residential reference building models developed for local, provincial or national building stocks for more realistic evaluations. Third, through the demonstration case in this paper, only the performance of two active cooling systems are compared. Therefore, future research is recommended to use the framework for the evaluation of other active cooling strategies and passive cooling strategies (see Section 2.1.3) as well as their combinations. Forth, future studies are suggested to implement additional discomfort/overheating indices besides the primary ones (i.e., *IOD*, *AWD*, and *CCOR*) to complement the overheating assessments.

In addition to the research recommendations on undemonstrated parts of the framework, future research is recommended to improve the performance indices suggested by the framework (i.e., *IOD* and *AWD*). The new metric for the indoor environment and occupant comfort should include more comfort parameters such as relative humidity, metabolic rate, clothing factor, and air velocity to better reflect the occupant's thermal sensation. At the same time, the new metric for the outdoor environment should include more outdoor thermal parameters such as solar radiation, relative humidity, etc. Future research is also encouraged to define a well-defined post-processing procedure to establish sensitivity and optimization analysis. It further extends the functionality of the current framework to optimize the cooling strategies for the buildings in different typologies and climates.

5. Conclusion

In this paper, a generic simulation-based framework is developed to evaluate the climate change overheating resistivity of cooling strategies in varying climates. Following the framework yields consistent results contributing to comparative studies among cooling strategies. The framework requires four key decisions: 1) specify weather data characterization (Section 2.1.1), 2) identify building characterization (Section 2.1.2), 3) identify and design/size the cooling strategies to be compared (Section 2.1.3), and 4) specify performance indicators and comfort models (Section 2.1.4). 23 cities are suggested as reference cities worldwide based on the rate of growth and population covering zones 1 to 6 in ASHRAE 169.1 classification. The framework considers all function types (i.e., residential and non-residential), comfort categories (i.e., I, II, III, and IV), cooling strategies (i.e., conditioned air, non-conditioned air, and mixed/hybrid mode). Three metrics are implemented namely, Indoor Overheating Degree (IOD), Ambient Warmness Degree (AWD), and Climate Change Overheating Resistivity (CCOR) allowing for a multi-zonal approach in the quantification of intensity and frequency of overheating during the zonal occupied hours.

Subsequently, the framework is tested by comparing sufficiently-sized VRF unit with DOAS and VAV cooling strategies in New Delhi, Cairo, Buenos Aires, Brussels, Toronto, and Stockholm. It was concluded that the VRF unit with DOAS results in reduced maximum indoor operative temperature and Exceedance Hours (EH) compared to VAV system. More importantly, the results showed that the building equipped with the former are more resistant to overheating impact of climate. It should be mentioned that the demonstration case is aimed to show that the framework is working well in conducting a universal comparison among cooling strategies. The validation of the results achieved in this study is required by using the framework in real multi-zonal reference buildings by using more reliable and accurate future climate data.

Declaration of competing interest

The authors declare that they have no known competing financial interests or personal relationships that could have appeared to influence the work reported in this paper.

Acknowledgement

This research was funded by the Walloon Region under the call 'Actions de Recherche Concertées 2019 (ARC)' (funding number: ARC 19/23–05) and the project OCCuPANt, on the Impacts Of Climate Change on the indoor environmental and energy PerformAnce of buildiNgs in Belgium during summer. The authors would like to gratefully acknowledge the Walloon Region and the University of Liege for funding. We would like to also acknowledge the Sustainable Building Design (SBD) lab at the Faculty of Applied Sciences at the University of Liege for valuable support during the content analysis and curation of the data. This study is a part of the International Energy Agency (IEA) EBC Annex 80 – "Resilient cooling of buildings" project activities to define resilient cooling in residential buildings.

References

[1] S. Attia, et al., Resilient cooling of buildings to protect against heat waves and power outages: key concepts and definition, Energy Build. (Mar. 2021) 110869, https://doi.org/10.1016/j.enbuild.2021.110869.

[2] H. Hooyberghs, S. Verbeke, D. Lauwaet, H. Costa, G. Floater, K. De Ridder, Influence of climate change on summer cooling costs and heat stress in urban office buildings, Climatic Change 144 (4) (Oct. 2017) 721–735, https://doi.org/10.1007/s10584-017-2058-1.

[3] R. Khosla, et al., Cooling for sustainable development, Nat. Sustain 4 (3) (2021) 201–208, https://doi.org/10.1038/s41893-020-00627-w.

[4] C. Zhang et al., "Resilient cooling strategies- a critical review and qualitative assessment," *Energy Build.* , In press., 2021.

[5] U. Berardi, P. Jafarpur, Assessing the impact of climate change on building heating and cooling energy demand in Canada, Renew. Sustain. Energy Rev. 121 (2020) 109681, https://doi.org/10.1016/j.rser.2019.109681.

[6] J. Izar-Tenorio, P. Jaramillo, W.M. Griffin, M. Small, Impacts of projected climate change scenarios on heating and cooling demand for industrial broiler chicken farming in the Eastern US, J. Clean. Prod. 255 (2020) 120306, https://doi.org/10.1016/j.jclepro.2020.120306.

[7] M.A.D. Larsen, S. Petrović, A. Radoszynski, R. McKenna, O. Balyk, Climate change impacts on trends and extremes in future heating and cooling demands over Europe, Energy Build. 226 (2020) 110397, https://doi.org/10.1016/j.enbuild.2020.110397.

[8] W. Luan, X. Li, Rapid urbanization and its driving mechanism in the Pan-Third Pole region, Sci. Total Environ. 750 (Jan. 2021) 141270, https://doi.org/10.1016/j.scitotenv.2020.141270.

[9] A. O' Donovan, M.D. Murphy, P.D. O'Sullivan, Passive control strategies for cooling a non-residential nearly zero energy office: simulated comfort resilience now and in the future, Energy Build. 231 (Jan. 2021) 110607, https://doi.org/10.1016/j.enbuild.2020.110607.

[10] G. Chiesa, A. Zajch, Contrasting climate-based approaches and building simulations for the investigation of Earth-to-air heat exchanger (EAHE) cooling sensitivity to building dimensions and future climate scenarios in North America, Energy Build. 227 (2020) 110410, https://doi.org/10.1016/j.enbuild.2020.110410.

[11] J.M. Rey-Hernández, C. Yousif, D. Gatt, E. Velasco-Gómez, J. San José-Alonso, F. J. Rey-Martínez, Modelling the long-term effect of climate change on a zero energy and carbon dioxide building through energy efficiency and renewables, Energy Build. 174 (2018) 85–96, https://doi.org/10.1016/j.enbuild.2018.06.006.

[12] A. Ibrahim, S.L. Pelsmakers, Low-energy housing retrofit in North England: overheating risks and possible mitigation strategies, Build. Serv. Eng. Technol. 39 (2) (Mar. 2018), https://doi.org/10.1177/0143624418754386. Art. no. 2.

[13] W. Feist, B. Kaufmann, J. Schnieders, O. Kah, Passive House Planning Package, *Passive House Institute*, Darmstadt, Germany, 2015.

[14] M. Hamdy, S. Carlucci, P.-J. Hoes, J.L.M. Hensen, The impact of climate change on the overheating risk in dwellings—a Dutch case study, Build. Environ. 122 (Sep. 2017) 307–323, https://doi.org/10.1016/j.buildenv.2017.06.031.

[15] K.J. Lomas, Y. Ji, Resilience of naturally ventilated buildings to climate change: advanced natural ventilation and hospital wards, Energy Build. 41 (6) (Jun. 2009) 629–653, https://doi.org/10.1016/j.enbuild.2009.01.001.

[16] V.I. Hanby, S.T. Smith, Simulation of the future performance of low-energy evaporative cooling systems using UKCP09 climate projections, Build. Environ. 55 (2012) 110–116, https://doi.org/10.1016/j.buildenv.2011.12.018.

[17] K.J. Lomas, R. Giridharan, Thermal comfort standards, measured internal temperatures and thermal resilience to climate change of free-running buildings: a case-study of hospital wards, Build. Environ. 55 (Sep. 2012) 57–72, https://doi.org/10.1016/j.buildenv.2011.12.006.

[18] R. Gupta, M. Gregg, Using UK climate change projections to adapt existing English homes for a warming climate, Build. Environ. 55 (2012) 20–42, https://doi.org/10.1016/j.buildenv.2012.01.014.

[19] S.M. Sajjadian, J. Lewis, S. Sharples, The potential of phase change materials to reduce domestic cooling energy loads for current and future UK climates, Energy Build. 93 (2015) 83–89, https://doi.org/10.1016/j.enbuild.2015.02.029.

[20] L. Pagliano, S. Carlucci, F. Causone, A. Moazami, G. Cattarin, Energy retrofit for a climate resilient child care centre, Energy Build. 127 (Sep. 2016) 1117–1132, https://doi.org/10.1016/j.enbuild.2016.05.092.

[21] R. Barbosa, R. Vicente, R. Santos, Climate change and thermal comfort in Southern Europe housing: a case study from Lisbon, Build. Environ. 92 (Oct. 2015) 440–451, https://doi.org/10.1016/j.buildenv.2015.05.019.

[22] P.M. Congedo, C. Baglivo, A.K. Seyhan, R. Marchetti, Worldwide dynamic predictive analysis of building performance under long-term climate change conditions, J. Build Eng. 42 (Oct. 2021) 103057, https://doi.org/10.1016/j.jobe.2021.103057.

[23] A. Dodoo, L. Gustavsson, F. Bonakdar, Effects of future climate change scenarios on overheating risk and primary energy use for Swedish residential buildings, Energy. Procedia 61 (Jan. 2014) 1179–1182, https://doi.org/10.1016/j.egypro.2014.11.1048.

[24] C.A. Alves, D.H.S. Duarte, F.L.T. Gonçalves, Residential buildings' thermal performance and comfort for the elderly under climate changes context in the city of São Paulo, Brazil, Energy Build. 114 (Feb. 2016) 62–71, https://doi.org/10.1016/j.enbuild.2015.06.044.

[25] A.D. Peacock, D.P. Jenkins, D. Kane, Investigating the potential of overheating in UK dwellings as a consequence of extant climate change, Energy Pol. 38 (7) (Jul. 2010) 3277–3288, https://doi.org/10.1016/j.enpol.2010.01.021.

[26] D.P. Van Vuuren, et al., The representative concentration pathways: an overview, Climatic Change 109 (1) (2011) 5–31, https://doi.org/10.1007/s10584-011-0148-z.

[27] A. Cibse Guide, A. Cibse Guide, Environmetnal Design, 2006, Chartered Institution of Building Services Engineers, London, UK, 2006.

[28] M. Herrera, et al., A review of current and future weather data for building simulation, Build. Serv. Eng. Technol. 38 (5) (2017) 602–627, https://doi.org/10.1177/0143624417705937.

[29] A. Moazami, V.M. Nik, S. Carlucci, S. Geving, Impacts of future weather data typology on building energy performance – investigating long-term patterns of climate change and extreme weather conditions, Appl. Energy 238 (Mar. 2019) 696–720, https://doi.org/10.1016/j.apenergy.2019.01.085.

[30] J. Bravo Dias, G. Carrilho da Graça, P.M.M. Soares, Comparison of methodologies for generation of future weather data for building thermal energy simulation, Energy Build. 206 (Jan. 2020) 109556, https://doi.org/10.1016/j.enbuild.2019.109556.

[31] Ansi/Ashrae Standard 169.1, Standard 169.1-2013: climatic data for building design standards, Climatic Data. Build. Des. Stand. (2013).

[32] A. Mohajerani, J. Bakaric, T. Jeffrey-Bailey, The urban heat island effect, its causes, and mitigation, with reference to the thermal properties of asphalt concrete, J. Environ. Manag. 197 (2017) 522–538, https://doi.org/10.1016/j.jenvman.2017.03.095.

[33] Ansi/Ashrae Standard 90.1, Standard 90.1-2013: energy standards for buildings except low-rise residential buildings, Climatic Data. Build. Des. Stand. (2019).

[34] ISO 18523-1, "'ISO 18523-1: Energy Performance of Buildings — Schedule and Condition of Building, Zone and Space Usage for Energy Calculation — Part 1: Non-residential buildings.,'" P. Geneva, Switzerland, 2016.

[35] ISO 18523-2, "'ISO 18523-2: Energy Performance of Buildings — Schedule and Condition of Building, Zone and Space Usage for Energy Calculation — Part 2: Residential buildings.,'" P. Geneva, Switzerland, 2017.

[36] ISO 17772-1, *"ISO 17772-1: Energy Performance of* Buildings - Indoor Environmental Quality. Part 1: Indoor Environmental Input Parameters for the Design and Assessment of Energy Performance in Buildings". Geneva, Switzerland, 2017.

[37] S.P. Corgnati, E. Fabrizio, M. Filippi, V. Monetti, Reference buildings for cost optimal analysis: method of definition and application, Appl. Energy 102 (2013) 983–993, https://doi.org/10.1016/j.apenergy.2012.06.001.

[38] Erika Guolo, Lorenza Pistore, Piercarlo Romagnoni, The role of the reference building in the evaluation of energy efficiency measures for large stocks of public buildings, E3S Web Conf. 111 (2019) 3017, https://doi.org/10.1051/e3sconf/201911103017.

[39] S. Attia, N. Shadmanfar, F. Ricci, Developing two benchmark models for nearly zero energy schools, Appl. Energy 263 (Apr. 2020) 114614, https://doi.org/10.1016/j.apenergy.2020.114614.

[40] P. Marrone, P. Gori, F. Asdrubali, L. Evangelisti, L. Calcagnini, G. Grazieschi, Energy benchmarking in educational buildings through cluster analysis of energy retrofitting, Energies 11 (3) (2018) 649, https://doi.org/10.3390/en11030649.

[41] P. Hernandez, K. Burke, J.O. Lewis, Development of energy performance benchmarks and building energy ratings for non-domestic buildings: an example for Irish primary schools, Energy Build. 40 (3) (Jan. 2008) 249–254, https://doi.org/10.1016/j.enbuild.2007.02.020.

[42] M. Khoshbakht, Z. Gou, K. Dupre, Energy use characteristics and benchmarking for higher education buildings, Energy Build. 164 (2018) 61–76, https://doi.org/10.1016/j.enbuild.2018.01.001.

[43] H.S. Park, M. Lee, H. Kang, T. Hong, J. Jeong, Development of a new energy benchmark for improving the operational rating system of office buildings using various data-mining techniques, Appl. Energy 173 (2016) 225–237, https://doi.org/10.1016/j.apenergy.2016.04.035.

[44] M. Shahrestani, R. Yao, G.K. Cook, A review of existing building benchmarks and the development of a set of reference office buildings for England and Wales, Intell. Build. Int. 6 (1) (2014) 41–64, https://doi.org/10.1080/17508975.2013.828586.

[45] Us Doe, Commercial prototype building models, Build. Energy. Codes. Progr. (2020) [Online]. Available: https://www.energycodes.gov/development/commercial/prototype_models.

[46] Us Doe, Residential prototype building models, Build. Energy. Codes. Progr. (2020) [Online]. Available: https://www.energycodes.gov/development/residential/iecc_models.

[47] ISO 17772-2, *"ISO 17772-2: Energy Performance of* Buildings - Overall Energy Performance Assessment Procedures. Part 2: Guideline for Using Indoor Environmental Input Parameters for the Design and Assessment of Energy Performance of Buildings". Geneva, Switzerland, 2018.

[48] T. Parkinson, R. de Dear, G. Brager, Nudging the adaptive thermal comfort model, Energy Build. 206 (2020) 109559, https://doi.org/10.1016/j.enbuild.2019.109559.

[49] R. Rahif, D. Amaripadath, S. Attia, Review on time-integrated overheating evaluation methods for residential buildings in temperate climates of Europe, Energy Build. 252 (Dec. 2021) 111463, https://doi.org/10.1016/j.enbuild.2021.111463.

[50] S. Carlucci, L. Pagliano, A review of indices for the long-term evaluation of the general thermal comfort conditions in buildings, Energy Build. 53 (Oct. 2012) 194–205, https://doi.org/10.1016/j.enbuild.2012.06.015.

[51] ASHRAE, ANSI/ASHRAE Standard 55-2017, Thermal Environmental Conditions for Human Occupancy, ASHRAE, Atlanta, 2017.

[52] *ISO 7730, ISO 7730: Ergonomics Of the Thermal Environment.* Analytical Determination and Interpretation of Thermal Comfort Using Calculation of the PMV and PPD Indices and Local Thermal Comfort Criteria, International Standards Organization Geneva, 2004.

[53] M. Hendel, K. Azos-Diaz, B. Tremeac, Behavioral adaptation to heat-related health risks in cities, Energy Build. 152 (Oct. 2017) 823–829, https://doi.org/10.1016/j.enbuild.2016.11.063.

[54] L. Yang, H. Yan, J.C. Lam, Thermal comfort and building energy consumption implications – a review, Appl. Energy 115 (Feb. 2014) 164–173, https://doi.org/10.1016/j.apenergy.2013.10.062.

[55] W.A. Andreasi, R. Lamberts, C. Cândido, Thermal acceptability assessment in buildings located in hot and humid regions in Brazil, Build. Environ. 45 (5) (May 2010), https://doi.org/10.1016/j.buildenv.2009.11.005. Art. no. 5.

[56] R. De Dear, G.S. Brager, "Developing an adaptive model of thermal comfort and preference," UC Berkeley: center for the Built Environment [Online]. Available: https://escholarship.org/uc/item/4qq2p9c6, 1998. (Accessed 3 February 2020).

[57] P.O. Fanger, J. Toftum, Extension of the PMV model to non-air-conditioned buildings in warm climates, Energy Build. 34 (6) (2002) 533–536, https://doi.org/10.1016/S0378-7788(02)00003-8.

[58] D. Khovalyg, et al., Critical review of standards for indoor thermal environment and air quality, Energy Build. (2020) 109819, https://doi.org/10.1016/j.enbuild.2020.109819.

[59] S. Carlucci, L. Bai, R. de Dear, L. Yang, Review of adaptive thermal comfort models in built environmental regulatory documents, Build. Environ. 137 (Jun. 2018) 73–89, https://doi.org/10.1016/j.buildenv.2018.03.053.

[60] D.B. Crawley, J.W. Hand, M. Kummert, B.T. Griffith, Contrasting the capabilities of building energy performance simulation programs, Build. Environ. 43 (4) (2008) 661–673, https://doi.org/10.1016/j.buildenv.2006.10.027.

[61] ANSI/ASHRAE Handbook, "Handbook–2017: Fundamentals," American Society of Heating, Refrigerating and Air Conditioning Engineers: Atlanta, GA, USA, 2009.

[62] D. Kim, S. J. Cox, H. Cho, and P. Im, "Evaluation of energy savings potential of variable refrigerant flow (VRF) from variable air volume (VAV) in the U.S. climate locations," Energy Rep., vol. 3, pp. 85–93, Nov. 2017, doi: 10.1016/j.egyr.2017.05.002.

[63] M.J. Witte, R.H. Henninger, D.B. Crawley, Experience testing energyplus with the iea hvac bestest E300-E545 series and iea hvac bestest fuel-fired furnace series, Proc. Sim. Build 2 (1) (2006) 1–8.

[64] X. Zhou, T. Hong, D. Yan, Comparison of HVAC System Modeling in EnergyPlus, DeST and DOE-2.1 E, 7, 2014, pp. 21–33, https://doi.org/10.1007/s12273-013-0150-7, 1.

[65] ISO 15927-4, "'ISO 15927-4: Hygrothermal Performance of Buildings — Calculation and Presentation of Climatic Data — Part 4: Hourly Data for Assessing the Annual Energy Use for Heating and cooling'." P. Geneva, Switzerland, 2005.

[66] Ipcc and Core Writing Team, Summary for policymakers, Clim. Change 2014: Synthesis Report. Contribution of Working Groups I, II and III to the Fifth Assessment Report of the Intergovernmental Panel on Climate Change (2014) 2–34.

[67] K.E. Taylor, R.J. Stouffer, G.A. Meehl, An overview of CMIP5 and the experiment design, Bull. Am. Meteorol. Soc. 93 (4) (2012) 485–498, https://doi.org/10.1175/BAMS-D-11-00094.1.

[68] R. Judkoff, J. Nevmark, International Energy Agency Building Energy Simulation Test (BESTEST) and Diagnostic Method (No. NREL/TP–472-6231), National Renewable Energy Lab. Colorado, United States, 1995.
[69] R.A. Raustad, A Variable Refrigerant Flow Heat Pump Computer Model in EnergyPlus, Univ. of Central Florida, Orlando, FL (United States), 2013.
[70] R. Zhang, K. Sun, T. Hong, Y. Yura, R. Hinokuma, A novel Variable Refrigerant Flow (VRF) heat recovery system model: development and validation, Energy Build. 168 (Jun. 2018) 399–412, https://doi.org/10.1016/j.enbuild.2018.03.028.
[71] H. Holder, DOAS & humidity control, ASHRAE J. 50 (5) (2008) 34.
[72] D.B. Lu, D.M. Warsinger, Energy savings of retrofitting residential buildings with variable air volume systems across different climates, J. Build Eng. 30 (Jul. 2020) 101223, https://doi.org/10.1016/j.jobe.2020.101223.
[73] T.N. Aynur, Y. Hwang, R. Radermacher, Simulation of a VAV air conditioning system in an existing building for the cooling mode, Energy Build. 41 (9) (2009) 922–929, https://doi.org/10.1016/j.enbuild.2009.03.015.
[74] S. Goel, et al., "Enhancements to ASHRAE Standard 90.1 Prototype Building Models," Pacific Northwest National Lab.(PNNL), Richland, WA (United States), 2014.
[75] B.A. Thornton, et al., "Achieving the 30% Goal: Energy and Cost Savings Analysis of ASHRAE Standard 90.1-2010," Pacific Northwest National Lab.(PNNL), Richland, WA (United States), 2011.
[76] S.P. Corgnati, E. Fabrizio, D. Raimondo, M. Filippi, Categories of Indoor Environmental Quality and Building Energy Demand for Heating and Cooling, 4, 2011, pp. 97–105, https://doi.org/10.1007/s12273-011-0023-x, 2.
[77] S. Attia, Net Zero Energy Buildings (NZEB): Concepts, Frameworks and Roadmap for Project Analysis and Implementation, Butterworth-Heinemann, Quebec, Canada, 2018.
[78] N. Fumo, P. Mago, R. Luck, Methodology to estimate building energy consumption using EnergyPlus Benchmark Models, Energy Build. 42 (12) (2010) 2331–2337, https://doi.org/10.1016/j.enbuild.2010.07.027.
[79] R. Hendron, R. Anderson, C. Christensen, M. Eastment, P. Reeves, Development of an Energy Savings Benchmark for All Residential End-Uses, National Renewable Energy Lab., Golden, CO (US), 2004.
[80] P. Torcelini, et al., DOE Commercial Building Benchmark Models, National Renewable Energy Lab.(NREL), Golden, CO (United States), 2008.
[81] X. Luo, T. Hong, Y. Chen, M.A. Piette, Electric load shape benchmarking for small- and medium-sized commercial buildings, Appl. Energy 204 (2017) 715–725, https://doi.org/10.1016/j.apenergy.2017.07.108.
[82] J. Evers, C. Struck, R. van Herpen, J. Hensen, A. Wijsman, W. Plokker, Robuustheid voor klimaatvariaties: een vergelijking van klimatiseringsconcepten met behulp van gebouwsimulatie, Bouwfysica 20 (3) (2009) 2–7.
[83] N. Eskin, H. Türkmen, Analysis of annual heating and cooling energy requirements for office buildings in different climates in Turkey, Energy Build. 40 (5) (2008) 763–773, https://doi.org/10.1016/j.enbuild.2007.05.008.
[84] M.-T. Ke, K.-L. Weng, C.-M. Chiang, Performance evaluation of an innovative fan-coil unit: low-temperature differential variable air volume FCU, Energy Build. 39 (6) (2007) 702–708, https://doi.org/10.1016/j.enbuild.2006.06.011.
[85] Y. Pan, H. Zhou, Z. Huang, Y. Zeng, W. Long, Measurement and simulation of indoor air quality and energy consumption in two Shanghai office buildings with variable air volume systems, Energy Build. 35 (9) (2003) 877–891, https://doi.org/10.1016/S0378-7788(02)00245-1.
[86] S. Sekhar, C.J. Yat, Energy simulation approach to air-conditioning system evaluation, Build. Environ. 33 (6) (1998) 397–408, https://doi.org/10.1016/S0360-1323(97)00056-5.
[87] S. Yuan, R. Perez, Multiple-zone ventilation and temperature control of a single-duct VAV system using model predictive strategy, Energy Build. 38 (10) (2006) 1248–1261, https://doi.org/10.1016/j.enbuild.2006.03.007.
[88] V.M. Nik, S. Coccolo, J. Kämpf, J.-L. Scartezzini, Investigating the importance of future climate typology on estimating the energy performance of buildings in the EPFL campus, Energy. Procedia 122 (2017) 1087–1092, https://doi.org/10.1016/j.egypro.2017.07.434.

Appendix D

Chapter 4: *Historical and future weather data for dynamic building simulations in Belgium using the regional climate model MAR: typical and extreme meteorological year and heatwaves*

Earth Syst. Sci. Data, 14, 3039–3051, 2022
https://doi.org/10.5194/essd-14-3039-2022

Open Access Earth System Science Data

Historical and future weather data for dynamic building simulations in Belgium using the regional climate model MAR: typical and extreme meteorological year and heatwaves

Sébastien Doutreloup[1], Xavier Fettweis[1], Ramin Rahif[2], Essam Elnagar[3], Mohsen S. Pourkiaei[4], Deepak Amaripadath[2], and Shady Attia[2]

[1]Laboratory of Climatology and Topoclimatology, Department de Geography, UR SPHERES, University of Liège, Liège 4000, Belgium
[2]Sustainable Building Design Lab, Dept. UEE, Faculty of Applied Sciences, University of Liège, Liège 4000, Belgium
[3]Thermodynamics Laboratory, Aerospace and Mechanical Engineering Department, Faculty of Applied Sciences, University of Liège, Liège 4000, Belgium
[4]Atmospheres and Monitoring lab (SAM), UR SPHERES, University of Liège, Arlon Campus Environment, Avenue de Longwy 185 6700 Arlon, Belgium

Correspondence: Sébastien Doutreloup (s.doutreloup@uliege.be)

Received: 9 November 2021 – Discussion started: 15 February 2022
Revised: 1 June 2022 – Accepted: 5 June 2022 – Published: 6 July 2022

Abstract. Increasing temperatures due to global warming will influence building, heating, and cooling practices. Therefore, this data set aims to provide formatted and adapted meteorological data for specific users who work in building design, architecture, building energy management systems, modelling renewable energy conversion systems, or others interested in this kind of projected weather data. These meteorological data are produced from the regional climate model MAR (Modèle Atmosphérique Régional in French) simulations. This regional model, adapted and validated over Belgium, is forced firstly, by the ERA5 reanalysis, which represents the closest climate to reality and secondly, by three Earth system models (ESMs) from the Sixth Coupled Model Intercomparison Project database, namely, BCC-CSM2-MR, MPI-ESM.1.2, and MIROC6. The main advantage of using the MAR model is that the generated weather data have a high resolution (hourly data and 5 km) and are spatially and temporally homogeneous. The generated weather data follow two protocols. On the one hand, the Typical Meteorological Year (TMY) and eXtreme Meteorological Year (XMY) files are generated largely inspired by the method proposed by the standard ISO15927-4, allowing the reconstruction of typical and extreme years, while keeping a plausible variability of the meteorological data. On the other hand, the heatwave event (HWE) meteorological data are generated according to a method used to detect the heatwave events and to classify them according to three criteria of the heatwave (the most intense, the longest duration, and the highest temperature). All generated weather data are freely available on the open online repository Zenodo (https://doi.org/10.5281/zenodo.5606983, Doutreloup and Fettweis, 2021) and these data are produced within the framework of the research project OCCuPANt (https://www.occupant.uliege.be/ (last access: 24 June 2022) – ULiège).

Published by Copernicus Publications.

1 Introduction

On a global scale, the warmest (SSP5-8.5) scenario from the IPCC last assessment report (IPCC, 2021) suggests a temperature increase of +5 °C by 2100. However, the regions of the world will not warm up at the same speed or intensity. Some regions, such as the poles, will warm faster and to higher levels than equatorial regions (Lee et al., 2021). Over the temperate regions, such as western Europe, the temperature is expected to increase between +1 and +5 °C in 2100, depending on the climate models and greenhouse gas emission scenarios used (Termonia et al., 2018; RMI, 2020; IPCC, 2021).

Moreover, IPCC (2021) affirm that extreme events will become more probable and more intense. In particular, the maximum temperature is expected to increase faster (sometimes up to twice) than the mean temperature (Seneviratne et al., 2021). Over western-central Europe, maximum temperatures are projected to increase up to +7 °C for a global increase of +5 °C (Seneviratne et al., 2021).

More concretely, in the summer, hot extremes (including heatwaves) are already increasing and will continue to strengthen with global warming, both in intensity and frequency (Suarez-Gutierrez et al., 2020; Seneviratne et al., 2021; Dunn et al., 2020). The consequences of these heatwaves will affect human health (Fouillet et al., 2006), agriculture, the comfort and health of life inside buildings (Bruffaerts et al., 2018; Sherwood and Huber, 2010; Buysse et al., 2010), and the energy demand, especially for cooling systems (Larsen et al., 2020). This is what motivated some previous studies in Belgium to represent the energy needs for heating and cooling under average and extreme weather conditions (Ramon et al., 2019).

Energy efficiency and living comfort are precisely what motivates the ULiège OCCuPANt project (Impacts Of Climate Change on the indoor environmental and energy PerformAnce of buildiNgs in Belgium during summer, https://www.occupant.uliege.be/, last access: 24 June 2022), in which climate data are involved. The OCCuPANt project aims to evaluate the energy performance and vulnerability of building inhabitants in the context of climate change. Acquiring reliable current and future climate data is vital in any study related to climate change and defines its quality (Pérez-Andreu and al., 2018).

The purpose of this data set is to propose meteorological data coming from a fine-resolution regional climate model over Belgium and neighbouring regions. These data will then be used to anticipate future climate changes, which will influence both the production of heating and cooling demands as well as the electrical grids on larger scales. These changes will require innovations in building design and systems, which will necessarily take time. Thus, the more they are anticipated, the better we will find solutions. The use of a regional model allows the building of spatially and temporally continuous and homogeneous past and future meteorological data, according to different warming scenarios for some Belgian cities. This regional model is fed by the ERA-5 reanalysis model (Hersbach et al., 2020) to simulate the past climate (1980–2020), and also by three different Earth system models (ESMs) from the Sixth Coupled Model Intercomparison Project (CMIP6) database (Wu et al., 2019; Tatebe et al., 2019; Gutjahr et al., 2019) to obtain different future projections and associated uncertainties for the same scenario SSP5-8.5.

The future climate data are very useful to predict the variations in heating and cooling demands in buildings. The characterisation of a minimum outdoor temperature under future scenarios is necessary to estimate the heating and cooling season needs. This can result in rethinking building designs and making them resilient against the impact of climate change. For instance, in the heating-dominated region of Belgium, the concept of building design focuses more on heat retention to decrease heating energy use during the winter. However, warming weather conditions in the last decades meant that this design concept caused significant overheating problems during the summer. Therefore, it is necessary to predict the future performance of buildings and adapt them to the variations in outdoor weather conditions. Designing cooling systems that can last for 100 years is challenging. However, it is possible to increase the preparedness of buildings for climate change through passive design strategies, the use of active heating/cooling systems, or both. Both active and passive solutions may need regular replacements over the building's lifespan.

For each city, considered period, model, and scenario, two synthetic files (in CSV format) are generated, largely inspired by the method in ISO-15927-4. These are a Typical Meteorological Year (TMY) file and an eXtreme Meteorological Year (XMY) file. In addition to these synthetic files, files focused on heatwaves are also generated, namely, a file for the most intense heatwave event, one for the warmest heatwave, one for the longest heatwave, and one containing all the heatwaves detected within a specific period. These files are described in detail in the Methodology section.

2 Methodology

2.1 MAR model and area of interest

The regional climate model used in this study is the Modèle Atmosphérique Régional model (hereafter MAR) in its version 3.11.4 (Kittel, 2021). The main role of MAR is to downscale a global model or reanalysis to get weather outputs at a finer spatial and temporal resolution (Fig. 1). As shown in Fig. 1, MAR is a 3-dimensional atmospheric model coupled to a 1-dimensional transfer scheme between the surface, vegetation, and atmosphere (Ridder and Gallée, 1998). The MAR model also includes an urban island module, which modifies the city grid points to simulate an urban heat island through a modification of the surface albedo (fixed to

0.1) and an absence of vegetation, which influence the thermal and humidity exchanges between soil and atmosphere. Initially, the MAR model was developed for both Greenland (Fettweis et al., 2013) and Antarctica ice sheets (Agosta et al., 2019; Kittel et al., 2021). However, it has recently been successfully adapted to temperate regions such as Belgium (Fettweis et al., 2017; Doutreloup et al., 2019; Wyard et al., 2021). In the framework of this study, MAR is initially forced every 6 h at its lateral boundaries (temperature, wind, and specific humidity) by the reanalysis ERA5 (hereafter called MAR-ERA5), which is available at a horizontal resolution of ∼ 31 km (Hersbach et al., 2020). Different kinds of observations (in situ weather observations, radar data, satellites, etc.) are 6-hourly assimilated into ERA5 to be closest to the observed climate. In this way, the simulations of MAR-ERA5 can be considered as the closest simulation to the current observed climate.

Then, the MAR model has been forced every 6 h by three ESMs from the CMIP6 database (Eyring et al., 2016). These ESMs do not contain any observational data and represent only an evolution of the average and interannual variability of the climatic parameters over long periods. These models contain two characteristic periods: one in the past from 1980 to 2014 (hereafter called the "historical" scenario) and another in the future from 2015 to 2100 according to different SSP scenarios (SSP5-8.5, SSP3-7.0, and SSP2-4.5). The selection and description of each of these ESMs and a comparison with MAR-ERA5 over the historical period are presented in the next section.

The atmospheric variables used to force MAR every 6 h at each vertical level are temperature, surface pressure, wind, specific humidity, and the sea surface temperature over the North Sea from both ERA5 reanalysis (from 1980 to 2020) and the three ESMs (from 1980 to 2100). The spatial resolution of MAR is 5 km over an integration domain (120×90 grid cells) centred over Belgium, as shown in Fig. 2, to build hourly outputs.

The choice of 12 cities is motivated, on the one hand, by the size of the cities which must be sufficient to show a temperature increase compared to the neighbouring countryside and, on the other hand, to best represent the climate spatial variability observed in Belgium. For example, the city of Oostende is strongly influenced by the thermal inertia of the sea, while the city of Arlon has a more continental climate.

2.2 Forcing models and MAR simulations

2.2.1 Choice of representative Earth system models

The Sixth Coupled Model Intercomparison Project (CMIP6; Eyring et al., 2016) database contains about 30 ESMs from many scientific institutes around the world. For practical reasons, we cannot regionalise all these ESMs. Thus, we had to select a few representative ESMs for our region of interest, western Europe.

Our choice was based on two criteria. The first criterion is that the ESM should represent (with the lowest possible bias) the main atmospheric circulation in the free atmosphere over western Europe by evaluating the geopotential height at 500 hPa and the temperature at 700 hPa during summer and winter, with respect to ERA5 over 1980–2014 based on the skill score method developed by Connolley and Bracegirdle (2007). After selecting the ESMs that meet this first criterion, the second criterion is to choose three ESMs representing the CMIP6 models spread in 2100 for the same scenario (SSP5-8.5 here). Namely, we keep only three ESMs (see Table A1): BCC-CSM2-MR (Wu et al., 2019), MPI-ESM.1.2 (Gutjahr et al., 2019), and MIROC6 (Tatebe et al., 2019). The ESM BCC-CSM2-MR simulates warming close to the ensemble mean of the 30 ESMs for the 2100 horizon using the SSP5-8.5 scenario, the ESM MIROC6 simulates larger warming than the ensemble mean, and the ESM MPI-ESM.1.2 simulates lower warming than the ensemble mean by 2100. The use of these three models allows us to obtain a first approximation of the uncertainty from ESMs without having to downscale all 30 available models of CMIP6.

2.2.2 Future socio-economic scenarios

Shared Socio-economic Pathways (SSPs; Riahi et al., 2017) are scenarios of global socio-economic evolution projected to 2100. These SSPs are used to develop greenhouse gas (GHG) emission scenarios associated with different climate policies and are used to force each future ESM. There are three main scenarios, namely SSP2-4.5 (intermediate GHGs), SSP3-7.0 (high GHGs) and SSP5-8.5 (very high GHGs), causing global warming for 2100 to increase respectively. For more details about these scenarios, we refer to Riahi et al. (2017). Finally, it should be noted that the historical scenario mentioned in Sect. 2.1 is forced by the greenhouse gas concentrations observed over the period of 1980–2014.

For the same practical reasons that led us to choose only three ESMs out of the 30 available models, we cannot afford to calculate every SSP scenario of each ESM. However, as the ESMs cannot represent general circulation changes (Eyring et al., 2021), the use of one scenario or another will not cause more blocking anticyclones leading to more persistent heatwaves, for example. Thus, whichever scenario is used will only reflect temperature changes in relation to its GHG concentrations. Hence, only the SSP5-8.5 scenario has been calculated and the other scenarios (SSP3-7.0 and SSP2-4.5) are derived from the MAR simulations forced by the ESMs using the SSP5-8.5 scenario, since the warming rates from lower scenarios are included in the scenario SSP5-8.5, but for a different earlier time period. Thus, for each scenario (SSP3-7.0 and SSP2-4.5), the equivalent warming period in the SSP5-8.5 scenario has been found according to these three steps:

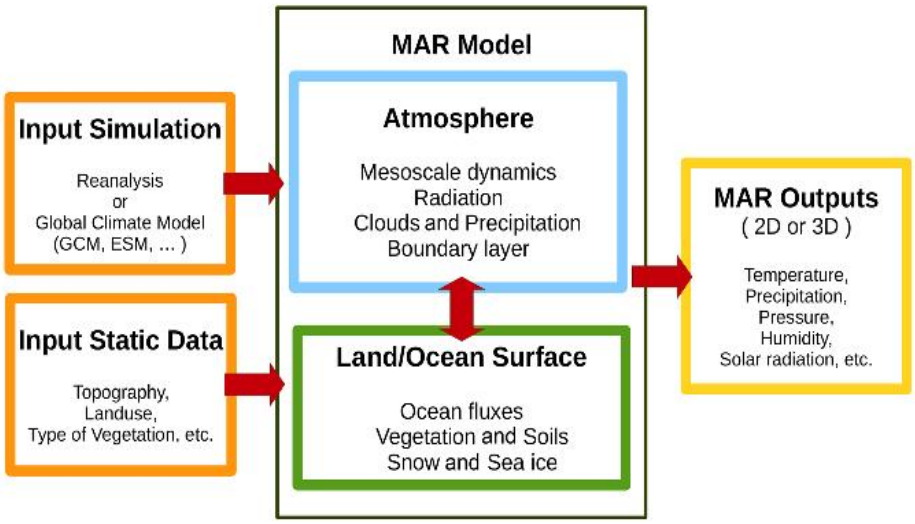

Figure 1. Workflow of the MAR model. The MAR model (black box) needs to be forced by a reanalysis model or global model (upper orange box) and by static data (lower orange box). The result of the MAR simulation gives meteorological variables in two or three dimensions (yellow box).

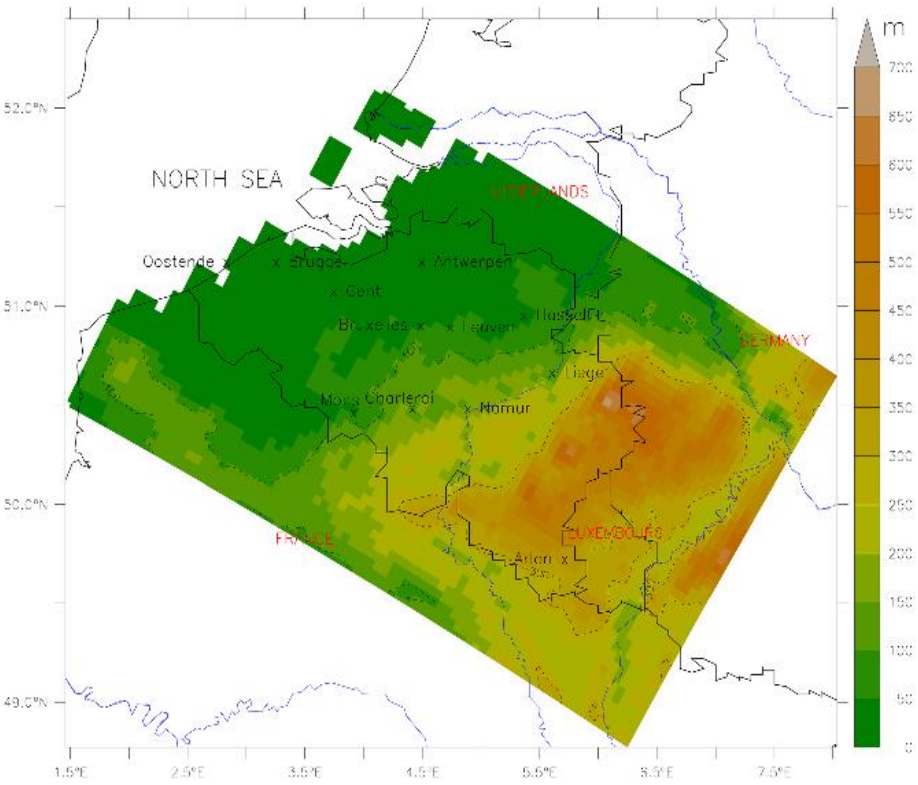

Figure 2. Model topography (colour background and dashed black line, both in metres above sea level), localisation of cities (black letters) used in this dataset for Belgium, and localisation of neighbouring countries (in red letters).

1. The raw 2 m annual mean temperature of each ESM and each scenario has been aggregated over Belgium to the horizon 2100.

2. For each ESM, the equivalent 20-year period from the SSP5-8.5 scenario has been chosen as the period with the closest mean and the closest interannual variability of the 2 m annual temperature, compared to the future 20-year period (i.e. 2021–2040, 2041–2060, ...) from the two other scenarios (SSP3-7.5 and SSP2-4.5).

3. Once the equivalent warming period has been identified, the data of this period are extracted out of the SSP5-8.5-forced MAR simulations for both SSP3-7.5 and SSP2-4.5 scenarios.

For example, the data of MAR-MPI for SSP3-7.0 over 2081–2100 are the outputs of MAR-MPI using SSP5-8.5 over the period 2066–2085.

This method is open to discussion for several reasons. Firstly, the climate does not react in a linear way to an increase of GHG flowing through the different SSP scenarios. Moreover, with an equal warming rate, but different periods, the earth, atmosphere and ocean systems will not have the same (spatial and temporal) responses due to their inertia. Despite these precautions, this methodology allows us, on the one hand, to derive a quick estimation without additional computer time. On the other hand, it remains valid as a first approximation, especially since the most interesting weather variable in this study is temperature, which is, by construction, the least sensitive to these issues.

2.2.3 Evaluation of the MAR simulations

To verify that these ESM-forced MAR simulations can be used to anticipate future periods, it is necessary to evaluate them over the overlapping period between the ERA5 reanalyses and the historical scenario (namely, 1980–2014). The aim is to determine if they can represent the average and climate variability over the Belgian territory for this period as observed (i.e. ERA5 in our case). So, we compare the three MAR simulations forced by the three ESMs with the MAR simulation forced by the ERA5 reanalyses. As the most important variable for this database is the temperature at 2 m above ground level (a.g.l.) and an important secondary variable is the incoming solar radiation, the mean and standard deviation of these data over the period 1980–2014 and over the Belgian territory are compared in Table 1 and Fig. 3. These values are compared on an annual scale and on a summer scale since the OCCuPANt project focuses on heatwaves.

The results of this comparison presented in Table 1 indicate that the incoming solar radiations and temperature at 2 m a.g.l. values proposed by the three MAR simulations forced by the ESMs are mostly close to the average simulated by MAR-ERA5, with (not statistically significant) biases between MAR forced by the ESMs and MAR-ERA5 lower than the standard deviation (i.e. the interannual variability) of MAR-ERA5. We can also note that the interannual variability of the MAR simulations forced by the ESMs is close to the interannual variability of the MAR-ERA5 simulation. We can then conclude that the MAR simulations forced by the ESMs can represent the mean climate simulated by MAR-ERA5 and its interannual variability with success, except MAR-MIR, which significantly overestimates temperature and solar radiation in summer. Knowing that MAR-MIR simulated the largest warming in 2100, this simulation needs to be considered as the extreme climate we could have.

2.3 Generating the Typical Meteorological Year and eXtreme Meteorological Year files

The Typical Meteorological Year (TMY) and the eXtreme Meteorological Year (XMY) are data sets that are widely used by building designers and others to model renewable energy conversion systems (Wilcox and Marion, 2008). The TMYs are the synthetic years (on an hourly basis) constructed by representative typical months (Barnaby and Crawley, 2011), which are selected by comparing the distribution of each month within the long-term (minimum of 10 years) distribution of that month for the available observations or modelled data (using Finkelstein–Schafer statistics (Finkelstein and Schafer, 1971). The XMY is the extension of the TMY weather data and is formed by selecting the most deviating (i.e. extreme) months over a certain data set instead of typical months (Ferrari and Lee, 2008). There are many methods to reconstruct this kind of weather file (Ramon et al., 2019), but for this study, a protocol for the construction of these typical years has been developed based on the ISO15927-4 (European Standard, 2005) and is described briefly below.

The method consists of reconstituting each month of the typical (extreme) year with the most typical (extreme) month present in the considered period for a considered city. The comparison is essentially based on two variables, namely, temperature at 2 m a.g.l. and incoming solar radiation. The choice of these two climatic parameters is related to the fact that they both influence the comfort inside the buildings. Therefore, we generate files with the typical year according to the temperature at 2 m a.g.l. and a typical year according to the incoming solar radiation.

Here are the steps to find the most typical (extreme) month for each climatic parameter:

1. Converting an hourly file into a daily file: from all the hourly data from all the same calendar months available within the selected period, the daily mean of the climatic parameter is computed.

2. Selecting the typical (extreme) month: for each calendar month, the percentile 50 (95) of the climatic parameter is calculated over the studied period to find the month that is the closest to the 50 percentile (95) of this climatic parameter.

3. Extracting hourly data of this typical (extreme) month: finally, the hourly weather values of this typical (extreme) month are stored in the file of the typical (extreme) year.

The hourly weather variables available in the TMY and XMY files are described in Table 2.

Table 1. Comparison of MAR-ERA5 (i.e. MAR forced by the reanalysis ERA5) with MAR-BCC (i.e. MAR forced by BCC-CSM2-MR), MAR-MPI (i.e. MAR forced by MPI-ESM.1.2), and MAR-MIR (i.e. MAR forced by MIROC6) to mean temperature at 2 m above ground level and mean incoming solar radiation over Belgium's territory during 1980 2014 (mean value ± standard error).

1980–2014 over Belgian territory	Timescale	MAR-ERA5	MAR-BCC	MAR-MPI	MAR-MIR
Mean temperature at 2 m a.g.l. (in °C)	annual	10.1 ± 6.2	10.3 ± 6.0	10.1 ± 6.4	10.4 +/-7.2
	summer	17.7 ± 1.3	17.6 ± 1.7	18.6 ± 1.2	19.9 ± 1.1
Mean incoming solar radiation (in $W m^{-2}$)	annual	119 ± 78	122 ± 79	116 ± 83	134 ± 85
	summer	213 ± 20	221 ± 20	224 ± 22	239 ± 25

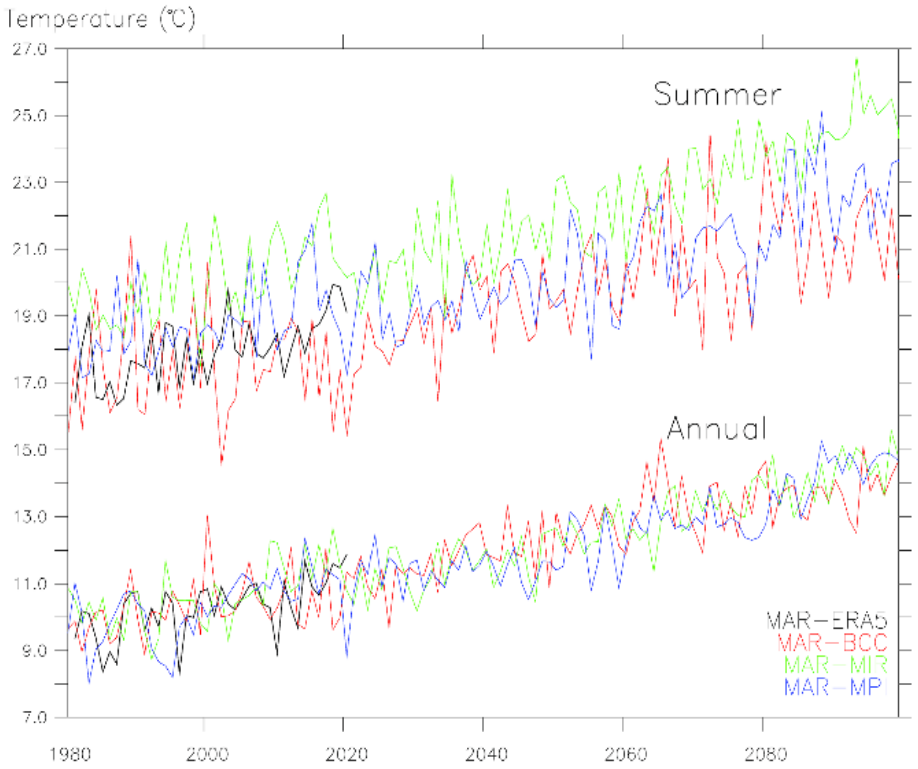

Figure 3. Annual mean temperature (in °C, lower lines) and annual summer temperature (in °C, upper lines) of MAR forced by ERA5 reanalysis (in black lines between 1980 and 2020), MAR-BCC (i.e. MAR forced by BCC-CSM2-MR in red lines), MAR-MPI (i.e. MAR forced by MPI-ESM.1.2 in blue lines), and MAR-MIR (i.e. MAR forced by MIROC6 in green lines) between 1980 and 2100 according to the scenario SSP5-8.5. The average is computed here over the whole integration domain, excluding the ocean.

2.4 Definition of a heatwave and generating heatwave event files

In Belgium, heatwaves are officially defined by two definitions: a retrospective one and a prospective one. The retrospective heatwave is defined as periods of at least five consecutive days with a maximum temperature higher than 25 °C, of which, at least 3 days within this period has a maximum temperature higher than 30 °C (RMI, 2020). The prospective heatwave is a period with a predicted minimum temperature of 18.2 °C or more and a maximum temperature of 29.6 °C or higher, both for three consecutive days (Brits et al., 2009).

However, these definitions are static and do not consider the local climate of each region. For example, in the highlands (with altitudes above 300 m in Fig. 2) where it is on average colder, these heatwave criteria are not necessarily met, even though this region also experiences a heatwave. Moreover, when comparing the different ESMs, this fixed heatwave definition criterion could induce artefacts, since each ESM has its own variability and biases over the current climate. For these reasons, we have used the statistical definition of a heatwave from Ouzeau et al. (2016), computed for each MAR pixel regardless of its basic climate and each ESM independently of its own internal variability.

The calculation method, according to Ouzeau et al. (2016), is as follows and it is illustrated in Fig. 4:

- For the period 1980–2014 (which corresponds to the "historical" scenario in the ESMs), for each pixel and each MAR simulation, we calculate three thresholds de-

Table 2. Name, level, and units of all weather variables used in the produced weather files.

Weather variable name	Level	Units
Dry bulb temperature	2 m a.g.l.	°C
Relative humidity	2 m a.g.l.	%
Global horizontal radiation	Ground (horizontal surface)	$W m^{-2}$
Diffuse solar radiation	Ground (horizontal surface)	$W m^{-2}$
Direct normal radiation	Ground (horizontal surface)	$W m^{-2}$
Wind speed	10 m a.g.l.	$m s^{-1}$
Wind direction	10 m a.g.l.	north degrees
Dew point temperature	2 m a.g.l.	°C
Atmospheric pressure	ground	Pa
Cloudiness	All troposphere	tenths
Sky temperature	All troposphere	K (according to Duffie and Beckman, 2013)
Specific humidity	2 m a.g.l.	$kg kg^{-1}$
Precipitation	Ground	mm

fined by three percentiles of the daily mean temperature: Sint = 95th percentile, Sdeb = 97.5th percentile, and Spic = 99.5th percentile.

- A heatwave is detected when the daily mean temperature reaches Spic. The duration of this event is the number of days between the first day when the daily mean temperature is equal to or greater than Sdeb, and either when the daily mean temperature falls below Sint or when the daily mean temperature falls below Sdeb for at least three consecutive days.
- In this data set, we add a condition compared to Ouzeau et al. (2016), which is that the minimum duration of the heatwave must be at least five consecutive days, otherwise the heatwave event is not considered as such.

Once the heatwave events (called HWE hereafter) are detected, we can characterise them according to three criteria:

1. the duration, which is the number of consecutive days of the HWE;
2. the maximal daily mean temperature reached during the HWE;
3. the global intensity, which is calculated by the cumulative difference between the temperature and the Sdeb threshold during the HWE, divided by the difference between Spic and Sdeb.

The hourly data provided in each HWE file are the same as for the TMY and XMY files (see section above). For each period, each city, each scenario, and each forcing, four files are created:

- a file containing hourly weather data for the longest HWE;
- a file containing the hourly weather data of the HWE characterised by the highest daily average temperature;
- a file containing the hourly weather data of the HWE characterised by the highest intensity;
- a file that concatenates all the hourly weather data of all the HWEs present in a period, for each city, each scenario, and each MAR model.

Finally, the HWE files contain only the period corresponding to a heatwave event. However, depending on the purpose of the users, the effects of a heatwave can also be dependent on the period preceding and/or following it. Thus, a suggestion for users could be to combine HWE files with files of typical or extreme years in order to obtain simulations of a normal year with one or more heatwaves. We have not built these files so that users can decide whether to combine these files or not, and to prepare them according to their own constraints and interests.

3 The data set

3.1 Data availability

The data described in this article can be freely accessed on the Zenodo open-access repository: https://doi.org/10.5281/zenodo.5606983 (Doutreloup and Fettweis, 2021). As the files are numerous, each zipped folder contains all the data for each city concerned with this data set.

3.2 Structure of each file

All files are in a CSV format and are comma-separated. The file names are formatted in such a way that they contain all the information about the origin of the file. Each file name is composed as follows:

- for TMY or XMY:
  CityName_Type_Period_Scenario_MARmodel
  _ClimaticParameter.csv;

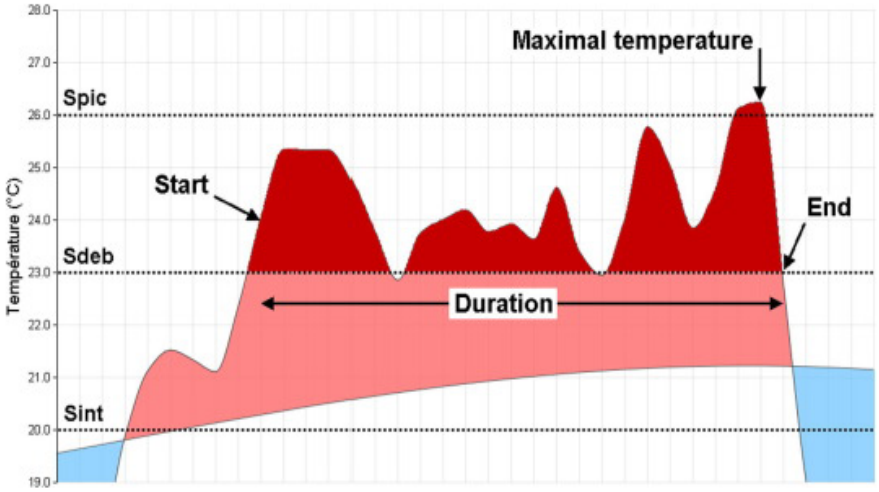

Figure 4. Figure and legend from Ouzeau et al. (2016): characterisation of a heatwave from a daily mean temperature indicator over France (example of a time series from 30 June to 5 August 1983). Duration (start and end), maximal temperature, and global intensity (red area of the plot). Temperatures above (below) the climatological line (1981–2010 reference period) are represented by the pink (blue) area. (For an interpretation of the references to colour in this figure legend, the reader is referred to Ouzeau et al., 2016).

– for heatwaves: CityName_Type_Period_Scenario _MARmodel.csv;

with

– city name: the name of the city considered in this file;

– type: the nature of this file, namely, TMY (typical meteorological year), XMY (extreme meteorological year), HWE-HI (most intense heatwave event), HWE-HT (warmest heatwave event), HWE-LD (longest heatwave event), and HWE-all (all heatwave events);

– period: the time period considered;

– scenario: the IPCC scenario of the ESM considered, namely, "hist", "SSP5-8.5", "SSP3-7.0", and "SSP2-4.5" (note that for MAR-ERA5, the name of the scenario is set by default to "hist" even if the ERA5 forcing does not contain any scenario);

– MAR model: the version of MAR used, namely, MAR-ERA5, MAR-BCC, MAR-MPI or MAR-MIR.

For TMY and XMY files, the header is composed of the task number (which is a reference number for internal use in the OCCuPANt project), the name of the city, and the name of the different variables accompanied by their unit. For HWE files, the header is composed of the task number (same remark as above), the name of the city, the characterisation of the heatwave (longest, warmest, and most intense) accompanied by its period, and the name of the different variables accompanied by their unit. Then comes the weather data with the time variable in the first column. Weather data are in universal time and leap year mode for the MAR-ERA5 and in no-leap year mode for MAR-BCC, MAR-MPI, and MAR-MIR.

A short example of how to select the desired data and files, as well as an example of how to use them, is provided in Appendix A for Liège-City.

4 Conclusion

The goal of this data set is to provide formatted and adapted meteorological data for specific users who work in building designing, architecture, building energy management systems, modelling renewable energy conversion systems, or other people interested in this kind of data. These weather data are derived from the regional climate MAR model. This regional model, adapted and validated over Belgium, is forced by a reanalysis and three ESMs. On the one hand, MAR is forced by the ERA5 reanalysis to represent the closest climate to reality. On the other hand, MAR is forced by three ESMs from the CMIP6 database, namely, BCC-CSM2-MR, MPI-ESM.1.2, and MIROC6. The main advantage of using the MAR model is that the generated weather data at a high resolution are spatially and temporally homogeneous.

The generated weather data follow two protocols. Firstly, the TMY and XMY meteorological data are generated largely inspired by the method proposed by the standard ISO15927-4, allowing the reconstruction of typical and extreme years, while keeping the plausible variability of the meteorological data. Secondly, the meteorological data concerning heatwaves (HWE) are generated according to the method proposed by Ouzeau et al. (2016) to detect the heatwave events and classify them according to three criteria of the heatwave. The OCCuPANt project, in which this paper is included, aims to identify the highest temperature, the longest heatwave duration, and the most intense heatwave event. Finally, all generated weather data are open source and freely available on the open

repository Zenodo (https://doi.org/10.5281/zenodo.5606983, Doutreloup and Fettweis, 2021).

Appendix A: Example for Liège city

The Liège folder contains 596 files. This is a huge amount of files, so to find your way around, we suggest the following method for TMY and XMY files:

1. choose a typical or extreme year, i.e. select XMY for an extreme year;
2. choose the parameter that determines the typical or extreme year (TT for temperature and SWD for incoming solar radiation), i.e. if you want a year with extreme incoming solar radiation (i.e. sunshine), you should select SWDbased;
3. choose the reference period, i.e. 2085–2100 for the end of the century;
4. choose the socio-economic scenario, i.e. "ssp585" for a world that continues to use fossil fuels according to the SSP5-8.5 scenario;
5. choose one of the 3 MAR models, i.e. MAR-BCC for the MAR model forced by BCC-CSM2-MR;
6. finally, the choice is made for the file:

   Liège-City_XMY2085-2100_ssp585_MAR-BCC_SWDbased.csv.

This file selection method is a proposal, but each user is free to develop their own method and, of course, the user can use several files to compare them. For example, if the user wants to compare typical and extreme temperatures for the end of the century and for the two selected parameters with MAR-BCC, the user gets Fig. A1. Figure A1 clearly shows that the extreme year temperature based on temperature is much higher than the typical year temperature. On the other hand, the extreme year temperature based on incoming solar radiation is much lower – especially in January – than the typical year temperature, because extreme radiation in winter usually means cold weather.

The method is almost identical for the heatwave files, except that there are no parameters to determine the typical and extreme years; instead, the user has to choose if they want to look at the longest, the most intense, the hottest, or all heatwaves present within the period. Therefore, if the user wants to compare the longest heatwave (HWE-LD) over the same period and for the same model and scenario as the example above, the user must choose the file: Liège-City_HWE-LD_2085-2100_ssp585_MAR-BCC.csv

Figure A2 compares the temperature evolution during the warmest heatwave, obtained from each of the MAR-BCC, MAR-MPI, and MAR-MIR simulations. The header of each file shows the warmest daily average temperature, namely, 37.2 °C for MAR-BCC, 35.3 °C for MAR-MPI, and 37.8 °C for MAR-MIR. However, it can be seen in Fig. A2 that the hourly temperatures obviously rise much higher than these daily average values and, in this case, rise to ∼44 °C for MAR-BCC and MAR-MIR, and ∼42 °C for MAR-MPI.

Table A1. Full name, abbreviation name, lead institution, and references of the Earth system model (ESM) used in this study.

Full name of the ESM	Abbreviation name of the ESM	Lead institution	References
BCC-CSM2-MR	BCC	Beijing Climate Centre	Wu et al. (2019)
MPI-ESM1-2-HR	MPI	Max Planck Institute	Gutjahr et al. (2019)
MIROC6	MIR	Japanese modelling community	Tatebe et al. (2019)

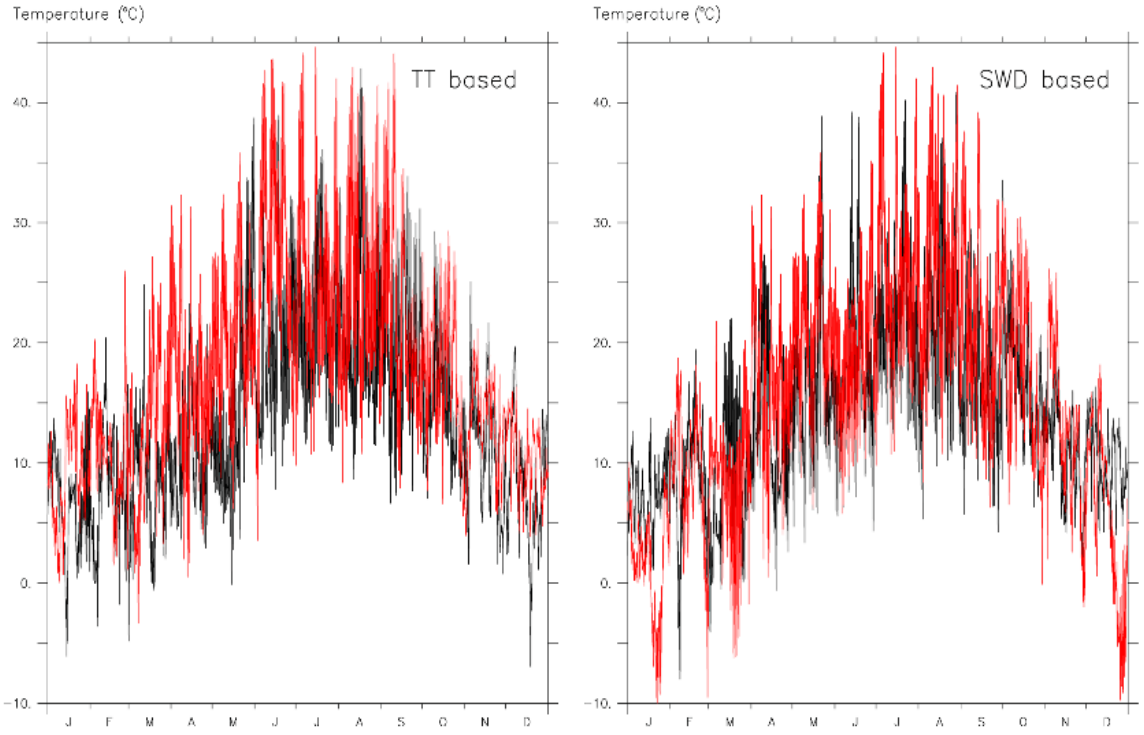

Figure A1. Typical (black) and extreme (red) temperature for Liège city, simulated by MAR forced by BCC-CSM2-MR, with the scenario SSP5-8.5 for the period 2085–2100. The typical/extreme months are based on temperature (left) and incoming solar radiation (right). These data are extracted from these files: Liège-City_TMY2085-2100_ssp585_MAR-BCC_TTbased.csv, Liège-City_XMY2085-2100_ssp585_MAR-BCC_TTbased.csv, Liège-City_TMY2085-2100_ssp585_MAR-BCC_SWDbased.csv, and Liège-City_XMY2085-2100_ssp585_MAR-BCC_SWDbased.csv.

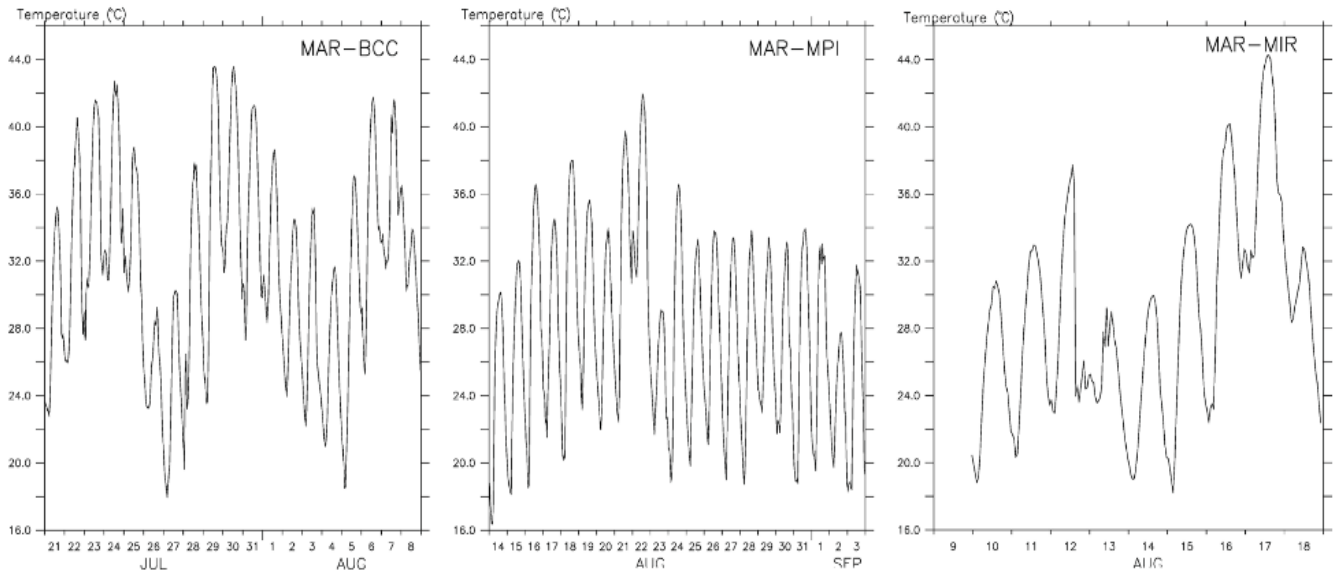

Figure A2. Temperature during warmest heatwave events for Liège city simulated by MAR-BCC (i.e. MAR forced by BCC-CSM2-MR), MAR-MPI (i.e. MAR forced by MPI-ESM.1.2), and MAR-MIR (i.e. MAR forced by MIROC6), with the scenario SSP5-8.5 for the period 2085–2100. These data are, respectively, extracted from these files: Liège-City_HWE-HT_2085-2100_ssp585_MAR-BCC.csv, Liège-City_HWE-HT_2085-2100_ssp585_MAR-MPI.csv, and Liège-City_HWE-HT_2085-2100_ssp585_MAR-MIR.csv.

Author contributions. SD, XF, RR, EE, MSP, DA and SA participated in the conceptualisation of this paper. SD and XF designed the experiments and methodology, and SD carried them out. SD prepared and created figures and data. XF oversaw the research. SD wrote the initial manuscript and SD, XF, RR, EE, MSP, DA and SA participated in the revisions. SA leads the project administration.

Competing interests. The contact author has declared that neither they nor their co-authors have any competing interests.

Disclaimer. Publisher's note: Copernicus Publications remains neutral with regard to jurisdictional claims in published maps and institutional affiliations.

Acknowledgements. The authors would like to gratefully acknowledge the Walloon Region and Liège University for the funding. Computational resources have been provided by the Consortium des Équipements de Calcul Intensif (CÉCI), funded by the Fonds de la Recherche Scientifique de Belgique (F.R.S.-FNRS), under grant no. 2.5020.11 and by the Walloon Region.

Financial support. This research was partially funded by the Walloon Region, under the call "Actions de Recherche Concertées 2019 (ARC)" and the project OCCuPANt, on the Impacts Of Climate Change on the indoor environmental and energy PerformAnce of buildiNgs in Belgium during summer.

Review statement. This paper was edited by David Carlson and reviewed by two anonymous referees.

References

Agosta, C., Amory, C., Kittel, C., Orsi, A., Favier, V., Gallée, H., van den Broeke, M. R., Lenaerts, J. T. M., van Wessem, J. M., van de Berg, W. J., and Fettweis, X.: Estimation of the Antarctic surface mass balance using the regional climate model MAR (1979–2015) and identification of dominant processes, The Cryosphere, 13, 281–296, https://doi.org/10.5194/tc-13-281-2019, 2019.

Barnaby, C. S. and Crawley, U. B.: Weather data for building performance simulation, in: Building Performance Simulation for Design and Operation, edited by: Hensen J. L. M. and Lamberts R., Routledge, London, https://doi.org/10.4324/9780203891612, 2011.

Bruffaerts, N., De Smedt, T., Delcloo, A., Simons, K., Hoebeke, L., Verstraeten, C., Van Nieuwenhuyse, A., Packeu, A., and Hendrickx, M.: Comparative long-term trend analysis of daily weather conditions with daily pollen concentrations in Brussels, Belgium, Int. J. Biometeorol., 62, 483–491, https://doi.org/10.1007/s00484-017-1457-3, 2018.

Buysse, D. J., Cheng, Y., Germain, A., Moul, D. E., Franzen, P. L., Fletcher, M., and Monk, T. H.: Night-to-night sleep variability in older adults with and without chronic insomnia, Sleep Med., 11, 56–64, https://doi.org/10.1016/j.sleep.2009.02.010, 2010.

Connolley, W. M. and Bracegirdle, T. J.: An Antarctic assessment of IPCC AR4 coupled models, Geophys. Res. Lett., 34, L22505, https://doi.org/10.1029/2007GL031648, 2007.

Doutreloup, S. and Fettweis X.: Typical & Extreme Meteorological Year and Heatwaves for Dynamic Building Simulations in Belgium based on MAR model Simulations (version 1.0.0), Zenodo [data set], https://doi.org/10.5281/zenodo.5606983, 2021.

Doutreloup, S., Wyard, C., Amory, C., Kittel, C., Erpicum, M., and Fettweis, X.: Sensitivity to Convective Schemes on Precipitation Simulated by the Regional Climate Model MAR over Belgium (1987–2017), Atmosphere, 10, 34, https://doi.org/10.3390/atmos10010034, 2019.

Duffie, J. A. and Beckman, W. A.: Solar Engineering of Thermal Processes, 4th edn., John Wiley & Sons, Inc., Hoboken, New Jersey, ISBN 978-0-470-87366-3, 2013.

Dunn, R. J. H., Alexander, L. V., Donat, M. G., Zhang, X., Bador, M., Herold, N., Lippmann, T., Allan, R., Aguilar, E., Barry, A. A., Brunet, M., Caesar, J., Chagnaud, G., Cheng, V., Cinco, T., Durre, I., Guzman, R. de, Htay, T. M., Ibadullah, W. M. W., Ibrahim, M. K. I. B., Khoshkam, M., Kruger, A., Kubota, H., Leng, T. W., Lim, G., Li-Sha, L., Marengo, J., Mbatha, S., McGree, S., Menne, M., Skansi, M. de los M., Ngwenya, S., Nkrumah, F., Oonariya, C., Pabon-Caicedo, J. D., Panthou, G., Pham, C., Rahimzadeh, F., Ramos, A., Salgado, E., Salinger, J., Sané, Y., Sopaheluwakan, A., Srivastava, A., Sun, Y., Timbal, B., Trachow, N., Trewin, B., Schrier, G. van der, Vazquez-Aguirre, J., Vasquez, R., Villarroel, C., Vincent, L., Vischel, T., Vose, R., and Yussof, M. N. B. H.: Development of an Updated Global Land In Situ-Based Data Set of Temperature and Precipitation Extremes: HadEX3, J. Geophys. Res.-Atmos., 125, e2019JD032263, https://doi.org/10.1029/2019JD032263, 2020.

European Standard: EN ISO 15927-4:2005 Hygrothermal performance of buildings – calculation and presentation of climatic data – Part 4: Hourly data for assessing the annual energy use for heating and cooling (ISO 15927-4:2005), 2005.

Eyring, V., Bony, S., Meehl, G. A., Senior, C. A., Stevens, B., Stouffer, R. J., and Taylor, K. E.: Overview of the Coupled Model Intercomparison Project Phase 6 (CMIP6) experimental design and organization, Geosci. Model Dev., 9, 1937–1958, https://doi.org/10.5194/gmd-9-1937-2016, 2016.

Eyring, V., Gillett, N. P., Achuta Rao, K. M., Barimalala, R., Barreiro Parrillo, M., Bellouin, N., Cassou, C., Durack, P. J., Kosaka, Y., McGregor, S., Min, S., Morgenstern, O., and Sun, Y.: Human Influence on the Climate System, in: Climate Change 2021: The Physical Science Basis. Contribution of Working Group I to the Sixth Assessment Report of the Intergovernmental Panel on Climate Change, edited by: Masson-Delmotte, V., Zhai, P., Pirani, A., Connors, S. L., Péan, C., Berger, S., Caud, N., Chen, Y., Goldfarb, L., Gomis, M. I., Huang, M., Leitzell, K., Lonnoy, E., Matthews, J. B. R., Maycock, T. K., Waterfield, T., Yelekçi, O., Yu, R., and Zhou, B., Cambridge University Press, Cambridge, United Kingdom and New York, NY, USA, 423–552, https://www.ipcc.ch/report/ar6/wg1/downloads/report/IPCC_AR6_WGI_Chapter03.pdf (last access: 28 June 2022), 2021.

Ferrari, D. and Lee, T.: Beyond TMY: Climate data for specific applications, in: Proceedings 3rd International Solar Energy Society conference – Asia Pacific region (ISES-AP-08), Sydney, 25–28 November 2008, http://exemplary.com.

au/download/FerrariLeeBeyondTMYpaperWC0093.pdf (last access: 24 June 2022), 2008.

Fettweis, X., Franco, B., Tedesco, M., van Angelen, J. H., Lenaerts, J. T. M., van den Broeke, M. R., and Gallée, H.: Estimating the Greenland ice sheet surface mass balance contribution to future sea level rise using the regional atmospheric climate model MAR, The Cryosphere, 7, 469–489, https://doi.org/10.5194/tc-7-469-2013, 2013.

Fettweis X., Wyard C., Doutreloup S., and Belleflamme A.: Noël 2010 en Belgique: neige en Flandre et pluie en Haute-Ardenne, Bull. Société Géographique Liège, 68, 97–107, 2017.

Finkelstein, J. M. and Schafer, R. E.: Improved goodness-of-fit tests, Biometrika, 58, 641–645, https://doi.org/10.1093/biomet/58.3.641, 1971.

Fouillet, A., Rey, G., Laurent, F., Pavillon, G., Bellec, S., Guihenneuc-Jouyaux, C., Clavel, J., Jougla, E., and Hémon, D.: Excess mortality related to the August 2003 heat wave in France, Int. Arch. Occup. Environ. Health, 80, 16–24, https://doi.org/10.1007/s00420-006-0089-4, 2006.

Gutjahr, O., Putrasahan, D., Lohmann, K., Jungclaus, J. H., von Storch, J.-S., Brüggemann, N., Haak, H., and Stössel, A.: Max Planck Institute Earth System Model (MPI-ESM1.2) for the High-Resolution Model Intercomparison Project (HighResMIP), Geosci. Model Dev., 12, 3241–3281, https://doi.org/10.5194/gmd-12-3241-2019, 2019.

Hersbach, H., Bell, B., Berrisford, P., Hirahara, S., Horányi, A., Muñoz-Sabater, J., Nicolas, J., Peubey, C., Radu, R., Schepers, D., Simmons, A., Soci, C., Abdalla, S., Abellan, X., Balsamo, G., Bechtold, P., Biavati, G., Bidlot, J., Bonavita, M., Chiara, G. D., Dahlgren, P., Dee, D., Diamantakis, M., Dragani, R., Flemming, J., Forbes, R., Fuentes, M., Geer, A., Haimberger, L., Healy, S., Hogan, R. J., Hólm, E., Janisková, M., Keeley, S., Laloyaux, P., Lopez, P., Lupu, C., Radnoti, G., Rosnay, P. de, Rozum, I., Vamborg, F., Villaume, S., and Thépaut, J.-N.: The ERA5 global reanalysis, Q. J. Roy. Meteor. Soc., 146, 1999–2049, https://doi.org/10.1002/qj.3803, 2020.

IPCC: Summary for Policymakers, in: Climate Change 2021: The Physical Science Basis. Contribution of Working Group I to the Sixth Assessment Report of the Intergovernmental Panel on Climate Change, edited by: Masson-Delmotte, V., Zhai, P., Pirani, A., Connors, S. L., Péan, C., Berger, S., Caud, N., Chen, Y., Goldfarb, L., Gomis, M. I., Huang, M., Leitzell, K., Lonnoy, E., Matthews, J. B. R., Maycock, T. K., Waterfield, T., Yelekçi, O., Yu, R., and Zhou, B., Cambridge University Press, Cambridge, United Kingdom and New York, NY, USA, 3−−32, https://www.ipcc.ch/report/ar6/wg1/downloads/report/IPCC_AR6_WGI_SPM.pdf (last access: 28 June 2022), 2021.

Kittel, C.: Present and future sensitivity of the Antarctic surface mass balance to oceanic and atmospheric forcings: insights with the regional climate model MAR, PhD Thesis, Université de Liège, Liège, Belgique, Liège, https://hdl.handle.net/2268/258491 (last access: 24 June 2022), 2021.

Kittel, C., Amory, C., Agosta, C., Jourdain, N. C., Hofer, S., Delhasse, A., Doutreloup, S., Huot, P.-V., Lang, C., Fichefet, T., and Fettweis, X.: Diverging future surface mass balance between the Antarctic ice shelves and grounded ice sheet, The Cryosphere, 15, 1215–1236, https://doi.org/10.5194/tc-15-1215-2021, 2021.

Larsen, M. A. D., Petrović, S., Radoszynski, A. M., McKenna, R., and Balyk, O.: Climate change impacts on trends and extremes in future heating and cooling demands over Europe, Energy Build., 226, 110397, https://doi.org/10.1016/j.enbuild.2020.110397, 2020.

Lee, J. Y., Marotzke, J., Bala, G., Cao, L., Corti, S., Dunne, J. P., Engelbrecht, F., Fischer, E., Fyfe, J. C., Jones, C., Maycock, A., Mutemi, J., Ndiaye, O., Panickal, S., and Zhou, T.: Future Global Climate: Scenario-Based Projections and Near-Term Information, Camb. Univ. Press, Climate Change 2021: The Physical Science Basis. Contribution of Working Group I to the Sixth Assessment Report of the Intergovernmental Panel on Climate Change, edited by: Masson-Delmotte, V., Zhai, P., Pirani, A., Connors, S. L., Péan, C., Berger, S., Caud, N., Chen, Y., Goldfarb, L., Gomis, M. I., Huang, M., Leitzell, K., Lonnoy, E., Matthews, J. B. R., Maycock, T. K., Waterfield, T., Yelekçi, O., Yu, R., and Zhou, B., Cambridge University Press, Cambridge, United Kingdom and New York, NY, USA, 553–672, https://www.ipcc.ch/report/ar6/wg1/downloads/report/IPCC_AR6_WGI_Chapter04.pdf (last access: 28 June 2022), 2021.

Ouzeau, G., Soubeyroux, J.-M., Schneider, M., Vautard, R., and Planton, S.: Heat waves analysis over France in present and future climate: Application of a new method on the EURO-CORDEX ensemble, Clim. Serv., 4, 1–12, https://doi.org/10.1016/j.cliser.2016.09.002, 2016.

Pérez-Andreu V., Aparicio-Fernández C., Martínez-Ibernón A., and Vivancos J.-L.: Impact of climate change on heating and cooling energy demand in a residential building in a Mediterranean climate, Energy, 165, 63–74, https://doi.org/10.1016/j.energy.2018.09.015, 2018.

Ramon, D., Allacker, K., van Lipzig, N. P. M., De Troyer, F., and Wouters, H.: Future Weather Data for Dynamic Building Energy Simulations: Overview of Available Data and Presentation of Newly Derived Data for Belgium, in: Energy Sustainability in Built and Urban Environments, 1st edn., edited by: Motoasca, E., Agarwal, A. K., and Breesch, H., Springer, Singapore, 111–138, ISBN 978-981-13-3283-8, https://doi.org/10.1007/978-981-13-3284-5_6, 2019.

Riahi, K., van Vuuren, D. P., Kriegler, E., Edmonds, J., O'Neill, B. C., Fujimori, S., Bauer, N., Calvin, K., Dellink, R., Fricko, O., Lutz, W., Popp, A., Cuaresma, J. C., Kc, S., Leimbach, M., Jiang, L., Kram, T., Rao, S., Emmerling, J., Ebi, K., Hasegawa, T., Havlik, P., Humpenöder, F., Da Silva, L. A., Smith, S., Stehfest, E., Bosetti, V., Eom, J., Gernaat, D., Masui, T., Rogelj, J., Strefler, J., Drouet, L., Krey, V., Luderer, G., Harmsen, M., Takahashi, K., Baumstark, L., Doelman, J. C., Kainuma, M., Klimont, Z., Marangoni, G., Lotze-Campen, H., Obersteiner, M., Tabeau, A., and Tavoni, M.: The Shared Socioeconomic Pathways and their energy, land use, and greenhouse gas emissions implications: An overview, Global Environ. Chang., 42, 153–168, https://doi.org/10.1016/j.gloenvcha.2016.05.009, 2017.

Ridder, K. D. and Gallée, H.: Land Surface–Induced Regional Climate Change in Southern Israel, J. Appl. Meteorol. Climatol., 37, 1470–1485, https://doi.org/10.1175/1520-0450(1998)037<1470:LSIRCC>2.0.CO;2, 1998.

RMI: Rapport climatique 2020 de l'information aux services climatiques, edited by: Gellens, D., Royal Meteorological Institute of Belgium, Brussels, ISSN 2033-8562, https://www.meteo.

be/resources/misc/climate_report/RapportClimatique-2020.pdf (last access: 24 June 2022), 2020.

Seneviratne, S. I., Zhang, X., Adnan, M., Badi, W., Dereczynski, C., Di Luca, A., Ghosh, S., Iskandar, I., Kossin, J., Lewis, S., Otto, F., Pinto, I., Satoh, M., Vicente-Serrano, S. M., Wehner, M., and Zhou, B.: Weather and Climate Extreme Events in a Changing Climate, in: Climate Change 2021: The Physical Science Basis. Contribution of Working Group I to the Sixth Assessment Report of the Intergovernmental Panel on Climate Change, edited by: Masson-Delmotte, V., Zhai, P., Pirani, A., Connors, S. L., Péan, C., Berger, S., Caud, N., Chen, Y., Goldfarb, L., Gomis, M. I., Huang, M., Leitzell, K., Lonnoy, E., Matthews, J. B. R., Maycock, T. K., Waterfield, T., Yelekçi, O., Yu, R., and Zhou, B., Cambridge University Press, Cambridge, United Kingdom and New York, NY, USA, pp. 1513–1766, https://www.ipcc.ch/report/ar6/wg1/downloads/report/IPCC_AR6_WGI_Chapter11.pdf (last access: 28 June 2022), 2021.

Sherwood, S. C. and Huber, M.: An adaptability limit to climate change due to heat stress, P. Natl. Acad. Sci. USA, 107, 9552–9555, https://doi.org/10.1073/pnas.0913352107, 2010.

Suarez-Gutierrez, L., Müller, W. A., Li, C., and Marotzke, J.: Hotspots of extreme heat under global warming, Clim. Dynam., 55, 429–447, https://doi.org/10.1007/s00382-020-05263-w, 2020.

Tatebe, H., Ogura, T., Nitta, T., Komuro, Y., Ogochi, K., Takemura, T., Sudo, K., Sekiguchi, M., Abe, M., Saito, F., Chikira, M., Watanabe, S., Mori, M., Hirota, N., Kawatani, Y., Mochizuki, T., Yoshimura, K., Takata, K., O'ishi, R., Yamazaki, D., Suzuki, T., Kurogi, M., Kataoka, T., Watanabe, M., and Kimoto, M.: Description and basic evaluation of simulated mean state, internal variability, and climate sensitivity in MIROC6, Geosci. Model Dev., 12, 2727–2765, https://doi.org/10.5194/gmd-12-2727-2019, 2019.

Termonia, P., Van Schaeybroeck, B., De Cruz, L., De Troch, R., Caluwaerts, S., Giot, O., Hamdi, R., Vannitsem, S., Duchêne, F., Willems, P., Tabari, H., Van Uytven, E., Hosseinzadehtalaei, P., Van Lipzig, N., Wouters, H., Vanden Broucke, S., van Ypersele, J.-P., Marbaix, P., Villanueva-Birriel, C., Fettweis, X., Wyard, C., Scholzen, C., Doutreloup, S., De Ridder, K., Gobin, A., Lauwaet, D., Stavrakou, T., Bauwens, M., Müller, J.-F., Luyten, P., Ponsar, S., Van den Eynde, D., and Pottiaux, E.: The CORDEX.be initiative as a foundation for climate services in Belgium, Clim. Serv., 11, 49–61, https://doi.org/10.1016/j.cliser.2018.05.001, 2018.

Brits E., Boone I., Verhagen B., Dispas M., Vanoyen H., Van der Stede Y., and Van Nieuwenhuyse A.: Climate change and health: set-up of monitoring of potential effects of climate change on human health and on the health of animals in Belgium. Unit environment and health, Brussels, Belgium, https://www.belspo.be/belspo/organisation/publ/pub_ostc/agora/ragjj146_en.pdf (last access: 28 June 2022), 2009.

Wilcox, S. and Marion, W.: Users Manual for TMY3 Data Sets, Technical report NREL/TP-581-43156, Task No. PVA7.6101, https://www.nrel.gov/docs/fy08osti/43156.pdf, 2008.

Wu, T., Lu, Y., Fang, Y., Xin, X., Li, L., Li, W., Jie, W., Zhang, J., Liu, Y., Zhang, L., Zhang, F., Zhang, Y., Wu, F., Li, J., Chu, M., Wang, Z., Shi, X., Liu, X., Wei, M., Huang, A., Zhang, Y., and Liu, X.: The Beijing Climate Center Climate System Model (BCC-CSM): the main progress from CMIP5 to CMIP6 , Geosci. Model Dev., 12, 1573–1600, https://doi.org/10.5194/gmd-12-1573-2019, 2019.

Wyard, C., Scholzen, C., Doutreloup, S., Hallot, É., and Fettweis, X.: Future evolution of the hydroclimatic conditions favouring floods in the south-east of Belgium by 2100 using a regional climate model, Int. J. Climatol., 41, 647–662, https://doi.org/10.1002/joc.6642, 2021.

s

Appendix E

Chapter 5: *Climate change sensitive overheating assessment in dwellings: a case study in Belgium*

BS 2021 1-3 SEPT BRUGES
INTERNATIONAL BUILDING PERFORMANCE SIMULATION ASSOCIATION

Climate Change Sensitive Overheating Assessment in Dwellings: A Case Study in Belgium

Ramin Rahif[1], Abdulrahman Fani[1], Piotr Kosinski[2], Shady Attia[1]
[1]Sustainable Building Design Lab, Dept. UEE, Faculty of Applied Sciences, Université de Liege, Belgium
[2]Faculty of Geoengineering, University of Warmia and Mazury in Olsztyn, Heweliusza Street 10, 10-724 Olsztyn, Poland

Abstract

Due to the current rate of global warming, overheating in buildings is expected to be more frequent and intense in future climates. High indoor temperature affects occupant productivity, comfort, and health. Thus, it is necessary to predict the thermal performance of buildings concerning climate change. This paper applies a climate change sensitive overheating assessment method to a lightweight timber house in Eupen, Belgium. Three metrics are used, namely Indoor Overheating Degree (IOD), Ambient Warmness Degree (AWD), and Building Climate Vulnerability Factor ($BCVF$). The overheating risk is assessed under four climate scenarios representing historical and future scenarios using dynamic simulation tool EnergyPlus v9.0. This method accounts for overheating severity and frequency, considering zonal occupancy profiles and thermal comfort models. The results indicate $BCVF$<1 for the Passive House case study showing its high potential in suppressing the outdoor thermal stress in the long-term. Finally, the increase in ventilation rate proves to be an adequate measure by decreasing the zonal peak temperatures up to 10°C and indoor overheating risk by ~60%.

Key Innovations

- Warm discomfort during the heating period is contained within the overheating analysis
- Lower base temperature for calculation of AWD is considered
- Climate change-sensitive overheating assessment is applied on a high-performance building in the Belgian context

Practical Implications

This paper provides a basis for the field experts in climate-resilient building design. It makes them aware of expected overheating risks in future climates and consider adaptation strategies in early-design stages.

Introduction

Overheating in buildings during sweltering weather conditions has become one of the main concerns in many countries (Eames, 2016; Laouadi et al., 2020). High indoor temperatures have significant impacts on occupant productivity, comfort, and health (Tanabe et al., 2013). During the extreme summer of 2003, more than 35,000 people died in Europe due to excessive heat stress (Brücker, 2005). This necessitates the definition of a reliable performance prediction methodology to indicate the vulnerability/resilience of buildings to high outdoor temperatures. Several studies assessed indoor overheating risk in residential buildings (Elsharkawy & Zahiri, 2020; Gamero-Salinas et al., 2020; Tian et al., 2020; Zukowska et al., 2019). Carlucci and Pagliano (2012) presented an overview of long-term thermal discomfort evaluation methods and grouped them into homogenous families. However, the thermal performance and overheating risk of buildings in relation to climate change are not appropriately addressed. Rahif and Attia (2021) investigated the overheating assessment methodologies to distinguish between short- and long-term methods. They found out that the only study that provides a climate change sensitive approach is the study of (Hamdy et al., 2017). In our paper, we apply this method to a Passive House (Attia & Gobin, 2020; Fani, 2020) in Belgium to predict its thermal performance in future climates.

Methodology

This study is a part of an ongoing project investigating the influence of climate change on occupant thermal comfort and overheating risk in Belgian residential building stock. Accordingly, a Passive House case study is simulated with minimum and maximum ventilation rates under four climate scenarios using dynamic simulation tool EnergyPlus v9.0. The monthly energy consumption and hourly indoor air temperature is calibrated by recorded data in 2015-2018 using ASHRAE 140 (2017) iterative method (Attia & Gobin, 2020). It is based on the calculation of Normalized Mean Bias Error (NMBE) and the Coefficient of Variation of Root Square Mean Error (CV(RSME)). Finally, the potential of ventilative cooling is calculated as a mitigation strategy. The results of the simulations are then post-processed and visualized using MATLAB.

Case study description

The case study is located in Eupen (50°37′40″N, 6°02′11″E, 298 m) municipality with a temperate oceanic climate (Figure 1). The local climate can be characterized by 2678 HDD and 285 CDD for the period 1976-2004 (Ramon et al., 2019). The house is built in two levels (see Figure 2) and is a four-façade lightweight timber construction with a total area of 174 m^2. The building complies with the Belgian Passive House requirements where the annual net energy for heating should fall below 150 MJ/m^2.

https://doi.org/10.26868/25222708.2021.30125

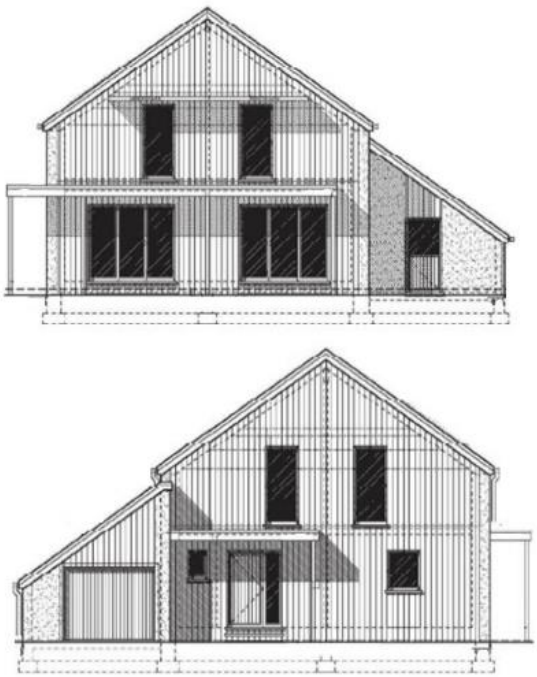

Figure 1: South-view (upper) and north-view (lower) of case study, Eupen, Belgium (derived from: http//energie.wallonie.be).

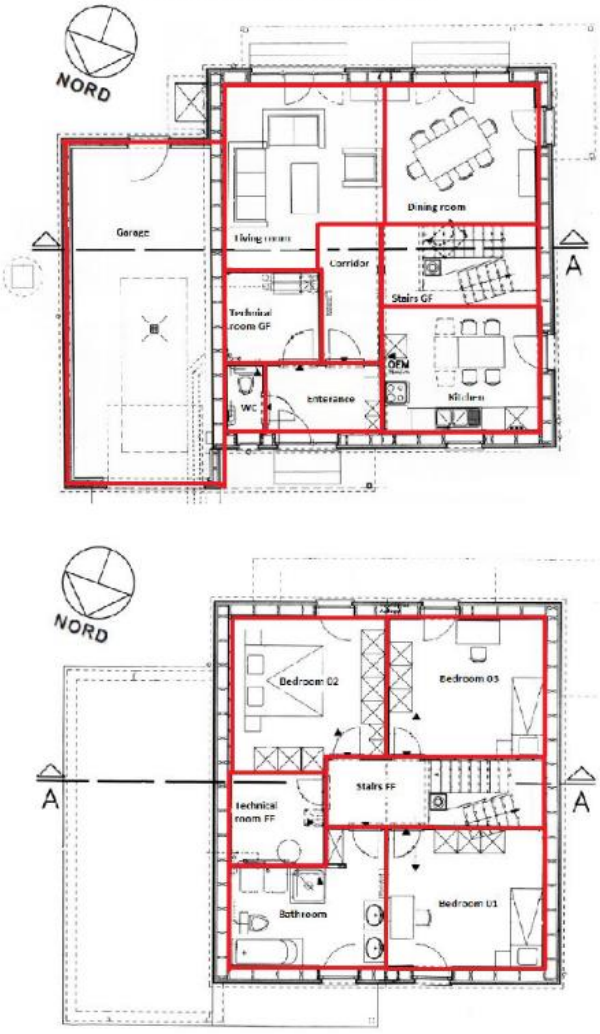

Figure 2: Case study plan: ground floor (upper), first floor (lower) (derived from: http//energie.wallonie.be).

The external wall conductivity is 0.132 W/m^{2}K insulated by mineral wool (6 cm) and cellulose (25 cm). Therefore, the thermal bridge caused by the mainframe in wood is eliminated. The building is heated by a pellet stove located in the stairs zone on the ground floor, and a gas water boiler supplies domestic hot water. The blower door test indicates the infiltration rate of 0.5 vol/h for a pressure difference of 50 Pa between the indoor and outdoor environments. South- and west-oriented ground floor zones (dining room, living room, and kitchen) and south-oriented bedrooms on the first floor are equipped with permanent solar shading devices.

The house is occupied by two adults and two children. Assumptions are made for the internal gains induced by equipment and the occupants considering weekdays and weekend occupancy scenarios.

Overheating assessment method

The overheating assessment method is based on three metrics called Indoor Overheating Degree (*IOD*), Ambient Warmness Degree (*AWD*) and Building Climate Vulnerability Factor (*BCVF*) (Hamdy et al., 2017).

IOD is a multi-zonal indicator that quantifies the indoor overheating risk taking into account severity and frequency of high indoor temperatures,

$$IOD = \frac{\sum_{z=1}^{Z}\sum_{i=1}^{N_{occ}(z)}\left[\left(T_{op,i,z}-T_{op,i,z,comfort}\right)^{+}\times t_{i,z}\right]}{\sum_{z=1}^{Z}\sum_{i=1}^{N_{occ}(z)} t_{i,z}} \quad (1)$$

Where i is occupied hour counter, z is building zone counter, Z is number of total building zones, N_{occ} is number of all occupied hours, $T_{op,i,z}$ is indoor operative temperature of time step i and zone z, and $T_{op,i,z,comfort}$ is the static or adaptive thermal comfort limit of time step i and zone z. *IOD* enables the implementation of multiple thermal comfort models in different building zones. We assumed a fixed temperature limit of 26°C based on the static comfort model CIBSE Guide A for the bedrooms. This selection is made since adaptation actions performed by occupants are limited during the sleeping period. For all other living areas, category II of the adaptive thermal comfort model EN 15251 is considered as one of the most commonly used comfort standards worldwide (Attia et al., 2019).

AWD indicates the severity and frequency of high outdoor temperatures according to a predefined base temperature,

$$AWD_{14°C} = \frac{\sum_{i=1}^{N}\left[\left(T_{a,i}-T_b\right)^{+}\times t_i\right]}{\sum_{i=1}^{N} t_i} \quad (2)$$

Where N is total number of building occupied hours, $T_{a,i}$ is outdoor air temperature in time step i, and T_b is outdoor base temperature. T_b is determined based on building characteristics and is equal to an outdoor air temperature threshold, which above necessitates the operation of any means of passive or active cooling systems. Due to high insulation levels and overheating risk in Passive Houses, T_b of 14 °C is considered.

By assuming a linear correlation between *IOD* and *AWD*, *BCVF* is the slope of regression line that predicts the vulnerability of the building to overheating risk in relation to climate change,

https://doi.org/10.26868/25222708.2021.30125

$$BCVF = \frac{IOD}{AWD_{18°C}} \quad (3)$$

$BCVF<1$ shows that the building can suppress the outdoor thermal stress, and $BCVF>1$ means that the building becomes overheated by increasing outdoor air temperature. The three above metrics help to estimate the ability of a building to maintain an acceptable indoor thermal environment in a warming climate.

Climate scenarios

The applied method requires two historical and two future weather datasets. For this aim, we used (i) average scenario representing historical climate using the weather data for the moderate year of 1965, (ii) extreme scenario that is the extreme data recorded in 2003, (iii) future normal scenario that is the normal climate projection of the year 1976 to 2100 with an increase of 2°C in average temperature due to global warming effect, (iv) future extreme scenario that is the extreme climate projection of the year 1976 to 2100 with an increase of 4°C in average temperature due to global warming effect and 1.4°C due to the urban heat island effect (Hamdy et al., 2017). The annual distribution of daily mean outdoor temperatures under four climate scenarios are shown in Figure 3.

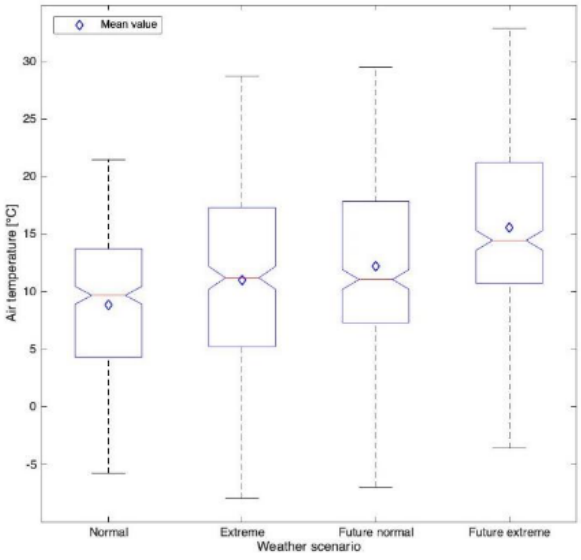

Figure 3: Annual distribution of daily mean outdoor air temperature under four climate scenarios.

Results

For each climate scenario, the case study with the minimum (0.9 l/s.m^2) and maximum (5 and 8 ac/h for bedrooms and living areas respectively) ventilation rates are simulated for annual periods (Hamdy et al., 2017). Therefore, the total number of simulations is 8. Figure 4 shows the trend of IOD in different climate scenarios represented by AWD. It is clear that the risk of indoor overheating increases as the average outdoor temperature increases. The slope of regression lines, 0.5269 for minimum ventilation rate, and 0.2443 for maximum ventilation rate, are the values of $BCVF$. It shows that the building with low ventilation rate has less potential to suppress the increased outdoor thermal stress in future climates. Figure 5 shows the annual distribution of hourly indoor operative temperature in different building zones under the future extreme scenario. Due to relatively higher solar gains through large glazing areas and orientation, the dining room, living room, and kitchen reach higher temperatures than the other zones. Figure 5 indicates that the maximum ventilation rate significantly decreases the upper margins of indoor operative temperature (up to ~10°C); however, high-temperature abnormalities emerge.

The potential of ventilative cooling is calculated based on the percentage of reduction in IOD. For this aim, the contribution of ventilative cooling $C_{\text{ventilation}}$ is defined as,

$$C_{\text{ventilation}} = IOD_{\text{min ventilation rate}} - IOD_{\text{max ventilation rate}} \quad (4)$$

The potential of ventilative cooling $P_{\text{ventilation}}$ is derived by normalizing the $C_{\text{ventilation}}$ over the $IOD_{\text{min ventilation rate}}$,

$$P_{\text{ventilation}} = \frac{C_{\text{ventilation}}}{IOD_{\text{min ventilation rate}}} \quad (5)$$

A new set of simulations are performed according to the minimum and maximum ventilation rates suggested by NBN D50-001 (1991) in Annex 4. All results regarding the potential of ventilative cooling (two sets of minimum and maximum ventilation rates) are depicted in Figure 6. The ventilative cooling potential decreases as global warming continues and it will be more challenging to mitigate the risk of overheating by only relying on ventilative cooling strategy.

Discussion

Findings and recommendations

More intense and frequent overheating events are expected as a result of climate change. This paper evaluates the thermal performance of a Passive House in a changing climate. Our study indicates that the buildings in compliance with the Passive House standard can suppress outdoor thermal stress. Figure 4 shows a substantial reduction in IOD in all scenarios for maximum ventilation rate. Higher ventilation rate decreases the vulnerability of the building to climate change by 53%. Figure 5 shows that in maximum ventilation rate, mean daily indoor operative temperature is reduced in the dining room, living room, and kitchen as high-risk zones by 7.5°C, 4°C, and 6°C, respectively. 5 ac/h for bedrooms and 8 ac/h for living areas has a significant potential of ~60% in overheating risk reduction (see Figure 6). However, Figure 6 shows that the effectiveness of ventilative cooling is predicted to be decreased by 3.74% in future extreme scenario compared to normal historical scenario. It means that although ventilative cooling is a resilient technology, its performance is expected to degrade with the continuation of global warming (Roetzel et al., 2010).

We recommend the Belgian government and experts in the field to take actions in defining accurate overheating calculation methods besides the requirements for active and passive mitigation strategies.

https://doi.org/10.26868/25222708.2021.30125

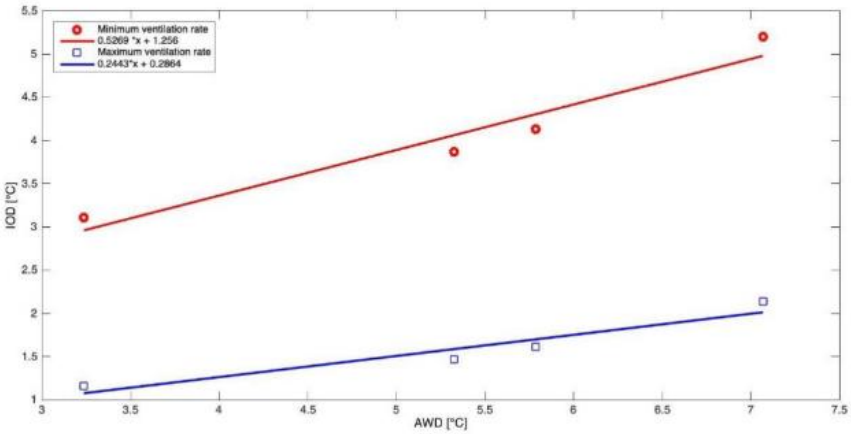

Figure 4. The Indoor Overheating Degree (IOD) presented by the Ambient Warmness Degree (AWD) under four climate scenarios for minimum (0.9 l/s.m²) and maximum (5 and 8 ac/h for bedrooms and living areas) ventilation rates. The slope of the regression lines shows the Building Climate Vulnerability Factor (BCVF).

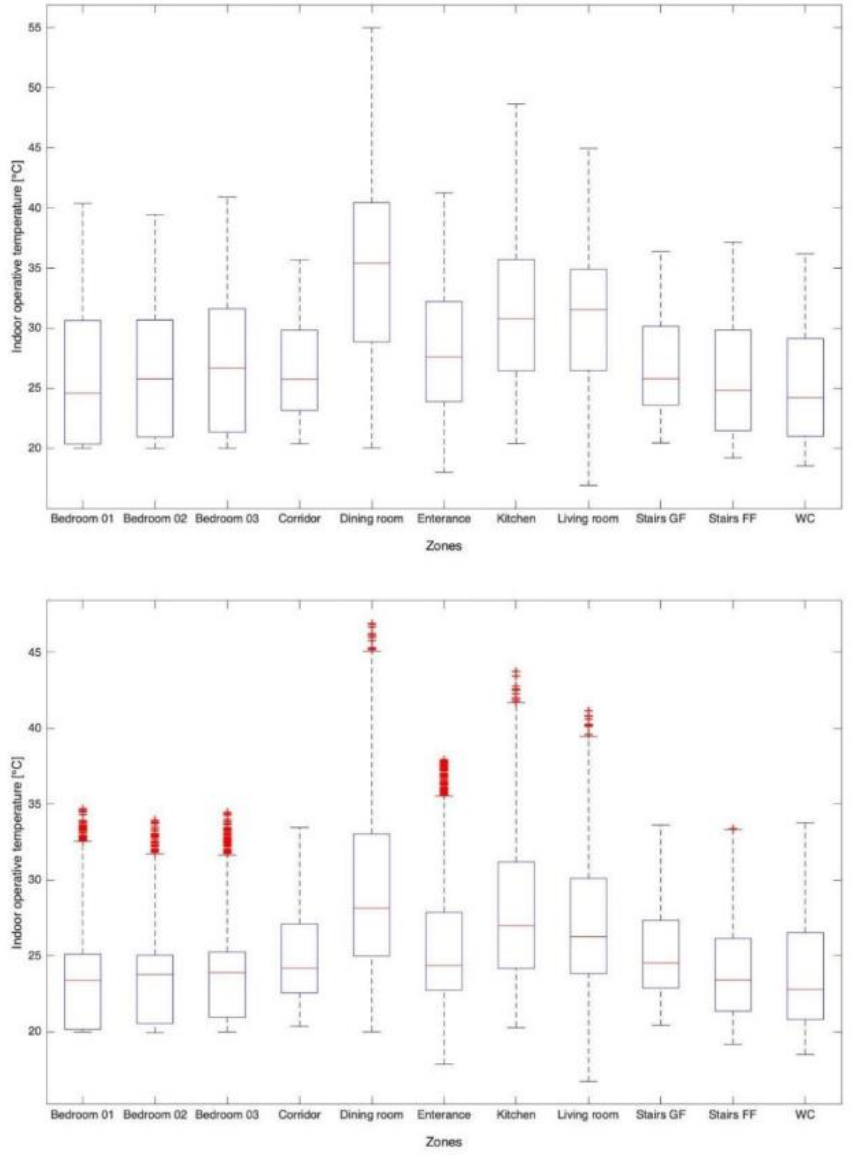

Figure 5. Annual distribution of hourly indoor operative temperature for minimum (top) and maximum (bottom) ventilation rates under future extreme scenarios for all living areas.

https://doi.org/10.26868/25222708.2021.30125

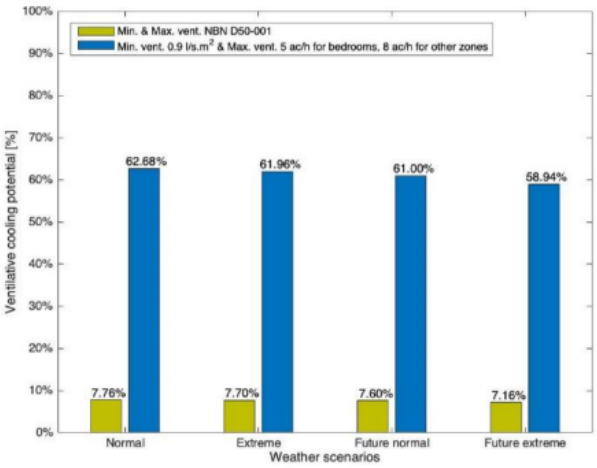

Figure 6. The potential of ventilative cooling to reduce the risk of overheating is expressed as a percentage of IOD for minimum and maximum ventilation rates.

We recommend exploring the potential of natural ventilation which is capable of 23-94% cooling demand reduction in future climates (Gilani & O'Brien, 2020). Mechanical ventilation increases building resiliency to climate change (Burman & Mumovic, 2018); however, it will increase energy consumption. Therefore, we recommend a full life-cycle assessment to balance energy efficiency and overheating resilience in the long-term. Also, we recommend the joint application of ventilative cooling with additional measures such as an increase in building thermal mass or solar shading devices.

Strengths and limitations

The first strength of our study relies on the validity of our simulation model due to the abundance and availability of data on the case study. Besides, we have implemented a novel method regarding climate change sensitive overheating assessment with some modifications. We extended the duration of our evaluation to the annual period. This enables us to consider the overheating risk during the winter season as well. Also, we defined a lower outdoor base temperature in the calculation of *AWD*. This is because the high-performance buildings with increased insulation levels are more prone to the risk of overheating (Attia, 2018) and needed to be cooled in lower outdoor temperatures.

The main limitation of the current study methodology is the neglect of solar radiation in the calculation of *AWD* which highly affects the results for *BCVF*. Besides, we only evaluate the potential of ventilative cooling. We hence do not account for the combined or individual effect of other measures such as an increase in thermal mass, glazing, solar shading devices, and building orientation. Also, we neglected the behavioral and spatial thermal adaptation in our assessments (Attia, 2020b).

Implication on practice and future research

One implication of our research is to include and address our modified methodology in future revisions of the national interpretation of the Energy Performance of Building Directive (EPBD). There is a need for major revisions in EPBD regulations to include and consider more precisely thermal comfort along with the energy calculation methods. The current rule for building stock in Belgium sets a static threshold of 23°C as comfort criterion and ignores the occupant adaptation opportunities. This approach overestimates the discomfort hours and increases energy consumption by forcing the installation and operation of active cooling systems. Thus, there is a need for further investigation in developing accurate and distinct thermal comfort models (static, adaptive, and hybrid) for naturally ventilated, mechanically cooled, and mixed-mode buildings. We strongly recommend a multi-zonal approach for overheating assessment, which allows the designer to set zone-based comfort models (e.g., static model for bedrooms) and identify the zones at higher risk of overheating (Attia, 2020a). For future research, there is a need for future weather files with more accurate sky conditions and solar radiation factor. We also recommend developing national and regional benchmark models to test the suggested overheating method in different climatic conditions and building stock (Attia et al., 2020).

Conclusion

This paper applies a state-of-the-art overheating assessment methodology based on three metrics, namely Indoor overheating Degree (*IOD*), Ambient Warmness Degree (*AWD*), and Building Climate Vulnerability Factor (*BCVF*) on a case study in Eupen, Belgium. The lightweight timber construction Passive House shows its high potential to suppress annual overheating risk in future climates. However, provisions are required in the dining room, living room, and the kitchen as the most vulnerable zones due to the relatively high solar gains. The ventilation strategy proved to be an adequate measure in reducing the indoor overheating risk, but its potential will decrease with continuation of global warming.

Acknowledgment

This research was partially funded by the Walloon Region under the call 'Actions de Recherche Concertées 2019 (ARC)' and the project OCCuPANt, on the Impacts Of Climate Change on the indoor environmental and energy PerformAnce of buildiNgs in Belgium during summer. The authors would like to gratefully acknowledge the Walloon Region and Liege University for funding. We would like to also acknowledge the Sustainable Building Design lab for valuable support during the content analysis and curation of the data. This study is a part of the International Energy Agency Annex 80 project activities to define resilient cooling in residential buildings.

References

ANSI/ASHRAE. (2017). Standard 140-2017: Standard Method of Test for the Evaluation of Building Energy Analysis Computer Programs. ASHRAE, Atlanta, USA.

Attia, S. (2018). Net Zero Energy Buildings (NZEB): Concepts, frameworks and roadmap for project

analysis and implementation. Butterworth-Heinemann. Quebec, Canada.

Attia, S. (2020a). Goede praktijken voor zonwering en EPB - berekening. Pixii - Passiefhuis Platform, Expert day Zomercomfort, Gent, Belgium. Available from: http://hdl.handle.net/2268/251437 (Accessed: 2020-12-11)

Attia, S. (2020b). Spatial and Behavioral Thermal Adaptation in Net Zero Energy Buildings: An Exploratory Investigation. Sustainability, 12(19), 7961. https://doi.org/10.3390/su12197961

Attia, S., & Gobin, C. (2020). Climate Change Effects on Belgian Households: A Case Study of a Nearly Zero Energy Building. Energies, 13(20), 5357. https://doi.org/10.3390/en13205357

Attia, S., Lacombe, T., Rakotondramiarana, H. T., Garde, F., & Roshan, G. (2019). Analysis tool for bioclimatic design strategies in hot humid climates. Sustainable Cities and Society, 45, 8–24. https://doi.org/10.1016/j.scs.2018.11.025

Attia, S., Shadmanfar, N., & Ricci, F. (2020). Developing two benchmark models for nearly zero energy schools. Applied Energy, 263, 114614. https://doi.org/10.1016/j.apenergy.2020.114614

Brücker, G. (2005). Vulnerable populations: Lessons learnt from the summer 2003 heat waves in Europe. Eurosurveillance, 10(7), 1–2.

Burman, E., & Mumovic, D. (2018). The impact of ventilation strategy on overheating resilience and energy performance of schools against climate change: The evidence from two UK secondary schools. 7th International Building Physics Conference, IBPC2018. Syracuse University, Syracuse, USA.

Carlucci, S., & Pagliano, L. (2012). A review of indices for the long-term evaluation of the general thermal comfort conditions in buildings. Energy and Buildings, 53, 194–205. https://doi.org/10.1016/j.enbuild.2012.06.015

CEN. (2007). EN 15251: Indoor environmental input parameters for design and assessment of energy performance of buildings addressing indoor air quality, thermal environment, lighting and acoustics. European Committee for Standardization, Brussels, Belgium.

Chartered Institution of Building Service Engineers (CIBSE). (2015). CIBSE Guide A: Environmetnal Design. Eighth ed.. CIBSE, London, UK.

Eames, M. E. (2016). An update of the UK's design summer years: Probabilistic design summer years for enhanced overheating risk analysis in building design. Building Services Engineering Research and Technology, 37(5), 503–522. https://doi.org/10.1177%2F0143624416631131

Elsharkawy, H., & Zahiri, S. (2020). The significance of occupancy profiles in determining post retrofit indoor thermal comfort, overheating risk and building energy performance. Building and Environment, 172, 106676. https://doi.org/10.1016/j.buildenv.2020.106676

Fani, A. R. (2020). Master thesis: Evaluation of the overheating risk and the potential of ventilative cooling: A case study in Belgium. University of Liege, Liege, Belgium.

Gamero-Salinas, J. C., Monge-Barrio, A., & Sánchez-Ostiz, A. (2020). Overheating risk assessment of different dwellings during the hottest season of a warm tropical climate. Building and Environment, 171, 106664. https://doi.org/10.1016/j.buildenv.2020.106664

Gilani, S., & O'Brien, W. (2020). Natural ventilation usability under climate change in Canada and the United States. Building Research & Information, 1–20. https://doi.org/10.1080/09613218.2020.1760775

Hamdy, M., Carlucci, S., Hoes, P.-J., & Hensen, J. L. M. (2017). The impact of climate change on the overheating risk in dwellings—A Dutch case study. Building and Environment, 122, 307–323. https://doi.org/10.1016/j.buildenv.2017.06.031

Laouadi, A., Gaur, A., Lacasse, M., Bartko, M., & Armstrong, M. (2020). Development of reference summer weather years for analysis of overheating risk in buildings. Journal of Building Performance Simulation, 13(3), 301–319. https://doi.org/10.1080/19401493.2020.1727954

NBN, D. (1991). Standard 50-001: Dispositifs de ventilation dans les bâtiments d'habitation. NBN, Brussels, Belgium.

Rahif, R., & Attia, S. (2021). Critical Review on Overheating Matrices for Residential Building Design. Energy and Buildings, under publication.

Ramon, D., Allacker, K., van Lipzig, N. P. M., De Troyer, F., & Wouters, H. (2019). Future Weather Data for Dynamic Building Energy Simulations: Overview of Available Data and Presentation of Newly Derived Data for Belgium. In Energy Sustainability in Built and Urban Environments (pp. 111–138). Springer Singapore. https://doi.org/10.1007/978-981-13-3284-5_6

Roetzel, A., Tsangrassoulis, A., Dietrich, U., & Busching, S. (2010). A review of occupant control on natural ventilation. Renewable and Sustainable Energy Reviews, 14(3), 1001–1013. https://doi.org/10.1016/j.rser.2009.11.005

Tanabe, S., Iwahashi, Y., Tsushima, S., & Nishihara, N. (2013). Thermal comfort and productivity in offices under mandatory electricity savings after the Great East Japan earthquake. Architectural Science Review,

56(1), 4–13. https://doi.org/10.1080/00038628.2012.744296

Tian, Z., Zhang, S., Deng, J., & Dorota Hrynyszyn, B. (2020). Evaluation on Overheating Risk of a Typical Norwegian Residential Building under Future Extreme Weather Conditions. Energies, 13(3), 658. https://doi.org/10.3390/en13030658

Zukowska, D., Ananida, M., Kolarik, J., Sarey Khanie, M., & Rammer Nielsen, T. (2019). Solar control solutions for reducing overheating risks in retrofitted Danish apartment buildings from the period 1850-1900 – A simulation-based study. E3S Web of Conferences, 111, 03051. Bucharest, Romania. https://doi.org/10.1051/e3sconf/201911103051

Appendix F

Chapter 6: *Impact of climate change on nearly zero-energy dwelling in temperate climate: thermal comfort, HVAC energy performance, and GHG emissions*

Building and Environment 223 (2022) 109397

Contents lists available at ScienceDirect

Building and Environment

journal homepage: www.elsevier.com/locate/buildenv

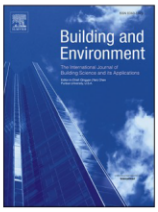

Impact of climate change on nearly zero-energy dwelling in temperate climate: Time-integrated discomfort, HVAC energy performance, and GHG emissions

Ramin Rahif [a,*], Alireza Norouziasas [a], Essam Elnagar [b], Sébastien Doutreloup [c], Seyed Mohsen Pourkiaei [d], Deepak Amaripadath [a], Anne-Claude Romain [d], Xavier Fettweis [c], Shady Attia [a]

[a] Sustainable Building Design Lab, Dept. UEE, Faculty of Applied Sciences, University of Liège, Belgium
[b] Thermodynamics Laboratory, Aerospace and Mechanical Engineering Department, Faculty of Applied Sciences, Université de Liège, 4000, Liège, Belgium
[c] Laboratory of Climatology and Topoclimatology, Department of Geography, UR SPHERES, University of Liège, Belgium
[d] University of Liège, Faculty of Sciences, Department of Environmental Science and Management, Sensing of Atmospheres and Monitoring (SAM), Avenue de Longwy 185, 6700, Arlon, Belgium

ARTICLE INFO

Keywords:
Global warming
Heating energy use
Cooling energy use
Primary energy use
Overheating
Overcooling

ABSTRACT

Global warming is widely recognized to affect the built environment in several ways. This paper projects the current and future climate scenarios on a nearly zero-energy dwelling in Brussels. Initially, a time-integrated discomfort assessment is carried out for the base case without any active cooling system. It is found that overheating risk will increase up to 528%, whereas the overcooling risk will decrease up to 32% by the end of the century. It is also resulted that the overheating risk will overlap the overcooling risk by 2090s under high emission scenarios. Subsequently, two commonly applied HVAC strategies are considered, including a gas-fired boiler + an air conditioner (S01) and a reversible air-to-water heat pump (S02). In general, S02 shows ~6–13% and 15–27% less HVAC primary energy use and GHG emissions compared to S01, respectively. By conducting the sensitivity analysis, it is found that the choice of the HVAC strategy, heating set-point, and cooling set-point are among the most influential parameters determining the HVAC primary energy use. Finally, some future recommendations are provided for practice and future research.

1. Introduction

Climate change arising from natural or anthropogenic sources causes long-term shifts in temperatures and weather patterns. According to Intergovernmental Panel on Climate Change (IPCC) Sixth Assessment Report (AR6), the average global surface temperature is expected to increase in the range of 1–5.7°*C* depending on the Shared Socioeconomic Pathway (SSP) scenario [1]. In addition, the Urban Heat Island (UHI) effect is recognized in more than 400 cities around the world [2,3]. The UHI effect, defined as "*relatively atmospheric warmth of urban areas compared to the surrounding countryside*", is predicted to increase the ambient temperature in cities by 5–10°*C* [4,5]. It is necessary to project such warming weather conditions on buildings to predict the changes in comfort conditions as well as Heating Ventilation, and Air Conditioning (HVAC) energy use and Green House Gas (GHG) emissions.

The impact of climate change on thermal comfort in different locations will vary depending on the climate. In temperate climates, a major anticipated impact of climate change is the increase of overheating occurrence and associated health hazards for the occupants in buildings [6–10]. Overheating affects the occupants' comfort [11], productivity [12] and health, where in severe cases can lead to illness and death [13,14]. In total, over 35,000 people died in Europe during the summer 2003 heatwave [15], in which 14,729 deaths are reported in France [16], 2139 in England and Wales [17], up to 2200 in the Netherlands [18], and 1175 in Belgium [19]. Therefore, there is a need to evaluate the future thermal performance of the buildings and equip them, if necessary, with sustainable and resilient cooling solutions to ensure the comfort and well-being of the occupants.

Several methods are introduced in the scientific literature to evaluate

* Corresponding author.
E-mail address: ramin.rahif@uliege.be (R. Rahif).

https://doi.org/10.1016/j.buildenv.2022.109397
Received 28 February 2022; Received in revised form 7 July 2022; Accepted 11 July 2022
Available online 1 August 2022

thermal comfort, described as *"the condition of mind that expresses satisfaction with the thermal environment and is assessed by subjective evaluation"* [20]. Recently, a new group of methods have been proposed (which are the focus of the current study) to assess the thermal comfort over a span of time in buildings that are named as *time-integrated, long-term, or chronic comfort evaluation methods* [20–23]. In other words, they quantify the accumulation of discomfort stimuli over a specific period. Most of those methods are aimed at assessing the overheating discomfort (asymmetric), whereas some deal with both overheating and overcooling discomfort (symmetric), and only a few of them developed for overcooling discomfort [24,25]. Previous studies reviewed such methods highlighting their strengths and limitations [21,25–27].

According to European Commission (EC), the buildings in the EU account for 40% of energy consumption and 36% of Green House Gas (GHG) emissions [28]. Heating and cooling make for the majority of building energy use in Europe, accounting for 70% of total energy consumption in residential units [29]. This highlights the potential of buildings, in particular HVAC systems, in reducing energy consumption and GHG emissions [30]. Climate change influences the HVAC size and energy demand [31]. With the continuation of global warming, energy demand for heating and cooling is predicted to decrease and increase, respectively [32]. However, the rate of change in different locations will vary depending on the climate [33]. Consequently, the future climatic forecasts must be included in the building energy simulations to better understand the trend of energy consumption and GHG emissions for the HVAC components as the major energy consumers in the buildings.

Table 1 lists some studies that discussed the impact of climate change on time-integrated discomfort, heating demand, cooling demand, and GHG emissions in residential buildings in Europe. Sajjadian et al. [34] evaluated a four-story flat in compliance with the Passive House standard in London. By applying future weather data obtained from morphing the UK Climate Impact Program (UKCIP) monthly climate data using CCWorldWeatherGen tool, a significant shift towards less overcooling was resulted from 2011 to 2080. It was also found that the overall energy consumption decreases because of considerably higher reduction in the heating demand compared to the increase in the cooling demand. Attia S. and Gobin C [35]. evaluated a nearly Zero-Energy Building (nZEB) located in Eupen municipality in Belgium using the future weather data downscaled by the regional climate model (MAR) "Modèle Atmosphérique Régional". The outcomes of the study showed that the passive design strategies could not prevent overheating in naturally ventilated and highly insulated case study. Considering EN15251 adaptive comfort model, the overheating hours rises 700 h, 845 h, and 1441 h by 2100 for the RCP4.5, RCP6, and RCP8 scenarios, respectively. They also suggested that the active cooling strategies may become the most practical option if the overheating hazards are not addressed during the building design. Ciancio V. et al. [36] studied the impact of climate change on energy demands in 19 European cities covering the main Köppen-Geiger climate classes (B - arid; C – temperate; D - continental; E – polar). A representative case study consisting of three floors and three apartments was considered for all cities. The weather data are obtained from real observations (current: 2020) and CCWorldWeatherGen tool (future: 2050 and 2080). It was found that in cities such as Copenhagen, Gothenburg and Paris the CO_2 emissions tend to decrease, whereas in some other cities such as Milan, Porto, and Berlin, the CO_2 emissions tend to increase. Taken together all the examined cities, they found that the increase in cooling demands will offset the decrease in heating demands; therefore, the energy consumption and CO_2 emissions will rise globally. It was also found that in cities such as Copenhagen, Gothenburg, London, and Prague, it will become necessary to install active cooling systems (if not present) to ensure comfort conditions in the future. In addition to the above-mentioned studies, other similar studies can be found at building scale [36–48] and building stock scale [49–51] in the scientific literature (see Table 1).

Despite the numerous studies on climate change impact assessment in buildings, there is relatively less comprehensive research including all aspects of time-integrated discomfort, HVAC primary energy use, and GHG emissions. They mostly lack a multizonal and asymmetric assessment of time-integrated discomfort [21] with high-resolution climate

Table 1
Summary of the recent studies on the impact of climate change on Time-integrated Discomfort (TiD), Heating Demand (HD), Cooling Demand (CD), and GHG Emissions (GE) in residential buildings in Europe.

Author(s)	Ref.	Year	Building type (study scale)	Location	Focus
Frank Th.	[41]	2005	Multistory residential unit (building scale)	Zurich–Kloten, Switzerland	HD, CD
Olonscheck M. et al.	[51]	2011	Residential buildings (building stock scale)	Germany	HD, CD, GE
Nik V. and Kalagasidis AS.	[50]	2013	Residential buildings (building stock scale)	Stockholm, Sweden	HD, CD
Jylhä K. et al.	[52]	2015	Detached residential house (building scale)	Southern Finland	HD, CD
Van Hooff T. et at.	[45]	2016	Terraced dwelling (building scale)	De Bilt, Netherlands	HD, CD
Sabunas A. and Kanapickas A.	[38]	2017	Four-story residential unit (building scale)	Kaunas, Lithuania	HD, CD
Sajjadian SM.	[34]	2017	Four-story residential unit (building scale)	London, UK	TiD, HD, CD
Tettey U. et al.	[39]	2017	Multi-story residential unit (building scale)	Växjö, Sweden	HD, CD
Andrić I. et al.	[43]	2017	Six-story detached residential unit (building scale)	6 cities including Madrid, Spain & Milan, Italy, & Hamburg, Germany	HD
Pérez-Andreu V. et al.	[47]	2018	Single-family detached house (building scale)	Valencia, Spain	TiD, HD, CD
Ciancio V. et al.	[44]	2019	Three-story residential unit (building scale)	Aberdeen, Scotland & Prague, Czech & Palermo, Italy	HD, CD
Moazami A. et al.	[46]	2019	16 building types including high- and mid-rise residential units (building scale)	Geneva, Switzerland	HD, CD
Attia S. and Gobin C.	[35]	2020	Three-story single-family detached house (building scale)	Eupen, Belgium	TiD
Ciancio V. et al.	[36]	2020	Three-story representative apartment (building scale)	19 European cities	HD, CD, GE
Machard A. et al.	[37]	2020	Single-story residential unit (building scale)	Paris, France	HD, CD
Shen J. et al.	[40]	2020	A flat in multi-family apartment (building scale)	Rome, Italy & Stockholm, Sweden	TiD
De Masi R. F. et al.	[48]	2021	Single-family representative house (building scale)	Benevento, Italy	HD, CD
Yang Y. et al.	[49]	2021	Residential buildings (building stock scale)	38 European cities	TiD, HD, CD
Pajek L. et al.	[42]	2022	Single-family detached unit (building scale)	Moscow, Russia & Ljubljana, Slovenia & Milan, Italy & Athens, Greece & Porto, Portugal	HD, CD

data [53]. In addition, most studies are carried out by a unique assumption on the type of the HVAC system without detailed information on their modelling procedure. The above is more evident in the studies performed in temperate climates in Europe. Therefore, as members of the International Energy Agency (IEA) EBC Annex 80 – "Resilient cooling of buildings" project, we developed this paper to address the abovementioned knowledge gap inspired by the framework developed within the project [8]. The aim of this research is to extend the knowledge on thermal comfort and energy performance of residential buildings in the context of climate change and broaden the comparative analysis among HVAC strategies to come up with the most sustainable solutions. The research questions are:

- Q1: What will be the changes in outdoor weather conditions assuming different emission scenarios for Brussels?
- Q2: To what extent climate change will affect time-integrated discomfort in a naturally ventilated nearly zero-energy dwelling?
- Q3: What will be the changes in HVAC primary energy use and GHG emissions under the operation of commonly applied HVAC systems?
- Q4: What are the influential parameters (i.e., weather data, the choice of the HVAC system, the HVAC performance characteristic, and set-point temperatures) in determining the HVAC primary energy use?

This paper provides a valuable contribution to the new body of knowledge from an international perspective by providing a clear picture of climate change impact assessment in temperate oceanic climates (Cfb) according to Köppen-Geiger-Peel climate classification [54]. Such climate is particularly dominant in Western Europe in cities like Amsterdam, Brussels, Copenhagen, London, and Paris. As can be seen in Fig. 1, in addition to European cities, some major cities such as Auckland, Bogotá, Canberra, Nairobi, Vancouver, and Santa Fe have a similar climate in other regions around the world. This paper also applies a multizonal method in quantification of time-integrated discomfort in buildings. More importantly, a new fit-to-purpose metric called *"Indoor overcooling Degree (IOcD)"* is proposed to provide a full asymmetric assessment together with a previously developed metric called *"Indoor Overheating Degree (IOhD)"* [10]. This paper also compares two HVAC strategies, including a gas-fired boiler for heating + Air Conditioner (AC) for cooling and a reversible air-to-water heat pump for both heating and cooling. Both strategies include mechanical ventilation with a heat recovery system. The detailed information on their sizing is provided while incorporating the uncertainties in the input parameters (uncertainty analysis). Last but not least, this paper includes sensitivity analysis (SA) to identify the most influential factors affecting the HVAC primary energy use.

For policymakers, this paper sheds light on the importance of climate change-sensitive comfort evaluations and criteria to be embedded in the building codes. This can result in comfort benefits and helps the construction sector towards climate change proof residential buildings. This paper also informs the building professionals about the future of HVAC related energy use and GHG emissions and how their choice of the HVAC system can affect them. The current paper is organized as follows. In Section 2, the methodology is provided, including the boundary conditions (Section 2.1), climate data (Section 2.2), building model (Section 2.3), time-integrated discomfort evaluation (Section 2.4), and HVAC strategies (Section 2.5). Section 3 presents the results. Section 4 discusses the key findings, recommendations, strengths, limitations, and implications on the practice of the study and suggests potential future research. And, Section 5 concludes the paper.

2. Methodology

Fig. 2 shows an overview of the current paper's methodology. In the first stage, the base case building model is created and simulated to analyze the indoor thermal conditions in different weather scenarios. In the second stage, two different designs for the HVAC system (i.e., S01 and S02) are considered. DesignBuilder v7.0.0 software is used to create the building and HVAC models, which is a comprehensive and intuitive Graphical User Interface (GUI) for the EnergyPlus simulation engine. In the second stage, the exported Input Data File (.idf) from DesignBuilder is fed into JEPlus and JEPlus + EA open-source software to perform the uncertainty and sensitivity analysis, respectively. JEPlus is a tool to manage complex parametric analysis based on the EnergyPlus simulation engine, while JEPlus + EA is an extension for JEPlus to conduct full-factorial, Monte Carlo, global sensitivity, and constrained multi-objective optimization [55]. In total, over 16000 simulations are run in 72 h using a workstation with CPU: AMD 3990X - 64 × 2.9 GHz, Cache: 256 MB, RAM: 64 GB, and Graphics card: 24 GB (2 × 32 GB). The post-processing and visualizations are done using a homemade MATLAB script.

2.1. Boundary conditions

In this section, the boundary conditions assumed for the current study are presented. First, the study is performed on a representative case in Belgium characterized by temperate climate. In such heating-dominated regions, the focus of building design is mainly on heat preservation during the winter season. This is achieved via highly insulated and airtight design concepts hindering heat dissipation during

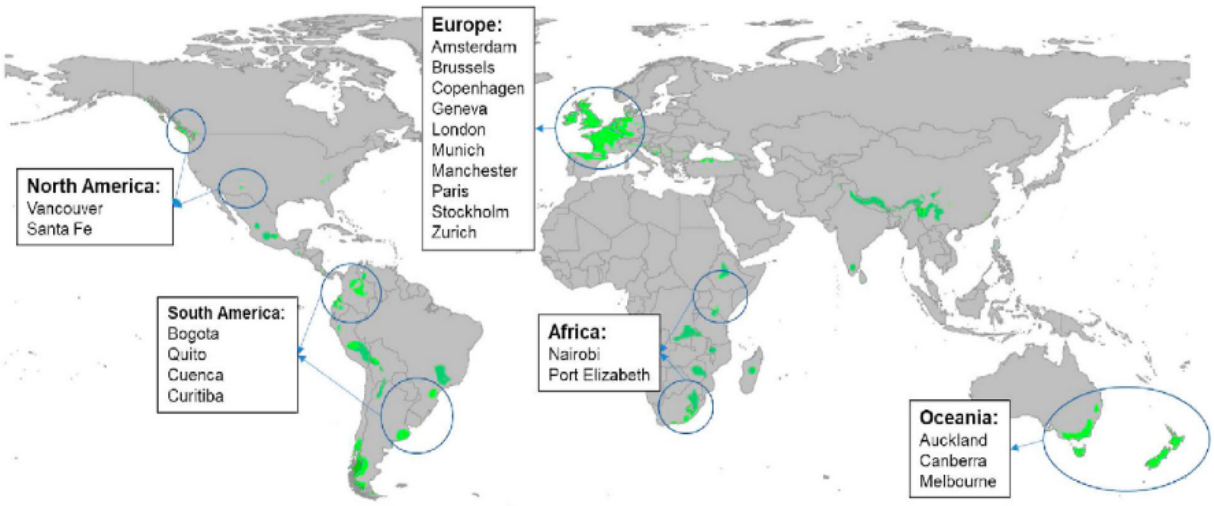

Fig. 1. Cities with temperate oceanic climate (Cfb) worldwide [54].

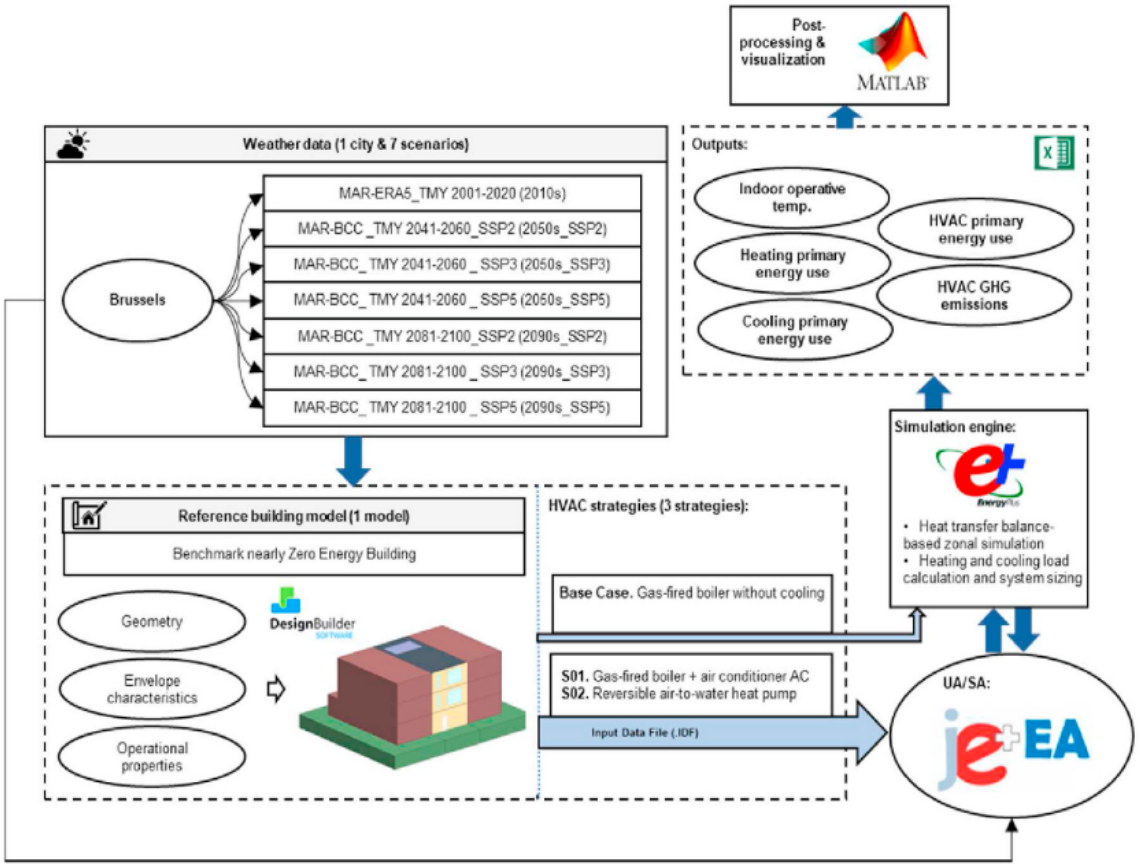

Fig. 2. Study conceptual framework (SCF).

the summer season. Therefore, by only relying on passive measures, it may become difficult in the future to prevent overheating issues. It should be mentioned that the provisions are required (e.g., reference building model, climate data, GHG emissions intensity, etc.) to the generalizability of the results to other temperate regions.

Second, the study's focus is restricted to the comparison of two commonly applied HVAC strategies. As the first HVAC strategy, an air conditioner is added to provide cooling along with the existing gas-fired boiler for heating. It is a cost-effective measure because there is no need for ductwork, and it requires minor changes to the building for fitting the components. As the second HVAC strategy, a reversible air-to-water heat pump is implemented that provides heating, cooling, and consistent Domestic Hot Water (DHW). Unlike air-to-air heat pumps, air-to-water heat pumps do not require additional systems to provide DHW. The air-to-water heat pumps are suitable for households for replacing the traditional boilers with a more environmentally friendly option with a relatively high installation cost. Other boundary conditions of the current study are that a) there is no consideration regarding degradation of building envelope and the HVAC components and b) there is no consideration regarding the evolution of GHG emissions factor based on the energy mix of the electricity production.

2.2. Climate data

Acquiring reliable current and future climate data is vital in any study related to climate change and defines its quality [47]. In this paper, the climate data are based on the General Circulation Model (GCM) outputs. The GCMs are used to estimate the climate projections, whereas they are not directly applicable to building simulations due to high spatial and temporal resolutions. It is necessary to transform them into compatible climate data using downscaling techniques (statistical or dynamical methods). For this aim, the regional climate model (MAR) *"Modèle Atmosphérique Régional"* was used in its version 3.11.14 [56], which is a dynamical method resulting in physically consistent climate parameters and extreme weather events. MAR is adapted and widely validated for Belgium region [57–59].

MAR is derived by coupling a three-dimensional atmospheric model to a one-dimensional transfer scheme between the atmosphere, vegetation, and surface [60]. To calculate the climate data used in this paper, two different methods were implemented. First, MAR was forced every 6 h in its lateral boundaries by reanalysis ERA5 [61] assimilated by different sources of observations (e.g., in-situ weather station, radar data, satellites, etc.) between 1980 and 2014. This can be considered as the reconstruction of observed climate data. Second, MAR was forced every 6 h by Earth System Model (ESM) BCC-CSM2-MR (which approximately follow the mean temperature of all ESMs over Belgium up to 2100) from the Sixth Coupled Model Intercomparison Project (CMIP6) that represents the mean evolution of climate parameters between 1980 and 2014 with the historical scenario and 2015–2100 with the SSPs [62]. ESM forced MAR was then validated by comparing to MAR ERA5 simulations to verify whether it can be used to generate future climate data [56].

ESMs for future periods are based on Shared Socioeconomic Pathways (SSPs). SSPs are projected scenarios of global socioeconomic evolution by 2100. SSPs are used to quantify Green House Gas (GHG) emissions associated with different climate policies. The future climate data in this paper consists of three SSPs, 1) SSP2 – medium challenges to mitigation and adaptation (1.8°*C* estimated global warming by 2100), 2) SSP3 – high challenges to mitigation and adaptation (3.6°*C* estimated global warming by 2100), and 3) SSP5 – high challenges to mitigation and low challenges to adaptation (4.4°*C* estimated global warming by 2100) [63,64].

After obtaining the results of MAR forced by BCC-CSM2-MR, the Typical Meteorological Years (TMYs) are constructed over 20 years for three different periods 2001–2020 (hereafter 2010s), 2041–2060 (hereafter 2050s), and 2081–2100 (hereafter 2090s). TMYs are

synthetic years (on an hourly basis) formed by typical representative months selected from the target period (e.g., 2001–2020) (i.e., January from 2001, February from 2012, etc.). The typical months are chosen by comparing the distribution of each month in the long-term distribution of that month for the available modelled or observed data (minimum 10 years) using Finkelstein-Shafer statistics. The protocol by ISO 15927–4 [23] was used to create the TMYs. The weather data in this paper are derived for Brussels (Köppen–Geiger climate zone: Cfb, Marine west coast and warm summer) from Ref. [56]. The selection of the periods and emission scenarios (SSPs) for the weather files in this paper are inspired by the recommendations of the dynamic simulation guideline developed within International Energy Agency (IEA) EBC Annex 80 – "Resilient cooling of buildings" project [65] as well as a previous study in the literature [8].

2.3. Building model

A reference building model representing a typical terraced dwelling in Belgium is adopted for this study based on the work of [66]. The building is located in Brussels (50°83′79″, 4°44′10″, 13 m) and was renovated after 2010 to comply with the nearly Zero-Energy Building (nZEB) requirements. The envelope is externally insulated, and photovoltaic panels are mounted on the roof. The building was constructed in three floors and has north- and south-facing glazing areas. The reference building is presented in Fig. 3.

The datasets regarding the building model in.dsb (DesignBuilder model data) and.idf (EnergyPlus input data file) formats are extracted from Ref. [67]. The multizonal building model includes the conditioned zones categorized as, 1) living areas (living room and open kitchen as one zone), 2) office room, 3) three bedrooms, and 4) five short-presence areas (two corridors, two bathrooms, one WC).

The building is occupied by a family of two parents (above 45 years old) and two children (seven and ten years old). The occupancy schedules are specified based on ISO 18253–2 [68] with a density of 43 m^2/person. ISO 18253–2 provides occupancy schedules for a four-member family with 46 years old householders. According to Ref. [66], the same occupancy schedules are defined for weekdays and weekends. Based on the data collected in the surveys, the lighting power intensity of 10 W/m^2 is assigned for the living areas, while the lighting power intensity of 8 W/m^2 is assigned for the bedrooms. The lighting schedules are tuned for the winter season and validated by using the outcomes of national energy reports provided by the Flemish Energy Agency (FEA) and IP Belgium. Table A1 in Annex A summarizes the characteristics of the calibrated building model.

In the base case building model, the heating is provided by a gas-fired boiler with a hydronic loop coupled to the radiators and there is no active cooling. The temperature set-points for heating are set to 21°C in living areas, 18°C in bedrooms, and 18°C in short-presence areas. The building is naturally ventilated during the occupied hours in the summer with control on minimum indoor air temperature of 24°C. Mechanical ventilation with a heat recovery system is also operating to provide minimum fresh air of 25 m^3/h according to NBN D50-001. In addition, the Photovoltaic (PV) panels are attached to the roof adjacent to the northern edge. The PV panels have Crystalline Silicon cell type (36 cells in series) with an active area of 0.34 m^2 and rated electric power output of 61 Watt. The PV panels are connected to a DC to AC converter with an efficiency of 0.95. According to Ref. [66], the on-site electricity generation of PV panels is 3000 kWh/year.

2.4. Time-integrated discomfort evaluation

The time-integrated discomfort evaluation in buildings requires the determination of indicators and underlying thermal comfort models (if required). The time-integrated discomfort indicators can be symmetric (overheating- and overcooling-specific) or asymmetric (overheating-specific or overcooling-specific) [21]. Following the recommendations of the guidelines developed in International Energy Agency (IEA) EBC Annex 80 – "Resilient cooling of buildings" project [65,69] and the scientific literature [8,21], an asymmetric index called Indoor Overheating Degree (IOhD) [10] is selected to estimate the overheating discomfort. Afterwards, a new asymmetric index is proposed in this study named as Indoor Overcooling Degree (IOcD) to quantify the overcooling discomfort separately. The *IOhD* and *IOcD* indices accumulate heating and cooling degree hours over the total number of zonal occupied hours, respectively. The formulas to calculate the *IOhD* and *IOcD* are,

$$\mathrm{IOhD} \equiv \frac{\sum_{z\ 1}^{Z}\sum_{i\ 1}^{N_{occ}(z)}\left[\left(T_{in,z,i} - T_{comf,upper,z,i}\right)^{+} \times t_{i,z}\right]}{\sum_{z\ 1}^{Z}\sum_{i\ 1}^{N_{occ}(z)} t_{i,z}} \tag{1}$$

$$\mathrm{IOcD} \equiv \frac{\sum_{z\ 1}^{Z}\sum_{i\ 1}^{N_{occ}(z)}\left[\left(T_{comf,lower,z,i} - T_{in,z,i}\right)^{+} \times t_{i,z}\right]}{\sum_{z\ 1}^{Z}\sum_{i\ 1}^{N_{occ}(z)} t_{i,z}} \tag{2}$$

Where Z [−] is the number of total building conditioned zones, $N_{occ}(z)$ [−] is the total number of occupied hours in zone z, $T_{in,o,z}$ is the indoor operative temperature in zone z at hour i, $T_{comf,upper,z,i}$ is maximum comfort threshold in zone z at hour i, $T_{comf,lower,z,i}$ is minimum comfort threshold in zone z at hour i. The $T_{comf,lower,z,i}$ and $T_{comf,upper,z,i}$ can be derived from the static or adaptive comfort models in the standards such as ISO 17772, EN 16798, ASHRAE 55, CIBSE Guide A, etc.

The *IOhD* and *IOcD* are multizonal indices that quantify, with a single

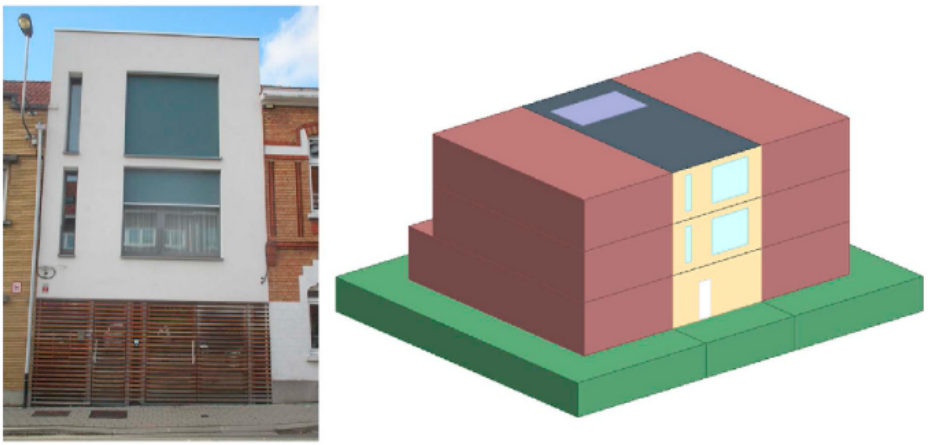

Fig. 3. The representative nearly zero-energy terraced dwelling in Belgium.

value, the intensity and frequency of discomfort in a building. Such a multizonal approach allows depicting real-world circumstances in buildings, encompassing zones with variable thermal comfort models (i.e., static and adaptive) and requirements (e.g., comfort categories), as well as tracking the occupied hours in each zone. This makes it easier to reflect the zone-based occupant behavior and adaptation opportunities. Therefore, the time-integrated discomfort assessment via those metrics is adaptable and allows for personalization at the zone level under real and artificial conditions.

In this paper, the comfort models are obtained from ISO 17772-1 standard. ISO 17772–1 provides category-based static (Cat. I, Cat. II, Cat. II and Cat. IV) and adaptive (Cat. I, Cat. II, and Cat. III) comfort models. Category II is selected in this study that is recommended for new buildings and renovations [21,25]. For the bedrooms, the static comfort model is chosen due to the limited occupant adaptation actions during the sleeping period [70]. The static comfort model in ISO 17772–1 is provided in PMV/PPD ranges that can be translated into the operative temperature ranges by setting assumptions on relative humidity (=40% for the heating season and = 60% for the cooling season), air velocity (<0.1 m/s), metabolic rate (~1.2 met), and clothing factor (~0.5 clo for summer and ~1 clo for winter). Consequently, $20°C$ and $26°C$ are assigned for the bedrooms as the lower limit and upper limit of comfort, respectively. For other zones, the adaptive comfort model is selected that is recommended for naturally ventilated buildings. The adaptive comfort model in ISO 17772–1 is provided via the formulas for the upper and lower limit of comfort based on the weighted running mean outdoor air temperature T_{rmo} [71]. The formulas to calculate the upper and lower limits in Category II are,

$$T_{comf,upper,z,i} = 0.33T_{rmo} + 18.8 + 3 \quad (3)$$

$$T_{comf,lower,z,i} = 0.33T_{rmo} + 18.8 - 4 \quad (4)$$

2.5. HVAC strategies

2.5.1. Gas-fired boiler (heating) + air conditioner (cooling)

As the first HVAC strategy (S01), a split Air Conditioner (AC) is added to the base case to provide cooling without changing the existing gas-fired boiler system (see Section 2.3). A gas-fired boiler connects to flow splitters and mixers together with a circulating pump to provide hot water for heating and domestic use. A conventional split AC, as implied by its name, consists of an indoor and an outdoor unit. The outdoor unit includes an air-cooled condenser, a condenser fan, and a compressor, while the indoor unit includes an evaporator, an expansion valve, and a distribution fan. The AC circulates the indoor air and cools it before the supply node by passing it over the evaporator coil. The AC cooling capacity is controlled by varying the indoor unit fan speed or AC/DC compressor inverter. The AC deals with both sensible and latent heat loads.

The gas-fired boiler is modelled in DesignBuilder using Hot Water Plant Loop module. It requires the boiler definition in terms of fuel type, rated heating capacity, rated thermal efficiency, and design flow rates. The amount of fuel used in the boiler is calculated by the combination of rated thermal efficiency and normalized efficiency performance curve. The performance curve is set to the default curve as CondensingBoilerEff and shows the fraction of nominal thermal efficiency of the boiler based on the hot water temperature leaving the boiler.

The AC in DesignBuilder can be implemented by using a unitary single zone module. The unitary single zone module allows modelling a constant volume direct-expansion cooling via the DX cooling coil. The DX cooling coil uses the combination of the rated Sensible Heat Ratio (SHR), rated total cooling capacity, rated air volume flow rate, and rated *EER*. It also requires the definition of availability schedules which is considered identical to the occupancy schedules in this study. In this paper, to define the DX coil performance under a range of conditions, the default performance curves are selected from the EnergyPlus database. For instance, DXClgCoilTotalClgCap/EnergyInputRatioFuncTemperature are selected that are bi-quadratic curves representing the total cooling capacity/Energy Input Ratio (EIR) as a function of temperature curves. In other words, they show the variations in total cooling capacity/EIR as a function of the wet-bulb temperature of the inlet air passing over the cooling coil and the dry-bulb temperature of the air entering the condenser coil. The output of this curve is then multiplied by the rated cooling capacity/EIR to show the total cooling capacity/EIR at a specific temperature operating condition.

2.5.2. Reversible air-to-water heat pump (heating & cooling)

As the second HVAC strategy (S02), a reversible air-to-water heat pump is implemented to provide both heating and cooling. Similar to the AC system, the reversible air-to-water heat pump has an indoor and an outdoor unit. In the heating mode, the outdoor unit coil operates as an evaporator by extracting the heat from the outdoor air by forcing the refrigerant to transform from the liquid phase to the gas phase. The gas is then compressed in the compressor to increase its temperature. The indoor unit coil acts as a condenser and transfers the heat from the gas into the hydronic loop. The heated water is stored in a tank with a supplemental electric heater. The stored hot water can serve the DHW or can be circulated in radiators, fan coils, or radiant surfaces. This process can be easily reversed to provide the chilled water during the cooling season using a 4-way valve (the evaporator becomes condenser, and the condenser becomes evaporator).

To model a reversible heat pump in DesignBuilder, different hot- and chilled-water loops should be defined. For hot water loop, an air-to-water heat pump module is implemented that consists of an air-to-water DX compression coil as a primary source connected to a water tank with a supplemental heater as a secondary/additional source for heating. The DX coil object calculates the air-side heating capacity in parallel to the water-side temperature gradient at a given condenser flow rate. To define the performance of the DX coil in different operating conditions in terms of the *COP* and total heating capacity, ASHPLowTCAPFT (heating capacity function of evaporator wet-bulb temperature) and ASHPLowTCOPFT (heating COP function of evaporator wet-bulb temperature) bi-quadratic curves are selected from the EnergyPlus database. For the chilled water loop, a high-temperature chilled water loop is defined consisting of an air-cooled condenser, an evaporator, and a compressor to supply chilled water at ~$18°C$. The performance curves and the characteristics of the components for the chilled water loop are derived from the manufacturer's data.

For both S01 and S02, all thermal capacities and design flow rates are auto-sized by EnergyPlus based on the external design conditions and the building configuration. For this aim, the summer and winter design data should be specified that are simplified weather data based on the most extreme days. The auto-sizing feature uses design day weather data to specify outside conditions when auto-sizing the HVAC components based on ASHRAE sizing method [72]. The design data for cooling consists of maximum dry-bulb temperature, coincident wet-bulb temperature, and minimum dry-bulb temperature. The design data for heating consists of minimum dry-bulb temperature, wind speed, and wind direction. For each period, the degree of confidence of the design data should be selected. In other words, the probability that the design data will occur in reality should be defined. This can be done based on the dry- or wet-bulb temperatures with 99.6%, 99%, and 98% confidence (i.e., 0.4%, 1%, and 2% chance of more extreme weather occurrence). 99.6% confidence is assumed in this paper. The auto-sizing feature sizes the HVAC components in a way to fit the loads and maintain comfort for all periods except for more extreme conditions than the design data. In this paper, the design data are derived from the current weather data (i.e., 2010s) and kept the same considering a non-climate change responsive design (i.e., the HVAC components are not re-sized based on the future summer and winter design data) [8]. In both strategies, the existing mechanical ventilation with a heat recovery system is kept providing minimum fresh air of 25 m^3/h according to NBN

D50-001. Both strategies are among widely available (TRL~9) and applicable HVAC systems in temperate climates [73]. All the input values to model S01 and S02 are listed in Table 2.

2.6. Uncertainty and sensitivity analysis method

This section provides an overview of the Uncertainty Analysis (UA) and the Sensitivity Analysis (SA) and their application in this study.

The UA is the practice of quantifying the variability of the output parameters due to the variability of the input parameters in an input/output dataset. It results in the estimation of statistical factors such as mean, median, and population quantiles of the output parameters. A sampling-based uncertainty analysis called Latin Hypercube Sampling (LHS) [74] is used in this study where a set of probability distribution of the input parameters are sampled to be propagated within the simulation model to obtain the distribution of the selected output parameters. The LHS method is extensively used due to relatively its small sample size (low computational cost) and efficient stratification properties [75]. Details for the LHS can be found in Refs. [76,77].

The SA studies to what extent the variations in the input parameters qualitatively or quantitatively vary the output parameters [78]. The SA can be divided into local SA and global SA. The latter is used in this study that characterizes the effect of the input parameters over the entire input space and helps discard the parameters with negligible effect in order to reduce the computational burden [79]. For this aim, the Morris method is used [80]. The Morris method uses a set of randomized One variable at a Time (OAT) design experiments [79] that vary only one parameter keeping the other parameters constant in each run. The main advantage of the Morris method is the low computational cost; however, it is not able to distinguish non-linear interactions between the input and output parameters [81].

Since this paper deals with modelling the HVAC systems in the future, it is necessary to account for the evolution of some key parameters characterizing their performance. Accordingly, some of those parameters are selected as input parameters for UA/SA, including the *COP* of the air-to-water heat pump (in heating mode) *"P0"*, gas-fired boiler efficiency *"P1"*, EER of the air-to-water heat pump (in cooling mode) and the AC *"P2 & P3"*, and mechanical ventilation fan efficiency *"P4"*. Due to foreseen advancements in the HVAC industry in the future, the input parameters are defined as improving ranges (i.e., the current values from the manufacturer's data are considered as the minimum value). In addition, in line with the work of [31], the set point temperatures for heating *"P5 & P6"* and cooling *"P7"* are added as the input parameters for the UA/SA. All the input parameter ranges regarding the HVAC systems are listed in Table 2. The output parameters are defined to fit the scope of the current paper including the heating primary energy use [kWh/m^2] *"t0"*, cooling primary energy use [kWh/m^2] *"t1"*, HVAC primary energy use [kWh/m^2] *"t2"*, and HVAC GHG emissions [ton] *"t3"*.

The SA is performed for S01 and S02 individually and combined (i.e., considering the building model as a discrete input parameter *"M"*). This allows exploring the most influential parameters affecting the HVAC primary energy use for each of the HVAC systems individually as well as to rank the effect of decision making regarding the type of the HVAC system on its primary energy use.

In this paper, JEPlus parametric tool is used to perform UA based on the LHS method and JEPlus + EA is used to perform SA based on the Morris method with a sample size of 600, max generations 300, and first population size of 50.

3. Results

3.1. Evolution of outdoor weather conditions

Fig. 4 shows the monthly outdoor air temperature for current and future TMYs for Brussels resulted from MAR forced by BCC-CSM2-MR

Table 2
The HVAC model inputs for S01 and S02.

	Gas-fired boiler + air conditioner (S01)	Reversible air-to-water heat Pump (S02)
Target zones (heating)	Living & kitchen, office, bedroom 01, bedroom 02, bedroom 03, corridors, WC, bathroom 01, and bathroom 02	Living & kitchen, office, bedroom 01, bedroom 02, bedroom 03, corridors, WC, bathroom 01, and bathroom 02
Target zones (cooling)	Living & kitchen, office, bedroom 01, bedroom 02, and bedroom 03	Living & kitchen, office, bedroom 01, bedroom 02, and bedroom 03
Target zones (ventilation)	Living & kitchen, office, bedroom 01, bedroom 02, bedroom 03, WC, bathroom 01, and bathroom 02	Living & kitchen, office, bedroom 01, bedroom 02, bedroom 03, WC, bathroom 01, and bathroom 02
Set-point temperatures [°C]	[Min: 20°C, Int: 0.5°C, Max: 22] for heating (living & kitchen and office) – [Min:17°C, Int:0.5°C, Max:19°C] for heating (bedrooms and short-presence areas e.g., corridors, bathrooms, and WC) -[Min: 23°C, Int: 0.5°C, Max: 25°C] for cooling	[Min: 20°C, Int: 0.5°C, Max: 22] for heating (living & kitchen and office) – [Min:17°C, Int:0.5°C, Max:19°C] for heating (bedrooms and short-presence areas e.g., corridors, bathrooms, and WC) -[Min: 23°C, Int: 0.5°C, Max: 25°C] for cooling
Ventilation rates [m^3/h]	25 m^3/h	25 m^3/h
Fuel type	Natural gas (heating)/ electricity (cooling)	Electricity
Heating	Gas-fired condensing boiler	Air-to-water DX compression
Cooling	Air-to-air DX expansion	Air-to-water DX expansion
Condenser type (cooling)	Air-cooled	Air-cooled
Total cooling capacity [W]	Auto-sized to design days	Auto-sized to design days
Rated EER [–]	[Min: 5.8, Int: 0.5, Max: 8.8]	[Min: 5.4, Int: 0.5, Max: 8.4]
Total heating capacity [W]	Auto-sized to design days	Auto-sized to design days
Rated thermal efficiency/ COP [–]	[Min: 0.88, Int: 0.02, Max: 0.98]	[Min: 4.6, Int: 0.5, Max: 7.6]
Rated Sensible Heat Ratio (SHR)	Auto-sized	–
Coil performance curve type	Bi-Quadratic	Bi-Quadratic
Indoor unit	VAV ADU (cooling)/ water radiator (heating)	Radiant surface heating and cooling (underfloor pipes)
Radiant surface hydronic tubing inside diameter [m]/length [m]/ number of circuits	N/A	0.013 m/auto-sized/one per surface
Rated supply air flow rates (cooling) [m3/s]	Auto-sized	N/A
Design supply air temperature (cooling) [°C]	14°C	N/A
Radiator/radiant surface design capacity [W]	Auto-sized (heating)	Auto-sized (heating and cooling)
Radiator/radiant surface maximum water flow rate [m^3/s]	Auto-sized (heating)	Auto-sized (heating and cooling)
Radiant surface heating/ cooling control throttling range [°C]	N/A	0.5°C
Min/max/design plant loop hot water flow rate [m^3/s]	Auto-sized (variable flow)	Auto-sized (variable flow)
Reference entering hot water temperature [°C]	80°C	35°C
Min/max/design plant loop chilled water flow rate [m^3/s]	N/A	Auto-sized (variable flow)
	N/A	18°C

(continued on next page)

Table 2 (*continued*)

	Gas-fired boiler + air conditioner (S01)	Reversible air-to-water heat Pump (S02)
Design entering chilled water temperature [°C]		
Tank volume [m^3]	N/A	Auto sized
Water tank internal heating element maximum capacity [W]/control type/fuel type/thermal efficiency [–]	N/A	Auto-sized/cycle/ electricity/0.9
Radiant surface condensation control type	N/A	Simple off
AHU type	Variable volume	Constant volume
AHU Fan	Efficiency [Min: 0.70, Int: 0.04, Max: 0.90]/ pressure rise: 600 pa/ motor efficiency: 0.90	Efficiency [Min: 0.70, Int: 0.04, Max: 0.90]/ pressure rise: 600 pa/ motor efficiency: 0.90
AHU design supply flow rate	Auto-sized	Auto-sized
AHU Heat recovery efficiency [–]/heat exchanger type/Frost control type	92%/plate/none	92%/plate/none

Earth System Model (ESM). In addition, Table 3 provides weather summaries per scenario in terms of Heating Degree Days (HDD10°*C*), Cooling Degree Days (CDD18°*C*), average, hottest, and coldest yearly air temperature, and annual cumulative horizontal solar radiation.

According to the weather files used in this paper, the monthly outdoor air temperature is expected to increase between 1.11°*C* to 4.11°*C* in 2090s_SSP5 compared to 2010s. The maximum and minimum changes occur in July and April, respectively. In general, the increases are larger in the summer (July to August) than in the spring (April to June). On an annual basis, there is an increase in air temperature 1.1°*C* by 2050s and 1.6°*C* by 2090s considering the SSP2 scenario, 1.3°*C* by 2050s and 2.6°*C* by 2090s considering the SSP3 scenario, and 1.6°*C* by 2050s and 3.2°*C* by 2090s considering the SSP5 scenario. The *HDD10°C* decreases 24% by 2050s and 42% by 2090s, whereas the *CDD18°C* increases 21% by 2050s and 60% by 2090s averaged over SSPs. The highest hottest temperature 34.7°*C* is resulted for 2090s_SSP3 and the lowest coldest temperature −7.1°*C* is resulted for 2010s. In general, the coldest air temperature during the year increases 3.63°*C* by 2050s and 4.2°*C* by 2090, while the hottest air temperature increases 1.4°*C* by 2050s and 3.7°*C* by 2090s averaged over SSPs. With the increase of *HDD10°C* and the coldest air temperature during the year, it is expected that the average and peak heating loads will decrease in buildings. On the other hand, with the increase of *CDD18°C* and the hottest air temperature during the year, it is expected that the average and peak cooling loads will increase [82–84]. Based on the climate data in this paper, the annual cumulative horizontal solar radiation inconsistently varies between 1024 kWh/m^2 and 1132 kWh/m^2 among different scenarios.

3.2. Time-integrated discomfort

In this section, the result of time-integrated discomfort assessment for the base case building model is described by analyzing the Indoor Overheating Degree (IOhD) and the Indoor Overcooling Degree (IOcD) indices. The *IOhD* and *IOcD* represent the intensity and frequency of

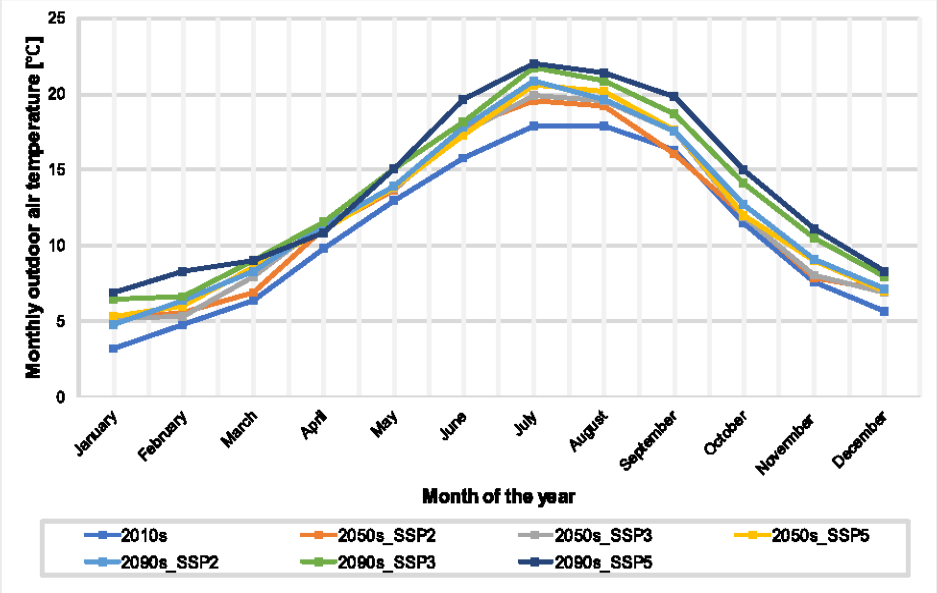

Fig. 4. Monthly outdoor air temperature for current and future TMYs for Brussels resulted from MAR forced by BCG-CSM2-MR Earth System Model (ESM).

Table 3
Summary of weather scenarios in terms of HDD10°*C*, HDD18°*C*, average yearly temperature, hottest temperature (99%), coldest temperature (1%), and annual cumulative horizontal solar radiation.

	HDD10°*C* [Kh]	CDD18°*C* [Kh]	Average yearly temperature [°*C*]	Hottest temperature (99%) [°*C*]	Coldest temperature (1%) [°*C*]	Annual cumulative horizontal solar radiation [kWh/m^2]
2010s	929	294	10.8	29.8	−7.1	1024.83
2050s_SSP2	738	342	11.9	29.6	−2.3	1111.67
2050s_SSP3	698	343	12.1	31.7	−3.7	1068.57
2050s_SSP5	665	390	12.4	31.9	−4.4	1132.63
2090s_SSP2	672	364	12.4	31.4	−6.9	1092.26
2090s_SSP3	510	488	13.4	34.7	−1.8	1056.92
2090s_SSP5	455	569	14	34.5	0.2	1090.91

overheating and overcooling discomfort considering zonal comfort criteria, respectively. Fig. 5 shows the *IOhD* and *IOcD* for different climate scenarios assuming the static comfort model for the bedrooms and the adaptive comfort model for other zones based on ISO 17772–1 (see Section 2.4).

The *IOhD* increases between 109 and 200% by 2050s and between 154 and 528% by 2090s. On the other hand, the *IOcD* decreases between 11 and 23% by 2050s and between 21 and 32% by 2090s. The overheating discomfort has relatively more variations compared to the overcooling discomfort. It means that the heating system performance (i.e., gas-fired boiler coupled to water radiators) will be less affected by climate change than the cooling system performance (i.e., natural ventilation). It is normal since the effectiveness of natural ventilation is highly dependent on outdoor thermal conditions [85]. Therefore, with the increase in outdoor air temperatures, the cooling effect of natural ventilation will decrease leading to an escalation in the overheating discomfort.

In addition, the results show that the *IOhD* in the current weather scenario (i.e., 2010s) is 85% lower than the *IOcD*. With the continuation of global warming, however, the situation will be reversed. The *IOhD* will become 3.8% and 21% more compared to *IOcD* considering 2090s_SSP3 and 2090s_SSP5, respectively. Therefore, it is predicted in this paper that the overheating discomfort will overlap the overcooling discomfort and will become the major cause of discomfort if the building lacks a proper active cooling system. This is in line with the findings of [12,35,86–88] that the use of active cooling systems along with the passive ones will become inexorable to cope with the overheating impact of climate change in buildings.

The result for the overcooling assessment shows that even though the building is equipped with a heating system, the high values between 0.76°*C* to 0.51°*C* are resulted for *IOcD*. It is since the lower limit of comfort for the static comfort model is 20°*C*, whereas the radiators are left half-open by the occupants to meet a set-point temperature of 18°*C* in the bedrooms and short-presence areas [66]. It makes these zones to be accounted as discomfortable during the heating season according to the thermal comfort model. Overall, a low heating set-point temperature can decrease the final heating energy use but forfeits thermal comfort [31].

3.3. Primary energy use and GHG emissions

This section presents the results of the simulations regarding the ranges of heating primary energy use, cooling primary energy use, HVAC primary energy use, and HVAC GHG emissions for S01 and S02. All HVAC components are considered while calculating the HVAC primary energy use and GHG emissions including the heating system, cooling system, and mechanical ventilation. Fig. 6 shows the distribution of the heating primary energy use and the cooling primary energy use for different variations of the input parameters. The point clouds for S01 and S02 are distinguished and colored by the weather scenarios. Moving from the current to future weather scenarios, the points tend towards lower heating primary energy use and higher cooling primary energy use in both S01 and S02.

Fig. 7 depicts the minimum, maximum, median, mean, 25% quartile, 75% quartile, and standard deviation for heating, cooling, and HVAC primary energy use for S01 and S02 under different weather scenarios. To derive the primary energy use, the final energy use is converted using the Primary Energy Factor (PEF) 2.5 for electricity from the grid and 1 for natural gas [89]. The final heating energy use for S01 includes the natural gas consumption of the boiler and electricity consumption of the pump and for S02 includes the electricity consumption of the compressor, the condenser pump, the evaporator fan, and the tank supplementary internal heating coil. The final cooling energy use for S01 includes the electricity consumption of the compressor, the condenser fan, and the evaporator fan and for S02 includes the electricity consumption of the compressor, the evaporator pump, and the condenser fan.

For heating, S01 has ~60% more mean heating primary energy use compared to S02 averaged over all climate scenarios. The mean heating primary energy use for S01 decreases between 19 and 37% from 2010s to 2050s and between 34 and 64% from 2010s to 2090s. While for S02, it decreases between 24 and 38% from 2010s to 2050s and between 32 and 74% from 2010s to 2090s. For cooling, S01 has between 37% and 56% less mean primary energy use than S02. The lowest value is calculated for 2090s_SSP5 and the highest value is calculated for 2010s. It shows that S01 has superior cooling energy performance than S02 in the current climate scenario; however, this superiority will diminish with the increase in outdoor temperatures. The mean cooling primary energy use

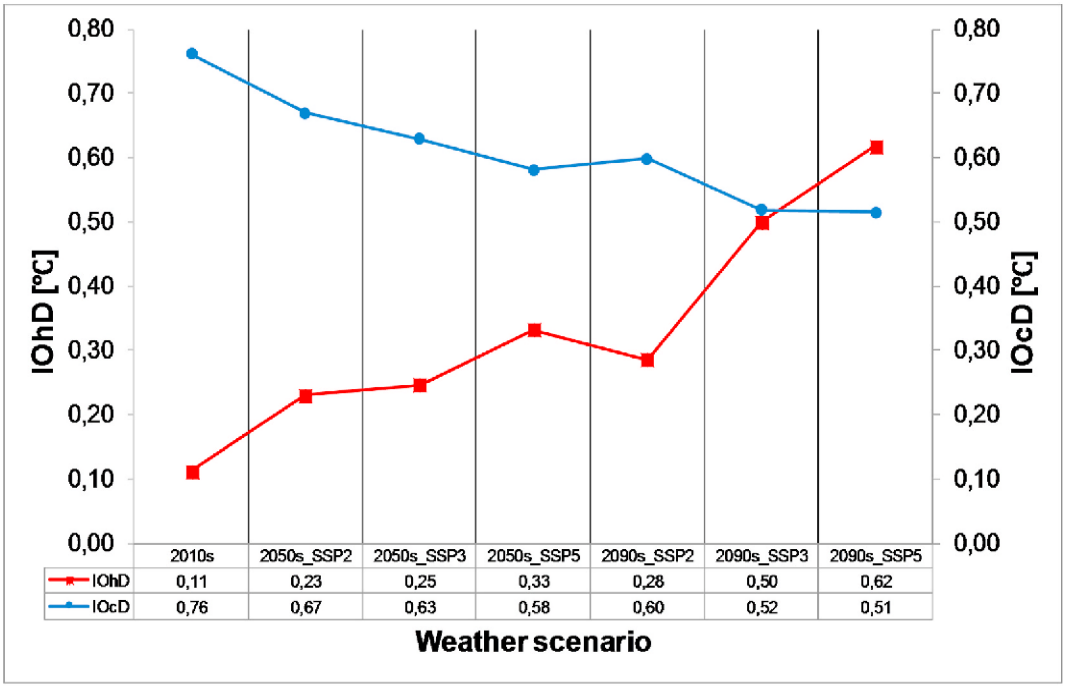

Fig. 5. IOhD and IOcD presented by weather scenario.

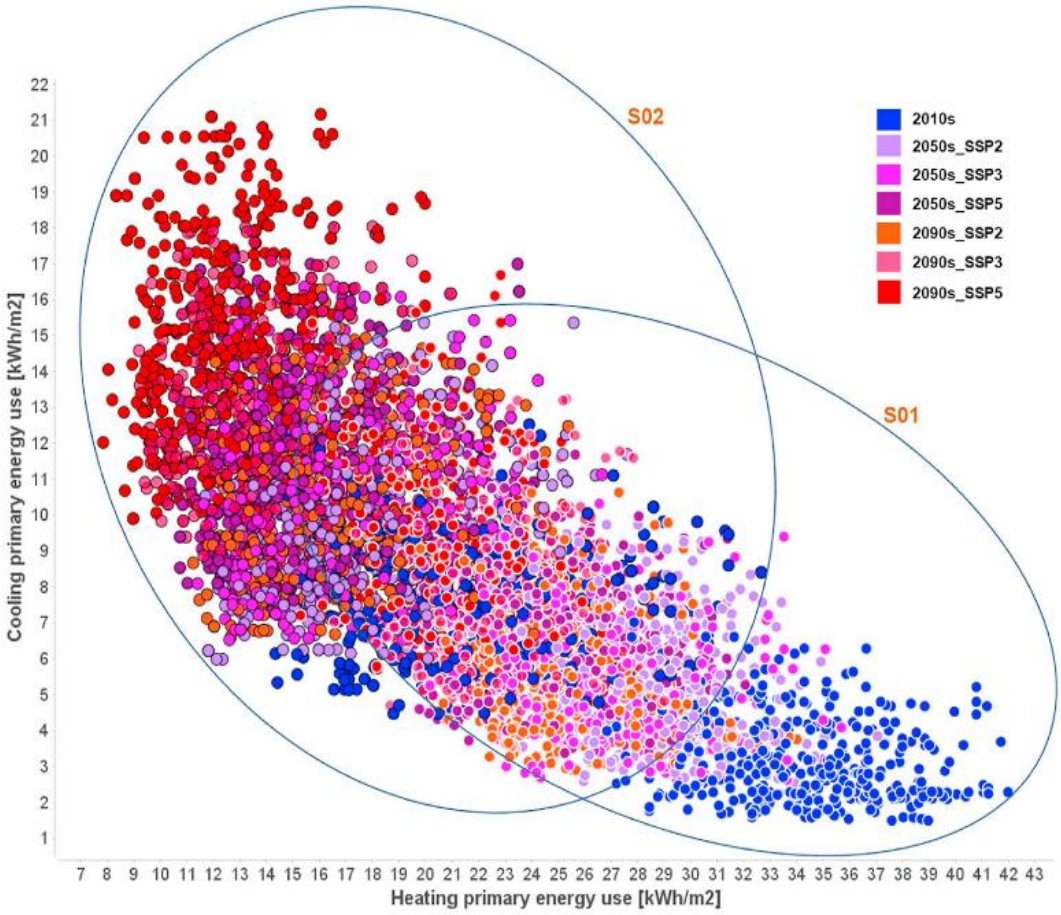

Fig. 6. Scatter plot based on heating and cooling primary energy use colour categorized by weather scenarios for all simulation cases. The point clouds for the case with S01 and S02 are distinguished. (For interpretation of the references to colour in this figure legend, the reader is referred to the Web version of this article.)

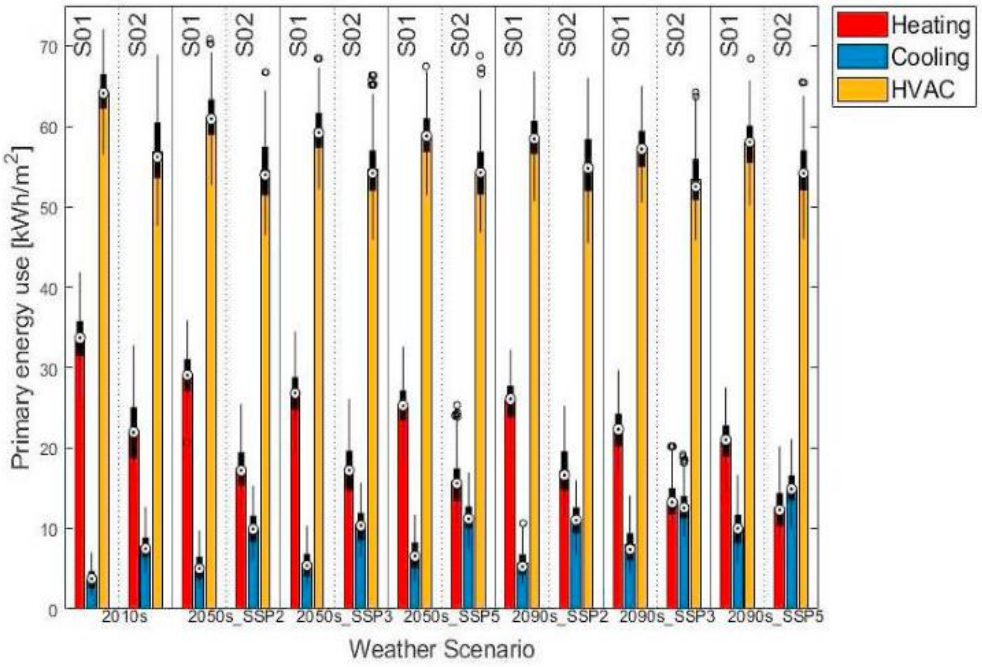

Fig. 7. Bar plots and box plots showing the heating, cooling, and HVAC primary energy use under different weather scenarios.

for S01 increases between 39 and 50% from 2010s to 2050s and between 43 and 65% from 2010s to 2090s. While for S02, it increases between 21 and 33% from 2010s to 2050s and between 28 and 50% from 2010s to 2090s.

The difference between the mean heating and cooling primary energy use for S02 is between 0.73 and 14.06 kWh/m^2. The cooling primary energy use overlaps the heating primary energy use by 2.76 kWh/m^2 in 2090s_SSP5 for S02. It is due to the fact that, a) there is a marginal difference between the *COP* of heating and EER of cooling for the reversible air-to-water heat pump, and b) the *CDD18°C* is 114 Kh more than *HDD10°C* in 2090s_SSP5. For S01, the difference between the mean heating and cooling primary energy use is between 11.07 and 30.66 kWh/m^2 where always the heating primary energy use is more than the cooling primary energy use. Even though the climate-related parameters (i.e., *CDD* and *HDD*) show more need for cooling than heating in 2090s_SSP5, due to the relatively low efficiency of the gas-fired boiler in S01, it remains the major energy consumer in the HVAC system.

Overall, because of lower final heating energy use in S02, the final HVAC energy use is ~29.04 kWh/m^2 less in S02 compared to S01. The difference becomes smaller in terms of the primary energy use due to higher PEF of the electricity than natural gas. S02 has ~4.84 kWh/m^2 less HVAC primary energy use compared to S01. The HVAC primary energy use decreases ~7% for S01 and ~4% for S02 by 2090s compared to 2010s.

The HVAC GHG emissions are calculated using the electricity and natural gas emission intensity derived from the European Environment Agency (EEA) and the report by Joint Research Center (JRC) of the European Commission (EC) [90]. Electricity's GHG intensity is assumed to be 0.161 tCO_2e/MWh and the natural gas's emission intensity is assumed to be 0.240 tCO_2e/MWh. Fig. 8 shows the GHG emissions related to heating, cooling, and ventilation for S01 and S02. It shows a decrease in future GHG emissions that is closely in relation to the warming weather conditions and the decrease in building heating primary energy use. Overall, the HVAC GHG emissions for S02 is lower between 15 and 27% than S01 thanks to lower HVAC primary energy use and lower emission intensity for electricity than natural gas. For S01, the mean HVAC GHG emissions decreases 14%, while for S02, a decrease of 3% is resulted by 2090s. Table B1 in Annex B summarizes the minimum, maximum, median, mean, 25% quartile, 75% quartile, and standards deviation for heating, cooling, and HVAC primary energy use as well as GHG emissions.

3.4. Sensitivity analysis

In this section, the results of Sensitivity Analysis (SA) are presented. Fig. 9 depicts the parallel coordinates showing the interactions between the input and output parameters during the SA process. Fig. 10 plots the Morris SA outcomes considering the HVAC primary energy use as the output parameter. In Fig. 10, the standard deviation of elementary effect (sigma) is an expression of the interaction effect of each input parameter (e.g., *W, T, P0, P1,* ...) (i.e., high-order or curvature effects) on the output parameter (i.e., HVAC primary energy use). And, the absolute mean of elementary effect (Mu*) is a measurement of the overall effect of each input parameter (e.g., *W, T, P0, P1,* ...) on the output parameter (i.e., HVAC primary energy use) avoiding the cancellation effect [91, 92]. The SA is performed for both S01 and S02 individually and combined (i.e., considering the building model as a discrete input parameter *"M"*).

The findings of this study show that the most influential parameters considering, a) only S01 are cooling set-point *"P7"*, weather scenario *"W"*, and heating set-point for living & kitchen and office *"P5"*, b) only S02 are fan efficiency *"P4"*, heating *COP "P0"*, and cooling set-point *"P7"*, and c) both S01 and S02 are building model (HVAC strategy) *"T"*, heating set-point for living & kitchen and office *"P5"*, and cooling set-point *"P7"*.

Fig. 10 shows that the standard deviation is always strictly positive, therefore none of the influential parameters has a perfectly linear effect on the outcomes. For only S01 case, the largest values of standard deviation (sigma) tend to be associated with the most influential parameters (*"P7" and "W"*). Therefore, *"P7" and "W"* are influential and non-linear/interacting parameters for only S01 case. It means that there is a link between those parameters' amount of influence and their involvement in the curvature effects (i.e., interaction effects). On the other hand, the most influential parameters, *"P4", "P0", and "P7"* for only S02 case and *"T", "P5"*, and *"P7"* for both S01 and S02 case, are not associated with the highest values of sigma. Therefore, those parameters are influential and non-interacting, meaning that while the magnitude of their effect is consistently high for the perturbations in the parameter space, the variation of their elementary effect is quite minor.

The average impact of *"W"* for the combined case (S01 & S02) is low, but the standard deviation is high. This suggests that in particular circumstances (associated with the implementation of S01 system), the weather scenario can have a significant impact on the HVAC primary

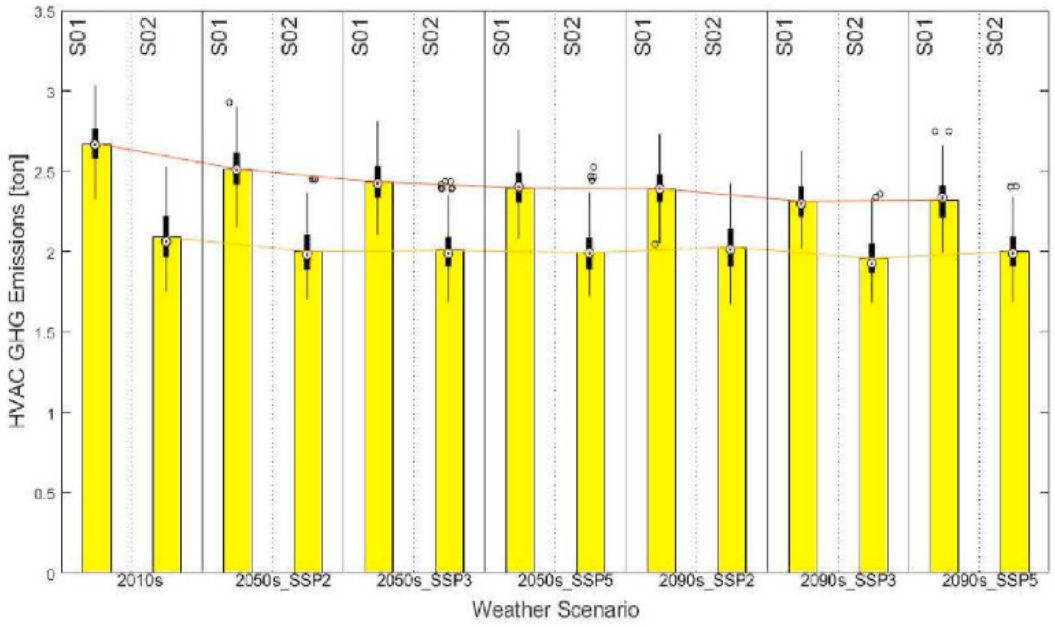

Fig. 8. Bar plots (means) and box plots of GHG emissions by HVAC systems for different weather scenarios.

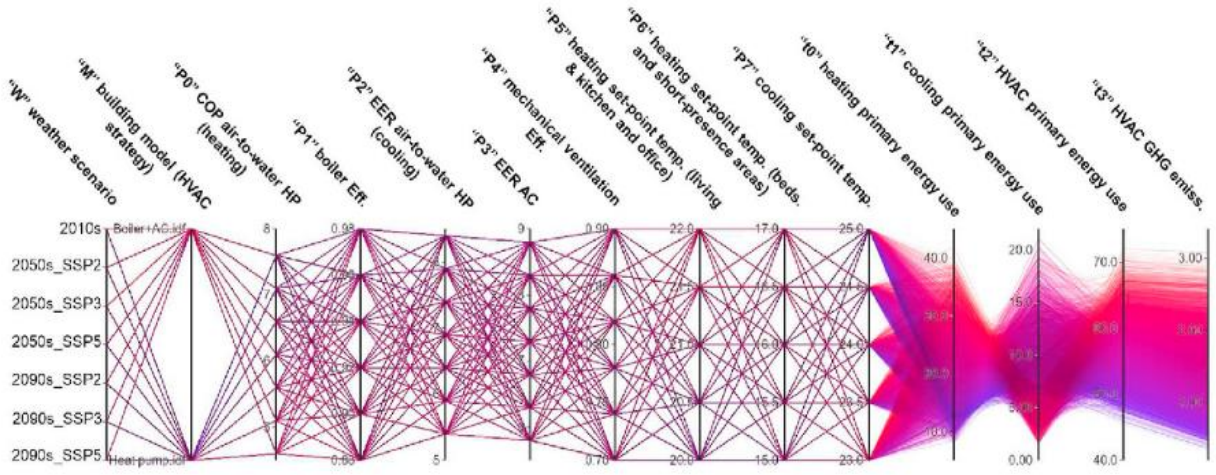

Fig. 9. Parallel coordinates to show the interactions between the input and output parameters in multi-dimensional space of Morris SA (combined case). The lines are colored by HVAC primary energy use.

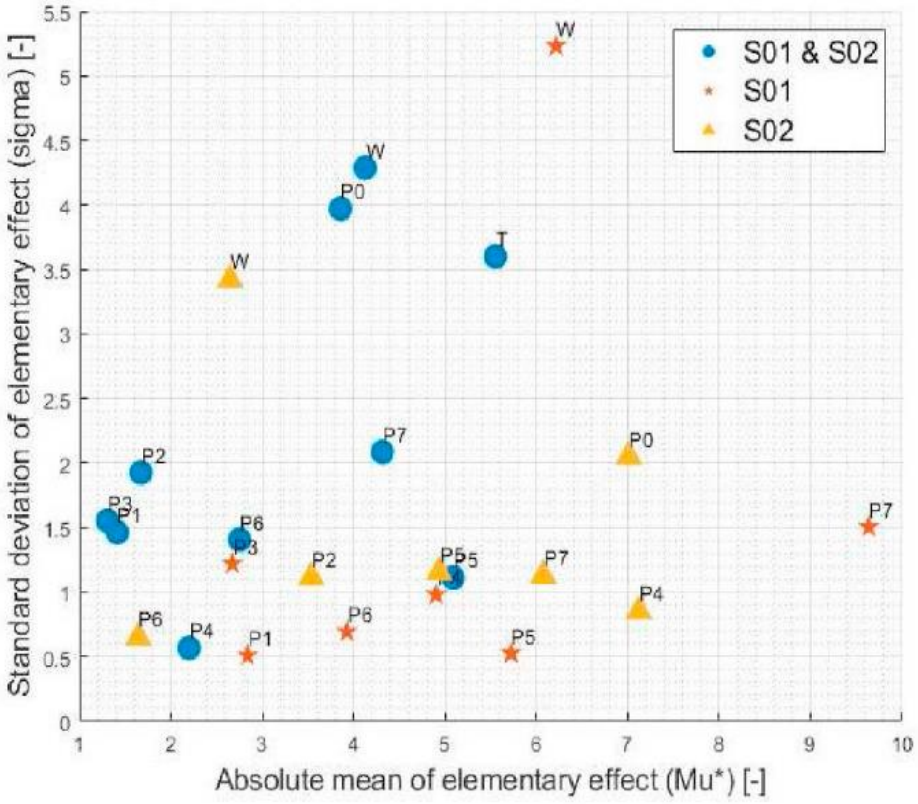

Fig. 10. The Morris sensitivity analysis results, sigma presented by Mu*. The analyses are run for S01 and S02, individually and combined. The output parameter is HVAC primary energy use.

energy use. Table 4 summarizes the input parameters for SA and Morris stats for all cases.

4. Discussion

4.1. Findings and recommendations

According to the Intergovernmental Panel on Climate Change (IPCC), the average global air temperature increased during the past 100 years and will continue to increase due to the release of GHG into the atmosphere. In this paper, the future weather data (MAR BCC-CSM2-MR based on SSP2, SSP3, and SSP5 scenarios) for Brussels city show an increase in the mean annual air temperature ~1.33°C by 2050s and ~2.46°C by 2090s. As shown in Fig. 4, with the continuation of global warming, the cooling seasons will be further extended to the shoulder seasons. The winter seasons will become warmer, and the outdoor air temperatures in the range of ~15°C to ~18°C will be experienced more. Also, the heatwave events can take place more frequently during the cooling season (i.e., in close occasions) which can make the recovery stage [93] for buildings troublesome. Overall, the future trends of outdoor air temperature show that the cooling energy demand in buildings will increase, in addition to the peak cooling loads, whereas the heating energy demand and peak heating loads will decrease.

The results in Fig. 5 show an increase up to ~324% in overheating discomfort and a decrease up to ~28% in overcooling discomfort by 2090s. It means that climate change is negatively correlated with the comfort of hot summer days and positively correlated with the comfort of cold winter days. In addition, the rise of internal gains due to growing

Table 4
Sensitivity analysis input parameters and Morris stats.

	Parameter	Type	[Discrete values]/[Min., Int., Max.]	Num. of values	Mu			Mu*			Sigma		
					S1	S2	S1 & S2	S1	S2	S1 & S2	S1	S2	S1 & S2
W	Weather data	Disc.	[2010s, 2050s_SSP2, 2050s_SSP3, 2050s_SSP5, 2090s_SSP2, 2090s_SSP3, 2090s_SSP5]	7	−6.13	−2.30	−3.72	6.21	2.65	4.12	5.23	3.42	4.28
T	Building model (HVAC strategy)	Disc.	[Reversible heat pump, gas-fired boiler + AC]	2	–	–	−5.26	–	–	5.55	–	–	3.60
P0	HP heating COP	Disc.	[4.6,0.5,7.6]	7	–	−7.01	−3.85	–	7.01	3.85	–	2.05	3.97
P1	Gas-fired boiler eff.	Disc.	[0.88,0.02,0.98]	6	−2.83	–	−1.41	2.83	–	1.41	0.50	–	1.46
P2	HP cooling EER	Disc.	[5.4,0.5,8.4]	7	–	−3.53	−1.67	–	3.53	1.67	–	1.11	1.92
P3	AC cooling EER	Disc.	[5.8,0.5,8.8]	7	−2.67	–	−1.30	2.67	–	1.30	1.22	–	1.55
P4	Fan eff.	Disc.	[0.7,0.04,0.9]	6	−4.90	−7.12	−1.45	4.90	7.12	2.20	0.98	0.85	0.56
P5	Heating Set point (Living & Kitchen and office)	Disc.	[20,0.5,22]	5	5.72	4.93	5.09	5.72	4.93	5.09	0.52	1.15	1.11
P6	Heating set point (Beds. and short- presence areas)	Disc.	[17,0.5,19]	5	3.92	1.64	2.75	3.92	1.64	2.75	0.69	0.65	1.40
P7	Cooling set point	Disc.	[23,0.5,25]	5	−9.63	−6.07	−4.31	9.63	6.07	4.31	1.50	1.13	2.08

occupancy densities, lifting up comfort expectations, and ageing population growth are reported in previous studies [94–96]. The above will increase the use of active cooling technologies to guarantee favourable and safe indoor thermal environments in the future.

As mentioned earlier, buildings in EU have a major share in energy consumption and GHG emissions. Enhancing building energy efficiency thus plays a critical part in reaching the European Green Deal's ambitious objective of carbon neutrality by 2050. Improvements in building design and systems (e.g., high insulation, efficient electricity-based HVAC systems, etc.) may reduce the direct GHG emissions from the buildings, but it shifts the emissions to the electricity or heating production sector. As shown in Section 3.3, the replacement of a gas-fired boiler + AC with a more efficient reversible heat pump can decrease the final energy use of the building. Whereas, by converting the final energy use to the primary energy use, the difference in the primary energy use between both systems becomes very small (due to the high Primary Energy Factor *"PEF"* for electricity). Therefore, to benefit more from the electrification in buildings in reducing the GHG emissions, it is necessary for the electricity sector to, 1) reduce the losses during the conversion and transformation process (e.g., transmission losses, distribution losses, fuel processing, etc.), and 2) move more towards decarbonized or renewable energy.

According to the results, S02 shows 15–27% lower GHG emissions than S01, considering the current electricity supply conditions (i.e., PEF and energy mix) in Belgium. It shows that the transition from fossil fuel-based (e.g., S01) to more efficient and electricity-based (e.g., S02) HVAC systems can assist a country like Belgium in achieving carbon neutrality and helps in the fight against climate change. It is since, in Belgium, the electricity is generated mostly from renewable energy sources such as wind, solar, and hydro as well as nuclear power [97], implying that future increases in electricity use for heating and cooling will have minimal effects on GHG emissions.

To summarize the significant recommendations, the list below is provided:

- To compensate for the rise of cooling demand in buildings because of climate change, it is recommended to consider highly efficient active cooling systems in combination with passive cooling techniques during the construction of new buildings and the renovation of existing ones.
- In the Belgian context, it is recommended to support electricity-based HVAC systems to enhance the carbon neutrality of buildings. This is valid due to the current energy mix for electricity production in Belgium [97]. The generalizability of the idea to other regions needs further provisions.
- It is recommended to further explore the potential of the reversible air-to-water heat pump coupled with a proper ventilation system as promising heating and cooling strategy in buildings.
- It is also recommended to implement *IOhD* and *IOcD* as principal indicators in time-integrated discomfort evaluations. Designers and decision-makers can use these indicators for a multizonal evaluation of time-integrated discomfort under the operation of different HVAC systems.

4.2. Strengths and limitations

The first strength of the study relies on the validity of the weather data used for the simulations. The weather data in this study are based on the MAR model that has a high spatial resolution (~5 km), detailed parameterization (takes into account the mesoscale phenomena), and is tuned for the studied region (i.e., Belgium). The study's strength also relates to the selection of a reference building model that represents nearly zero-energy terraced dwellings in Belgium. The simulation model was developed and calibrated in a previous study by some authors of the current paper [66]. This study also compares two commonly applied HVAC strategies in Belgium (gas-fired boiler + AC and reversible air-to-water heat pump) providing detailed information on the system design and sizing. Another strength of the study relates to the application of Uncertainty Analysis (UA) and Sensitivity Analysis (SA). This allows not only to take into account the uncertainties in the HVAC input parameters but also to find the most influential factors affecting the HVAC primary energy use.

However, the study has some limitations. First, in determining time-integrated discomfort, it is also vital to consider relative humidity and other comfort factors such as clothing insulation, metabolic rate, and air velocity. Within the current study's evaluation paradigm, those criteria are ignored. Second, subjective ranges of uncertainty are defined due to the scarcity of data on future predictions of the parameters characterizing the performance of the selected HVAC systems. Third, the degradation of the HVAC systems over time and their replacement with new technologies are neglected. Fourth, the study assesses only three periods (e.g., 2010s, 2050s, and 2090s) based on three SSPs (SSP2, SSP3, and SSP5), disregarding the intermediate periods (e.g., 2030s, 2040s, 2060s, etc.) or other SSP scenarios (e.g., SSP1-1.9 *"very low GHG emissions"* and SSP1-2.6 *"low GHG emissions"*). Therefore, more accurate studies are suggested to overcome the limitations of this paper.

4.3. Implication on practice and future research

Interpreting the outcomes of the current study implies that future revisions of the building codes and regulations must provide provisions regarding the use of active cooling systems. They must include overheating criteria beyond there is a need for the installation of active cooling systems. The overheating compliance must be achieved not only considering the current climate conditions but also for the standardized future climate predictions. The provisions must also incorporate the maximum allowable limits for cooling energy use in addition to the limits for heating energy use. The study enlightens the building designers and professionals regarding the design for climate change. In heating-dominated regions such as Brussels, the focus is mainly to preserve the heat during the winter season to reduce heating energy use, whereas this study shows that overheating and cooling energy use will become dominant in the future. Therefore, together with the comfort and efficiency standards, prudent building design is a key measure to avoid inefficient and uncomfortable units in the coming decades.

This study reveals some future research ideas. First, future research is recommended to perform the same study and compare the results by implementing the weather data obtained from other sources such as CORDEX, Meteonorm, WeatherShift, and CCWorldWeatherGen. Second, it is recommended for future research to analyze the reference buildings representing other building typologies (detached single-family houses, apartment blocks, etc.). Third, future research is encouraged to evaluate other HVAC technologies with more accurate prospective value ranges characterizing their performance. Fourth, future study is needed to enhance the suggested time-integrated discomfort indices (i.e., *IOcD* and *IOhD*). To better reflect the occupant's thermal experience, the new metrics should incorporate more comfort parameters such as relative humidity, metabolic rate, clothing factor, and air velocity.

5. Conclusion

This paper provides a climate change impact assessment for a nearly Zero-Energy dwelling in terms of time-integrated discomfort, HVAC energy performance, and HVAC GHG emissions. In total, seven weather scenarios are used based on regional climate model (MAR) *"Modèle Atmosphérique Régional"* including, the TMYs for 2001–2020 (2010s), 2041–2060 (2050s: SSP2, SSP3, and SSP5), and 2081–2100 (2090s: SSP2, SSP3, and SSP5). In the first stage, a time-integrated discomfort assessment is carried out on the naturally ventilated base case. In the second stage, two commonly applied HVAC strategies including a gas-fired boiler + an air conditioner (AC) (S01) and a reversible air-to-water heat pump (S02) are compared. It is concluded that.

- based on the climate data resulted from MAR forced by BCC-CSM2-MR Earth System Model (ESM), climate change will decrease *HDD10°C* by 42% and increase *CDD18°C* by 60% averaged over three emission scenarios (i.e., SSP2, SSP3, and SSP5) in Brussels by 2090s. Such variations are expected to shift this region from a heating-dominated to a cooling-dominated one.
- with the continuation of global warming, the overheating risk quantified by Indoor Overheating Degree (IOhD) metric will increase between 154 and 528%, whereas the overcooling risk quantified by Indoor Overcooling Degree (IOcD) metric will decrease between 21 and 32% by the end of this century. It is estimated that the overheating risk may overlap the overcooling risk by 2090s under the high emission scenario (i.e., SSP5).
- by 2090s, the HVAC primary energy use decreases ~7% for S01 and ~4% for S02. For S01, the HVAC GHG emissions decrease 14%, while for S02, a decrease of 3% is predicted by 2090s. Overall, the HVAC GHG emissions for S02 is lower between 15 and 27% than S01 thanks to lower heating primary energy use and carbon emission intensity for electricity than natural gas.
- the most influential parameters on the HVAC primary energy use are, a) heating set-point, cooling set-point, and weather scenario for S01, and b) fan efficiency, heating COP, and cooling set-point for S02. The choice of the HVAC system is the most influential parameter while considering it as an input parameter for the sensitivity analysis. Therefore, the selection of the HVAC system during the early-design stages plays a crucial role in determining the energy efficiency in buildings.

Overall, to reach the EU objective of 55% reduction in emissions by 2030 (Fit for 55), it is necessary to advance in four aspects of, a) embracing the end-user electrification in the residential sector, b) improving the efficiency of the building systems, c) reducing the losses during the conversion and transformation process for electricity production, and d) decarbonization of the electricity sector. For this to happen, the current energy renovation rates [98] and replacement of traditional building systems should be accelerated in parallel to increasing the efficiency and share of renewable energy sources in the electricity sector.

CRediT authorship contribution statement

Ramin Rahif: Writing – original draft, Visualization, Validation, Methodology, Investigation, Formal analysis, Data curation, Conceptualization. **Alireza Norouziasas:** Writing – original draft, Visualization, Investigation. **Essam Elnagar:** Writing – review & editing, Validation, Software. **Sébastien Doutreloup:** Writing – review & editing, Validation, Investigation, Formal analysis, Data curation. **Seyed Mohsen Pourkiaei:** Validation, Formal analysis, Data curation. **Deepak Amaripadath:** Writing – original draft, Formal analysis, Data curation, Conceptualization. **Anne-Claude Romain:** Writing – review & editing, Validation, Conceptualization. **Xavier Fettweis:** Writing – review & editing, Validation, Resources, Data curation. **Shady Attia:** Writing – review & editing, Supervision, Resources, Project administration, Funding acquisition, Conceptualization.

Declaration of competing interest

The authors declare that they have no known competing financial interests or personal relationships that could have appeared to influence the work reported in this paper.

Data availability

Data will be made available on request.

Acknowledgments

This research was funded by the Walloon Region under the call 'Actions de Recherche Concertées 2019 (ARC)' (funding number: ARC 19/23-05) and the project OCCuPANt, on the Impacts Of Climate Change on the indoor environmental and energy PerformAnce of buildiNgs in Belgium during summer. The authors would like to gratefully acknowledge the Walloon Region and the University of Liege for funding. We would like to also acknowledge the Sustainable Building Design (SBD) lab at the Faculty of Applied Sciences at the University of Liege for the use of 64-processor workstation during the computation. This study is a part of the International Energy Agency (IEA) EBC Annex 80 – "Resilient cooling of buildings" project activities to define resilient cooling in residential buildings. We also appreciate the guidance and support provided by Mr. Patrick Van Beeck. No potential competing interest was reported by the authors.

Appendix A

Table A.1 summarizes the envelope and operational characteristics of the reference building used for the current study. The building was constructed in the 1930s and renovated after 2010. It was shifted from D to A grade after the renovation according to the Energy Performance Certificate (EPC) rating scheme.

Table A.1
General description of the case study [66].

Description	Value
Number of floors	3
Total area [m^2]	259
Conditioned area [m^2]	173
Unconditioned area [m^2]	86
Number of occupants	4
Total volume [m^3]	873
Window-wall ratio [%]	19
Window U-value [W/m^2K]	1.2
Window G-value [−]	0.6
Solar Heat Gain Coefficient (SHGC) [−]	0.6
Wall surface absorptance [−]	0.9
External wall U-value [W/m^2K]	0.4
Roof U-value [W/m^2K]	0.3
Ground U-value [W/m^2K]	0.3
Attic floor U-value [W/m^2K]	0.8
Airtightness (50 Pa $m^3/h.m^2$) [ACH]	1.58
Occupancy density [m^2/person]	43
Lighting power density [W/m^2]	8–10
Occupancy, lighting, and equipment schedules	Ref. [66]
Holidays	(Easter) start: 30/03 end: 05/04, total: 7 days (Summer) start: 01/08 end: 155/08, total: 15 days (All saint's day) start: 28/10 end: 05/11, total: 7 days (Christmas) start: 24/12 end: 01/01, total: 7 days

Appendix B

Table B.1 summarizes the minimum, maximum, median, mean, 25% quartile, 75% quartile, and standard deviation for heating, cooling, and HVAC primary energy use as well as HVAC GHG emissions.

Table B.1
Minimum, maximum, median, mean, Q1 (25%), Q3 (75%), and standard deviation of heating, cooling, and HVAC primary energy use, and HVAC GHG emissions for the simulation cases.

	No. cases	Min. heating/ cooling/HVAC/ GHG emiss.	Max. heating/ cooling/HVAC/ GHG emiss.	Med. Heating/ cooling/HVAC/ GHG emiss.	Mean heating/ cooling/HVAC/ GHG emiss.	Q1 (25%) heating/ cooling/HVAC/ GHG emiss.	Q3 (75%) heating/ cooling/HVAC/ GHG emiss.	StdDev. heating/ cooling/HVAC/ GHG emiss.
2010s S01	485	26.61/1.49/ 56.43/2.32	41.97/7.01/ 72.04/3.03	33.94/3.05/ 64.09/2.66	33.97/3.31/ 64.22/2.67	31.49/2.28/62.19/ 2.57	36.37/4.23/66.46/ 2.76	3.25/1.20/2.90/ 0.13
2010s S02	493	14.34/4.47/ 47.61/1.74	32.66/12.52/ 68.93/2.53	21.46/7.48/ 56.16/2.06	21.63/7.56/ 56.88/2.08	18.26/6.12/53.49/ 1.96	24.37/8.84/60.49/ 2.22	3.96/1.68/4.50/ 0.16
2050s SSP2 S01	410	20.27/2.53/ 52.69/2.14	37.05/9.73/ 70.81/2.92	28.72/5.28/ 60.89/2.51	28.49/5.51/ 61.07/2.51	26.56/3.93/58.92/ 2.41	30.18/6.80/63.37/ 2.61	2.72/1.77/3.17/ 0.13
2050s SSP2 S02	503	11.69/5.98/ 46.41/1.70	27.60/15.35/ 66.69/2.44	16.86/9.25/ 53.93/1.97	17.38/9.57/ 54.49/2.00	15.05/7.90/51.40/ 1.88	19.31/10.84/ 57.42/2.10	3.17/2.11/3.93/ 0.14
2050s SSP3 S01	411	19.95/2.63/ 52.11/2.10	35.69/10.32/ 68.43/2.81	26.35/5.31/ 59.18/2.42	26.71/5.50/ 59.41/2.43	24.64/4.21/57.28/ 2.33	28.75/6.51/61.67/ 2.53	2.92/1.68/3.15/ 0.13
2050s SSP3 S02	479	11.41/6.52/ 45.88/1.68	26.65/16.35/ 66.30/2.43	15.68/10.48/ 54.16/1.98	16.35/10.59/ 54.65/2.00	13.99/8.83/51.91/ 1.90	18.48/11.93/ 56.98/2.09	2.99/2.21/3.96/ 0.14
2050s SSP5 S01	465	18.26/3.37/ 51.43/2.07	32.05/11.68/ 67.45/2.75	24.56/6.48/ 58.79/2.40	24.71/6.66/ 58.87/2.39	22.36/5.31/56.74/ 2.30	26.81/7.81/60.97/ 2.49	2.99/1.81/3.11/ 0.13
2050s SSP5 S02	482	10.56/7.31/ 46.81/1.71	24.08/17.17/ 68.77/2.52	15.17/11.24/ 54.24/1.99	15.63/11.35/ 54.29/1.99	13.31/9.43/51.49/ 1.89	17.31/12.81/ 56.84/2.08	2.96/2.30/3.74/ 0.13

(continued on next page)

Table B.1 (*continued*)

	No. cases	Min. heating/ cooling/HVAC/ GHG emiss.	Max. heating/ cooling/HVAC/ GHG emiss.	Med. Heating/ cooling/HVAC/ GHG emiss.	Mean heating/ cooling/HVAC/ GHG emiss.	Q1 (25%) heating/ cooling/HVAC/ GHG emiss.	Q3 (75%) heating/ cooling/HVAC/ GHG emiss.	StdDev. heating/ cooling/HVAC/ GHG emiss.
2090s SSP2 S01	515	19.55/2.89/ 50.63/2.04	34.02/10.62/ 66.79/2.73	25.00/5.60/ 58.43/2.39	25.24/5.82/ 58.49/2.38	23.32/4.43/56.52/ 2.30	26.90/6.93/60.66/ 2.48	2.61/1.72/2.98/ 0.13
2090s SSP2 S02	481	11.24/6.49/ 45.47/1.66	25.37/16.27/ 66.02/2.42	15.90/10.46/ 54.81/2.01	16.29/10.61/ 55.21/2.02	13.93/8.93/51.88/ 1.90	18.37/12.22/ 58.43/2.14	2.88/2.14/4.14/ 0.15
2090s SSP3 S01	509	15.56/4.54/ 50.51/2.01	29.00/14.36/ 64.98/2.62	21.94/7.76/ 57.13/2.29	22.16/8.04/ 57.28/2.31	20.49/6.41/54.96/ 2.21	23.96/9.52/59.43/ 2.40	2.51/2.14/3.19/ 0.13
2090s SSP3 S02	463	9.19/8.86/45.83/ 1.68	20.94/18.03/ 64.19/2.35	13.28/12.90/ 52.47/1.92	13.78/13.04/ 53.30/1.95	11.64/11.32/ 50.79/1.86	15.83/14.63/ 55.90/2.05	2.67/2.24/3.60/ 0.13
2090s SSP5 S01	433	14.93/5.69/ 50.12/1.99	26.79/16.68/ 68.41/2.74	20.43/9.25/ 58.01/2.33	20.62/9.54/ 57.92/2.32	18.98/7.95/55.45/ 2.21	22.42/10.89/ 50.11/2.41	2.47/2.21/3.35/ 0.14
2090s SSP5 S02	470	7.84/9.90/45.96/ 1.68	19.99/21.16/ 65.47/2.40	12.20/15.16/ 54.15/1.98	12.41/15.17/ 54.53/2.00	10.73/13.02/ 51.97/1.90	13.86/17.29/ 57.01/2.09	2.25/2.71/3.64/ 0.13

■ Heating, cooling, and HVAC primary energy use: [kWh/m^2], HVAC GHG emissions: [ton].

References

[1] IPCC WGII core writing team, Summary for Policymakers: Climate Change 2022 - Impacts, Adaptation, and Vulnerability, IPCC Geneva, Switzerland, 2022, p. 7 [Online]. Available: https://www.ipcc.ch/report/ar6/wg2/downloads/report/IPCC_AR6_WGII_FinalDraft_FullReport.pdf. (Accessed 21 June 2022).

[2] M. Santamouris, Innovating to zero the building sector in Europe: minimising the energy consumption, eradication of the energy poverty and mitigating the local climate change, Sol. Energy 128 (2016) 61–94, https://doi.org/10.1016/j.solener.2016.01.021.

[3] M. Santamouris, et al., Urban heat island and overheating characteristics in Sydney, Australia. An analysis of multiyear measurements, Sustainability 9 (5) (2017) 712, https://doi.org/10.3390/su9050712.

[4] S.I. Bohnenstengel, S. Evans, P.A. Clark, S.E. Belcher, Simulations of the London urban heat island, Q. J. R. Meteorol. Soc. 137 (659) (Jul. 2011) 1625–1640, https://doi.org/10.1002/qj.855.

[5] T. Oke, The heat island of the urban boundary layer: characteristics, causes and effects, Wind Clim. Cities (1995) 81–107, https://doi.org/10.1007/978-94-017-3686-2_5.

[6] M. Gustin, R.S. McLeod, K.J. Lomas, Forecasting indoor temperatures during heatwaves using time series models, Build. Environ. 143 (Oct. 2018) 727–739, https://doi.org/10.1016/j.buildenv.2018.07.045.

[7] D.P. Jenkins, V. Ingram, S.A. Simpson, S. Patidar, Methods for assessing domestic overheating for future building regulation compliance, Energy Pol. 56 (May 2013) 684–692, https://doi.org/10.1016/j.enpol.2013.01.030.

[8] R. Rahif, M. Hamdy, S. Homaei, C. Zhang, P. Holzer, S. Attia, Simulation-based framework to evaluate resistivity of cooling strategies in buildings against overheating impact of climate change, Build. Environ. (2022), 108599, https://doi.org/10.1016/j.buildenv.2021.108599.

[9] R. Rahif, A. Fani, S. Attia, Climate change sensitive overheating assessment in dwellings: a case study in Belgium, Bruges, Belgium, in: Proceeding of the International Building Simulation Conference, 2021, pp. 30125–30131 [Online]. Available: http://hdl.handle.net/2268/263260.

[10] M. Hamdy, S. Carlucci, P.-J. Hoes, J.L.M. Hensen, The impact of climate change on the overheating risk in dwellings—a Dutch case study, Build. Environ. 122 (Sep. 2017) 307–323, https://doi.org/10.1016/j.buildenv.2017.06.031.

[11] L. Lan, K. Tsuzuki, Y. Liu, Z. Lian, Thermal environment and sleep quality: a review, Energy Build. 149 (2017) 101–113, https://doi.org/10.1016/j.enbuild.2017.05.043Get.

[12] H. Hooyberghs, S. Verbeke, D. Lauwaet, H. Costa, G. Floater, K. De Ridder, Influence of climate change on summer cooling costs and heat stress in urban office buildings, Clim. Change 144 (4) (Oct. 2017) 721–735, https://doi.org/10.1007/s10584-017-2058-1.

[13] B.G. Armstrong, et al., Association of mortality with high temperatures in a temperate climate: England and Wales, J. Epidemiol. Community Health 65 (4) (Apr. 2011), https://doi.org/10.1136/jech.2009.093161. Art. no. 4.

[14] E.M. Kilbourne, Heat waves and hot environments, Public Health Consequences Disasters 245 (1997) 269.

[15] G. Brücker, Vulnerable populations: lessons learnt from the summer 2003 heat waves in Europe, Euro Surveill. 10 (7) (2005) 1–2, https://doi.org/10.2807/esm.10.07.00551-en.

[16] A. Fouillet, et al., Excess mortality related to the August 2003 heat wave in France, Int. Arch. Occup. Environ. Health 80 (1) (2006) 16–24, https://doi.org/10.1007/s00420-006-0089-4.

[17] H. Johnson, S. Kovats, G. McGregor, J. Stedman, M. Gibbs, H. Walton, The impact of the 2003 heat wave on daily mortality in England and Wales and the use of rapid weekly mortality estimates, Euro Surveill. 10 (7) (2005) 15–16, https://doi.org/10.2807/esm.10.07.00558-en.

[18] J. Garssen, C. Harmsen, J. De Beer, The effect of the summer 2003 heat wave on mortality in The Netherlands, Euro Surveill. 10 (7) (2005) 13SP 557–614, https://doi.org/10.2807/esm.10.07.00557-en.

[19] J.-M. Robine, et al., Death toll exceeded 70,000 in Europe during the summer of 2003, C. R. Biol. 331 (2) (Feb. 2008), https://doi.org/10.1016/j.crvi.2007.12.001. Art. no. 2.

[20] Ansi/Ashrae Standard 55, Standard 55–2020: Thermal Environmental Conditions for Human Occupancy, American Society of Heating, Refrigerating and Air Conditioning Engineers, Atlanta, GA, USA, 2020.

[21] R. Rahif, D. Amaripadath, S. Attia, Review on time-integrated overheating evaluation methods for residential buildings in temperate climates of Europe, Energy Build. 252 (Dec. 2021), 111463, https://doi.org/10.1016/j.enbuild.2021.111463.

[22] R.S. McLeod, M. Swainson, Chronic overheating in low carbon urban developments in a temperate climate, Renew. Sustain. Energy Rev. 74 (Jul. 2017) 201–220, https://doi.org/10.1016/j.rser.2016.09.106.

[23] Iso 15927-4, ISO 15927-4: Hygrothermal Performance of Buildings — Calculation and Presentation of Climatic Data — Part 4: Hourly Data for Assessing the Annual Energy Use for Heating and Cooling, 2005. Geneva, Switzerland.

[24] M. Beshir, J.D. Ramsey, Heat stress indices: a review paper, Int. J. Ind. Ergon. 3 (2) (1988) 89–102.

[25] S. Carlucci, L. Pagliano, A review of indices for the long-term evaluation of the general thermal comfort conditions in buildings, Energy Build. 53 (Oct. 2012) 194–205, https://doi.org/10.1016/j.enbuild.2012.06.015.

[26] S. Carlucci, Thermal Comfort Assessment of Buildings, Springer, 2013, https://doi.org/10.1007/978-88-470-5238-3.

[27] Zero Carbon Hub, Impacts of Overheating: Evidence Review, Zero Carbon Hub, London, England, 2015.

[28] European Commission – Department: Energy, Energy Efficiency in Buildings, Brussels, Belgium, 2020 [Online]. Available: https://ec.europa.eu/info/news/focus-energy-efficiency-buildings-2020-lut-17_en. (Accessed 23 June 2022).

[29] G. Martinopoulos, K.T. Papakostas, A.M. Papadopoulos, A comparative review of heating systems in EU countries, based on efficiency and fuel cost, Renew. Sustain. Energy Rev. 90 (Jul. 2018) 687–699, https://doi.org/10.1016/j.rser.2018.03.060.

[30] É. Mata, J. Wanemark, V.M. Nik, A. Sasic Kalagasidis, Economic feasibility of building retrofitting mitigation potentials: climate change uncertainties for Swedish cities, Appl. Energy 242 (May 2019) 1022–1035, https://doi.org/10.1016/j.apenergy.2019.03.042.

[31] P. Jafarpur, U. Berardi, Effects of climate changes on building energy demand and thermal comfort in Canadian office buildings adopting different temperature setpoints, J. Build. Eng. 42 (Oct. 2021), 102725, https://doi.org/10.1016/j.jobe.2021.102725.

[32] T. Wilbanks, et al., Effects of Climate Change on Energy Production and Use in the United States, *US Dep.* Energy Publ., 2008, p. 12.

[33] H. Radhi, Evaluating the potential impact of global warming on the UAE residential buildings – a contribution to reduce the CO2 emissions, Build. Environ. 44 (12) (Dec. 2009) 2451–2462, https://doi.org/10.1016/j.buildenv.2009.04.006.

[34] S.M. Sajjadian, Performance evaluation of well-insulated versions of contemporary wall systems—a case study of London for a warmer climate, Buildings 7 (1) (2017) 6, https://doi.org/10.3390/buildings7010006.

[35] S. Attia, C. Gobin, Climate change effects on Belgian households: a case study of a nearly zero energy building, Energies 13 (20) (2020) 5357, https://doi.org/10.3390/en13205357.

[36] V. Ciancio, F. Salata, S. Falasca, G. Curci, I. Golasi, P. de Wilde, Energy demands of buildings in the framework of climate change: an investigation across Europe,

Sustain. Cities Soc. 60 (Sep. 2020), 102213, https://doi.org/10.1016/j.scs.2020.102213.
[37] A. Machard, C. Inard, J.-M. Alessandrini, C. Pelé, J. Ribéron, A methodology for assembling future weather files including heatwaves for building thermal simulations from the European coordinated regional downscaling experiment (EURO-CORDEX) climate data, Energies 13 (13) (2020) 3424, https://doi.org/10.3390/en13133424.
[38] A. Sabunas, A. Kanapickas, Estimation of climate change impact on energy consumption in a residential building in Kaunas, Lithuania, using HEED Software, 2017 10-12 May 2017, in: Int. Sci. Conf. "Environmental Clim. Technol vol. 128, *CONECT*, Riga Latv, Sep. 2017, pp. 92–99, https://doi.org/10.1016/j.egypro.2017.09.020.
[39] U.Y.A. Tettey, A. Dodoo, L. Gustavsson, Energy use implications of different design strategies for multi-storey residential buildings under future climates, Energy 138 (Nov. 2017) 846–860, https://doi.org/10.1016/j.energy.2017.07.123.
[40] J. Shen, B. Copertaro, L. Sangelantoni, X. Zhang, H. Suo, X. Guan, An early-stage analysis of climate-adaptive designs for multi-family buildings under future climate scenario: case studies in Rome, Italy and Stockholm, Sweden, J. Build. Eng. 27 (Jan. 2020), 100972, https://doi.org/10.1016/j.jobe.2019.100972.
[41] T. Frank, Climate change impacts on building heating and cooling energy demand in Switzerland, Res. Inspires 125 Years EMPA 37 (11) (Nov. 2005) 1175–1185, https://doi.org/10.1016/j.enbuild.2005.06.019.
[42] L. Pajek, J. Potočnik, M. Košir, The effect of a warming climate on the relevance of passive design measures for heating and cooling of European single-family detached buildings, Energy Build. 261 (Apr. 2022), 111947, https://doi.org/10.1016/j.enbuild.2022.111947.
[43] I. Andrić, A. Pina, P. Ferrão, J. Fournier, B. Lacarrière, O. Le Corre, The impact of climate change on building heat demand in different climate types, Energy Build. 149 (Aug. 2017) 225–234, https://doi.org/10.1016/j.enbuild.2017.05.047.
[44] V. Ciancio, et al., Resilience of a building to future climate conditions in three European cities, Energies 12 (23) (2019) 4506.
[45] T. van Hooff, B. Blocken, H.J.P. Timmermans, J.L.M. Hensen, Analysis of the predicted effect of passive climate adaptation measures on energy demand for cooling and heating in a residential building, Energy 94 (Jan. 2016) 811–820, https://doi.org/10.1016/j.energy.2015.11.036.
[46] A. Moazami, V.M. Nik, S. Carlucci, S. Geving, Impacts of future weather data typology on building energy performance – investigating long-term patterns of climate change and extreme weather conditions, Appl. Energy 238 (Mar. 2019) 696–720, https://doi.org/10.1016/j.apenergy.2019.01.085.
[47] V. Pérez-Andreu, C. Aparicio-Fernández, A. Martínez-Ibernón, J.-L. Vivancos, Impact of climate change on heating and cooling energy demand in a residential building in a Mediterranean climate, Energy 165 (Dec. 2018) 63–74, https://doi.org/10.1016/j.energy.2018.09.015.
[48] R.F. De Masi, A. Gigante, S. Ruggiero, G.P. Vanoli, Impact of weather data and climate change projections in the refurbishment design of residential buildings in cooling dominated climate, Appl. Energy 303 (Dec. 2021), 117584, https://doi.org/10.1016/j.apenergy.2021.117584.
[49] Y. Yang, K. Javanroodi, V.M. Nik, Climate change and energy performance of European residential building stocks – a comprehensive impact assessment using climate big data from the coordinated regional climate downscaling experiment, Appl. Energy 298 (Sep. 2021), 117246, https://doi.org/10.1016/j.apenergy.2021.117246.
[50] V.M. Nik, A. Sasic Kalagasidis, Impact study of the climate change on the energy performance of the building stock in Stockholm considering four climate uncertainties, Build. Environ. 60 (Feb. 2013) 291–304, https://doi.org/10.1016/j.buildenv.2012.11.005.
[51] M. Olonscheck, A. Holsten, J.P. Kropp, Heating and cooling energy demand and related emissions of the German residential building stock under climate change, Energy Pol. 39 (9) (Sep. 2011) 4795–4806, https://doi.org/10.1016/j.enpol.2011.06.041.
[52] K. Jylhä, et al., Energy demand for the heating and cooling of residential houses in Finland in a changing climate, Energy Build. 99 (Jul. 2015) 104–116, https://doi.org/10.1016/j.enbuild.2015.04.001.
[53] D. Mauree, E. Naboni, S. Coccolo, A.T.D. Perera, V.M. Nik, J.-L. Scartezzini, A review of assessment methods for the urban environment and its energy sustainability to guarantee climate adaptation of future cities, Renew. Sustain. Energy Rev. 112 (Sep. 2019) 733–746, https://doi.org/10.1016/j.rser.2019.06.005.
[54] M.C. Peel, B.L. Finlayson, T.A. McMahon, Updated world map of the Köppen-Geiger climate classification, Hydrol. Earth Syst. Sci. 11 (5) (Oct. 2007) 1633–1644, https://doi.org/10.5194/hess-11-1633-2007.
[55] Y. Zhang, L. Jankovic, An interactive optimisation engine for building energy performance simulation, United States, in: Presented at the IBPSA Building Simulation Conference, 2017 [Online]. Available: http://www.ibpsa.org/proceedings/BS2017/BS2017_607.pdf.
[56] S. Doutreloup, et al., Historical and future weather data for dynamic building simulations in Belgium using the regional climate model MAR: typical and extreme meteorological year and heatwaves, Earth Syst. Sci. Data 14 (7) (2022) 3039–3051, https://doi.org/10.5194/essd-14-3039-2022.
[57] X. Fettweis, C. Wyard, S. Doutreloup, A. Belleflamme, Noël 2010 en Belgique: neige en Flandre et pluie en Haute-Ardenne, Bull. Société Géographique Liège 68 (2017) 97–107.
[58] C. Wyard, C. Scholzen, S. Doutreloup, É. Hallot, X. Fettweis, Future evolution of the hydroclimatic conditions favouring floods in the south-east of Belgium by 2100 using a regional climate model, Int. J. Climatol. 41 (1) (2021) 647–662, https://doi.org/10.1002/joc.6642.
[59] S. Doutreloup, C. Wyard, C. Amory, C. Kittel, M. Erpicum, X. Fettweis, Sensitivity to convective schemes on precipitation simulated by the regional climate model MAR over Belgium (1987–2017), Atmosphere 10 (1) (2019) 34, https://doi.org/10.3390/atmos10010034.
[60] K. De Ridder, H. Gallée, Land surface–induced regional climate change in southern Israel, J. Appl. Meteorol. 37 (11) (1998) 1470–1485, https://doi.org/10.1175/1520-0450(1998)037<1470:LSIRCC>2.0.CO;2.
[61] H. Hersbach, et al., The ERA5 global reanalysis, Q. J. R. Meteorol. Soc. 146 (730) (2020) 1999–2049, https://doi.org/10.1002/qj.3803.
[62] V. Eyring, et al., Overview of the coupled model Intercomparison project phase 6 (CMIP6) experimental design and organization, Geosci. Model Dev. (GMD) 9 (5) (2016) 1937–1958, https://doi.org/10.5194/gmd-9-1937-2016.
[63] K. Riahi, et al., The Shared Socioeconomic Pathways and their energy, land use, and greenhouse gas emissions implications: an overview, Global Environ. Change 42 (Jan. 2017) 153–168, https://doi.org/10.1016/j.gloenvcha.2016.05.009.
[64] V. Masson-Delmotte, et al., Climate Change 2021: the Physical Science Basis Contribution of Working Group I to the Sixth Assessment Report of the Intergovernmental Panel on Climate Change, 2021.
[65] C. Zhang, et al., IEA EBC Annex 80 - Dynamic Simulation Guideline for the Performance Testing of Resilient Cooling Strategies, Aaalborg University, Dec. 2021 [Online]. Available: https://hdl.handle.net/2268/266179.
[66] S. Attia, T. Canonge, M. Popineau, M. Cuchet, Developing a benchmark model for renovated, nearly zero-energy, terraced dwellings, Appl. Energy 306 (Jan. 2022), 118128, https://doi.org/10.1016/j.apenergy.2021.118128.
[67] S. Attia, Benchmark model for nearly-zero-energy terraced dwellings, Harvard Dataverse, Cambridge, United States, https://dataverse.harvard.edu/dataset.xhtml?persistentId=doi:10.7910/DVN/GJI84W. (Accessed 29 November 2021).
[68] Iso 18523-2, "ISO 18523-2: Energy Performance of Buildings — Schedule and Condition of Building, Zone and Space Usage for Energy Calculation — Part 2: Residential Buildings, 2017. Geneva, Switzerland.
[69] S. Attia, et al., Framework to Evaluate the Resilience of Different Cooling Technologies, IEA Annex 80 – Resilient Cool. Build., 2021, https://doi.org/10.13140/RG.2.2.24588.13447.
[70] A. Cibse Guide, A. Cibse Guide, Environmetnal Design, Chartered Institution of Building Services Engineers, London, UK, 2015, 2015.
[71] Iso 17772-1, ISO 17772-1: Energy performance of Buildings - Indoor Environmental Quality. Part 1: Indoor Environmental Input Parameters for the Design and Assessment of Energy Performance in Buildings", 2017. Geneva, Switzerland.
[72] Ansi/Ashrae Handbook, Handbook–2017: Fundamentals, American Society of Heating, Refrigerating and Air Conditioning Engineers, Atlanta, GA, USA, 2017.
[73] C. Zhang, et al., Resilient cooling strategies – a critical review and qualitative assessment, Energy Build. 251 (Nov. 2021), 111312, https://doi.org/10.1016/j.enbuild.2021.111312.
[74] M. Stein, Large sample properties of simulations using Latin hypercube sampling, Technometrics 29 (2) (1987) 143–151, https://doi.org/10.1080/00401706.1987.10488205.
[75] F. Domínguez-Muñoz, J.M. Cejudo-López, A. Carrillo-Andrés, Uncertainty in peak cooling load calculations, Energy Build. 42 (7) (Jul. 2010) 1010–1018, https://doi.org/10.1016/j.enbuild.2010.01.013.
[76] M.D. McKay, R.J. Beckman, W.J. Conover, A comparison of three methods for selecting values of input variables in the analysis of output from a computer code, Technometrics 42 (1) (2000) 55–61, https://doi.org/10.1080/00401706.2000.10485979.
[77] J.C. Helton, J.D. Johnson, C.J. Sallaberry, C.B. Storlie, Survey of sampling-based methods for uncertainty and sensitivity analysis, Reliab. Eng. Syst. Saf. 91 (10–11) (2006) 1175–1209, https://doi.org/10.1016/j.ress.2005.11.017.
[78] A. Saltelli, S. Tarantola, F. Campolongo, Sensitivity analysis as an ingredient of modeling, Stat. Sci. (2000) 377–395.
[79] M. Balesdent, L. Brevaul, S. Lacaze, S. Missoum, J. Morio, 8 - methods for high-dimensional and computationally intensive models, in: J. Morio, M. Balesdent (Eds.), Estimation of Rare Event Probabilities in Complex Aerospace and Other Systems, Woodhead Publishing, 2016, pp. 109–136, https://doi.org/10.1016/B978-0-08-100091-5.00008-3.
[80] M.D. Morris, Factorial sampling plans for preliminary computational experiments, Technometrics 33 (2) (1991) 161–174, https://doi.org/10.1080/00401706.1991.10484804.
[81] P. Ekström, R. Broed, Sensitivity Analysis Methods and a Biosphere Test Case Implemented in EIKOS, Posiva Working Report 2006-31, 2006. Tech. rep. Posiva Oy, Eurajoki, Finland.
[82] K. Papakostas, N. Kyriakis, Heating and cooling degree-hours for Athens and Thessaloniki, Greece, Renew. Energy 30 (12) (2005) 1873–1880, https://doi.org/10.1016/j.renene.2004.12.002.
[83] D.J. Sailor, Relating residential and commercial sector electricity loads to climate—evaluating state level sensitivities and vulnerabilities, Energy 26 (7) (Jul. 2001) 645–657, https://doi.org/10.1016/S0360-5442(01)00023-8.
[84] A. Ploskić, Q. Wang, Evaluating the potential of reducing peak heating load of a multi-family house using novel heat recovery system, Appl. Therm. Eng. 130 (Feb. 2018) 1182–1190, https://doi.org/10.1016/j.applthermaleng.2017.11.072.
[85] S. Gilani, W. O'Brien, Natural ventilation usability under climate change in Canada and the United States, Build. Res. Inf. 49 (4) (2021) 367–386, https://doi.org/10.1080/09613218.2020.1760775.
[86] H. Wang, Q. Chen, Impact of climate change heating and cooling energy use in buildings in the United States, Energy Build. 82 (Oct. 2014) 428–436, https://doi.org/10.1016/j.enbuild.2014.07.034.

[87] A.D. Peacock, D.P. Jenkins, D. Kane, Investigating the potential of overheating in UK dwellings as a consequence of extant climate change, Large-Scale Wind Power Electr. Mark. Regul. Pap. 38 (7) (Jul. 2010) 3277–3288, https://doi.org/10.1016/j.enpol.2010.01.021.

[88] R. Gupta, M. Gregg, Using UK climate change projections to adapt existing English homes for a warming climate, Build. Environ. 55 (2012) 20–42, https://doi.org/10.1016/j.buildenv.2012.01.014.

[89] IBGE, Performance Energétique des Bâtiments: Guide des exigences et des procédures de la réglementation Travaux PEB en Région de Bruxelles Capitale, 2017. Brussels, Belgium.

[90] B. Koffi, A. Cerutti, M. Duerr, A. Iancu, A. Kona, G. Janssens-Maenhout, CoM Default Emission Factors for the Member States of the European Union, Eur. Comm. Jt. Res. Cent. JRC, 2017.

[91] F. Campolongo, J. Cariboni, A. Saltelli, W. Schoutens, Enhancing the Morris method, in: Proceedings of the 4th International Conference on Sensitivity Analysis of Model Output, 2005, pp. 369–379. Santa Fe, NM.

[92] S. Bertagnolio, Evidence-based Model Calibration for Efficient Building Energy Services, University of Liege, Belgium, 2012 [Online]. Available: http://hdl.handle.net/2268/125650.

[93] S. Attia, et al., Resilient cooling of buildings to protect against heat waves and power outages: key concepts and definition, Energy Build. 239 (May 2021), 110869, https://doi.org/10.1016/j.enbuild.2021.110869.

[94] W. Luan, X. Li, Rapid urbanization and its driving mechanism in the Pan-Third Pole region, Sci. Total Environ. 750 (Jan. 2021), 141270, https://doi.org/10.1016/j.scitotenv.2020.141270.

[95] M. Luo, et al., The dynamics of thermal comfort expectations: the problem, challenge and impication, Build. Environ. 95 (Jan. 2016) 322–329, https://doi.org/10.1016/j.buildenv.2015.07.015.

[96] United Nations, World Population Prospects, 2017 Revision; 2017, U. N. N. Y., 2014.

[97] International Energy Agency (IEA), Data &statistics [Online]. Available: https://www.iea.org/countries/belgium, 2020. (Accessed 28 June 2022).

[98] European Commission, A renovation wave for Europe—greening our buildings, creating jobs, improving lives, Commun. Comm. Eur. Parliam. Counc. Eur. Econ. Soc. Comm. Comm. Reg 662 (2020) 1–26.

Appendix G

Chapter 7: *Overheating analysis of optimized nearly Zero-Energy dwelling during current and future heatwaves coincided with cooling system outage*

Energy & Buildings 287 (2023) 112998

Contents lists available at ScienceDirect

Energy & Buildings

journal homepage: www.elsevier.com/locate/enb

Overheating analysis of optimized nearly Zero-Energy dwelling during current and future heatwaves coincided with cooling system outage

Ramin Rahif [a,*], Mostafa Kazemi [b], Shady Attia [a]

[a] Sustainable Building Design Lab, Dept. UEE, Faculty of Applied Sciences, University of Liège, Belgium
[b] GeMMe Building Materials, Department of Urban and Environmental Engineering (UEE), Faculty of Applied Sciences, University of Liège, 4000, Liège, Belgium

ARTICLE INFO

Article history:
Received 24 November 2022
Revised 8 March 2023
Accepted 14 March 2023
Available online 18 March 2023

Keywords:
Climate change
Optimization
Residential building
Thermal comfort
HVAC
Final energy use

ABSTRACT

It is expected that heatwaves will strike more frequently and with higher temperatures with the continuation of global warming. More extreme heatwaves concurrent with disruptions in the cooling system can lead to significant overheating problems in buildings affecting occupants' health, productivity, and comfort. This paper projects current and future heatwaves on an optimized nearly Zero-Energy terraced dwelling in Brussels, assuming the outage of the cooling system. Initially, a multi-objective optimization is performed considering 13 passive design strategies using the Genetic Algorithm (GA) based on the Non-dominated Sorting Genetic Algorithm 2 (NSGA-II) method. It is found that high ventilation rate, low infiltration rate, high insulation, high thermal mass, integration of green roof, and application of operable roller blinds are beneficial in reducing the final HVAC energy use up to 32% and enhancing thermal comfort up to 46%. Subsequently, three optimal solutions are selected and analyzed under the highest maximal temperature heatwaves detected during the 2001–2020, 2041–2060, and 2081–2100 periods. It is found that non of the optimal solutions are able to fully suppress overheating during heatwaves and the cooling system outage. The indoor operative temperatures reach more than 29 °C, which can cause serious health issues for the occupants. The situation will be exacerbated in the future since an increase in maximum Heat Index (HI) between 0.28 °C and 0.49 °C, an increase in the maximum operative temperature between 1.34 °C and 2.33 °C, and a decrease in Thermal Autonomy (TA) between 17% and 28% are estimated. Finally, some recommendations are provided for practice and future research.

1. Introduction

1.1. Background

Climate change is the long-term shift in weather patterns due to natural causes (e.g., variations in solar cycles) or human activities (mainly due to the use of fossil fuels). The Intergovernmental Panel on Climate Change (IPCC) Sixth Assessment Report (AR6) [1] predicted that the average global surface temperature will increase between 1 and 5.7 °C by the end of the century. Similarly, the European Environment Agency (EEA) foresees an increase in average air temperature between 2.5 °C and 4 °C by 2071–2100 over Europe. The situation will be worse in cities due to the Urban Heat Island (UHI) effect. According to [2,3], the ambient temperature in cities is 5 °C-10 °C higher compared to the surrounding areas. This undesirable warming can exacerbate existing problems in large cities, such as water scarcity, air pollution, and heatwaves.

Although there is no commonly accepted definition of heatwaves, they are understood to be a period of sweltering weather that can or cannot be accompanied by high humidity levels, usually with an obvious effect on humans or natural systems [4]. Heatwaves usually happen due to the trapped air in a specific region that can last for two or more days during the hot season. As climate change continues to raise global temperatures, the heatwaves start earlier in some places around the world [5]. It is also found that with the continuation of global warming, future heatwaves will tend to be longer and more severe [6]. In late June and July 2019, most European countries experienced consecutive days above 30 °C, and some countries, such as Belgium, France, Germany, the Netherlands, and the UK, set a new all-time high [7]. Such extreme heatwave events can lead to water shortages, blackouts, and overheating problems in buildings [8].

Overheating or accumulation of heat in buildings forfeits occupants' productivity, comfort, and health, which in severe cases can lead to heat exhaustion, dehydration, and heat stroke [9,10]. According to the UK Housing Health and Safety Rating System (HHSRS), indoor temperatures above 25 °C can increase mortality

* Corresponding author.
E-mail address: ramin.rahif@uliege.be (R. Rahif).

https://doi.org/10.1016/j.enbuild.2023.112998
0378-7788/

rates [11]. Over 2500 excess deaths were reported across Europe during the summer 2019 heatwaves [12], of which 716 died in Belgium [13], 1435 in France [14], 400 in the Netherlands [15], 900 in the UK [16], and 500 in Germany [17]. It is urged to optimize and enhance the thermal performance of buildings so that they act as a shelter and keep the occupants safe during hot weather conditions.

Optimization is the procedure of making a design or a system perform as perfectly or most effectively as possible [18]. In other words, it is the process of identifying designs that minimize or maximize a specific goal. Simulation-based optimization is undoubtedly a great approach to reach many design targets, opening a new era for building designers and modellers. Several simulation programs have been introduced in recent decades to perform building optimization, such as DesignBuilder, BuildSimHub, jEPlus + EA, Autodesk Insight, etc. It should be noted that the aim of optimization in Building Performance Simulation (BPS) is not necessarily to find globally optimal solutions to a problem due to the limitations of the simulation program itself [19] or the nature of the problem [20]. The optimization methods and their applications are extensively reviewed in some previous studies [18,20–23].

1.2. Literature review

Several studies have been conducted to optimize the energy efficiency and thermal comfort of buildings in different regions by considering various input factors and employing metaheuristic algorithms. These studies have demonstrated promising results in terms of reducing energy consumption and improving thermal comfort. Chegari et al. [24] optimized a two-floor residential unit in Morocco by considering thermo-physical parameters of the building envelope as the input factor. They aimed at minimizing the computation time via the integration of Artificial Neural Networks (ANN) coupled with multiple metaheuristic algorithms such as Multi-Objective Particle Swarm Optimization (MOPSO), Multi-Objective Genetic Algorithm (MOGA), and Non-dominated Sorting Genetic Algorithm 2 (NSGA-II). They found that the coupling between ANN and MOPSO has the greatest desired performance among others by reducing the total heating and cooling thermal needs by 74.52% while enhancing the indoor thermal comfort (quantified by degree-hours *"Dh"*) by 4.32%. Vukadinović et al. [25] discussed a performed optimization for a detached passive house building in Serbia based on the NSGA-II method. The optimization variables include the parameters of the passive solar design, such as glazing type, window shading, wall construction, and the window-to-wall ratio of each façade individually. Prior to optimization, a sensitivity analysis is conducted using the Latin hypercube Sampling (LHS) method to identify the most influential variables affecting the optimization objectives: heating energy use, cooling energy use, and thermal comfort (quantified by discomfort hours *"DH"*). They found that low-emissivity glazing, high thermal capacity and insulation levels for the opaque elements, and no/smallest shading for south facing façade are beneficial in achieving optimal thermal comfort and heating energy performance. Bre et al. [26] carried out a multi-objective optimization to improve energy efficiency and thermal comfort in a single-family house in Argentina. They used a novel metamodel-based approach by dynamic coupling between NSGA-II and ANN metamodels, which were trained previously by the results of building performance simulations. In total, 12 discrete and categorial design variables, such as shading dimension, solar absorptance, window type, roof type, and external/internal wall type, are considered input factors. It was claimed that the presented method is able to reduce the number of simulations by up to 75% without affecting the accuracy of the results. In addition to the abovementioned studies, some other similar studies exist [27–33] that are analyzed in Table 1 based on four criteria (i.e., multi-objective, multizonal modeling, reference case study, and comprehensive or specific input factors). It is clear that, except [26] conducted for a case study in a hot and humid climate, other reviewed studies either do not have a comprehensive approach to selecting the input factors for the optimization (i.e., they focus on specific elements such as HVAC control parameters, solar design parameters, etc.) or fail to fulfill at least one of the specified criteria.

Numerous studies have examined the risk of overheating and indoor thermal comfort in different types of buildings during heatwaves, with some focusing on specific regions and employing different analysis methods. Ozarisoy [34] studied thermal comfort conditions in a prototype terraced building located in Watford, UK, from May to September 2018. It was found that indoor operative temperatures remain relatively high during the heatwaves, ranging from 26.5 °C to 32.5 °C. The situation is worse in the bedrooms on the first floor, where indoor operative temperatures exceed EN 15251 Category II upper limit for 15% of the hours. Laouadi et el. [35] assessed overheating risk in a typical detached house (assuming old and current construction practice) located in Ontario, Canada, during the extreme heatwave from 5th to 11th July 2010. They applied the CIBSE TM52 [36], Passive House

Table 1
Summary of some studies that optimized thermal comfort in residential buildings.

Author(s)	Country	Case study	Optimization method	Features			
				Multi-objective	Multizonal modeling	Reference case study	Comprehensive (C) or Specific (S) input factors
Chegari et al. (2021) [24]	Morocco	Two-floor residential unit	ANN coupled to MOPSO, MOGA, and NSGA-II	✓	✓	✓	S (envelope thermo-physical parameters)
Vukadinović et al. (2021) [25]	Serbia	Detached passive house	NSGA-II	✓	✓	×	S (Passive solar design factors)
Ebrahimi-Moghadam et al. (2020) [45]	Iran	Residential tower	GA(1)	✓	✓	×	S (light shelves)
Bre et al. (2020) [26]	Argentina	Single-family house	ANN coupled to NSGA-II	✓	✓	✓	C
Gou et al. (2018) [27]	China	Apartment building	ANN coupled to NSGA-II	✓	✓	×	C
Li et al. (2017) [28]	China	Simple model & typical residential unit	Proposed method, GenOpt®, and ANN	✓	✓	×	C
Ascione et al. (2015) [29]	Turkey & Italy	Six-story residential building	MPC(2)	✓	✓	✓	S (HVAC system control parameters)
Yu et al. (2015) [31]	China	Three-story typical residential building	ANN coupled to NSGA-II	✓	×	✓	C

(1) **GA:** Genetic Algorithm,
(2) **MPC:** Model Predictive Control

Institute (PHI) [37], and heat stress (using transient Standard Effective Temperature "t-SET" index) methods to analyze overheating considering four different passive measures (combination of interior and exterior solar shadings with window opening). The results showed that naturally ventilated buildings cannot fully satisfy the overheating criteria during the heatwaves according to the abovementioned methods. It was also found that older and leakier houses are less prone to overheating than highly-insulated and airtight buildings. Zhou et al. [38] analyzed overheating risk in a room (dimensions: 5 m × 3 m × 2.5 m) of a residential unit located in Zurich, Switzerland, during the heatwave from 24th July to 9th August 2018. Four different orientations (north, south, east, and west) are assumed for the test room, and 26.5 °C is set as the overheating threshold. The results showed 51.3%, 44.3%, 51.3%, and 35.7% hours of exceedance during the heatwave for east, south, west, and north-facing orientations, respectively, where indoor operative temperature and relative humidity reach up to 27.8 °C and 60.9%, respectively. In addition to the abovementioned studies, some other similar studies exist [39–44] that are analyzed in Table 2. Among the reviewed studies, only [41] incorporates future heatwaves in the analysis; however, only comfort indices are used for overheating evaluations. Other studies neglect climate change scenarios and fail to picture future overheating incidents under more severe heatwaves.

1.3. Knowledge gap, aim, and research questions

Despite several studies on building optimization and thermal comfort analysis during heatwave events, there is relatively less research that couples both. Most studies perform optimization to find the best combinations of passive design strategies but do not proceed with the evaluation of optimal solutions under extreme events. In addition, most studies dealing with overheating risk during heatwave events are performed for passive houses or assume that the cooling system is running without any disruption in air-conditioned ones. The latter is not the case in reality due to probable failure in the cooling system. In addition, very limited studies incorporate climate change scenarios to forecast the impact of aggravating heatwaves on overheating risks in buildings. Therefore, as members of the International Energy Agency (IEA) EBC Annex 80 – "Resilient cooling of buildings" project, we carried out this research to address the abovementioned knowledge gap inspired by the frameworks and guidelines developed within the project [46–48]. This research aims to broaden the knowledge on overheating risk evaluations in high-performance residential buildings during critical conditions in the context of climate change. The research questions are:

- Q1: What will be the changes in outdoor weather conditions assuming a plausible scenario for climate change in Brussels?
- Q2: How to optimize the building for final HVAC energy use and thermal comfort using passive design strategies?
- Q3: How will optimal solutions perform in current and future heatwave scenarios coinciding with the outage of the cooling system?

1.4. Paper contribution

This study contributes to the new body of knowledge from an international perspective by performing multi-objective optimization and overheating analysis for a case study in a temperate oceanic climate (Cfb) according to the Köppen-Geiger-Peel climate classification. Such a climate is particularly dominant in Western Europe, in addition to some other major cities around the world, such as Vancouver, Auckland, Canberra, Nairobi, etc. The results and findings can be generalized to those cities with some provisions. It should be mentioned that the applicability range of the results and findings of the current study is limited to the temperate

Table 2
Summary of some studies that analyzed overheating in residential buildings during heatwaves using multiple indices.

Author(s)	Country	Case study	Indices	Features			
				Climate change	Short-term (S) or Long-term (L) heatwaves	Static (S) or Adaptive (A) comfort model	Heat stress (H) or Comfort (C) indices
Ozarisoy (2022) [34]	UK	Three-story terraced building	Indoor Operative Temperature (IOpT), Relative Humidity (RH), & Percentage of Exceedance Hours (% EH)	×	L	S & A	C
Laouadi et al. (2020) [35]	Canada	Typical detached home	Percentage of Exceedance Hours (% EH), Degree Hours (DH), Daily Weighted Exceedance (DWE), & transient Standard Effective Temperature (t-SET)	×	S	S & A	H & C
Zhou et al. (2020) [38]	Switzerland	A room in a residential building	Indoor Operative Temperature (IOpT), Relative Humidity (RH), Heat Index (HI) & Percentage of Exceedance Hours (%EH)	×	L	S	H & C
Kwok et al. (2017) [39]	Hong Kong	Four types of public rental housing	Air Temperature (AT), Standard Predicted Mean Vote (SPMV), Adjusted Predicted Mean Vote (APMV), & Percentage of Exceedance Hours (%EH)	×	L	S & A	C
Porritt et al. (2012) [40]	UK	A row of three terraced house	Indoor Operative Temperature (IOpT) & Degree Hours (DH)	×	L	S	C
Sakka et al. (2012) [42]	Greece	Apartments & detached houses	Air Temperature (AT) & Percentage of Exceedance Hours (%EH)	×	S & L	S	C
Porritt et al. (2011) [41]	UK	A row of three terraced house	Air Temperature (AT), Degree Hours (DH), & peak occupied operative temperature reduction	✓	S	S	C

oceanic climate; therefore, similar studies must be conducted to achieve valid and reliable results concerning other climates. In addition, this paper considers a wide range of passive design strategies as input factors for the optimization of a benchmark nearly Zero-Energy terraced building in Belgium. The findings are representative and can be extended to other buildings in the same typology to enhance energy efficiency and thermal comfort. Furthermore, this paper performs overheating analysis under current and future heatwaves and provides a clear picture of climate change impact assessment in buildings that are being built according to the current legislation in Belgium. Last but not least, this paper analyzes overheating during heatwaves coinciding with the cooling system outage shedding light on the importance of building thermal analysis under abnormal conditions.

2. Methodology

Fig. 1 shows the Study Conceptual Framework (SCF) adopted for the current study. The methodology consists of two main stages. In the first stage, a multi-objective optimization is performed to minimize the final HVAC energy use and thermal comfort, considering 13 passive design strategies. Three optimal solutions are then selected on the resulting Pareto front to proceed with the second stage. In the second stage, the simulations are performed for the selected optimal solutions during the short-term heatwave events assuming the outage of the cooling system.

DesignBuilder v7.0.0 software is used in both stages, which is a Graphical User Interface (GUI) for the EnergyPlus simulation engine. EnergyPlus, developed by the U.S. Department of Energy

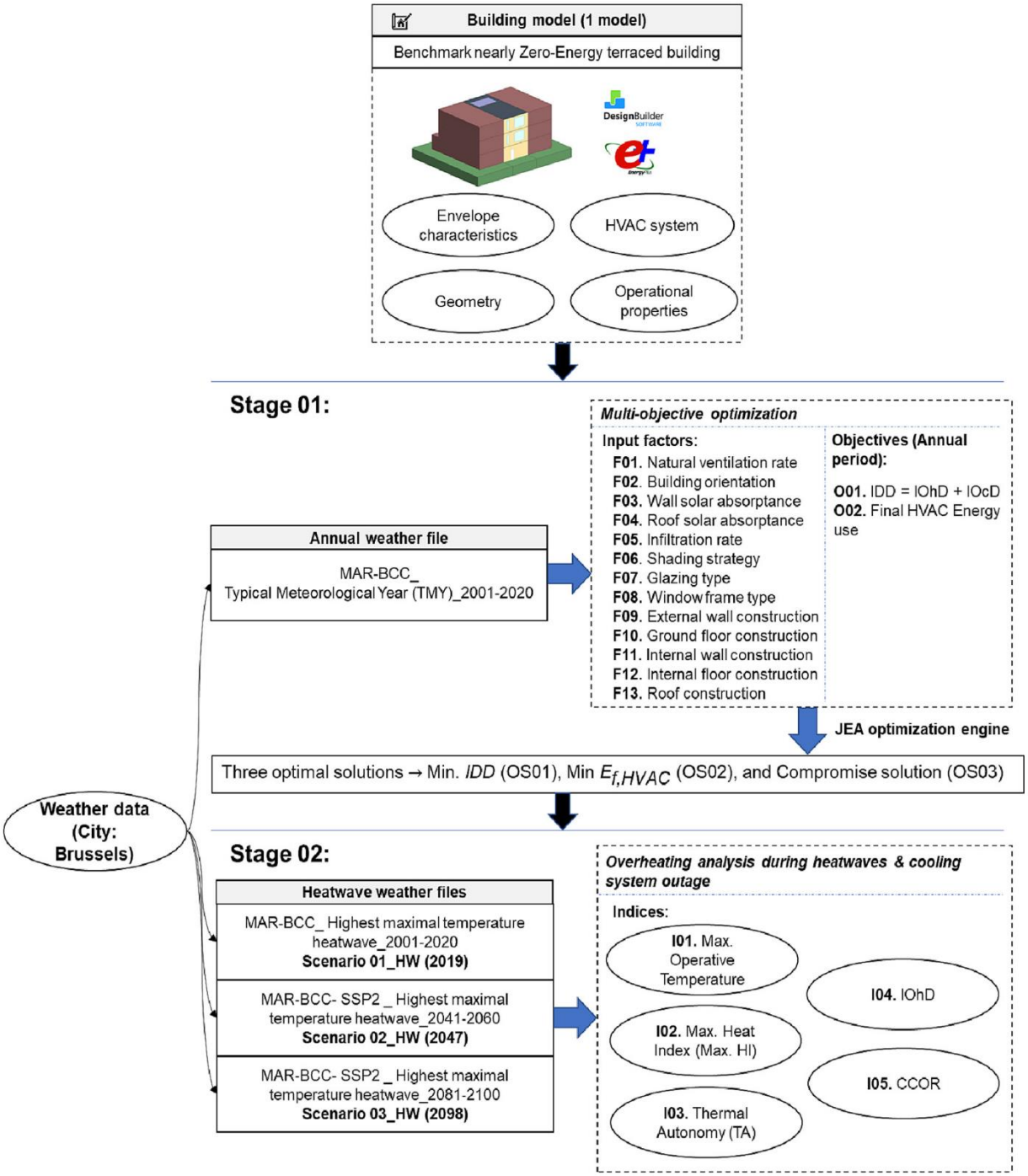

Fig. 1. Study Conceptual Framework (SCF).

(U.S. DOE), is accounted as one of the twenty major energy simulation programs [49], in which the simulation results are in close agreement with other well-known tools such as ESP-r, TRNSYS, DOE-2.1E, and IDA-ICE. DesignBuilder is validated based on a procedure specified by ANSI/ASHRAE 140, *"Method of Test for Evaluating Building Performance Simulation Software"* [50]. DesignBuilder uses Genetic Algorithm (GA) for optimization based on the Non-dominated Sorting Genetic Algorithm 2 (NSGA-II) method. NSGA-II method provides a feasible trade-off between a well-converged and well-distributed set of solutions and is highly effective in classifying the competing objectives. In this study, a combination of Energy Management System (EMS) and Python codes is also used to implement all the desired input variables for optimization. In total, over 4100 simulations are run in 48 h using a workstation with CPU: AMD 3990X – 64 × 2.9 GHz, Cache: 256 MB, RAM: 64 GB, and Graphics card: 24 GB (2 × 32 GB). The post-processing and visualizations are done using the CBE Clima tool [51] and a homemade MATLAB script [52].

2.1. Boundary conditions

This section is allocated to explain the boundary conditions of the current study. First, the focus is restricted to a case study located in a temperate oceanic climate (Cfb). Such a climate generally has cool summers and mild winters, with a relatively low-temperature gradient between different seasons. In Cfb climate regions, the Heating Degree Days (HDD) overlap the Cooling Degree Days (CDD); therefore, they are recognized as heating-dominated regions. In such regions, the building design concept is more on heat preservation during the cold seasons to reduce heating energy consumption. This results in highly insulated and airtight buildings that are more prone to overheating during the summer [53,54].

The second boundary condition assumed for this paper relies on the selection of single building typology representing the nearly Zero-Energy terraced dwellings in Belgium. This is because (i) newly built/renovated Passive house complying buildings are at a higher risk of overheating compared to less insulated old buildings [55–57], (ii) people spend most of their time at home [58], especially after the COVID pandemic and the rising tendency toward remote working [59], and (iii) overheating during the sleeping period at homes is identified as a critical risk for the occupants' health [60,61].

2.2. Building model

This paper selects a benchmark terraced dwelling in Belgium as the case study based on the work of [62]. The building is located in Woluwe-Saint-Lambert municipality in Brussels. As shown in Fig. 2, it was constructed in three floors and renovated in 2010 to comply with the nearly Zero-Energy Building (nZEB) requirements. The envelope was externally insulated during the renovation, and photovoltaic panels were added to the roof for on-site electricity generation of 3000 kWh/year. The multizonal building model includes the conditioned zones categorized as (i) living areas (living room and open kitchen as one zone), (ii) office room, (iii) bedrooms, and (iv) short-presence areas (two corridors, two bathrooms, one WC) [63].

Table 3 provides an overview of the general building's characteristics. The building has a total area of 259 m^2 and is occupied by a four-member family (two adults and two children). The occupancy schedules are derived differently for weekdays and weekends from ISO 18253–2 [33]. The lighting power density of 8 W/m^2 for the bedrooms and 10 W/m^2 for other zones are set based on the data collected from the surveys. The lighting densities are adjusted for the winter season and validated using the reports published by IP Belgium and the Flemish Energy Agency (FEA). The building model in this paper is obtained from [63], which has been checked against the public statistics and verified through model calibration and utility bill comparison between 2015 and 2019.

In its original mode, the building is naturally ventilated and heated by a gas-fired boiler coupled with water radiators. In addition, a mechanical ventilation system with heat recovery operates to provide a minimum fresh air of 25 m3/h during the occupied hours according to the Belgian norm NBN D50-001. Based on the findings of [64,65], this paper replaces the gas-fired boiler with a reversible air-to-water heat pump to provide heating and cooling along with natural ventilation (mixed-mode). The set-point temperatures for heating and cooling modes and the minimum and maximum indoor temperatures for natural ventilation are listed in Table 3. The HVAC components' design flow rates and thermal capacities are auto-sized by EnergyPlus based on the building configuration and external weather conditions using the ASHRAE siz-

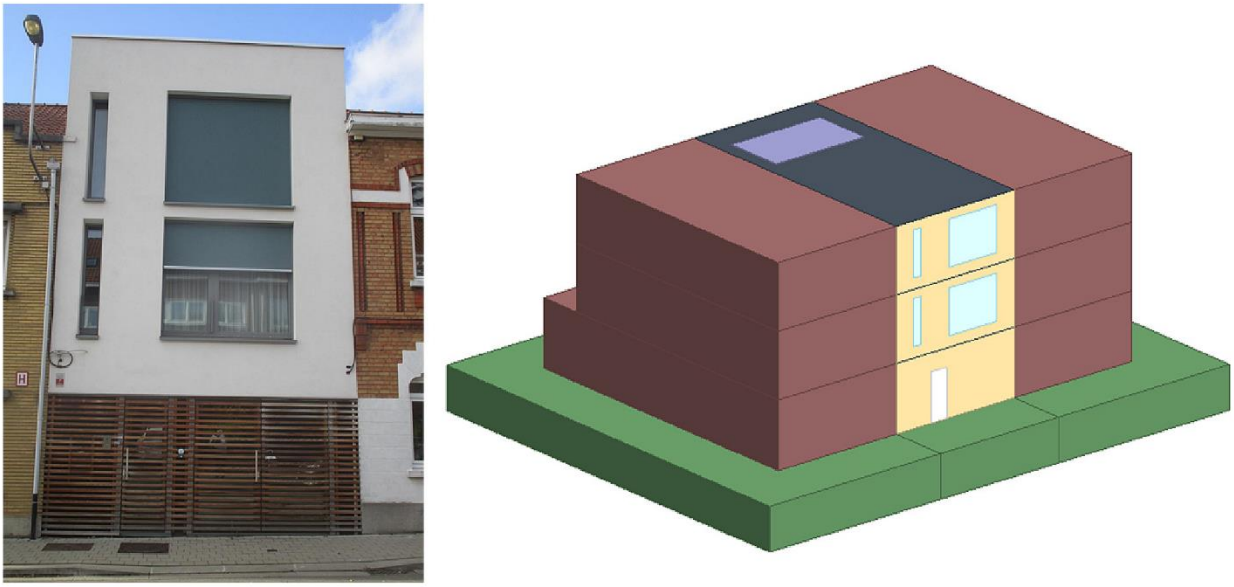

Fig. 2. The benchmark nearly Zero-Energy terraced dwelling in Belgium: (left) south-facing façade and (right) DesignBuilder simulation model.

Table 3
General description of the case study's construction, operational, and HVAC characteristics derived from [62,64].

Description	Value
Number of floors	3
Total area [m^2]	259
Conditioned area [m^2]	173
Unconditioned area [m^2]	86
Number of occupants	4
Total volume [m^3]	873
Window-wall ratio [%]	19
Occupancy density [m^2/person]	43
Occupancy, lighting, and equipment schedules	Ref. [62]
Lighting power density [W/m^2]	8 (bedrooms) & 10 (other zones)
Holidays	(Easter) start: 30/03 end: 05/04, total: 7 days (Summer) start: 01/08 end: 155/08, total: 15 days (All saint's day) start: 28/10 end: 05/11, total: 7 days (Christmas) start: 24/12 end: 01/01, total: 7 days
HVAC System type	Reversible air-to-water heat pump + mechanical ventilation
Heated and cooled zones	Heated: Living & kitchen, office, bedroom 01, bedroom 02, bedroom 03, corridors, WC, bathroom 01, and bathroom 02; Cooled: Living & kitchen, office, bedroom 01, bedroom 02, and bedroom 03
HVAC schedule	– occupancy schedules in Ref. [62]
Heating and cooling capacities [W]	Auto-sized to design days
Heating and cooling schedules [h]	Occupied hours
Set-point temperatures [°C]	21 °C for heating (living & kitchen, and office); 18 °C for heating (bedrooms and short-presence areas, e.g., corridors, bathrooms, and WC); 24 °C for cooling (all areas)
Maximum indoor temperature for natural ventilation [°C]	23.5 °C for all areas
Minimum indoor temperature for natural ventilation [°C]	21.5 °C for living & kitchen and office; 19 °C for bedrooms and short-presence areas, e.g., corridors, bathrooms, and WC
Minimum ventilation rate [m^3/h]	25

ing method [66]. The auto-sizing feature sizes the HVAC components in a way to fulfil the heating/cooling loads for all periods except for more extreme conditions than the design days (i.e., there is still a chance of overcooling/overheating in the building). In line with the authors' previous works [47,64], the availability schedule of the HVAC system is considered identical to the occupancy schedules defined in [62].

2.3. Climate data

Obtaining high-quality and detailed climate data is crucial in any study related to climate change and adaptation decisions [67]. The current study uses climate data based on the General Circulation Model (GCM) outputs. GCM outputs are not directly applicable to building simulations due to their high spatial and temporal resolution. They should be transformed using statistical or dynamical downscaling techniques in order to generate compatible weather data. For this aim, a dynamical downscaling technique called the Regional Climate Model (MAR) *"Modèle Atmosphérique Régional"* (in version 3.11.14) [68] was used to generate the weather data in this paper. MAR is calculated by coupling a three-dimensional atmospheric model to a one-dimensional transfer scheme between the surface, vegetation, and atmosphere [69]. MAR results in physically consistent climate parameters and extreme weather events and is widely adapted for Belgium [70,71].

Two different methods were used to ensure the validity of future weather data:

- **MAR ERA5:** In this method, MAR was initially forced every 6 h by its lateral boundaries (temperature, specific humidity, and etc.) based on the reanalysis ERA5 [72] assimilated by different sources of observation between 1980 and 2014. The sources of observation were in-situ weather stations, satellites, etc. Therefore, MAR ERA5 is assumed to be the reconstruction of the observed climate data.
- **MAR BCC-CSM2-MR:** In this method, MAR was forced based on the Earth System Model (ESM) BCC-CSM2-ME (mean temperature of all ESMs up to 2100 over Belgium) from the 6th Coupled Model Intercomparison Project (CMIP6). CMIP6 characterizes the average evolution of climate parameters between 1980 and 2014 based on observations and 2015–2100 based on Shared Socioeconomic Pathway (SSP) scenarios [73]. SSPs are used to project the Green House Gas (GHG) emission scenarios based on global socioeconomic evolution by 2100. In other words, they quantify the GHG emissions under different global climate policies. In total, there are five SSPs, i) SSP1-1.9 – CO_2 -emissions cut to net zero around 2050 (1.4 °C estimated global warming by 2100), ii) SSP1-2.6 – CO_2 emissions cut to net zero around 2075 (1.8 °C estimated global warming by 2100), iii) SSP2-4.5 – CO_2 emissions around current levels until 2050, then falling but not reaching net zero by 2100 (2.7 °C estimated global warming by 2100), iv) SSP3-7.0 – CO_2 emissions double by 2100 (3.6 °C estimated global warming by 2100), and v) SSP5-8.5 – CO_2 emissions triple by 2075 (4.4 °C estimated global warming by 2100) [74,75]. In this paper, the SSP2-4.5 scenario is selected, which is the most plausible scenario according to [76], in which the evaluation of 1184 IPCC AR5 [77] and 127 IPCC AR6 [1,74] scenarios are compared to observations over 2005–2020 [78] and projections to 2021–2050 from the International Energy Agency's (IEA) 2021 World Energy Outlook (WEO) [79]. From the perspective of the IPCC scenarios, it is evident from [76] that the globe is not now very far off the Fossil Fuel and Industry (FFI) emission trajectory envisioned in IPCC scenarios to be consistent with meeting 2 °C policy goals and all plausible scenarios fall between 2 °C and 3 °C by 2100 (global warming estimation in SSP2-4.5). This is also in line with the IPCC AR6 [1], which recently determined that mid-range scenarios (e.g., SSP2-4.5) are more likely and high-emission scenarios (e.g., SSP5-8.5) have a low likelihood.

MAR BCC-CSM2-MR was validated using the results of MAR ERA5 to confirm whether it can be used to calculate future climate data [68].

This paper uses the annual weather data for the optimization stage based on the protocol defined by ISO 15927–4 [80]. Accordingly, the Typical Meteorological Year (TMY) is used for the period 2001–2020 based on the outcomes of MAR BCC-CSM2-MR. TMYs are widely used by building designers and modelers [81] since they are accounted to be reasonably accurate and useful in estimating long-term building energy and thermal performance [82].

During the second stage of this paper, the heatwave weather data are used. According to the Royal Meteorological Institute (RMI) of Belgium, a heatwave is a period of a minimum of five consecutive days with a maximum air temperature higher than 25 °C, in which at least three days have a maximum air temperature higher than 30 °C [83]. The above definition is static and does not consider the climate variations in different regions. In addition, a fixed threshold for heatwave definition leads to artifacts when comparing the data obtained from different ESMs, since each ESM has its own biases and variations. The heatwave weather data used in the second stage are derived based on a statistical method by [84] coupled to the RMI static heatwave definition. Therefore, they lack the abovementioned limitations. The calculation method was based on three principles, which can be found in [68]. All the heatwaves are characterized based on three criteria, including duration (number of consecutive days during the heatwave period), maximal temperature (maximum daily mean air temperature), and intensity (the cumulative difference between the air temperature and S_{deb} during the heatwave period, divided by the difference between S_{deb} and S_{pic}). S_{deb} and S_{pic} are 97.5%, and 99.5% percentiles of the reference period air temperature dataset, respectively. In this paper, the highest maximal temperature heatwaves are selected during three different periods, including 2001–2020 (historical scenario), 2041–2060 (mid-future scenario), and 2081–2100 (future scenario). The selection of the periods is based on the recommendations of the dynamic simulation guideline provided by the International Energy Agency (IEA) EBC Annex 80 – "Resilient cooling of buildings" project [46,85] and a previous study in the scientific literature [47]. All the weather data in this paper are obtained from [68].

2.4. Stages of analysis

As mentioned earlier, this paper consists of optimizing passive cooling design strategies (Stage 01) and a short-term analysis during heatwave events and the cooling system outage (Stage 02). The following sections (i.e., Section 2.4.1 and Section 2.4.2) are allocated to describe each stage and its corresponding indicators.

2.4.1. Stage 01: Optimization using passive design strategies

Optimization in building design is the practice of using mathematical models to formulate a design problem in order to select the optimal design solutions among many other alternatives. In this paper, the NSGA-II algorithm is used to determine non-dominated design solutions developed by the combinations of 13 passive design strategies (see Table 4) to minimize final HVAC energy use and Indoor Discomfort Degree (IDD). The NSGA-II multi-objective genetic algorithm method [86] is widely used to optimize the design of new buildings and the renovation of existing ones [87–89]. The NSGA-II is based on crowding distance sorting mechanisms and is defined by some main features such as generation population size, crossover probability, mutation probability, the maximum number of generations, and the number of objectives. Based on the literature analysis and considering the available computational capacity, the following parameters are set for the analysis in this paper, (i) generation population size = 50, (ii) crossover probability = 1, (iii) mutation probability = 0.4, (iv) the maximum number of generations = 400, and (v) number of objectives = 2.

In this paper, the input factors for optimization are selected among those representing passive and bioclimatic design strategies. For this aim, a set of 13 design strategies are chosen based on the literature review [90–93], in order to determine their relative impact on thermal comfort and energy performance of the studied model. Those strategies are applicable to the examined model considering its components and climate. All the input factors' characteristics, including type, minimum/maximum/step value (for numeric factors), and options (for non-numeric factors), are listed in Table 4. The objective functions are based on two indicators, final HVAC energy use ($E_{f,HVAC}$) for energy efficiency analysis and Indoor Discomfort Degree (IDD) for thermal comfort analysis. The final HVAC Energy use includes the electricity consumption of the compressor, condenser/evaporator pump, condenser/evaporator fan, and tank supplementary internal heating coil for the reversible air-to-water heat pump system. The optimization process is conducted using the Typical Metrological Year (TMY) weather data for the period 2001–2020 (see Section 2.3).

In this paper, the Indoor Discomfort Degree (IDD) indicator is proposed for thermal comfort assessment, inspired by the recommendations of the guidelines developed in the International Energy Agency (IEA) EBC Annex 80 – "Resilient cooling of buildings" project [46,48,94] and the scientific literature [47,64,95]. *IDD* [°C] is a symmetric time-integrated thermal discomfort index that sums up Indoor Overheating Degree (IOhD) [°C] and Indoor Overcooling Degree (IOcD) [°C] [64,94]. *IOhD* and *IOcD* are multizonal indices that accumulate the heating and cooling degree hours over the total number of zonal occupied hours, respectively. The multizonal feature of *IOhD* and *IOcD* allows for the implementation of zone-specific thermal comfort models (i.e., static or adaptive) and requirements (e.g., comfort categories) tracking the zonal occupied hours. The formulas to calculate *IDD*, *IOhD*, and *IOcD* are as follows,

$$IDD = IOhD + IOcD (1).$$

$$IOhD \equiv \frac{\sum_{z=1}^{Z}\sum_{i=1}^{N_{occ(z)}}\left[\left(T_{in,z,i}-T_{comf,upper,z,i}\right)^{+}\times h_{i,z}\right]}{\sum_{z=1}^{Z}\sum_{i=1}^{N_{occ(z)}} h_{i,z}} \quad (2).$$

$$IOcD \equiv \frac{\sum_{z=1}^{Z}\sum_{i=1}^{N_{occ(z)}}\left[\left(T_{comf,lower,z,i}-T_{in,z,i}\right)^{+}\times h_{i,z}\right]}{\sum_{z=1}^{Z}\sum_{i=1}^{N_{occ(z)}} h_{i,z}} \quad (3).$$

Where Z [-] is the total number of building zones, z is zone counter, $N_{occ}(z)$ [-] is the total number of occupied hours in zone z, i is hour counter, $T_{in,o,z}$ is the indoor operative temperature in zone z at hour i, $T_{comf,upper,z,i}$ is maximum comfort threshold in zone z at hour i, $T_{comf,lower,z,i}$ is the minimum comfort threshold in zone z at hour i. This paper refers to ISO 17772–1 standard to define the upper and lower limits of comfort (i.e., $T_{comf,upper,z,i}$ and $T_{comf,lower,z,i}$). ISO 17772–1 standard provides category-based static (Cat. I, Cat. II, Cat. II and Cat. IV) and adaptive (Cat. I, Cat. II, and Cat. III) thermal comfort criteria. This paper selects, (i) the static criterion that is recommended to actively heated and cooled buildings [47] and (ii) Category II that is recommended for new buildings and renovations [96]. As a result, $T_{comf,upper,z,i}$ and $T_{comf,lower,z,i}$ are set to 26 °C and 20 °C, respectively, assuming a sedentary activity for the occupants (1.2 met) as well as clothing factors of 0.5 clo for summer and 1 clo for winter. It should be noted that the target zones for the calculation of *IDD* are living + kitchen, bedroom 01, bedroom 02, and office.

2.4.2. Stage 02: Overheating analysis during heatwaves and cooling system outage

In Stage 02, a set of optimal solutions obtained from Stage 01 is analyzed under short-term heatwave conditions coinciding with the outage of the cooling system. The heatwave weather data used

Table 4
The ranges/options of input factors for optimization.

	Factor	Type	Min. value Options	Max. value	Step	Number of values / options
F1	Natural ventilation rate [ac/h]	Discrete	1	5	2	3
F2	Building orientation [°]	Discrete	135	315	180	2
F3	Wall solar absorptance [-]	Discrete	0.40	0.90	0.10	6
F4	Roof solar absorptance [-]	Discrete	0.40	0.80	0.10	5
F5	Infiltration rate [ac/h]	Discrete	0.10	1.20	0.10	12
F6	Shading strategy[1]	Discrete	No shading, Electrochromic glazing, Roller blind, venetian blind			4
F7	Glazing type	Discrete	Thermochromic, U0.8[2]-SHGC0.2[3], U0.8-SHGC0.5, U0.8-SHGC0.8, U0.9-SHGC0.2, U0.9-SHGC0.5, U0.9-SHGC0.8, U1-SHGC0.2, U1-SHGC0.5, U1-SHGC0.8, U1.1-SHGC0.2, U1.1-SHGC0.5, U1.1-SHGC0.8, U1.2-SHGC0.2, U1.2-SHGC0.5, U1.2-SHGC0.8			16
F8	Window frame type	Discrete	Aluminum frame with no thermal break, Aluminum frame with thermal break, Painted wood, UPVC			4
F9	External wall construction	Discrete	U0.1-ThM1000[4], U0.1-ThM2000, U0.1-ThM3000, U0.2-ThM1000, U0.2-ThM2000, U0.2-ThM3000, U0.3-ThM1000, U0.3-ThM2000, U0.3-ThM3000			9
F10	Ground floor construction	Discrete	U0.1-ThM1000, U0.1-ThM2000, U0.1-ThM3000, U0.2-ThM1000, U0.2-ThM2000, U0.2-ThM3000, U0.3-ThM1000, U0.3-ThM2000, U0.3-ThM3000			9
F11	Internal wall construction	Discrete	U1-ThM1000, U1-ThM2000, U1-ThM3000, U1.5-ThM1000, U1.5-ThM2000, U1.5-ThM3000, U2-ThM1000, U2-ThM2000, U2-ThM3000			9
F12	Internal floor construction	Discrete	U0.8-ThM1000, U0.8-ThM2000, U0.8-ThM3000, U0.9-ThM1000, U0.9-ThM2000, U0.9-ThM3000, U1-ThM1000, U1-ThM2000, U1-ThM3000			9
F13	Roof construction	Discrete	U0.1-ThM1000, U0.1-ThM1000 + GR[5], U0.1-ThM2000, U0.1-ThM2000 + GR, U0.1-ThM3000, U0.1-ThM3000 + GR, U0.2-ThM1000, U0.2-ThM1000 + GR, U0.2-ThM2000, U0.2-ThM2000 + GR, U0.2-ThM3000, U0.2-ThM3000 + GR, U0.3-ThM1000, U0.3-ThM1000 + GR, U0.3-ThM2000, U0.3-ThM2000 + GR, U0.3-ThM3000, U0.3-ThM3000 + GR			18

[1] all shading devices are positioned outside and controlled by inside air temperature set-point of 24 °C during occupied hours
[2] U-Value (thermal conductivity) [W/m^{2}K],
[3] Solar Heat Gain Coefficient [-],
[4] Thermal Mass [KJ/m^{2}K], and
[5] Green Roof → substrate layer = 15 cm, drainage layer = 5 cm, plant height = 0.1 m, leaf reflectivity = 0.22, and leaf emissivity = 0.95 [97].

in this stage represents the heatwaves with the highest maximal temperature over three periods, including 2001–2020 (historical), 2041–2060 (mid-future), and 2081–2100 (future) (see Section 2.3).

Initially, a zonal thermal comfort analysis is carried out using three fit-to-purpose indices, including maximum operative temperature (derived from air temperature, mean radiant temperature, and air velocity), maximum Heat Index (HI) [98], and Thermal Autonomy (TA) [99]. *HI* metric, also known as the apparent temperature, is a metric that quantifies the human body's thermal sensation by coupling relative humidity (RH) and air temperature (T_{air}). *HI* [°C] metric is proposed by RELi 2.0. [98] guideline developed by U.S. Green Building Council (USGBC) to ensure thermal safety or thermally habitable conditions in buildings during the power outages. The formula to calculate *HI* has resulted from multiple regression analyses performed by [100] that requires adjustments for different ranges of air temperature and relative humidity. *HI* is calculated via Rothfusz's equation as below,

$$HI = -42.379 + 2.04901523 \times T_{air} + 10.1333127 \times RH - 0.22475541 \times T_{air} \times RH - 0.00683783 \times T_{air}^2 - 0.05481717 \times RH^2 + 0.00122874 \times T_{air}^2 \times RH + 0.00085282 \times T_{air} \times RH^2 - 0.00000199 \times T_{air}^2 \times RH^2 \quad (4).$$

$$where if RH < 13\% \&\& 26.66°C < T_{air} < 44.44°C : adjustment(subtracted) = [(13 - RH)/4] \times SQRT\{[17 - ABS(T - 95)]/17\}$$

$$if RH > 85\% \&\& 26.66°C < T_{air} < 30.55°C : adjustment(added) = [(RH - 85)/10] \times [(87 - T_{air})/5]$$

Where *SQRT* and *ABS* are square root function and absolute value, respectively. The US National Oceanic and Atmospheric Administration (NOAA) defines different ranges for *HI* index based on their effect on the human body (see Table 5). *HI* has become popular in environmental health research and has been widely used in previous studies [101–104].

Thermal Autonomy (TA) [%] index is defined as *"the percentage of the occupied time over a period where a thermal zone meets or*

Table 5
Classification of the Heat Index ranges based on the effect on the human body.

Classification	Heat Index	Effect on the body
Caution	26.6 °C – 32.2 °C	Possible fatigue with prolonged exposure and/or physical activity
Extreme caution	32.2 °C – 39.4 °C	Heat stroke, heat cramps, or heat exhaustion possible with prolonged exposure and/or physical activity
Danger	39.4 °C – 51.1 °C	Heat cramps or heat exhaustion likely, and heat stroke possible with prolonged exposure and/or physical activity
Extreme danger	More than 51.1 °C	Heat stroke highly likely

exceeds a given set of thermal comfort acceptability criteria through passive means only" [99]. *TA* puts forward the building construction as the main factor in defining the building's thermal performance. It is different from the conventional design approach of ensuring thermal comfort via a prosthetic mechanical system remedially. Therefore, *TA* fits to the aim of the current study at this stage while evaluating the building's thermal performance assuming the outage of the active cooling system. The formula to calculate *TA* is,

$$TA = \frac{\sum_{i=1}^{occupiedhours} wf_i}{\sum_{i=1}^{occupiedhours} h_i} where \begin{cases} wf_i = 1; T_{in} < T_{comfort,upper} \\ wf_i = 0; T_{in} > T_{comfort,upper} \end{cases} \quad (5)$$

Where wf_i is the weighting factor [-], T_{in} is indoor operative or air temperature [°C], and $T_{comfort,upper}$ is the maximum temperature threshold.

Subsequently, the resistivity of building to overcome the increasing risk of overheating due to climate change is assessed using the Climate Change Overheating Resistivity (CCOR) index developed in [47]. *CCOR* metric shows the rate of change in indoor overheating risk represented by *IOhD* metric (See Section 2.4.1) with the change in outdoor weather conditions represented by the Ambient Warmness Degree (AWD) metric. In other words, it couples the indoor and outdoor environments to assess the ability of the building to withstand the warming outdoor weather conditions. *AWD* metric is used to quantify the severity of outdoor thermal conditions by averaging the Cooling Degree hours (CDh) calculated for a base temperature (T_b) of 18 °C over the total number of building occupied hours [94]. The formulas to calculate *AWD* and *CCOR* are,

$$AWD = \frac{\sum_{i=1}^{N_{occ,building}} [(T_{out,a,i} - T_b)^+ \times h]}{\sum_{i=1}^{N_{occ,building}} h_i} \quad (6)$$

$$\frac{1}{CCOR} = \frac{\sum_{Sc-1}^{Sc=M} (IOhD_{Sc} - \bar{IOhD}) \times (AWD_{Sc} - \bar{AWD})}{\sum_{Sc-1}^{Sc=M} (AWD_{Sc} - \bar{AWD})^2} \quad (7)$$

Where $T_{out,a,i}$ is the outdoor dry-bulb air temperature and *N* is the total number of building occupied hours, *Sc* is the weather scenario counter, *M* is the total number of weather scenarios, and $\bar{IOhD}$ and $\bar{AWD}$ are the averages of all *IOhDs* and *AWDs* calculated for different scenarios. Only the positive values of $(T_{out,a,i}-T_b)^+$ are taken into account in the summation. CCOR> 1 means that the building is able to suppress the increasing outdoor thermal stress due to climate change, and CCOR< 1 means that the building is unable to suppress the increasing outdoor thermal stress due to climate change. *CCOR* metric is recommended by Thermal Conditions Task Force [48] and Dynamic Simulation Task force [46] in (IEA) EBC Annex 80 – "Resilient cooling of buildings" project.

3. Results

3.1. Outdoor weather conditions

Fig. 3 shows the daily outdoor dry-bulb air temperature for the Typical Meteorological Year (TMY) generated for Brussels considering the 2001–2020 period based on the Regional Climate Model (MAR) "Modèle Atmosphérique Régional" (BCC-CSM2-MR). Heating Degree Days (HDD10 °C) 929 °C. days and Cooling Degree Days (CDD18 °C) 294 °C. days are calculated, showing that Brussels is generally a heating-dominated region with an annual average air temperature 10.83 °C. January and February are the coldest months, with a mean air temperature 3.18 °C and 4.75 °C, respectively. At the same time, July and August are the hottest months, with a mean air temperature 17.88 °C and 17.86 °C, respectively. The minimum air temperature −11.5 °C (-7.1 °C assuming 1% percentile) is estimated during January, and the maximum air temperature 36.8 °C (29.8 °C assuming 99% percentile) is estimated during July. It is clear from Fig. 3 that the fluctuations between the day and night temperatures during the summer are higher than in the winter. In the cold months (January, February, and December), the average day and night temperature difference is 3 °C; in the hot months (June, July, August, and September), it becomes 8 °C. Also, April has the highest standard deviation 8.07 °C, making it the month with the highest temperature gradient.

As explained in Section 2.3, the highest maximal temperature heatwaves are selected during three periods, including 2001–2020 (historical scenario), 2041–2060 (mid-future scenario), and 2081–2100 (future scenario). It should be noted that the mid-future and future scenarios are based on the SSP2-4.5 emission scenario. According to the heatwave characterization in [68], the highest maximal temperature heatwave occurred in 2019 during the 2001–2020 period and will occur in 2047 and 2098 during the 2041–2060 and 2081–2100 periods, respectively.

Fig. 4 shows the heat maps representing the distribution of outdoor air temperature for the years with the highest maximal temperature heatwave (i.e., 2019, 2047, and 2098). It also provides weather summaries, including Heating Degree Days (HDD10 °C), Cooling Degree Days (CDD18 °C), average, hottest, and coldest yearly air temperature, and annual cumulative horizontal solar radiation. According to the results, the average annual air temperature will increase 1.4 °C in 2047 and 4 °C in 2098 compared to 2019. *HDD10 °C* decreases 18.29% in 2047 and 55.52% in 2098, whereas *CDD18 °C* increases 39% in 2047 and 148.94% in 2098

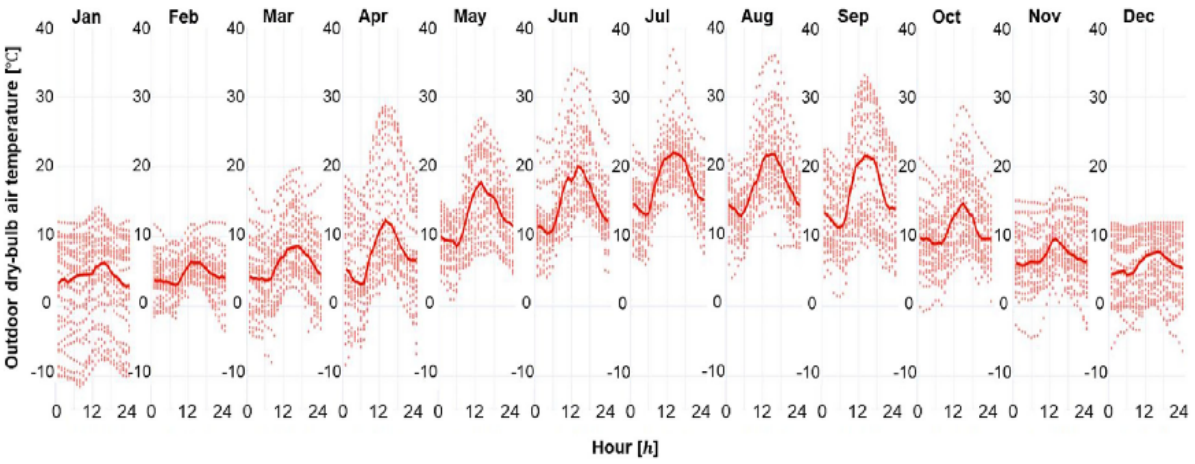

Fig. 3. The graph shows the daily outdoor dry-bulb temperature for different months in Brussels for the TMY of the period 2001–2020.

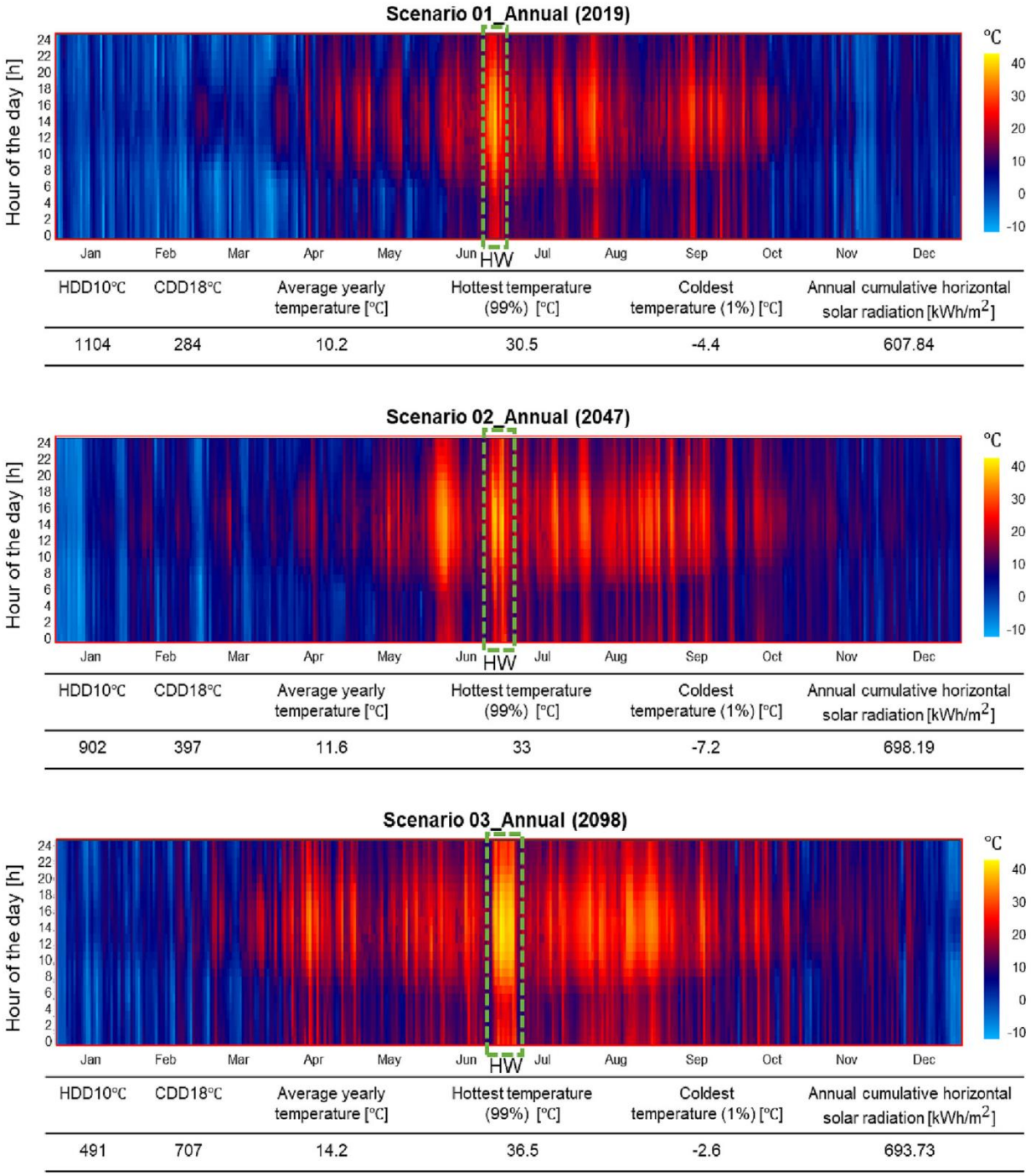

Fig. 4. The heat maps and weather summary for 2019, 2047 (under SP2-4.5 emission scenario), and 2083 (under SP2-4.5 emission scenario). The heatwaves are distinguished with green dashed lines. (For interpretation of the references to colour in this figure legend, the reader is referred to the web version of this article.)

compared to 2019. With the decrease of *HDD10* °*C* and the increase of *CDD18* °*C*, the average heating and cooling loads in buildings are expected to decrease and increase, respectively [105–107]. The highest hottest air temperature 36.5 °*C* is estimated in 2098, and the lowest coldest temperature −7.2 °*C* is estimated in 2047. Based on the climate data in this paper, the annual cumulative horizontal solar radiation inconsistently varies between 607.84 kWh/m^2 and 698.19 kWh/m^2 among the weather scenarios.

Fig. 5 depicts hourly outdoor dry-bulb air temperature during the highest maximal temperature heatwaves, and Table 6 summarizes their main characteristics. The heatwave detection is based on a statistical method [84] by calculating the three percentiles of the daily mean air temperature over the 2001–2020 period, including S_{int} = 23.8 °*C* (95th percentile) S_{deb} = 26.9 °*C* (97.5th percentile) and S_{pic} = 33.2 °*C* (99.5th percentile). The highest maximal temperature heatwaves generally start in late June and end by the end of the month or early July, depending on the duration of the event. According to the heatwave data used in this paper, the duration and average air temperature of heatwaves will increase with the continuation of global warming. The highest maximal temperature heatwave detected in 2019 lasted for 120 h (five days), while it increases to 168 h (seven days) by 2047 and 240 h (10 days) by 2098. Similarly, the average air temperature during the detected heatwaves in 2047 and 2098 will increase 3.28% and 12.15%, respectively, compared to the one in 2019. The intensity of heatwave as the cumulative difference between the air temperature and S_{deb}, divided by the difference between S_{deb} and S_{pic}, increases 115% by 2047 and 498% by 2098 due to the increase in temperature and duration of future heatwaves.

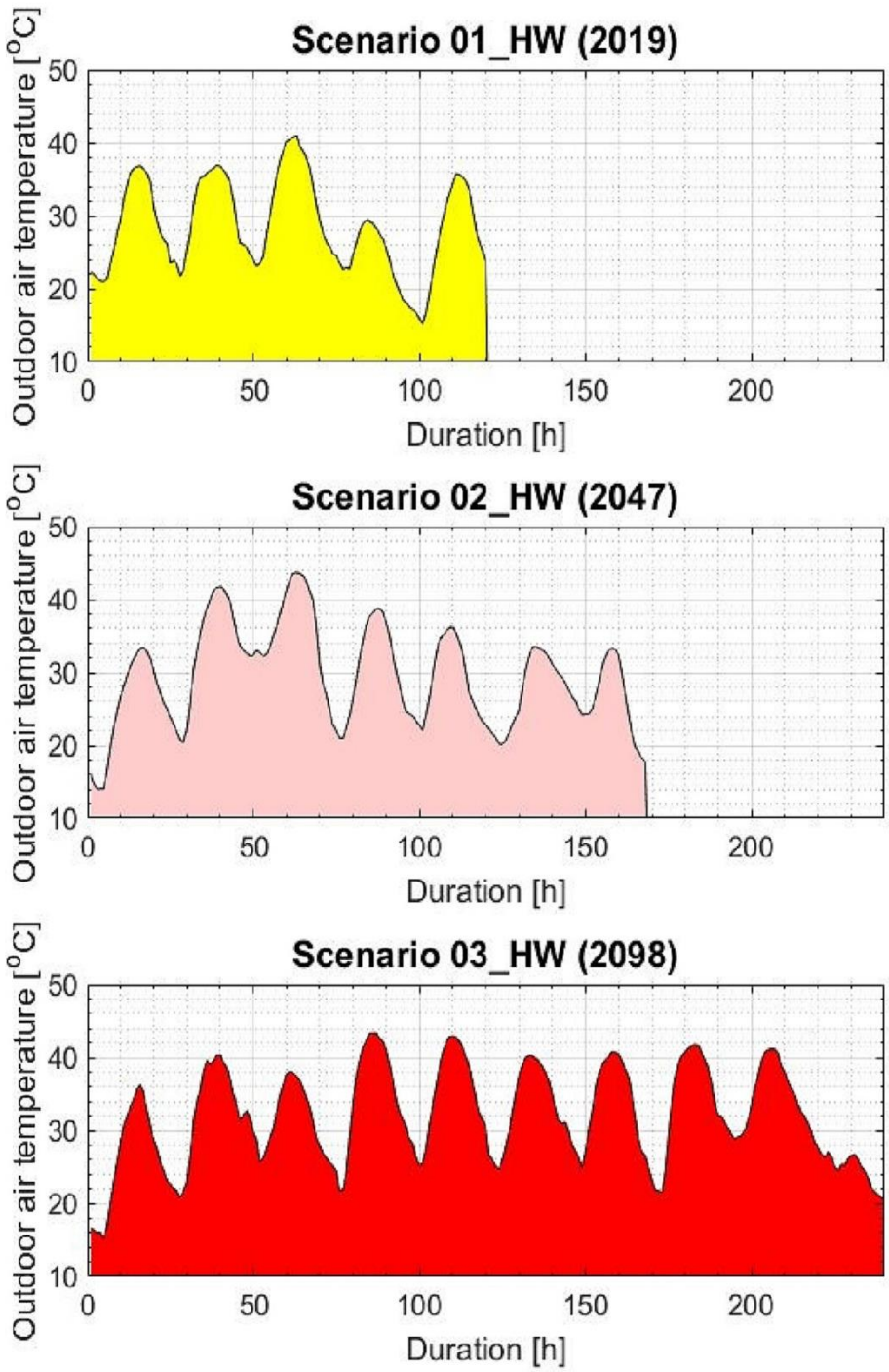

Fig. 5. Hourly outdoor air temperature during the highest maximal temperature heatwaves detected in 2019 for 2001–2020, 2047 for 2041–2060, and 2098 for 2081–2100.

Table 6
Summary of main parameters characterizing the three highest maximal temperature heatwaves: Scenario 01 HW (2019), Scenario 02 HW (2047), and Scenario 03 HW (2098).

	Scenario 01_HW (2019)	Scenario 02_HW (2047)	Scenario 03_HW (2098)
Date	25 Jun-29 Jun	25 Jun-01 Jul	26 Jun-05 Jul
Duration [days]	5	7	10
Intensity [-]	1.38	2.98	8.29
Max. Air Temperature [°C]	41.02	43.64	43.37
Avg. Air Temperature [°C]	28.64	29.58	32.12

3.2. Optimal solutions

Fig. 6 shows the optimization solution space to minimize final HVAC energy use ($E_{f,HVAC}$) and Indoor Discomfort Degree (IDD). The optimization problem can be mathematically expressed as,

$$min\{E_{f,HVAC}(x), IDD(x)\} for x \in X subject to WD(x) = TMY_{2001-2020} (8)$$

In multi-objective optimization, a set of solutions that are non-dominated by each other but are superior to the rest of solutions in the search space are denoted as the Pareto front or set of the optimal solutions in the space of objective functions. This means that

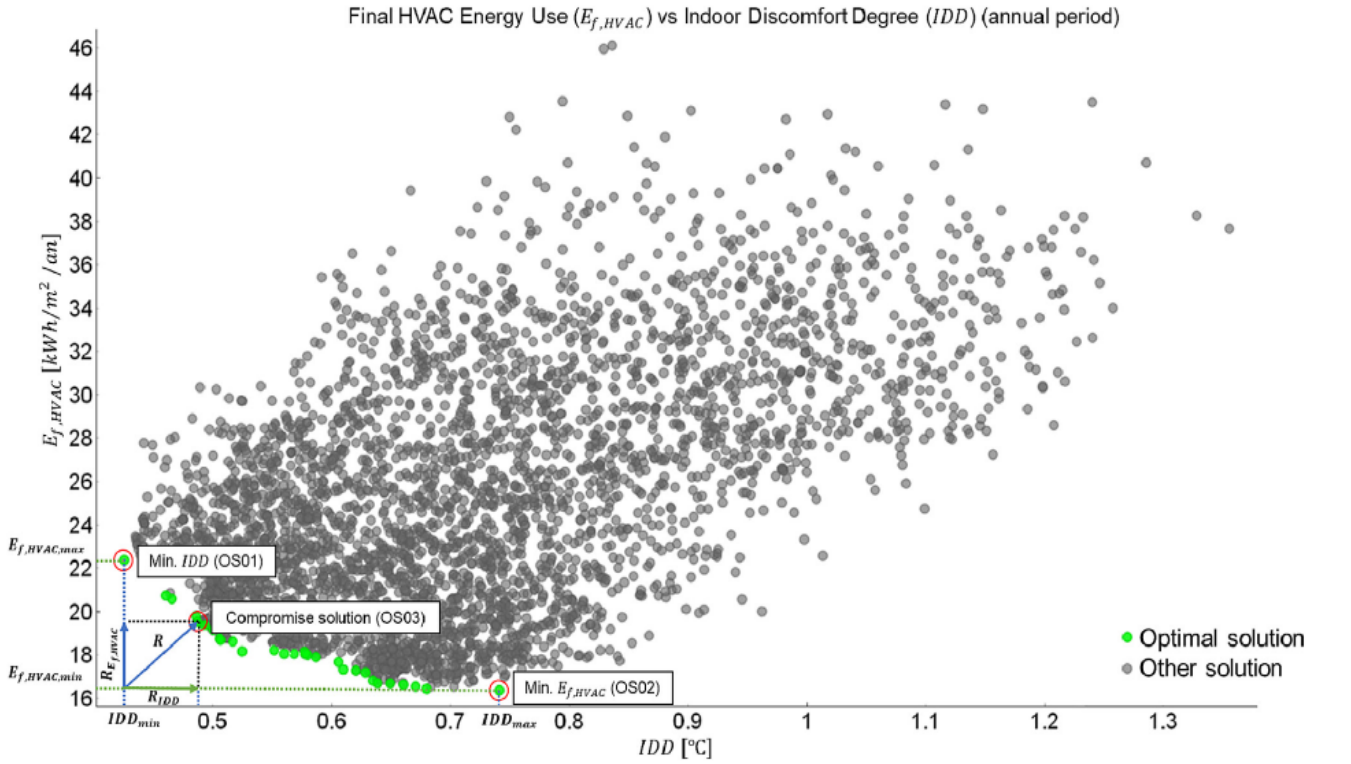

Fig. 6. Scatter plot of final HVAC energy use ($E_{f,HVAC}$) vs. Indoor Discomfort Degree (IDD) for all optimization cases, with green Pareto front and three optimal solutions distinguished. (For interpretation of the references to colour in this figure legend, the reader is referred to the web version of this article.)

no single solution can be found that is superior to all other solutions in terms of all objectives, making it impossible to simultaneously improve all objectives by altering the vector of design variables in a Pareto front made up of numerous non-dominated solutions. As a result, each solution of the Pareto front includes at least one objective inferior to another solution in that Pareto front, although both are superior to others in the rest of search space. In this paper, the selection of optimal solutions from the resulting Pareto front depends on the trade-off between both objective functions. As illustrated in Fig. 6, the Pareto front can be normalized considering the minimum and maximum values of the objective functions via coefficients $R_{E_{f,HVAC}}$ and R_{IDD}. The optimal solution OS01 is the most thermally comfortable solution (i.e., $R_{IDD} = 0$) with the highest final HVAC energy use (i.e., $R_{E_{f,HVAC}} = 1$). Differently, the optimal solution OS02 is the most energy-efficient solution (i.e., $R_{E_{f,HVAC}} = 0$) with the highest discomfort (i.e., $R_{IDD} = 1$). In addition, the optimal solution OS03 (or compromise solution) is selected as a trade-off, using $R_{E_{f,HVAC}}$ and R_{IDD} weighting factors (Eq. (9) and Eq. (10)). The compromise solution OS03 is characterized by the minimum value of $\bar{R}$ using the following equations,

$$f(\vec{X})_{OS03} = R_{E_{f,HVAC}}.E_{f,HVAC}(\vec{X}_{E_{f,HVAC},R_{E_{f,HVAC}}}) + R_{IDD}.IDD(\vec{X}_{IDD,R_{IDD}}) \quad (8)$$

$$R_{E_{f,HVAC}} = \frac{E_{f,HVAC}(\vec{X}_{E_{f,HVAC},R_{E_{f,HVAC}}}) - E_{f,HVAC_{min}}}{E_{f,HVAC_{max}} - E_{f,HVAC_{min}}} \quad (9)$$

$$R_{IDD} = \frac{R_{IDD}.IDD(\vec{X}_{IDD,R_{IDD}}) - IDD_{min}}{IDD_{max} - IDD_{min}} \quad (10)$$

$$\bar{R} = \sqrt{R^2_{E_{f,HVAC}} + R^2_{IDD}} \quad (11)$$

Table 7 summarizes the combinations of input factors and the outputs for the three selected optimal solutions (OS01, OS02, and OS03). F1-F13 are the input factors considered during the optimization process (see Table 4) that characterize each optimal solution. In addition to the optimization objectives/outputs, Table 7 lists additional outputs such as cooling energy use, heating energy use, Indoor Overheating Degree (IOhD), and Indoor Overcooling Degree (IOcD). In order to get the parameter values in Table 7, the optimization output (with a distinction of Pareto front and other solutions) is exported in.csv format from DesignBuilder, which includes all characteristics (i.e., input factors and outputs) of each solution. The exported.csv file is then imported into the Orange data analysis and visualization tool. Using the interactive feature in Orange, initially, the input factors' and outputs' values for the Min. IDD (OS01) and Min $E_{f,HVAC}$ (OS02) cases are extracted and recorded. Subsequently, the $\bar{R}$ is calculated for the rest of the solutions in the Pareto front to find the case with minimum R value (i.e., compromise solution) and extract corresponding input factors' and outputs' values.

It should be noted that $E_{f,HVAC}$ and IDD for the base case are 24.19 kWh/m^2 and 0.80 °C, respectively. OS01 has the lowest IDD value of 0.425 °C and the highest $E_{f,HVAC}$ value of 22.37 kWh/m^2 among all optimal solutions. On the other hand, OS02 has the highest IDD value of 0.741 °C and the lowest $E_{f,HVAC}$ value of 16.36 kWh/m^2 among all optimal solutions. OS03 has IDD value of 0.487 °C and $E_{f,HVAC}$ value of 19.53 kWh/m^2, falling between the minimum and maximum ranges of IDD and $E_{f,HVAC}$ owned by OS01 and OS02. OS01 has 2118.31 kWh higher cooling energy use, 674.4 kWh lower heating energy use, 91% higher overheating discomfort, and 44% lower overcooling discomfort compared to OS02. It is since: (i) the south-oriented zones that are more exposed to the sun in S01 (i.e., living + kitchen and bedroom 02 zones) have larger glazing areas than S02 (i.e., bedroom 01 and office zones), (ii) south-oriented zones (with larger glazing areas) in S01 has relatively higher occupancy hours compared to S02 (note that the HVAC operates and IDD is calculated during occupied hours; e.g., the living + kitchen zone with higher occupancy hours has more influence on the final HVAC energy use and IDD than the office), (iii) the solar heat gains through the envelope and glazing areas is higher in S01 than S02 due to higher wall solar absorptance, roof solar absorptance, and Solar Heat Gain Coefficients (SHGC) of windows.

Table 7
The characteristics of the selected optimal solutions: minimum Indoor Discomfort Degree (IDD) case (OS01), minimum final HVAC energy use ($E_{f,HVAC}$) case (OS02), and compromise solution case (OS03).

Optimal solutions													
Min. IDD (OS01)	**Factors**												
	F1	F2	F3	F4	F5	F6	F7	F8	F9	F10	F11	F12	F13
	5	135	0.50	0.60	0.10	Roller blind	U0.8-SHGC0.8	UPVC	U0.1-ThM3000	U0.1-ThM2000	U1-ThM3000W	U1-ThM3000W	U0.1-ThM3000 + GR
	Outputs												
	Final HVAC energy use [kWh/m^2]	Cooling energy use [kWh]	Heating energy use [kWh]	IDD [°C]	IOcD [°C]	IOhD [°C]							
	22.37	2435.01	1331.18	0.425	0.413	0.012							
Min. $E_{f,HVAC}$ (OS02)	**Factors**												
	F1	F2	F3	F4	F5	F6	F7	F8	F9	F10	F11	F12	F13
	5	315	0.40	0.40	0.10	Roller blind	U0.8-SHGC0.2	UPVC	U0.1-ThM3000	U0.1-ThM1000	U1-ThM3000W	U0.8-ThM3000	U0.1-ThM2000 + GR
	Outputs												
	Final HVAC energy use [kWh/m^2]	Cooling energy use [kWh]	Heating energy use [kWh]	IDD [°C]	IOcD [°C]	IOhD [°C]							
	16.36	316.70	2005.58	0.741	0.741	0.001							
Compromise solution (OS03)	**Factors**												
	F1	F2	F3	F4	F5	F6	F7	F8	F9	F10	F11	F12	F13
	5	135	0.80	0.50	0.10	Roller blind	U0.8-SHGC0.5	Painted wood	U0.1-ThM3000	U0.1-ThM1000	U1-ThM3000W	U1 - ThM3000	U0.1-ThM3000 + GR
	Outputs												
	Final HVAC energy use [kWh/m^2]	Cooling energy use [kWh]	Heating energy use [kWh]	IDD [°C]	IOcD [°C]	IOhD [°C]							
	19.53	1535.56	1559.79	0.487	0.487	0.004							

There are some factors that are common between the selected optimal solutions. The first common factor is the natural ventilation rate of 5 ac/h, which is the maximum specified value. This is in line with the findings of previous research [94,108–110] on the positive impact of high natural ventilation rates on improved cooling energy efficiency and summer comfort. It is since high rates of natural ventilation in mixed-mode buildings can adequately provide fresh outdoor airflow to maintain comfort during intermediate and summer seasons and delay the operation of active cooling systems. However, its potential is expected to diminish with the continuation of global warming [94,108,110,111]. The second common factor is the infiltration rate of 0.1 ac/h, which is the minimum specified value. Previous research [112–114] also confirmed that the infiltration rate negatively correlates with HVAC energy consumption and thermal comfort in buildings. It is because the infiltration rate is an uncontrolled phenomenon and consistently blows cold air in the winter and hot air in the summer into the building, adding to the heating and cooling loads. The third common factor is the lowest specified U-value for building envelope components. This shows that high insulation levels in an actively heated and cooled building in a temperate climate contribute to both energy-saving and thermal comfort. It is because high insulation levels can prevent the unwanted heat flux from the indoor environment in the winter and to the indoor environment in the summer. The same result is achieved in [115] for an envelope-dominated building with low levels of internal gains in a temperate climate. The fourth common factor is the highest specified thermal mass value of 3000 KJ/m^{2}K for envelope components. High thermal mass sets a high heat storage capacity for the building. It can help dampen the hot and cold peak temperatures, and if coupled with active systems, it helps in lowering the overall HVAC energy consumption [116]. The fifth common factor is the integration of green roofs. Like insulation, green roofs enhance the roofs' insulation, minimizing heat transfer [117]. Therefore, they can help reduce heating and cooling loads and improve thermal comfort in air-conditioned buildings [118]. The sixth common factor is the application of roller blinds as a shading strategy. Even though operable shading devices have limited benefits in lowering heating loads and overcooling discomfort, they are helpful in reducing cooling loads and overheating discomfort. According to the optimization objectives in this study, roller blinds are the best choice for achieving optimal thermal comfort and final HVAC energy use.

3.3. Thermal comfort assessment during heatwaves for optimized solutions

3.3.1. Zonal analysis

Fig. 7, Fig. 8, and Fig. 9 show the zonal indoor operative temperature for OS01, OS02, and OS03 during Scenario 01 HW (2019), Scenario 02 HW (2047), and Scenario 03 HW (2098) concurrent with the outage of the cooling system. Full-year simulations are per-

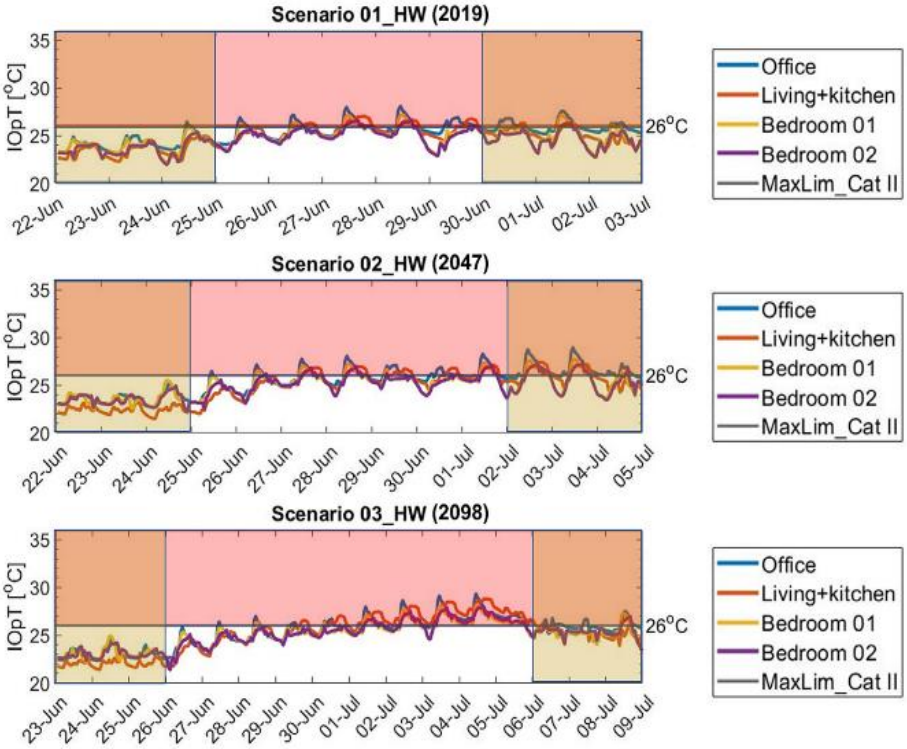

Fig. 7. The plots show the indoor operative temperature for different zones during the three heatwave scenarios for OS01 (including three days shoulder periods).

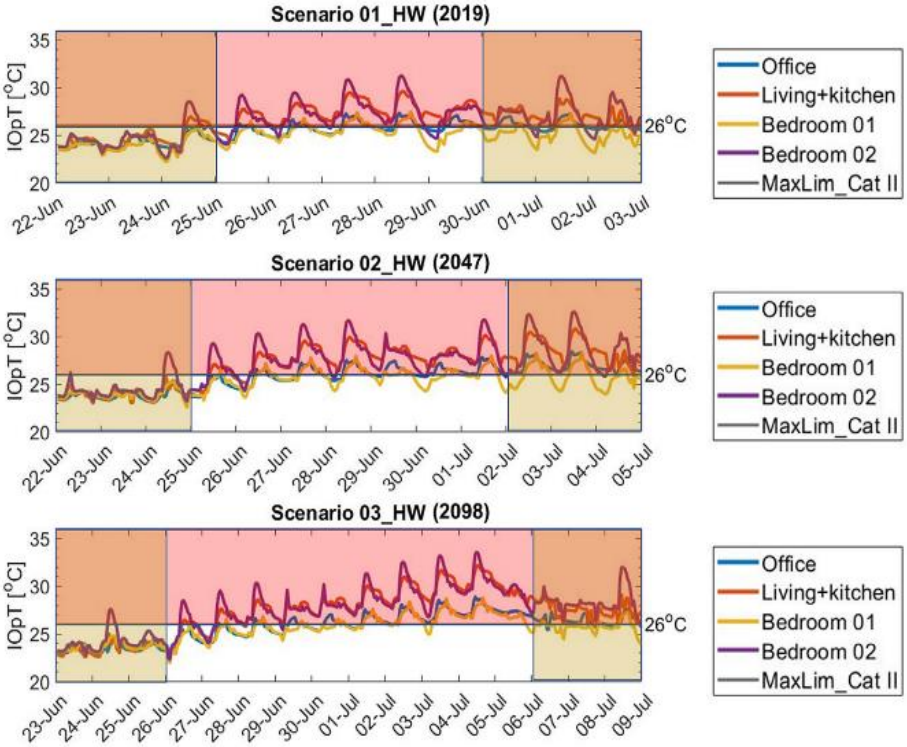

Fig. 8. The plots show the indoor operative temperature for different zones during the three heatwave scenarios for OS02 (including three days shoulder periods).

formed; only heatwaves and three-days shoulder periods are reported in the graphs. The shoulder periods are intended to indicate the building's thermal state before and after the heatwave occurrence.

The results show that OS02 is the only case that can fully maintain the indoor operative temperature within the comfort limits before the heatwaves start by only relying on passive measures. It means that OS01 and OS02 require active cooling to prevent overheating even during normal conditions. During the heatwaves, all three optimal solutions deviate from the maximum comfort limit of 26 °C (according to the Cat II static comfort model in ISO 17772–1) by different extents. For OS01, the maximum operative temperature reaches 32.86 °C in the most critical zone (i.e., bedroom 02) in the 2019 heatwave and increases up to 34.53 °C in the 2098 heatwave. For OS02, the maximum operative temperature reaches 28.09 °C in the most critical zone (i.e., office) in the

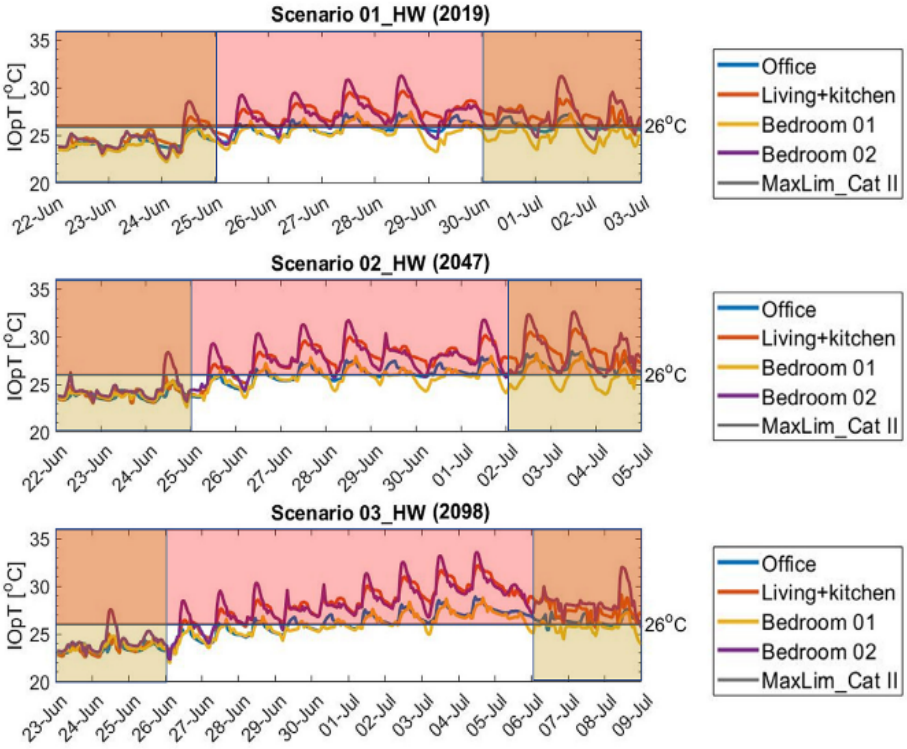

Fig. 9. The plots show the indoor operative temperature for different zones during the three heatwave scenarios for OS03 (including three days shoulder periods).

2019 heatwave and increases up to 29.35 °C in the 2098 heatwave. For OS03, the maximum operative temperature reaches 31.27 °C in the most critical zone (i.e., bedroom 02) in the 2019 heatwave and increases up to 33.64 °C in the 2098 heatwave. Furthermore, the indoor operative temperatures for the bedrooms significantly exceed, in all cases, the healthy sleeping temperature limit of 24 °C recommended by the World Health Organization (WHO). The results also show that non of the cases are able to recover right away after the termination of the heatwave period. The situation is worse for OS01 and OS03, in which the indoor operative temperatures remain at similar ranges as during the heatwaves.

Table 8 summarizes the zonal maximum operative temperature, maximum Heat Index (HI), and Thermal Autonomy (TA) for OS01, OS02, and OS03 during Scenario 01 HW (2019), Scenario 02 HW (2047), and Scenario 03 HW (2098) concurrent with the outage of the cooling system. According to RELi 2.0, *HI* should not go beyond 32.2 °C, corresponding to the "Extreme Caution" threshold (see Table 5) for residential units during the hot season. The results show that OS01 and OS02 fail to keep the abovementioned limit for Bedroom 02 in all three heatwave scenarios. The maximum *HI* values between 33.61 °C and 34.43 °C result for bedroom 02 in OS01 and between 32.29 °C and 32.80 °C in OS02. Therefore, there is a risk of heat stroke, cramp, or exhaustion for the occupants in Bedroom 02 with prolonged exposure and/or physical activity. On the other hand, OS02 can successfully maintain the maximum threshold of 32.2 °C in all scenarios.

Thermal Autonomy (TA) index correlates thermal comfort, building fabric, building operation, and climate [99]. It shows to what extent the building is able to maintain the comfort criteria autonomously (i.e., without the need for active heating and cooling) during occupied hours. In general, climate change causes a decrease in *TA* during heatwaves between 17% and 28% in selected optimal solutions. OS01 has *TA* values of 37.30% in Scenario 01_HW (2019), 32.68% in Scenario 02_HW (2047), and 28.056% in Scenario 03_HW (2098) averaged over all zones. OS02 has *TA* values of 83.70% in Scenario 01_HW (2019), 73.23% in Scenario 02_HW (2047), and 69.14% in Scenario 03_HW (2098) averaged over all zones. OS03 has *TA* values of 57.1% in Scenario 01_HW (2019), 43.17% in Scenario 02_HW (2047), and 40.68% in Scenario 03_HW (2098) averaged over all zones. Consequently, OS02 and OS01 are identified as the most autonomous and the least autonomous cases during the heatwaves, respectively.

3.3.2. Resistivity to overheating impact of climate change

The analyses of the Indoor Overheating Degree (IOhD), Ambient Warmness Degree (AWD) and Climate Change Overheating Resistivity (CCOR) are presented in this section. *IOhD* represents the frequency and intensity of overheating by implementing zonal comfort criteria. *AWD* shows the outdoor thermal severity by accumulating the cooling degree hours averaged over total building occupied hours. *CCOR* couples *IOhD* and *AWD* (i.e., couples indoor and outdoor environments) to quantify the extent of variation in *IOhD* corresponding to a variation in *AWD*. In other words, *CCOR* is the inverse of the slope of the linear regression line between *IOhD* and *AWD*. As shown in Fig. 10, there is a direct correlation between IOhD and AWD; that is, when *AWD* increases, *IOhD* increases as well. The severity of heatwaves is represented by *AWD* in Fig. 10 as follows: AWD for the 2019 heatwave = 4.871 °C, AWD for the 2047 heatwave = 6.3 °C, and AWD for the 2098 heatwave = 8.855 °C.

This study calculated the highest *IOhD* value of 1.84 °C for sOS01 in the 2098 heatwave. It means that the building configuration (i.e., the combination of passive design strategies) in OS01 leads to the highest risk of overheating in the future. The results also show that the difference in *IOhD* between the three optimal cases increases with worsening heatwave events in the future. In the 2019 heatwave, the *IOhD* difference between OS01 and OS02 is 0.87 °C, and it increases up to 1.57 °C in the 2098 heatwave. This shows that OS01 will be affected more by intensifying heatwave events due to climate change. This is also confirmed by *CCOR* values for the selected optimal solutions that vary between 4.63 and 21.16. OS01 has the lowest *CCOR* of 4.63, representing the case that will be affected the most by climate change (i.e., least resistant case). On the other hand, OS02 has the highest *CCOR* of 21.16 and therefore

Table 8
Summary of the maximum operative temperature, maximum Heat Index (HI), and Thermal Autonomy (TA) in different zones during the three heatwaves scenarios in OS01, OS02, and OS03.

OS01				
Scenario 01_HW (2019)				
Zone	Office	Living + kitchen	Bedroom 01	Bedroom 02
Max. Op. temperature [°C]	28.19	30.26	28.18	32.86
Max. Heat Index (HI) [°C]	29.29	31.35	29.19	33.61
Thermal autonomy (TA) [%]	36.36	23.10	65.15	24.62
Scenario 02_HW (2047)				
Max. Op. temperature [°C]	29.61	31.75	29.25	34.53
Max. Heat Index (HI) [°C]	29.60	31.31	29.05	33.60
Thermal autonomy (TA) [%]	31.73	26.28	48.07	24.67
Scenario 03_HW (2098)				
Max. Op. temperature [°C]	30.06	33.31	29.83	35.61
Max. Heat Index (HI) [°C]	29.59	32.21	29.20	34.43
Thermal autonomy (TA) [%]	31.71	23.43	38.80	20.31
OS02				
Scenario 01_HW (2019)				
Max. Op. temperature [°C]	28.09	27.03	27.19	26.68
Max. Heat Index (HI) [°C]	29.54	27.94	28.33	27.77
Thermal autonomy (TA) [%]	73.10	84.47	85.60	91.66
Scenario 02_HW (2047)				
Max. Op. temperature [°C]	28.94	27.38	27.72	27.35
Max. Heat Index (HI) [°C]	29.37	28.05	27.97	27.71
Thermal autonomy (TA) [%]	60.89	73.07	78.84	80.12
Scenario 03_HW (2098)				
Max. Op. temperature [°C]	29.35	28.80	28.27	27.95
Max. Heat Index (HI) [°C]	29.19	29.24	28.36	28.63
Thermal autonomy (TA) [%]	62.76	63.80	75	75
OS03				
Scenario 01_HW (2019)				
Max. Op. temperature [°C]	27.36	29.63	28.48	31.27
Max. Heat Index (HI) [°C]	28.63	30.99	28.67	32.34
Thermal autonomy (TA) [%]	71.59	31.81	84.47	40.53
Scenario 02_HW (2047)				
Max. Op. temperature [°C]	28.49	30.85	28.30	32.68
Max. Heat Index (HI) [°C]	28.84	30.80	28.39	32.29
Thermal autonomy (TA) [%]	46.79	28.48	68.91	28.52
Scenario 03_HW (2098)				
Max. Op. temperature [°C]	28.91	32.23	28.83	33.64
Max. Heat Index (HI) [°C]	28.70	31.36	28.90	32.80
Thermal autonomy (TA) [%]	46.61	26.04	65.36	24.74

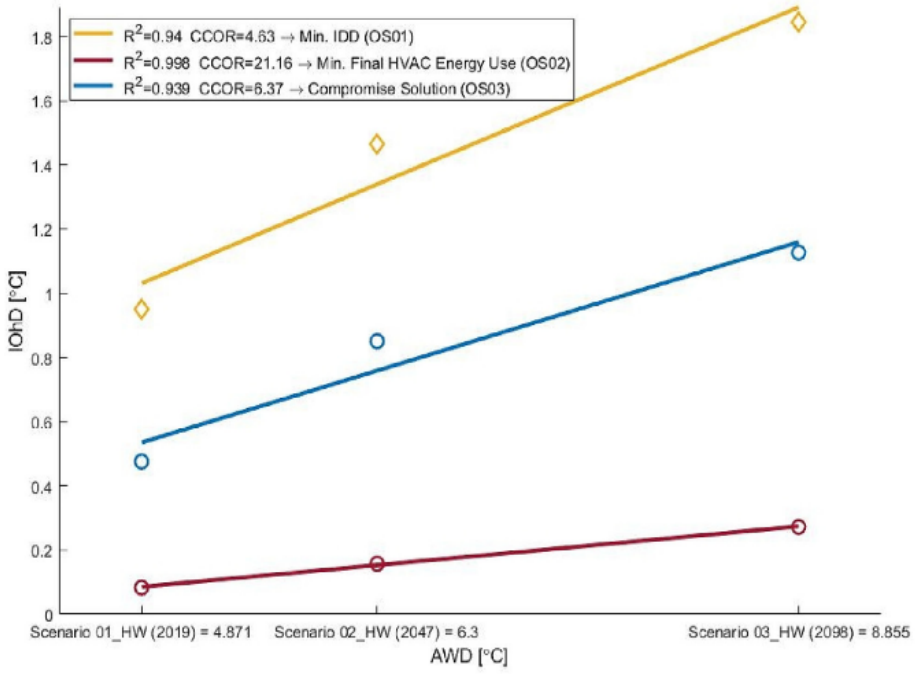

Fig. 10. Indoor Overheating Degree (IOhD) vs. Ambient Warmness Degree (AWD). The inverse of the slope of the regression line shows the Climate Change Overheating Resistivity (CCOR) for each optimal solution.

is the most resistant case. Finally, the relative potential to adapt to climate change P [94] is calculated. P is the difference in *IOhDs* between optimal solutions in the 2098 heatwave $(\Delta IOhD_{i,j,Scenario03\_HW(2098)})^{+}$ divided by $Max[IOhD_{i,Scenario03\_HW(2098)}, IOhD_{j,Scenario03\_HW(2098)}]$ where i,j = OS01, OS02, or OS03. By calculating P, OS02 shows 83% and 75% more potential to adapt to climate change compared to OS01 and OS03, respectively.

4. Discussion

4.1. Findings and recommendations

According to the Intergovernmental Panel on Climate Change (IPCC), the average global air temperature increased in the past 100 years and will continue to increase due to natural and anthropogenic reasons. The weather data in this paper (derived from MAR BCC-CSM2-MR based on IPCC SSP2-4.5 emission scenario) show an increase in annual mean air temperature 1.4 °C by 2047 and 3.6 °C by 2098 compared to 2019 in Brussels. As illustrated in Fig. 4, the cooling seasons are predicted to extend to shoulder seasons. At the same time, the heating seasons will become warmer and outdoor air temperatures in the range of 15 °C to 18 °C will be experienced more. The *HDD10*°C will decrease 55% and *CDD18*°C will increase 148%, shifting Brussels from a heating-dominated region to a cooling-dominated one by the end of the century. In addition, as shown in Fig. 5, the intensity and duration of heatwaves will increase. More severe heatwaves are expected to (i) make it more troublesome for buildings to maintain a thermally safe indoor environment by only relying on passive cooling strategies [119] and (ii) lead to scarcity or failure of the power supply more frequently due to the heavy use of air conditioning [120].

Building design optimization aims to reach energy and cost-effective design with optimum performance in specific circumstances. The combinations of design factors that lead to optimal solutions depend on some parameters, such as climate and building operational properties. In general, to optimize the final HVAC energy use and thermal comfort in any building using passive design strategies, there is a need for making a trade-off between reducing heating energy use/overcooling and cooling energy use/overheating. As shown in Section 3.2, for this specific case study (i.e., nearly Zero-Energy terraced dwelling) and climatic region (i.e., temperate), high ventilation rate, low infiltration rate, high insulation, high thermal mass, integration of green roof, and application of operable roller blinds are found to contribute to both energy efficiency up to 32% and thermal comfort up to 46%. Whilst some factors such as orientation, roof/wall solar absorptance, and Solar Heat Gain Coefficient (SHGC) of windows differ between the best solutions in terms of energy efficiency and thermal comfort. As shown in Table 7, the building orientation towards less exposure to the sun in mostly occupied zones coupled with lower values of wall/roof solar absorptance and windows' SHGC can reduce the cooling energy use, whereas increasing the heating energy use and overcooling discomfort. Differently, the building orientation towards more exposure to the sun in mostly occupied zones coupled with higher values of wall/roof solar absorptance and windows' SHGC can reduce the symmetric thermal discomfort arising mainly from overcooling. Therefore, it works the opposite during the summer and forfeits cooling energy use and summer comfort. This shows that in heating-dominated regions, it is not always the solution to increase solar heat gains to optimize final HVAC energy use and thermal comfort. It is since such a measure may significantly increase the cooling energy use, which can overlap, in some cases, the heating energy use. This is more important considering the impact of climate change and warming weather conditions, which will change the building design concept in temperate regions from heat preserving to heat dissipating to enhance energy efficiency and thermal comfort.

Occupants' exposure to extreme heat in buildings can reach dangerous levels if the mechanical cooling system becomes inoperable. In Fig. 7, Fig. 8, and Fig. 9, it is shown that none of the optimal solutions can fully suppress overheating during concurrent heatwaves and the cooling system outage. The indoor operative temperatures go beyond 29 °C, which can cause serious health issues to the occupants, especially elderly and vulnerable groups. The situation will be aggravated by climate change. By comparing the current and future heatwaves (see Table 8), there is an increase in maximum Heat Index (HI) between 0.28 °C and 0.49 °C, an increase in the maximum operative temperature between 1.34 °C and 2.33 °C, and a decrease in *TA* between 17% and 28% by 2098 over the three selected optimal solutions. Therefore, provisions are required to increase the preparedness of the buildings against more severe and abnormal conditions to avoid any potential health and comfort issues in the future.

To summarize the main recommendations, the list below is provided:

- It is recommended to analyze the actively heated and cooled buildings not only in normal but also in abnormal conditions such as concurrent heatwave and the outage of the HVAC system. It reveals whether the building can withstand such unprecedented events and keep the indoor environment safe for the occupants.
- Back-up cooling and energy storage systems (e.g., batteries, fuel cells, etc.) should be considered in buildings that fail to maintain a thermally safe environment by only relying on passive measures.
- Due to the continuation of global warming, it is recommended to detach from heat-preserving design concept in temperate regions. The future weather predictions show that such regions will shift from heating-dominated to cooling-dominated ones in the coming decades.
- It is recommended to analyze new buildings and renovations under climate change scenarios to ensure their future performance. It is now imperative that new buildings are designed to be adaptable to a changing climate.
- The use of optimization techniques is recommended during the early design stages of new buildings and the renovation of existing ones. Optimized buildings improve energy, cost, operational efficiency, occupant comfort, and equipment lifecycle [121–123].

4.2. Strengths and limitations

There are numerous methods to conduct scientific research, each with its strengths and limitations. The first strength of the current study is related to the validity of the weather data used for the simulations. As mentioned in Section 2.3, the weather data in this paper are based on the Regional Climate Model (MAR) *"Modèle Atmosphérique Régional"* [68] that has high temporal and spatial resolution (~5 km), detailed parametrization (including mesoscale phenomena), and is tuned for the studied region. In addition, the heatwaves are derived using a statistical method [84], which is adaptable to the studied climate, periods, and geographic region. The second strength of the study relies on the selection of a reference building model as the case study. Therefore, the results are representative and helpful in developing and revising the national or regional building codes. The reference model was developed and validated by some authors of the current paper in a previous study [63]. Third, the paper entails an advanced multi-objective optimization to identify the best combinations of the passive design strategies to enhance energy efficiency and

thermal comfort. Fourth, this paper uses multiple indices to evaluate the overheating risk during heatwaves, including maximum indoor operative temperature, Heat Index (HI), Thermal Autonomy (TA), and Indoor Overheating Degree (IOhD). Such a multi-indicator approach allows to evaluate the building's thermal performance through a more composite, complex, and informative way. Fifth, this paper considers not only current climatic conditions but also future weather projections to analyze the variations in indoor overheating risk due to global warming.

It is plausible that several limitations may have influenced the results obtained. First, the study only assesses three periods (i.e., TMYs for 2010–2020, 2041–2060, and 2081–2100) based on the most likely SSP2-4.5 emission scenario. Therefore, it ignores the intermediate periods (i.e., 2021–2040 and 2061–2080) and other emission scenarios (i.e., SSP1-1.9 *"very low GHG emissions"* and SSP1-2.6 *"low GHG emissions"*, SSP3-7.0 *"high GHG emissions"*, and SSP5-8.5 *"very high GHG emissions"*). Second, this paper lacks Uncertainty Analysis (UA) and Sensitivity Analysis (SA) to take into account the uncertainties in modelling inputs and to find the most influential factors affecting the final HVAC energy use and thermal comfort. Third, only the indoor operative temperature and relative humidity (latter only in calculating Heat Index *"HI"*) are considered while evaluating thermal comfort. However, it is also crucial to consider other comfort factors such as occupant's metabolic rate, clothing insulation, and air velocity. Therefore, more accurate studies are suggested to overcome the limitations of the current paper.

4.3. Implication on practice and future research

The present findings suggest several courses of action to revise current building codes to incorporate compliance criteria during heatwave events. In addition, the new legislation must provide provisions to enhance the preparedness and resistivity of building against global warming. This study also enlightens building professionals, designers, and constructors about the design for climate change. The heat-preserving design concept for buildings in heating-dominated regions should change since it can significantly increase cooling energy use and overheating problems in the future. This study also sheds light on the importance of developing guidelines that include criteria for acute hazard preparation and mitigation strategies as well as chronic risk prevention during abnormal conditions such as power or cooling system outage. Finally, the study establishes a foundation for (IEA) EBC Annex 80 – "Resilient cooling of buildings" project to test and compare different cooling strategies during short-term heatwave events in different climatic zones worldwide. The findings and results will be disseminated publicly to raise awareness about adapting the buildings to such disruptive events.

The findings suggest the following directions for future research. First, future studies should perform similar analyses in other building typologies and climatic regions. In particular, for the Belgian context, the post-World War II buildings are recommended to be studied as the main challenge in renovation schemes [124,125]. Second, further work needs to be carried out by comparing the future weather data obtained from different sources, such as WeatherShift, CORDEX, CCWorldWeatherGen, and Meteonorm. Third, more research is required to improve thermal comfort and overheating indices to incorporate six major comfort parameters (i.e., metabolic rate, clothing factor, relative humidity, air velocity, radiant temperature, and air temperature). Fourth, future research is recommended to perform complementary optimization analyses with different objectives related to cost and environmental impacts. Fifth, the effect of other predicted future global warming scenarios (e.g., SSP1-1.9, SSP1-2.6, SSP3-7.0, and SSP5-8.5) and heatwaves (e.g., the longest and most intense) is of value to be studied in future research. Sixth, further work is recommended to examine the impact of the change of other climate parameters (e.g., wind and humidity) due to climate change on optimal passive design strategies.

5. Conclusion

This paper performs overheating analysis for an optimized nearly Zero-Energy terraced dwelling in Belgium under extreme conditions in two stages. In the first stage, a multi-objective optimization is performed to minimize the final HVAC energy use and thermal discomfort (sum of Indoor Overheating Degree "IOhD" and Indoor Overcooling Degree "IOcD"), considering 13 passive design strategies. In the second stage, three optimal solutions are selected from the resulting Pareto front to analyze the overheating risk during concurrent heatwaves and the cooling system outage. The weather data used in this paper are derived from the Regional Climate Model (MAR) *"Modèle Atmosphérique Régional"*. This paper concludes that, i) even under an optimistic emission scenario of SSP2-4.5, the cooling degree days will overlap the heating degree days by the end of the century in a heating-dominated region like Brussels, ii) high ventilation rate, low infiltration rate, high insulation, high thermal mass, integration of green roof, and application of operable roller blinds can be effective in enhancing thermal comfort and energy performance in similar buildings and climates, and iii) overheating in buildings (even in optimized ones) during abnormal conditions such as heatwaves coincided with the cooling system outage can reach critical and unhealthy levels for the occupants. Overall, overheating in buildings is felt and recognized as a major issue arising from climate change in many regions around the world. There is a need today for additional adaptation and provisions to enhance the preparedness of buildings. Multiple effective strategies have been developed so far that can limit the health, productivity, and well-being impacts of overheating. Governments and policymakers can play a critical role in limiting overheating by encouraging proactive adaptation. This can be achieved by establishing a clear path for well-adapted building stock with quantitative targets backed up with appropriate inspection, enforcement, and access to finance [126].

Data availability

Data will be made available on request.

Declaration of Competing Interest

The authors declare that they have no known competing financial interests or personal relationships that could have appeared to influence the work reported in this paper.

Acknowledgments

This research was funded by the Walloon Region under the call 'Actions de Recherche Concertées 2019 (ARC)' (funding number: ARC 19/23-05) and the project OCCuPANt, on the Impacts Of Climate Change on the indoor environmental and energy PerformAnce of buildiNgs in Belgium during summer. The authors would like to gratefully acknowledge the Walloon Region and the University of Liege for funding. We would like to also acknowledge the Sustainable Building Design (SBD) lab at the Faculty of Applied Sciences at the University of Liege for the use of 64-processor workstation during the computation. This study is a part of the International Energy Agency (IEA) EBC Annex 80 – "Resilient cooling of buildings" project activities to define resilient cooling in residential buildings. No potential competing interest was reported by the authors.

References

[1] IPCC WGII core writing team, "Summary for Policymakers: Climate Change 2022 - Impacts, Adaptation, and Vulnerability.," p.7, IPCC Geneva, Switzerland, 2022. Accessed: Jun. 21, 2022. [Online]. Available: https://www.ipcc.ch/report/ar6/wg2/downloads/report/IPCC_AR6_WGII_FinalDraft_FullReport.pdf

[2] S.I. Bohnenstengel, S. Evans, P.A. Clark, S.E. Belcher, Simulations of the London urban heat island, Q. J. R. Meteorol. Soc. 137 (659) (Jul. 2011) 1625–1640, https://doi.org/10.1002/qj.855.

[3] T. Oke, "The heat island of the urban boundary layer: characteristics, causes and effects", *Wind Clim*, Cities (1995) 81–107, https://doi.org/10.1007/978-94-017-3686-2_5.

[4] G. McGregor, "Heatwaves and health: Guidance on warning-system development", World Meteorological Organisation [Online]. Available: World Health Organisation (2015). https://www.who.int/globalchange/publications/heatwaves-health-guidance/en/.

[5] A. Witze, Extreme heatwaves: surprising lessons from the record warmth, Nature 608 (7923) (2022) 464–465, https://doi.org/10.1038/d41586-022-02114-y.

[6] S.J. Brown, Future changes in heatwave severity, duration and frequency due to climate change for the most populous cities, Weather Clim. Extrem. 30 (Dec. 2020), https://doi.org/10.1016/j.wace.2020.100278.

[7] S. Baker, "Europe is battling an unprecedented heat wave, which has set records in 3 countries and is linked to at least 4 deaths," *Business Insider*, Insider Inc., Jul. 25, 2019.

[8] S. Attia, C. Gobin, Climate Change Effects on Belgian Households: A Case Study of a Nearly Zero Energy Building, Energies 13 (20) (2020) 5357, https://doi.org/10.3390/en13205357.

[9] L. Lan, K. Tsuzuki, Y. Liu, Z. Lian, Thermal environment and sleep quality: A review, Energy Build. 149 (2017) 101–113, https://doi.org/10.1016/j.enbuild.2017.05.043Get.

[10] H. Hooyberghs, S. Verbeke, D. Lauwaet, H. Costa, G. Floater, K. De Ridder, Influence of climate change on summer cooling costs and heat stress in urban office buildings, Clim. Change 144 (4) (Oct. 2017) 721–735, https://doi.org/10.1007/s10584-017-2058-1.

[11] HHSRS, "HHSRS Guidance for Landlords and Property-Related Professionals," London, UK, 2006. [Online]. Available: https://www.gov.uk/government/publications/housing-health-and-safety-rating-system-guidance-for-landlords-and-property-related-professionals

[12] Climate Centre, "European summer heatwaves the most lethal disaster of 2019, says international research group," May 05, 2020. https://www.climatecentre.org/565/european-summer-heatwaves-the-most-lethal-disaster-of-2019-says-international-research-group/ (accessed Jun. 10, 2022).

[13] "In ons land vielen tijdens en vlak na hittegolven 716 doden meer," *De Morgen*, Oct. 03, 2019. Accessed: Jun. 10, 2022. [Online]. Available: https://www.demorgen.be/nieuws/in-ons-land-vielen-tijdens-en-vlak-na-hittegolven-716-doden-meer~b710b9c6/?referrer=https%3A%2F%2Fen.wikipedia.org%2F

[14] Climate Centre, "New official data in Europe exposes heatwaves as still the 'silent killer' of the elderly," Sep. 09, 2019. https://www.climatecentre.org/737/new-official-data-in-europe-exposes-heatwaves-as-still-the-a-silent-killera-of-the-elderly/ (accessed Jun. 10, 2022).

[15] "Heatwave caused nearly 400 more deaths in Netherlands: stats agency," *Reuters*, Aug. 09, 2019. Accessed: Jun. 10, 2022. [Online]. Available: https://www.reuters.com/article/us-weather-netherlands/heatwave-caused-nearly-400-more-deaths-in-netherlands-stats-agency-idUSKCN1UZ0GA?il=0

[16] D. Carrington, "Heatwaves in 2019 led to almost 900 extra deaths in England," *The Guardian*, Jan. 07, 2020. Accessed: Jun. 10, 2022. [Online]. Available: https://www.theguardian.com/world/2020/jan/07/heatwaves-in-2019-led-to-almost-900-extra-deaths-in-england

[17] B. Raddatz, "Almost 500 heat deaths in Berlin last year," Robert Koch Institute, Aug. 29, 2019. Accessed: Jun. 10, 2022. [Online]. Available: https://www.rbb24.de/panorama/thema/2019/klimawandel/beitraege/statistik-hitzetote-sommer-2018-robert-koch-institut.html

[18] A.-T. Nguyen, S. Reiter, P. Rigo, A review on simulation-based optimization methods applied to building performance analysis, Appl. Energy 113 (2014) 1043–1058, https://doi.org/10.1016/j.apenergy.2013.08.061Get, rights and content.

[19] M. Wetter, J. Wright, A comparison of deterministic and probabilistic optimization algorithms for nonsmooth simulation-based optimization, Build. Environ. 39 (8) (2004) 989–999, https://doi.org/10.1016/j.buildenv.2004.01.022.

[20] R. Banos, F. Manzano-Agugliaro, F. Montoya, C. Gil, A. Alcayde, J. Gómez, Optimization methods applied to renewable and sustainable energy: A review, Renew. Sustain. Energy Rev. 15 (4) (2011) 1753–1766, https://doi.org/10.1016/j.rser.2010.12.008.

[21] F. Kheiri, A review on optimization methods applied in energy-efficient building geometry and envelope design, Renew. Sustain. Energy Rev. 92 (Sep. 2018) 897–920, https://doi.org/10.1016/j.rser.2018.04.080.

[22] N. Gunantara, A review of multi-objective optimization: Methods and its applications, Cogent Eng. 5 (1) (2018) 1502242, https://doi.org/10.1080/23311916.2018.1502242.

[23] V. Machairas, A. Tsangrassoulis, K. Axarli, Algorithms for optimization of building design: A review, Renew. Sustain. Energy Rev. 31 (2014) 101–112, https://doi.org/10.1016/j.rser.2013.11.036.

[24] B. Chegari, M. Tabaa, E. Simeu, F. Moutaouakkil, H. Medromi, Multi-objective optimization of building energy performance and indoor thermal comfort by combining artificial neural networks and metaheuristic algorithms, Energy Build. 239 (May 2021), https://doi.org/10.1016/j.enbuild.2021.110839.

[25] A. Vukadinović, J. Radosavljević, A. Đorđević, M. Protić, N. Petrović, Multi-objective optimization of energy performance for a detached residential building with a sunspace using the NSGA-II genetic algorithm, Sol. Energy 224 (Aug. 2021) 1426–1444, https://doi.org/10.1016/j.solener.2021.06.082.

[26] F. Bre, N. Roman, V.D. Fachinotti, An efficient metamodel-based method to carry out multi-objective building performance optimizations, Energy Build. 206 (Jan. 2020), https://doi.org/10.1016/j.enbuild.2019.109576.

[27] S. Gou, V.M. Nik, J.-L. Scartezzini, Q. Zhao, Z. Li, Passive design optimization of newly-built residential buildings in Shanghai for improving indoor thermal comfort while reducing building energy demand, Energy Build. 169 (Jun. 2018) 484–506, https://doi.org/10.1016/j.enbuild.2017.09.095.

[28] K. Li, L. Pan, W. Xue, H. Jiang, and H. Mao, "Multi-Objective Optimization for Energy Performance Improvement of Residential Buildings: A Comparative Study," *Energies*, vol. 10, no. 2, 2017, doi: 10.3390/en10020245.

[29] F. Ascione, N. Bianco, R.F. De Masi, G.M. Mauro, G.P. Vanoli, Design of the Building Envelope: A Novel Multi-Objective Approach for the Optimization of Energy Performance and Thermal Comfort, Sustainability 7 (8) (2015) 10809–10836, https://doi.org/10.3390/su70810809.

[30] F. Ascione, N. Bianco, C. De Stasio, G.M. Mauro, G.P. Vanoli, Simulation-based model predictive control by the multi-objective optimization of building energy performance and thermal comfort, Energy Build. 111 (Jan. 2016) 131–144, https://doi.org/10.1016/j.enbuild.2015.11.033.

[31] W. Yu, B. Li, H. Jia, M. Zhang, D. Wang, Application of multi-objective genetic algorithm to optimize energy efficiency and thermal comfort in building design, Energy Build. 88 (Feb. 2015) 135–143, https://doi.org/10.1016/j.enbuild.2014.11.063.

[32] F. Ascione, N. Bianco, G. Maria Mauro, D.F. Napolitano, Building envelope design: Multi-objective optimization to minimize energy consumption, global cost and thermal discomfort. Application to different Italian climatic zones, Energy 174 (May 2019) 359–374, https://doi.org/10.1016/j.energy.2019.02.182.

[33] A. O' Donovan, M. D. Murphy, and P. D. O'Sullivan, "Passive control strategies for cooling a non-residential nearly zero energy office: Simulated comfort resilience now and in the future," *Energy Build.*, vol. 231, p. 110607, Jan. 2021, doi: 10.1016/j.enbuild.2020.110607.

[34] B. Ozarisoy, Energy effectiveness of passive cooling design strategies to reduce the impact of long-term heatwaves on occupants' thermal comfort in Europe: Climate change and mitigation, J. Clean. Prod. 330 (Jan. 2022), https://doi.org/10.1016/j.jclepro.2021.129675.

[35] A. Laouadi, M. Bartko, M.A. Lacasse, A new methodology of evaluation of overheating in buildings, Energy Build. 226 (Nov. 2020), https://doi.org/10.1016/j.enbuild.2020.110360.

[36] CIBSE TM52, *CIBSE TM52: The limits of thermal comfort: avoiding overheating in European buildings.* Chartered Institution of Building Services Engineers, London, UK: Chartered Institution of Building Services Engineers, London, UK, 2013.

[37] W. Feist, B. Kaufmann, J. Schnieders, O. Kah, Passive house planning package, Passive House Inst. Darmstadt Ger. (2015).

[38] X. Zhou, J. Carmeliet, M. Sulzer, D. Derome, Energy-efficient mitigation measures for improving indoor thermal comfort during heat waves, Appl. Energy 278 (Nov. 2020), https://doi.org/10.1016/j.apenergy.2020.115620.

[39] Y.T. Kwok et al., Thermal comfort and energy performance of public rental housing under typical and near-extreme weather conditions in Hong Kong, Energy Build. 156 (Dec. 2017) 390–403, https://doi.org/10.1016/j.enbuild.2017.09.067.

[40] S.M. Porritt, P.C. Cropper, L. Shao, C.I. Goodier, Ranking of interventions to reduce dwelling overheating during heat waves, Energy Build. 55 (Dec. 2012) 16–27, https://doi.org/10.1016/j.enbuild.2012.01.043.

[41] S. Porritt, L. Shao, P. Cropper, C. Goodier, Adapting dwellings for heat waves, Sustain. Cities Soc. 1 (2) (Jul. 2011) 81–90, https://doi.org/10.1016/j.scs.2011.02.004.

[42] A. Sakka, M. Santamouris, I. Livada, F. Nicol, M. Wilson, On the thermal performance of low income housing during heat waves, Energy Build. 49 (Jun. 2012) 69–77, https://doi.org/10.1016/j.enbuild.2012.01.023.

[43] A. Baniassadi, J. Heusinger, D.J. Sailor, Energy efficiency vs resiliency to extreme heat and power outages: The role of evolving building energy codes, Build. Environ. 139 (Jul. 2018) 86–94, https://doi.org/10.1016/j.buildenv.2018.05.024.

[44] A. Baniassadi, D.J. Sailor, Synergies and trade-offs between energy efficiency and resiliency to extreme heat – A case study, Build. Environ. 132 (Mar. 2018) 263–272, https://doi.org/10.1016/j.buildenv.2018.01.037.

[45] A. Ebrahimi-Moghadam, P. Ildarabadi, K. Aliakbari, F. Fadaee, Sensitivity analysis and multi-objective optimization of energy consumption and thermal comfort by using interior light shelves in residential buildings, Renew. Energy 159 (Oct. 2020) 736–755, https://doi.org/10.1016/j.renene.2020.05.127.

[46] C. Zhang *et al.*, "IEA EBC Annex 80 - Dynamic simulation guideline for the performance testing of resilient cooling strategies: Version 2," Aaalborg University, DCE Technical Reports 306, 2023.

[47] R. Rahif, M. Hamdy, S. Homaei, C. Zhang, P. Holzer, and S. Attia, "Simulation-based framework to evaluate resistivity of cooling strategies in buildings against overheating impact of climate change," *Build. Environ.*, p. 108599, 2022, doi: 10.1016/j.buildenv.2021.108599.
[48] S. Attia et al., "Framework to evaluate the resilience of different cooling technologies", *IEA Annex 80 – Resilient Cool*, Build. (2021), https://doi.org/10.13140/RG.2.2.24588.13447.
[49] D.B. Crawley, J.W. Hand, M. Kummert, B.T. Griffith, Contrasting the capabilities of building energy performance simulation programs, Build. Environ. 43 (4) (2008) 661–673, https://doi.org/10.1016/j.buildenv.2006.10.027.
[50] ANSI/ASHRAE 140-2017, *Standard 140-2017: Standard Method of Test for the Evaluation of Building Energy Analysis Computer Programs*. American Society of Heating, Refrigerating and Air Conditioning Engineers: Atlanta, GA, USA, 2017.
[51] G. Betti, F. Tatarini, S. Schiavon, and C. Nguyen, "CBE Clima Tool. Version 0.4.6.," *Center for the Built Environment, University of California Berkeley*. https://clima.cbe.berkeley.edu (accessed Aug. 19, 2022).
[52] R. Rahif, S. Attia, IOhD (Calculation & illustration), IOcD (Calculation & illustration), AWD (Calculation & illustration), ACD (Calculation & illustration), CCOhR (Calculation), CCOcR (Calculation), Zonal OpT (illustration), and HWs (illustration) v01, Zenodo (Nov. 2022), https://doi.org/10.5281/zenodo.7326901.
[53] R.S. McLeod, M. Swainson, Chronic overheating in low carbon urban developments in a temperate climate, Renew. Sustain. Energy Rev. 74 (Jul. 2017) 201–220, https://doi.org/10.1016/j.rser.2016.09.106.
[54] K.J. Lomas, S.M. Porritt, Overheating in buildings: lessons from research, Build. Res. Inf. (2017), https://doi.org/10.1080/09613218.2017.1256136.
[55] R. Mitchell, S. Natarajan, Overheating risk in Passivhaus dwellings, Build. Serv. Eng. Res. Technol. 40 (4) (2019) 446–469, https://doi.org/10.1177/0143624419842000.
[56] N. Artmann, H. Manz, P. Heiselberg, Parameter study on performance of building cooling by night-time ventilation, Renew. Energy 33 (12) (2008) 2589–2598, https://doi.org/10.1016/j.renene.2008.02.025.
[57] V. Badescu, N. Laaser, R. Crutescu, Warm season cooling requirements for passive buildings in Southeastern Europe (Romania), Energy 35 (8) (2010) 3284–3300, https://doi.org/10.1016/j.energy.2010.04.013.
[58] S.S. Intille, Designing a home of the future, IEEE Pervasive Comput. 1 (2) (2002) 76–82, https://doi.org/10.1109/MPRV.2002.1012340.
[59] S. Phillips, Working through the pandemic: Accelerating the transition to remote working, Bus. Inf. Rev. 37 (3) (2020) 129–134, https://doi.org/10.1177/0266382120953087.
[60] Zero Carbon Hub, Impacts of Overheating: Evidence Review, Zero Carbon Hub, London, England, 2015.
[61] R.S. Kovats, S. Hajat, Heat Stress and Public Health: A Critical Review, Annu. Rev. Public Health 29 (1) (Mar. 2008) 41–55, https://doi.org/10.1146/annurev.publhealth.29.020907.090843.
[62] S. Attia, T. Canonge, M. Popineau, M. Cuchet, Developing a benchmark model for renovated, nearly zero-energy, terraced dwellings, Appl. Energy 306 (Jan. 2022), https://doi.org/10.1016/j.apenergy.2021.118128.
[63] S. Attia, Benchmark model for nearly-zero-energy terraced dwellings, Harv. Dataverse Camb. U. S. (2021), https://doi.org/10.7910/DVN/GJI84W.
[64] R. Rahif et al., Impact of climate change on nearly zero-energy dwelling in temperate climate: Time-integrated discomfort, HVAC energy performance, and GHG emissions, Build. Environ. 223 (Sep. 2022), https://doi.org/10.1016/j.buildenv.2022.109397.
[65] E. Elnagar, A. Zeoli, R. Rahif, S. Attia, V. Lemort, A qualitative assessment of integrated active cooling systems: A review with a focus on system flexibility and climate resilience, Renew. Sustain. Energy Rev. 175 (Apr. 2023), https://doi.org/10.1016/j.rser.2023.113179.
[66] ANSI/ASHRAE Handbook, *Handbook–2017: Fundamentals*. American Society of Heating, Refrigerating and Air Conditioning Engineers: Atlanta, GA, USA, 2017.
[67] V. Pêrez-Andreu, C. Aparicio-Fernández, A. Martínez-Ibernón, J.-L. Vivancos, Impact of climate change on heating and cooling energy demand in a residential building in a Mediterranean climate, Energy 165 (Dec. 2018) 63–74, https://doi.org/10.1016/j.energy.2018.09.015.
[68] S. Doutreloup et al., Historical and future weather data for dynamic building simulations in Belgium using the regional climate model MAR: typical and extreme meteorological year and heatwaves, Earth Syst. Sci. Data 14 (7) (2022) 3039–3051, https://doi.org/10.5194/essd-14-3039-2022.
[69] K. De Ridder, H. Gallée, Land surface–induced regional climate change in southern Israel, J. Appl. Meteorol. 37 (11) (1998) 1470–1485, https://doi.org/10.1175/1520-0450(1998)037<1470:LSIRCC>2.0.CO;2.
[70] S. Doutreloup, C. Wyard, C. Amory, C. Kittel, M. Erpicum, X. Fettweis, Sensitivity to convective schemes on precipitation simulated by the regional climate model MAR over Belgium (1987–2017), Atmos. 10 (1) (2019) 34, https://doi.org/10.3390/atmos10010034.
[71] C. Wyard, C. Scholzen, S. Doutreloup, É. Hallot, X. Fettweis, Future evolution of the hydroclimatic conditions favouring floods in the south-east of Belgium by 2100 using a regional climate model, Int. J. Climatol. 41 (1) (2021) 647–662, https://doi.org/10.1002/joc.6642.
[72] H. Hersbach et al., The ERA5 global reanalysis, Q. J. R. Meteorol. Soc. 146 (730) (2020) 1999–2049, https://doi.org/10.1002/qj.3803.
[73] V. Eyring et al., Overview of the Coupled Model Intercomparison Project Phase 6 (CMIP6) experimental design and organization, Geosci. Model Dev. 9 (5) (2016) 1937–1958, https://doi.org/10.5194/gmd-9-1937-2016.
[74] K. Riahi et al., The Shared Socioeconomic Pathways and their energy, land use, and greenhouse gas emissions implications: An overview, Glob. Environ. Change 42 (Jan. 2017) 153–168, https://doi.org/10.1016/j.gloenvcha.2016.05.009.
[75] V. Masson-Delmotte *et al.*, "Climate Change 2021: The Physical Science Basis Contribution of Working Group I to the Sixth Assessment Report of the Intergovernmental Panel on Climate Change," 2021.
[76] R. Pielke Jr, M.G. Burgess, J. Ritchie, Plausible 2005–2050 emissions scenarios project between 2° C and 3° C of warming by 2100, Environ. Res. Lett. 17 (2) (2022), https://doi.org/10.1088/1748-9326/ac4ebf.
[77] R.K. Pachauri et al., Climate change 2014: synthesis report. Contribution of Working Groups I, II and III to the fifth assessment report of the Intergovernmental Panel on Climate Change, Ipcc, 2014.
[78] Global Carbon Project, Supplemental data of Global Carbon Budget 2021 (Version 1.0), Glob. Carbon Proj. 2021 (2021).
[79] L. Cozzi et al., World energy outlook 2020, Int. Energy Agency Paris Fr. (2020) 1–461.
[80] ISO 15927-4, "'ISO 15927-4: Hygrothermal performance of buildings — Calculation and presentation of climatic data — Part 4: Hourly data for assessing the annual energy use for heating and cooling'.," p. Geneva, Switzerland, 2005.
[81] S. Wilcox and W. Marion, "Users Manual for TMY3 Data Sets, Technical report NREL/TP-581-43156, Task No. PVA7.6101," National Renewable Energy Laboratory Golden, CO, 2008. Accessed: Oct. 10, 2022. [Online]. Available: https://www.nrel.gov/docs/fy08osti/43156.pdf, 2008
[82] C.S. Barnaby, U.B. Crawley, Weather data for building performance simulation, Build. Perform. Simul. Des. Oper. (2012) 61–79, https://doi.org/10.4324/9780203891612.
[83] RMI, "Rapport climatique 2020 de l'information aux services climatiques, edited by: Gellens, D., Royal Meteorological Institute of Belgium, Brussels, ISSN 2033-8562," 2020. Accessed: Aug. 31, 2022. [Online]. Available: https://www.meteo.be/resources/misc/climate report/RapportClimatique-2020.pdf
[84] G. Ouzeau, J.-M. Soubeyroux, M. Schneider, R. Vautard, S. Planton, Heat waves analysis over France in present and future climate: Application of a new method on the EURO-CORDEX ensemble, Clim. Serv. 4 (Dec. 2016) 1–12, https://doi.org/10.1016/j.cliser.2016.09.002.
[85] S. Attia et al., Resilient cooling of buildings to protect against heat waves and power outages: Key concepts and definition, Energy Build. 239 (May 2021), https://doi.org/10.1016/j.enbuild.2021.110869.
[86] K. Deb, A. Pratap, S. Agarwal, T. Meyarivan, A fast and elitist multiobjective genetic algorithm: NSGA-II, IEEE Trans. Evol. Comput. 6 (2) (2002) 182–197, https://doi.org/10.1109/4235.996017.
[87] L. Magnier, F. Haghighat, Multiobjective optimization of building design using TRNSYS simulations, genetic algorithm, and Artificial Neural Network, Build. Environ. 45 (3) (2010) 739–746, https://doi.org/10.1016/j.buildenv.2009.08.016.
[88] F.P. Chantrelle, H. Lahmidi, W. Keilholz, M. El Mankibi, P. Michel, Development of a multicriteria tool for optimizing the renovation of buildings, Appl. Energy 88 (4) (2011) 1386–1394, https://doi.org/10.1016/j.apenergy.2010.10.002.
[89] S. Carlucci, G. Cattarin, F. Causone, L. Pagliano, Multi-objective optimization of a nearly zero-energy building based on thermal and visual discomfort minimization using a non-dominated sorting genetic algorithm (NSGA-II), Energy Build. 104 (2015) 378–394.
[90] J.C. Gamero-Salinas, A. Monge-Barrio, A. Sánchez-Ostiz, Overheating risk assessment of different dwellings during the hottest season of a warm tropical climate, Build. Environ. 171 (Mar. 2020), https://doi.org/10.1016/j.buildenv.2020.106664.
[91] W.A. Mahar, G. Verbeeck, S. Reiter, S. Attia, Sensitivity analysis of passive design strategies for residential buildings in cold semi-arid climates, Sustainability 12 (3) (2020) 1091, https://doi.org/10.3390/su12031091.
[92] J. Mukkavaara, F. Shadram, An integrated optimization and sensitivity analysis approach to support the life cycle energy trade-off in building design, Energy Build. 253 (Dec. 2021), https://doi.org/10.1016/j.enbuild.2021.111529.
[93] K. Menberg, Y. Heo, R. Choudhary, Sensitivity analysis methods for building energy models: Comparing computational costs and extractable information, Energy Build. 133 (Dec. 2016) 433–445, https://doi.org/10.1016/j.enbuild.2016.10.005.
[94] M. Hamdy, S. Carlucci, P.-J. Hoes, J.L.M. Hensen, The impact of climate change on the overheating risk in dwellings—A Dutch case study, Build. Environ. 122 (Sep. 2017) 307–323, https://doi.org/10.1016/j.buildenv.2017.06.031.
[95] R. Rahif, D. Amaripadath, S. Attia, Review on Time-Integrated Overheating Evaluation Methods for Residential Buildings in Temperate Climates of Europe, Energy Build. 252 (Dec. 2021), https://doi.org/10.1016/j.enbuild.2021.111463.
[96] S. Carlucci, L. Pagliano, A review of indices for the long-term evaluation of the general thermal comfort conditions in buildings, Energy Build. 53 (Oct. 2012) 194–205, https://doi.org/10.1016/j.enbuild.2012.06.015.
[97] M. Kazemi, L. Courard, Modelling hygrothermal conditions of unsaturated substrate and drainage layers for the thermal resistance assessment of green roof: Effect of coarse recycled materials, Energy Build. 250 (Nov. 2021), https://doi.org/10.1016/j.enbuild.2021.111315.

[98] RELi 2.0., "Rating Guidelines for Resilient Design + Construction," U.S. Green Building Council, Feb. 2020.
[99] B. Levitt, M. Ubbelohde, G. Loisos, and N. Brown, "Thermal autonomy as metric and design process," presented at the CaGBC National Conference and Expo: Pushing the Boundary-Net Positive Buildings, 2013, pp. 47–58.
[100] L.P. Rothfusz, N.S.R. Headquarters, The heat index equation (or, more than you ever wanted to know about heat index), Ft. Worth Tex. Natl. Ocean. Atmospheric Adm. Natl. Weather Serv. Off. Meteorol. 9023 (1990).
[101] M. Zune, L. Rodrigues, M. Gillott, The vulnerability of homes to overheating in Myanmar today and in the future: A heat index analysis of measured and simulated data, Energy Build. 223 (2020), https://doi.org/10.1016/j.enbuild.2020.110201.
[102] A.R. Rempel, J. Danis, A.W. Rempel, M. Fowler, S. Mishra, Improving the passive survivability of residential buildings during extreme heat events in the Pacific Northwest, Appl. Energy 321 (Sep. 2022), https://doi.org/10.1016/j.apenergy.2022.119323.
[103] E.S. Quigley, K. Lomas, "Performance of medium-rise, thermally lightweight apartment buildings during a heat wave", presented at the Proceedings of 10th Windsor Conference: Rethinking Comfort, London, UK, Apr, Windsor, 2018, pp. 32–47.
[104] K. Sun, M. Specian, T. Hong, Nexus of thermal resilience and energy efficiency in buildings: A case study of a nursing home, Build. Environ. 177 (Jun. 2020), https://doi.org/10.1016/j.buildenv.2020.106842.
[105] K. Papakostas, N. Kyriakis, Heating and cooling degree-hours for Athens and Thessaloniki, Greece, Renew. Energy 30 (12) (2005) 1873–1880, https://doi.org/10.1016/j.renene.2004.12.002.
[106] D.J. Sailor, Relating residential and commercial sector electricity loads to climate—evaluating state level sensitivities and vulnerabilities, Energy 26 (7) (Jul. 2001) 645–657, https://doi.org/10.1016/S0360-5442(01)00023-8.
[107] A. Ploskić, Q. Wang, Evaluating the potential of reducing peak heating load of a multi-family house using novel heat recovery system, Appl. Therm. Eng. 130 (Feb. 2018) 1182–1190, https://doi.org/10.1016/j.applthermaleng.2017.11.072.
[108] R. Rahif A. Fani S. Attia Climate Change Sensitive Overheating Assessment in Dwellings: A Case Study in Belgium Proceeding of the International Building Simulation Conference 2021 Bruges, Belgium 30125 30131 [Online]. Available:
[109] R. Becker, I. Goldberger, M. Paciuk, Improving energy performance of school buildings while ensuring indoor air quality ventilation, Build. Environ. 42 (9) (2007) 3261–3276, https://doi.org/10.1016/j.buildenv.2006.08.016.
[110] M. Gil-Baez, Á. Barrios-Padura, M. Molina-Huelva, R. Chacartegui, Natural ventilation systems in 21st-century for near zero energy school buildings, Energy 137 (2017) 1186–1200, https://doi.org/10.1016/j.energy.2017.05.188.
[111] E. Tavakoli, A. O'Donovan, M. Kolokotroni, P.D. O'Sullivan, Evaluating the indoor thermal resilience of ventilative cooling in non-residential low energy buildings: A review, Build. Environ. 222 (Aug. 2022), https://doi.org/10.1016/j.buildenv.2022.109376.
[112] K. Hassouneh, A. Alshboul, A. Al-Salaymeh, Influence of infiltration on the energy losses in residential buildings in Amman, Sustain. Cities Soc. 5 (2012) 2–7, https://doi.org/10.1016/j.scs.2012.09.004.
[113] U. Mathur, R. Damle, Impact of air infiltration rate on the thermal transmittance value of building envelope, J. Build. Eng. 40 (Aug. 2021), https://doi.org/10.1016/j.jobe.2021.102302.
[114] J. Jokisalo, J. Kurnitski, M. Korpi, T. Kalamees, J. Vinha, Building leakage, infiltration, and energy performance analyses for Finnish detached houses, Build. Environ. 44 (2) (2009) 377–387, https://doi.org/10.1016/j.buildenv.2008.03.014.
[115] J. Lee, J. Kim, D. Song, J. Kim, C. Jang, Impact of external insulation and internal thermal density upon energy consumption of buildings in a temperate climate with four distinct seasons, Renew. Sustain. Energy Rev. 75 (Aug. 2017) 1081–1088, https://doi.org/10.1016/j.rser.2016.11.087.
[116] S.A. Al-Sanea, M.F. Zedan, S.N. Al-Hussain, Effect of thermal mass on performance of insulated building walls and the concept of energy savings potential, Spec. Issue Therm. Energy Manag. Process Ind. 89 (1) (Jan. 2012) 430–442, https://doi.org/10.1016/j.apenergy.2011.08.009.
[117] J. Goussous, H. Siam, H. Alzoubi, Prospects of green roof technology for energy and thermal benefits in buildings: Case of Jordan, Sustain. Cities Soc. 14 (Feb. 2015) 425–440, https://doi.org/10.1016/j.scs.2014.05.012.
[118] A. Sfakianaki, E. Pagalou, K. Pavlou, M. Santamouris, M. Assimakopoulos, Theoretical and experimental analysis of the thermal behaviour of a green roof system installed in two residential buildings in Athens, Greece, Int. J. Energy Res. 33 (12) (2009) 1059–1069, https://doi.org/10.1002/er.1535.
[119] B. Stone et al., Climate change and infrastructure risk: Indoor heat exposure during a concurrent heat wave and blackout event in Phoenix, Arizona, Urban Clim. 36 (Mar. 2021), https://doi.org/10.1016/j.uclim.2021.100787.
[120] B. Stone Jr et al., Compound climate and infrastructure events: how electrical grid failure alters heat wave risk, Environ. Sci. Technol. 55 (10) (2021) 6957–6964, https://doi.org/10.1021/acs.est.1c00024.
[121] M. Hamdy, K. Sirén, S. Attia, Impact of financial assumptions on the cost optimality towards nearly zero energy buildings – A case study, Energy Build. 153 (Oct. 2017) 421–438, https://doi.org/10.1016/j.enbuild.2017.08.018.
[122] T. Hong, Z. Wang, X. Luo, W. Zhang, State-of-the-art on research and applications of machine learning in the building life cycle, Energy Build. 212 (Apr. 2020), https://doi.org/10.1016/j.enbuild.2020.109831.
[123] M. Ferrara, E. Fabrizio, J. Virgone, M. Filippi, Energy systems in cost-optimized design of nearly zero-energy buildings, Autom. Constr. 70 (2016) 109–127, https://doi.org/10.1016/j.autcon.2016.06.007.
[124] G. Ruellan, M. Cools, S. Attia, Analysis of the determining factors for the renovation of the Walloon residential building stock, Sustainability 13 (4) (2021) 2221, https://doi.org/10.3390/su13042221.
[125] S. Attia, A. Mustafa, N. Gir1y, M. Popineau, M. Cuchet, N. Gulirmak, Developing two benchmark models for post-world war II residential buildings, Energy Build. 244 (Aug. 2021), https://doi.org/10.1016/j.enbuild.2021.111052.
[126] T. Dooks, "Risks to health, wellbeing and productivity from overheating in buildings," *Clim. Change Comm.*, Jul. 2022, Accessed: Oct. 10, 2022. [Online]. Available: https://www.theccc.org.uk/publication/risks-to-health-wellbeing-and-productivity-from-overheating-in-buildings/